The link between true larvae and parasitic forms within Isopoda – insights from the fossil record

Dissertation an der Fakultät für Biologie der Ludwig-Maximilians-Universität München
zur Erlangung des Doktorgrades der Naturwissenschaften (Dr. rer nat.)

Vorgelegt von Mario Schädel
München / Tübingen, 2022

Diese Dissertation wurde unter Leitung von Prof. Dr. Joachim T. Haug im Bereich Zoologie an der Ludwig-Maximilians-Universität München angefertigt.

Erstgutachter:	Prof. Dr. Joachim T. Haug
Zweitgutachter:	Prof. Dr. Roland Melzer
Tag der Abgabe:	27.01.2022
Tag der Mündlichen Prüfung:	29.09.2022

Eidesstattliche Erklärung

Ich versichere hiermit an Eides statt, dass die vorgelegte Dissertation von mir selbständig und ohne unerlaubte Hilfe angefertigt ist.

Tübingen, 19.10.2022   Mario Schädel

Erklärung

Hiermit erkläre ich, dass die Dissertation nicht ganz oder in wesentlichen Teilen einer anderen Prüfungskommission vorgelegt worden ist. Darüberhinaus erkläre ich, dass ich mich nicht anderweitig (mit oder ohne Erfolg) einer Doktorprüfung unterzogen habe.

Tübingen, 19.10.2022   Mario Schädel

Table of Contents

List of publications incorporated in this thesis

I   SCHÄDEL, M., HYŽNÝ, M. & HAUG, J. T. 2021. Ontogenetic development captured in amber – the first record of aquatic representatives of Isopoda in Cretaceous amber from Myanmar. Nauplius 29, e2021003. https://doi.org/10.1590/2358-2936e2021003

II   SCHÄDEL, M., PERRICHOT, V. & HAUG, J. T. 2019. Exceptionally preserved cryptoniscium larvae – morphological details of rare isopod crustaceans from French Cretaceous Vendean amber. *Palaeontologia Electronica*, 22.3.71, 1–45. https://doi.org/10.26879/977

III   SCHÄDEL, M., HÖRNIG, M. K., HYŽNÝ, M., & HAUG, J. T. 2021. Mass occurrence of small isopodan crustaceans in 100-million-year-old amber: an extraordinary view on behaviour of extinct organisms. PalZ, 1-17. https://doi.org/10.1007/s12542-021-_00564-9

IV   VAN DER WAL, S., SCHÄDEL, M., EKRT, B., HAUG, J. T. 2021. Description and ontogeny of a 40-million-year-old parasitic isopodan crustacean: *Parvucymoides dvorakorum* gen. et sp. nov. PeerJ. https://doi.org/10.7717/peerj.12317

V   SCHÄDEL, M., HYŽNÝ, M., NAGLER, C. & HAUG, J. T. (unpublished manuscript). Fossil relatives of extant parasitic crustaceans from the Mesozoic of Europe.

Author contributions to manuscripts included in this thesis

This thesis contains the results of the research conducted from 2018 until 2021 in the course of my doctoral studies at the Ludwig-Maximilians-Universität München under the supervision of Prof. Dr. Joachim T. Haug. The author contribution declarations below are based on the CRediT taxonomy (https://credit.niso.org).

I   SCHÄDEL, M., PERRICHOT, V. & HAUG, J. T. 2019

Conceptualization: MS, JTH; Data curation: MS, VP, JTH; Formal Analysis: MS; Funding acquisition JTH, VP; Investigation: MS, VP, JTH; Methodology: MS, JTH; Project administration: MS, JTH; Resources: VP, JTH; Software: MS; Supervision: JTH; Visualization: MS, VP, JTH; Writing – original draft: MS; Writing – review & editing: MS, JTH, VP.

II   SCHÄDEL, M., HYŽNÝ, M., & HAUG, J. T. 2021

Conceptualization: MS, MH, JTH; Data curation: MS; Formal Analysis: MS; Funding acquisition: MH, JTH; Investigation: MS; Methodology: MS, JTH; Project administration: MS, MH, JTH; Resources: MH, JTH; Supervision: JTH; Visualization: MS; Writing – original draft: MS; Writing – review & editing: MS, MH, JTH

III   SCHÄDEL, M., HÖRNIG, M. K., HYŽNÝ, M., & HAUG, J. T. 2021

Conceptualization: MS, MKH, MH, JTH; Data curation: MS, MKH; Formal Analysis: MS; Funding acquisition: MKH, MH, JTH; Investigation: MS; Methodology: MS, MKH, JTH; Project administration: MS, JTH; Resources: MKH, MH, JTH; Software: MS; Supervision: JTH; Visualization: MS, MKH; Writing – original draft: MS, MKH; Writing – review & editing: MS, MKH, MH, JTH.

IV VAN DER WAL, S., SCHÄDEL, M., EKRT, B., HAUG, J. T. 2021
Conceptualization: SW, MS, JTH; Data curation: SW, MS; Formal Analysis: SW; Funding acquisition: SW, BE, JTH; Investigation: SW, MS; Methodology: SW, MS, JTH; Project administration: SW, JTH; Resources: BE, JTH; Software: SW, MS; Supervision: JTH; Visualization: SW, MS; Writing – original draft: SW, MS; Writing – review & editing: SW, MS, BE, JTH.

V SCHÄDEL, M., HYŽNÝ, M., NAGLER, C. & HAUG, J. T. (unpublished manuscript)
Conceptualization: MS, MH, CN, JTH; Data curation: MS, CN; Formal Analysis: MS; Funding acquisition: MH, CN, JTH; Investigation: MS, MH; Methodology: MS; Project administration: MS, MH; Resources: MS, CN, JTH; Software: MS; Supervision: JTH; Visualization: MS; Writing – original draft: MS; Writing – review & editing: MS, MH, JTH.

……………………………………   ………………………………………...
Ort, Datum   Mario Schädel

……………………………………   ………………………………………...
Ort, Datum   Joachim T. Haug

Summary

Isopoda is a species-rich ingroup of Eucrustacea (crustaceans and insects), whose representatives live in a variety of habitats from the deep sea to arid terrestrial landscapes. Isopoda is very diverse regarding the life styles which are present in its species. There are herbivorous and detritivorous species as well as predators and scavengers. Parasitism, as an interaction between animals where one animal exploits resources from the other to it's disadvantage, is far from being a fringe phenomenon inside Isopoda – a large proportion of species in Isopoda are either parasites or micro-predators (also referred to as temporary parasites). Parasitic forms (in the wider sense, including micro-predators) of Isopoda can be found in a few ingroups, which are generally thought to be closely related or to form a monophyletic group. Among the parasitic forms there are many species whose development includes a strong ecological and morphological differentiation between the immatures and the adults (larval development). Despite the ecological importance in modern ecosystems, the fossil record of parasitic forms of Isopoda is rather sparse.

The aim of this study was to recognise and thoroughly document potentially parasitic forms of Isopoda in the fossil record, using modern imaging techniques. By interpreting the systematic positions of the extinct species, the fossil forms could be compared with closely related extant forms for which there are observations of their behaviour in their natural environment. The goal was also to recognise potentially immature forms, which could provide insights into the evolution of developmental patterns within Isopoda, especially with respect to the parasitic forms in which there seems to be a stronger tendency for differentiation between adults and their offspring. Fossils have the potential to yield combinations of characters that are not present in extant species and are thereby important to reconstruct the evolution of characters. Fossils of such value were explicitly searched for. Furthermore, the fossils inspected in the studies of this dissertation should be used to provide a temporal context to the evolution of parasitism and larval development within Isopoda.

Two well-preserved fossils of presumably non-parasitic forms within the group Cymothoida (in which there are also parasitic forms) from fossilised mid-Cretaceous resin were studied (study I). One of them was interpreted as an immature, which resembles the other, larger, specimen, which is assumed to be of a later developmental stage, in most aspects of the body morphology – except for the absence of a well developed leg on the posterior-most walking leg, which absence in immatures is an apomorphy of the group

Mancoidea, which comprises Isopoda. This represents, together with a recently published fossil of the same site, the oldest record of an immature specimen in Isopoda.

Multiple minute fossils of the group Epicaridea (parasites of crustaceans) from two different mid- and Late Cretaceous amber localities (studies I and III) were studied. They represent the oldest body fossils of the group Epicaridea, which has a rich record of fossil traces which its representatives left on their host (growth responses by the host) while feeding on them. Based on the available morphological features, the fossils were identified as either larvae (of the cryptoniscium stage) or paedomorphic adult males. Their presence in the fossil record suggests that the complex life cycle that is found in extant species of Epicaridea was already present in the Cretaceous.

An assemblage of multiple strongly compressed fossils from the Eocene of the Czech Republic was documented (study IV). The specimens were identified as being either close relatives to or representatives of group Cymothoidae (mostly parasites of fishes in the extant fauna). This marks the first and therefore oldest reliable record of this lineage in the fossil record. The assemblage contains specimens of different body sizes. Together with differences in the overall body shape this indicates the presence of immature stages.

Fossils of *Urda*, an extinct, potentially non-monophyletic group with a unique combination of characters, were analysed (study V). The fossils are interpreted as the closest so far known relatives of the extant group Gnathiidae (temporary parasites of fishes), with which representatives they share a number of apomorphic characters; a convincing apomorphy for *Urda* could not be found. The fossils, for which there is no indication that they represent remains of immatures, are very similar in many aspects to immature forms of Gnathiidae, in contrast to which they, however, lack the paedomorphic absence of legs on one segment of the trunk. The occurrence of some fossils of Urda on fossils of fishes suggests a syn-vivo interaction, such as parasitism or commensalism. Fossils of *Urda* provide important information about the character evolution towards modern, fish-parasites of the group Gnathiidae.

The evolution of larvae within Isopoda seems to be deeply interlinked with the evolution of parasitism. The fossil record yields specimens with a larval development that date back to the mid-Cretaceous. These specimens simultaneously represent the oldest fossils which can be identified as belonging to extant groups in which all species have a parasitic life style. Close relatives of extant parasites date back even further, to the Lower Jurassic. Overall, despite still being patchy, the fossil record of Isopoda provides unique

insights into the evolution of parasitic forms as well as into the differentiation between adults and immature forms.

1 Introduction

1.1 General background to the group Isopoda

Isopoda Latreille, 1817 is a diverse group of crustaceans, with a worldwide distribution and well over 10000 described extant species (Boyko et al. 2008). Isopoda is not only species-rich but also yields a high diversity of body shapes. Besides from the more typical body shape, like for example that of a woodlouse, there are very thin and elongated (Wägele 1981) as well as distinctly flattened disc-shaped forms (Moreira 1971), but also individuals without a sclerotised exoskeleton (Shiino 1954). Also from an ecological perspective Isopoda yields a high diversity. Unlike woodlice, which as their name suggests, live in a terrestrial environment, many other species within Isopoda live underwater and from those many live in the sea or in brackish environments (Poore & Bruce 2012). Isopoda can be seen as a primarily marine group, meaning that besides that most species are marine (Boyko et al. 2008), also the direct ancestor of Isopoda likely lived in the ocean (Brusca & Wilson 1991). Today, representatives of Isopoda inhabit a wide range of habitats from the deep sea (Lins et al. 2012) to freshwater (Brasil-Lima & De Lima Barros 1998) and arid terrestrial landscapes (Schmidt 2008). Oniscidea is, within Isopoda, the only group that successfully managed to produce animals with a fully terrestrial lifestyle and by this is also a very species-rich group (more than 3500 species) (Brusca et al. 2001; Schmalfuss 2003; Boyko et al. 2008). Feeding types differ drastically between different lineages of Isopoda; for example, there are detritivores (Arrontes 1990), suspension feeders (Wägele 1987; Si et al. 2002) and scavengers (Lowry & Dempsey 2006) as well as specialised herbivores (Daniel et al. 1991), predators (Wägele 1985) and parasites (Nagler & Haug 2016; Nagler et al. 2020).

1.2 Development in Isopoda

Isopoda is an ingroup of Peracarida; by this, its representatives share a form of prolonged maternal brood care. The eggs are carried in a brood pouch located on the ventral side of the female, which is made up of flat overlapping protrusions of the walking legs and the posterior-most appendage of the head (oostegites); the offspring is also carried in the brood pouch after it has hatched from the eggs for some time (Wägele 1989; Ax 2000 p. 174).

Isopoda is also an ingroup of Mancoidea (=Mancoida; Spelaeogriphacea + Cumacea + Tanaidacea + Isopoda), which itself is an ingroup of Peracarida, the most outstanding autapomorphy of Mancoidea is the manca stage – an immature life stage, in which only the posterior-most walking leg (post-ocular segment 13) is not yet fully developed (Watling 1981; Ax 2000 p. 176; Boyko & Wolff 2014).

Like in other ingroups of Peracarida, the offspring within most species of Isopoda strongly resembles the adult, which is by some authors referred to as the offspring hatching as 'miniature versions of the adult' (Boyko & Wolff 2014 p. 210). However, it has been shown for another ingroup of Peracarida, Amphipoda (Lang et al. 2007), that despite the overall resemblance there are still a lot of differences between the freshly hatched immatures and the adults (Haug 2019). Overall, the lesser extent of differentiation between adults and their offspring in Peracarida seems to be linked with a loss of true larval stages and outside of Isopoda there are no records so far of species in which the offspring is strongly differing from the adults apart from its size (Martin et al. 2014). Yet, within a few ingroups of Isopoda there are immature forms which qualify as true larvae according to most characterisations of the term 'larva' (cf. Haug 2020).

In Epicaridea Latreille, 1825 the offspring undergoes three distinct phases until reaching sexual maturity. These phases can be distinguished morphologically but also there are ecological differences between the phases. The entire immature phase, from being released from the brood pouch to reaching sexual maturity lasts about 10-30 days (Caroli 1928; Anderson 1975). The first stage is termed epicaridium. In this stage the immatures, after being released from the brood pouch of the female live as part of the plankton and differ from the adults, amongst other things, by having a much less elongated body shape (Dale & Anderson 1982). The epicaridium lacks a fully developed leg on post-ocular segment 13 (Dale & Anderson 1982); it therefore corresponds to the manca stage. During this stage the immatures search for suitable host animals, which are copepods of the group Calanoida Sars, 1903. After attaching to a copepod, the immatures moult into the microniscium stage, which differs from the epicaridium stage in being more elongated and having less differentiated appendages of the trunk. It feeds on the haemolymph of the copepod, causing a negative effect on the fitness of the copepod (Anderson 1975; Uye & Murase 1997). Whilst being attached to the copepod, the microniscium, supposedly without moulting, grows rapidly and the seventh leg of the trunk grows to the same size as the preceding legs (Anderson & Dale 1981).

After the microniscium stage the immatures develop to the cryptoniscium stage, which is again mobile and has well differentiated and specialised trunk appendages (Dale & Anderson 1982). The cryptoniscia can swim actively (Fraisse 1878) and search for the subsequent (final) host, which usually is a crustacean (Markham 1986; but see Pascual et al. 2002). The lifecycle of Epicaridea consequently comprises two distinct dispersal phases in which the animals search for hosts. During the entire immature phase, including the time they are attached to a planktic copepod, the animals can be subject to passive transportation of up to 100 km (Owens & Rothlisberg 1991). The cryptoniscium stage is often indistinguishable from the males, which in some lineages retain the morphology of the cryptoniscium, especially in species with protandric development (development through the larval stages to a sexually mature male and then to a sexually female) (Hosie 2008). Within Epicaridea there are different modes of development that can happen after undergoing the three distinct immature phases. In some lineages there is a strictly protandric development (every female was once a male), in others the is sex determined by presence of other conspecific individuals on final host – if a female is present on the host, the newly arriving individual develops to a male (Wägele 1989). In general, the males are much smaller than females (Shimomura et al. 2005) and the females often loose their bilateral symmetry (Williams & An 2009). In some species the adults are located underneath the thoracic shield or inside the body of their host. In those species the adults are often much less sclerotised than the immature individuals (Shiino 1954). By this, the immatures of Epicaridea fulfil several (morphological and ecological) criteria of the term 'larva' and can thus be interpreted as secondarily evolved morpho- and eco-larvae (strong morphological and ecological differentiation from the adults) (Haug 2020).

In Gnathiidae the immatures can also be interpreted as morpho- and eco-larvae. The immatures within Gnathiidae feed on the blood of fish which they retrieve by piercing through the skin of the fish (Alaş et al. 2009). The adults have been reported to be non-feeding (Upton 1987). The mouthparts of the immatures are specialised for piercing and sucking, whereas the mouthparts of the adults are subject to distinct sexual dimorphism (Thing et al. 2015). In males the mandibles are enlarged; in contrast, the adult females lack mandibles (Brusca & Iverson 1985). The females die shortly after releasing the offspring, while the males live much longer after reproduction (Smit & Davies 2004). In many species within Gnathiidae the non-feeding stages form 'harems', consisting of one male and many females and/or late immature stages (Tanaka 2007). The development from the last feeding

immature stage towards the adult male seems to include one additional moult, which is not observed in the development towards the adult female (Wägele 1988).

In Cymothoidae the immatures differ morphologically as well as in their behaviour from the adults. The immatures have large plumose setae on the appendages, that allow them to swim effectively (Thamban et al. 2015). As soon as a suitable host (usually a fish) is found they attach to it and loose the large swimming setae; after that the individuals can no longer swim well, even though representatives of some species differ not much in the overall appearance (van der Wal & Haug 2020). All species within Cymothoidae are thought to have a strict protandric development (Brusca 1981). In many species, especially those where the adults are located in confined spaces, the overall morphology changes gradually, from moult to moult, so that especially the mature females can look drastically different from the mobile (swimming) immature stages. Individuals that inhabit a confined space on either side of the host, such as the gill chamber, can loose their bilateral symmetry (Aneesh et al. 2020). Because of the modifications of the adults, and because the loss of the swimming setae represents a sudden change in both a morphological aspects as well as a ecological aspect, the immature stages qualify well as ecolarvae and morpholarvae (sensu Haug 2020).

1.3   Parasitism in general

Parasitism denotes a close interaction between two animals in which one animal benefits, usually by receiving nourishment, whilst the other one experiences a disadvantage through the interaction (Zelmer 1998). However, there is no universally acknowledged characterisation of the term 'parasitism' and so the term is applied differently, depending on the author and often also depending on the group of animals to which the term is applied. Nevertheless, there are obvious cases of parasitism where there is little or no dispute regarding the use of the term. One such example would be the pork tapeworm *Taenia solium*, which infests two different species of mammals in its lifecycle. In this case the parasite feeds on the host, reduces their fitness, is protected by the body of the host and depends strongly on the presence of its host in a way, that only certain life stages can temporarily survive outside of the host (Pawlowski 2002).

In other cases the use of the term 'parasitism' is more ambiguous, because there needs to be made a distinction between parasitism and other feeding types or life habits.

Predation is probably the most important feeding type from which parasitism needs to be distinguished. As with parasitism, the term 'predation' can also not unambiguously be characterised and there are some aspects where the same behaviour might be labelled as predation by one author but as something different by others. The question whether both the feeding organism and the organism that is fed on need to be animals applies for both parasitism and predation in the same way. One example for when the term predation is used for feeding on a plant is 'seed predation' (Labandeira & Li 2021). However, since the focus of this dissertation is on animals feeding on animals, only the cases in which both the feeding and the being-fed-on individual are animals are considered here. Possible terms from which predation is often separated are detritivory and planktivory. Both terms denote feeding habits in which the prey organisms are usually much smaller in size compared to the animal which feeds on them.

Apart from the size of the prey, predation is also delimited by other factors such as the question whether the being fed on animal has been killed or whether it has been killed by the feeding organism (distinction from scavenging). The case when an animal is not yet dead when it is consumed by another animal is of course most relevant for the distinction between form of predation and parasitism.

Micropredation describes an animal feeding on another living animal. Examples of such are fishes feeding on fins and scales of other fish (Lavoué et al. 2017). Another case which is often labelled as micropredation is mosquitoes feeding on the blood of vertebrates. Consequently the question arises how micropredation differs from parasitism in a narrow sense. The level of dependence, for example measured in the frequency and the duration of the interaction is often used to distinguish micropredation from parasitism; in this aspect the parasites interrupt the feeding process less often stay on the host for longer periods of time (Lafferty & Kuris 2002). This is of course a 'soft boundary' and the same interactions are labelled differently depending on the author and micro-predation is often used synonymous to 'temporary parasitism' (Smit et al. 2003 vs. Artim et al. 2015).

Parasitoidism is another mode of life that is sometimes distinguished from parasitism or used as a sub-part of parasitism. Parasitoids feed on other living animals, with a high level on dependence, just like parasites do, yet the host of parasitoids die after the interaction, e.g. when the parasitoid ruptures the hull body wall of the host for dispersal and reproduction. This distinction seems only to be relevant for the final host of the parasite/parasitoid, because otherwise the most obvious parasites would also needed to be called parasitoids, as the

intermediate hosts are often killed or weakened so they will be killed by predators (Ducháček & Lamka 2003).

Whether or not parasites have to feed on the body of the host is another factor regarding the usage of the term. One form of interaction where the benefiting animal feeds not on the host is often referred to as cleptoparasitism (parasitism through theft). A popular example of cleptoparasitism is the interaction between frigate birds (e.g. *Fregata magnificens*) and other piscivorous birds, which they sometimes force to regurgitate their food in order to feed on it (Brockmann & Barnard 1979). The process of exploiting the feeding behaviour of another species is called brood parasitism, here the parasite also does not necessarily feed on the host itself but on resources that the hosts accumulated. The probably most famous example are some species of cuckoos (Cuculidae) which place eggs in nests of other bird species in order not to have to feed their offspring; this behaviour is thus also called 'cuckooism' (Breed et al. 2012). More complex but trophically similar interactions can be found in interactions in which social insects are exploited, where this behaviour is referred to as 'social parasitism' (Buschinger 2009; Rabeling 2020).
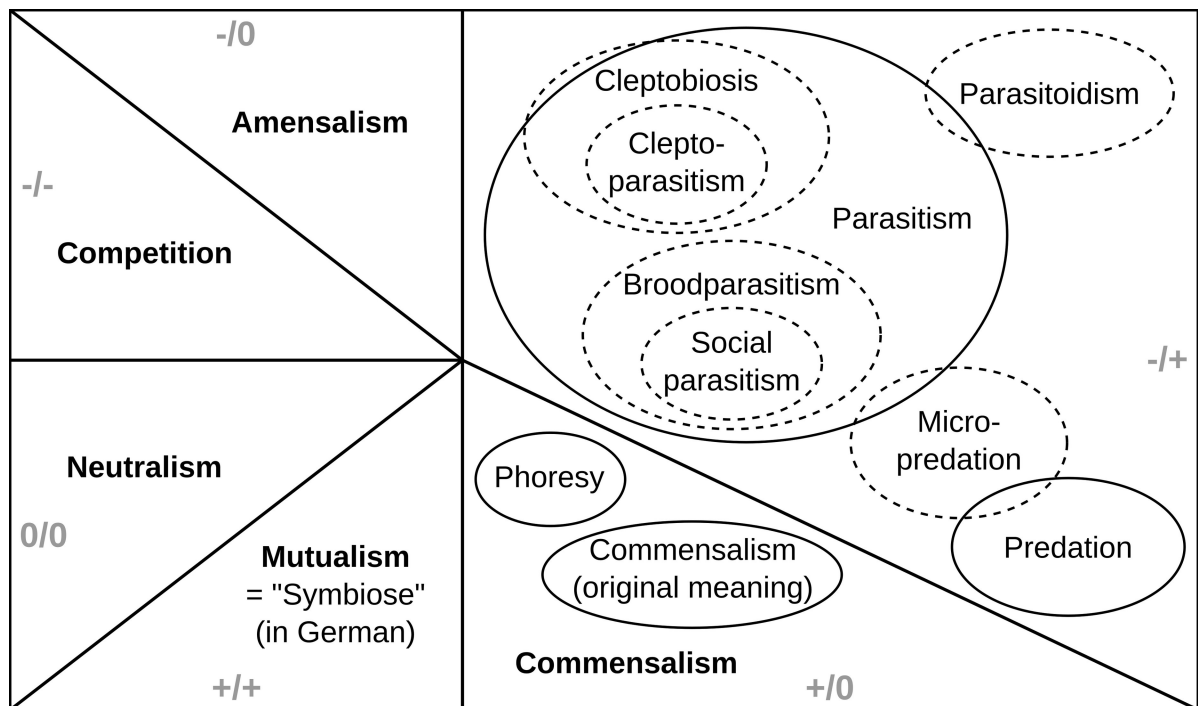
Figure 1: Simplified Venn diagram representation of different modes direct interactions between two animal species divided after the net payoff of the interaction (in grey letters) (modified after Morin 2011). Terms where the usage and the overlaps with other terms are not clearly defined are denoted by dashed lines.

Commensalism is an interaction between two species, where one species receives a benefit, while there is no substantial negative effect for the other species (Morin 2011; Fig. 1). Originally, the term has been used to such interactions where the benefit is trophic in nature, nowadays most authors used the term also for other forms of interactions that do not include a food component, such as phoresy (transport through attaching to other organisms) (White et al. 2017). Phoresy has often been discussed as a possible precursor to parasitism (in its narrower sense), due to the close nature of the interaction (Bartlow & Agosta 2021; Skawina 2021). In practice, commensalistic interactions and especially phoresy are often hard to distinguish from other forms of interactions such as parasitism and mutualism (both species receive mutual benefits from the interaction), even when looking at extant species (Leung & Poulin 2008).

1.4 Parasitism in Isopoda

The term 'parasitic isopods' is strongly linked to 5 ingroups of Isopoda – Corallanidae, Aegidae, Cymothoidae, Epicaridea and Gnathiidae (e.g. Nagler et al. 2017). However, the term parasitic, depending on how it is applied may not be a suitable term to describe the behaviour that is prevalent in some of these groups.

Corallanidae Hansen, 1890 contains species that mostly feed on living fishes but also on other vertebrates such as marine turtles (Delaney 1989). In most species the feeding behaviour is typical for micro-predation/temporary parasitism by only feeding on their prey/host for a short time followed by periods of hiding in safe environments, such as reef crevices or within sponges (Delaney 1984, 1989). On the other hand there are some reports of individuals being found on fishes in sheltering spots such as the gill cavities or the nostrils (Bowman 1977; Delaney 1984), which could suggest that at least some individuals feed on the same fish for extended periods of time. Some species of Corallanidae are not restricted to vertebrates as source of nutrition: At least one species has been reported to prey on smaller crustaceans such as opossum shrimps (Mysida) (Guzman et al. 1988). A population of another species has been reported to attach to larger shrimps as immatures and to stay and on them for a considerable amount of time (Ota 2019). The seemingly obligatory nature of the interaction allows for it to be referred to as parasitism even in a very narrow sense, forming

an exception from the prevalent micro-predatory behaviour within Corallanidae (parasitism in a wider sense).

Tridentella Richardson, 1905 is a small group of species which previously have been interpreted to be within Corallanidae but now are interpreted to form a separate, closely related group (Bruce 1984; Delaney 1989). Representatives of *Tridentella* share a similar lifestyle with representatives of Corallanidae. Individuals of most species temporarily attach to and feed on fishes *(Delaney & Brusca 1985)*. As in Corallanidae, there are also reports of individuals found in sheltering places on fishes, such as in the nasal cavities (Heard, pers. comm. in Bruce 1984).

In Aegidae White, 1850 individuals of most species temporarily attach externally to fishes and feed on their blood. Therefore, representatives of Aegidae are often referred to as micro-predators rather than parasites (e.g. Öktener et al. 2020). Some species have been found associated with sponges (Porifera) (Bruce 1983) and sea squirts (Ascidia) (Wetzer 1990); however, it is not clear whether these interactions involves a feeding process, especially as species inhabiting sponges have also been found feeding on fishes (Saito & Saito 2011). Similar to representatives of Corallanidae and *Tridentella*, individuals of some species are found in sheltering spaces on fishes, such as the gill cavities (de Lima et al. 2005; Saito & Saito 2011).

Most representatives of Cymothoidae Leach, 1818 are obligate parasites of fishes (Brusca 1981). While in their immature stages individuals are able to actively swim and to repeatedly attack their prey/hosts and their behaviour could be described as temporary parasitism or micro-predation (Segal 1987), the adult forms lack much of the setation on the appendages and by this their ability to swim in an effective manner. Once fully mature, representatives of Cymothoidae stay on their host indefinitely (Brusca 1981). Flight reactions when fishes are removed from water or when they are caught in nets are common and can lead to confusion regarding the host preferences of species, as some individuals are able to re-attach to other fish of other species in the same net, while re-attachments (e.g. when the host fish is attacked) are unlikely to happen on a regular basis in nature (Brusca 1981). Many species show a high host specificity and specificity regarding their attachment site and their mode of attachment, at least regarding the hosts they choose before moulting into the reproductive stages (Brusca 1981; Bunkley-Williams & Williams 1998). In Cymothoidae there are externally attaching forms as well as forms that inhabit the mouth and gill cavities and forms that from outside burrow deeply into the body of their host (Bunkley-Williams &

Williams 1998). While representatives of most species of Cymothoidae feed on fishes, males of some species are parasites or micro-predators of shrimps (Caridea), that attach externally to the shrimps (Lemos de Castro 1985; Grassini 1994; Wunderlich et al. 2011), similar to some species of Corallanidae (Ota 2019).

Representatives of Epicaridea throughout their life have phases when they are obligatory parasites. As introduced above, all individuals undergo a complex life cycle that involves two different hosts. The first (intermediate host) is a planktic copepod of the group Calanoidea (Uye & Murase 1997) to which freshly hatched immatures (epicaridium stage) attach. After feeding on the immediate host, the individuals detach from it and search for the final host which for almost all species is a crustacean. There is a vast variety of groups of crustaceans that can be final hosts, ranging from shrimps (Caridea) – from which the group Epicaridea has its name – over seed shrimps (Ostracoda) (Rybakov 1998), barnacles (Cirripedia) (Wägele 1989), crabs (Brachyura) (Torres Jordá 2003), to amphipods (Sars 1899) and isopods (Nielsen & Strömberg 1965). Some species of Epicaridea are even parasitic on other parasites (hyperparasitism) such as parasitic barnacles (Rhizocephala) (Williams & Boyko 2012) and even other species of Epicaridea (Rybakov 1990). While the females are permanently associated with their hosts, males of certain lineages within Epicaridea which retain a larval morphology (paedomorphosis within a protandric life cycle) (Hosie 2008) can still swim and switch between hosts to inseminate multiple females (Nielsen & Strömberg 1973). Adult forms of Epicaridea are located either outside – often underneath the thoracic shield inside the gill chamber (Beck 1980) – or inside the hosts body (Shiino 1954). Some, but not all, of the apparent endoparasites are technically outside the body of the host in thin invaginations of the hosts body (Atkins 1933). There are also interesting cases where the female parasite lives inside the body of another female representative of Isopoda of another species but feeds in an obligatory way on the eggs of the host, which are outside the body of the host in the brood pouch, rather than on the host individual itself (Holdich 1975).

In Gnathiidae Leach, 1814 only the immature stages feed. They do so by temporarily attaching to fishes and taking up a large amount of blood using piercing-sucking mouthparts; afterwards they detach and hide in cryptic habitats such as between corals, in sand, in wood borings but also inside other organisms such as sponges (Porifera) or sea squirts (Ascidia) (Smit & Davies 2004; Alaş et al. 2009). For the adult forms there is no indication for a feeding process (Upton 1987).

Representatives of Gnathiidae are often referred to as parasites (Smit & Davies 2004; e.g. Nagel 2009; Wilson et al. 2011b) rather than micro-predators (Penfold et al. 2008; Artim et al. 2015), while the time of the actual inter-species interaction is rather short (see discussion in van der Wal & Haug 2019). Some species have the ability to feed on non-vertebrates such as sea slugs (Sacoglossa) and worms (Annelida) as well, when the preferred prey/host is not available (Nicholson et al. 2019). There are also reports of immature individuals stealing food that has already been swallowed from other conspecific individuals, which has been referrd to as cleptoparasitism (Shodipo et al. 2019). Van der Wal and Haug (2019) argued that this interaction should rather be referred to as hyperparasitism because the process of feeding involves the penetration of the integument of the being fed on individual and the retrieval of food that has already been consumed.

Representatives of Cirolanidae Dana, 1852 are generally understood as scavengers and predators (Bruce 1986). Nevertheless, there are numerous records of micro-predatory behaviour with fishes as prey, especially from circumstances where the fish were restricted in their movement (caged, in fishing nets, or hooked on fishing lines) (Vásquez-Yeomans et al. 2011). Yet, there are also observations from the wild where fishes were attacked by representatives of Cirolanidae when they were resting (Stepien & Brusca 1985; Robin et al. 2018). In some cases the gill cavities or, through the anus, the abdominal cavity of the fish were entered, causing severe damage by feeding on the organs, ultimately leading to the death of the prey (Stepien & Brusca 1985), similar in the overall effect to that what parasitoids have on their hosts. There seems not to be a preference for living fish compared to carcasses of fish, rather the opposite (Vásquez-Yeomans et al. 2011), which further corroborates the view of Cirolanidae as a group of scavengers, predators and occasional micropredators (Brusca 1981). Representatives of Cirolanidae have been reconstructed to be morphologically close to the ancestor of some (if not all; see next section) groups with parasitic forms/micropredators (Dreyer & Wägele 2001, 2002) and the predatory behaviour within the group has been argued as a potential precursor to the parasitic behaviour in the related groups (Wägele 1989).

1.5 Relationships between Isopoda ingroups with parasitic forms

The relationships between ingroups of Isopoda, including those with micro-predatious and or parasitic forms – namely Corallanidae, *Tridentella*, Aegidae, Cymothoidae, Epicaridea and Gnathiidae – has been debated for several decades and as of now there seems to be no clear consensus. Nevertheless, all parasitic forms can be identified as representatives of the group Scutocoxifera Dreyer and Wägele, 2002, which is characterised by the presence of flat scutiform sclerites derived from the coxae of the trunk legs and the lateral-most parts of the tergites; their presence is also the autapomorphy of the group (Dreyer & Wägele 2002).

Wägele (1989) found the group Gnathiidae (alongside with the group *Protognathia*; but see (Wilson 1996) to be the sister group to a group that comprises the groups *Anuropus*, Cirolanidae, and the remainder groups with parasitic forms. Within this group Wägele (1989) found Cirolanidae – labelled as potentially non-monophyletic – to be the sister group of all groups with parasitic forms, except for Gnathiidae; alternatively it could be the group from which the parasitic forms, except for Gnathiidae, arose. According to Wägele (1989) within the group comprising only the parasitic forms Aegidae, Cymothoidae and Epicaridea form a natural group and Cymothoidae and Aegidae form a group that arose from within a non-monophyletic Aegidae (Fig. 1B).

Brusca and Wilson (1991) found Epicaridea and Gnathiidae to be in a sister group relationship and Anthuridea, *Anuropus* and the remainder of groups with parasitic forms to form a monophyletic group in which Cirlolanidae is not included and in which the groups with parasitic forms form another monophyletic group (Fig. 1 A). Similar to the relationships proposed by Wägele (1989), this would mean that parasitic behaviour evolved at least two times independently within Isopoda (alternatively the parasitic life style was abandoned and readopted later).
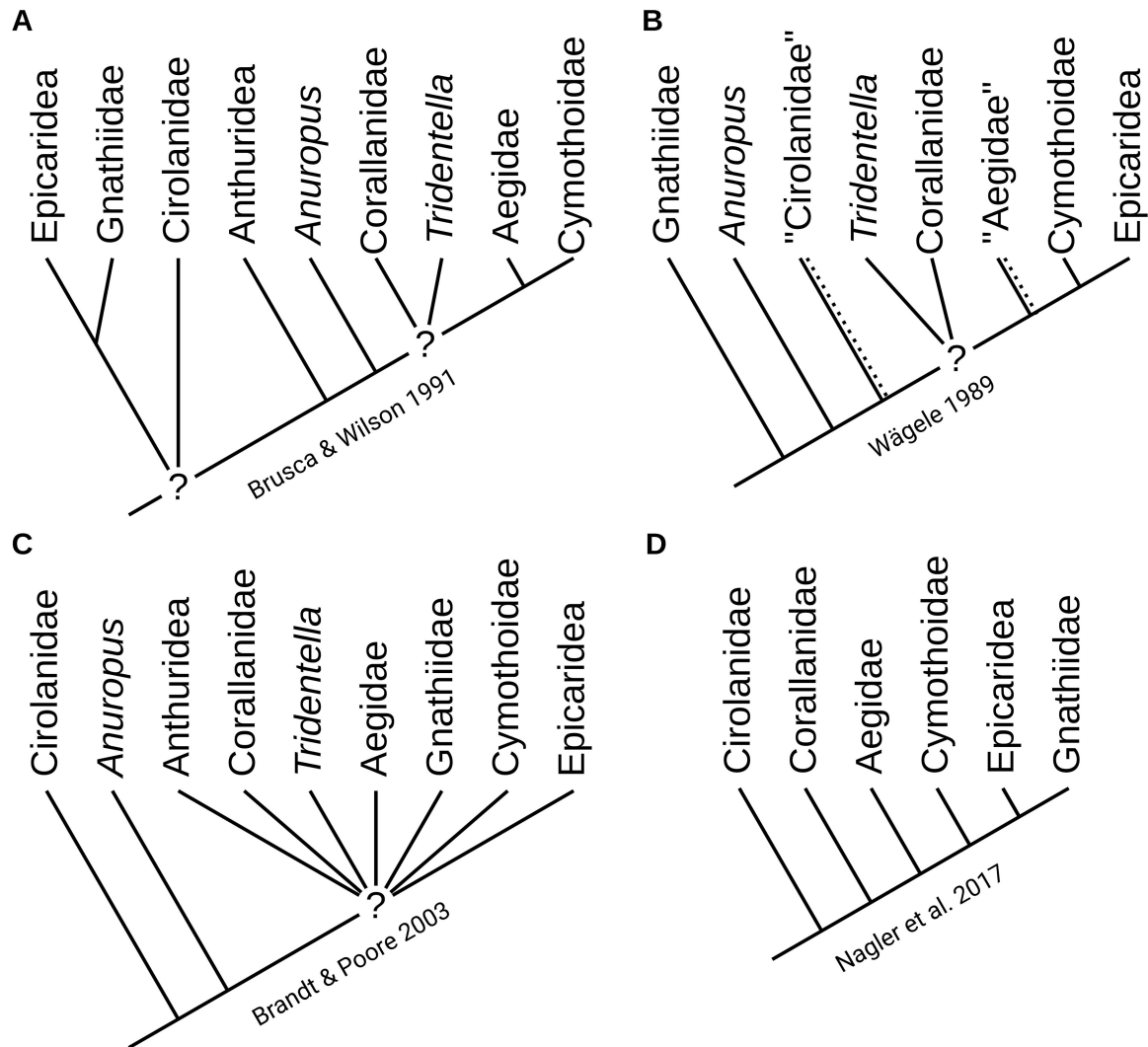
Figure 2: Trees depicting results of different phylogenetic analyses and proposed relationships between ingroups of Scutocoxifera, including the ingroups of Isopoda with parasitic representatives. **A:** modified after Brusca & Wilson (1991, fig. 14). **B:** modified after Wägele (1989 fig. 93). **C:** modified after Brandt & Poore (2003, fig. 6A). **D:** Nagler et al. (2017, fig. 7).

Brandt and Poore (2003) found all Isopoda ingroups with parasitic forms alongside with the group Anthuridea to form a natural group which they found to be closely related to the groups *Anuropus* and Cirolanidae (Fig. 1 C). However, the taxonomic classification which they provided (Brandt & Poore 2003 tab. 3) only partly reflects their findings.

Nagler et al. (2017) recently argued for a relationship between the ingroups of Isopoda with parasitic forms in which a parasitic life style could have theoretically evolved

only once. Here, the groups with parasitic form a monophyletic group which is in a sister group relationship with Cirolanidae and within this group Corallanidae is the sister group to the remainder groups. According to Nagler et al. (2017) Aegidae is the sister group to a group comprising Cymothoidae, Epicaridea and Gnathiidae. Similar to Brusca and Wilson (1991), they found Epicaridea to be the sister group of Gnathiidae (Fig. 1 D), while the rest of the proposed tree topology is very similar to that of Wägele (1989) and the evolutionary scenario proposed by Dreyer and Wägele (2001, fig. 12). The topology presented in Nagler et al. (2017) is identical to the parsimony trees based on morphological characters presented in Wilson (2009, figs. 3–4).

1.6   Isopoda in the fossil record (in general)

The fossil record of Isopoda dates back as far as to the late Carboniferous. With an age of about 300 million years, *Hesslerella shermani* Schram, 1970 from Mason Creek (Illinois, USA) is the oldest fossil remain of a representative of Isopoda (Schram 1970) and one of only two remains of Isopoda from the Carboniferous (Racheboeuf et al. 2009). From the Permian there are an additional 8 formally described species (but see discussion in study V) and the fossil record of the group in the Triassic comprises another 12 species (Schädel et al. 2020). From the Jurassic onwards the fossil record of Isopoda is denser and more or less continuous towards the present (Karasawa et al. 1992; Wieder & Feldmann 1992; Hyžný et al. 2013; De Angeli & Quaggiotto 2014). Throughout its extent the fossil record of Isopoda is by far not as rich as the fossil record of other groups of crustaceans (which not include Isopoda) such as Brachyura (e.g. Luque et al. 2017). Nevertheless, fossil remains of Isopoda are known from many field sites that yield complete and un-distorted remains of arthropods and are even abundant in some deposits (Walther 1904; Haack 1933).

Generally, there are two different modes in which remains of Isopoda are preserved in the fossil record: preservation in sediment and preservation in fossilised resin (amber). Fossil remains of Isopoda preserved in sediment often lack delicate structures such as appendages and especially the distal parts of them. The missing parts are either not preserved, destroyed during a mechanical preparation process or are even missing prior to the hardening of the sediment (pre-diagenetic). Additionally, sediments from many field sites, and especially those which yield well preserved fossils of arthropods, are often strongly

compressed (Fig. 3), which further limits the insights that can be gained about the morphology of the once living animals (e.g. Schädel et al. 2020).

The fashion in which representatives of Isopoda usually moult has a strong influence on the quality of the sediment fossil record of the group, as many fossils can be interpreted as preserved moults (Fig. 3) rather than carcasses (Wieder & Feldmann 1989; Daley & Drage 2016). Representatives of Isopoda mostly moult in a two-step process: the posterior part of the body (post-ocular segments 11-19) undergoes the moulting first and the moult is stripped off in one part; the anterior part of the body subsequently undergoes a moulting process in which the old exoskeletal parts are removed in several smaller pieces (Tait 1918). For rare exceptions where the entire exoskeleton is moulted in one piece see Anderson and Dale (1981), Panakkool-Thamban and Kappalli (2020) and George (George 1972). As a consequence, many fossil remains which can be identified as belonging to representatives of Isopoda are exoskeletal remains of the posterior body region ('posterior moults').

Arthropod fossils in amber usually have more and finer details preserved and observable as compared to fossils preserved in sediment. Amber fossils often are or can be made accessible from multiple angles, allowing for more aspects of the body being optically observable within a single specimen (e.g. Sidorchuk 2013). Despite being a medium produced by plants, amber yields not only remains of terrestrial organisms that fit into the view of a typical 'amber forest' fauna, but also (to a lesser extent) remains of aquatic organisms and even those of species for which marine environment is assumed (Girard et al. 2008; Saint Martin et al. 2015; Xing et al. 2018; Yu et al. 2019; Wang et al. 2020). How aquatic organisms can get trapped in resin has been speculated for a long time; recent actualistic experiments (Schmidt & Dilcher 2007) as well as fossils that clearly suggest an entrapment of living aquatic organisms (Serrano-Sánchez et al. 2015) suggest aquatic organisms can get trapped in still liquid resin that is submerged in water, which could for example happen in a swamp or a temporarily flooded forest. Fossils of Isopoda are not particularly abundant but occur in most proliferous and well studied amber deposits (Penney 2010).
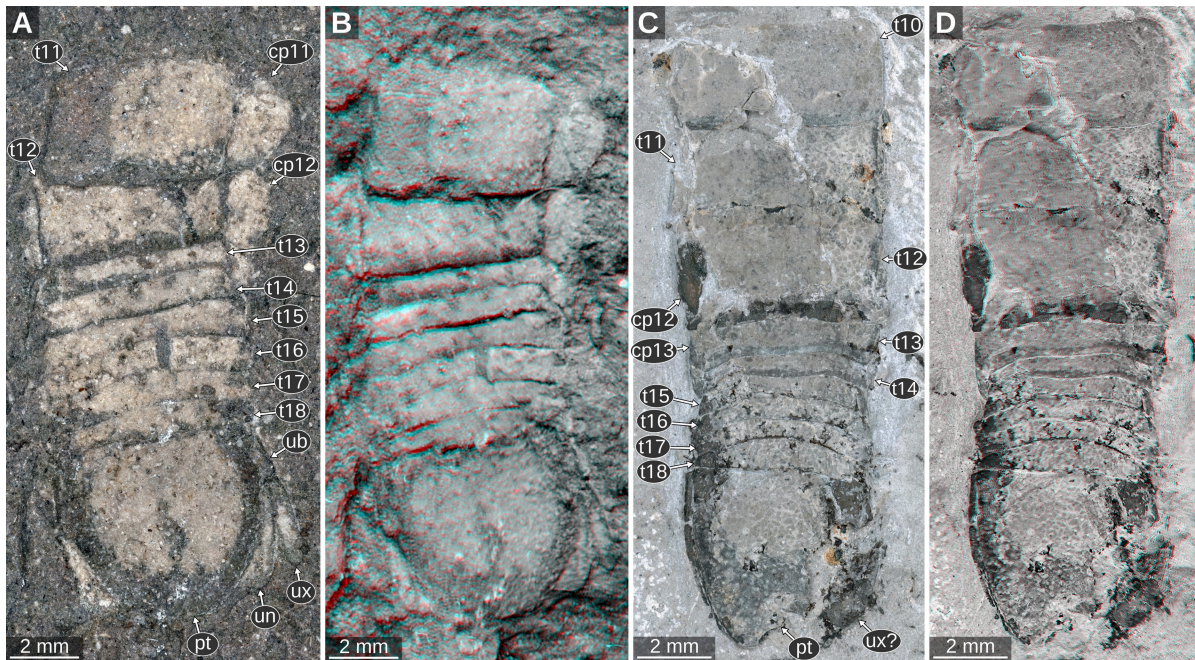
Figure 3: Two fossil remains of representatives of Isopoda with a typical mode of preservation. **A–B:** Collection of the University of Tübingen, without accession number (located at NC/08/A/13), Müllingen, Kanton Aargau, Switzerland, Lower Jurassic ('Lias α'). **B:** red-cyan stereo anaglyph version of A. **C–D:** Collesction of the State Museum of Natural History Stuttgart, SMNS 65510a, Sonnenbühl-Willmandingen, Baden-Württemberg, Germany, Kimmeridgian (Upper Cretaceous). **D:** red-cyan stereo anaglyph version of C. Abbreviations: **cp11–13**, coxal plates of post-ocular segments 11–13; **t11–18**, tergites of post-ocular segments 11–18; **pt**, pleotelson; **ub**, uropod basipod; **un**, uropod endopod; **ux?**, possibly uropod exopod.

1.7   Parasitic forms of Isopoda in the fossil record

Parasitic behaviour from representatives of Isopoda has left a surprisingly high amount of traces in the fossil record, compared to the number of body fossils of Isopoda that can be linked with parasitism. However, traces are in most cases the only thing left behind by the parasites. There is a plethora of fossil traces that can confidently be linked to representatives of Epicaridea parasitising larger crustaceans. The traces consist of swellings of the branchial chambers of shrimps, lobsters and crabs that are very similar to those found in modern environments and date back as far as to the Late Jurassic (Bell 1863; Bachmayer 1948; Radwański 1972; Wienberg Rasmussen et al. 2008; Robins et al. 2013; Klompmaker et al. 2014, 2018; Klompmaker & Boxshall 2015; Fraaije et al. 2019; Robins & Klompmaker

2019). Despite several attempts using modern imaging techniques, no parasite has yet been found inside the swellings (Robin 2021).

So far, despite fossils of Isopoda not being rare and many of the extant species having a parasitic life style (Boyko et al. 2008), there are only a few records of body fossils of parasitic forms. Robin et al. (2018) described fossil Isopoda remains with a morphology very similar to that in extant species of Cirolanidae which are located on the bodies of fossil electric rays (Torpediniformes). The authors concluded that the assemblage could either be the result of a syn-vivo interaction (parasitism/micro-predation) or due to a scavenging behaviour of the representatives of Isopoda. A similar assemblage has been shown by Bowman (1971) – a single fossil representative of Isopoda located on a fossil mackerel shark (*Lamna* sp.); however, in this case the preservation of the presumed parasite or scavenger is very poor and therefore not allowing for a precise systematic interpretation.

Apart from the many species named *Palaega* (non-monophyletic 'form genus'), which by some early authors (e.g. Zittel 1887) have been referred to as representatives of Aegidae, two species have been specifically attributed to this group (Polz 2005; Hansen & Hansen 2010). However, also these attributions are based on the overall similarity (of the preserved body parts) with extant species of Aegidae rather than on apomorphies; the attributions have consequently been questioned by Wilson et al. (2011a).

Prior to the work contained in this dissertation there were two records of specialised larval forms which only occur in the group Epicaridea, which representatives are parasites and hyperparasites of crustaceans. The records come from two different amber deposits. One is from Chiapas amber from the Miocene of Mexico (Serrano-Sánchez et al. 2016), the other record is from Vendean amber from the Late Cretaceous of France (Néraudeau et al. 2017). The fossils from the Late Cretaceous of France which are briefly mentioned in Néraudeau et al. (2017) are described and discussed in more detail in study II.

Nagler et al. (Nagler et al. 2016) reported the presence of remains of Isopoda on fossil fishes from the Late Jurassic Solnhofen limestones, which they tentatively interpreted as representatives of Cymothoidae which extant species comprise parasites of fishes (but see discussion in study V and below). Fossils of *Urda* from the Middle Jurassic of Bielefeld (Germany) have been interpreted as parasites of fishes (Nagler et al. 2017); the corresponding fossils are restudied in study V.

1.8   Research questions

- How can immature and specifically true larval forms within Isopoda be identified in the fossil record?

- How old are the earliest records of immature stages and specifically true larvae within Isopoda?

- Are there morphological differences between extinct and extant larvae within Isopoda?

- Are there extinct forms with a heterochronic developmental pattern when compared to extant relatives?

- How can parasitic forms of Isopoda be recognised in the fossil record?

- Are there morphologies within Isopoda that are different from those in extant species which can be linked with parasitism?

- Are all fossil larval forms linked with a parasitic ecology, as in modern lineages of Isopoda?

1.9   Aims and scope of the dissertation

- thorough documentation of fossil remains of Isopoda that could be either from larval and/or parasitic forms, using modern imaging techniques

- providing systematic interpretations of the studied fossils based on apomorphic characters

- comparison of the studied fossil specimens with other fossils and with extant specimens of closely related species with a special emphasis on the body parts that are relevant in an ecological context

- study of the evolution of parasitism by studying the fossil remains that can be linked with parasitic behaviour in a functional or phylogenetic way

- discussion of the effect of ontogenetic development on the evolution of parasitism within Isopoda and vice versa

1.10 Methods

1.10.1   Measurements

Living organisms and fossil remains of them are 3-dimensional objects. Measurements of them were mostly performed in 2-dimensional images of the objects (including orthographic projections of 3D volumetric data). This requires appropriate projections and low optical distortion. In some cases the former requirement was not fulfilled (fossils in amber pieces). In such cases the position of in focus images within stacks of images with equal and known spacing was used to determine the true length of the objects. Measurements of 2-dimensional images were performed using ImageJ (Schneider et al. 2012, public domain) and Inkscape (Inkscape Project, inkscape.org, GPL v.3 license).

1.10.2   Microscopic and Macro-photographic imaging

Macro-photographic images were obtained from a variety of camera setups including different DSLR camera bodies (Canon EOS REBEL T3i, Canon EOS 70D DSLR, Canon EOS 700D, Canon EOS 750D, Nikon D7200) and different lenses (Canon EF-S18-55mm f/3.5-5.6, Canon MP-E 65 mm f/2.8 1-5x, Laowa 100mm f/2.8 2x). In most cases a set of twin flashes (e.g. Meike MT24) was used to illuminate the objects. Small objects were placed on a microscopy table (different models) to adjust the distance of the fossil relative to the camera.

Microscopic images were obtained from two models of digital microscopes (Keyence VHX-6000 and Keyence BZ9000) using different inbuilt light sources. Pieces of amber were photographed in dry state, fully submerged in water (fluorescence microscopy) or partly wetted with water or glycerol and concealed with a cover slip. For the Keyence BZ9000, which is a reversed microscope, a special dish (modified petri dish with a glass window) was constructed in order to photograph amber pieces fully submerged in water and to optimize for the working distance of high magnification microscope objectives.

1.10.3   Fluorescence imaging

The epifluorescent quality of organic structures of extant and fossil organic structures was utilized by inducing epifluorescence using exciting light of different wavelengths and

filtering out light of undesired wavelength when photographing the objects (Eklund et al. 2018). This was done using a Keyence BZ-9000 digital fluorescence microscope. The digital microscope has a modular set of filters to produce exciting light of different spectra of wavelengths along with filters that allow only the light produced by the fluorescence to pass through to the camera sensor.

Tab. 1: Filter setups used with the Keyence BZ9000 digital microscope which produced good results.

Wavelength excitation (center of spectrum)	Wavelength dichoitic filter (mounted in front of the sensor)	Typically use
360 nm	400 nm	DAPI stains
470 nm	495 nm	GFP stains
545 nm	565 nm	TRITC stains

Additionally, epifluorescence was used in macro photography with the aid of a 10 W TATTU U2S ultraviolet light torch with a ZWB2 filter, which emits light of 365 nm wavelength and a UV light filter mounted on the camera objective (cf. Tischlinger & Arratia 2013). In a different macro photography setup epifluorescence was induced by equipping white-light lamps with low-cost cyan filters from red-cyan stereo glasses. The light produced by the fluorescence was the filtered by a red filter ('green-orange fluorescence', Haug et al. 2009; Haug & Haug 2011).

Small strongly fluorecent fibers (dust particles) can cause artefacts (circular glow around the particles) caused by when merging focal planes, especially when using UV light. To minimize this effect, in some cases the blue colour channel was removed from the image stacks prior to merging the focal planes. This was done using the command line program ImageMagick (Apache 2.0 license) automated using GNU Bash shell scripts.

1.10.4   Cross-polarised light

Where suitable, cross-polarised light was used in both microscopy and macro-photography in order to reduce the amount of reflections (Bengtson 2000). By this, the technique can also massively increase the contrast between fossil material and the surrounding sediment matrix.

1.10.5   Depth of field

To overcome the limitation of the depth of field when photographing with high magnification, sets ('stacks') of multiple images of the same view with different areas of the object being in focus were recorded ('focus stacking'). These stacks were then combined to single images with all desired parts of the photographed object being in focus ('extended depth of field') (Pieper & Korpel 1983; Itoh et al. 1989).

This process is fully implemented in the utilized digital microscopes. However, in case of the Keyence BZ9000 the stacks of images were exported rather than combined to in-focus images by the microscopes software. When the merging of the image stacks was not performed by the software of the microscopes, different open source programs were used to perform this task. These include CombineZP (Alan Hadley, GPL license), CZBatch (Alan Hadley, batch processing version of CombineZP, GPL license), ENFUSE (GPL v. 1.2 license) and MacroFusion (graphical interface for ENFUSE, GPL license). CombineZP and CZBatch are designed for the Windows operating systems but were mostly used on Linux through the software WINE (Alexandre Julliard, LGPL license). GNU Bash (GPL v. 3 licence) was used to execute shell scripts to automate repetitive tasks such as arranging large numbers of image files into folders or executing command line programs such as ENFUSE.

1.10.6   Panoramic stitching

When photographing with high magnification, the field of view can be too small to depict the entire desired object. To overcome this limitation, multiple images were combined to a larger panoramic image. For this different programs were used. These programs include the software of the Keyence VHX6000 digital microscope as well as hardware independent programs. Open source programs used for this task include the 'Grid/Collection Stitching' plugin (Preibisch *et al.* 2009, GPL license) for ImageJ or TrakEM2 (Cardona et al. 2012, GPL v. 2 license). Some panoramic images were created manually using the 'unified

transform tool' and layer masks in GIMP (GNU Image Manipulation Program, GPL v. 3.0 license).

1.10.7 HDR

Some photographed objects had very dark and very bright surfaces side by side (e.g. dark fossil material in a sediment matrix with white grains). For these objects it was necessary to combine the information of two or more images to obtain an image without under- or overexposed areas (Fraser et al. 2009). This method is implemented in the Keyence VHX6000 digital microscope, however in most cases this was done hardware independent using software such as ENFUSE and MacroFusion.

1.10.8 Image Processing and Graphic Design

The images were optimised for colour, brightness, contrast and sharpness using GIMP. Uninformative background (i.e. the base on which the object was placed when photographing it) was removed using layer masks in GIMP. For aesthetic purposes sediment background was simulated using the stamp tool in GIMP in order to enlarge the field of view of the images, so that there are no gaps in the figure plates. Wherever this technique was applied, the modified area was labelled accordingly. Colour markings were created using layer masks, the 'colorize' and the 'drop shadow' function in GIMP. Inkscape was used to create line drawings as well as to arrange the figure plates and to add labels. The perceptibility of colours used in the figures was ensured by choosing appropriate colour palettes and by simulating colour vision impairment. Appropriate colour maps were retrieved from different sources: e.g. the web application iWantHue (GPL-3 licence, available at https://medialab.github.io/iwanthue/) and the website of Paul Tol (https://personal.sron.nl/~pault/). Color Oracle (Bernhard Jenny and Nathaniel V. Kelso, MIT license) and Daltonize (Jörg Dietric, https://github.com/joergdietrich/daltonize, GPL v. 2 license) were used to simulate the most common impairments. Unfortunately, this was not done in the earlier publications included in this thesis.

1.10.9 Micro Computer Tomography

Micro computer tomography (μCT) was performed at two facilities with different devices: Zoological State Collection of Bavaria in Munich (ZSM), 'phoenix nanotom m' (Baker Hughes); Zoological Institute and Museum, University of Greifswald, Zeiss Xradia XCT-200 (Carl Zeiss Microscopy GmbH), equipped with switchable scintillator-objective lens units. Both devices were operated using the recommended software provided by the manufacturer. In all cases the samples were rotated 360 degrees. For data produced by the 'phoenix nanotom m', it was necessary to convert the original images into an image volume (stack of virtual slices, .tif images) using software that is not provided by the manufacturer. For this, VGStudio MAX v.2.2 (Volume Graphics, proprietary) was used.

1.10.10 3D image processing

In order to find meaning in the 3D information generated by micro computer tomography, it is most often necessary to create virtual models of the scanned objects which then can be inspected and rendered to 2D images for illustrative purposes. These models can be divided into two categories: volumetric models and surface models.

Volumetric models are based on the radiometric information of the smallest units of the image data: voxels (three-dimensional pixels). This type of model has the advantage of being close to the original data, requiring only few choices to be made by the creator of the model. In the simplest case the creator has to set a threshold that determines which grey value is necessary for a voxel to be visible. The volumetric models included in this dissertation were created using the volume rendering software Drishti (Limaye 2012, MIT license). Unlike many other software, Drishti allows to have two-dimensional transfer functions. This means that not only the grey value of the voxel itself determines its final visibility and appearance but also the grey values of its neighbouring voxels, resulting in more ways to fine-tune the appearance and usually in a higher quality of the final model. Drishti also allowed to exclude irrelevant areas of the volume by adding clipping planes and carving away visible voxels that are not part of the fossil (e.g. sediment particles or air bubbles in amber). In one case a rough manualimage segmentation was performed, in order to separate the fossil from further enclosed particles using TrakEM2 (Cardona et al. 2012, GPL v.3 license) prior to the volume rendering process.

The disadvantage of volumetric models is that the model can be a inaccurate representation of the preserved biological structures if there is little contrast between biological structure and the surrounding material. Artefacts of the µCT scanning process (e.g. 'beam hardening') can also drastically decrease the quality of volumetric models. Surface models based on manually or semi-automatically labelled areas of virtual slices ('image segmentation') can represent a viable alternative of addition to volumetric models. However, here the image segmentation process requires more choices to be made by the creator, which can lead to misinterpretations that can only be recognized if one compares the model with the corresponding image data. Image segmentation was performed using TrakEM2. Some of the models were smoothened prior to exporting as surface models using 3DSlicer (Fedorov et al. 2012; Kikinis et al. 2014, BSD-style license). In some only a selection of slices was manually segmented using TrakEM2, which was then used as input for the program Biomedisa (Lösel et al. 2020, EUPL v. 1.2 license), which then labelled the interspersed virtual slices automatically following a semi-supervised machine learning approach.

Where necessary, the models were modified using the decimate, remesh and subdivision surface modifiers in Blender. Within Blender, the surface models were illuminated using a combination of 'sun' and 'world' lights and were finally converted into 2D images using ray-trace rendering (cf. Sutton et al. 2014). An external add-on for Blender was used to import multiple surface models (.obj files) at once ('p2or' 2021, GPL v. 2 license, available at https://blender.stackexchange.com/a/31825/31447, GPL v. 2 license).

1.10.11   Stereo

Stereo photography is a simple and practical way to capture and display 3-dimensional shapes obtaining pairs of 2-dimensional images of slightly different angles (Wheatstone 1838). Unlike in photogrammetry, no digital 3D model has to be computed. Instead the stereo vision of the human body is used to perform the task of creating a 3D image. One possibility for this is presenting the stereo images side by side and the view of the observer needs to adjust in a way that allows perceiving the images as a 3D object. However, this requires some training for the observer. Therefore for the figures in the manuscripts of this thesis, the stereo images are presented stacked on top of each other, the upper one with 50% transparency, the left view of the image with the green and blue colour channels removed and the right view with the red colour channel removed ('red-cyan stereo anaglyph'). This

way, the resulting image can be viewed through low-cost red-cyan stereo glasses (Rollmann 1853). This task was performed manually using GIMP. Other stereo images were created directly from 3D volumetric data using Drishti.

For objects with little relief it was possible to capture stereo pairs of images using an older consumer grade flatbed scanner. Older models of flatbed scanners facilitate charge-coupled device (CCD) sensors, which optical properties allow for a change in viewing angle if an object is moved on the scanning window. This effect only takes place in left-right direction with respect to the portrait mode of scanned documents (Schubert 2000). For viewers with stereo vision impairment the program kataglyph (GPL v.3.0, available at https://github.com/mcranium/kataglyph) was developed, which allows to extract grayscale images of both views from red-cyan stereo anaglyphs and to present them as an animated wiggle (.gif) image. The same operation can easily be replicated using graphics programs such as GIMP.

1.10.12   Data Analysis and Visualization

Data entry and prepararation was done using Libreoffice Calc (Mozilla Public Licence v. 2). All analyses were preformed using different versions of the R programming language (R Core Team 2021, GPL v. 2 license). Additional to the functions provided by R reading, manipulating and data visualisation was done using functions of the following packages: readr (Wickham et al. 2021, MIT license), reshape2 (Wickham 2007, MIT license), dplyr (Wickham et al. 2020, MIT license), ggplot2 (Wickham 2009, MIT license), ggrepel (Slowikowski 2019, GPL v. 3 license), ggtext (Wilke 2020, GPL v. 2 license) and gridExtra (Auguie & Antonov 2017, GPL v. 2 license). Principal Component analyses (PCA) were performed using the base R functions and functions from FactoMineR (Husson et al. 2020, GPL v. 2 license) and factoextra (Kassambara & Mundt 2020, GPL v. 2 license). Geological scales were applied using the R package deeptime (Gearty 2021, GPL v. 2 license).
Morphological data of different species were plotted along with a phylogenetic tree using the R packages ape (Paradis et al. 2021, GPL v. 2), phytools (Revell 2017, GPL v. 2) and paleotree (Bapst & Wagner 2019, CCO license).

Body outline shapes of different biological and palaeontological specimens were quantified using an elliptic Fourier transformation. The outlines, which were obtained from photographs and drawings, were converted into binary (black and white) bitmap images. To

alleviate this task ImageMagick (Apache 2.0 license) was used to batch resize and to convert images between different file types. The images were then read in into an R environment, the shapes were converted into Fourier series, aligned and a PCA was performed to reduce the dimensionality of the data. This was done using the package momocs (Bonhomme et al. 2014, GPL v. 3 licence).

1.10.13   Maps

Maps were created in Inkscape by importing sets of vector graphics, using QGIS (qgis.org, GPL v.2) along with the QuickOSM plugin (Etienne Trimaille, GPL v. 2 license) and by facilitating the R packages sf (Pebesma 2018), rnaturalearth (South 2017) and tmap (Tennekes 2018). The geographic data used for the maps were retrieved from Natural Earth (naturalearthdata.com, public domain), and OpenStreetMap (openstreetmap.org, ODbL license). Geological map data was retrieved fom the Geological service of France http://www.geocatalogue.fr/Detail.do?id=4162, intellectual property of the organisation). A palaeogeographic map was retrieved from Scotese (2016) (PALEOMAP Project, www.earthbyte.org/paleomap-paleoatlas-for-gplates) and processed using QGIS. Palaeolatitudes were calculated using the R package chronosphere (Kocsis & Raja 2020, GPL v. 3 license).

1.10.14   Use of proprietary software

A special emphasis was given to the use of free and open source software to increase the reproducibility and the accessibility of the workflow. Most of the digital work was done using GNU/Linux operating systems. The use of non-free software, except for those tasks that involved controlling commercially manufactured devices such as digital microscopes and μCT scanners, was not necessary to accomplish the performed tasks and similar results could have been produced using free software.

2 Projects and results

2.1 Study I: SCHÄDEL, HYŽNÝ & HAUG 2021

Authors: Schädel, M., Hyžný, M. & Haug, J. T.

Title: Ontogenetic development captured in amber – the first record of aquatic representatives of Isopoda in Cretaceous amber from Myanmar

Journal: Nauplius

Article number: e2021003

Pages: 1–29

DOI: https://doi.org/10.1590/2358-2936e2021003

Ontogenetic development captured in amber – the first record of aquatic representatives of Isopoda in Cretaceous amber from Myanmar

Mario Schädel[1]   ⓘ orcid.org/0000-0001-7945-4205

Matúš Hyžný[2]   ⓘ orcid.org/0000-0002-8960-2846

Joachim T. Haug[1,3]   ⓘ orcid.org/0000-0001-8254-8472

1 Ludwig-Maximilians-Universität München, Department of Biology II, Zoomorphology group. Großhaderner Straße 2, 82152 Planegg-Martinsried, Germany.

2 Comenius University in Bratislava, Department of Geology and Paleontology. Mlynská dolina, Ilkovičova 6, 842 15 Bratislava, Slovakia.

3 Ludwig-Maximilians-Universität München, GeoBio-Center. Richard-Wagner-Str. 10, 80333 München, Germany.

ZOOBANK: http://zoobank.org/urn:lsid:zoobank.org:pub:4817F86A-F0E9-41F8-B841-6B0A5ABE0221

ABSTRACT

Two fossils from Burmese amber are the subject of this study. The specimens differ in size; yet, they appear to be conspecific because of the profound morphological similarity. The fossils are interpreted as representatives of Isopoda, more precisely of the group Cymothoida, due to the presence of a triangular basipod of the uropod. Cymothoida comprises parasitic forms of Isopoda as well as many other types of feeding-habits. The morphology in the studied fossils suggests that they are not representatives of any of the parasitic ingroups of Cymothoida. Since there are no other findings of Isopoda from the Cretaceous with the same morphological features, the fossils at hand are described as a new species – *Electrolana madelineae* sp. nov. The smaller specimen lacks well-developed walking appendages on trunk segment seven; it can thus be interpreted as a manca stage (immature) individual. The systematic affinity and the functional morphology of the herein described fossils, as well as three seed shrimps (Ostracoda) in close proximity to one of the specimens, and the presence of pyrite in the amber piece points towards an aquatic lifestyle and a preservation in moist conditions. In addition, we review the fossil record of immature forms of Isopoda.

KEYWORDS

Juvenile, manca, ontogeny, pyrite, taphonomy

INTRODUCTION

General background

The majority of representatives of Isopoda are marine, with a high diversity of body shapes and fulfilling various ecological functions (Wägele, 1989; Brusca and Wilson, 1991; Brandt and Poore, 2003; Poore and Bruce, 2012). Oniscidea is the only lineage within Isopoda that successfully managed to establish a full terrestrial lifestyle, with more than 4,000 species (Brusca *et al.*, 2001; Schmalfuss, 2003).

The oldest fossil record of the group Isopoda in general reaches back into the Middle Pennsylvanian (Late Carboniferous, about 300 million years old) of Illinois (*Hesslerella shermani* Schram, 1970 from Mazon Creek). The Palaeozoic and most of the Mesozoic fossils of Isopoda are marine forms. Cretaceous amber from Myanmar (Cenomanian, about 99 million years old; Shi *et al.,* 2012) includes the oldest record of terrestrial representatives of Isopoda. However, the diversification of the terrestrial lifestyle must have occurred earlier, as the presence of several oniscidean lineages in Burmese amber suggests (Broly *et al.*, 2015; Poinar, 2018; Ross, 2019; Yu *et al.*, 2019).

Isopoda is an ingroup of Peracarida, hence its representatives share a special mode of brood care: the eggs develop in a brood pouch of the female, that is made-up of protrusions from the walking appendages (oostegites). This specialization is also preserved in the fossil record of Isopoda (Broly *et al.*, 2017) and other peracaridan lineages, including rather enigmatic extinct groups, such as Pygocephalomorpha (Pazinato *et al.*, 2016).

The extended brood care in Peracarida appears to be coupled with the loss of true larval stages during individual development (see discussion in Haug, 2020). In many lineages of Peracarida the offspring is thought to hatch from the egg as 'miniature versions of the adult' (Boyko and Wolff, 2014: 210); yet, this expression seems to be only a matter of detail, because, naturally, there are (small) differences between immatures and adults (Haug, 2019).

Within Peracarida one major lineage evolved a particular mode of post-embryonic ontogenetic development. Mancoidea is characterized by a specialized stage, a so-called manca stage, representing a strong autapomorphy of the group (Ax, 2000). Manca stage individuals lack fully developed appendages on the segment that holds the posterior-most walking appendages in the adult (Wägele, 1989; Ax, 2000; Boyko and Wolff, 2014) while already possessing fully functional appendages on the further posterior (pleon) segments. As Isopoda is an ingroup of Mancoida, manca stages are also found in representatives of Isopoda.

Within the group Cymothoida parasitic forms evolved. These parasitize fishes, crustaceans and occasionally other organisms (*e.g.* Cephalopoda; Hosie, 2008; Poore and Bruce, 2012). Parasites of crustaceans (Epicaridea) appear to have evolved from fish parasites (Dreyer and Wägele, 2001; Nagler *et al.*, 2017). Within Cymothoida, the parasitic feeding strategy likely evolved from a more generalist (hunting/scavenging) feeding type (Wägele, 1989; Nagler *et al.*, 2017). Within two of the parasitic lineages (Epicaridea and Gnathiidae) secondarily differentiated early post-embryonic stages evolved, that are generally considered to represent true larval stages (Boyko and Wolff, 2014) as they clearly fulfil numerous criteria such as: differing significantly from the adult in morphology and ecology; possessing structures that will be reduced later in ontogeny; being dispersal stages and also undergoing distinct metamorphosis (see Haug, 2020 for a longer discussion of the term 'larva' and its criteria).

Fossils of these parasitic lineages are quite rare, but often show characters that identify them as such and can give a clue about the systematic affinity of the fossils (Hansen and Hansen, 2010; Serrano-Sánchez *et al.*, 2015; Nagler *et al.*, 2017; Néraudeau *et al.*, 2017; Schädel *et al.*, 2019b). However, the systematic affinity of non-parasitic cymothoidans is often more problematic because many groups have only small-scaled apomorphic features that are unlikely to be accessible in fossils. Different approaches have been applied to solve the problem of systematic uncertainty by taxonomic practice. An overview of non-parasitic cymothoidans is given in Hyžný *et al.* (2013). Wieder and Feldmann (1992) tried to solve the problem by assigning new species to existing widespread groups with extant representatives – such as Cirolana. Jarzembowski *et al.* (2014) erected a new 'collective group' (= form-genus) for their non-parasitic cymothoidan fossil species.

Aside from these problems with the identification of fossil specimens, the main problem when dealing with new species is, that many ingroups of Cymothoida – such as Cirolanidae and many of its ingroups – cannot be characterized by apomorphic features and the monophyly of some of the groups is questionable (see discussion below).

Aims of this study

In this study we present the oldest currently known representatives of Cymothoida, which are preserved in amber. In most non-amber fossil sites, fossils of Isopoda are either strongly compressed or lack delicate structures such as the antennae. Thanks to the preservation in fossil resin, microscopic images, as well as micro-CT data, could be obtained. Based on two conspecific specimens we can show morphological differences that can be explained by ontogenetic development. The phylogenetic affinity is carefully discussed with respect to systematic problems within the group Cymothoida.

Geological settings

Burmese amber ('Burmite') refers to fossilized resin that is excavated in the Hukawng Valley in the northern part of Myanmar (Fig. 1A, map). Burmese amber has been dated to an age of *ca.* 99 million years (Cenomanian, Late Cretaceous) (Shi *et al.*, 2012). To prevent confusion with the younger, Late Cretaceous Tilin amber from central Myanmar (Zheng *et al.*,

2018), the amber from the Hukawng Valley is also termed Kachin amber. Palaeo-geographically, the Burmese amber site is located on the southern margin of the Eurasian Plate (Fig. 1B, map) and has a palaeolatitude of less than 22°N (Seton *et al.*, 2012; Mathews *et al*, 2016; Müller *et al.*, 2016; Scotese and Wright, 2018). The global temperature during the time of the amber deposition (early Cenomanian) is reconstructed to be relatively high and the decrease in temperature with increasing latitude was probably much lower than today (Voigt *et al.*, 2003; Price *et al.*, 2012); therefore a warm tropical climate can be assumed for the palaeoenvironment.

Material and Methods

Material

The two amber pieces in this study (Fig. S1A) have been commercially obtained by Mark Pankowski (Rockville, Maryland, USA), who kindly donated the pieces to the Natural History Museum Vienna (Naturhistorisches Museum Wien, NHMW), where the pieces are housed under the collection numbers 2017/0052/0001 and 2017/0052/0002. Further information on the geological background, except for the trade-name 'Burmese amber', is not available. The amber pieces likely stem from the mining areas near Noje Bum (Hukawng Valley, Kachin State, Myanmar), from where most of the commercially available Burmese amber pieces originate.
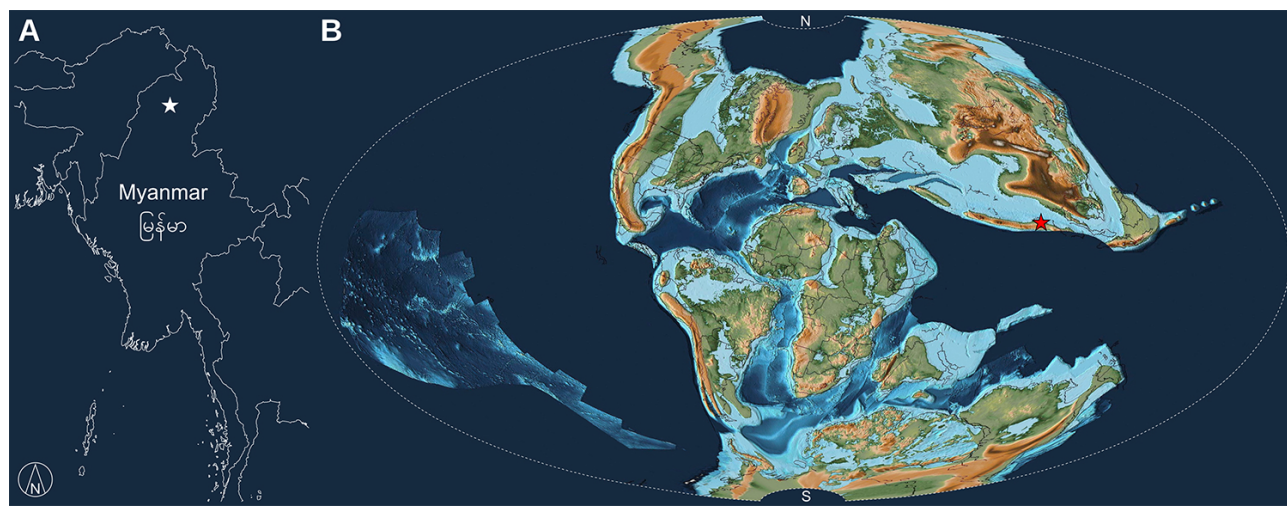
Figure 1. A: Map of Myanmar, white star marks the location of the Burmese amber mining sites near the town Noje Bum, base map from OpenStreetMap (openstreetmap.org); **B:** palaeogeographic world map, Aitov projection, 100 million years in the past, base image from PALEOMAP project (Scotese, 2016), red star marks the location of the Burmese amber sites.

Imaging

Microscopic images were gathered using a Keyence VHX-6000 digital microscope (VHX in the following). The implemented focus-merging function was used to overcome the limitations of the depth of field resulting from the high magnifications. Additionally, the implemented panoramic stitching function was applied in some cases to create high resolution images of larger objects. In-focus images from different view angles were gathered for further processing. In cases where the implemented focus-merging and panoramic stitching functions did not provide good results, stacks of images or individual in-focus images were recorded for further processing.

A Keyence BZ9000 digital fluorescence microscope (BZ in the following) was used to gather further microscopic images. Incident light with an excitation wavelength center of 545 nm (generally used for rhodamine-based stains, 'TRITC' filter cube) revealed the best contrast among the available fluorescence light sources (Haug *et al.*, 2011). Using the same microscope (BZ), transmitted-light microscopy was also performed. The native grey-value images gathered from the BZ9000 were saved for later processing.

For x-ray computer tomography (micro-CT) a Baker Hughes (General Electric) 'phoenix nanotom m' computer tomograph with a wolfram target on a cvd diamond was used along with the recommended acquisition software 'datos|x'. The scan was performed under a voltage of 100 kV. The amber piece was rotated 360 degrees in 1440 steps. The total scan time was 72 minutes. The final volume data was reconstructed using VGStudio MAX 2.2.6.80630 (Volume Graphics, proprietary). The achieved voxel size for the resulting stack of images (Fig. S5) was 2.81295 μm.

Processing

CombineZP (Alan Hadley, GPL) and Macrofusion (based on the Enfuse image blending algorithm, GPL) were used for combining stacks of images automatically to a single in-focus image (Mayer *et al.*, 2011). Drishti 2.6.4 was used for volume rendering of the micro-CT data (Hörnig *et al.*, 2016; Kypke and Solodovnikov, 2018). In one case, more than one transfer function was applied to show structures with different x-ray qualities. Two-dimensional images and red-cyan anaglyphs were exported from Drishti for further processing. GIMP 2.10 (GPL) was used to optimize the histogram, and enhance color, brightness and contrast of the final images. GIMP was also used to manually create panoramic images, background removal and to apply color markings to images (using layer masks, the colorize function and applying a shadow filter). Red-cyan stereo anaglyphs were created, using GIMP, to display three-dimensional structures (desaturation tool, colorize tool & layer transparency) (following Haug *et al.*, 2013).

QGIS 3.4.11 (GPL license) was used to assemble the maps. The map data for the map of Myanmar was obtained from OpenStreetMap (openstreetmap. org, ODbL license) via the QuickOSM plugin for QGIS. The palaeo-geographic map was retrieved from Scotese (2016) (PALEOMAP Project, www. earthbyte.org/paleomap-paleoatlas-for-gplates) and reprojected into Aitov projection (EPSG 53043) using QGIS. The palaeolatitude was calculated using the R package chronosphere (Kocsis and Raja 2020, GPL license) including multiple models (Seton *et al.*, 2012; Matthews *et al.*, 2016; Müller *et al.*, 2016; Scotese and Wright 2018). Inkscape (versions 0.92.3 and 0.92.4, GPL) was used to assemble the figure plates.

Use of generic names

Throughout the text, generic names are written in italics only when they are part of a binomial species name. This is a direct consequence of applying rank free nomenclature and, in addition, enhances the distinction between species names and names of higher systematic groups (with the exception of monospecific genera, all genus-ranked taxa are higher systematic groups and should represent monophyletic groups; *cf.* Schädel *et al.*, 2019b).

RESULTS

Description of specimen NHMW 2017/0052/0002 (smaller specimen)

The body is composed of a distinct head (postocular segments 1–6, cephalothorax) and a trunk (postocular segments 7–19). The trunk is divided into two functional tagmata: the anterior trunk (pereon, postocular segments 7–13; posterior thorax) and the pleon (posterior trunk, postocular segments 14–19).

The last segment of the pleon is conjoined with the telson forming a pleotelson.

Body ovoid in dorsal view, tapering posteriorly, about 2.5 times longer than wide, widest at about half of the length. Dorsal surface with head capsule, tergites (robust dorsal sclerotization of the trunk segments) and pleotelson; surface largely with small rhomboid scales (Fig. 2A).

Head with anterior margin roughly semi-circular in dorsal view (Fig. 2A).

Eyes well developed, positioned laterally on the head, extending to the posterior margin of the head; ommatidia organised in an hexagonal array of at least 6 by 8 ommatidia (Fig. 2A–D).

Anteroventral side of the head with a complex formed by frontal lamina, clypeus and labrum. Anterior-most part (frontal lamina) with rhomboid anterior part, posterior part narrow with parallel lateral sides, prominent also in dorsal view; subsequent part (clypeus) connected to frontal lamina, but separated by a suture, triangular, shorter than wide, much wider than the posterior part of the frontal lamina; posterior-most part (labrum) connected to clypeus, but separated by a suture, about as wide as the posterior side of the clypeus (Fig. 3E).

Antennula (appendage of postocular segment 1) subdivided into a set of proximal peduncle elements and a set of distal flagellum elements; with at least two elongated peduncle elements and three or more, much shorter flagellum elements (distal elements not well visible) (Fig. 2A, B).

Antenna (appendage of postocular segment 2) subdivided into a set of proximal peduncle elements and a set of distal flagellum elements; three elongated peduncle elements and ten much shorter flagellum elements; proximal flagellum element about as wide as peduncle elements; flagellum elements continuously decreasing in width towards the distal most element; peduncle elements with setae on the distal margin, setae about one third of the length of the corresponding peduncle element (Fig. 2A, B).

Mandible (appendage of postocular segment 3) well developed, with proximal coxa and distal palp; mediodistal part ('pars incisivus', 'mandibular incisor') moderately broad; palp on the lateral side of the mandible ('mandibular palp'), well developed, composed of three or more elements; distal tip of mandibular palp with short setae (Fig. 3E).

Maxillula (appendage of postocular segment 4) narrow, distal tip with at least four setae (Fig. 3E).
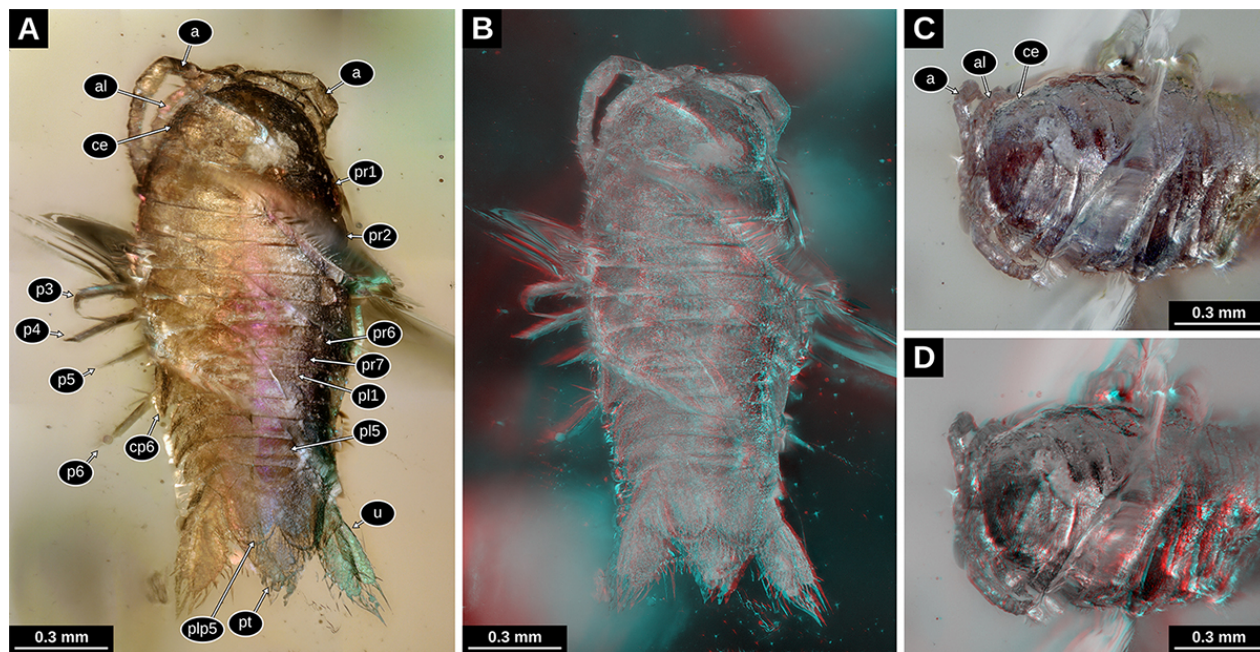
Figure 2. Paratype of *Electrolana madelineae* sp. nov. (NHMW 2017/0052/0002). **A**: Habitus in dorsal view, white light microscopy, coaxial light and polarising filter, 300x (VHX); **B**: habitus in dorsal view, red-cyan stereo anaglyph, white light microscopy, 200x (VHX); **C**: head region in antero-dorsal view, white light microscopy, 200x (VHX); **D**: head region in antero-dorsal view, red-cyan stereo anaglyph, white light microscopy, 200x (VHX). a, antenna; al, antennula; ce, compound eye; cp6, coxal plate of trunk segment 6; p3–6, trunk appendages 3–6; pl, pleon segments 1–5; plp5, pleopod 5; pr1–7, trunk segments 1–7; pt, pleotelson; u, uropod.
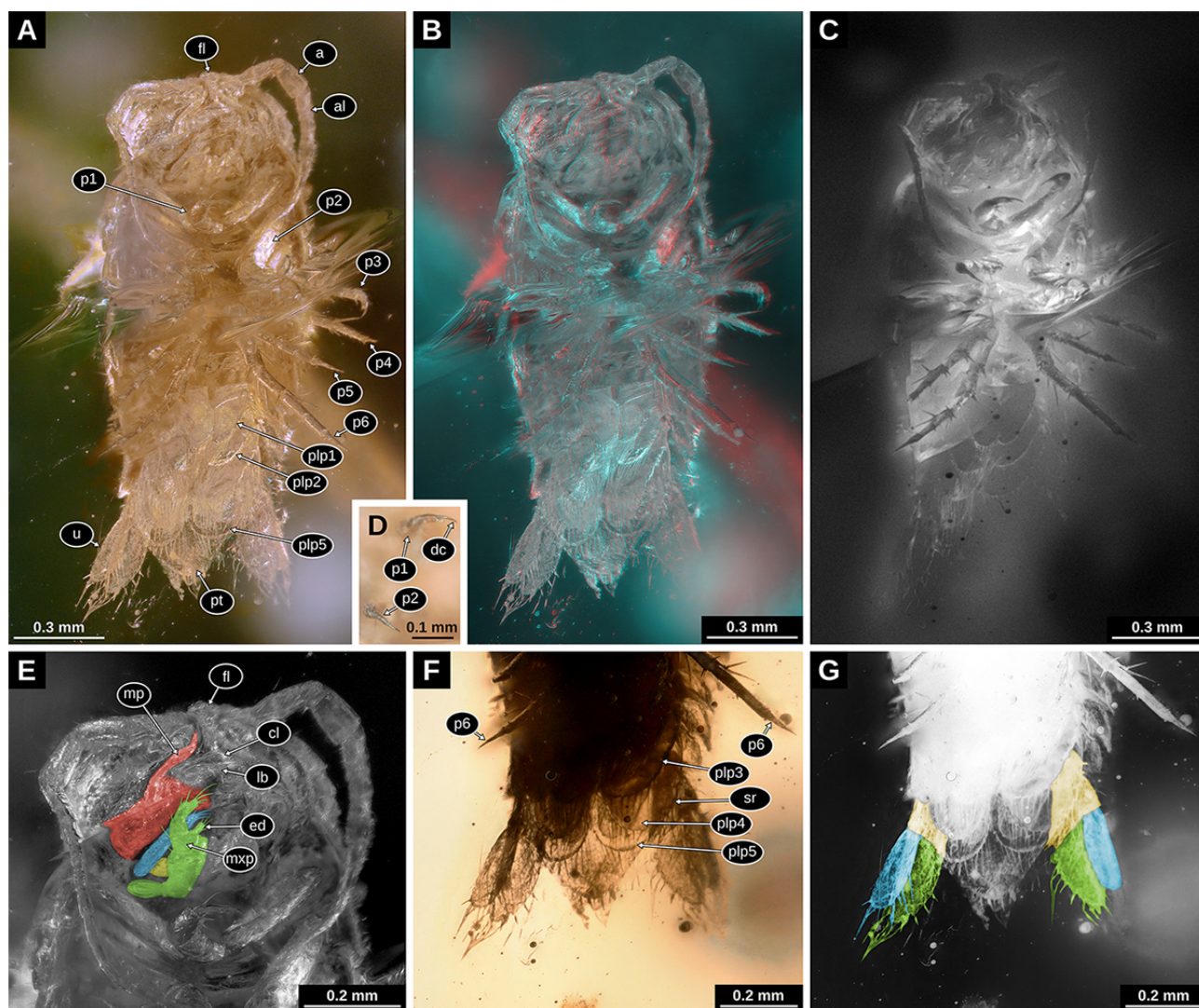
Figure 3. Paratype of *Electrolana madelineae* sp. nov. (NHMW 2017/0052/0002). **A**: Habitus in ventral view, white light microscopy, 300x (VHX); **B**: habitus in ventral view, red-cyan stereo anaglyph, white light microscopy, 200x; **C**: habitus in ventral view, epifluorescence microscopy, 4x (BZ); **D**: distal region of trunk appendages 1 and 2 in ventral view, right body side, white light microscopy, 300x (VHX); **E**: head in ventral view, white light microscopy, desaturated with colour markings, red mandible, blue maxillula, yellow maxilla, green maxilliped, 300x (VHX); **F**: pleon region in ventral view, white light microscopy, 300x (VHX); **G**: pleon region in ventral view, white light microscopy, desaturated and inverted, with color markings, yellow basipod, green endopod, blue exopod, 300x (VHX). a, antenna; al, antennula; cl, clypeus; dc, dorsal claw; ed, endite of the maxilliped; fl, frontal lamina; lb, labrum; mp, mandibular palp; mxp, maxilliped; p1–6, trunk appendages 1–6; plp1–5, pleopod 1–5; pt, pleotelson; sr, serration pattern; u, uropod.

Maxilla (appendage of postocular segment 5) present, but concealed by the appendage of the succeeding segment (Fig. 3E).

Maxilliped (appendage of postocular segment 6) composed of two proximal elements and a latero-distal palp (endopod?) inserting on the second element; proximal element elongated, originating on the postero-lateral side of the head and oriented medially along the ventral side of the head; distal element roughly rectangular, longer than broad; median margins of the distal elements of the left and right body side meeting each other along the medio-sagittal plane; distal element bearing an endite on the distal side and palp on the latero-distal side; endite narrow, with at least 4 prominent setae on the distal tip; palp composed of three elements; palp elements distally decreasing in width, each element with setae on the latero-distal corners; 4 prominent setae and multiple short setae on the distal tip of the palp (Fig. 3E).

Anterior trunk (pereon, postocular segments 7–13) dorsoventrally compressed, with 7 free tergites (tergites not conjoined with those of other segments).

Tergite of trunk segment 1 with concave anterior margin; longer along the lateral margins than along the midline; lateral margins gently convex (Fig. 2A, B).

Tergites of trunk segments 2–5 relatively uniform in shape, without concave anterior margins, shorter than the tergite of trunk segment 1 (Fig. 2A, B).

Tergite of trunk segment 6 about as long as the preceding tergites, with concave posterior margin (Fig. 2A, B).

Trunk segment 6 with a well-developed coxal plate (derivative of the proximal leg element); coxal plate triangular, with pointed postero-distal tip (Fig. 2A, B).

Tergite of trunk segment 7 (postocular segments 13) shorter than the preceding tergites, laterally encompassed by the tergite of trunk segment 6; without well-developed coxal plates (Fig. 2A, B).

Trunk segments 1–6 (postocular segments 7–12) with well-developed legs (thoracopods 2–7; pereopods 1–6); trunk segment 7 (postocular segment 13) without well-developed legs; trunk appendages 1–6 composed of 7 elements (coxa, basipod , and the five endopod elements: ischium, merus, carpus, propodus, dactylus); coxa not forming a distinct movable leg element, but forming scale-like extensions of the tergites (coxal plates) (Fig. 3A–C).

Distal part of trunk appendage 1 (distal to the coxa) with long basipod; ischium, merus and carpus much shorter than basipod; propodus moderately curved inward (median side concave), with setae on the median side and one long seta on the distal side; dactylus moderately curved inward, with two distinct tips ('claws') on the distal end, the more prominent one, in extension to the convex lateral side of the dactylus ('dorsal claw'; *cf.* Wägele, 1989; Wilson, 2009) distinct and much larger than the tip in extension to the concave median side of the dactylus ('ventral claw'; *cf.* Wägele, 1989; Wilson, 2009); dorsal claw with about the same level of curvature as the rest of the dactylus (Fig. 3A–D).

Distal part of trunk appendage 2 similar to trunk appendage 1; carpus triangular in anterior view; dorsal claw of dactylus distinct, but possible curvature not observable due to the viewing angle (Fig. 3A–D).

Distal part of trunk appendage 3 with small spines distally on the propodus; dactylus moderately curved; dorsal claw of the dactylus distinct and moderately curved (Fig. 3A–C).

Distal part of trunk appendage 4 with leg elements roughly cylindrical, all of them tapering distally; strong spines on the latero-distal side of the merus; propodus not curved; dactylus not curved (Fig. 3A–C).

Distal part of trunk appendage 5 with basipod long and antero-posteriorly compressed, distally increasing in width; ischium much shorter than basipod, antero-posteriorly compressed, distally increasing in width; merus antero-posteriorly compressed, about as long as ischium, more slender than ischium, with strong distal spines on the median side, with two strong and long spines on the lateral side; propodus roughly cylindrical, tapering distally; dactylus straight and conical, possible curvature only in the distal-most part (Fig. 3A–C).

Distal part of trunk appendage 6 with basipod long, antero-posteriorly compressed, distally increasing in width, with one strong distal spine on the median side and one strong distal spine on the lateral side; ischium similar to basipod, but of only about one third of the length of the basipod; merus not distally increasing in width, slightly antero-posteriorly compressed, two long and strong distal spines on the lateral side, strong but shorter distal spines on the median side; carpus and propodus sub-cylindrical, both with short distal spines on the median side; dactylus conical with pointed tip (Fig. 3A–C).

Posterior trunk, pleon (postocular segments 14–19) dorsoventrally compressed, with 5 free tergites.

Tergite of pleon segment 1 (postocular segment 14) short, laterally covered by the tergites of the preceding trunk segments 6 and 7 (Fig. 2A, B).

Tergite of pleon segment 2–4 (postocular segments 15–17) of about the same length and width, distinctly longer than the tergite of pleon segment 1 (postocular segment 14), lateral sides bent posteriorly and with pointed tips (Fig. 2A, B).

Tergite of pleon segment 5 (postocular segment 18) distinctly longer than the preceding segments, lateral margin with less distinct pointed tip (Fig. 2A, B).

Tergite of pleon segment 6 (postocular segment 19) conjoined with telson (pleotelson), triangular (angle between posterolateral margins about 75°), slightly

longer than wide, posterior tip rounded, posterior margin with 6 setae grouped around the posterior tip, serration pattern on the anterior part of the posterior margin (Figs. 2A, B, 3A, B, 3F, G).

Pleon segments 1–5 (postocular segments 14–18) with similarly shaped, flattened, appendages (pleopods), inserting on the ventral side of the body, composed of a proximal element (basipod) and two distal elements inserting on the basipod (endopod and exopod). Pleopods increasing in size from pleopod 1 to pleopod 5 (Fig. 3A–C, F, G).

Pleopod 1 basipod wider than long, with distal margin oblique, resulting median margin being much longer than lateral margin; endopod not visible, probably covered by the exopod; exopod longer than wide, median margin convex; distal margin rounded; distal margin with about 8 long setae (Fig. 3A–C).

Pleopod 2 basipod and endopod not visible; exopod similar to that of pleon segment 1, serration pattern at the distal margin (Fig. 3A–C).

Pleopod 3 basipod and endopod not visible; exopod similar to that of the preceding segments (Fig. 3A–C, F, G).

Pleopod 4 basipod not visible; exopod similar in shape to those of the preceding segments, with distinct serration pattern on the distal margin, setae inserting on the convex parts of the serration pattern; endopod narrower than the exopod, distal tip of endopod reaching more distally than the tip of the exopod (Fig. 3A–C, F, G).

Pleopod 5 basipod not visible; endopod more slender than exopod, no setae on distal margin; exopod with rounded distal margin, distal margin with long setae, serration pattern of the distal margin weaker than that in the exopod of pleopod 4 (Fig. 3A–C, F, G).

Pleon segment 6 (postocular segment 19) with appendages inserting on the ventrolateral side of the body (uropods). Basipod roughly triangular in shape, lateral margins without visible setae; endopod elongated, longer than wide, about 2.5 times, distal margin rounded, strong and long setae on the distal margin and the distal part of the median margin; exopod elongated, more slender than the endopod, longer than wide, about 3 times, distal margin rounded, some weak setae on the lateral margins, strong and long setae on the distal margin and the distal part of the median margin (Fig. 3A–C, F, G).

Measurements of specimen NHMW 2017/0052/0002 (smaller specimen)

Body length (without appendages) 1.72 mm; maximal body width (without appendages) 0.70 mm; head length 0.35 mm; head width 0.51 mm; antenna length (two-dimensional measurement) 0.71 mm (left), 0.85 mm (right); anterior trunk length 0.64 mm; trunk tergite 1 length 0.14 mm; trunk tergite 2 length 0.09 mm; trunk tergite 3 length 0.10 mm; trunk tergite 4 length 0.09 mm; trunk tergite 5 length 0.08 mm; trunk tergite 6 length 0.08 mm; trunk tergite 7 length 0.06; pleon length without pleotelson 0.33 mm; pleon segment 1 length 0.04 mm; pleon tergite 2 length 0.06 mm; pleon tergite 3 length 0.07 mm; pleon tergite 4 length 0.07 mm; pleon tergite 5 length 0.09 mm; pleotelson length 0.39 mm.

Syn-inclusions of specimen NHMW 2017/0052/0002 (smaller specimen)

Isolated leg, Euarthropoda (Fig. S2A); isolated distal element of a leg, Euarthropoda (Fig. S2B); mite (Arachnida: Acari) (Fig. S2C–E); possible cuticle remains, Euarthropoda (Fig. S2F); multiple needle-like objects, possibly plant hairs or setae of euarthropodans (Fig. S2G).

Description of specimen NHMW 2017/0052/0001 (larger specimen)

Body organization, see description above. Body drop shaped (dorsal view), tapering posteriorly, about 2.2 times longer than wide, widest at about half of the length (Figs. 4A, 5A–C, 6). Dorsal surface with head capsule, tergites (robust dorsal sclerotizations of the trunk segments) and the pleotelson.

Head with anterior margin roughly half-circular in dorsal view (Fig. 5A).

Eyes well developed, positioned laterally on the head (Fig. 4E). Anterior margin of the head without distinct median process (rostrum), separated from the frontal lamina (Fig. S1D).

Antennula (appendage of postocular segment 1) subdivided into a set of proximal peduncle elements and a set of distal flagellum elements; with three elongated peduncle elements and nine or more, much shorter, flagellum elements (Figs. 4B,C, E, 5A).
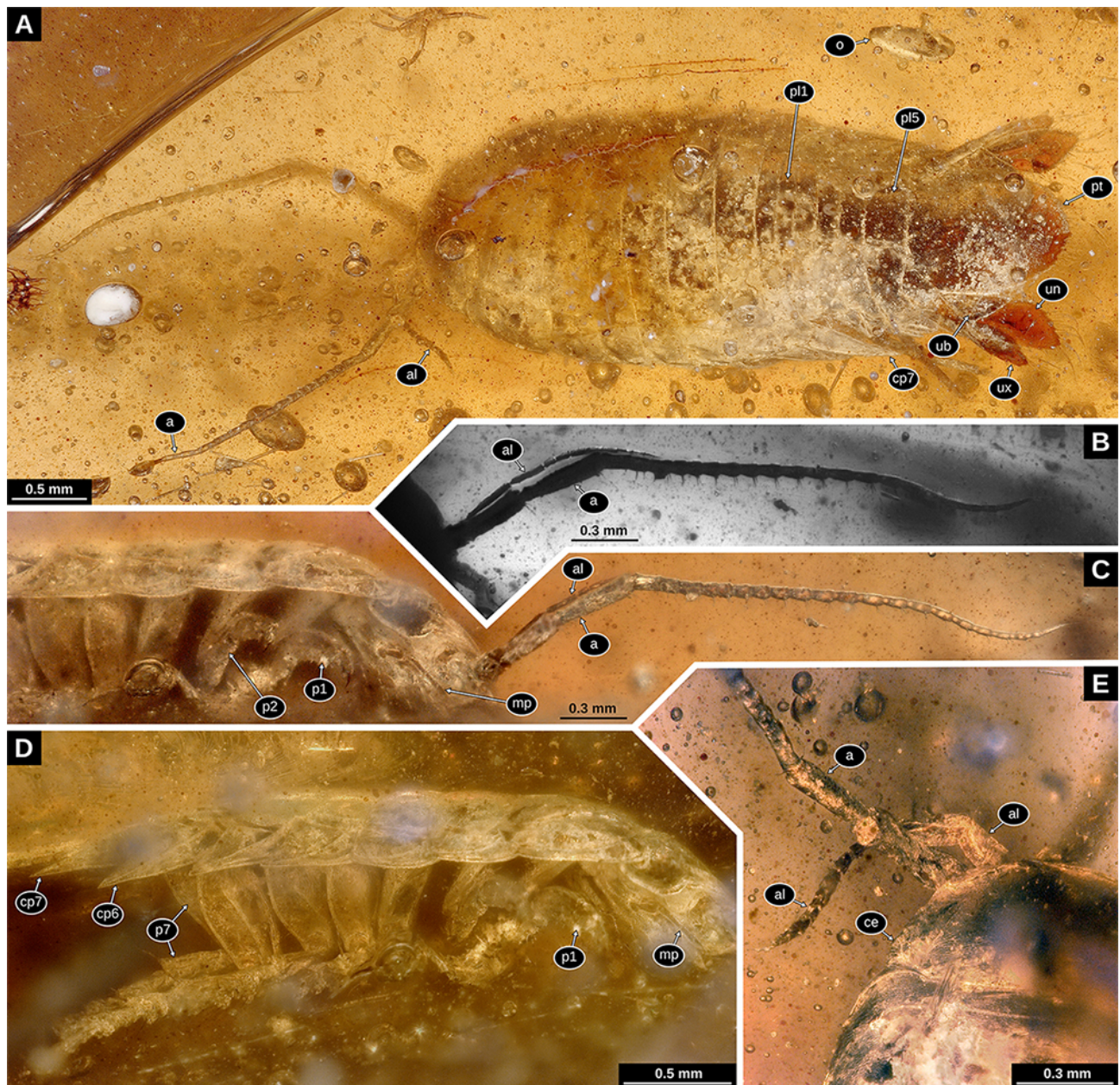
Figure 4. Holotype of *Electrolana madelineae* sp. nov. (NHMW 2017/0052/0001). **A**: Habitus in dorsal view, white light microscopy, 200x (VHX). **B**: anterior head region in ventro-lateral view, transmitted light microscopy, 4x (BZ); **C**: anterior body region in ventro-lateral view, white light microscopy, 200x (VHX); **D**: anterior trunk region in ventro-lateral view, white light microscopy, 150x (VHX); **E**: head region in dorsal view, left body side, white light microscopy, 200x (VHX). a, antenna; al, antennula; ce, compound eye; cp6–7, coxal plate of trunk segment 6–7; mp, mandibular palp; o, seed shrimp (Ostracoda); p1–7, trunk appendages 1–7; pt, pleotelson; ub, uropod basipod; un, uropod endopod; ux, uropod exopod.

Antenna (appendage of postocular segment 2) subdivided into a set of proximal peduncle elements and a set of distal flagellum elements; three elongated peduncle elements and twenty-two much shorter flagellum elements; proximal peduncle element about two times longer than wide; second and third peduncle element of about the same shape and size, much longer than the proximal peduncle element, a set of two setae on the ventral side of the distal end of the elements; proximal flagellum element distinctly narrower than the peduncle elements; flagellum elements continuously decreasing in width towards the distal most element, a set of two setae on the ventral side of the distal end of the elements; long seta on the distal end of the distal most flagellum element (Figs. 4A–C, 5A–D).
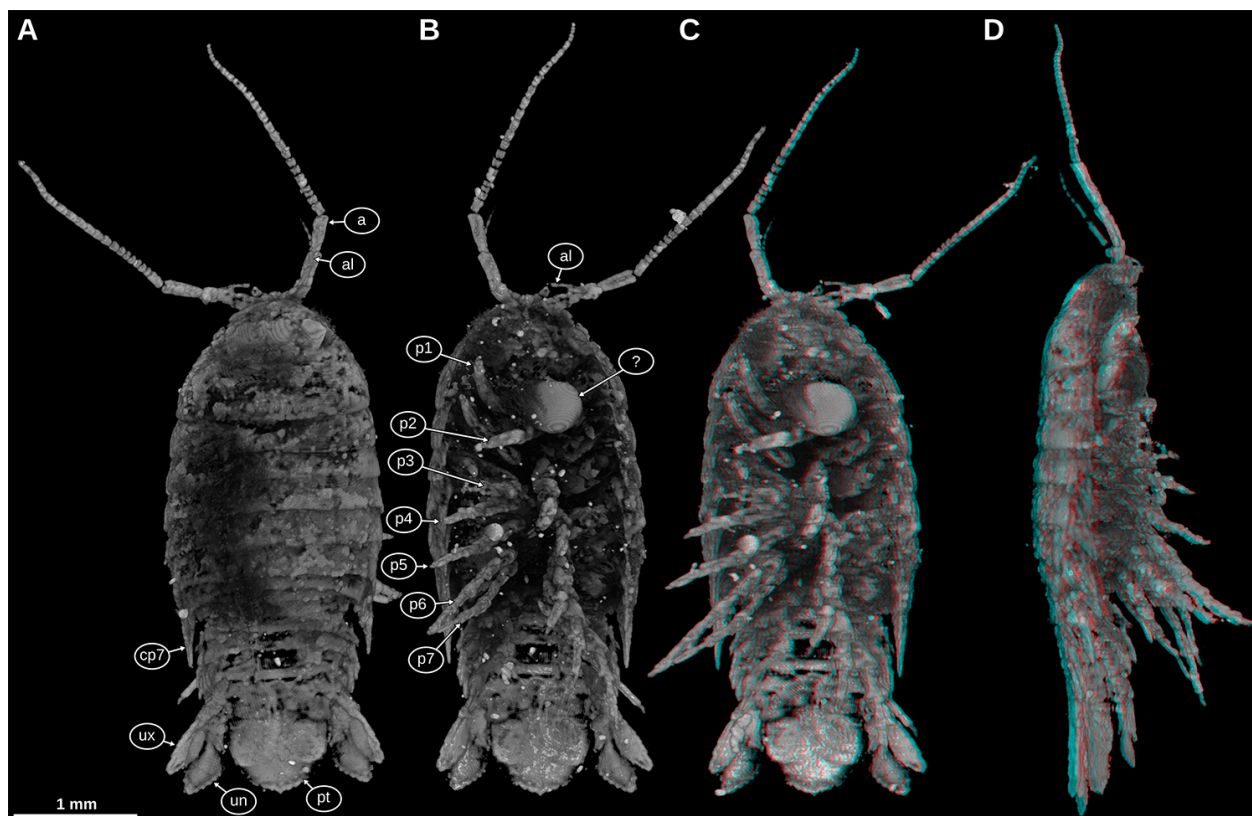
Figure 5: Holotype of *Electrolana madelineae* sp. nov. (NHMW 2017/0052/0001), volume rendering images based on micro-CT data. **A**: Habitus in dorsal view, orthographic projection; **B**: habitus in ventral view, orthographic projection; **C**: habitus in ventral view, red-cyan stereo anaglyph, perspective projection; **D**: habitus in lateral view, right body side, red-cyan stereo anaglyph, perspective projection. a, antenna; al, antennula; cp7, coxal plate of trunk segment 7; p1–6, trunk appendages 1–6; pt, pleotelson; un, uropod endopod; ux, uropod exopod; ?, unknown material forming an irregular bubble.

Mandible (appendage of postocular segment 3) well developed, with coxa and distal palp; mandibular palp well developed, composed of a wide proximal element and one or more much narrower distal elements, distal elements together about three times longer than proximal element (Fig. 4C).

Anterior trunk (pereon, postocular segments 7–13) dorsoventrally compressed, with 7 free tergites (tergites not conjoined with those of other segments).

Tergite of trunk segment 1 (postocular segment 7) with concave anterior margin; longer along the lateral margins than along the midline; lateral margins convex (Figs. 4A, 5A).

Tergites of trunk segments 2–5 (postocular segments 8–11) relatively uniform in shape, without concave anterior margins, shorter than the tergite of trunk segment 1 (Figs. 4A, 5A).

Tergite of trunk segment 6 (postocular segment 12) about as long as the preceding tergites, with gently concave posterior margin (Fig. 4A).

Tergite of trunk segment 7 (postocular segment 13) much shorter along the midline than the preceding tergites, laterally not encompassed by the tergite of trunk segment 6 (Fig. 4A).

Trunk segment 1 (postocular segment 7) seemingly without coxal plate (derivative of the proximal leg element, laterally adjoining the tergite); trunk segment 2 and 3 with sub-rectangular coxal plates, ridge on the dorsal side of the plate curved, distally approaching the lateral margin; trunk segment 4–7 (postocular segments 10–13) with well-developed triangular coxal plates, plates triangular, with pointed postero-distal tip, increasing in size towards trunk segment 7 (postocular segment 13); coxal plates 6 and 7 (postocular segment 12-13) with oblique straight ridge on the dorsal side of the plate, distally joining the postero-distal corner; coxal plate of trunk segment 7 very conspicuous in dorsal view, extending distally to the level of pleon segment 5 (postocular segment 18) (Figs. 4A, D, 5A–D).
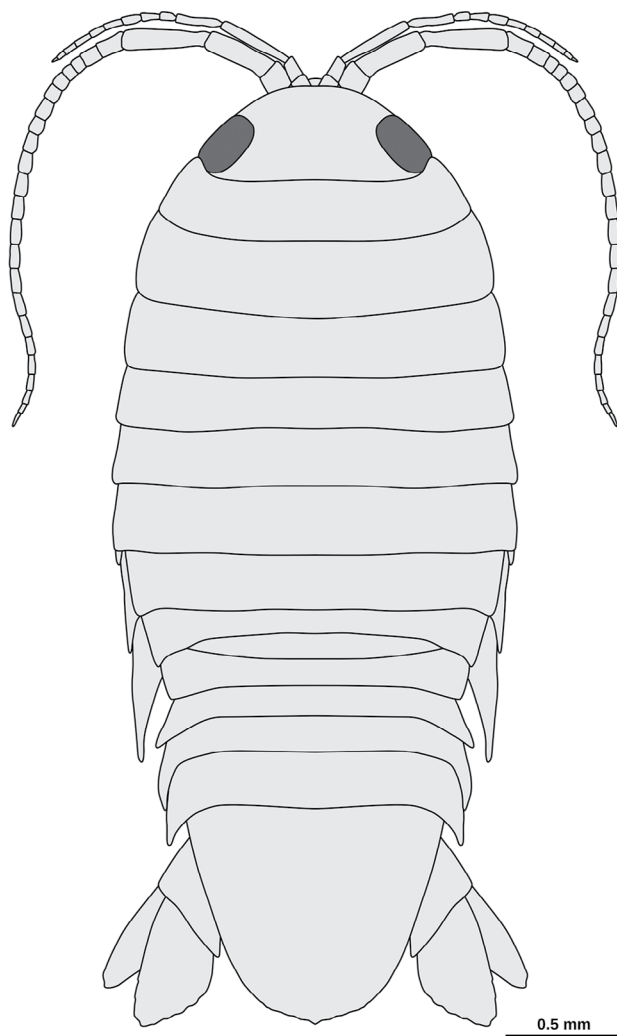
Figure 6. Drawing of the holotype of *Electrolana madelineae* sp. nov. (NHMW 2017/0052/0001), dorsal view, composite of microscopic images and micro-CT scan data.

Trunk segments 1–7 (postocular segment 7–13) with well-developed legs (thoracopods 2–7, pereopods 1–6); trunk appendages composed of 7 elements (coxa, basipod, and the five endopod elements: ischium, merus, carpus, propodus, dactylus); coxa not forming a distinct movable leg element but forming scale-like extensions of the tergites (coxal plates) (Figs. 4C, D, 5B–D).

Distal part of trunk appendage 1 (distal to the coxa; postocular segment 7) with long basipod; ischium, merus and carpus much shorter than basipod; propodus slightly curved inward (median side concave), with setae on the median side; dactylus much shorter and narrower than the propodus, curved inward, with a distinct claw, claw curved inward and

much darker than the rest of the dactylus (Figs. 4C, 5B–D and volume data).

Distal part of trunk appendage 2 similar to trunk appendage 1; ischium much shorter than basipod; merus and carpus shorter than ischium, carpus triangular in posterior view (Figs. 4C, 5B–D and volume data).

Distal part of trunk appendage 3 roughly similar to the two preceding trunk appendages; propodus slightly curved inward (Fig. 5C and volume data).

Distal part of trunk appendage 4 longer than trunk appendage 3; carpus distally increasing in width; propodus straight and roughly cylindrical; dactylus short and straight (Fig. 5C and volume data).

Distal part of trunk appendage 5 (postocular segment 11) longer than trunk appendage 4; basipod broad, with posterior margin convex, median ridge along the midline of the lateral surface; ischium almost as long as basipod; merus and carpus of about half of the ischium, each distally increasing in width and slightly compressed in antero-posterior direction; propodus slightly compressed in antero-posterior direction, median margin slightly concave; dactylus short and pointed, very weakly curved inward (Figs. 4D, 5C, D and volume data).

Distal part of trunk appendage 6 (postocular segment 12) longer than trunk appendage 5 (longest trunk appendage); basipod broad, with posterior margin convex, median ridge along the midline of the lateral surface; ischium long and slender, distally increasing in width and more antero-posteriorly compressed; merus and carpus of similar shape, both antero-posteriorly compressed, distally increasing in width; propodus slightly compressed in antero-posterior direction, median margin slightly concave; dactylus short and pointed, very weakly curved inward (Figs. 4D, 5C, D and volume data).

Distal part of trunk appendage 7 similar to trunk appendage 6, but distinctly shorter; ischium with long seta distally on the lateral side; merus with seta distally on the lateral side (Fig. 5C, D and volume data).

Posterior trunk, pleon (postocular segments 14–19) dorsoventrally compressed, with 5 free tergites.

Tergite of pleon segment 1 short, laterally covered by the tergites of the preceding trunk segment 7 (Figs. 4A, 5A, 7A).
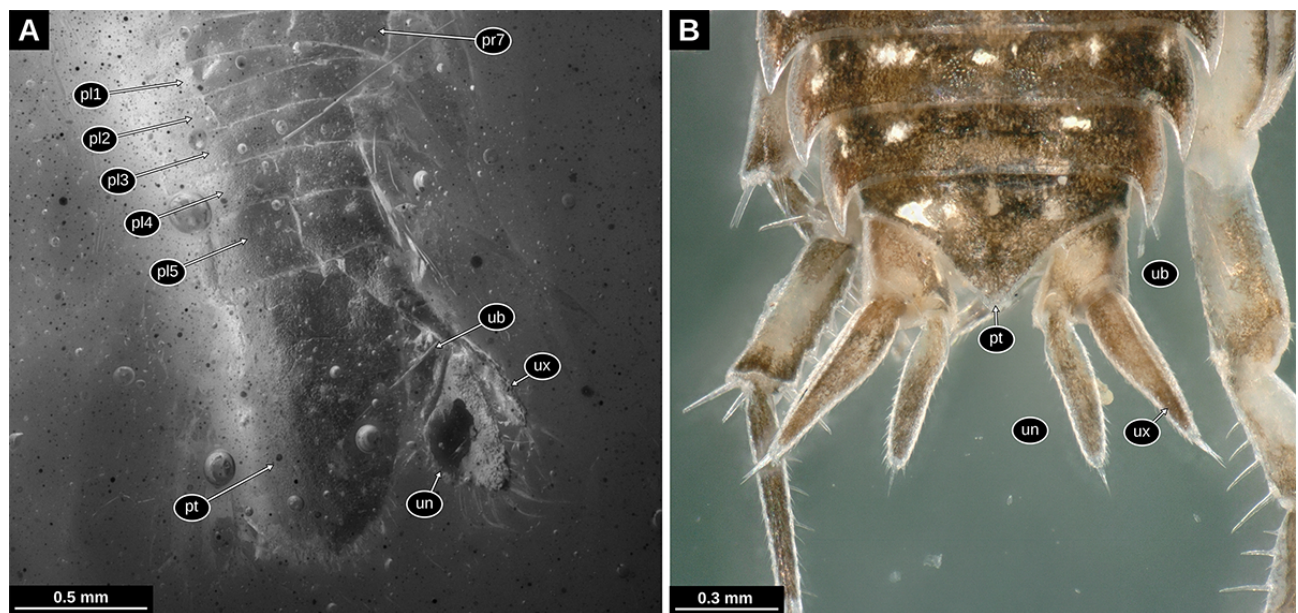
Figure 7. Comparison of the uropod morphology between *Electrolana madelineae* sp. nov. and an extant representative of Oniscidea. **A**: Holotype of *Electrolana madelineae* sp. nov. (NHMW 2017/0052/0001), pleon region in latero-dorsal view, epifluorescence microscopy, 4x (BZ); **B**: *Philoscia* cf. *muscorum* (Scopoli, 1763), posterior pleon region in dorsal view, white light microscopy, 200x (VHX). pl, pleon segments 1–5; pr7, trunk segment 7; pt, pleotelson; ub, uropod basipod; un, uropod endopod; ux, uropod exopod.

Tergites of pleon segments 2–4 (postocular segments 15–17) of about the same length and width, slightly longer than the tergite of pleon segment 1, lateral sides bent posteriorly and with pointed tips (Figs. 4A, 5A, 7A).

Tergite of pleon segment 5 (postocular segment 18) distinctly longer than the preceding segments (Figs. 4A, 5A, 7A).

Tergite of pleon segment 6 (postocular segment 19) conjoined with the telson (pleotelson) half-oval, slightly longer than wide; anterior margin straight; posterior tip rounded with median notch/tooth, posterior margin with numerous setae grouped in the posterior-most part (Figs. 4A, 7A).

Pleon segments 1–4 (postocular segments 14–17) with appendages not visible (not preserved, not visible and without x-ray contrast). Appendage of pleon segment 5 (pleopod 5; postocular segment 18) with only exopod visible, exopod broad, flattened and with rounded posterior margin, numerous long setae on the distal margin (Fig. 5B, C).

Pleon segment 6 (postocular segment 19) with appendages roughly similar to those of the preceding segments but inserting on the ventrolateral side of the body (uropods). Uropod basipod roughly triangular in shape, lateral margins without visible setae; endopod

elongated, about 2 times longer than wide, median margin with weak angle, fine setae on the lateral margin, strong and long setae on the distal margin and the distal part of the median margin; exopod elongated, more slender than the endopod, about 3 times longer than wide, distal margin with an acute angle, strong and long setae on the distal margin and the distal part of the median margin (Figs. 4A, 5B, C, 7A).

Measurements of specimen NHMW 2017/0052/0001 (larger specimen)

Body length (without appendages) 4.00 mm; maximal body width (without appendages) 1.79 mm; head length 0.58 mm; head width 1.01 mm; antennula length (two-dimensional measurement) 0.95 mm (left), 0.81 mm (right); antenna length (two-dimensional measurement) 2.38 mm, peduncle length 0.76 mm, flagellum length 1.62 mm (left), 2.62 mm, peduncle length 0.85 mm, flagellum length 1.77 mm (right); anterior trunk length 1.93 mm; trunk tergite 1 length 0.57 mm; trunk tergite 2 length 0.25 mm; trunk tergite 3 length 0.22 mm; trunk tergite 4 length 0.26 mm; trunk tergite 5 length 0.29 mm; trunk tergite 6 length 0.25 mm; trunk tergite 7 length 0.12;

pleon length without pleotelson 0.72 mm; pleon segment 1 length 0.12 mm; pleon tergite 2 length 0.13 mm; pleon tergite 3 length 0.14 mm; pleon tergite 4 length 0.15 mm; pleon tergite 5 length 0.26 mm; pleotelson length 0.93 mm.

Syn-inclusions of specimen NHMW 2017/0052/0001 (larger specimen)

Fly, Diptera *cf.* Psychodidae (Fig. S3A, B); Alavesia (Fig. S3C, D); beetle, Coleoptera (Fig. S3E, F); remains, Euarthropoda (Fig. S4A); two isolated but closely grouped legs, Euarthropoda (Fig. S4B–C); isolated leg, Euarthropoda (Fig. S4D); three individuals of seed shrimps, Ostracoda (Fig. S4E–G).

DISCUSSION

Conspecificity of the two specimens and ontogenetic changes

Except for the body size, the two herein studied specimens are overall very similar.

Nevertheless, there are morphological differences between the two studied fossil specimens: 1) The antennae are proportionally longer, more slender and consist of a larger number of flagellum elements in the larger specimen (Fig. 3A *vs.* Fig. 4C). 2) The trunk appendage 7 is only well developed in the larger specimen (Fig. 3A–C *vs.* Fig. 4D). 3) The posterior margin of the pleotelson is more rounded and less triangular in shape in the larger specimen (Fig. 2A *vs.* Fig. 5A). 4) The distal ends of the uropods are more acute and less rounded in the larger specimen (Fig. 3F *vs.* Fig. 4A). Considering the similarity between the two specimens and that the differences can easily be explained by ontogenetic changes, it appears most likely that the two specimens are conspecific.

Most representatives of Isopoda develop at first in a specialised brood pouch of the female (Boyko and Wolff, 2014). Early post-embryonic stages lack a well-developed seventh trunk appendage (manca stage; Ax, 2000; Boyko and Wolff, 2014). The seventh pair of trunk appendages develops well after the immature offspring escapes from the brood pouch; the development of these appendages marks the end of the manca stage (Boyko and Wolff, 2014). The smaller specimen (NHMW 2017/0052/0002) can clearly be interpreted as a manca stage, due to the absence of a well-developed seventh trunk appendage.

The transition between the manca stage and the (following) juvenile or adult stage in the herein described Cretaceous species must have occurred while the individuals were 1.72 to 4 mm long. This of course cannot be generalized for the entire population, as there can be considerable variation in the sizes of individuals (*cf.* size ranges of manca stages in Bruce, 1986; Brusca *et al.*, 1995). Only in the group Bathynomus manca stage individuals are much larger (up to 60 mm body length) – likely due to the enormous size of the adults (Soong and Mok, 1994).

After 'Dyar's law' (Dyar, 1890) or 'Brook's law' (Fowler, 1904) the growth in representatives of Euarthropoda measured in areas of the bodies that are not affected by inter-moult growth, follows a constant coefficient ('*r*' in the following). The application of Dyar's law/Brook's law certainly has its limitations, since with some exception, *e.g.*, (most) flying insects, the number of moults in the life of individuals is not limited ('life-long growth'). A decrease of the growth coefficient *r* with increasing size and age, especially after reaching maturity, has to be expected. Nevertheless, in early stages of the development of non-insectan crustaceans, such as those of the group Isopoda, a more or less linear growth with each moult can be expected (Minelli and Fusco, 2013).

Assuming a linear growth, the growth coefficient *r* can be calculated with the following formula, when a certain length before (X_{i-n}) and after (X_i) the moult or multiple (n) moulting events are known.

$$r = (X_i/X_{i-n})^{1/n}$$

Growth coefficients of 1.2 to 1.44 have been shown for extant aquatic forms of Isopoda, that have not yet reached sexual maturity (Strong and Daborn, 1979; Luxmoore, 1981; Johansen, 2000). Assuming that both fossils are neither especially small nor large for their respective ontogenetic stage, the most likely assumption is that there are two or three intermediate instars (three or four moults) between them (Tab. 1).

Table 1. Growth coefficients calculated for *Electrolana madelineae* sp. nov. for different numbers of moults assumed to have happened between the preserved stages, calculated based on the overall-body length of the holotype and the paratype.

n (Number of potential moulting events)	Growth coefficient
1	2.33
2	1.52
3	1.32
4	1.23
5	1.18

Systematic interpretation of the herein described fossils

With the presence of a manca stage juvenile, the herein studied species can be considered as a representative of Mancoidea (including Cumacea, Mictacea, Spelaeogriphacea, Tanaidacea and Isopoda; Ax, 2000). Though there are no apomorphic features for Isopoda visible in the fossils, the overall morphology only matches Isopoda and not any of the other mancoideans ingroups. Specialised proximal elements of the trunk appendages 2–7 (coxal plates) are an autapomorphy of the group Scutocoxifera (Dreyer and Wägele, 2002), which is an ingroup of Isopoda. The triangular shaped basipod of the uropods (Fig. 3F, G) is an autapomorphy of Cymothoida (a large ingroup of Scutocoxifera) (Wägele, 1989).

Terrestrial representatives of Isopoda (Oniscidea) are not an ingroup of Cymothoida, and the herein studied fossils differ from terrestrial forms in many aspects. In oniscideans the number of antennulae elements is reduced (Tabacaru and Danielopol, 1996), the mandibular palp is absent (Tabacaru and Danielopol, 1996), the border between tergites and coxal plates is usually indistinct (Gruner, 1954), and the endopod of the uropods is rod-shaped (Wägele, 1989; Broly *et al.*, 2013).

The interpretation of the herein described fossils can be further narrowed down by ruling out ingroups of Cymothoida – the narrowest group to which the herein described fossils could be determined, using apomorphic character states that are visible in the fossils ('basal delimitation of the systematic interpretation'). Some ingroups of Cymothoida can be ruled out, as they have apomorphic states where the herein described fossils have plesiomorphic character states ('distal delimitation of the systematic interpretation'). This second step of the systematic

interpretation can contribute to a better understanding of the palaeoecology of the herein described fossils.

The relationship between the different lineages within Cymothoida is far from being fully understood. This way, many different ingroups of Cymothoida need to be considered. To limit the length of this section, only a selection cymothoidan lineages is discussed here. A more complete comparison between the herein described fossils and the different ingroups of Cymothoida can be found in Tab. S1.

Representatives of the groups Gnathiidae and Protognathia can be distinguished from the herein described fossils because, in Gnathiidae and Protognathia, the appendages on the trunk segment seven are absent (possibly an extreme post-displacement of their development, *cf.* manca stage; Wägele and Brandt, 1988; Wägele, 1989).

Representatives of Corallanidae, Aegidae and Cymothoidae (fish parasites) and Epicaridea (mostly crustacean parasites) can be distinguished from the herein described fossils because in those groups the dactylus is firmly conjoined with its claw, forming a hook-like compound structure (prehensile condition, Fig. 8C, dactylus). In Cymothoidae this applies for trunk appendages 1–7, in Aegidae this applies for trunk appendages 1–3, and in Corallanidae this applies at least for trunk appendage 1 (Wägele, 1989; Nagler *et al.*, 2017). This is in contrast to the herein described fossil (Fig. 8A dactylus), where the separation between the dactylus and its claw is clearly visible (*e.g.*, Figs. 3C, D, 4C).

Representatives of the group Tridentella (= Tridentellidae) can be distinguished from the herein described fossils, because the maxilliped endite is elongated and extends at least to the level of the third element of the maxilliped palp (Wägele, 1989; Bruce, 2008), whereas this is not the case in the herein described fossils (Fig. 3A, C).

Figure 8. Comparison of the distal part of trunk appendage 1 in different lineages of Cymothoida. **A**: *Electrolana madelineae* n. sp., schematic reconstruction; **B**: *Cirolana australiense* Hale, 1925, redrawn from Bruce (1986, fig. 114L); **C**: *Elthusa vulgaris* (Stimpson, 1857), drawn after van der Wal and Haug (2020, fig. 16B). d, dactylus, dc, claws of dactylus, pp, propodus.

Well preserved fossils of the group Urda show clear morphological features that can be attributed to a parasitic lifestyle (dactylus and claw of trunk appendages 1–7 strongly curved and hook-like) (Nagler *et al.*, 2017). In Urda, aside from the morphology of the appendages, the tergites of the anterior trunk are proportionally much longer than the corresponding tergites of the pleon (Stolley, 1910).

Most of the remainder lineages of Cymothoida are collectively referred to as Cirolanidae. Representatives of Cirolanidae are characterised by an overall plesiomorphic appearance (Wägele, 1989). Brandt and Poore (2003) argued that Cirolanidae could be characterised by apomorphic characters of the mandible (tridentate incisor with the posterior tooth the most prominent and mandible spine row on a fleshy lobe); however, one of these putative apomorphic character states (tridentate incisor with the posterior tooth the most prominent) can also be found in Corallanidae (see figures in Delaney, 1989). These characters of the mouthparts, however, are very prone to become unrecognisable in the course of further specialization of the mouthparts. For the parasitic lineages of Cymothoidae – which are well characterized by their specialised mouthparts — a cirolanid-like, scavenging ancestor has been reconstructed (Menzies *et al.*, 1955; Brusca, 1981; Dreyer and Wägele, 2001). This way — even if the extant, non-parasitic, representatives of Cymothoida form a monophylum (Cirolanidae) — fossils with a cirolanid-like morphology must not necessarily belong to Cirolanidae.

Palaega is a 'form genus' (assemblage based on rough similarity) that likely comprises many different Isopoda lineages (Feldmann and Rust, 2006). Palaega is largely synonymous with Bathynomus (Wieder and Feldmann, 1989; Feldmann, 1990; Martin and Kuck, 1990; Hyžný *et al.*, 2019). Individual Cretaceous species that have been assigned to Palaega are discussed below regarding a possible conspecificity with the herein described fossils. Representatives of Bathynomus can be distinguished from the herein described fossils, because in Bathynomus the posterior margin of the pleotelson has a characteristic serration (Bruce, 1986).

Representatives of the group Pseudopalaega Mezzalira and Martins-Neto, 1992 can be distinguished from the herein described fossils, because representatives of Pseudopalaega have a strongly dorsoventrally-flattened, oval body and prominent, laterally-projecting coxal plates.

The herein described fossils resemble representatives of Natatolana in having relatively broad basipods in trunk appendages 5–7. Representatives of Natatolana can be distinguished from the herein described fossils, because in Natatolana the basipod of trunk appendage 7 is broader in its distal half and has plumose setae on the anterior margin as well as at the postero-distal angle (Keable, 2006).

The herein described fossils resemble representatives of Metacirolana in the overall morphology; however, in Metacirolana the clypeus forms a ventrally projected blade (Bruce, 1986; Sidabalok and Bruce, 2018). In the larger herein described specimen

this character is not visible; in the smaller specimen the clypeus is not projected (Fig. 3A–E). Yet, this is uninformative, as we could not find information whether this character is present in extant manca stage individuals of Metacirolana.

The groups Aatolana, Pseudolana, Plakolana, Odysseylana, Neocirolana, Eurylana, Baharilana, and Cirolana cannot securely be ruled out from the systematic interpretation of the herein described fossils and each of the groups might potentially include the fossils at hand. The fossils could, however, also belong to a different lineage within Cymothoida that has no extant representatives.

Brunnaega tomhurleyi Wilson, 2011 is very similar to the herein described fossils and could potentially be closely related. At this point it needs to be pointed out that the name Brunnaega is based on the "shared anatomical similarity" between *Brunnaega tomhurleyi* and *Brunnaega roeperi* Polz, 2005 (Wilson *et al.*, 2011: 1056) — consequently, Brunnaega should not be treated as a systematic group (see also Hyžný *et al.*, 2013).

Species delimitation

All representatives of Isopoda that have been formally described from Burmese amber are terrestrial forms (Oniscidea) (Broly *et al.*, 2015; Poinar, 2018; Ross, 2019). Recently, some specimens that are syn-inclusions to an ammonite, have been presented, including remains of presumed non-oniscidean representatives of Isopoda (Yu *et al.*, 2018). However, the limited information from the provided microscopic images is not sufficient to give precise systematic interpretations. Also, the specimens presented in Yu *et al.* (2018) do not morphologically resemble the herein presented specimens in many aspects.

Burmese amber is of earliest Late Cretaceous age (Shi *et al.*, 2012; Yu *et al.*, 2018). To limit the discussion about potential conspecificities to a reasonable set of species we only considered species with records from the Cretaceous; this includes occurrences that are *ca.* 45 million years older and 32 million years younger. To further limit the length of this section, not all of the Cretaceous species are discussed below — for a

comparison of the herein describe fossils with the remainder species, see Tab. S2.

As discussed above, *B. tomhurleyi* is very similar to the herein described fossils. Yet, *B. tomhurleyi* can be distinguished from the herein described fossils, because in *B. tomhurleyi* the lateral sides of the tergites of pleon segment 1 and 5 are each concealed by the tergites of the respective preceding segment.

Cymatoga jazykowii von Eichwald, 1863 from the Cretaceous of Uljanowsk (Volga Federal District, Russia) has never been figured. The description raises doubts, whether it even is a fossil representative of Isopoda at all — it states that there are 8 or 9 segments of the anterior trunk (von Eichwald, 1863).

*Cirolana cottreaui (*Roger, 1946) has a trapezoid pleotelson (posteriorly truncated), whereas in the fossils at hand the pleotelson is half-oval in shape and not truncated.

In *Cirolana enigma* Wieder and Feldman, 1992 the anterior margin of the pleotelson is distinctly convex, which is not the case for the fossils at hand.

Cirolana garassinoi Feldmann, 2009 has relatively large uropods and the uropod endopods are very broad on the distal side (their distal margins are almost straight). In the fossils at hand the uropods are not that large and the broadest level of the uropod endopods is much closer to the proximal side.

Natatolana poblana Vega and Bruce, 2019 is not easy to differentiate from the herein described specimens due to preservation of the *N. poblana* types. All of the *N. poblana* types have a relatively more acute pleotelson posterior margin when compared to the larger specimen at hand. The smaller specimen at hand is similar to the *N. poblana* types, yet there is considerable size variation in the figured specimens (at least 35%, measured by pleotelson length), but not much variance in the shape of the posterior margin of the pleotelson, suggesting that young individuals of *N. poblana* also do not have a pleotelson morphology as in the fossils at hand. In addition to the small morphological differences it has to be considered that the type occurrence of *N. poblana* is *ca.* 30 million years older than Burmese amber and also remote from a palaeogeographical point of view. The affinity of *N. poblana* to the group Natatolana is questionable, as

the apomorphic characters of Natatolana as listed in Keable (2006) are not visible or not even preserved in the types of *N. poblana*.

Cymothoidana websteri Jarzembowski *et al.*, 2014 differs from the fossils at hand in having a much more triangular shaped pleotelson, comparably large uropods and the shape of the uropod endopod (in *C. websteri* with a straight lateral margin).

Representatives of Isopoda preserved in amber

Fossils of Isopoda usually do not make up a high proportion of inclusions in amber — compared to the vast number of insect inclusions. Yet, they are known from many amber sites with each a rather low diversity when compared to other groups of Euarthropoda, such as Insecta, Araneae (spiders) and Acari (mites). By far the largest fraction of inclusions of representatives of Isopoda in amber is that of terrestrial forms (Oniscidea). A detailed list of fossil oniscideans in amber has been given in Broly *et al.* (2013). Aside from oniscideans there are aquatic larvae of epicarideans in Miocene amber from Chiapas (Mexico; Serrano-Sánchez *et al.*, 2016) and from Late Cretaceous Vendean amber (France; Néraudeau *et al.*, 2017; Schädel *et al.*, 2019b). The only record so far of a non-parasitic representative of Cymothoida ("Cirolanidae") is from Eocene Baltic amber (southern coast of Baltic sea; Weitschat *et al.*, 2002; Wichard *et al.*, 2009).

Burmese amber is Earliest Cenomanian in age, which corresponds to a numeric age of about 99 million years (Shi *et al.*, 2012). So far, only two species of Isopoda have been formally described from Burmese amber: *Myanmariscus deboiseae* Broly, Maillet and Ross, 2015 and *Palaeoarmadillo microsoma* Poinar, 2018 (Broly *et al.*, 2015; Poinar, 2018). Additionally, there is another record of Oniscidea, interpreted as a representative of Tylidae, yet without formal description (Zhang, 2017; referenced in Ross, 2019). Additionally, there have been three specimens of Isopoda figured in Yu *et al.* (2019). However, with the images that are available, it cannot be ruled out that those specimens are representatives of *P. microsoma*.

Marine animals in Burmese amber

Amber is a typical terrestrial product as it derives from tree sap. The tolerance of trees towards a moist environment is quite limited for most trees with the exception of very specialised trees, such as mangroves or swamp cypresses. Thus, for a long time, aquatic organisms preserved in amber have been explained by smaller bodies of water that frequently occur in any type of forest (streams, small pools, flooded tree holes, etc.).

In Burmese amber there are records of insect larvae with supposed aquatic lifestyles (Zhao *et al.*, 2019; Schädel *et al.*, 2020). Additionally, there are inclusions of organisms that could also be linked to a marine lifestyle, such as seed shrimps (Xing *et al.*, 2018), pholadid bivalves (Mao *et al.*, 2018; Smith and Ross, 2018), snails (Gastropoda) and an ammonite shell (Yu *et al.*, 2019). An earlier record of alleged marine snails (Yu *et al.*, 2018) is likely a product of misinterpretation (they are likely representatives of the terrestrial groups Cochlostomatidae or Diplommatinidae; M. Harzhauser, pers. comm., 2019). Along with the animals preserved within the fossilized resin, marine animals that are attached to amber pieces (sea feathers, corals and oysters; Mao *et al.*, 2018) suggest a near shore environment for the Burmese amber forest.

Palaeoecology inferred from the systematic interpretation

The plesiomorphic condition for representatives of Isopoda is to live in a marine habitat. The transition from a marine habitat to limnic habitats occurred in many lineages of Isopoda, however Oniscidea is the only group to have established a terrestrial mode of life (Wägele, 1989; Brusca and Wilson, 1991; Broly *et al.*, 2013). Despite the preservation in amber, as a terrestrial substance (see discussion below), from a systematic perspective it is unlikely, that the herein presented fossils were terrestrial organisms.

Limnic habitats are inhabited by many lineages of Cymothoida, also including the parasitic lineages within the group such as Cymothoidae (Brusca, 1981) and Epicaridea (Chopra, 1923). Many representatives of ingroups of Cymothoida with plesiomorphic feeding strategies (Cirolanidae) such as Eurydice,

Pseudolana, Cirolana, Anopsilana, Hansenolana, and Natatolana live in estuarine environments (Bruce, 1986); even mangrove muds are inhabited by cymothoidans (*e.g.*, Limicolana; Bruce, 1986). There are also true freshwater species among non-parasitic cymothoidans, with probably more than one lineage being linked to ground water and cave systems (Bruce, 1986; Wägele, 1989). In conclusion, it is likely that the herein presented fossil specimens once lived in a marine or brackish environment. However, the systematic position of the fossils alone cannot provide much certainty in this regard, as the ecology of extant species is so diverse.

Functional morphology

Dense rows of long setae on pleopods, uropods and pleotelson such as those in the here described specimens are frequent among aquatic representatives of Isopoda — yet not in terrestrial forms. This might be due to the different respiratory function of the pleopods in oniscideans (Wägele, 1989). Also, setae increase the surface area of body parts, which is crucial for efficient propulsion by stroking motions of movable body parts. In the case of the pleopods and the pleotelson, increasing the surface area with dense rows of setae is seen in many aquatic species (*e.g.*, Bruce, 1986); this would however probably be disadvantageous in a terrestrial environment, because this could result in an increased adhesion of moist particles to the animal. The same applies for the wide second leg element (basipod) in trunk appendages 5–7 in the herein described fossils (Fig. 4D). Such widened basipods often occur in swimming species, *e.g.*, in the group Natatolana, but also in many species of Cirolana. In representatives of Natatolana and Politolana the basipod of the more posterior appendages of the anterior trunk is additionally equipped with long setae (Kensley and Schotte, 1989), which are not apparent in the fossils at hand (*cf.* Fig. 4D).

The morphology of the antennal flagellum in the fossils at hand, with many small elements and short setae on the ventral side, is very similar to the morphology in many aquatic cymothoidans (*cf.* figures in Bruce, 1986; Brusca *et al.*, 1995). The high surface area of such types of antennulae suggests that this would be disadvantageous in terrestrial environments that oniscideans typically inhabit — *e.g.* due to the adhesion to moist objects.

Syn-inclusions

Syn-inclusions of the smaller fossil at hand (NHMW 2017/0052/0002) are various unidentifiable euarthropodan remains (Fig. S2A, B, F) and a mite that is located in very close proximity or in contact with a gas-filled bubble (Fig. S2C–E). Also, several enigmatic needle-shaped objects are present in the amber piece (Fig. S2G). These could possibly be plant hairs or setae of euarthropodans. No inclusion within this amber piece, except for the specimens of Isopoda itself, shows any specialization for a specific environment or could be identified to a systematic level that would allow palaeoecological conclusions to be drawn.

Syn-inclusions of the larger fossil at hand (NHMW 2017/0052/0001) are an adult midge (*cf.* Psychodidae; Fig. S3A, B), an adult fly (Alavesia; V. Baranov, pers. comm., 2019; Fig. S3C, D), a beetle (Coleoptera; Fig. S3D, E), various unidentified euarthropodan remains (Fig. S4A–D) and three seed shrimp specimens (Fig. S4E–G).

The group Alavesia (Diptera: Atelestidae) has so far only been recorded from Burmese amber with one, not (yet) formally described, species (Grimaldi *et al.*, 2002). Extant species of Alavesia have been found at an ephemerous river in proximity to pools of standing water (Sinclair and Kirk-Spriggs, 2010). The larvae, even of the extant representatives of Atelestidae, are unknown and the adults are assumed to feed on flowering plants (Sinclair and Kirk-Spriggs, 2010; Sinclair, 2017). Thus, the value of the Alavesia specimen for ecological reconstruction is very limited.

The presumed psychodid specimen resembles *Bamara groehni* Stebner *et al.*, 2015 in many aspects; but especially the claspers (male genitalia) differ distinctly. The phylogenetic interpretation of the specimen in this study (and even that of *B. groehni*) is too broad to draw any ecological conclusions, as the eligible extant relatives are ecologically very diverse. The only other non-parasitic representative of Cymothoida which is preserved in amber, is from the Eocene Baltic amber and also is accompanied by (freshwater) seed shrimps (Weitschat *et al.*, 2002).

Abiotic taphonomic indicators

The two amber pieces containing the fossils at hand have a very different macroscopic appearance (Supplementary file 1: Fig. S1A). The amber piece containing the smaller specimen (NHMW 2017/0052/0002) is very clear and almost devoid of impurities. The amber piece containing the larger specimen, on the other hand, is much less transparent due to a high abundance of small-scale impurities. These impurities comprise dead organic matter (plant and animal remains) as well as a distinct type of many very small spherical inclusion of reddish colour. This kind of impurity has also been reported for other Cretaceous amber sites (Girard *et al.*, 2011; 2013; Quinney *et al.*, 2015). Girard *et al.* (2011) and likely represent fossilized tree sap double emulsions (Lozano *et al.*, 2020).

Due to these impurities, a stratified build-up is apparent in the matrix of the amber piece NHMW 2017/0052/0001. Aquatic taphocoenoses are often associated with a stratified build-up of the amber matrix (Serrano-Sánchez *et al.*, 2015; Schädel *et al.*, 2019b).

The stratification within the amber piece containing the larger specimen (NHMW 2017/0052/0001) also affects the arrangement of bubbles (Fig. 9). A large fraction of bubbles within the amber piece is confined to a narrow layer, in alignment with the stratification pattern. The content of the bubbles in the layer has the same x-ray contrast as the air outside the amber piece (Fig. S1B, C), leading to the interpretation that these bubbles are gas filled to the time of observation. The presence of crystals (presumably pyrite) within many of the bubbles, that make up the dense layer, renders it unlikely that the bubbles were gas filled to the time the resin was still fluid (although re-sublimation cannot be ruled-out entirely). Inclusions of water — often alongside with a gas phase — occur in various amber deposits (Ross, 1997; 1998; Poinar *et al.*, 1999), including Burmese amber (see fig. 1 in Caterino and Maddison, 2018). From Baltic amber there is even a record of a seed shrimp (Ostracoda) embedded in a water filled bubble (Keyser and Weitschat, 2005). The circumstances under which such abiotic inclusions form are still poorly studied. Experiments on synthetic resins have shown that resins are permeable to water (Hashimoto *et al.*, 2005). For fossil natural resins permeability has been shown for gases, and permeability for fluids is also suggested (Hopfenberg *et al.*, 1988 and references therein). Cases of extreme dehydration (mummification) within Baltic amber that allowed for ultrastructure preservation have been explained to be the result of the absorption of water by terpenes and/or saccharides within the resin (Poinar and Hess, 1982).
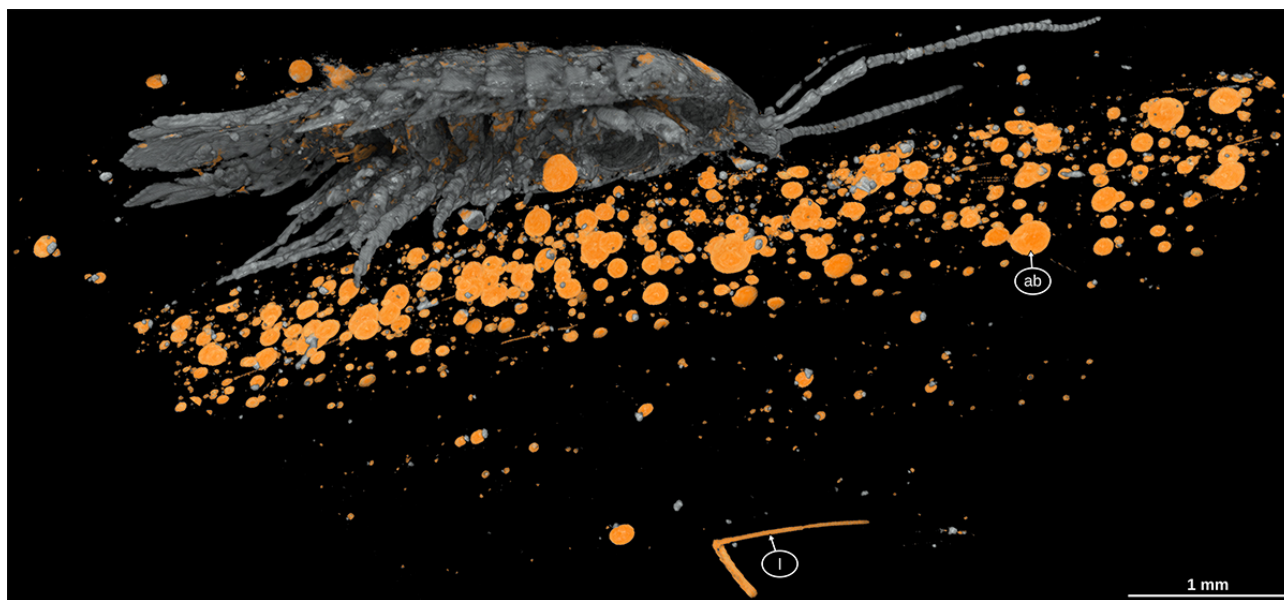
Figure 9. Holotype of *Electrolana madelineae* sp. nov. (NHMW 2017/0052/0001), habitus in ventrolateral view and surrounding objects in the resin, volume rendering image, two different transfer functions and clipping planes applied, orange colour transfer function solely depicts extremely low-x-ray contrast areas (gas phase). ab, air bubble; l, leg, Euarthropoda.

From the micro-CT scan it becomes apparent that a mineral with high x-ray contrast is present in the body cavities of the larger fossil at hand and in gas filled bubbles surrounding it (Fig. S1B, C). Pyrite is an iron sulfide (FeS_2) with cubic (= isometric) crystals that would match the structures seen in the micro-CT scan. Pyrite is a common mineral in sedimentary environments and is formed by bacterial activity in chemically reducing conditions. The presence of enough sulfate ions (SO_4^{2-}) in the water of the environment is a prerequisite for the formation of pyrite (Knight *et al.*, 2010) and can be provided, for example, by nearby gypsum deposits. The crystals do not penetrate the surface of the fossil. Thus, this kind of preservation can be interpreted as an incomplete pseudomorph of pyrite after the fossil arthropod (pyrite casting the shape of the fossil organisms). Pseudomorphs of pyrite after fossils are a common phenomenon but are usually known from hard-shelled marine animals such as ammonites (Hudson, 1982) but have also been reported for amber inclusions (Knight *et al.*, 2010). Pyrite is not uncommon in Burmese amber and has been interpreted as an indicator for the presence of sulfate rich water before (Schlüter, 1978; Smith and Ross, 2018). Pyrite is also present in other supposedly aquatic taphocoenoses in amber (Serrano-Sánchez *et al.*, 2015; 2016; Smith and Ross, 2018).

There is a bubble-like object with a similarly high radiometric density as the presumed pyrite crystals (Figs. 5B, C, S1C, D). However, it lacks apparent crystal structures, and therefore its nature and cause remains unexplained. Similar structures have been found associated with burrowing bivalves (Pholadidae) in Burmese amber. Spectrometric tests have revealed that those cavities are filled with carbonate-rich material (Smith and Ross, 2018).

A reasonable interpretation of the taphonomic situation in the amber piece NHMW 2017/0052/0001 is that resin was recurrently released into a body of water, causing a stratification and the entrapment of water between two layers of resin flow. The entrapped water formed bubbles within the still fluid resin. Subsequently, the water permeated out of the resin. This latter process could have happened well after the resin polymerized and formed amber.

Preservation of aquatic organisms in amber

In most amber sites, organisms with a supposed aquatic lifestyle are extremely rare in comparison to terrestrial organisms. This does not necessarily apply for adults of organisms with aquatic larvae.

Typical interpretations of the preservation of aquatic organisms in fossil resins include dead and dried up specimens being transported to the resin by wind (Weitschat *et al.*, 2002) or still hydrated specimens being transported by spray (Schmidt *et al.*, 2018).

The herein presented specimens show no signs of desiccation, such as collapsed fine structures in areas of the body that are less sclerotized. Also, the fossils are very complete, *i.e.*, no delicate structures such as flagellum articles of the antenna are missing. This suggests, that the individuals were not exposed to desiccation or strong mechanical forces (*e.g.*, transport by spray).

Experiments in a modern day swamp have shown that resin, when submerged in water, stays fluid for a long time (reduced evaporation of volatiles) and aquatic animals can be caught in still-fluid submerged resin by autonomous movement (Schmidt and Dilcher, 2007). This process is also the best explanation for some instances found in Campo La Granja (Chiapas) amber, where, for example, traces of torn-off side-swimmer (Amphipoda) legs have been found. Such an arrangement is only possible when the side-swimmers were still alive when they got embedded in the resin (Serrano-Sánchez *et al.*, 2015). Similar explanations have been given for microorganisms preserved in amber (Waggoner, 1994).

In close proximity to the larger specimen (NHMW 2017/0052/0001) three seed shrimps (Ostracoda) are preserved. The larger specimen and the seed shrimps are all on one side of the above mentioned layer of bubbles whereas the much larger side of the amber piece is devoid of seed shrimps or other organisms for which an aquatic environment can be reconstructed. This high abundance in a small volume of amber also points towards an *in situ* entrapment rather than towards a transport of aquatic organisms by wind or spray.

With several different aquatic organisms preserved in Burmese amber (Mao *et al.*, 2018; Smith and Ross,

2018; Xing *et al.*, 2018; Yu *et al.*, 2019), including marine ones, it appears to be the most consistent interpretation that the forest that produced the fossilised resin was close to a marine environment and at least parts of the forest were flooded temporarily.

Fossil record of early developmental stages in Isopoda

Most representatives of Isopoda have hatchlings that are very similar in their outer morphology to the corresponding adults (Boyko and Wolff, 2014), at least at first sight. Consequently, it is very difficult to identify whether a fossil specimen is of a very early stage of development or a small adult. Yet, there are two factors, which sometimes allow for a better identification of the individual developmental stage of a fossil representative of Isopoda: (1) The so-called manca stage is characterized by the absence of well-developed legs on trunk segment 7 (postocular segment 13; Boyko and Wolff, 2014). Before the individual becomes adult, within a single moult, a well-developed leg appears at this segment (Boyko and Wolff, 2014). The resulting, not yet adult, individuals are often termed 'juveniles' (Boyko and Wolff, 2014). The fossil record of manca stage individuals is very sparse. The smaller specimen presented in this study (Fig. 10A) represents only the second fossil record of this life stage that can undoubtedly be identified as such. The other record is from terrestrial representatives of Isopoda (Oniscidea) in Miocene Mexican amber (Fig. 10B) (Broly *et al.*, 2017). From Burmese amber there is also another short note on presumable hatchlings of terrestrial representatives of Isopoda (Poinar, 2018); however, the quality of the illustration does not allow to reliably evaluating this observation. (2) Within Epicaridea, which itself is an ingroup of Cymothoida, a developmental pattern had secondarily evolved, resulting in (true) larvae that are distinct from the corresponding adults (see discussion in Haug, 2020). Fossil larvae of Epicaridea have been found in two amber sites. One record is from the Cretaceous of France, with multiple specimens likely corresponding to a single species (Fig. 10C; Schädel *et al.*, 2019b). The other record is from the Miocene of Mexico with several specimens that likely correspond to different species (Fig. 10D–H) (Serrano-Sánchez *et al.*, 2016).

Taxonomy

Euarthropoda (*sensu* Walossek, 1999)

Eucrustacea (*sensu* Walossek, 1999)

Peracarida Calman, 1904

Isopoda Latreille, 1817

Scutocoxifera Dreyer and Wägele, 2002

Cymothoida Wägele, 1989

***Electrolana* gen. nov.**

Zoobank: urn:lsid:zoobank.org:act:D069AD30-5BE0-44DB-B436-4A04B7FE8CDF

Etymology. Latinized spelling of the Greek word ḗlektron for amber with the suffix *-lana*, originating from the name Cirolana.

Remarks. The name *Electrolana* gen. nov. is erected to provide a binomial name for the species below. Since only one species will be included as of this study, no diagnosis can be given.

***Electrolana madelineae* sp. nov.**
Figs. 2–6, 7A, 8A, 9, 10A, S1, S6–8

Zoobank: urn:lsid:zoobank.org:act:8D1A3CC8-B700-4819-85A9-4ACBA02966D0

Etymology. After Madeline Pankowski of Rockville, Maryland, USA, daughter of Mark Pankowski who donated the types to the Museum of Natural History in Vienna.

Material examined. Holotype: NHMW 2017/0052/0001, Natural History Museum Vienna. Paratype: NHMW 2017/0052/0002, Natural History Museum Vienna.

Ontogenetic stage of the type. The paratype is of a manca stage; the holotype is a post-manca juvenile or an adult.

Type locality. Near Noje Bum, Hukawng Valley, Kachin State, Myanmar.
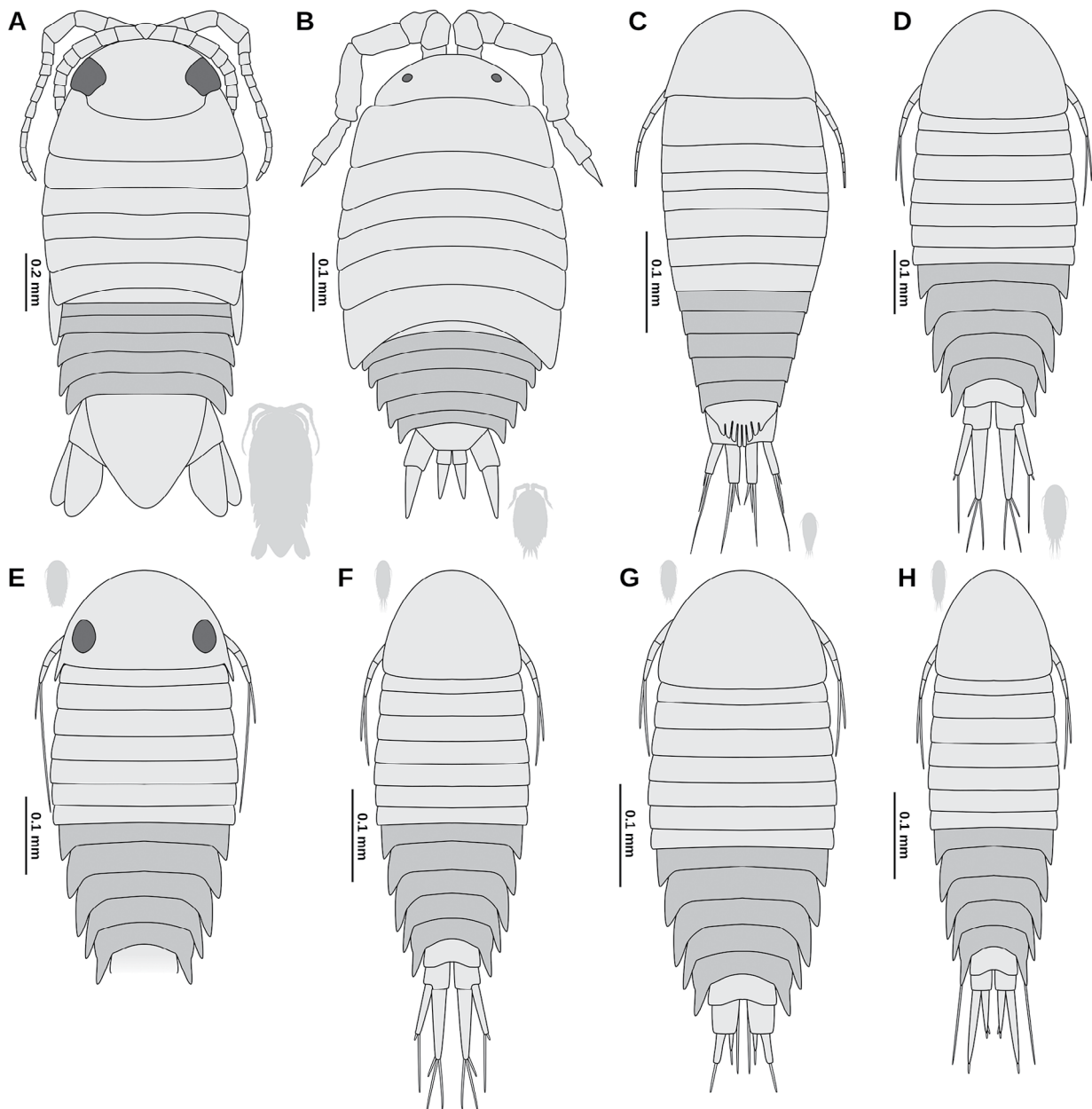
Figure 10. Graphical summary of all known manca-stage or larval fossils of Isopoda, reconstruction line drawings, free pleon tergites (postocular segments 14–18) in darker grey. **A.** Paratype of *Electrolana madelineae* sp. nov. (NHMW 2017/0052/0002); **B**: *Aquitanoscia chiapasensis* Broly *et al.*, 2017; **C**: *Vacuotheca dupeorum* Schädel *et al.*, 2019b; **D**: IHNFG-4951-Ep1 ('specimen 2') Serrano Sanchez *et al.* (2016); **E**: openstreetmap.org IHNFG-4964-Ep2 ('specimen 5b') Serrano Sanchez *et al.* (2016); **F**: IHNFG-5321-Ep1 ('specimen 6') Serrano Sanchez *et al.* (2016); **G**: IHNFG-4971-Ep1 ('specimen 3') Serrano Sanchez *et al.* (2016); **H**: IHNFG-4939-Ep1 ('specimen 1') Serrano Sanchez *et al.* (2016).

Type stratum. Unknown stratum, 98.8 million years, earliest Cenomanian, earliest Late Cretaceous, after Shi *et al.* (2012).

Differential diagnosis. Body drop shaped in dorsal view, tapering posteriorly, about 2.5 to 2.2 times longer than wide; tergite of trunk segment 1 about twice as long as succeeding segments; dactylus and claws of trunk appendages 1–3 gently curved inwards, not hook-like; coxal plates well developed, triangular in trunk segments 4–7 (postocular segments 10–13); basipod of trunk appendage 6 broad, posterior margin convex, median ridge along the mid-line of the lateral surface; coxal plate of trunk segment 7 (postocular segment 13) very conspicuous in dorsal view, extending distally to the level of pleon segment 5;

tergites of pleon segments 1–5 (postocular segments 14–18) free; tergite of pleon segment 1 (postocular segment 14) short, laterally covered by the tergite of trunk segment 7 (postocular segment 13); basipod of pleopod 1 (postocular segment 14) wider than long; pleopod 1 not operculate, concealing the succeeding pleopods; tergite of pleon segment 5 (postocular segment 18) with free lateral margins, not covered by the tergite of the preceding segment; endopod of pleopod 5 (postocular segment 18) more slender than the corresponding exopod, no setae on the distal margin; pleotelson half-oval in shape, slightly longer than wide, straight anterior margin, without distinct ornamentation on the dorsal surface, posterior margin without large spines, posterior margin with numerous setae grouped in the posterior-most part; uropod endopod about twice as long as wide, with median angle, not 'truncated'.

Remarks on the differential diagnosis. Due to the limited set of characters available, using the current methods, this diagnosis will not be able to differentiate the new species from all fossil or extant species. Thus, this differential diagnosis should be seen as a short recap of the description with respect to the discussion above.

Systematic interpretation. Cymothoida *incertae sedis*, *nec* Anuropus, *nec* Tridentella, *nec* Corallanidae, *nec* Aegidae, *nec* Cymothoidae, *nec* Epicaridea, *nec* Gnathiidae, *nec* Protognathia, *nec* Urda, *nec* Bathynomus, *nec* Colopisthus, *nec* Boorlana, *nec* Parabathynomus, *nec* Bahalana, *nec* Arubolana, *nec* Cirolanides, *nec* Typhlocirolana, *nec* Turcolana, *nec* Speocirolana, *nec* Sphaeromides, *nec* Skotobaena, *nec* Sphaerolana, *nec* Atarbolana, *nec* Aphantolana, *nec* Annina, *nec* Pseudaega, *nec* Politolana, *nec* Oncilorpheus, *nec* Natatolana, *nec* Haptolana, *nec* Excirolana, *nec* Eurydice, *nec* Conilera, *nec* Dolicholana. The following extant ingroups of Cymothoida represent likely affinities for *Electrolana madelineae* sp. nov.: Aatolana, Pseudolana, Plakolana, Odysseylana, Neocirolana, Eurylana, Baharilana, and Cirolana.

Remarks on the systematic interpretation. The Latin term *nec* (= but not) is used to list ingroups of Cymothoida, to which *Electrolana madelineae* sp. nov. does not belong (as applied in Schädel *et al.*, 2019a).

Conclusion

The two herein presented specimens are interpreted as conspecific and represent different stages of individual development. The smaller specimen thus could be identified as a manca stage. The specimens represent a not previously described species, due to distinct morphological differences and the huge temporal distance to species with similar morphological features. An affinity to parasitic lineages within Cymothoida, which is the narrowest group to which the fossil specimens could be identified, could be excluded due to the visible absence of apomorphies of the parasitic ingroups. Both the systematic interpretation of the fossils themselves, as well as the surrounding taphonomic condition in one of the amber pieces (*e.g.*, seed shrimp syn-inclusions) suggest that at least one of the specimens became embedded in resin while submerged in water. The complete taphocoenoses suggest the presence of a water body in proximity to the resin producing tree but not necessarily brackish or marine conditions within this water body.

SUPPLEMENTARY MATERIAL

Supplementary file 1: Figure S1. A: overview image of the two amber pieces photographed under the same light settings, white light microscopy, 50x (VHX); **B:** holotype of *Electrolana madelineae* sp. nov. (NHMW 2017/0052/0001), cross section through the anterior trunk region, micro-CT image, reconstructed slice; **C:** holotype of *Electrolana madelineae* sp. nov. (NHMW 2017/0052/0001), cross section through the anterior trunk region, micro-CT image, reconstructed slice; **D:** holotype of *Electrolana madelineae* sp. nov. (NHMW 2017/0052/0001), head region in frontal view, red-cyan stereo anaglyph, volume rendering images based on micro-CT data. a, antenna; al, antennula; ab, air bubble; ap, air phase; fl, frontal lamina; py, pyrite; ?, unknown material forming an irregular bubble. https://doi.org/10.20363/mdb.u254_m-26.1

Supplementary file 2: Figure S2. Syn-inclusions of the paratype of *Electrolana madelineae* sp. nov. (NHMW 2017/0052/0002). **A:** Isolated leg, Euarthropoda , white light microscopy, 500x (VHX); **B:** isolated distal element of leg, Euarthropoda, white light microscopy, 500x (VHX); **C–E:** mite (Arachnida: Acari) in ventral view. **C:** white light microscopy, 300x (VHX); **D:** transmitted light microscopy, 20x (BZ); **E:** epifluorescence microscopy, 20x (BZ); **F:** possible cuticle remains, Euarthropoda, white light microscopy, 150x (VHX); **G:** multiple needle-like objects, possibly plant hairs or setae of euarthropodans, white light microscopy, 500x (VHX). https://doi.org/10.20363/mdb.u254_m-25.1

Supplementary file 3: Figure S3. Syn-inclusions of the holotype of *Electrolana madelineae* sp. nov. (NHMW 2017/0052/0001). **A, B:** Diptera *cf.* Psychodidae, habitus in ventral view, different illuminations, white light microscopy, 200x (VHX); **C, D:** *cf. Alavesia* (Empidoidea: Atelestidae), **C:** dorso-lateral view, white light microscopy, 100x (VHX),

D: ventro-lateral view, white light microscopy, 100x (VHX); **E, F:** beetle (Coleoptera), **E:** antero-dorsal view, white light microscopy, 200x (VHX), **F:** postero-ventral view, white light microscopy, 200x (VHX). https://doi.org/10.20363/mdb.u254_m-24.1

Supplementary file 4: Figure S4. Syn-inclusions of the holotype of *Electrolana madelineae* sp. nov. (NHMW 2017/0052/0001). **A:** remains, Euarthropoda, white light microscopy, 100x (VHX); **B:** two isolated but closely grouped legs, Euarthropoda, white light microscopy, 200x (VHX); **C:** detail of the upper leg from B, white light microscopy, 200x (VHX); **D:** isolated leg, Euarthropoda, white light microscopy, 100x (VHX); **E–G:** Ostracoda, three different specimens, white light microscopy, **E:** 200x (VHX), **F:** 500x (VHX), **G:** 300x (VHX).

https://doi.org/10.20363/mdb.u254_m-23.1

Supplementary file 5: Table S1. Morphological comparison between *Electrolana madelineae* sp. nov. and systematic groups within Scutocoxifera (Isopoda; Gruner, 1954; Ferrara and Lanza, 1978; Jansen, 1978; Bruce, 1981; 1986; 1994; 2008; Wägele and Brandt, 1988; Javed and Yasmeen, 1989; Wägele, 1989; Schotte, 1994; Brusca *et al.*, 1995; George and Longerbeam, 1997; Keable, 1998; 1999; 2006; Bruce and Olesen, 2002; Riseman and Brusca, 2002; Brandt and Poore, 2003; Bruce and Svavarsson, 2003; Moore and Brusca, 2003; Wilson, 2003; Wilson *et al.*, 2011; Jones and Nithyanandan, 2012; Paiva and Souza-Filho, 2015; Nagler *et al.*, 2017; Sidabalok and Bruce, 2018). Use the UTF-8 character encoding and commas as the only delimiters to open the file. https://doi.org/10.20363/mdb.u254_m-22.1

Supplementary file 6: Table S2. Morphological comparison between *Electrolana madelineae* sp. nov. and isopod species with occurrences in the Cretaceous (von Eichwald, 1863; Woodward, 1870; Stolley, 1910; Rathbun, 1935; Malzahn, 1968; Bowman, 1971; Spassky and Kravtsov, 1976; Wieder and Feldmann, 1992; Calzada and Gómez Pallerola, 1994; Fraaye and Summesberger, 1999; Feldmann and Goolaerts, 2005; Karasawa *et al.*, 2008; Feldmann, 2009; Feldmann and Charbonnier, 2011; Wilson *et al.*, 2011; Jarzembowski *et al.*, 2014; Vega *et al.*, 2019). Use the UTF-8 character encoding and commas as the only delimiters to

open the file. https://www.doi.org/10.20363/mdb.u254_m-21.1

Supplementary file 7: Figure S5. Reconstructed micro-CT-scan data in form of a stack of images (Tagged Image Format, TIF). https://doi.org/10.20363/mdb.u254_m-27.1

Supplementary file 8: Figure S6. Paratype of *Electrolana madelineae* sp. nov. (NHMW 2017/0052/0002), habitus in dorsal view, white light microscopy, 200x (VHX), stereo pair for parallel viewing. https://www.morphdbase.de/?M_Schaedel_20200502-M-29.1

Supplementary file 9: Figure S7. Paratype of *Electrolana madelineae* sp. nov. (NHMW 2017/0052/0002), head region in antero-dorsal view, white light microscopy, 200x (VHX), stereo pair for parallel viewing. https://www.morphdbase.de/?M_Schaedel_20200502-M-28.1

Supplementary file 10: Figure S8. Paratype of *Electrolana madelineae* sp. nov. (NHMW 2017/0052/0002), habitus in ventral view, white light microscopy, 200x, stereo pair for parallel viewing. https://www.morphdbase.de/?M_Schaedel_20200502-M-30.1

References

Anderson, G. and Dale, W.E. 1981. *Probopyrus pandalicola* (Packard) (Isopoda, Epicaridea): morphology and development of larvae in culture. *Crustaceana*, 41: 143–161.

Ax, P. 2000. The Phylogenetic System of the Metazoa. Multicellular Animals, Vol. 1. Berlin, Springer-Verlag, 154p.

Bowman, T.E. 1971. *Palaega lamnae*, new species (Crustacea: Isopoda) from the Upper Cretaceous of Texas. *Journal of Paleontology*, 45: 540–541.

Boyko, C.B. and Wolff, C. 2014. Isopoda and Tanaidacea. p. 210–212. In: J.W. Martin, J. Olesen, and J.T. Hoeg (eds), Atlas of crustacean Larvae. Baltimore, Johns Hopkins University Press.

Brandt, A. and Poore, G.C. 2003. Higher classification of the flabelliferan and related Isopoda based on a reappraisal of relationships. *Invertebrate Systematics*, 17: 893–923.

Broly, P.; Deville, P. and Maillet, S. 2013. The origin of terrestrial isopods (Crustacea: Isopoda: Oniscidea). *Evolutionary Ecology*, 27: 461–476.

Broly, P.; Maillet, S. and Ross, A.J. 2015. The first terrestrial isopod (Crustacea: Isopoda: Oniscidea) from Cretaceous Burmese amber of Myanmar. *Cretaceous Research*, 55: 220–228.

Broly, P.; Serrano-Sánchez, M. de L.; Rodríguez-García, S. and Vega, F.J. 2017. Fossil evidence of extended brood care in new Miocene Peracarida (Crustacea) from Mexico. *Journal of Systematic Palaeontology*, 15: 1037–1049.

Bruce, N. 1981. Cirolanidae (Crustacea: Isopoda) of Australia: diagnoses of *Cirolana* Leach, *Metacirolana* Nierstrasz, *Neocirolana* Hale, *Anopsilana* Paulian & Debouteville, and three new genera— *Natatolana, Politolana* and *Cartetolana*. *Marine and Freshwater Research*, 32: 945.

Bruce, N.L. 1986. Cirolanidae (Crustacea: Isopoda) of Australia. *Records of the Australian Museum, Supplement*, 6: 1–239.

Bruce, N.L. 1994. The marine isopod *Neocirolana* Hale, 1925 (Crustacea: Cirolanidae) from tropical Australian waters. *Memoirs of the Queensland Museum*, 37: 41–51.

Bruce, N.L. 2008. New species of *Tridentella* Richardson, 1905 (Isopoda: Cymothoida: Tridentellidae), tropical marine isopod crustaceans from the Banda Sea, Indonesia. *Zootaxa*, 1734: 43–58.

Bruce, N.L. and Olesen, J. 2002. Cirolanid isopods from the Andaman Sea off Phuket, Thailand, with description of two new species. *Phuket Marine Biological Center Special Publication*, 23: 109–131.

Bruce, N.L. and Svavarsson, J. 2003. A new genus and species of cirolanid isopod (Crustacea) from Zanzibar, Tanzania, western Indian Ocean. *Cahiers de Biologie Marine*, 44: 1–12.

Brusca, R.C. 1981. A monograph on the Isopoda Cymothoidae (Crustacea) of the eastern Pacific. *Zoological Journal of the Linnean Society*, 73: 117–199.

Brusca, R.C.; Coelho, V.R. and Taiti, S. 2001. Suborder Oniscidea (Terrestrial Isopods). Tree of life web project, http://tolweb.org/notes/?note_id=4179. Accessed on 4 December 2019.

Brusca, R.C.; Wetzer, R. and France, S.C. 1995. Cirolanidae (Crustacea: Isopoda: Flabellifera) of the Tropical Eastern Pacific. *Proceedings of the San Diego Society of Natural History*, 30: 1–96.

Brusca, R.C. and Wilson, G.D.F. 1991. A phylogenetic analysis of the Isopoda with some classificatory recommendations. *Memoirs of the Queensland Museum*, 31: 143–204.

Calman, W.T. 1904. XVIII.—On the classification of the Crustacea Malacostraca. *Annals and Magazine of Natural History*, 13: 144–158.

Calzada, S. and Gómez Pallerola, J.E. 1994. Un nuevo Isópod (Crustacea) de Sta. Maria de Meià. *Batalleria*, 4: 27–30.

Caterino, M.S. and Maddison, D.R. 2018. An early and mysterious histerid inquiline from Cretaceous Burmese amber (Coleoptera, Histeridae). *ZooKeys*, 733: 119–129.

Chopra, B. 1923. Bopyrid isopods parasitic on Indian Decapoda Macrura. *Records of the Indian Museum*, 25: 411–550.

Daley, A.C. and Drage, H.B. 2016. The fossil record of ecdysis, and trends in the moulting behaviour of trilobites. *Arthropod Structure & Development*, 45: 71–96.

Delaney, P.M. 1989. Phylogeny and biogeography of the marine isopod family Corallanidae (Crustacea, Isopoda, Flabellifera). *Contribution in Science, Natural History Museum of Los Angeles County*, 409: 1–75.

Dreyer, H. and Wägele, J.-W. 2001. Parasites of crustaceans (Isopoda: Bopyridae) evolved from fish parasites: molecular and morphological evidence. *Zoology*, 103: 157–178.

Dreyer, H. and Wägele, J.-W. 2002. The Scutocoxifera tax. nov. and the information content of nuclear ssu rDNA sequences for reconstruction of isopod phylogeny (Peracarida: Isopoda). *Journal of Crustacean Biology*, 22: 217–234.

Dyar, H.G. 1890. The number of molts of Lepidopterous larvae. *Psyche: A Journal of Entomology*, 5: 420–422.

Eichwald, E. von 1863. Beitrag zur nähern Kenntnis der in meiner Lethaea Rossica beschriebenen Illaenen und über einige Isopoden aus andern Formationen Russlands. *Société Impériale des Naturalistes de Moscou*, 36: 372–424.

Feldmann, R.M. 1990. Comment on the proposed precedence of *Bathynomus* A. Milne Edwards, 1879 (Crustacea, Isopoda) over Palaega Woodward, 1870. *Bulletin of Zoological Nomenclature*, 47: 290–291.

Feldmann, R.M. 2009. A new cirolanid isopod (Crustacea) from the Cretaceous of Lebanon: Dermoliths document the pre-molt condition. *Journal of Crustacean Biology*, 29: 373–378.

Feldmann, R.M. and Charbonnier, S. 2011. *Ibacus cottreaui* Roger, 1946, reassigned to the isopod genus *Cirolana* (Cymothoida: Cirolanidae). *Journal of Crustacean Biology*, 31: 317–319.

Feldmann, R.M. and Goolaerts, S. 2005. *Palaega rugosa*, a new species of fossil isopod (Crustacea) from Maastrichtian Rocks of Tunisia. *Journal of Paleontology*, 79: 1031–1035.

Feldmann, R.M. and Rust, S. 2006. *Palaega kakatahi* n. sp.: The first record of a marine fossil isopod from the Pliocene of New Zealand. *New Zealand Journal of Geology and Geophysics*, 49: 411–415.

Ferrara, F. and Lanza, B. 1978. *Skotobaena monodi*, espèce nouvelle de cirolanidé phréatobie de la Somalie (Crustacea Isopoda): (Pubblicazioni del centro di studio per la faunistica ed ecologia tropicali del c.n.r.: cxlii). *Monitore Zoologico Italiano. Supplemento*, 10: 105–112.

Fowler, G.H. 1904. Biscayan plankton collected during a cruise of H.M.S. "Research" 1900. Part xii. The Ostracoda. *Transactions of the Linnean Society of London*, 2: 219–336.

Fraaye, R.H. and Summesberger, H. 1999. New crustacean records from the Late Campanian of the Gschiefgraben (Cretaceous, Austria). *Beiträge zur Paläontologie*, 24: 1–6.

George, R.Y. and Longerbeam, A.A. 1997. Two new species of cirolanid isopod crustaceans from Onslow Bay and Hatteras Slope off North Carolina: *Eurydice bowmani* n. sp. and *Conilera menziesi* n. sp. *Journal of the Elisha Mitchell Scientific Society*, 113: 163–170.

Girard, V.; Breton, G.; Perrichot, V.; Bilotte, M.; Le Loeuff, J.; Nel, A.; Philippe, M. and Thevenard, F. 2013. The Cenomanian amber of Fourtou (Aude, Southern France): Taphonomy and palaeoecological implications. *Annales de Paléontologie*, 99: 301–315.

Girard, V.; Néraudeau, D.; Adl, S.M. and Breton, G. 2011. Protist-like inclusions in amber, as evidenced by Charentes amber. *European Journal of Protistology*, 47: 59–66.

Grimaldi, D.A.; Engel, M.S. and Nascimbene, P.C. 2002. Fossiliferous Cretaceous amber from Myanmar (Burma): its rediscovery, biotic diversity, and paleontological significance. *American Museum Novitates*, 3361: 1–71.

Gruner, H.-E. 1954. Über das Coxalglied der Pereiopoden der Isopoden (Crustacea). *Zoologischer Anzeiger*, 152: 312–317.

Hansen, T. and Hansen, J. 2010. First fossils of the isopod genus *Aega* Leach, 1815. *Journal of Paleontology*, 84: 141–147.

Hashimoto, M.; Tay, F.R.; Ito, S.; Sano, H.; Kaga, M. and Pashley, D.H. 2005. Permeability of adhesive resin films. *Journal of Biomedical Materials Research Part B: Applied Biomaterials*, 74B: 699–705.

Haug, C.; Kutschera, V.; Ahyong, S.; Vega, F.; Maas, A.; Waloszek, D. and Haug, J. 2013. Re-evaluation of the Mesozoic mantis shrimp *Ursquilla yehoachi* based on new material and the virtual peel technique. *Palaeontologia Electronica*, 16: 1–14.

Haug, C.; Mayer, G.; Kutschera, V.; Waloszek, D.; Maas, A. and Haug, J.T. 2011. Imaging and documenting Gammarideans. *International Journal of Zoology*, 2011: 1–9.

Haug, J.T. 2020. Why the term "larva" is ambiguous, or what makes a larva? *Acta Zoologica*, 101: 167–188.

Haug, J.T. 2019. Categories of developmental biology: Examples of ambiguities and how to deal with them. p. 93–102. In: G. Fusco (ed), Essays for Alessandro Minelli, Festschrift, 2. Padova, Padova University Press.

Haug, J.T.; Haug, C.; Kutschera, V.; Mayer, G.; Maas, A.; Liebau, S.; Castellani, C.; Wolfram, U.; Clarkson, E.N.K. and Waloszek, D. 2011. Autofluorescence imaging, an excellent tool for comparative morphology. *Journal of Microscopy*, 244: 259–272.

Hopfenberg, H.B.; Witchey, L.C.; Poinar, G.O.; Beck, C.W.; Chave, K.E.; Smith, S.V.; Horibe, Y. and Craig, H. 1988. Is the Air in Amber Ancient? *Science, New Series*, 241: 717–721.

Hörnig, M.K.; Sombke, A.; Haug, C.; Harzsch, S. and Haug, J.T. 2016. What nymphal morphology can tell us about parental investment – a group of cockroach hatchlings in Baltic Amber documented by a multi-method approach. *Palaeontologia Electronica*, 19: 1–20.

Hosie, A.M. 2008. Four new species and a new record of Cryptoniscoidea (Crustacea: Isopoda: Hemioniscidae and Crinoniscidae) parasitising stalked barnacles from New Zealand. *Zootaxa*, 1795: 1–28.

Hudson, J.D. 1982. Pyrite in ammonite bearing shales from the Jurassic of England and Germany. *Sedimentology*, 29: 639–667.

Hyžný, M.; Bruce, N.L. and Schlögl, J. 2013. An appraisal of the fossil record for the Cirolanidae (Malacostraca: Peracarida: Isopoda: Cymothoida), with a description of a new cirolanid isopod crustacean from the early Miocene of the Vienna Basin (Western Carpathians). *Palaeontology*, 56: 615–630.

Hyžný, M.; Pasini, G. and Garassino, A. 2019. Supergiants in Europe: on the cirolanid isopod *Bathynomus* A. Milne Edwards, 1879 (Malacostraca, Peracarida) from the Plio-Pleistocene of Italy. *Neues Jahrbuch für Geologie und Paläontologie - Abhandlungen*, 291: 283–298.

Jansen, K.P. 1978. A revision of the genus *Pseudaega* Thomson (Isopoda: Flabellifera: Cirolanidae) with diagnoses of four new species. *Journal of the Royal Society of New Zealand*, 8: 143–156.

Jarzembowski, E.A.; Wang, B.; Fang, Y. and Zhang, H. 2014. A new aquatic crustacean (Isopoda: Cymothoida) from the early Cretaceous of southern England and comparison with the Chinese and Iberian biotas. *Proceedings of the Geologists' Association*, 125: 446–451.

Javed, W. and Yasmeen, R. 1989. *Atarbolana setosa*, a new Cirolanid isopod from the Northern Arabian Sea. *Crustaceana*, 56: 78–82.

Johansen, P.-O. 2000. Contribution to the knowledge of growth and postmarsupial development of *Natatolana borealis* (Crustacea: Isopoda). *Journal of the Marine Biological Association of the United Kingdom*, 80: 623–632.

Jones, D.A. and Nithyanandan, M. 2012. Taxonomy and distribution of the genus *Eurydice* Leach, 1815 (Crustacea,

Isopoda, Cirolanidae) from the Arabian region, including three new species. *Zootaxa*, 3314: 45–57. Karasawa, H.; Ohara, M. and Kato, H. 2008. New records for Crustacea from the Arida Formation (Lower Cretaceous, Barremian) of Japan. *Boletín de la Sociedad Geológica Mexicana*, 60: 101–110.

Keable, S.J. 1998. A third species of *Aatolana* Bruce, 1993 (Crustacea: Isopoda: Cirolanidae). *Records of the Australian Museum*, 50: 19–26.

Keable, S.J. 1999. New species and records of *Plakolana* Bruce (Crustacea: Isopoda: Cirolanidae) from Australia. *Memoirs of The Queensland Museum*, 43: 763–775.

Keable, S.J. 2006. Taxonomic revision of *Natatolana* (Crustacea: Isopoda: Cirolanidae). *Records of the Australian Museum*, 58: 133–244.

Kensley, B. and Schotte, M. 1989. Guide to the marine isopod crustaceans of the Caribbean. Smithsonian Institution Pres, 308p.

Keyser, D. and Weitschat, W. 2005. First record of ostracods (Crustacea) in Baltic amber. *Hydrobiologia*, 538: 107–114.

Knight, T.K.; Bingham, P.S.; Grimaldi, D.A.; Anderson, K.; Lewis, R.D. and Savrda, C.E. 2010. A new Upper Cretaceous (Santonian) amber deposit from the Eutaw Formation of eastern Alabama, USA. *Cretaceous Research*, 31: 85–93.

Kocsis, A.T. and Raja, N.B. 2020. chronosphere: Earth system history variables (pre-release) (Version 0.3.0). Zenodo. http://doi.org/10.5281/zenodo.3525482. Accessed on 11 June 2020.

Kypke, J.L. and Solodovnikov, A. 2018. Every cloud has a silver lining: X-ray micro-CT reveals *Orsunius* rove beetle in Rovno amber from a specimen inaccessible to light microscopy. *Historical Biology*, 1–11.

Latreille, P.A. 1817. Le règne animal distribué d'après son organisation: pour servir de base a l'histoire naturelle des animaux et d'introduction a l'anatomie comparée. 3. Paris, Chez Déterville.

Lozano, R.P.; Pérez-de la Fuente, R.; Barrón, E.; Rodrigo, A.; Viejo, J.L. and Peñalver, E. 2020. Phloem sap in Cretaceous ambers as abundant double emulsions preserving organic and inorganic residues. *Scientific Reports*, 10: 9751.

Luxmoore, R.A. 1981. Moulting and growth in serolid isopods. *Journal of Experimental Marine Biology and Ecology*, 56: 63–85.

Malzahn, E. 1968. Über einen neuen Isopoden aus dem Hauterive Nordwestdeutschlands. *Geologisches Jahrbuch*, 86: 827–834.

Mao, Y.; Liang, K.; Su, Y.; Li, J.; Rao, X.; Zhang, H.; Xia, F.; Fu, Y.; Cai, C. and Huang, D. 2018. Various amberground marine animals on Burmese amber with discussions on its age. *Palaeoentomology*, 1: 91.

Martin, J.W. and Kuck, H.G. 1990. Case 2721 *Bathynomus* A. Milne Edwards 1879 (Crustacea Isopoda): proposed precedence over *Palaega* Woodward 1870. *Bulletin of Zoological Nomenclature*, 47: 27–29.

Matthews, K.J.; Maloney, K.T.; Zahirovic, S.; Williams, S.E.; Seton, M. and Müller, R.D. 2016. Global plate boundary evolution and kinematics since the late Paleozoic. *Global and Planetary Change*, 146: 226–250.

Menzies, R.J.; Bowman, T.E. and Alverson, F.G. 1955. Studies of the biology of the fish parasite *Livoneca convexa* Richardson (Crustacea, Isopoda, Cymothoidae). *Wasmann Journal of Biology*, 13: 277–295.

Mezzalira, S. and Martins-Neto, R.G. 1992. Novos crustáceos Paleozóicos do Estado de São Paulo, com descrição de novos taxa. *Acta Geologica Leopoldensia*, 36: 49–66.

Minelli, A. and Fusco, G. 2013. Arthropod Post-embryonic Development. p. 91–122. In: A. Minelli, G. Boxshall, and G. Fusco (eds), Arthropod Biology and Evolution. Berlin, Heidelberg, Springer Berlin Heidelberg.

Moore, W. and Brusca, R.C. 2003. A monograph on the isopod genus *Colopisthus* (Crustacea: Isopoda: Cirolanidae) with the description of a new genus. *Journal of Natural History*, 37: 1329–1399.

Müller, R.D.; Seton, M.; Zahirovic, S.; Williams, S.E.; Matthews, K.J.; Wright, N.M.; Shephard, G.E.; Maloney, K.T.; Barnett-Moore, N.; Hosseinpour, M.; Bower, D.J. and Cannon, J. 2016. Ocean Basin Evolution and Global-Scale Plate Reorganization Events Since Pangea Breakup. *Annual Review of Earth and Planetary Sciences*, 44: 107–138.

Nagler, C.; Hyžnỳ, M. and Haug, J.T. 2017. 168 million years old "marine lice" and the evolution of parasitism within isopods. *BMC Evolutionary Biology*, 17: 76.

Néraudeau, D.; Perrichot, V.; Batten, D.J.; Boura, A.; Girard, V.; Jeanneau, L.; Nohra, Y.A.; Polette, F.; Saint Martin, S. and Saint Martin, J.-P. 2017. Upper Cretaceous amber from Vendée, north-western France: age dating and geological, chemical, and palaeontological characteristics. *Cretaceous Research*, 70: 77–95.

Paiva, R.J.C. and Souza-Filho, J.F. 2015. A new species of *Dolicholana* Bruce, 1986 (Isopoda, Cymothoidea, Cirolanidae), the first record of the genus from the Atlantic Ocean. *Zootaxa*, 4039: 276.

Pazinato, P.G.; Soares, M.B. and Adami-Rodrigues, K. 2016. Systematic and palaeoecological significance of the first record of Pygocephalomorpha females bearing oöstegites (Malacostraca, Peracarida) from the lower Permian of southern Brazil. *Palaeontology*, 59: 817–826.

Poinar, G. 2018. A new genus of terrestrial isopods (Crustacea: Oniscidea: Armadillidae) in Myanmar amber. *Historical Biology*, 1–6.

Poinar, G.; Archibald, S.B. and Brown, A.E. 1999. New amber deposit provides evidence of Early Paleogene extinctions, paleoclimates and past distributions. *The Canadian Entomologist*, 131: 171–177.

Poinar, G.O. and Hess, R. 1982. Ultrastructure of 40-million-year-old insect tissue. *Science*, 215: 1241–1242.

Polz, H. 2005. Zwei neue Asselarten (Crustacea: Isopoda: Scutocoxifera) aus den Plattenkalken von Brunn (Oberkimmeridgium, Mittlere Frankenalb). *Archaeopteryx*, 23: 67–81.

Poore, G.C.B. and Bruce, N.L. 2012. Global Diversity of Marine Isopods (Except Asellota and Crustacean Symbionts). *PLoS ONE*, 7: e43529.

Price, G.D.; Williamson, T.; Henderson, R.A. and Gagan, M.K. 2012. Barremian–Cenomanian palaeotemperatures for Australian seas based on new oxygen-isotope data from belemnite rostra. *Palaeogeography, Palaeoclimatology, Palaeoecology*, 358–360: 27–39.

Quinney, A.; Mays, C.; Stilwell, J.D.; Zelenitsky, D.K. and Therrien, F. 2015. The range of bioinclusions and pseudoinclusions

preserved in a new Turonian (~90 Ma) amber occurrence from Southern Australia. *PLoS ONE*, 10: e0121307.

Rathbun, M.J. 1935. Fossil Crustacea of the Atlantic and Gulf Coastal Plain. Geological Society of America Special Papers, Vol. 2, 160p.

Riseman, S.F. and Brusca, R.C. 2002. Taxonomy, phylogeny and biogeography of *Politolana* Bruce, 1981 (Crustacea: Isopoda: Cirolanidae). *Zoological Journal of the Linnean Society*, 134: 57–140.

Ross, A. 1998. *Amber*. Cambridge, Harvard University Press, 76p.

Ross, A.J. 1997. Insects in amber. *Geology Today*, 13: 24–28.

Ross, A.J. 2019. Burmese (Myanmar) amber checklist and bibliography 2018. *Palaeoentomology*, 2: 22.

Schädel, M.; Müller, P. and Haug, J.T. 2020. Two remarkable fossil insect larvae from Burmese amber suggest the presence of a terminal filum in the direct stem lineage of dragonflies and damselflies (Odonata). *Rivista Italiana di Palaeontologia e Stratigrafia*, 126: 13–35.

Schädel, M.; Pazinato, P.G.; van der Wal, S. and Haug, J.T. 2019a. A fossil tanaidacean crustacean from the Middle Jurassic of southern Germany. *Palaeodiversity*, 12: 13–30.

Schädel, M.; Perrichot, V. and Haug, J. 2019b. Exceptionally preserved cryptoniscium larvae – morphological details of rare isopod crustaceans from French Cretaceous Vendean amber. *Palaeontologia Electronica*, 22.3.71: 1–46.

Schlüter, T. 1978. Zur systematik und palökologie harzkonservierter Arthropoda einer taphozönose aus dem Cenomanium von NW-Frankreich. *Berliner Geowissenschaftliche Abhandlungen Reihe A: Geologie und Paläontologie*, 9: 1–150.

Schmalfuss, H. 2003. World catalog of terrestrial isopods (Isopoda: Oniscidea). *Stuttgarter Beiträge zur Naturkunde, Serie A*, 654: 1–296.

Schmidt, A.R. and Dilcher, D.L. 2007. Aquatic organisms as amber inclusions and examples from a modern swamp forest. *Proceedings of the National Academy of Sciences*, 104: 16581–16585.

Schmidt, A.R.; Grabow, D.; Beimforde, C.; Perrichot, V.; Rikkinen, J.; Saint Martin, S.; Thiel, V. and Seyfullah, L.J. 2018. Marine microorganisms as amber inclusions: insights from coastal forests of New Caledonia. *Fossil Record*, 21: 213–221.

Schotte, M. 1994. *Annina mannai*, a new isopod from the Ganges river, west Bengal (Crustacea: Isopoda: Cirolanidae). *Proceedings of the Biological Society of Washington*, 107: 268–273.

Scotese, C.R. 2016. PALEOMAP PaleoAtlas for GPlates and the PaleoData Plotter Program, PALEOMAP Project, http://www.earthbyte.org/paleomap-paleoatlas-for-gplates/. Accessed on 11 June 2020.

Scotese, C.R. and Wright, N.M. 2018. PALEOMAP Paleodigital Elevation Models (PaleoDEMS) for the Phanerozoic PALEOMAP Project. Retrieved from https://www.earthbyte.org/paleodem-resource-scotese-and-wright-2018/. Accessed on 11 June 2020.

Serrano-Sánchez, M. de L.; Guerao, G.; Centeno García, E. and Vega, F.J. 2016. Crabs (Brachyura: Grapsoidea: Sesarmidae) as inclusions in Lower Miocene amber from Chiapas, Mexico. *Boletín de la Sociedad Geológica Mexicana*, 68: 37–43.

Serrano-Sánchez, M. de L.; Hegna, T.A.; Schaaf, P.; Pérez, L.; Centeno-García, E. and Vega, F.J. 2015. The aquatic and semiaquatic biota in Miocene amber from the Campo La Granja mine (Chiapas, Mexico): paleoenvironmental implications. *Journal of South American Earth Sciences*, 62: 243–256.

Serrano-Sánchez, M. de L.; Nagler, C.; Haug, C.; Haug, J.T.; Centeno-García, E. and Vega, F.J. 2016. The first fossil record of larval stages of parasitic isopods: cryptoniscus larvae preserved in Miocene amber. *Neues Jahrbuch für Geologie und Paläontologie-Abhandlungen*, 279: 97–106.

Seton, M.; Müller, R.D.; Zahirovic, S.; Gaina, C.; Torsvik, T.; Shephard, G.; Talsma, A.; Gurnis, M.; Turner, M.; Maus, S. and Chandler, M. 2012. Global continental and ocean basin reconstructions since 200Ma. *Earth-Science Reviews*, 113(3–4): 212–270.

Shi, G.; Grimaldi, D.A.; Harlow, G.E.; Wang, J.; Wang, J.; Yang, M.; Lei, W.; Li, Q. and Li, X. 2012. Age constraint on Burmese amber based on U–Pb dating of zircons. *Cretaceous Research*, 37: 155–163.

Sidabalok, C.M. and Bruce, N.L. 2018. Two new species and a new record of *Metacirolana* Kussakin, 1979 (Crustacea: Isopoda: Cirolanidae) from Indonesia. *Zootaxa*, 4370: 519–534.

Sinclair, B.J. 2017. Atelestidae. p. 1257–1260. In: A.H. Kirk-Spriggs and B.J. Sinclair (eds), Manual of Afrotropical Diptera. Volume 2. Nematocerous Diptera and lower Brachycera. Suricata, 5. Pretoria, South African National Biodiversity Institute.

Sinclair, B.J. and Kirk-Spriggs, A.H. 2010. *Alavesia* Waters and Arillo–a Cretaceous-era genus discovered extant on the Brandberg Massif, Namibia (Diptera: Atelestidae). *Systematic Entomology*, 35: 268–276.

Smith, R.D.A. and Ross, A.J. 2018. Amberground pholadid bivalve borings and inclusions in Burmese amber: implications for proximity of resin-producing forests to brackish waters, and the age of the amber. *Earth and Environmental Science Transactions of the Royal Society of Edinburgh*, 107: 239–247.

Soong, K. and Mok, H.-K. 1994. Size and maturity stage observations of the deep-sea isopod *Bathynomus doederleini* Ortmann, 1894 (Flabellifera: Cirolanidae), in Eastern Taiwan. *Journal of Crustacean Biology*, 14: 72–79.

Spassky, N.Y. and Kravtsov, A.G. 1976. The first find of an isopod in the Cenomanian of the Crimea. *Paleontologicheskii Zhurnal*, 10: 151–152.

Stebner, F.; Kraemer, M.M.S.; Ibáñez-Bernal, S. and Wagner, R. 2015. Moth flies and sand flies (Diptera: Psychodidae) in Cretaceous Burmese amber. *PeerJ*, 3: e1254.

Stolley, E. 1910. Über zwei neue Isopoden aus norddeutschem Mesozoikum. *Jahresbericht der Naturhistorischen Gesellschaft zu Hannover*, 60: 191–216.

Strong, K.W. and Daborn, G.R. 1979. Growth and energy utilisation of the intertidal isopod Idotea baltica (Pallas) (Crustacea: Isopoda). *Journal of Experimental Marine Biology and Ecology*, 41: 101–123.

Tabacaru, I. and Danielopol, D.L. 1996. Phylogénie des Isopodes terrestres. *Comptes rendus de l'Académie des sciences. Série 3, Sciences de la vie*, 319: 71–80.

Tait, J. 1918. V.—Experiments and Observations on Crustacea: Part II. Moulting of Isopods. *Proceedings of the Royal Society of Edinburgh*, 37: 59–68.

van der Wal, S. and Haug, J.T. 2020. Shape of attachment structures in parasitic isopodan crustaceans: the influence of attachment site and ontogeny. *PeerJ*, 8: e9181.

Vega, F.J.; Bruce, N.L.; González-León, O.; Jeremiah, J.; Serrano-Sánchez, M. de L.; Alvarado-Ortega, J. and Moreno-Bedmar, J.A. 2019. Lower Cretaceous marine isopods (Isopoda: Cirolanidae, Sphaeromatidae) from the San Juan Raya and Tlayúa formations, Puebla, Mexico. *Journal of Crustacean Biology*, 39: 121–135.

Voigt, S.; Wilmsen, M.; Mortimore, R.N. and Voigt, T. 2003. Cenomanian palaeotemperatures derived from the oxygen isotopic composition of brachiopods and belemnites: evaluation of Cretaceous palaeotemperature proxies. *International Journal of Earth Sciences*, 92: 285–299.

Wägele, J.-W. 1989. Evolution und phylogenetisches System der Isopoda: Stand der Forschung und neue Erkenntnisse. *Zoologica* (Stuttgart), 140: 1–262.

Wägele, J.-W. and Brandt, A. 1988. *Protognathia* n. gen. *bathypelagica* (Schultz, 1977) rediscovered in the Weddell Sea: A missing link between the Gnathiidae and the Cirolanidae (Crustacea, Isopoda). *Polar Biology*, 8: 359–365.

Waggoner, B.M. 1994. An aquatic microfossil assemblage from Cenomanian amber of France. *Lethaia*, 27: 77–84.

Waloszek, D. 1999. On the Cambrian diversity of Crustacea. p. 3–27. In: F.R. Schram and J.C. von Vaupel Klein (eds), Crustaceans and the Biodiversity Crisis. Proceedings of the Fourth International Crustacean Congress. Leiden, Brill.

Weitschat, W.; Brandt, A.; Coleman, C.O.; Andersen, N.M.; Myers, A.A. and Wichard, W. 2002. Taphocoenosis of an extraordinary arthropod community in Baltic amber. *Mitteilungen aus dem Geologisch-Paläontologischen Institut der Universität Hamburg*, 86: 189–210.

Wichard, W.; Gröhn, C. and Seredszus, F. 2009. Aquatic Insects in Baltic Amber - Wasserinsekten im Baltischen Bernstein. Remagen, Verlag Kessel, 336p.

Wieder, R.W. and Feldmann, R.M. 1989. *Palaega goedertorum*, a fossil isopod (Crustacea) from late Eocene to early Miocene rocks of Washington State. *Journal of Paleontology*, 63: 73–80.

Wieder, R.W. and Feldmann, R.M. 1992. Mesozoic and Cenozoic fossil isopods of North America. *Journal of Paleontology*, 66: 958–972.

Wilson, G.D.F. 2003. A new genus of Tainisopidae fam. nov. (Crustacea: Isopoda) from the Pilbara,Western Australia. *Zootaxa*, 245: 1–20.

Wilson, G.D.F.; Paterson, J.R. and Kear, B.P. 2011. Fossil isopods associated with a fish skeleton from the Lower Cretaceous of Queensland, Australia - direct evidence of a scavenging lifestyle in Mesozoic Cymothoida: Scavenging isopod crustaceans from the Lower Cretaceous. *Palaeontology*, 54: 1053–1068.

Woodward, H. 1870. I.—Contributions to British Fossil Crustacea. *Geological Magazine*, 7: 493.

Xing, L.; Sames, B.; McKellar, R.C.; Xi, D.; Bai, M. and Wan, X. 2018. A gigantic marine ostracod (Crustacea: Myodocopa) trapped in mid-Cretaceous Burmese amber. *Scientific Reports*, 8: 1365.

Yu, T.; Kelly, R.; Mu, L.; Ross, A.; Kennedy, J.; Broly, P.; Xia, F.; Zhang, H.; Wang, B. and Dilcher, D. 2019. An ammonite trapped in Burmese amber. *Proceedings of the National Academy of Sciences*, 116: 11345-11350.

Yu, T.-T.; Wang, B. and Jarzembowski, E. 2018. First record of marine gastropods (wentletraps) from mid-Cretaceous Burmese amber. *Palaeoworld*, 28: 508–513.

Zhang, W.W. 2017. Frozen dimensions. The fossil insects and other invertebrates in amber. Chongqing, Chongqing University Press, 692p.

Zhao, X.; Zhao, X.; Jarzembowski, E.A. and Wang, B. 2019. The first whirligig beetle larva from mid-Cretaceous Burmese amber (Coleoptera: Adephaga: Gyrinidae). *Cretaceous Research*, 99: 41–45.

Zheng, D.; Chang, S.-C.; Perrichot, V.; Dutta, S.; Rudra, A.; Mu, L.; Kelly, R.S.; Li, S.; Zhang, Q.; Zhang, Q.; Wong, J.; Wang, J.; Wang, H.; Fang, Y.; Zhang, H. and Wang, B. 2018. A Late Cretaceous amber biota from central Myanmar. *Nature Communications*, 9: 1–6.

2.2 Study II: Schädel, Perrichot. & Haug 2019

Authors: Schädel, M., Perrichot, V. & Haug, J. T.

Title: Exceptionally preserved cryptoniscium larvae – morphological details of rare isopod crustaceans from French Cretaceous Vendean amber

Journal: Palaeontologia Electronica

Article number: 22.3.71

Pages: 1–45

DOI: https://doi.org/10.26879/977
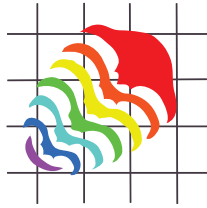
Exceptionally preserved cryptoniscium larvae - morphological details of rare isopod crustaceans from French Cretaceous Vendean amber

Mario Schädel, Vincent Perrichot, and Joachim T. Haug

ABSTRACT

Epicaridea is an ingroup of Isopoda that comprises only parasitic crustaceans. Within parasitic isopods, epicarideans represent a special case: throughout their ontogeny they switch from a small intermediate host (copepod) to a final host (various larger crustaceans), and develop through distinct larval phases (epicaridium, microniscium and cryptoniscium). Young males of some species retain a larval morphology. Recent findings of fossil epicarideans in amber from the Miocene of Mexico consisted in the only epicaridean body fossils, until one specimen has been figured from Cretaceous amber from France. Here we provide a detailed analysis of this specimen and 20 more specimens from the same locality. The presented specimens represent the oldest occurrence of epicaridean body fossils, extending their fossil record by 67 million years.

The fossils are exceptionally well preserved and, despite their small size of less than 0.5 mm, reveal even fine morphological details. The specimens correspond either to cryptoniscium larvae or males that have retained their larval morphology. There are no morphological features in the fossils that argue against conspecifity of all specimens. All character states found in the fossils are also present in extant species. Given the displayed combination of character states and the age difference, it is unlikely that the specimens are conspecific to any extant species nor to much younger fossils from the Miocene of Mexico. The species *Vacuotheca dupeorum* gen. et sp. nov. is described and interpreted as an epicaridean of uncertain affinities, but that is not part of the epicaridean ingroup Dajidae. Furthermore, multiple aspects of the evolutionary history of parasitic isopods and epicarideans in particular are discussed. This includes possible scenarios for host changes that could have led to the life cycle of modern epicarideans and the evolution of size within epicaridean larvae.

Mario Schädel. Ludwig-Maximilians-Universität München, Department of Biology II, Zoomorphology group, Großhaderner Straße 2, 82152 Planegg-Martinsried, Germany. mario.schaedel@palaeo-evo-devo.info
Vincent Perrichot. Univ. Rennes, CNRS, Géosciences Rennes, UMR 6118, 35000 Rennes, France. vincent.perrichot@univ-rennes1.fr
Joachim T. Haug. Ludwig-Maximilians-Universität München, Department of Biology II, Zoomorphology group, Großhaderner Straße 2, 82152 Planegg-Martinsried, Germany and Ludwig-Maximilians-Universität München, GeoBio-Center, Richard-Wagner-Str. 10, 80333 München, Germany. joachim.haug@palaeo-evo-devo.info

---

INTRODUCTION

General Background

Isopoda (woodlice and their relatives) is an enormously diverse group of malacostracan crustaceans. Having a marine origin, isopod species did not only master the transition to a fully terrestrial life (Oniscidea), they also inhabit deep sea and freshwater environments, and some groups even developed parasitic lifestyles (Williams and Bunkley-Williams, 2019). Some isopod species have been known as parasites of fishes and crustaceans for a long time (e.g., Müller, 1862). However, the evolution of these groups of parasites is still quite enigmatic to the present day.

Fossils can provide important clues to the early evolution of a group, by combining highly specialised modern-type features with more plesiomorphic aspects of the morphology. Fossils may provide evolutionary "steps-in between". Yet, in the case of parasitic isopods it is not so simple.

Isopod fossils are not very common in the fossil record in general and identifying a parasitic lifestyle based on fossil morphology is quite challenging (see discussion in Nagler and Haug, 2015). Thus, the record of parasitic isopod body fossil is, so far, highly limited.

Even when fossils are available, a solid understanding of the biology of the suspected extant relatives is required to interpret their significance. Also, hypotheses on the relationships between animal groups of interest should always be critically evaluated in light of the usually more detailed known extant species.

Whether all parasitic isopods belong to a monophyletic group that excludes non-parasitic species is still a matter of debate. It seems widely accepted that most fish parasites and some predatory and scavenging forms (Cirolanidae, Corallanidae, Tridentella, Aegidae, and Cymothoidae) are closely related and form the monophyletic group Cymothoida (Wägele, 1989; Brusca and Wilson, 1991; Dreyer and Wägele, 2001; Brandt and Poore, 2003). However, the position of Gnathiidae (only larval forms are fish parasites) and Epicaridea (parasites on crustaceans) is still under debate (Wägele, 1989; Brusca and Wilson, 1991; Dreyer and Wägele, 2001, 2002). Brusca and Wilson (1991) suggested a sister group relationship between Epicaridea and Gnathiidae (outside of Cymothoida), whereas Dreyer and Wägele (2001, 2002) suggested Epicaridea being the sister group of Cymothoidae (within Cymothoida).

The analysis of Nagler et al. (2017) combines close relationships proposed for Cymothoidae and Epicaridea (Wägele, 1989) and between Gnathiidae and Epicaridea (Brusca and Wilson, 1991) by interpreting a group including Gnathiidae and Epicaridea as a sister group to Cymothoidae. Support for this view is currently mainly provided by an exceptionally preserved fossil of the group Urda Münster, 1840, combining characters of Epicaridea, Gnathiidae and Cymothoidae (Nagler et al., 2017).

Isopoda is an ingroup of the diverse group Peracarida. All peracaridans share a unique specialisation: the adult female develops a brood pouch that is covered with sclerites protruding from the legs (oostegites), providing for prolonged maternal care. As a result, most species do not produce true larval offspring in the strict sense (for difficulties of the term see Haug, in press). The immatures, that leave the brood pouch, largely resemble the adults in morphology and ecology (but see discussion in Lang et al., 2007). This holds also true for the stem species of Isopoda (Ax, 2000).

In fish-parasitising isopods (mostly species of Aegidae and Cymothoidae) dispersal happens in the so-called manca stage or the subsequent juveniles. The manca stage lacks a fully developed seventh pereopod (thoracic appendage 8, appendage of post-ocular segment 13) that the adults have (Boyko and Wolff, 2014) but otherwise resembles the adult in the general body organisation. Yet, based on their ecological function (dispersal) they may be interpreted as functional larvae (if dispersal is considered a larval feature; see Haug, in press). In Cymothoidae subsequently gradual morphological changes in favour of a close parasite-host interaction can happen, which can, for example, lead to the loss of the bilateral symmetry in late stages of the individual development (e.g., van der Wal et al., 2019).

In epicarideans, much smaller offspring is released from the brood pouch and the ontogenesis can be separated in distinct steps with very different ecological functions corresponding to very different morphologies, too (Figure 1). In most epicarideans the ontogeny can be differentiated into three distinct true larval stages, accepted as such by most authors - epicaridium, microniscium and cryptoniscium - and the subsequent further development towards adults (Williams and Boyko, 2012; Boyko and Wolff, 2014).
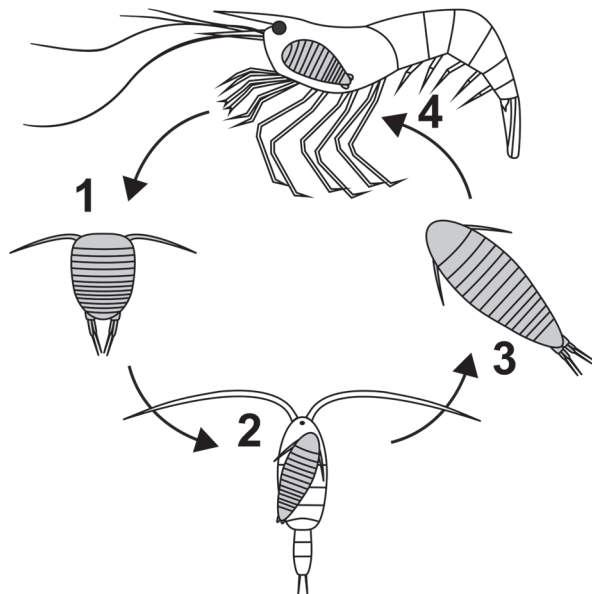
FIGURE 1. Sketched and simplified illustration of the life cycle of epicarideans. 1.1: Planktic epicaridium larva. 1.2: Microniscium larva feeding on a copepod (intermediate host). 1.3: Planktic cryptoniscium larva. 1.4: Adult feeding on a crustacean final host.

The Post-embryonic Ontogeny of Epicarideans

Epicaridium. With only one reported exception (Miyashita, 1940) epicaridean crustaceans hatch from their eggs as epicaridium larvae. The name of this larval type derives from its discovery on the definitive host, i.e., a caridean shrimp, where larvae were released from the brood pouch of the female (Fraisse, 1878). Epicaridium larvae are stout in appearance with short but wide thoracic segments. There is a clear distinction between the free trunk segments (segments that have a dorsal sclerite and not conjoined with others) into pereon-segments (posterior, free thoracic segments) and the pleon-segments regarding the morphology of the legs. At least the anterior pereopods are well differentiated. The pleopods bear distinct setae (Dale and Anderson, 1982).

After their release they become planktic and infest copepods (Boyko et al., 2013). The small epicaridium larvae grasp the appendages of the copepods and move to the trunk where they will moult and transform to the next distinct larval stage: the microniscium.

Microniscium. Relatively little is known about the life of microniscia, besides that they are parasitising copepods crustaceans. At some point (maybe still as epicaridia?) they pierce through the integument of the host and from then on feed on the host's body fluid (Pike pers. comm. in Marshall and Orr, 2013). Due to the relatively large size of the microniscium compared to its host it causes a tremendous negative effect on the reproductive rate of the copepods individual (Uye and Murase, 1997). It is also likely (but has not been reported yet) that the microniscium kills its host. In this case, the microniscium would rather correspond to a parasitoid than a parasite. The mechanism of detachment from this intermediate host and when or where moulting towards next stage happens remains to be investigated.

The epicarideans use the phase of attachment to the copepod with a steady income of nutrients to drastically change the overall body morphology. While the epicaridium is rather stout in appearance compared to the subsequent larval stages, it possesses well-developed setae and specialized, fully developed appendages (Anderson and Dale, 1981). The microniscium is more slender. Early microniscia lack fully developed thoracic appendages, and the seventh pereopod (last thoracic appendage) is missing entirely as well as the setation of the pleopods. The absence of the last thoracic appendage is reminiscent to the condition in manca stages in other isopod species. During the

microniscium larval stage a significant growth and a morphological change (supposedly without moulting) towards the morphology of the cryptoniscium stage can be observed (Anderson and Dale, 1981).

Cryptoniscium. The cryptoniscium is the last distinct larval stage that can be observed throughout the ontogeny of species of all epicaridean lineages. The cryptoniscium develops from a microniscium that is attached to a planktic copepod. Cryptoniscia are all still rather small and resemble microniscia in overall body shape (Nielsen and Strömberg, 1973). Similar to epicaridia, cryptoniscium larvae are planktic and in search for a host. They swim actively and at least some cryptoniscia are able to curl up (for protection?) (Fraisse, 1878). The overall morphology of cryptoniscium larvae is relatively uniform in all epicaridean species known from this stage (Anderson and Dale, 1981). The body is elongated with a convex dorsal and a concave ventral surface. The mouthparts form a sucking mouth cone. The seventh pereopod (thoracic appendage eight) is present and the dactyli of the pereopods, i.e., the terminal elements of posterior seven thoracic appendages, are recurved forming a functional subchelae with the proximal appendage elements. The pleopods have long natatory setae; the uropods are rod-shaped with long distal setae.

For the species *Entoniscoides okadai* Miyashita, 1940, it has been reported that the hatching stage has a cryptoniscium-like habitus. This was shown by the examination of the brood pouch of an adult female where pre-hatched and hatched larvae, with the appearance of a cryptoniscium, were observed. Furthermore, an embryonic stage resembling microniscium larvae has been described (although this statement is not directly evident from the provided photograph; Miyashita, 1940). Without free swimming epicaridia, it is likely that *Entoniscoides okadai* is not parasitising copepods. With respect to the current phylogenetic hypothesis it seems unlikely that this represents an ancestral feature, but is better understood as a decrease of step numbers during ontogeny along with an intensification in maternal care.

Later development and sex. The stage following the cryptoniscium has been termed 'bopyridium' by some authors (e.g., Oliveira and Masunari, 2006). Boyko and Wolf (2014) critically questioned the value of this term. We support their critical view. The term indicates the presence of a distinct stage of life, yet it refers to a phase of morphological transition between the cryptoniscium and the adult (including several moults) and cannot be properly outlined using morphological features. In other groups comparable stages of eucrustaceans would have been simply addressed as 'juveniles'.

The sexual development is highly variable within epicaridean species. It can be (1) strictly protandric, meaning that all individuals are males at first, or (2) depend on an external trigger, such as the presence of on adult female on the same host. Yet, also a direct, externally triggered, development from the cryptoniscium towards both sexes is possible (summarised in Wägele, 1989). Possible genotypic determination for both sexes has also been reported once (Hiraiwa, 1936). When a female dies on the alive host, adult males can also transform into functional females (Reverberi, 1947).

Hosie (2008) stated that in the epicaridean subgroup Cryptoniscoidea males are often not distinguishable from cryptoniscia. The author uses the term 'male' for all non-planktic cryptoniscoideans that show no signs of modification towards a female habitus. We think this practice is critical; it heavily depends on assumptions about the sexual development and behaviour of epicarideans, which has not been studied in detail for most species.

Epicaridean Ecology

The entire larval phase of epicaridean crustaceans lasts around 10 to 30 days (Caroli, 1928; Anderson, 1975). The dispersal of the larval stages strongly correlates with the length of the larval phases. A passive transportation of up to 100 km distance has been reported during the time of the larval development (Owens and Rothlisberg, 1991). Further spatial dispersal obviously depends on the mobility of the host.

As their name suggests, adult epicarideans can be found especially on caridean shrimps. However, they are not restricted to them as final hosts, but also infest a variety of other crustaceans including other isopod species (Nielsen and Strömberg, 1965). Some species are also hyperparasitic on other epicarideans (Rybakov, 1990) or rhizocephalans (parasitic barnacles) (Williams and Boyko, 2012). Epicarideans have even be reported infesting cephalopods (Pascual et al., 2002); the authors suggest that similar cases may have simply been overseen in the past due to their small size. Hence, cephalopods could indeed represent additional host species.

Given the planktic dispersal stages in Epicaridea and the multiplicity of hosts observable in only one species (Bourdon, 1968), it is surprising to note the apparent impacts of geographical bounda-

ries on the distribution of extant representatives. Markham (1968) mentioned the example of the epicaridean ingroup Orbioninae (Bopyroidea), which occurrence is restricted to the Indo-Pacific although suitable hosts are globally distributed.

Epicarideans are not limited to full marine environments but also occur in brackish estuarine habitats (Anderson and Dale, 1981). There are also records for species living in strict freshwater environments (Chopra, 1923).

Epicaridean Ingroup Relationships

As a result of their complex life cycle in combination with the presence of two planktic larval stages, associating larvae and adults is challenging. Thus, many species are known either as cryptoniscium larvae only (e.g., Schultz, 1975) or lack the description of this stage (e.g., Williams and An, 2009). This clearly affects the research on the systematics of the group, leading Boyko et al. (2013, p. 496) to the following assertion about the taxonomy within Epicaridea: "[…] genera are defined by the gross morphology of the females, and species by characters of cryptoniscium larvae." Future

studies have to overcome the taxonomic bias that has been caused by the arbitrary distinctions between species and higher level characters.

Very few studies have focused on the epicaridean ingroup relationships. Beside a few older publications (Shino, 1965; Markham, 1968; reviewed in Boyko and Williams, 2009) for which the results are non-replicable (lacking any description of methods), there are only three studies focusing on this issue (Wägele, 1989; Boyko et al., 2013; Boyko and Williams, 2015). These phylogenetic analyses are both limited with respect to the number of included epicaridean species and, as a consequence, are complementary rather than comparable (see Figure 2). Both found Entoniscidae as the sister group of Bopyridae and Dajidae inside Cryptoniscoidea.

Fossil Record of Epicaridea

Until recently, there was simply no report for epicaridean body fossils. Hitherto, the fossil record of Epicaridea was consisting of swellings observed from the branchial chambers of fossil decapod crustaceans. These swellings were first identified
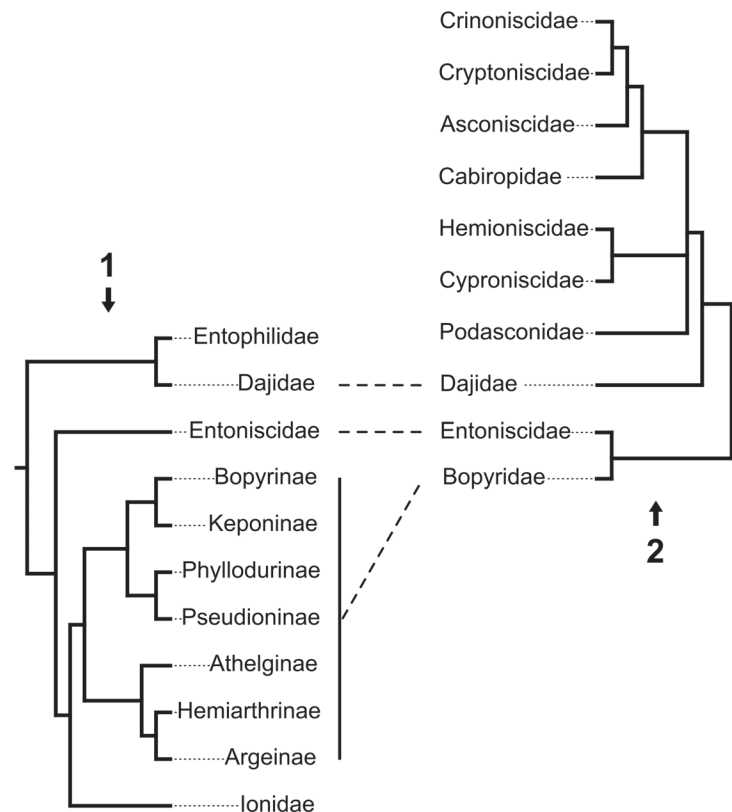
FIGURE 2. Confronting phylogenetic hypotheses in Epicaridea. Dashed lines represent supported monophyletic groups. **2.1:** Molecular phylogeny from Boyko et al. (2013). **2.2:** Phylogeny based on putative apomorphic morphological characters from Wägele (1989).

by Bell (1863) and attributed by actualism to the internal colonization of the gill chamber, as nowadays performed by adult bopyroideans.

These fossil deformations supposedly induced by epicarideans have been listed and reviewed by Markham (1968), Wienberg Rasmussen et al. (2008), Klompmaker et al. (2014) and Klompmaker and Boxhall (2015). Their oldest occurrence is reported from a lobster-like crustacean (Erymidae) from the Toarcian (Lower Jurassic) of Western New Guinea (Soergel, 1913). This occurrence is questionable, as the repository of the depicted specimen is unknown, and because there is no record for such swellings in the Middle Jurassic so far (see also Klompmaker et al., 2014; Klompmaker and Boxshall, 2015). Klompmaker et al. (2014) reported a 'peak' in infestation during the Late Jurassic and supposed that this, rather than being a sampling artefact, could be linked to synecological reasons (occurrence of potential host species, biological defence strategies, etc.). Klompmaker et al. (2014) furthermore showed that more different species of true crabs (Brachyura) were infected in comparison to the representatives of its sister group (squat lobster, hermit crabs, false crabs; all together Anomura/Anomala). Yet, anomuran/anomalan crustaceans seem to have been more frequently infected than brachyuran crabs when considering the number of infected individuals per taxon for a Cretaceous assemblage.

Klompmaker et al. (2014) also erected the ichnotaxon *Kanthyloma crusta* for these Epicaridea-caused swellings (see Klompmaker and Boxhall, 2015 for a further discussion regarding this nomenclatural practice). Attempts have been made to investigate the preservation of isopod body fossils within swellings in fossil crustaceans through computed tomography without success (N. Robin, 2019 pers. comm.). In experimental studies on the taphonomy of decapod crustaceans, remains of epicarideans are still present up to 25 days after the death of the infected host (Klompmaker et al., 2017).

A preservation type that could have the chance to preserve epicarideans is amber. That living arthropods submerged in water can get trapped by resin was experimentally shown (Schmidt and Dilcher, 2007) and can be explained by active or passive collision with the submerged resin (Figure 3). Yet, aquatic and especially marine organisms are relatively rare in amber considering their overall proportion in amber inclusions. However, there are some aquatic or even marine organisms in many amber localities (Schmidt et al., 2004; Key-
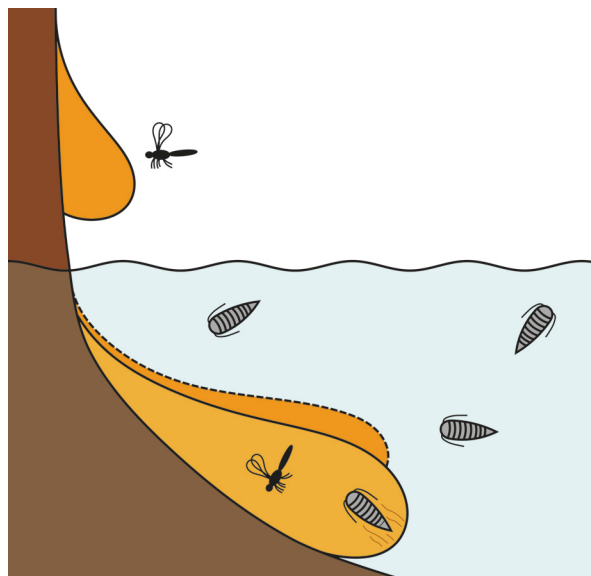
FIGURE 3. Illustration of possible entombment conditions suggested for Vendean amber: cryptoniscium larvae living in an aquatic environment close to the resin producing tree and getting trapped by making contact with submerged liquid resin.

ser and Weitschat, 2005; Girard et al., 2008; Saint Martin et al., 2015; Serrano-Sánchez et al., 2015, 2016; Xing et al., 2018).

More recently there were two reports of epicaridean body fossils preserved in amber. 1) There is a record from Miocene Mexican amber (Serrano-Sánchez et al., 2016). The fossils, which come from the Campo La Granja site, are clearly recognisable as larval epicarideans. These specimens were the first fossil record of epicaridean body fossils as well as a rare occurrence of fossil crustacean larvae in general. 2) Shortly after this primary description, Néraudeau et al. (2017) reported a second set of epicaridean larvae in the palaeontological content of a new French amber deposit. In this case, the fauna is significantly older than the Mexican epicarideans (about 90 million years) and allows access to better apparent morphological details.

Here, we describe 21 exceptionally well-preserved epicarideans from Cretaceous amber of Vendée, France. We further discuss the implications of the find for our understanding of the evolutionary history of epicaridean crustaceans. The aspect of body size for the known fossil epicaridean larvae in comparison to the extant representatives is discussed. Also, we critically discuss multiple possible scenarios that could have lead to the complex life cycle of extant epicarideans. The taphonomical implications of the herein presented fossils are discussed with respect to the circum-

6

stances that could have lead to their preservation in amber.

GEOLOGICAL SETTING

The Vendean amber deposit is located in northwestern France (Pays-de-la-Loire region) at La Robinière, a locality near the village of La Garnache (department of Vendée). The amber pieces were sampled with the help of local amateur palaeontologists at an only temporarily accessible outcrop (road construction works). Amber was only found in lignitic (dark, carbon rich) lenses within grey coloured clay in the initial digging site Garnache 1 but not in other nearby outcrops with similar lithology (Néraudeau et al., 2017). The stratigraphic correlation and dating of the sediment that contained the amber yielded severe difficulties, namely the inaccessibility of Garnache 1 and the insufficient resolution of the local geological map (Néraudeau et al., 2017). Néraudeau et al. (2017) used palynomorphs from Garnache 1 to date the amber bearing sediment by (relative) biostratigraphy. Based on their results they suggested a Turonian (Late Cretaceous) age for the sediment. The Turonian is correlated with an absolute age of 93.9 to 89.8 million years (Ogg et al., 2012, International Chronostratigraphic Chart v. 2018/08). Chemical analyses of the amber matrix favoured Cupressaceae related trees as the origin of the now fossilised resin (Nohra et al., 2015; Néraudeau et al., 2017).

The sediment surrounding the Vendean amber pieces was most likely deposited in an estuarine or lagoonal coastal environment within the Challans-Commequiers Basin (Néraudeau et al., 2017). Charentese amber of Southwest France is slightly older (latest Albian-earliest Cenomanian) and comes from a different geological basin (Aquitaine Basin) (Perrichot et al., 2010). The slightly older Albian (Early Cretaceous) "Iberian amber" was found in northern and eastern Spain (Penalver and Delclòs, 2010). Despite the spatial proximity today, the Iberian basins and the French basins with (arthropod bearing) Cretaceous amber do not directly correspond as they represent coastal regions of separated landmasses in the Cretaceous. Iberian amber comes from a series of geological basins (mainly Basque-Cantabrian Basin and Maestrat Basin) roughly portraying the coastline of the Iberian terrane during the Cretaceous (Penalver and Delclòs, 2010). Charentese amber (Aquitaine Basin) and Vendean amber were deposited in basins along the west coast of the European archipelago and are linked to coastal depositional environments including marine or brackish water-bodies near the amber trees (Girard et al., 2008; Perrichot et al., 2010; Saint Martin et al., 2015; Néraudeau et al., 2017). All Iberian amber localities are, just like Vendean amber, associated with lignitic sediments deposited in deltaic or estuarine environments and, in the case of the Basque-Cantabrian Basin (El Soplao), also with marine influence (Penalver and Delclòs, 2010).

Vendean amber, although the sample size is very limited, has already yielded a diverse spectrum of fossil arthropod species. A complete list is given in Néraudeau et al. (2017). Aquatic inclusions known in Vendean amber (apart from the herein described epicaridean crustaceans) are a water mite ("Hydracarina"), centric diatoms and one tanaidacean crustacean (Peracarida: Tanaidacea) (Saint Martin et al., 2015; Sánchez-García et al., 2016; Néraudeau et al., 2017).

MATERIAL AND METHODS

Material and Repository

The focus of this study is small epicaridean isopod specimens preserved in amber. The fossils are embedded in 17 pieces of Vendean amber. Vendean amber refers to Cretaceous amber found in the department of Vendée, France (Figure 4), which comprises a small collection of amber pieces found in the outcrop Garnache 1 (coordinates: 46°52.802' N 1°51.583' W., elevation 12 m). Vendean amber is dated to a Turonian (Late Cretaceous) age (93.9 to 89.8 million years old) (Néraudeau et al., 2017). The amber pieces studied herein originate from the private collection of Fanny Dupé, which has been donated to the collection of the Geological Department and Museum of the University Rennes 1 (IGR.GAR-8.1-1, IGR.GAR-8.1-2, IGR.GAR-8.2, IGR.GAR-28, IGR.GAR-41-1, IGR.GAR-41-2, IGR.GAR-48, IGR.GAR-51, IGR.GAR-53-1, IGR.GAR-53-2, IGR.GAR-64, IGR.GAR-65, IGR.GAR-89, IGR.GAR-90, IGR.GAR-92, IGR.GAR-93, IGR.GAR-94, IGR.GAR-95-1, IGR.GAR-95-2, IGR.GAR-97, IGR.GAR-98). Each piece contained either one or two visible larvae. Altogether the studied amber pieces bear 21 visible inclusions of epicarideans (see Appendix 1 for a more detailed description of the amber pieces).

The pieces were manually polished using a Buehler Metaserv 3000 polisher and Buehler CarbiMet silicon carbide papers to remove the altered, opaque outer surface of the amber samples. Whenever possible, a further polishing was made
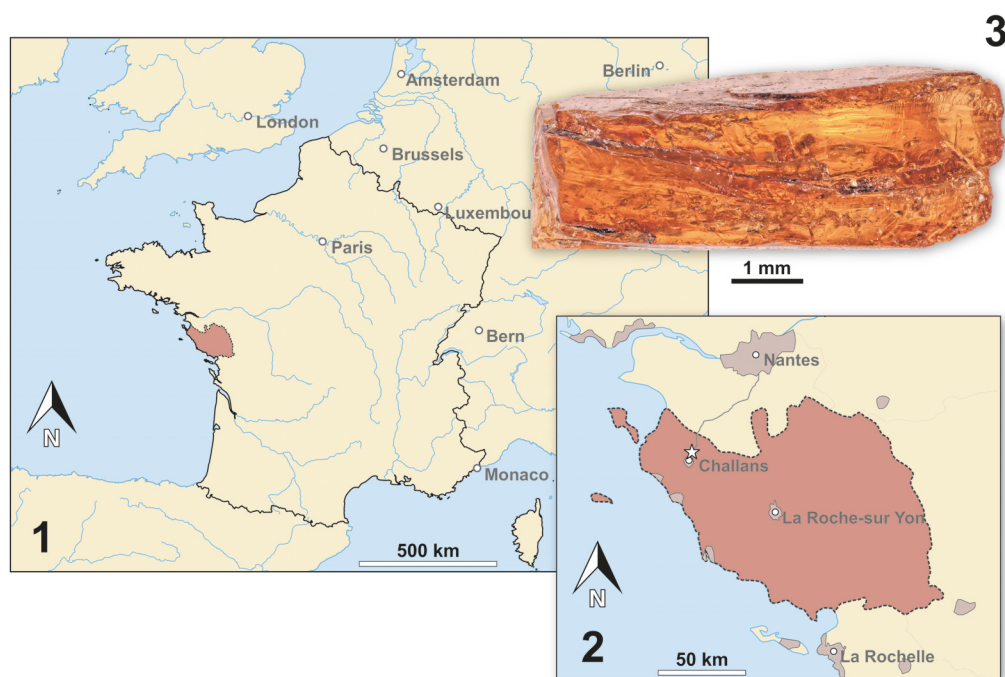
FIGURE 4. Map of France (**4.1**) and a detailed map of the Vendée department (reddish) (**4.2**). The fossil site is marked by a star. **4.3:** Photograph of a piece of Vendean amber - notice the layered build-up of the resin.

to obtain flat surfaces for optimal observation and imaging of the inclusions. Some pieces that contained multiple inclusions were cut using a scalpel blade as a microsaw in order to separate the syninclusions and facilitate their respective study.

Referencing

To precisely address each specimen (more than one specimen can occur with the same collection number) we amended the collection number with the suffix "-1" or "-2". A distinction between two neighbouring specimens is warranted by a study of the photographic images (Figures 5-9) and a description of the preservational circumstances of each specimen (Appendix 1).

Documentation Methods

Imaging was performed with a Keyence BZ-9000 epi-fluorescence inverted microscope and a Keyence VHX-6000 digital microscope with a 20-2000x lens. The pieces of amber were photographed fully submerged in water (fluorescence microscopy) or dry or partly wetted with a cover slip on top. For the fluorescence microscopy we experienced the best results using incident light with an excitation wavelength centre of 545 nm (generally used for rhodamine-based stains, 'TRITC' filter cube).

For some of the images gathered with the Keyence VHX-6000 digital microscope, the implemented focus-stacking method was used to create in-focus images. In all other cases, stacks of unprocessed images were saved for later customized image processing.

Image Processing

Using the VHX-6000 digital microscope the internal stacking algorithm was used for focus-stacking for some images. Additionally, single images were separately merged with CombineZP (Alan Hadley, GPL) for better results. Fluorescent microscopy images were also separately merged using CombineZP and Macrofusion/EnfuseGUI (both based on the Enfuse image blending algorithm, GPL). Panoramic image compositions were stitched "manually" in GIMP (GNU Image Project) or automatically stitched in Hugins (based on Enfuse and Enblend, GPL). The microphotographs were post-processed in GIMP and arranged and labeled in Inkscape (GPL). Graphs were plotted in R and manually adjusted in Inkscape without actions that could alter the position of data points relative to each other or the axes. Drawings and schemes were created in Inkscape and post processed in GIMP roughly applying the approach proposed by Coleman (2003).
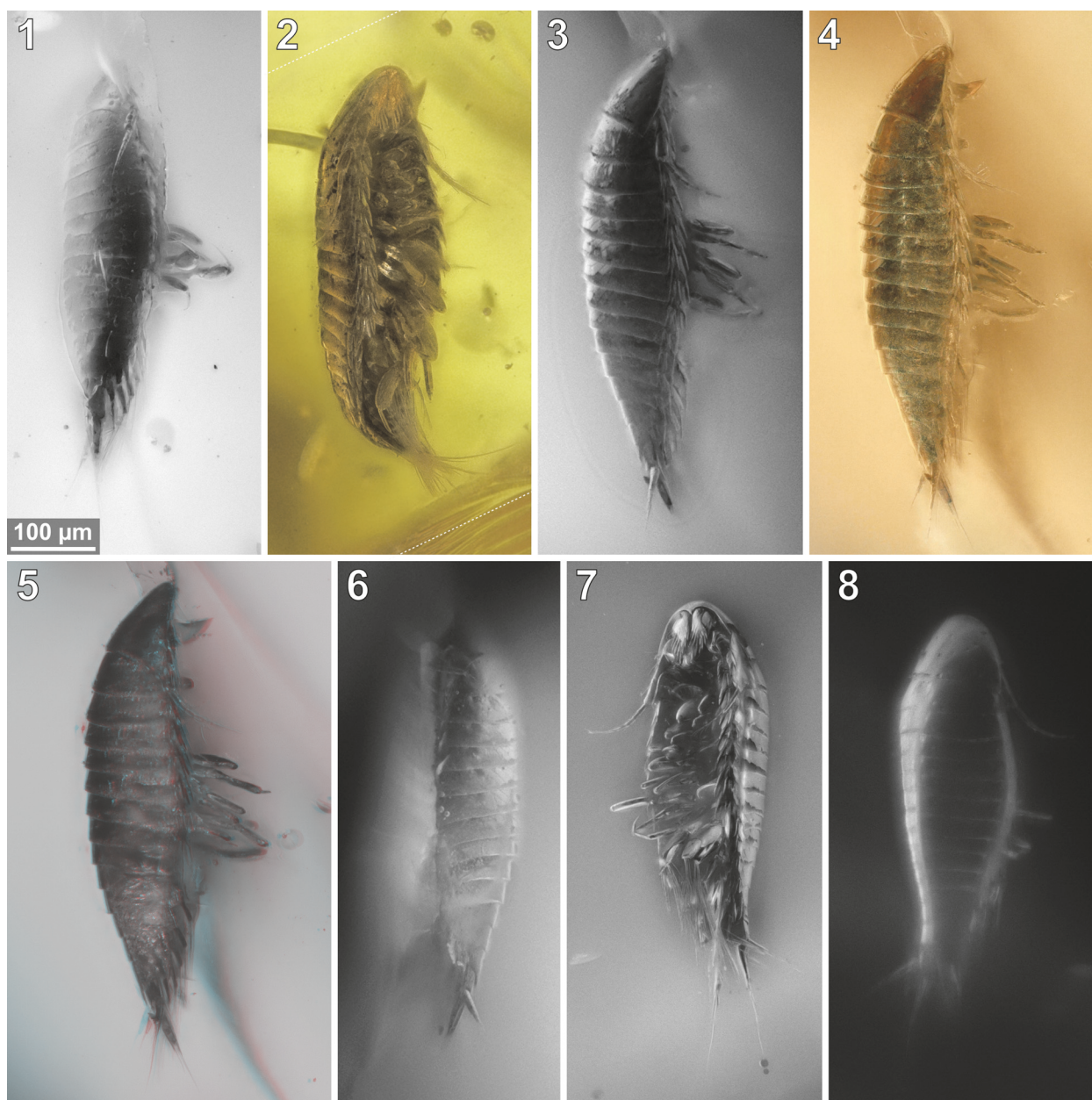
FIGURE 5. *Vacuotheca dupeorum* sp. nov., comparative overview of the type material sorted by collection number (same scale). **5.1:** Paratype IGR.GAR-8.1-1, lateral view, epifluorescence. **5.2:** Paratype IGR.GAR-8.1-2, latero-ventral view, reflected light. **5.3-5.6:** Paratype IGR.GAR-8.2, lateral view (5.3-5.5) and lateral view of the opposite side (5.6), epifluorescence (5.3, 5.6), reflected light (5.4) and 3D red-cyan anaglyph of reflected light micrograph (5.5). **5.7-5.8:** Holotype IGR.GAR-28, ventro-lateral view (5.7) and dorsal view (5.8), epifluorescence.

Phylogenetic trees in Figure 2 were created in R (ape, phytools and paleotree) from a manually written edge matrix, converted to a phylo-object and then both converted to a single "cophylo"-object. The final plot was afterwards adjusted and styled in Inkscape.

A phylogenetic tree, figured below, to illustrate character distributions among epicarideans, is based on the molecular phylogeny of Boyko et al. (2013) and the assignment to (genus-ranked) higher groups (Boyko et al., 2008). The tree topology was created with a manually written edge matrix in a spreadsheet file and converted to a phylo-object in R (ape and phylobase). The final plot along with matching character states (Appendix 2) was generated using the phylo.heatmap
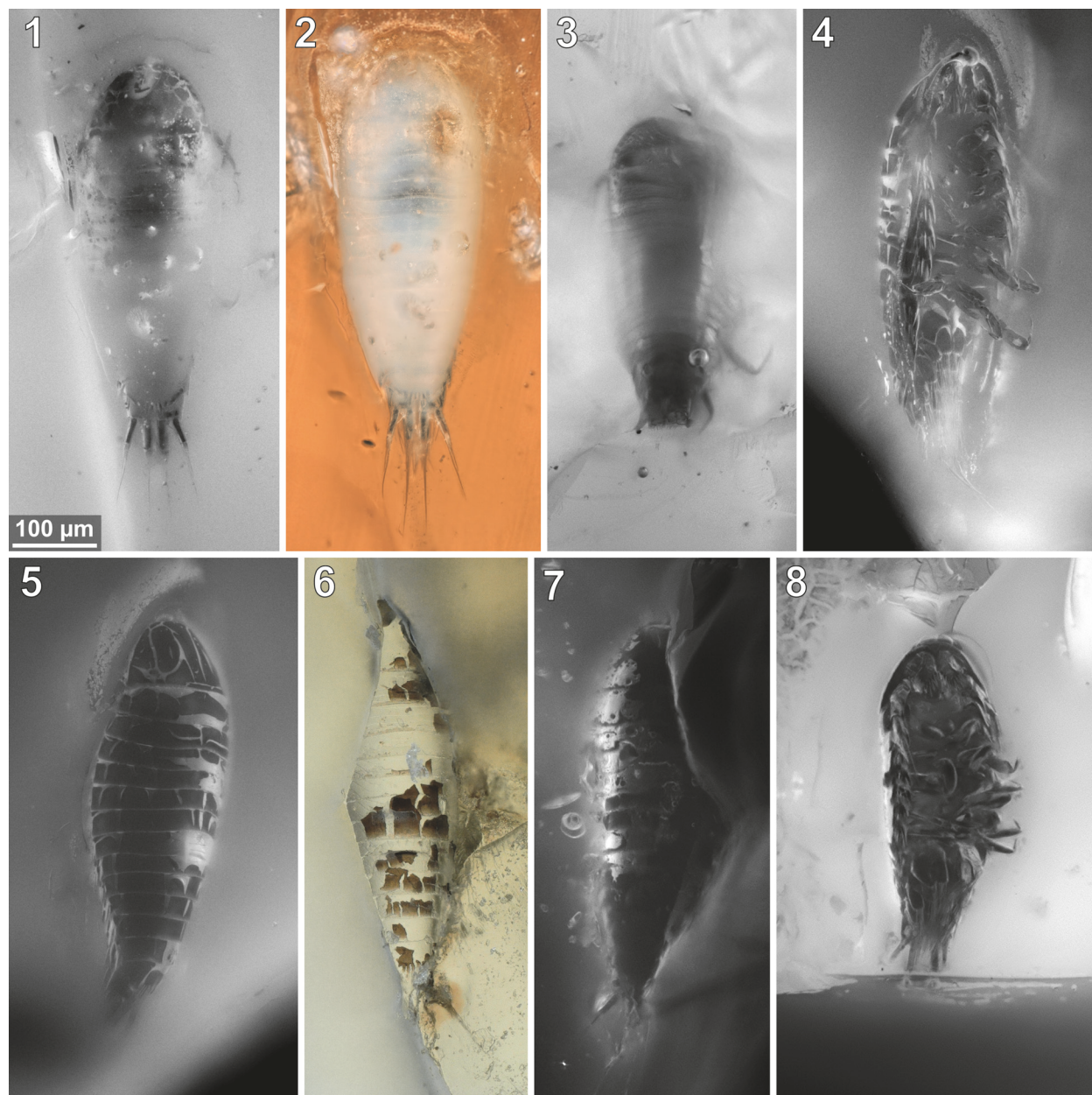
FIGURE 6. *Vacuotheca dupeorum* sp. nov., comparative overview of the type material sorted by collection number (same scale). **6.1-6.2:** Paratype IGR.GAR-41-1, dorsal view, epifluorescence (6.1) and reflected light (6.2). **6.3:** Paratype IGR.GAR-41-2, dorsal view, epifluorescence. **6.4-6.5:** Paratype IGR.GAR-48, ventrolateral view (6.4) and dorsal view (6.5). **6.6-6.7:** Paratype IGR.GAR-51, located at the surface of the amber piece and cracked in roughly frontal plane, ventral view of the dorsal surface (6.6) and dorsal view (6.7), reflected light (6.6) and epifluorescence (6.7). **6.8:** Paratype IGR.GAR-53-1, ventral view, epifluorescence.

function from the phytools package (Revell, 2017) and adjusted in Inkscape.

Measurements

Lengths of cryptoniscium larvae (Appendix 3) were collected from the literature or measured from scaled figures. If not declared otherwise, the body length is measured from the anterior-most point of the head-shield to the posterior-most point of the pleotelson (posteriormost tergite fused with telson). The correction for the z-depth (three-dimensional orientation of the specimens in the resin) was done by examination of the original stack of unprocessed images. The spatial distances between the focal planes of the images are uniform and could be extracted from the microscope. Thus, by count-
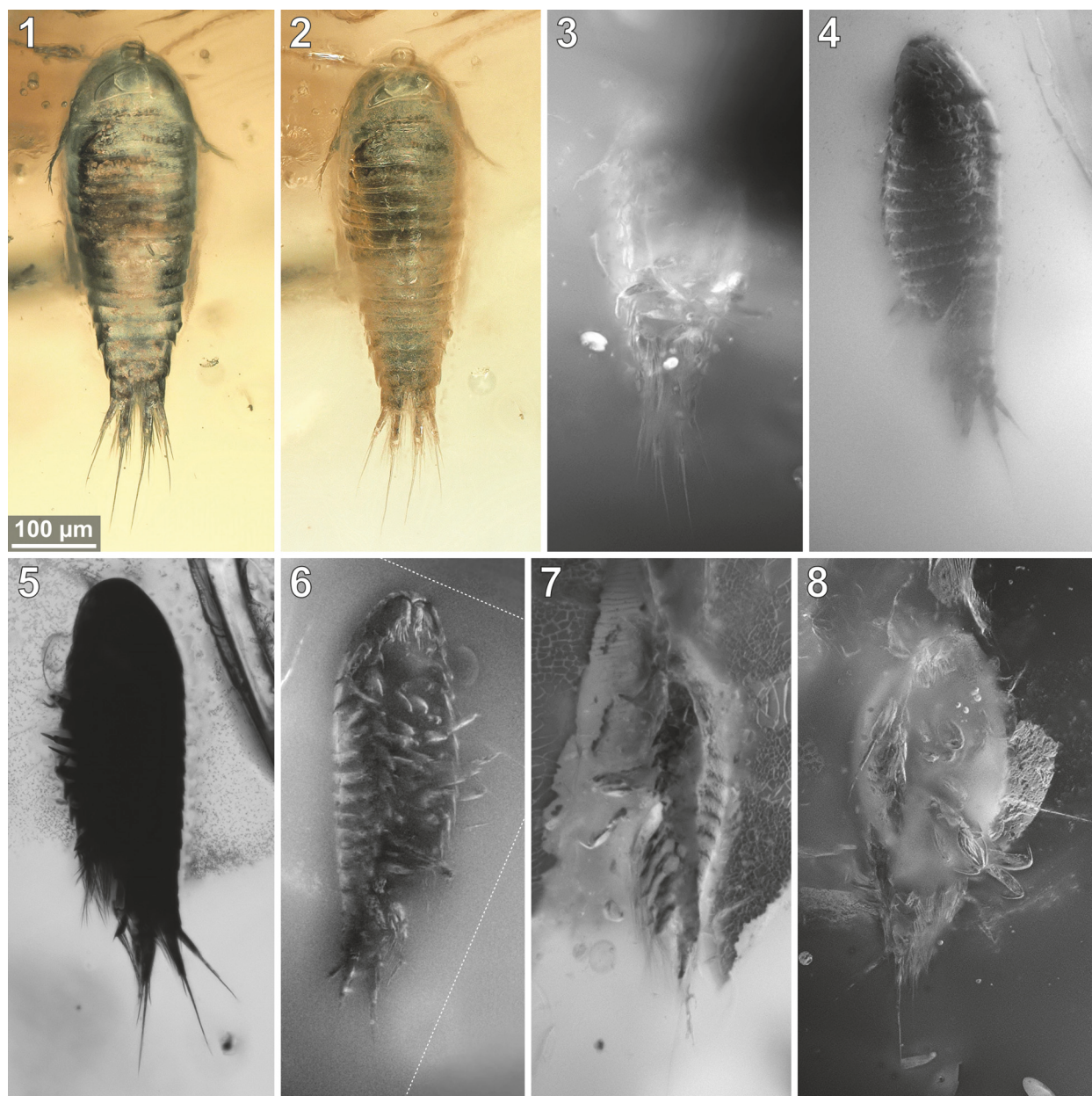
FIGURE 7. *Vacuotheca dupeorum* sp. nov., comparative overview of the type material sorted by collection number (same scale). **7.1-7.3:** Paratype IGR.GAR-53-2, dorsal view (7.1, 7.2) and ventral view (7.3), reflected light with (7.1) and without (7.2) polarising filter and epifluorescence (7.3). **7.4-7.6:** Paratype IGR.GAR-64, dorso-lateral view (7.4) and ventro-lateral view (7.5, 7.6), epifluorescence (7.4, 7.6) and transmitted light (7.5). **7.7:** Paratype IGR.GAR-65, lateral view, epifluorescence. **7.8:** Paratype IGR.GAR-89, ventro-lateral view, epifluorescence. Dashed lines mark areas with artificially created background.

ing interjacent images between structures in focus (defined and known pitches) the z-depth could be determined.

Nomenclature

The body of isopod crustaceans is organised into 20 segments, the ocular segment and 19 post-ocular segments, and the non-somitic telson. The segments form three distinct functional units or tagmata. The first seven segments form the functional head (cephalothorax) including the ocular segments and six appendage-bearing post-ocular segments (segments of antennula, antenna, mandible, maxillula, maxilla and maxilliped). The trunk is further subdivided into two tagmata. The anterior one (pereon) is formed by seven segments (post-ocular
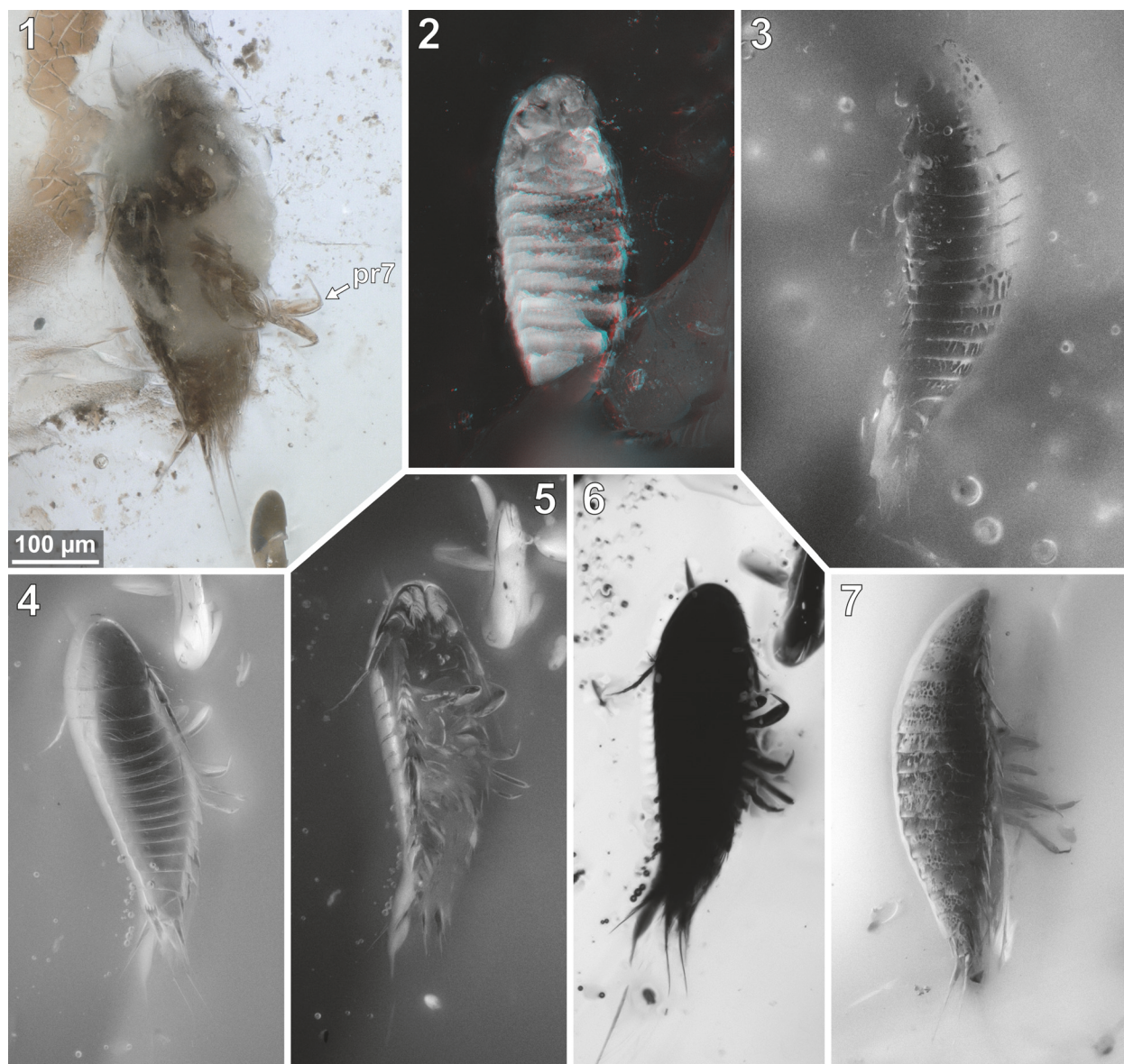
FIGURE 8. *Vacuotheca dupeorum* sp. nov., comparative overview of the type material sorted by collection number (same scale). **8.1:** Paratype IGR.GAR-89, ventro-lateral view, reflected light; **pr7**, pereopod 7. **8.2:** Paratype IGR.GAR-90, located at the surface of the amber piece and cracked in roughly frontal plane, ventral view of the dorsal surface, 3D red-cyan anaglyph of reflected light micrographs. **8.3:** Paratype IGR.GAR-92, lateral view, epifluorescence. **8.4-8.6:** dorsal view (8.4) and ventral view (8.5, 8.6), epifluorescence (8.4, 8.5) and transmitted light (8.6). **8.7:** Paratype IGR.GAR-94, lateral view, epifluorescence.

segments 7-13); each with a separated free tergite and a pair of uniramous walking appendages (thoracic appendages, thoracopods, pereopods). The third tagma, pleon, is formed by post-ocular segments 14-19 and the telson. Pleon segments 1-5 each have a separate free tergite and a pair of biramous swimming appendages (pleopods). Pleon segment six (post-ocular segment 19) is conjoined dorsally with the telson (pleotelson) and bears a pair of biramous appendages (uropods).

We herein use the term microniscium and cryptoniscium instead of microniscus larva and cryptoniscus larva to highlight the interpretation of this morphology as a distinct ontogenetic appearance rather than referring to the historical interpretation as (genus-ranked) animal groups (e.g., "Microniscidae" in Bonnier, 1900). Our intention hereby is to use terms that have no prior charge and to be more consistent with the term epicaridium.

FIGURE 9. *Vacuotheca dupeorum* sp. nov., comparative overview of the type material sorted by collection number (same scale). **9.1-9.3:** Paratype IGR.GAR-95-1, ventral view, reflected light (9.1), transmitted light (9.2) and epifluorescence (9.3). **9.4:** Paratype IGR.GAR-95-2, lateral view, epifluorescence. **9.5:** Paratype IGR.GAR-97, ventral view, epifluorescence. **9.6-9.7:** Paratype IGR.GAR-98, dorsal view, epifluorescence (9.6) and reflected light (9.7). Dashed lines mark areas with artificially created background.

In most cases where the terms microniscium and cryptoniscium have been used many authors did use incorrect plural forms. The correct plural form of microniscium is microniscia and for cryptoniscium is cryptoniscia (second/o-stem declension in a neuter case).

Taxonomic Practice

The International Code of Zoological Nomenclature (ICZN) recommends (no strict regulation) to write genus and species names in italic letters with the intention to separate the (binominal) species name from 'higher taxa' (ICZN 2012, App. B, 6.). However, in our view this is problematic because the genus, besides its function as part of the species name, also ideally represents a natural group (when not monospecific). Therefore we suggest writing generic names in italics when they are used as part of the species name but writing in regular letters when they are used to address natural

13
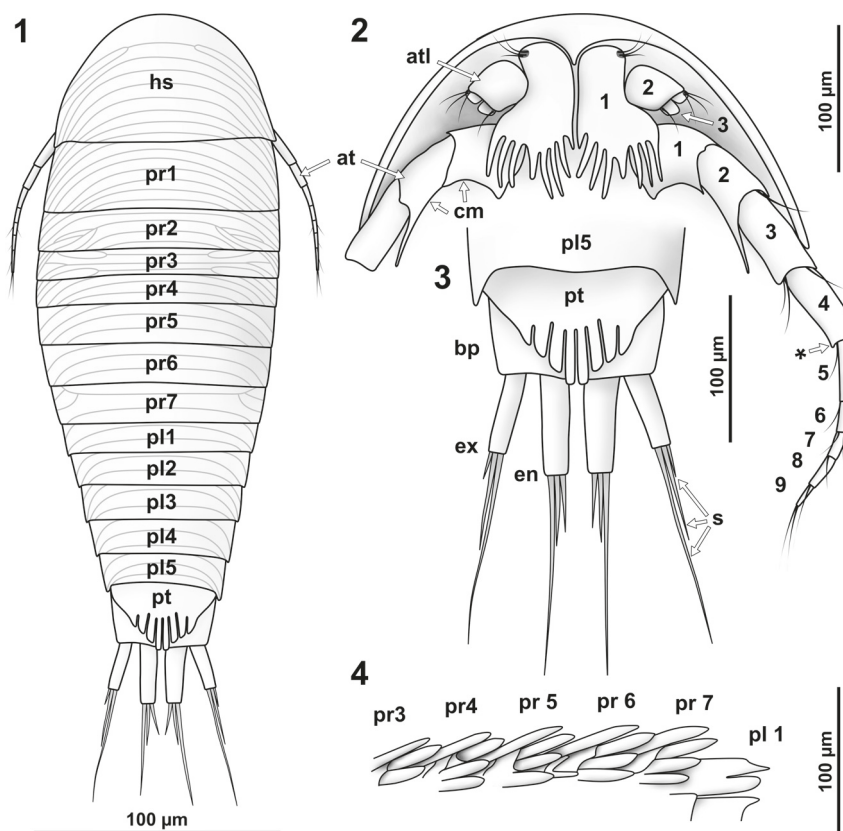
FIGURE 10. *Vacuotheca dupeorum* sp. nov., reconstructions and drawings. **10.1:** Reconstruction in dorsal view (based on multiple specimens) including the striation pattern (based on paratype IGR.GAR-93). **10.2:** Reconstruction based on paratype IGR.GAR-95-1 and holotype IGR.GAR-28, head shield in ventral view, numbers refer to the elements of antennula (numbers on the left side) and antenna (numbers on the right side). **10.3:** Drawing of the paratype IGR.GAR-41-1, uropod region in dorsal view. bs, basipod of the uropod; en, endopod of the uropod; ex, exopod of the uropod; **pl5**, pleon segment 5; **pt**, pleotelson (pleon segment 6 and telson). Drawing of the holotype IGR.GAR-28, coxal plates in ventro-lateral view, mirrored. **per3**-**per7**, pereon segments 3-7; **pl1**, pleon segment 1.

groups (e.g., the groundpattern of Drosophila). This should help the reader to differentiate between references to species vs. references to groups.

RESULTS

Summarizing Description

This description is based on multiple specimens (Figures 5-9). To warrant the traceability between characters and specimens, described characters are followed by an abbreviated reference to the specimens in which the described features were observed: e.g.,"IGR.GAR-8.1 specimen 2" is cited as "[8.1-2]". We tried to cover all characters that were recommended for future descriptions proposed by Nielsen and Strömberg (1965, 1973) wherever it was possible.

General Body Form

The general body form is strictly bilateral with the anterior-posterior body axis being the longest [all specimens]. The dorsal surface is convex with greatest dorsal-ventral extent at about half of the overall body length (Figure 5.4) [8.1-1, 8.2, 28, 48, 64, 92, 93, 94, 95-2]. The dorsal outline of the complete body (without appendages) is ovate to drop-shaped with the broadest point at about the half of the body length and tapering posteriorly (Figures 7.1, 10.1) [41-1, 41-2, 53-2, 95-1, 97, 98]. The ventral side of the animal (without appendages) is concave, and the resulting space is occupied by the appendages (Figure 5.7) [8.1-2, 28, 48, 53-1, 64, 89, 93, 95-1, 95-2, 97]. The overall size of the main body (excluding anterior and posterior appendages, i.e., antennula and uropods) ranges from 366 μm [53-1] to 495 μm [8.2] with a mean of 423
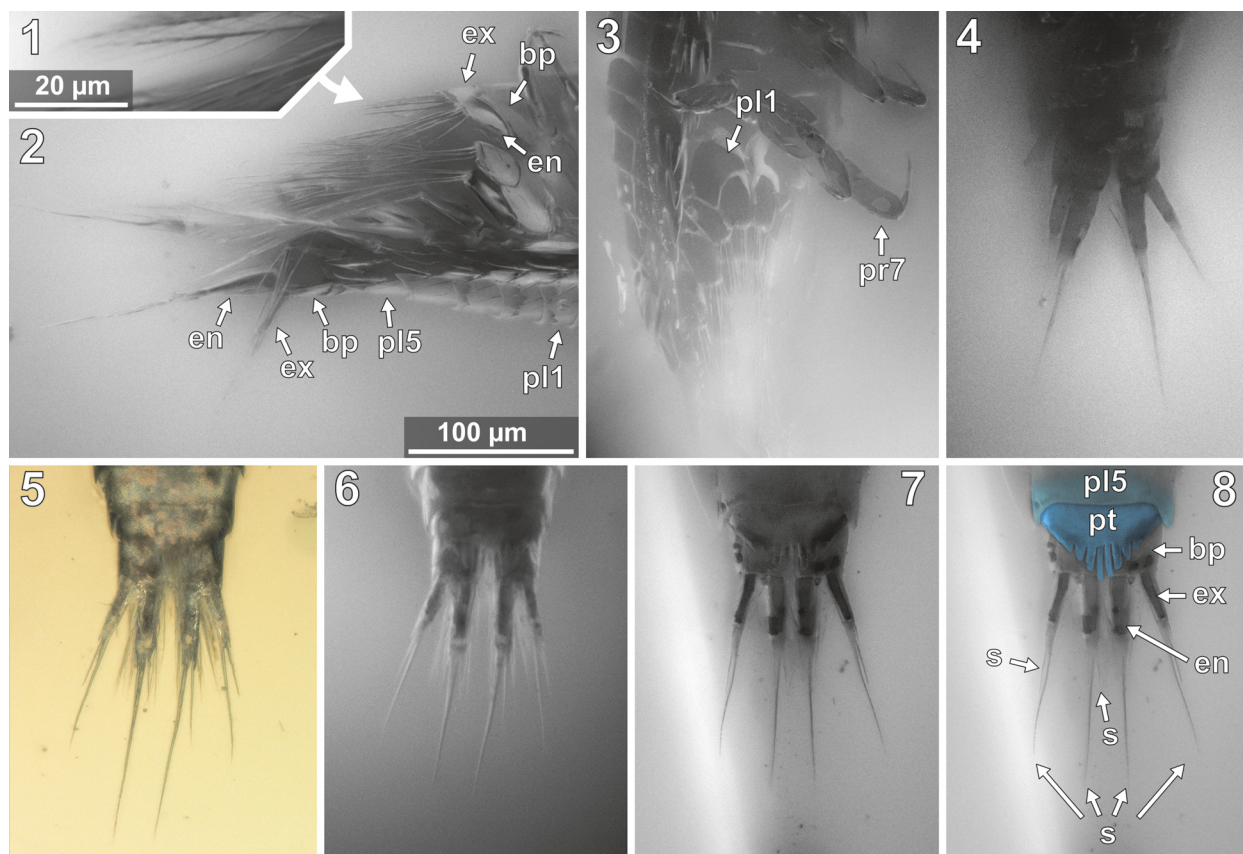
FIGURE 11. *Vacuotheca dupeorum* sp. nov., detailed images of the pleon and the uropod region (11.2-11.8 with same scale). **11.1:** Holotype IGR.GAR-28, setulose setae on pleopod 1, ventro-lateral view, epifluorescence. **11.2:** Holotype IGR.GAR-28, pleon and uropods in ventro-lateral view, epifluorescence. **bas**, basipod of pleopod 1; **en**, endopod of the pleopod 1; **ex**, exopod of the pleopod 1; **pl1** and **pl5**, pleopod segment 1 and 5; **up**, uropod segment. **11.3:** Paratype IGR.GAR-48, pleon region in ventral view, epifluorescence. **pr7**, propodus of pereopod 7. **11.4:** Paratype IGR.GAR-64, uropod region in dorsal view, epifluorescence. **11.5-11.6:** Paratype IGR.GAR-53-2, uropod region in dorsal view, reflected light (11.4) and epifluorescence (11.5). **11.7 - 11.8:** Paratype IGR.GAR-41, uropod region in dorsal view, epifluorescence. **bas**, basipod of the uropod; **en**, endopod of the uropod; **ex**, exopod of the uropod; **pl5**, pleon segment 5; **pt**, pleotelson (pleon segment 6 and telson); **st**, setae.

µm and a corresponding standard deviation of 32 µm.

Dorsal Sclerites

Dorsal areas of the ocular segment and post-ocular segments 1-6 (segments of antennula, antenna, mandibula, maxillula, maxilla and maxilliped) form a single dorsal sclerite, head shield. The dorsal surfaces of the post-ocular segments 7-18 (trunk segments 1-12) form free tergites. [8.1-1, 8.2, 28, 41-1, 48, 53-2, 64, 92, 93, 94]. The tergite of the post-ocular segment 19 (pleon segment 6, uropod segment) is conjoined with the telson [8.2, 41-1, 48, 53-2, 64, 92, 93, 94, 98] forming a pleotelson that is roughly triangular in dorsal view (Figures 10.3, 7.1, 11.8). The pleotelson has a rounded posterior corner and a toothed posterior margin [41-1, 48, 53-2, 64, 93, 98] bearing six straight posterior pointed teeth with blunt tips (Figure 11.6-11.8) [41-1, 53].

Head Shield

The anterior margin of the head shield is almost half-circular in dorsal view (Figure 6.1-2) [41-1, 41-2, 53-2, 64, 95-1, 98]. The head shield has a convex dorsal surface, and its ventral margins lie in one plane (Figure 5.4). A median posterior-pointed extension protrudes from the anterior margin of the head shield forming a triangular ventral plain surface and corresponding to lateral concave lateral spaces that are occupied by the antennulae (Figure 12.1) [8.1-2, 28, 48, 53-1, 64, 93, 95-1, 97].
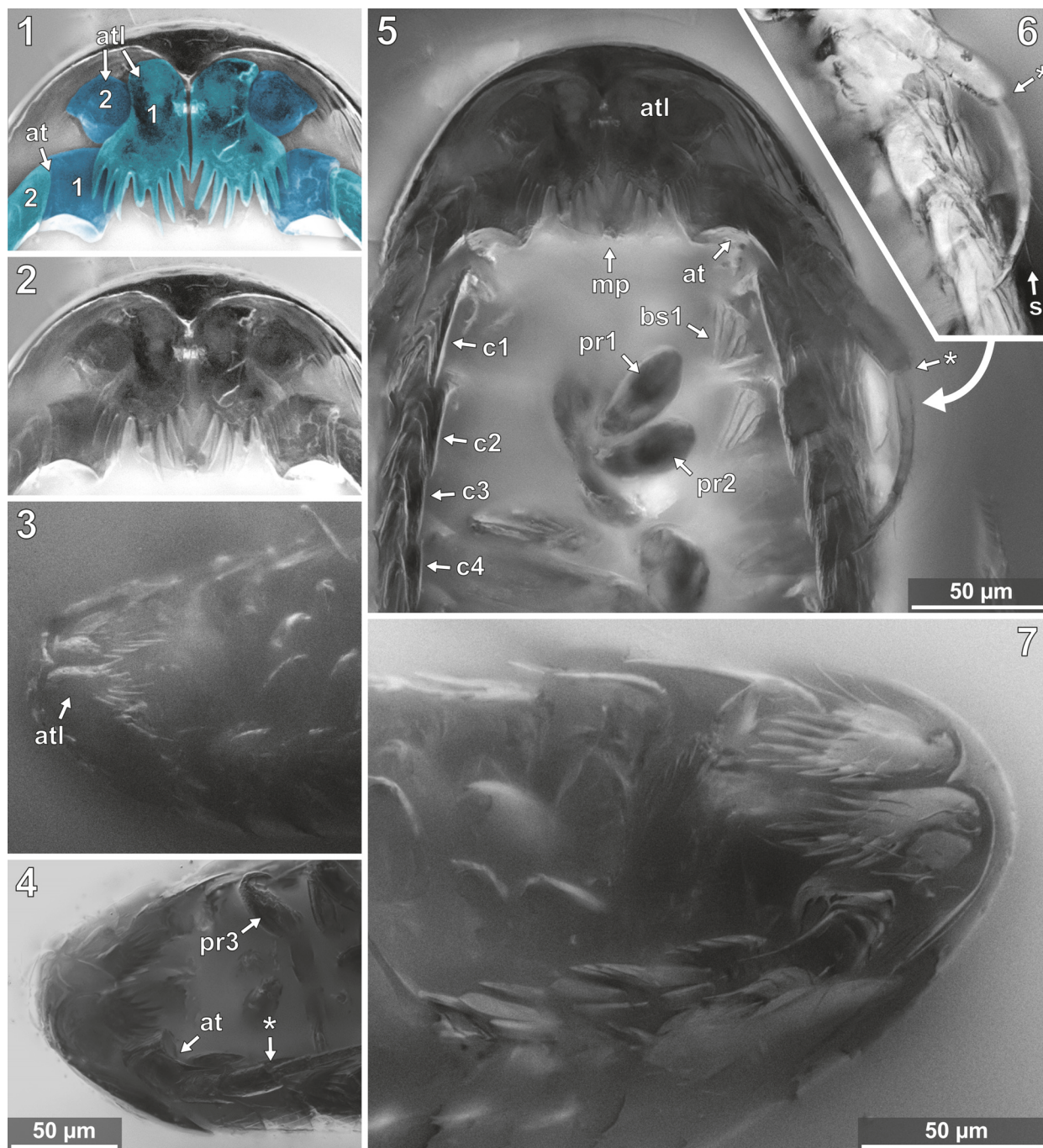
FIGURE 12. *Vacuotheca dupeorum* sp. nov., detailed images of the head region. **12.1-12.2:** Paratype IGR.GAR-95-1, head region in ventral view, epifluorescence, numbers refer to the elements of antennula (**atl**) and antenna (**ant**), in blue colour (12.1), same scale as 12.4. **12.3:** Paratype IGR.GAR-64, head region in ventro-lateral view, epifluorescence, same scale as 12.4. **12.4:** Paratype IGR.GAR-53-1, head region in ventro-lateral view, epifluorescence. **pr3**, propodus of pereopod 3; *, junction between antennal peduncle and flagellum (element 4 and element 5). **12.5-12.6:** Paratype IGR.GAR-95-1, head and pereon region in ventral view (12.5) and distal antenna elements in ventral view (12.6), epifluorescence, same scale. **bs1**, basipod of pereopod 1; **cp1-cp4**, coxal plates of pereon segments 1 to 4; **dc1-dc2**, dactsyli of pereopods 1 and 2; **mp**, mouthparts; **s**, seta. **12.7:** Holotype IGR.GAR-28, head region in ventro-lateral view, epifluorescence, compare to 10.2 for identification of details.
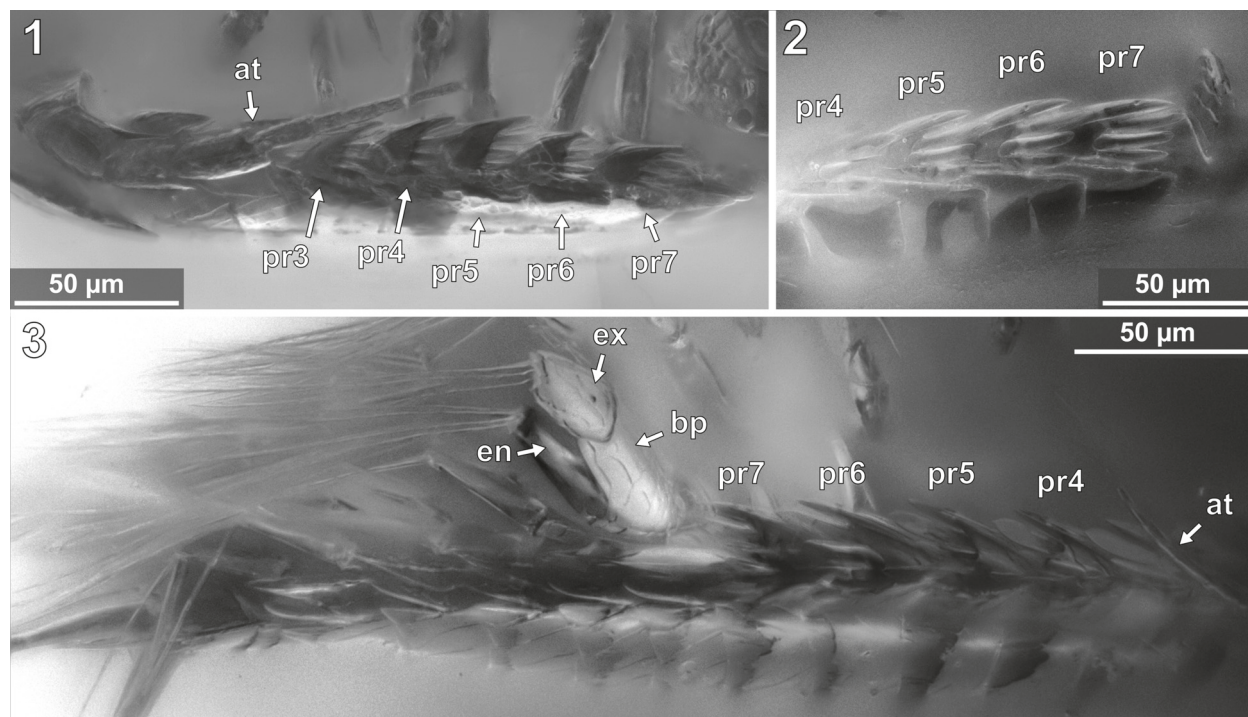
FIGURE 13. *Vacuotheca dupeorum* sp. nov., detailed images of the lateral body side. **13.1:** Paratype IGR.GAR-53-1, ventro-lateral view, epifluorescence. **at**, antenna; **pr3**-**pr7**, pereopod segments 3 to 7, arrows point to the corresponding coxal plates. **13.2:** Paratype IGR.GAR-48, ventro-lateral view, epifluorescence. **13.3:** Holotype IGR.GAR-28, ventro-lateral view, epifluorescence. **bp**, basipod of pleopod 1; **en**, endopod of pleopod 1; **ex**, exopod of pleopod 1.

Eye-structures are not apparent [8.1-1, 8.2, 28, 41-1, 48, 53-2, 64, 92, 93, 94, 98]. However, this must not necessarily mean that the living animal possessed no optical sensory organs (see discussion).

Tergites

The tergites have a convex dorsal surface, which anteriorly conforms with the head-shield. The preservation of the tergite surfaces is variable. In some specimens it appears smooth (Figure 5.4) [8.2, 28, 41-1, 48, 93, 98]. In other specimens the smooth surface is disrupted by large extensive or multiple small crater-like gaps (Figure 8.7) [8.1-1, 41-1, 51, 65, 94], which can appear darker or brighter with respect to the fluorescent characteristics of the surrounding surface areas. One specimen shows a fluent transition between the small and large gaps on the dorsal surface (Figure 8.3) [92].

In some of the specimens a striation pattern is visible, which consists of more or less parallel sometimes bifurcating lines, which appear brighter or darker under fluorescent light than the surrounding surface areas (Figure 8.4, 10.1) [8.2, 41-2, 48, 53-2, 92, 93, 98]. The striation has some variation between the specimens. Also, the position of the specimens and their accessibility by microscopy preclude further statement about the bilateral symmetry of the striation. The striation pattern is also preserved in specimens where the organic matter of the specimen is separated from the amber matrix (shrinking). Here, the surface of cavity in the resin bears the morphological information of the (putative) original surface of the animal. The striation pattern is thus depicted by the light refraction of the amber surface, which has kept it as a counterpart (Figure 6.6) [48, 51]. The ventro-lateral margins of the tergites of the pleon segments each have two pointed lobes directing posterior (Figure 13.3) [8.1-2, 28, 48, 53-1, 94].

Antennula

The antennula (appendage of post-ocular segment 1) consists of three peduncle elements and two flagella (Figures 10.2, 12.1-2) [28, 93, 95]. The first element has a large plate-like posterior-oriented extension bearing multiple teeth on its distal margin; the anterior margin is continuous and without a plate-like extension [8.1-2, 28, 48, 53-1, 64, 89, 93, 95-1, 97]. The first antennula element bears three setae antero-laterally and distally, all

arising close to each other (Figures 10.2, 12.2, 12.7, Appendix 4) [28, 48, 93, 95]. The functional ventral surface (originally anterior) of the antennula plates has sharp furrows that correspond to the proximal origins of the posterior pointing teeth of the posterior expansion of the first antennular element (Figure 12.7) [28, 93]. There are eight teeth on the plate-like posterior-oriented extension of the first antennula element in all specimens (where counting was possible) (Figures 10.2, 12.2, 12.3, 12.4, 12.7) [28, 53-1, 64, 95].

Element two is about as long as element one (without extension) and is roughly quadratic in ventral view [28, 53-1, 95]. Element two lacks teeth and plate-like extensions (Figures 10.2, 12.1-12.2) [28, 48, 53-1, 93, 95].

A presumably present third antennular element is not discernible from the microscopic photographs. It is the third element that usually bears two distal flagella, which are also apparent here. Each flagellum consists of a single element [28, 93, 95]. The anterior flagellum bears three delicate setae and the posterior flagellum bears at least one delicate seta (Appendix 4) [28].

Antenna

The antenna (appendage of post-ocular segment 1) is composed of nine elements, coxa, basipod and seven endopod elements, functionally organised into four peduncle elements [28, 53, 93, 95-1] and five flagellum elements (Figures 10.2, 12.5, 12.6) [8.1-1, 8.1-2, 8.2, 28, 53-1, 53-2, 89, 93, 94, 95-1]. In dorsal view the first two peduncle elements are always concealed by the body, and the third antennal element protrudes from the postero-lateral corner of the head shield (Figure 7.1) [8.1-1, 8.1-2, 8.2, 28, 64, 41-1, 41-2, 53-1, 53-2, 90, 93, 95-1, 97, 98].

The peduncle elements are distinctly wider than the flagellum elements [8.1-1, 8.1-2, 8.2, 28, 41-1, 41-2, 53-1, 53-2, 48, 93, 94, 95-1, 97]. Element one and two (coxa and basipod) together form a continuous concave median (functional posterior) margin that distally ends in the spine-like prolonged postero-distal corner of the second element (Figure 10.2, 12.4, 12.5) [28, 53-1, 95]. Element two bears at least one seta distally at its anterior (functional ventral) side. Element three bears three setae distally on the ventral side. Element 4 bears at least one seta distally on its anterior (functional ventral) side (Figure 10.2, Appendix 4 and 5) [28, 53-1].

The flagellum elements are barrel shaped to slightly conical and decrease in diameter distally

(Figure 12.6) [8.1-1, 8.1-2, 8.2, 28, 53-1, 89, 93, 94, 98]. Fifth antennal element (proximal flagellum article) with two distal setae (Figure 10.2) [8.1-1]; sixth element with at least one distal seta [53-2, 93, 95]; seventh element with two distal setae [8.1-1, 28]; eighth element with one distal seta [8.1-1, 53-2, 28]; ninth (distal-most) element with two distal setae (Figure 10.2, Appendix 4) [28, 53-2].

Mouthparts

The mouthparts (appendages of post-ocular segments 3-6; mandible, maxillula, maxilla, maxilliped) form a posteroventral-pointing cone (Figure 12.5) [28, 53, 93, 95]. The cone is concealed by an anterior larger sclerite that encompasses about two thirds of the perimeter of the cone and a smaller triangular posterior sclerite (only visible in the original stack of images, Appendix 4) [28, 53]. The cone is apically truncated with a narrow opening (Figure 12.2, Appendix 4) [28, 53, 95-1].

Pereopods (appendages of the pereon segments/post-ocular segments 7-13)

Each of the seven free thoracic segments bears a pair of appendages (pereopods). Each consists of seven elements. Element one, coxa, forms a plate like structure that lies in extension to the lateral margin of its corresponding tergite (coxal plates). Coxal plates bear posterior teeth (Figures 10.4, 13.2) [8.1-2, 8.2, 28, 48, 53-1, 89, 93, 95-1, 95-2, 97]. All coxal plates have four teeth (in specimens where the preservation allowed for counting) [28, 48, 53-1, 64]. Posterior to the coxal plates, in the pleon segments, are lateral extensions of the tergites that superficially resemble the coxal plate morphology (see description of tergites, Figure 13.3).

Element two (basipod) is large. Element three (ischium) is slightly shorter. Elements four and five (merus, carpus) are short. Element six (propodus) is large. Element seven (dactylus) is spine-like and slightly curved inwards. The thoracic appendages become progressively longer towards the posterior end of the body. The first two pereopods are both short, the third is longer, the fourth even more. The fifth pereopod is longer than the fourth and about as long or only slightly shorter than pereopods 6 and 7, which are the longest and about the same length (Figure 14.2, 15) [53-1].

Pereopod 1. The basipod is broad and with a concave space at the median side (Figure 12.5, 12.7 14.1) [28]. The propodus is broad and only weakly anterior-posteriorly compressed with an oval outline in anterior view (Figure 12.5, 14.1) [28, 53-1,
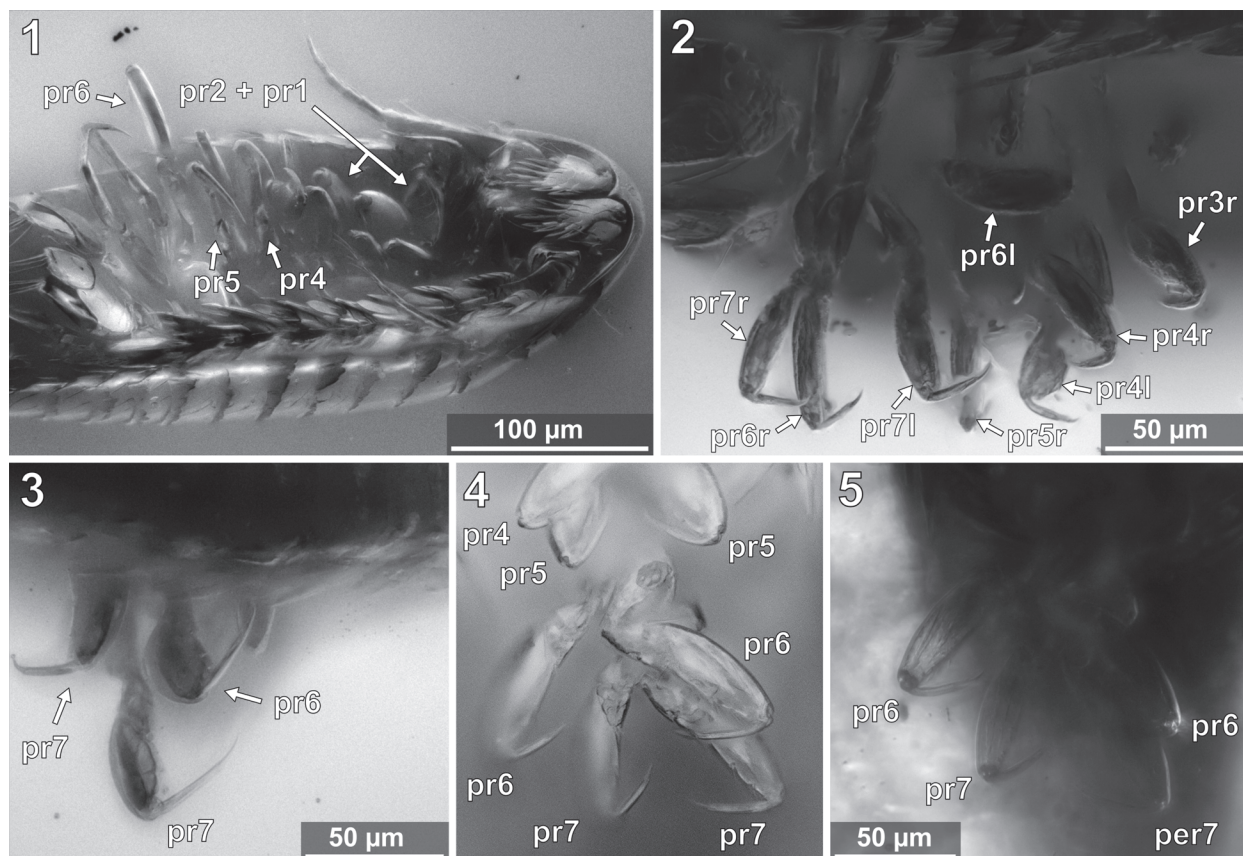
FIGURE 14. *Vacuotheca dupeorum* sp. nov., detailed images of the pereopods. **14.1:** Holotype IGR.GAR-28, ventro-lateral view, epifluorescence. **pr1-2** and **pr4-6**, pereopods 1-2 and 4-6. **14.2:** Paratype IGR.GAR-53-1, pereopods in lateral view, right side of the image is anterior, epifluorescence, for labels see Figure 15 (corresponding drawing with labels). **14.3:** Paratype IGR.GAR-8.1-1, posterior pereopods in lateral view, right side of the image is anterior, epifluorescence. **pr6-pr7**, pereopods 6 and 7. **14.4-14.5:** Paratype IGR.GAR-95-1, pereopods in ventral view, upper side of the image is anterior, same scale. **pr4-pr7**, pereopods 4 to 7.

95-1], the median margin of the propodus is distally with a soft angle. The dactylus is curved inward and with a pointed tip (Figure 14.1).

Pereopod 2. The propodus is weakly compressed in anterior-posterior axis, with an oval in outline in anterior view (Figure 14.1) [28, 53-1, 95-1], the median margin of the propodus is distally with a soft angle.

Pereopod 3. The basipod is long and slender, much narrower than in pereopod 1 (Figures 14-15) [53-1]; the propodus is weakly compressed in anterior-posterior axis, with an oval outline in anterior view (Figures 14-15) [28, 53-1, 95-1], the median margin of the propodus is distally with a soft angle and a set of two setae distal to the angle (Figure 12.4) [28, 53-1, 95-1]. The dactylus is curved inward and with a pointed tip (Figures 14-15).

Pereopod 4. The basipod is long and slender, much narrower than in pereopod 1 (Figures 14-15) [53-1]. The propodus is compressed in anterior-posterior axis (Figure 14.1) (resulting in an even

anterior and posterior surface) and longer and narrower as that of pereopods 1-3, the median margin of the propodus is distally with a distinct soft angle and a set of two setae distal to the angle (Figures 14-15) [28, 53-1, 95-1]. The dactylus is slightly curved inward and with a pointed tip (Figure 14.1-2).

Pereopod 5. The basipod is long and slender, much narrower than in pereopod 1 (Figures 14-15) [53-1]. The propodus is compressed in anterior-posterior axis (resulting in an even anterior and posterior surface) and longer and narrower as that of pereopods 1-3 (Figure 14.1), the median margin is distally with a set of two setae [28, 53-1, 95-1]. The dactylus is slightly curved inward and with a pointed tip (Figure 14.4).

Pereopod 6. The basipod is long and slender, much narrower than in pereopod 1 (Figures 14-15) [53-1]. The ischium is compressed in anterior-posterior axis with a convex lateral margin and a straight median margin (Figures 14-15) [53-1]. The

19
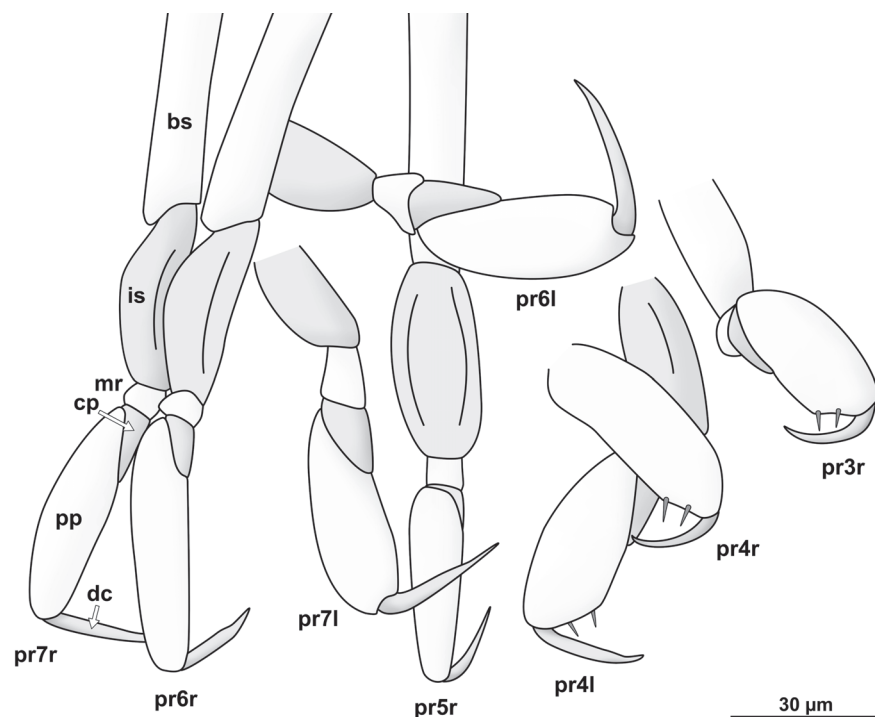
FIGURE 15. *Vacuotheca dupeorum* sp. nov., paratype IGR.GAR-53-1, drawing of pereopods 3 to 7 **(pr3–pr7). (r)**, right body side; **(l)**, left body side; **bs**, basipod; **is**, ischium; **mr**, merus; **cp**, carpus; **pr**, propodus; **dc**, dactylus. Notice the setae on the propodi of pereopods 3 and 4.

merus is short and roughly triangular in anterior view (Figures 14-15) [53-1, 89, 95-1]. The carpus is short and roughly triangular in anterior view (Figures 14-15) [53-1, 89, 95-1]. The propodus is antero-posteriorly compressed (resulting in an even anterior and posterior surface) and longer and narrower as that of pereopods 1-3 (Figure 14.1), the median margin is distally with a set of two setae [28, 53-1, 95-1] and with two proximo-distal strings of muscles distally attaching to the lateral and median side of the dactylus joint (Figure 14.5) [89, 95-1]. The dactylus is slightly curved inward and with a pointed tip.

Pereopod 7. The basipod is long and slender, much narrower than in pereopod 1 (Figures 14-15) [53-1]. The ischium is anterior-posteriorly compressed with a convex lateral margin and a straight median margin (Figures 14-15) [53-1]. The merus is short and roughly triangular in anterior view (Figures 14-15) [53-1, 89, 95-1]. The carpus is short and roughly triangular in anterior view (Figures 14-15) [53-1, 89, 95-1]. The propodus is antero-posteriorly compressed (resulting in an even anterior and posterior surface) and longer and narrower as that of pereopods 1-3, the median margin is distally with a set of two setae (Figure 14.4) [28, 53-1, 95-1] and with two proximo-distal strings of muscles distally attaching to the lateral and median side of

the dactylus joint (Figure 8.1) [89, 95-1]. The dactylus is slightly curved and with a pointed tip (Figure 14.3).

Pleopods (appendages of the pleon segments/ post-ocular segments 14-18)

The pleopods consist of a broad basipod which distally bears the median endopod and the lateral exopod (Figures 13.3, 11.2) [28, 48, 53-1, 97]. All elements are strongly compressed in anterior-posterior axis and roughly leaf-shaped. The endopods are broader and more massive than the corresponding exopods [28, 48, 53-1, 97].

Endopod and exopod bear long setae distally (Figure 11.2) [8.1-1, 8.1-2, 8.2, 28, 48, 53-1, 53-2, 64, 89, 97]. The setae originate in an obtuse angle from the pleopods and point posteriorly (Figure 11.2) [8.1-1, 28, 64]. Pleopod 1 is with at least five setae on the endopod and four setae on the exopod (Figure 11.2) [28]. Pleopod 2 is with at least five setae on the exopod [28]. Pleopod 3 is with at least three setae on the endopod and four setae on the exopod (Figure 11.2) [28].

At least in pleopods 1, the distal setae are setulose with delicate posterio-laterally protruding setulae. The setulae are less than 1 µm in diameter and ca. 15 µm long (Figure 11.1) [28].

Uropod (appendage of post-ocular segment 19)

The uropods consist of a basipod which distally bears the median endopod and the lateral exopod. The basipod of the uropods is massive and rectangular in dorso-ventral view [8.1-1, 41-1, 41-2, 53-1, 53-2, 64, 93, 98]. Basipods are apparently movable in relation to the trunk as specimens with (parallel) posterior pointed (Figure 11.7) [41-1, 41-2, 53-2] and somewhat spread (laterally diverging) basipods (Figure 11.4) [64, 98] suggest. Endopods and exopods are truncated cone-shaped (tapering distally). Endopods and exopods are apparently movable in relation to the basipod as the angle between both elements and the angle between each of the elements and the corresponding basipod vary in one specimen (Figure 11.4). Endo- and exopods are ovate to rectangular in cross-section (greatest diameter in dorsoventral direction) (Figure 6.3) [41-2]. The endopods are longer and thicker than the exopods (Figure 10.3, 11.4-8) [8.1-1, 8.2, 28, 53-1, 53-2, 64, 89, 98] and distally bear one long and one short seta (Figure 11.5) [53-2]. The exopods are about as long as the basipods (Figure 10.3, 11.4-8) [8.1-1, 53-2, 64, 28] and distally bear one long (about twice as long as the exopod) and one short seta (Figures 10.3, 11.5, 11.7) [53-2].

DISCUSSION

Systematic Interpretation

Assuming that the cone shaped feeding apparatus consists of appendages of more than one segment (four segments in Epicaridea), the functional head comprises at least four appendage-bearing segments, which is apomorphic for Euarthopoda (sensu Walossek, 1999, e.g., Haug et al., 2013). The trunk is divided in two distinct sets of segments (thorax and pleon), which are considered as an apomorphy of Eumalacostraca (Walossek, 1999).

The body is dorsoventrally flattened, and the tergite of the first thoracic segment (maxilliped) is conjoined with the tergites of the functional head. The lateral flagellum of the antennula is not well developed but consists only of a single short element. Also, all pereopods (appendages of post-ocular segments 7-13) lack an exopod. This combination of characters is unique and characterizes the group Isopoda (Ax et al., 2000; Wilson, 2009). All pereopods bear lateral plate-like extensions of the coxa (coxal plates), which is an autapomorphy of Scutocoxifera (Dreyer and Wägele, 2002). The mouthparts (mandible, maxillula, maxilla and maxil-

liped) form a cone-like structure, which is only known for parasitic isopods within Cymothoida (if including Gnathiidae).

The combination of the following characters is typical for larvae of the group Epicaridea (Latreille, 1825): body elongated and drop shaped; mouthparts forming a cone like structure; antennula with enlarged first element; pereopods with large propodi and thin, spine like and often curved dactyli; truncated cone-shaped uropod rami.

Within Epicaridea, a further determination providing identifications to monophyletic groups is not possible due to the absence of undisputed apomorphies in most groups. Within Epicaridea, Dajidae (Sars, 1883) is the only group with a well-accepted apomorphy that can be seen in the cryptoniscium stage. In Dajidae cryptoniscia have an oral cone with a conspicuous sucking disk (Bresciani, 1966; Schultz, 1975; Wägele, 1989).

Thus, the herein presented specimens can be interpreted as epicarideans that are not (latin: nec) part of the epicaridean ingroup Dajidae (Epicaridea nec Dajidae). We demonstrated that the morphology of the herein presented specimens fits perfectly with that of the cryptoniscium larvae of Epicaridea. However, the exact ontogenetic phase of the fossils cannot be determined with certainty. In some epicaridean lineages (Cryptoniscoidea) the adult male does (at least superficially) not differ morphologically from the cryptoniscium (Hosie, 2008). Therefore, the studied fossils could not only represent cryptoniscium larvae but also adult males with a paedomorphic morphology. Paedomorphic, strict-protandric males (as they occur in most cryptoniscoideans) have been recorded to switch between host animals on a regular basis to inseminate females and finally find a host that is not infected by other epicarideans where they transform into a female (Wägele, 1989).

Conspecifity

We assume conspecifity for the herein studied specimens. This is based on the lack of conspicuous morphological differences among the individuals (as lain out in the description). Also, the body size is relatively uniform with a standard deviation of 32 µm (7.5 % of the mean body size). Only the dorsal striation pattern is subject to some variation within the studied specimens (Figures 5.3, 5.4, 6.2, 6.6, 7.2, 8.3, 8.4, 9.7, 10, 14.8). However, without data on the degree of variability of the striation pattern in modern species, it is impossible to draw conclusions on the intra- and interspecific variability of this character in extinct species.

Striation

The dorsal surface as well as various other body regions of cryptoniscium larvae bears a surface pattern that superficially appears as lines (striae/striation). In the first extensive study focusing on the surface structure of cryptoniscia using scanning electron microscopy, Nielsen and Strömberg (1973) categorized striation patterns in two types. They characterized the striae on the dorsal side of the head shield as "rather broad cuticular ridges separated by narrow furrows." Striae on other parts of the body, like the pleopod basipod, were characterized as "pectinate scales." They also perfomed transmission electron microscopy to study the structure of the striae. By this, they found the striae to affect only the epicuticle but not the endocuticle. This distinction appears somewhat arbitrary because both types of striae are purely epicuticular, and both the "pectinate scales" and the ridges and furrows are asymmetric, as the transmission electron microscopy images show. It could be possible that both types differ only (gradually) in scale, collocation and manifestation of the fringes (ctenae).

Judging from the scale of the striae it is very likely that especially a dense striation pattern appears like a homogeneous surface in light microscopy and is thus been overlooked possibly partly here, but also more generally in the literature.

The visibility of this pattern in some of the herein studied fossils is highly dependent on the illumination of the specimen (e.g., compare Figure 6.1 vs. 6.2 or 7.1 vs. 7.2). The striation pattern is more or less pronounced in cryptoniscia of different epicaridean groups (Nielsen and Strömberg, 1973; Hosie, 2008). To our knowledge there is no information about the intraspecific variability of the striation for modern species that would be useful for the interpretation of future fossil findings.

Eyes

Although eyes are not visible in the studied specimens, we cannot conclude their absence. In many modern cryptoniscia the compound eyes are highly reduced so that they are only recognizable as dark spots beneath the dorsal surface of the head shield (Nielsen and Strömberg, 1973). Only one extant species of epicarideans has been recorded to have cryptoniscia with externally visible eyes, as well as a single fossil specimen (Schultz, 1975; Serrano-Sánchez et al., 2016).

Antennula

Wägele (1989) suggested that the toothed posterior projection of the first antennula element (antennular plate) could be an autapomorphy for Cryptoniscoidea. Based on figures and descriptions in taxonomic literature (summarized in Figure 16), we cannot support this assumption. Indeed, at least two species with a toothed margin of the antennula plate have been interpreted as representatives of Bopyroidea (*Probopyrus bithynis* Richardson, 1905, in Dale and Anderson, 1982) and *Leidya distorta* Comalia and Panceri, 1858, in Torres Jordá, 2003).

Also, Wägele (1989) suggested that a continuous margin of the antennula plate, in contrast to a toothed margin (orange colour compared to beige colour in Figure 16) could be an autapomorphy of monophyletic group combining Asconiscidae, Crinoniscidae and Cryptoniscidae. This must be seen as distinct from cases in which antennula element one has no distinct posterior projection (red in Figure 16). We support this assumption based on our study of literature. If future phylogenetic analyses support the monophyly of this group, we recommend the erection of a proper name for this group, as well as to include the two species *abyssorum* Bourdon, 1981, and *longicaudatus* Schultz, 1975, in it, which possess this specific structure (both known from cryptoniscia only and traditionally interpreted as Cryptoniscoidea incertae sedis).

Given that the distribution of a toothed antennula plate in cryptoniscia is not restricted to a single subgroup of Epicaridea, also a different polarity of the character than proposed by Wägele (1989) has to be considered. The toothed antennula plate could represent an autapomorphy of Epicaridea that has been lost several times independently.

The orientation of the mouthparts (sucking cone) seems to constrain the shape and size of the proximal element of the antennula. This seems to affect whether or not a posterior extension of the antennular plate is developed and also, if there is a posterior expansion it seems to affect the orientation of the antennular plate. Indeed, in species that have mouthparts anteriorly directed (e.g., *Probopyrus pandalicola*) the median margins of the first antennula element are not parallel but diverge posteriorly.

Little intraspecific variability in epicaridean species has been recorded regarding the number of these teeth. However, a few cases of intraspecific but also intra-individual differences have been recorded (Nielsen and Strömberg, 1973).
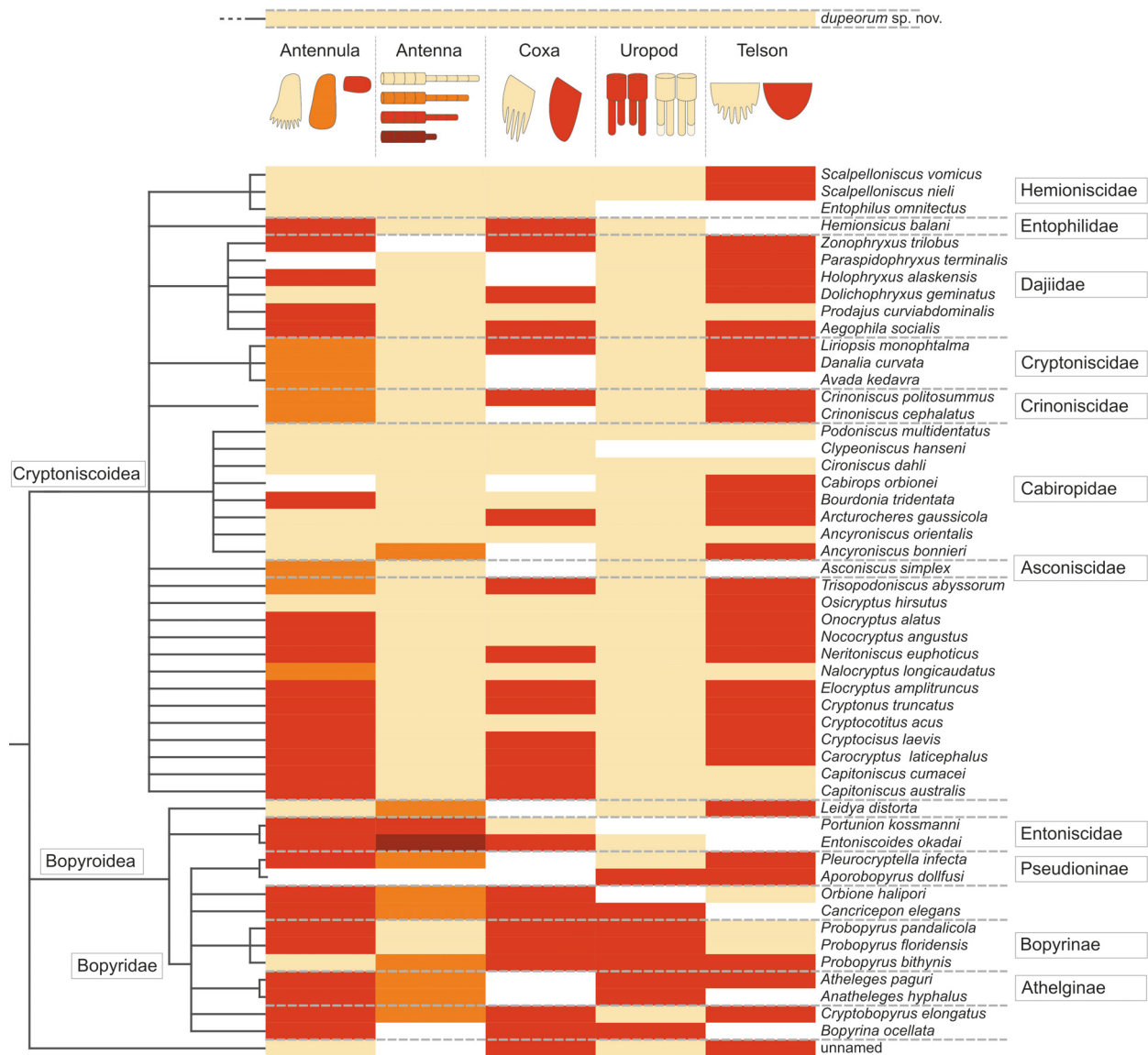
FIGURE 16. Phylogenetic tree of Epicaridea (Boyko et al., 2013) (topology on the left side, species names and taxonomic groups on the right side) mapped with characters gathered from descriptions and illustrations of literature. Characters are coded in colour as depicted in the illustration at the top. Beige is reserved for character states in *Vacuotheca dupeorum* gen. et sp. nov. (at the very top). Antenna: five flagellum elements (beige), four flagellum elements (orange), three flagellum elements (red), one flagellum elements (orange). Uropod: endopods longer or equal as exopods (beige), endopods shorter than exopods (red). Antennula: with posterior extension and teeth (beige), with posterior extension and without teeth (orange), without posterior extension (red). Coxa: coxal plates with teeth (beige), coxal plates without teeth (red). Telson: posterior margin with teeth (beige), posterior margin without teeth (red). (Fraisse, 1878; Giard and Bonnier, 1887; Bonnier, 1900; Thompson, 1901; Caullery, 1907; Miyashita, 1940; Nielsen and Strömberg, 1965; Bresciani, 1966; Bourdon, 1972, 1976, 1981; Holdich, 1975; Schultz, 1975, 1980; Kensley, 1979; Bourdon and Bruce, 1980; Anderson and Dale, 1981; Coyle and Mueller, 1981; Dale and Anderson, 1982; Adkinson and Collard, 1990; Rybakov, 1990; Pascual et al., 2002; Torres Jordá, 2003; Shimomura et al., 2005; Hosie, 2008; Boyko, 2015).

SCHÄDEL, PERRICHOT, & HAUG: CRETACEOUS EPICARIDEA

Antenna

Boyko and Williams (2015) mapped the antenna morphology of cryptoniscus larvae onto their molecular phylogeny and concluded that in Cryptoniscoidea (incl. Dajidae) the number of antennal flagellum elements is five (4+5 antennal elements) and four (4+4 antennal elements) for Bopyridae and Ionidae. In Entoniscidae they found one or three flagellum elements (4+1 or 4+3 antennal elements). However, we found an exception to this pattern. Two supposed species of Bopyridae, *Probopyrus pandalicola* and *Probopyrus floridensis,* have five antennal flagellum elements (Dale and Anderson, 1982).

The cryptoniscium larvae of some species of Probopyrus are not only aberrant compared to other bopyroideans regarding the antennal morphology (*floridensis* and *pandalicola*), but also in the shape of the antennula element one (Figure 16). *Probopyrus bithynis* is the only bopyroidean with an antennula plate, which is posteriorly toothed and allows two possible conclusions. The distribution of character states in natural groups of Epicaridea could be more heterogeneous than expected, or the phylogenetic position of Probopyrus species is incorrect.

The situation is further complicated because of some inconsistencies in the literature. The phylogenetic trees used for the character mapping (Boyko et al., 2013, fig. 4) and (Boyko and Williams, 2015, fig. 3) show a significant discrepancy with the text. In the phylogenetic trees Cryptoniscoidea appears to be the sister group of Dajidae whereas in the text Dajidae and Entophilinae are treated as ingroups of Cryptoniscoidea. This twist in topology is based on an, incorrectly labeled, undetermined cryptoniscoidean species (in the tree 'Cryptoniscoidea' should mean 'Cryptoniscoidea sp. indet.' Also, in Boyko and Williams (2015), the key provided for the identification of cryptoniscus larvae (mainly based on antennal morphology) is erroneous as it does not allow the final identification of Ionidae (although possible based on the character mapping).

Mouthparts

Due to the small size and the condensed arrangement of the mouthparts for most extant species, only descriptions of the external features of the feeding apparatus exist. The mouthparts in cryptoniscium larvae and paedomorphic males form a condensed and complex structure that has yet only been studied in detail for a single species (Goudeau, 1969, 1977). These mouth parts have

many features that are unique within Isopoda. The mandibles lack a conventional proximal joint, and the arrangement of muscles suggests that an active pro- and retraction of the complete mandible is possible. However, the orientation and the external shape of the mouthparts are highly variable among epicaridean species. In many species the mouthparts form a cone-like structure often referred to as "buccal cone"; in other species the cone-like shape is less distinct. The orientation of the apical opening of the concealed mouthpart-complex varies among epicaridean species. In some species the apical opening is located more anteriorly and can even be located medially between the proximal elements of the antennula (e.g., *Probopyrus pandalicola* depicted in Dale and Anderson, 1982). In Dajidae also a suction disc at the end of a short stalk occurs at the apical opening of the concealed mouthpart-complex (Wägele, 1989).

In herein presented specimens the mouthparts form a distinct cone and the apical opening of the cone points postero-ventrally (Figure 12.5, Appendix 4). In the putative sister groups of Epicaridea (Cymothoidae or Gnathiidae) the mouthparts are anteriorly projected but not between antennula and antenna. It is not clear which of these conditions is ancestral and which is derived. Comparative studies of the head morphology in larvae and adults between Epicaridea and suitable outgroups could provide information about the polarity of this character and could thus contribute to a better understanding of the phylogenetic position of Epicaridea within Cymothoida and the relationships within Epicaridea.

Proximal Region of Pereopods (post-ocular segments 7-13): Coxal Plates

Wägele (1989) interpreted the presence of coxal plates with a continuous margin as an autapomorphy for the group that comprises Asconiscidae, Crinoniscidae and Cryptoniscidae (Figure 2). It is indeed present in all species of this group, yet it is also present in many other groups (also within Cryptoniscoidea; see Figure 16).

Distal Parts of Pereopods (post-ocular segments 7-13)

Pereopods 1 and 2 (thoracic appendages 2 and 3) in the observed fossils are difficult to see as they do not protrude from the concave cavity in all of the specimens. Nevertheless, they are much shorter and have more robust propodi than the more posterior pereopods; which seems to be a

pattern in extant species as well. In general, the posteriormost pereopod (pereopod 7) of cryptoniscium larvae is always the longest of the pereopods. Some modern species have a very distinct differentiation between the morphology of pereopods 1 and 2 compared to pereopods 3 to 7. The former are usually short and robust with a short and often strongly curved dactylus and the latter long and slender with straight dactyli (e.g., *Bourdonia tridentata* Rybakov, 1990). In most species (e.g., *Cryptocisus laevis* Schultz, 1975), the antero-posterior transition between these morphologies is more gradual, which is also the case for the herein presented specimens (robust morphology of the propodi in pereopods 3 and 4, Figure 15).

In the herein presented specimens, as in many modern species, the lateral side of the propodus in the anterior-most pereopods fits into a concave space on the lateral side (medio-ventral side in tucked resting position) of the basipod (Figure 14.1). The armature of the median side of the propodus where the adducted dactylus is in contact varies among the extant cryptoniscium larvae. In the herein presented specimens two simple setae are present in pereopods 3 to 7 (Figures 14.2, 15, setae possibly also in pereopods 1 and 2 but not evident). The presence of two strong setae (often accompanied with a smaller more distal seta) is a common feature in extant species, but often additional setae are present or the setae are forked (e.g., *Aegophila socialis* Bresciani, 1966). This feature may be of systematic value, but small setae may have been overseen in species, which have not been studied using SEM or high magnification light-microscopy with appropriate contrasting methods.

In many descriptions of cryptoniscia a distinct tip of the dactylus has been illustrated (hardly visible here). SEM imaging (Nielsen and Strömberg, 1973, figure 43) has confirmed a distinct division between the proximal part of the dactylus (pectinate surface pattern) and the tip (smooth surface). The tip is interpreted as the claw (one of two claws in the ground pattern of Isopoda), which is curved and firmly connected to the dactylus in some groups of parasitic isopods (Wägele, 1989). In conclusion, the pereopod morphology of the herein presented specimens apparently lies within the range of modern cryptoniscia without exhibiting extreme patterns.

Pleopods

The setulose setae of the pleopods are barely visible in the processed images, except in one case (Figure 11.1) displaying convincing information after focus-stacking. The extreme delicacy of the setulae (less than 1 μm in diameter) provides a good example for the exceptional preservation potential of Vendean amber. Setulose pleopod setae have been reported for some modern cryptoniscium larvae (e.g., *Capitoniscus cumacei* Schultz, 1975). This structure is rarely included in descriptions of extant larvae, making its systematic value difficult to assess.

Uropods

In modern cryptoniscia, endopods can be longer, equal or shorter in length to the corresponding exopods, the latter condition only being found within Bopyridae (=Bopyrinae sensu Wägele, 1989) (red in Figure 16). This could even represent an autapomorphy of Bopyridae. Manca stages of groups closely related to Epicaridea do have an endopod that is longer than the exopod (Aegidae, Cymothoidae and Gnathiidae). Note that the adults of these groups are less informative as they are often morphologically very derived and with broader and leaf-shaped endo- and exopods, which are less comparable to the truncated-cone-shaped uropod rami of cryptoniscium larvae. The herein described specimens have endopods that are longer than the corresponding exopods. Combined with topological inference regarding the distribution of this character state, its presence within the herein described (oldest) fossil specimens is consistent with the ancestral feature of this length ratio.

Alternatively, Wägele (1989) suggested that uropod endopods that are longer than the corresponding exopods (in contrast to equally long endo- and exopods) could be an autapomorphy for Cryptoniscoidea. We judge this as a less parsimonious hypothesis as exopods that are longer than the endopods can be reconstructed for the ground pattern of Epicaridea. Also, the vice versa character state (endopods shorter than the exopods) is not explained by this assumption.

Telson

Judging from the literature (Figure 16) the distribution of a toothed posterior margin of the telson in cryptoniscium larvae is erratic and not linked to any natural group within Epicaridea. Considering the toothed structures on antennulae and coxal plates, we consider the possible existence of a regulatory gene complex responsible for the development of teeth-like extensions/constrictions on different parts of the body, as, if present, those pat-

terns often occur in multiple regions of the body. One explanation for the chaotic distribution of toothed/smooth character states (Figure 16) could be that this regulatory gene complex has already been present in the ground pattern of Epicaridea, and the formation of associated teeth structures has been suppressed in many lineages.

Summary of Morphological Characters and Suggested Systematic Interpretation

Based on shared character states the herein presented specimens could be interpreted as representatives of Cabiropidae (at least two species have the exact same combination of characters that are included in Figure 16). Nevertheless, none of the character states in the herein presented specimens can be considered autapomorphic for Cabiropidae, precluding a taxonomic treatment as representatives of that group. Based on current character mapping, none of the studied character states can confidently be considered autapomorphic for any epicaridean ingroup. The herein presented specimens can therefore be treated as "Epicaridea inc. sed. nec Dajidae" (unknown position within Epicaridea but not part of Dajidae). If the antennular plate with an entire posterior margin (Wägele, 1989) is considered a strict autapomorphy of Asconiscidae+Crinoniscidae+Cryptonisci- dae, then the herein presented specimens could be treated as Epicaridea inc. sed. nec Dajidae, nec Asconiscidae, nec Crinoniscidae, nec Cryptonisci- dae. Yet, as discussed above, the latter assumption should be tested for consistency in future phylogenetic studies.

Further Interpretations of Fossil Epicarideans from the Miocene of Chiapas

Crustacean larvae are extremely rare in the fossil record, making this report only the second one for Epicaridea. The primary finding has been only very recently reported from the Miocene amber of Mexico (Serrano-Sánchez et al., 2016).

The authors found two clusters (specimens 1, 3, 4 and 6 in contrast to specimens 2, 5a, 5b) based on the size of the specimens (Figure 17). However, the specimens of each size cluster differ enormously in the morphology of the uropods. Since these morphologies are not apparently cor- relating with the size clusters, Serrano-Sánchez et al. (2016) concluded that the specimens were unlikely to be conspecific within the clusters.

Specimens 1, 3 and 4 have massive and (at least in specimen 3) relatively long exopods but thin endopods. Specimens 2 and 6 have thin exo- pods and relatively long and massive endopods.

As stated above, exopods being longer and more massive than endopods is a character state found only within Bopyridae advocating for this to be autapomorphic of the group, although not as seen in by all bopyrid representatives (see discus- sion above). Consequently, the Mexican speci- mens 1, 3 and 4 can be interpreted as possible representatives of Bopyridae. As Serrano-Sánchez et al. (2016) stated, these specimens must not all be conspecific.

Serrano-Sánchez et al. (2016) tentatively sug- gested that specimen 2 and 6 could be conspecific, specimen 6 being the corresponding microniscium larva of specimen 2 (cryptoniscium). Microniscium larvae are generally said to have ill-defined appendages without developed setae on pleopods and uropods (Anderson and Dale, 1981; Wägele, 1989), features which are clearly displayed in specimen 6. Furthermore, microniscia, due to their parasitic — non swimming — lifestyle (Anderson and Dale 1981), are quite unlikely to be preserved in amber without their host nor have they ever been reported to detach from their host.

The size clusters observed by Serrano- Sánchez et al. (2016) are most likely the result of the coexistence of multiple species, showing large size-ranges (e.g., 0.8-2.8 mm in *Cryptocisus laevis* Schultz, 1975) and possibly paedomorphic adult males resembling the cryptoniscia.

Body Size

With a mean of 423 µm and the largest speci- men of only 495 µm in body size (excluding the uropods), the herein presented specimens are the smallest ever reported cryptoniscium larvae (Fig- ure 17, Appendix 2) regarding both fossil and extant occurences, its average body length being even smaller than the shortest length recorded for extant species. Also, only two extant species fall within or close to the range of the herein presented specimens body size or close (Figure 17): *Bopy- rina ocellata*, 450 µm (Román-Contreras and Romero-Rodríguez, 2013) and *Entoniscoides oka- dai*, 500 µm (Miyashita, 1940).

The Mexican specimens of the smaller size- cluster are slightly larger but still comparable in size to the Vendean specimen. The Mexican speci- mens that fall into the larger size cluster are dis- tinctly larger than the of herein presented specimens type specimens. Nevertheless, the specimens in the larger Miocene size class are rather small compared to the spectrum of body
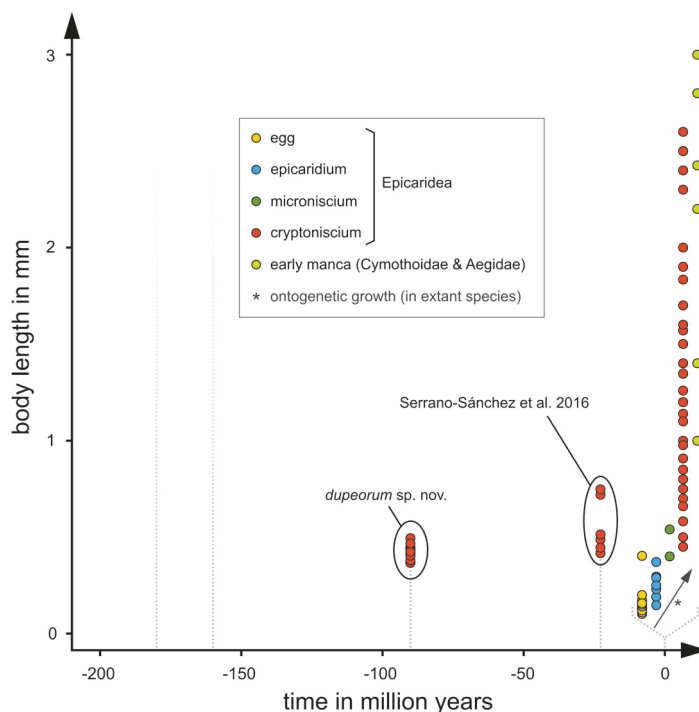
FIGURE 17. Body lengths of fossil epicaridean cryptoniscium larvae over time (all specimens) compared to cryptoniscium larvae and other developmental stages of modern epicaridean species and potential sistergroup taxa (smallest record of each species). The fading dotted lines at the left mark the earliest occurrences of trace fossils (precarious and affirmed) (Soergel, 1913; Klompmaker et al., 2014). The data from extant species is expanded for better visibility and is outlined by a dotted bracket. (Fraisse, 1878; Bonnier, 1900; Thompson, 1901; Caullery, 1907; Miyashita, 1940; Nielsen and Strömberg, 1965; Bresciani, 1966; Nielsen, 1967; Bourdon, 1972, 1972, 1976, 1981; Holdich, 1975; Schultz, 1975, 1980; Kensley, 1979; Bourdon and Bruce, 1980; Anderson and Dale, 1981; Coyle and Mueller, 1981; Dale and Anderson, 1982; Strömberg, 1983; Adkinson and Collard, 1990; Rybakov, 1990; Shields and Ward, 1998; Pascual et al., 2002; Torres Jordá, 2003; Shimomura et al., 2005; Hosie, 2008; Román-Contreras and Romero-Rodríguez, 2013; An et al., 2015; Serrano-Sánchez et al., 2016; Adlard and Lester, 1995; Atkins, 1933; Bruce, 2009; Brusca, 1978; McDermott, 2002; Romero-Rodríguez and Román-Contreras, 2008; Strömberg, 1971; Thamban et al., 2015; Truesdale and Mermilliod, 1977; Tsukamoto, 1981).

lengths in cryptoniscium larvae of extant species. The body size of modern cryptoniscia extends up to 2.6 mm (*Cryptocotitus acus* Schultz, 1975), which is more than five times longer than in herein presented specimens (longest specimen).

Epicaridea being a well-supported monophyletic group (Boyko et al., 2013), the small size of the fossils compared to the wide range in size for extant species questions the ancestral size of the epicaridean cryptoniscium. Although fossil data are limited here, the most parsimonious hypothesis suggests the ancestral larva were small and that body size has increased over time in some lineages.

The size of the cryptoniscium has to be influenced by the size of the intermediate host (copepod) that is parasitised by the microniscium stage. Although some calanoid copepods are much larger, most species are of 0.5 to 2 mm in length (Blaxter et al., 1998). Over time, an optimisation of the interaction between the microniscium larvae, and their hosts (copepods) could have led to a greater uptake of nutrients and the possibility for epicarideans to develop larger cryptoniscium larvae.

Evolutionary History of Epicarideans

The evolutionary history of the epicaridean lifestyle is still unresolved. Phylogenetic analyses support a close relationship with fish parasites, implying a fish-parasitic (or at least fish-associated) lifestyle for the common ancestor shared either with gnathiids (Brusca and Wilson, 1991; Brandt and Poore, 2003), cymothoids (Wägele, 1989; Dreyer and Wägele, 2001, 2002; Brandt and Poore, 2003) or both of these groups (Nagler et al., 2017). Dreyer and Wägele (2001) even suspected the possible sessile (attached) habit of the adult
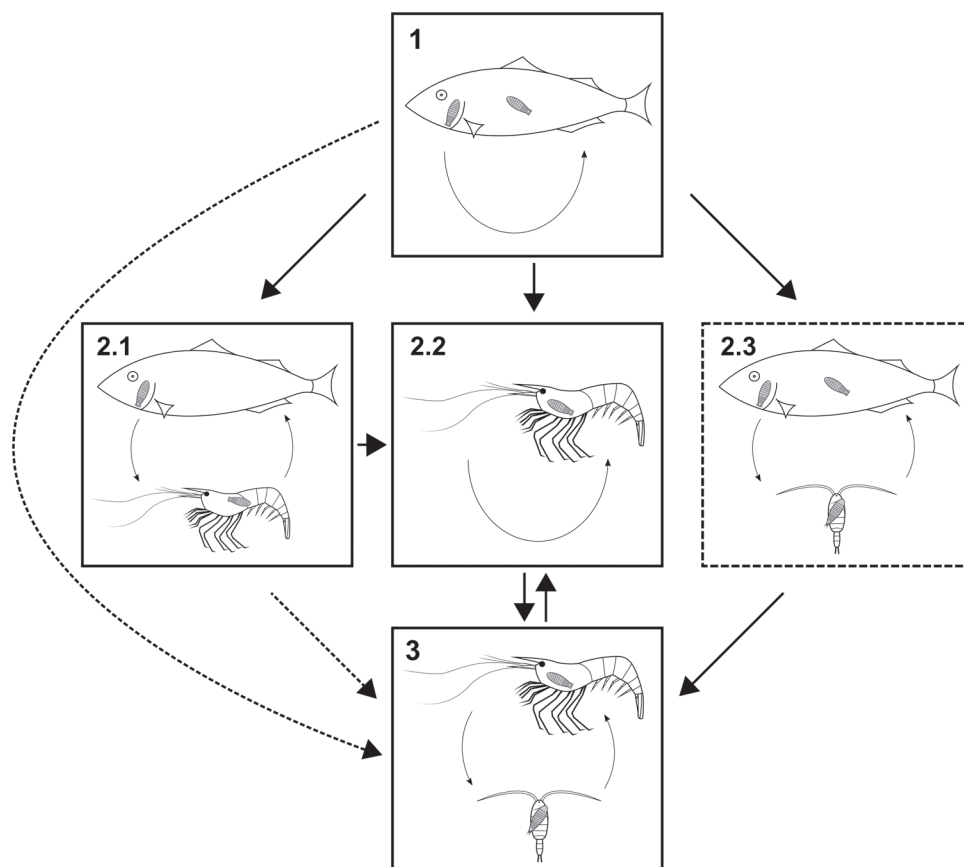
FIGURE 18. Possible evolutionary transitions between parasitic lifestyles in isopods (Cymothoida). Solid boxes, lifestyles with modern analogue; dashed box, lifestyle without modern analogue; solid arrows, likely transitions; dashed arrows, possible but less likely transitions. **18.1:** Strict fish parasites, larvae or larvae and adults are parasiting fish (Aegidae, Cymothoidae, Gnathiidae). **18.2.1:** Mixed fish and crustacean parasites, adult females parasitic to fish (some cymothoids). **18.2.2:** Crustacean parasites without copepod intermediate host (*Entoniscoides okadai,* Epicaridea). **18.2.3:** Larvae feed on copepods, adult females feed on fish. **18.3:** Larvae feed on copepods and adults are parasitic to other crustaceans.

common ancestor of cymothoids and epicarideans. Likewise, protandric sexual development (Brusca, 1981) could be an ancestral for both groups (Dreyer and Wägele, 2001). A transition from a fish to a crustacean host is not difficult to imagine. Males of Cymothoidae (*Thelota henseli*) have even been reported feeding on palaemonid shrimps (De Castro, 1985). The involvement of a smaller crustacean (copepod) as intermediate host complicates the evolutionary scenario of the epicaridean life cycle. Indeed, aside of a single species (*Entoniscoides okadai* Miyashita, 1940) that seems to lack the epicaridium stage (Miyashita, 1940), all epicaridean species feed on copepods as intermediate host (Wägele, 1989). This suggests that copepods have already been involved as hosts in the life cycle of the common ancestor of all modern species. This leaves several equivalently parsimonious scenarios for the host change (Figure 18). It

is possible that the life cycle of epicarideans evolved directly from a fish parasitic ancestor (Figure 18.1-18.3). This would have required the following significant evolutionary steps: (1) change in final host and adaption of cryptoniscium/adult for attachment onto decapods, (2) adaption to crustacean diet and (3) development of a specialised larva that, during this stage, attaches to a single copepod. However, some of these features could already have been present in the common ancestor of Epicaridea/Cymothoidae/Aegidae (Figure 18.2.1, 18.2.2, 18.2.3). Indeed, some representatives of Cymothoidae actually display an intermediate stage on a crustacean host (*Thelota henseli* De Castro, 1985) before colonizing their fish final host (Figure 18.2.1).

The lack of epicaridium larvae in one species of Epicaridea (*Entoniscoides okadai,* Miyashita, 1940) suggests that this species does not feed on

copepods but exclusively on the final host, a crustacean. A condition as in *Entoniscoides okadai* (Figure 18.2.2) could have evolved directly from fish parasitism (Figure18.1) or from mixed fish-crustacean parasitism (Figure 18.2.1). It is possible that the modern epicaridean life cycle evolved from a condition like in *Entoniscoides okadai* by adding an intermediate smaller crustacean host. However, there is no support for *Entoniscoides okadai* to represent an early branch within Epicaridea. Therefore, it is likely that this life cycle evolved from the regular epicaridean life cycle (Figure 18.3 to 18.2.2). Likewise, also a transitory lifestyle involving fished as final hosts and copepods as intermediate hosts (Figure 18.2.3) could be considered. Yet, this scenario lacks a known extant analogue.

In this regard, we stress out that epicarideans are not restricted to crustacean as hosts. Pascual et al. (2002), indeed, revealed in a spectacular way the presence of endoparasitic cryptoniscium-shaped life stages of epicarideans in squids. The authors of this report also emphasized that this may have been overseen for a long time due to the small size of the isopod parasites.

Preservational Biases

Scanning electron microscopy showed that the surface of cryptoniscium larvae (and males) is covered by fine grooves and fringes (e.g., Hosie, 2008). Due to the small scale of most of the surface structures, most of these surface structures could likely not be properly visualized in amber by light microscopy. Yet, some of the (larger scaled) surface structures, like the dorsal striation pattern, are visible in a few specimens. We explain this by two reasons. Some specimens are closer to the amber surface than others. The specimens located deeper in the amber are more difficult to photograph and also organic particles, cracks and cloudy areas of the resin can interfere with the microscopic results and therefore prevent surface structures to be observed. Yet, in some cases different surface structures are apparent in the same specimen (not affected by the location in amber, e.g., Figure 8.7). A cracked-open specimen (Figure 6.6) shows that (at least in some specimens) the exoskeleton is preserved in Vendean amber. Judging also from a specimen that shows a transition between a smooth and crater-like dorsal surface (Figure 8.3), we assume that these differences in the surface texture are caused by taphonomy rather than by differences in the original texture of the living animal.

Taphonomic Environment

Apart from the material studied herein, which was briefly mentioned and partially figured in Néraudeau et al. (2017), there is only one other record of epicaridean body fossils. Serrano-Sánchez et al. (2016) reported seven specimens (most likely cryptoniscia) from Miocene Chiapas amber (Mexico). All specimens come from the amber site Campo La Granja which is dissimilar to other Chiapas amber sites with respect to its high proportion of aquatic arthropod species and the stratified build-up of the resin (Serrano-Sánchez et al., 2015). The stratified build-up of the resin can also be seen in Vendean amber (Figure 4.3). However, in Campo La Granja amber the layers of resin are often intersected with grains of sand (Serrano-Sánchez et al., 2015), which has not been observed in Vendean amber. For Vendean amber Néraudeau et al. (2017) mentioned two categories of resin pieces: "stalactite-like" and "flat and multi-layered." Yet, all fossil epicarideans from Vendée were found in the flat and multilayered amber pieces. This raises the question whether the build-up of the resin is actually linked to a taphonomic environment.

How aquatic and especially brackish/marine organisms could have been trapped in amber has long been debated. Two main processes have been discussed. The organisms could have been transported to the resin producers by wind, spray or tides (Girard et al., 2008; Schmidt et al., 2018) or they could have lived in proximity to the resin producers (Serrano-Sánchez et al., 2015).

Schmidt and Dilcher (2007) supported the possibility of the latter process by observations in a modern swamp environment and showed that this kind of entrapment is not only possible, but also likely to happen when the resin producer is located in an environment with stagnant water, where at least few extant epicaridean species live (Chopra, 1923).

Resin is not soluble in water and has a hydrophobic surface that prevents the volatiles to leave the resin. Thus, the resin stays in a liquid condition for a longer period of time and can function as a submerged trap for living organisms (until water levels drop and the resin hardens). Dead material can also be overflown and subsequently embedded in resin (Schmidt and Dilcher, 2007). The authors observed that living animals can promote getting fully immersed in the resin by autonomous motion.

In Campo La Granja amber, taphonomic circumstances strongly point out that at least some

aquatic arthropod individuals must have been alive when trapped in the resin. This is dramatically shown by traces of torn off arthropod appendages leading to the corresponding bodies that lack exactly those appendages (Serrano-Sánchez et al., 2015). Although there is no such strong evidence for the entrapment of living aquatic arthropods in Vendean amber, a living condition still is the best scenario that explains the number and density of aquatic epicaridean larvae.

In this aspect, not only their large number of specimens in the French amber is informative, but also the fact that the French and the Mexican amber each include pieces that contain two specimens. This is quite remarkable and suggests a high density of larvae in the environment or a great chance for them to get stuck in the resin.

Even though the majority of extant epicaridean species is found in marine and brackish environments, there are also records of epicarideans living in true freshwater environments (Chopra, 1923). Thus, the herein described fossils alone cannot be used as an indicator for marine influence. However, many other findings such as plant pollen (Nohra et al., 2015), diatoms (Néraudeau et al., 2017; Saint Martin et al., 2015), dinoflagellates (Legrand et al., 2006), foraminifers (Legrand et al., 2006) and tanaidaceans (Sánchez-García et al., 2016) suggest a temporarily flooded near-shore palaeoenvironment that is comparable to extant cypress swamps.

The reconstructed coastal environment could have provided host species suitable for epicaridean larvae (crustaceans). However, only one crustacean species (Tanaidacea) has been recorded for Vendean amber (Sánchez-García et al., 2016; Néraudeau et al., 2017). Yet, no parasite-host relationship between epicarideans and tanaidaceans has ever been recorded, and the tanaidaceans known from Vendean amber are too small to represent final hosts of epicarideans (*Eurotanais seilacheri* in Sánchez-García et al., 2016).

TAXONOMIC ACT

EUARTHROPODA (sensu Walossek, 1999)
EUCRUSTACEA (sensu Walossek, 1999)
PERACARIDA Calman, 1904
ISOPODA Latreille, 1817
SCUTOCOXIFERA Dreyer et Wägele, 2002
CYMOTHOIDA Wägele, 1989
EPICARIDEA Latreille, 1825 (=Bopyridae Rafinesque, 1815 sensu Wägele, 1989)
VACUOTHECA gen. nov.

zoobank.org/91B40537-4598-4320-B602-AF530D19F51F

Type species. *Vacuotheca dupeorum* sp. nov. (type and only species).
Etymology. From the Latin words *vacuus* and *theca*, meaning empty case.
Remarks. The species cannot be interpreted with certainty as a representative of any already known epicaridean ingroup. Hence, it is required by the International Code of Zoological Nomenclature (ICZN, Chapter 2, Article 5 and App. B, 6.) to erect a new genus name. No diagnosis can be given for *Vacuotheca* gen. nov. as it includes only the type species (monospecific), and it cannot be differentiated which characters should diagnose the higher taxonomic unit. A possible alternative has been suggested by Lanham (1965). After Lanham, the uniqueness of a species name can be given by the species name along with detailed bibliographic information on the original description (uninomial nomenclature).

Vacuotheca dupeorum sp. nov.
Figures 5-15

zoobank.org/64997B3E-E77A-4095-A72C-726DC7710D39

v.2017   Epicaridean larva (depicted is the paratype IGR.GAR-8.1-2); Ne raudeau, Perrichot, Batten, Boura, Girard, Jeanneau, Nohra, Polette, S. Saint Martin, J. Saint Martin, Thomas, fig. 9A.
v.2014   Isopoda indet.; Perrichot and Néraudeau, tab. A1.

Etymology. From the last name of Fanny and André Dupé, who found and donated the amber specimens.
Holotype. IGR.GAR-28.
Paratypes. IGR.GAR-8.1-1, IGR.GAR-8.1-2, IGR.GAR-8.2, IGR.GAR-41-1, IGR.GAR-41-2, IGR.GAR-48, IGR.GAR-51, IGR.GAR-53-1, IGR.GAR-53-2, IGR.GAR-64, IGR.GAR-65, IGR.GAR-89, IGR.GAR-90, IGR.GAR-92, IGR.GAR-93, IGR.GAR-94, IGR.GAR-95-1, IGR.GAR-95-2, IGR.GAR-97, IGR.GAR-98. All deposited in the Geological Department and Museum of the University Rennes 1.
Ontogenetic stage of the types. Cryptoniscium larva or adult male (see discussion below).
Type locality. La Robinière (municipal of La Garnache, department of Vendée, France).
Type stratum. Unknown; Turonian age (Late Cretaceous) after Néraudeau et al. (2017).
Differential diagnosis. The cryptoniscium larva of *Vacuotheca dupeorum* sp. nov. differs from that of all (but one) known and sufficiently illustrated species in having an antennular plate (proximal element of the antennula) with 8 posteriorly directed teeth, the second antennular element having no

teeth-like projections, the antenna having 5 flagellum elements, the coxal plates having 4 posterior teeth on each segment, the endopod of the uropod being longer than the exopod and the telson having 6 posterior teeth. For the remaining species *Cironiscus dahli* Nielsen and Strömberg, 1967, *V. dupeorum* sp. nov. differs in the shape of the antennular plate (first element) and the size of the third antennular element. The unnamed fossil Miocene cryptoniscium larvae reported in Serrano-Sánchez et al. (2016) show too few details to morphologically differentiate all of the Mexican specimens from the *Vacuotheca dupeorum* sp. nov. type specimens. Only the slightly larger size of the Miocene fossils could be used as a morphological distinction.

Also, it remains the possibility that there is an extant epicaridean species that does not differ in the larval morphology from *V. dupeorum* sp. nov. in the above listed characters but could not be located in the literature by the authors of this study. However, the large time span of 90 million years between the occurrence of *V. dupeorum* sp. nov. (Cretaceous) to extant species, respectively 67 million years between the occurrence of *V. dupeorum* sp. nov. and the Miocene Mexican fossils makes it highly unlikely that they belong to an extant species in the sense of the biological or phylogenetic species concept.

Remark on the Citation of Dajidae. The group of Dajidae was not established by Giard and Bonnier (1887) as stated by many authors in the recent literature (e.g., Boyko et al., 2013 'WORMS') but by Sars (1883). Thus, the correct citation is: Dajidae Sars, 1883.

CONCLUSIONS

The studied fossils represent cryptoniscium larvae or paedomorphic males of a highly specialised group of parasitic isopod species (Epicaridea) that feed on crustaceans. Fossils of epicarideans are extremely rare and, so far, only known from one other location, extending the fossil record of Epicaridea by 67 million years. The fossils are very small but exceptionally well preserved. It was possible to date back many morphological features seen in extant cryptoniscium larvae to a Cretaceous age. All specimens appear to be conspecific and *Vacuotheca dupeorum* sp. nov. is described as a new species different from all known fossil and extant species in the morphology of the cryptoniscium larva. Extant epicaridean species have a much wider range in body size for the cryptoniscium stage larvae than the *V. dupeorum* sp. nov. type specimens. The evolution of the epicaridean life cycle as it is observed in the extant representatives is still enigmatic. Yet, some likely transitional conditions have been observed in extant representatives (although these conditions are likely not plesiomorphic). The herein presented specimens make a valid point for the hypothesis that at least some aquatic animals that are preserved in amber are indeed the result of entrapment that happened underwater.

REFERENCES

Adkinson, D.L. and Collard, S.B. 1990. Description of the cryptoniscium larva of *Entophilus omnitectus* Richardson, 1903 (Crustacea: Isopoda: Epicaridea) and records from the Gulf of Mexico. *Proceedings of the Biological Society of Washington*, 103:649-654.

Adlard, R.D. and Lester, R.J.G. 1995. The life-cycle and biology of *Anilocra pomacentri* (Isopoda, Cymothoidae), an ectoparasitic isopod of the coral-reef fish, *Chromis nitida* (Perciformes, Pomacentridae). *Australian Journal of Zoology,* 43:271–281.

Anderson, G. 1975. Larval metabolism of the epicaridian isopod parasite *Probopyrus pandalicola* and metabolic effects of *P. pandalicola* on its copepod intermediate host *Acartia tonsa*. *Comparative Biochemistry and Physiology Part A: Physiology*, 50:747-751. https://doi.org/10.1016/0300-9629(75)90140-1

Anderson, G. and Dale, W.E. 1981. *Probopyrus pandalicola* (Packard) (Isopoda, Epicaridea): morphology and development of larvae in culture. *Crustaceana*, 41:143-161. https://doi.org/10.1163/156854081X00192

An, J., Boyko, C.B., and Li, X. 2015. A review of bopyrids (Crustacea: Isopoda: Bopyridae) parasitic on caridean shrimps (Crustacea: Decapoda: Caridea) from China. *Bulletin of the American Museum of Natural History*, 399:1-85. https://doi.org/10.1206/amnb-921-00-01.1

Atkins, D. 1933. *Pinnotherion vermiforme* Giard and Bonnier, an entoniscid infecting *Pinnotheres pisum*. *Proceedings of the Zoological Society of London*, 103:319–363. https://doi.org/10.1111/j.1096-3642.1933.tb01598.x

Ax, P. 2000. *The Phylogenetic System of the Metazoa. Multicellular Animals*. Springer-Verlag, Berlin.

Bell, T. 1863. *A Monograph of the fossil Malacostracous Crustacea of Great Britain, Part II, Crustacea of the Gault and Greensand*. *Palaeontographical Society Monograph I, II*, Palaeontographical Society, London.

Béthoux, O. 2010. Optimality of phylogenetic nomenclatural procedures. *Organisms Diversity & Evolution*, 10:173-191. https://doi.org/10.1007/s13127-010-0005-3

Blaxter, J.H., Douglas, B., Tyler, P.A., and Mauchline, J. 1998. *The Biology of Calanoid Copepods* 33. Academic Press, San Diego.

Bonnier, J. 1900. *Contribution à l'étude des épicarides les Bopyridae*. Travaux de la Station Zoologique de Wimereux, Paris.

Bourdon, R. 1968. Les Bopyridae des mers européennes. *Mémoires du Muséum National d'Histoire naturelle (A)*, 50:77-424.

Bourdon, R. 1972. Epicarides de la Galathea Expedition. *Galathea Report*, 12:101-112.

Bourdon, R. 1976. Épicarides de Madagascar. I. *Bulletin du Muséum National d'Histoire Naturelle*, 3:353-392.

Bourdon, R. 1981. Trois nouveaux *Cryptoniscina* antarctique*s* abyssaux (Isopoda, Epicaridea). *Bulletin du Muséum National d'Histoire Naturelle*, 3:603-613.

Bourdon, R. and Bruce, N.L. 1980. *Ancyroniscus orientalis* sp. nov. (Isopoda: Epicaridea), nouveau cabiropside parasite de la « great barrier reef ». *Bulletin de l´Academie et de la Societe Lorraines des Sciences*, 19:21-26.

Boyko, C. 2015. A Revision of *Danalia* Giard, 1887, *Faba* Nierstrasz & Brender à Brandis, 1930 and *Zeuxokoma* Grygier, 1993 (Crustacea: Isopoda: Epicaridea: Cryptoniscoidea: Cryptoniscidae) with description of a new genus and four new species. *Bishop Museum Bulletin in Zoology*, 9:65-92.

Boyko, C., Bruce, N.L., Hadfield, K.A., Merrin, K.L., Ota, Y., Poore, G.C.B., Taiti, S., Schotte, M., and Wilson, G.D.F. (eds.). 2008. *World Register of Marine Species*. Retrieved August 7, 2018.

Boyko, C.B., Moss, J., Williams, J.D., and Shields, J.D. 2013. A molecular phylogeny of Bopyroidea and Cryptoniscoidea (Crustacea: Isopoda). *Systematics and Biodiversity*, 11:495-506. https://doi.org/10.1080/14772000.2013.865679

Boyko, C.B., Schotte, M., Boyko, C.B., Bruce, N.L., Merrin, K.L., Ota, Y., Poore, G.C.B., Taiti, S., Schotte, M., and Wilson, G.D.F. 2013. Dajidae Giard & Bonnier, 1887. *World Marine, Freshwater and Terrestrial Isopod Crustaceans Database.* Accessed through: World Register of Marine Species at http://www.marinespecies.org/aphia.php.

Boyko, C. and Williams, J. 2009. Crustacean parasites as phylogenetic indicators in decapod evolution, p. 197-220. In Martin, J., Crandall, K., and Felder, D. (eds.), *Decapod Crustacean Phylogenetics*. CRC Press, Boca Raton.

Boyko, C.B. and Williams, J.D. 2015. A new genus for *Entophilus mirabiledictu* Markham & Dworschak, 2005 (Crustacea: Isopoda: Cryptoniscoidea: Entophilidae) with remarks on morphological support for epicaridean superfamilies based on larval characters. *Systematic Parasitology*, 92:13-21. https://doi.org/10.1007/s11230-015-9578-8

Boyko, C.B. and Wolff, C. 2014. Isopoda and Tanaidacea, p. 210-212. In Martin, J.W., Olesen, J., and Hoeg, J.T. (eds.), *Atlas of Crustacean Larvae*. Johns Hopkins University Press, Baltimore.

Brandt, A. and Poore, G.C. 2003. Higher classification of the flabelliferan and related Isopoda based on a reappraisal of relationships. *Invertebrate Systematics*, 17:893-923. https://doi.org/10.1071/IS02032

Bresciani, J. 1966. *Aegophila socialis* gen. et sp. nov., an epicaridean parasitic on the isopod *Aega ventrosa* Sars. *Ophelia*, 3:99-112. https://doi.org/10.1080/00785326.1966.10409636

Bruce, N.L. 2009. *The marine fauna of New Zealand: Isopoda, Aegidae (Crustacea)*. Biodiversity Memoir. National Institute of Water and Atmospheric Research, Wellington.

Brusca, R.C. 1978. Studies on the cymothoid fish symbionts of the eastern Pacific (Isopoda, Cymothoidae) I. Biology of *Nerocila californica*. *Crustaceana* 34:141–154.

Brusca, R.C. 1981. A monograph on the Isopoda Cymothoidae (Crustacea) of the eastern Pacific. *Zoological Journal of the Linnean Society*, 73:117-199. https://doi.org/10.1111/j.1096-3642.1981.tb01592.x

Brusca, R.C. and Wilson, G.D.F. 1991. A phylogenetic analysis of the Isopoda with some classificatory recommendations. *Memoirs of the Queensland Museum*, 31:143-204.

Calman, W.T. 1904. XVIII. On the classification of the Crustacea Malacostraca. *Annals and Magazine of Natural History*, 13:144-158. https://doi.org/10.1080/00222930408562451

Caroli, E. 1928. La fase "micronisci" di Ione thoracica (Montagu) ottenuta per allevamento sui copepodi. *Accademia Nazionale dei Lincei Rendiconti*, 6:321-326.

Caullery, M. 1907. Recherches sur les Liriopsidae, Épicarides cryptonisciens parasites des Rhizocéphales. *Mittheilungren aus der Zoologischen Station zu Neapel*, 18:583-643.

Chopra, B. 1923. Bopyrid isopods parasitic on Indian Decapoda Macrura. *Records of the Indian Museum*, 25:411-550.

Cohen, K.M., Finney, S.C., Gibbard, P.L., and Fan, J.-X. 2013, updated. The ICS International Chronostratigraphic Chart. *Episodes,* 36:199-204.

Coleman, C. 2003. Digital inking: how to make perfect line drawings on computers. *Organisms Diversity & Evolution*, 3:303-304. https://doi.org/10.1078/1439-6092-00081

Coyle, K.O. and Mueller, G.J. 1981. Larval and juvenile stages of the isopod *Holophryxus alaskensis* (Epicarida, Dajidae) parasitic on decapods. *Canadian Journal of Fisheries and Aquatic Sciences*, 38:1438-1443. https://doi.org/10.1139/f81-190.

Dale, W.E. and Anderson, G. 1982. Comparison of morphologies of *Probopyrus bithynis*, *P. floridensis*, and *P. pandalicola* larvae reared in culture (Isopoda, Epicaridea). *Journal of Crustacean Biology*, 2:392-409. https://doi.org/10.2307/1548055

De Castro, A.L. 1985. Ectoparasitism of *Telotha henselii* (Von Martens) (Isopoda, Cymothoidae) on *Macrobrachium brasiliense* (Heller) (Decapoda, Palaemonidae). *Crustaceana,* 49:200-201. https://doi.org/10.1163/156854085X00440

de Queiroz, K. and Gauthier, J. 1990. Phylogeny as a central principle in taxonomy: phylogenetic definitions of taxon names. *Systematic Zoology*, 39:307. https://doi.org/10.2307/2992353

de Queiroz, K. and Gauthier, J. 1994. Toward a phylogenetic system of biological nomenclature. *Trends in Ecology & Evolution*, 9:27-31. https://doi.org/10.1016/0169-5347(94)90231-3

Dreyer, H. and Wägele, J.-W. 2001. Parasites of crustaceans (Isopoda: Bopyridae) evolved from fish parasites: molecular and morphological evidence. *Zoology*, 103:157-178.

Dreyer, H. and Wägele, J.-W. 2002. The Scutocoxifera tax. nov. and the information content of nuclear ssu rDNA sequences for reconstruction of isopod phylogeny (Peracarida: Isopoda). *Journal of Crustacean Biology*, 22:217-234. https://doi.org/10.1163/20021975-99990229

Fraisse, P. 1878. Die Gattung Cryptoniscus Fr. Müller. *Arbeiten aus dem Zoologisch-Zootomischen Institut in Würzburg*, 4:239-296.

Giard, A. and Bonnier, J.J. 1887. *Contributions à l'étude des Bopyriens*. Travaux de la Station Zoologique de Wimereux, 5. Imprimerie L. Danel, Lille.

Girard, V., Schmidt, A.R., Martin, S.S., Struwe, S., Perrichot, V., Martin, J.-P.S., Grosheny, D., Breton, G., and Néraudeau, D. 2008. Evidence for marine microfossils from amber. *Proceedings of the National Academy of Sciences*, 105:17426-17429. https://doi.org/10.1073/pnas.0804980105

Goudeau, M. 1969. Appareil buccal et mécanisme alimentaire chez l'Isopode Epicaride Hemioniscus balani Buchholz. *Archives de Zoologie Expérimentale et Générale*, 110:473-512.

Goudeau, M. 1977. Contribution à la biologie d'un crustacé parasite: *Hemioniscus balani* Buchholz, isopode épicaride. Nutrition, mues et croissance de la femelle et des Embryons. *Cahiers de Biologie Marine*, 18:201-242.

Haug, J.T., in press. Why the term "larva" is ambiguous, or what makes a larva? *Acta Zoologica*, 1-22. https://doi.org/10.1111/azo.12283

Haug, J.T. and Haug, C. 2016. "Intermetamorphic" developmental stages in 150 million-year-old achelatan lobsters - the case of the species *tenera* Oppel, 1862. *Arthropod Structure & Development*, 45:108-121. https://doi.org/10.1016/j.asd.2015.10.001

Haug, J.T., Maas, A., Haug, C., and Waloszek, D. 2013. Evolution of crustacean appendages, p. 34-73. In Watling, L. and Thiel, M. (eds.), *Functional Morphology and Diversity*. Oxford University Press, Oxford. https://doi.org/10.1093/acprof:osobl/9780195398038.003.0002

Hiraiwa, Y.K. 1936. Studies on a bopyrid, *Epipenaeon japonica* Thielemann. III. Development and life-cycle, with special reference to the sex differentiation in the bopyrid. *Journal of Science of the Hiroshima University (Zoology)*, 4:101-141.

Holdich, D.M. 1975. *Ancyroniscus bonnieri* (Isopoda, Epicaridea) infecting British populations of *Dynamene bidentata* (Isopoda, Sphaeromatidae). *Crustaceana*, 28:145-151. https://doi.org/10.1163/156854075X00694

Hosie, A.M. 2008. Four new species and a new record of Cryptoniscoidea (Crustacea: Isopoda: Hemioniscidae and Crinoniscidae) parasitising stalked barnacles from New Zealand. *Zootaxa*, 1795:1-28. https://doi.org/10.11646/zootaxa.1795.1.1

International Commission on Zoological Nomenclature. 2012. Retrieved June 8, 2018, from http://www.nhm.ac.uk/hosted-sites/iczn/code/.

Kensley, B. 1979. Redescription of *Zonophryxus trilobus* Richardson, with notes on the male and developmental stages (Crustacea: Isopoda: Dajidae). *Proceedings of the Biological Society of Washington*, 92:665-670.

Keyser, D. and Weitschat, W. 2005. First record of ostracods (Crustacea) in Baltic amber. *Hydrobiologia*, 538:107-114. https://doi.org/10.1007/s10750-004-5941-5

Klompmaker, A.A., Artal, P., Van Bakel, B.W.M., Fraaije, R.H.B., and Jagt, J.W.M. 2014. Parasites in the fossil record: a Cretaceous fauna with isopod-infested decapod crustaceans, infestation patterns through time, and a new ichnotaxon. *PLoS One*, 9:e92551. https://doi.org/10.1371/journal.pone.0092551

Klompmaker, A.A. and Boxshall, G.A. 2015. Fossil crustaceans as parasites and hosts. *Advances in Parasitology*, 90:233-289. https://doi.org/10.1016/bs.apar.2015.06.001

Klompmaker, A.A., Portell, R.W., and Frick, M.G. 2017. Comparative experimental taphonomy of eight marine arthropods indicates distinct differences in preservation potential. *Palaeontology*, 60:773-794. https://doi.org/10.1111/pala.12314

Lang, C., Krapp, T., and Melzer, R.R. 2007. Postembryonal development in Caprellidae: SEM description and comparison of ready-to-hatch juveniles and adults of two Mediterranean skeleton shrimps (Crustacea: Amphipoda). *Zootaxa*, 1605:1-32. https://doi.org/10.11646/zootaxa.1605.1.1

Lanham, U. 1965. Uninominal nomenclature. *Systematic Zoology*, 14:144-144.

Latreille, P.A. 1817. *Le règne animal distribué d'après son organisation: pour servir de base a l'histoire naturelle des animaux et d'introduction a l'anatomie comparée*. Chez Déterville, Paris.

Latreille, P.A. 1825. *Familles naturelles du règne animal, exposées succinctement et dans un ordre analytique, avec lindication de leurs genres*. J. B. Baillière, Paris. https://doi.org/10.5962/bhl.title.16094

Legrand, J., Viaud, J.M., Pouit, D., and Pons, D. 2006. Upper Cretaceous woody structures and associated microfloral data from western France. *7th European Paleobotany-Palynology Conference*, Prague, p. 80.

Markham, J.C. 1986. Evolution and zoogeography of the Isopoda Bopyridae, parasites of Crustacea Decapoda, p. 143-164. In Gore, R.H. and Heck, K.L. (eds.), *Crustacean Issues 4. Crustacean Biogeography*. A.A. Balkema, Rotterdam.

Marshall, S.M. and Orr, A.P. 1972. *The Biology of a Marine Copepod: Calanus finmarchicus (gunnerus)*. Oliver & Boyd, Edinburgh.

Mayr, E. 1940. Speciation phenomena in birds. *The American Naturalist*, 74:249-278.

Mayr, E. 1942. *Systematics and the Origin of Species, from the Viewpoint of a Zoologist*. Columbia University Press, New York.

McDermott, J.J. 2002. Relationships between the parasitic isopods *Stegias clibanarii* Richardson, 1904 and *Bopyrissa wolffi* Markham, 1978 (Bopyridae) and the intertidal hermit crab *Clibanarius tricolor* (Gibbes, 1850) (Anomura) in Bermuda. *Ophelia,* 56:33–42. https://doi.org/10.1080/00785236.2002.10409487

Miyashita. 1940. On an entoniscid with abbreviated development, *Entoniscoides okadai*, n. g., n. sp. *Annotationes Zoologicae Japonenses*, 19:149-157.

Müller, F. 1862. *Entoniscus porcellanae*, eine neue Schmarotzerassel. *Archiv für Naturgeschichte*, 28(1):10-18.

Nagler, C. and Haug, J.T. 2015. From fossil parasitoids to vectors. *Advances in Parasitology*, 90:137-200. https://doi.org/10.1016/bs.apar.2015.09.003

Nagler, C., Hyžný, M., and Haug, J.T. 2017. 168 million years old "marine lice" and the evolution of parasitism within isopods. *BMC Evolutionary Biology*, 17:76. https://doi.org/10.1186/s12862-017-0915-1

Néraudeau, D., Perrichot, V., Batten, D.J., Boura, A., Girard, V., Jeanneau, L., Nohra, Y.A., Polette, F., Saint Martin, S., and Saint Martin, J.-P. 2017. Upper Cretaceous amber from Vendée, north-western France: age dating and geological, chemical, and palaeontological characteristics. *Cretaceous Research*, 70:77-95. https://doi.org/10.1016/j.cretres.2016.10.001

Nielsen, S.-O. 1967. *Cironiscus dahli* gen. et sp. nov. (Crustacea, Epicaridea) with notes on host-parasite relations and distribution. *Sarsia*, 29:395-412. https://doi.org/10.1080/00364827.1967.10411096

Nielsen, S.-O. and Strömberg, J.-O. 1965. A new parasite of *Cirolana borealis* Lilljeborg belonging to the Cryptoniscinae (Crustacea Epicaridea). *Sarsia*, 18:37-62. https://doi.org/10.1080/00364827.1965.10409547

Nielsen, S.-O. and Strömberg, J.-O. 1973. Morphological characters of taxonomical importance in Cryptoniscina (Isopoda Epicaridea) A scanning electron microscopic study of cryptoniscus larvae. *Sarsia*, 52:75-96.

Nohra, Y., Perrichot, V., Jeanneau, L., and Azar, D. 2015. Chemical characterization and botanical origin of French ambers. *Journal of Natural Products*, 78:1284-1293. https://doi.org/10.1021/acs.jnatprod.5b00093

Ogg, J.G., Hinnov, L.A., and Huang, C. 2012. *The Geologic Time Scale*. Elsevier. https://doi.org/10.1016/B978-0-444-59425-9.00027-5

Oliveira, E. and Masunari, S. 2006. Distribuição temporal de densidade de *Aporobopyrus curtatus* (Richardson) (Crustacea, Isopoda, Bopyridae), um parasito de *Petrolisthes armatus* (Gibbes) (Crustacea, Anomura, Porcellanidae) na Ilha do Farol, Matinhos, Paraná, Brasil. *Revista Brasileira de Zoologia*, 23:1188-1195. https://doi.org/10.1590/S0101-81752006000400028

Owens, L. and Rothlisberg, P.C. 1991. Vertical migration and advection of bopyrid isopod cryptoniscid larvae in the Gulf of Carpentaria, Australia. *Journal of Plankton Research*, 13:779-787. https://doi.org/10.1093/plankt/13.4.779

Pascual, S., Vega, M.A., José Rocha, F., and Guerra, A. 2002. First report of an endoparasitic epicaridean isopod infecting cephalopods. *Journal of Wildlife Diseases*, 38:473-477. https://doi.org/10.7589/0090-3558-38.2.473

Penalver, E. and Delclòs, X. 2010. Spanish amber, p. 236-270. In Penney, D. (ed.), *Biodiversity of Fossils in Amber from the Major World Deposits*. Siri Scientific Press, Manchester.

Perrichot, V. and Néraudeau, D. 2014. Introduction to thematic volume "Fossil arthropods in Late Cretaceous Vendean amber (northwestern France)". *Paleontological Contributions*, 10A:1-4. https://doi.org/10.17161/PC.1808.15981

Perrichot, V., Néraudeau, D., and Tafforeau, P. 2010. Charentese amber, p. 192-207. In Penney, D. (ed.), *Biodiversity of Fossils in Amber from the Major World Deposits*. Siri Scientific Press, Manchester.

Rafinesque, C.S. 1815. *Analyse de la nature ou tableau de l'univers et des corps organisés*. Jean Barravecchia, Palermo.

Revell, L.J. 2017. *Phytools: Phylogenetic Tools for Comparative Biology (and Other Things)*. Retrieved April 25, 2018, from https://CRAN.R-project.org/package=phytools.

Reverberi, G. 1947. Ancora sulla trasformazione sperimentale del sesso nei Bopiridi. La trasformazione della femmine giovanili in maschi. *Pubblicazioni della Stazione Zoologica di Napoli*, 21:83-93.

Román-Contreras, R. and Romero-Rodríguez, J. 2013. Prevalence and reproduction of *Bopyrina abbreviata* (Isopoda, Bopyridae) in Laguna de Términos, SW Gulf of Mexico. *Journal of Crustacean Biology*, 33:641-650. https://doi.org/10.1163/1937240X-00002182

Romero-Rodríguez, J. and Román-Contreras, R. 2008. Aspects of the reproduction of *Bopyrinella thorii* (Richardson, 1904) (Isopoda, Bopyridae), a branchial parasite of *Thor floridanus* Kingsley, 1878 (Decapoda, Hippolytidae) in Bahía de la Ascensión, Mexican Caribbean. *Crustaceana*, 81:1201–1210. https://doi.org/10.1163/156854008X374522

Rybakov, A.V. 1990. *Bourdonia tridentata* gen. n., sp. n. (Isopoda: Cabiropsidae) a hyperparasite of *Bopyroides hippolytes* Kroyer from the shrimp *Pandalus borealis*. *Parazitologiia*, 24:408-416.

Saint Martin, S., Saint Martin, J.-P., Schmidt, A.R., Girard, V., Néraudeau, D., and Perrichot, V. 2015. The intriguing marine diatom genus *Corethron* in Late Cretaceous amber from Vendée (France). *Cretaceous Research*, 52:64-72. https://doi.org/10.1016/j.cretres.2014.07.006

Sánchez-García, A., Peñalver, E., Bird, G.J., Perrichot, V., and Delclòs, X. 2016. Palaeobiology of tanaidaceans (Crustacea: Peracarida) from Cretaceous ambers: extending the scarce fossil record of a diverse peracarid group. *Zoological Journal of the Linnean Society*, 178:492-522. https://doi.org/10.1111/zoj.12427

Sars, G.O. 1883. Oversigt af Norges Crustaceer med foreloebige Bemaerkninger over de nye eller mindrebekjendte Arter. *Videnskabs-Selskabet i Christiana*, 18:68-75.

Schmidt, A.R. and Dilcher, D.L. 2007. Aquatic organisms as amber inclusions and examples from a modern swamp forest. *Proceedings of the National Academy of Sciences*, 104:16581-16585. https://doi.org/10.1073/pnas.0707949104

Schmidt, A.R., Grabow, D., Beimforde, C., Perrichot, V., Rikkinen, J., Saint Martin, S., Thiel, V., and Seyfullah, L.J. 2018. Marine microorganisms as amber inclusions: insights from coastal forests of New Caledonia. *Fossil Record*, 21:213-221. https://doi.org/10.5194/fr-21-213-2018

Schmidt, A.R., Schönborn, W., and Schäfer, U. 2004. Diverse fossil amoebae in German Mesozoic amber. *Palaeontology*, 47:185-197. https://doi.org/10.1111/j.0031-0239.2004.00368.x

Schultz, G.A. 1975. Bathypelagic isopod Crustacea from the Antarctic and southern seas, p. 69-128. In Schultz, G.A. (ed.), *Biology of the Antarctic Seas V*. American Geophysical Union, Richmond, Virginia.

Schultz, G.A. 1980. *Arcturocheres gaussicola* n. sp. (Cabiropsidae) parasite on *Antarcturus gaussianus* Vanhöffen (Arcturidae) from Antarctica (Isopoda). *Crustaceana*, 39:153-156. https://doi.org/10.1163/156854080X00058

Serrano-Sánchez, M. de L., Hegna, T.A., Schaaf, P., Pérez, L., Centeno-García, E., and Vega, F.J. 2015. The aquatic and semiaquatic biota in Miocene amber from the Campo La Granja mine (Chiapas, Mexico): paleoenvironmental implications. *Journal of South American Earth Sciences*, 62:243-256. https://doi.org/10.1016/j.jsames.2015.06.007

Serrano-Sánchez, M. de L., Nagler, C., Haug, C., Haug, J.T., Centeno-García, E., and Vega, F.J. 2016. The first fossil record of larval stages of parasitic isopods: cryptoniscus larvae preserved in Miocene amber. *Neues Jahrbuch für Geologie und Paläontologie-Abhandlungen*, 279:97-106. https://doi.org/10.1127/njgpa/2016/0543

Shields, J.D. and Ward, L.A. 1998. *Tiarinion texopallium*, new species, an entoniscid isopod infesting majid crabs (*Tiarinia* spp.) from the Great Barrier Reef, Australia. *Journal of Crustacean Biology*, 18:590-596. https://doi.org/10.1163/193724098X00412

Shimomura, M., Ohtsuka, S., and Naito, K. 2005. *Prodajus curviabdominalis* n. sp. (Isopoda: Epicaridea: Dajidae), an ectoparasite of mysids, with notes on morphological changes, behaviour and life-cycle. *Systematic Parasitology*, 60:39-57. https://doi.org/10.1007/s11230-004-1375-8

Shino, S.M. 1965. Phylogeny of the genera within the family Bopyridae. *Bulletin du Museum National d'Histoire Naturelle, Series 2*, 37:462-465.

Strömberg, J.-O. 1971. Contribution to the embryology of bopyrid isopods with special reference to *Bopyroides, Hemiarthrus*, and *Pseudione* (Isopoda, Epicaridea). *Sarsia* 47:1–46. https://doi.org/10.1080/00364827.1971.10411191

Strömberg, J.-O. 1983. A redescription of *Onisocryptus sagittus* Schultz 1977 (Epicaridea, Cryptoniscina) with notes on hosts, distribution and family relationships. *Polar Biology*, 2:87-94. https://doi.org/10.1007/BF00303173

Thamban, A.P., Kappalli, S., Kottarathil, H.A., Gopinathan, A., and Paul, T.J. 2015. *Cymothoa frontalis*, a cymothoid isopod parasitizing the belonid fish *Strongylura strongylura* from the Malabar Coast (Kerala, India): redescription, description, prevalence and life cycle. *Zoological Studies* 54:42. https://doi.org/10.1186/s40555-015-0118-7

Thompson, M.T. 1901. A new isopod parasitic on the hermit crab. *Bulletin of the U.S. Fisheries Commission*, 21:53-56.

Torres Jordá, M. 2003. Estudio de la Relación Entre el Parásito *Leidya Distorta* (Isopoda: Bopyridae) y su Hospedador *Uca uruguayensis* (Brachyura: Ocypodidae), y Descripción de los Estadíos Larvales de *L. Distorta*. Doctoral thesis, Universidad de Buenos Aires, Buenos Aires.

Truesdale, F.M. and Mermilliod, W.J. 1977. Some observations on the host-parasite relationship of *Macrobrachium ohione* (Smith) (Decapoda, Palaemonidae) and *Probopyrus bithynis* Richardson (Isopoda, Bopyridae). *Crustaceana,* 32:216–220.

Tsukamoto, R.Y. 1981. *Bopyrina ocellata* (Czerniavsky, 1868), isópode parasita assinalada pela primeira vez no Atlântico Sul (Epicaridea, Bopyridae). Morfologia, desenvolvimento e distribuição geográfica. *Ciência e Cultura,* 33:394–401.

Uye, S. and Murase, A. 1997. Infertility of the planktonic copepod *Calanus sinicus* caused by parasitism by a larval epicaridian isopod. *Plankton Biology & Ecology*, 44:97-99.

van der Wal, S., Smit, N.J., and Hadfield, K.A. 2019. Review of the fish parasitic genus *Elthusa* Schioedte & Meinert, 1884 (Crustacea, Isopoda, Cymothoidae) from South Africa, including the description of three new species. *ZooKeys*, 841:1-37. https://doi.org/10.3897/zookeys.841.32364

von Soergel, W. 1913. Lias und Dogger von Jefbei und Fialpopo (Misólarchipel), p. 586-650. In Boehm G. (ed.), *Geologische Mitteilungen aus dem Indo-Australischen Archipel. Neues Jahrbuch für Mineralogie.* E. Schweizerbartsche Verlagsbuchhandlung, Stuttgart.

Wägele, J.-W. 1989. *Evolution und phylogenetisches System der Isopoda: Stand der Forschung und neue Erkenntnisse. Zoologica.* Schweizerbart, Stuttgart.

Walossek, D. and Müller, K.J. 1998. Cambrian 'Orsten'-type arthropods and the phylogeny of Crustacea, p. 139-153. In Fortey, R.A. and Thomas, R.H. (eds.), *Arthropod Relationships. The Systematics Association Special Volume Series*. Springer Netherlands, Dordrecht. https://doi.org/10.1007/978-94-011-4904-4_12

Walossek, D. 1999. On the Cambrian diversity of Crustacea. *Crustaceans and the Biodiversity Crisis. Proceedings of the Fourth International Crustacean Congress,* Brill, Leiden, p. 3-27.

Wienberg Rasmussen, H., Jakobsen, S.L., and Collins, J.S.H. 2008. Raninidae infested by parasitic Isopoda (Epicaridea). *Bulletin of the Mizunami Fossil Museum*, 34:31-49.

Williams, J.D. and An, J. 2009. The cryptogenic parasitic isopod *Orthione griffenis* Markham, 2004 from the eastern and western Pacific. *Integrative and Comparative Biology*, 49:114-126. https://doi.org/10.1093/icb/icp021

Williams, J.D. and Boyko, C.B. 2012. The global diversity of parasitic isopods associated with crustacean hosts (Isopoda: Bopyroidea and Cryptoniscoidea). *PLoS One*, 7:e35350. https://doi.org/10.1371/journal.pone.0035350

Williams, E.H. and Bunkley-Williams, L. 2019. Life cycle and life history strategies of parasitic Crustacea, p. 179-266. In Smit, N.J., Bruce, N.L., and Hadfield, K.A. (eds.), *Parasitic Crustacea. State of Knowledge and Future Trends. Zoological Monographs 3*. Springer International Publishing, Cham. https://doi.org/10.1007/978-3-030-17385-2_5

Wilson, G.D. 2009. The phylogenetic position of the Isopoda in the Peracarida (Crustacea: Malacostraca). *Arthropod Systematics & Phylogeny*, 67:159-198.

Xing, L., Sames, B., McKellar, R.C., Xi, D., Bai, M., and Wan, X. 2018. A gigantic marine ostracod (Crustacea: Myodocopa) trapped in mid-Cretaceous Burmese amber. *Scientific Reports*, 8:1365. https://doi.org/10.1038/s41598-018-19877-y

APPENDIX 1.

Preservation of the type specimens.

IGR.GAR-8.1: two specimens.

IGR.GAR-8.1-1: lateral view from the right body side; good visibility restricted to some areas; posterior pereopods (thoracic appendages), distal part of the antenna and uropods visible.

IGR.GAR-8.1-2: ventro-lateral view from the right body side; is depicted in Néraudeau (2017); covered with a layer of glue.

IGR.GAR-8.2: one specimen; visible from both lateral views; good visibility from the right body side and minor visibility from the left body side; antenna, dorsal striation pattern and coxal plates visible.

IGR.GAR-28 (holotype): one specimen; visible from two directions, ventrolateral view from the left body side and latero-dorsal view from the right body side; very good visibility; antennular plates, second and third antennula elements, antenna, oral cone, pereopods (thoracic append-ages), coxal plates, pleopods and uropods visible.

IGR.GAR-41: two specimens.

IGR.GAR-41-1: dorsal view; good visibility only in the posterior region; dorsal shape of the head shield, dorsal outline, telson and uropods visible.

IGR.GAR-41-2: dorsal view, bad visibility except for the uropod region; uropods partly broken off, showing cross-sections of endo- and exopods.

IGR.GAR-48: one specimen; visible from two directions, latero-dorsal view from the left body side and ventro-lateral view from the right body side; relatively good visibility from both sides; dorsal surface including striation pattern, antennular plates, coxal plates, posterior pereopods (thoracic appendages) and first pleopods visible.

IGR.GAR-51: one specimen, ventral view; inclusion is cracked open and the interior surface of the cavity is visible, large parts of the right body side missing; dorsal striation pattern and telson ornamentation visible.

IGR.GAR-53: two specimens.

IGR.GAR-53-1: ventral view; very good visibility except for the uropods; antennulae, antennae, mouthparts, pereopods (thoracic appendages) and anterior pleopods visible.

IGR.GAR-53-2: visible from dorsal and ventral view; good visibility from dorsal view and bad vis-ibility from ventral view; antennae, dorsal striation pattern, telson and uropods visible.

IGR.GAR-64: one specimen; latero-ventral view from the left body side; bad visibility; antennular plates, rough shapes of pereopods (thoracic appendages) and pleopods and uropods visible.

IGR.GAR-65: one specimen; postero-lateral view from the left body side; relatively good visibility; body on the left side partially abraded (grinded off during preparation); posterior pereopods (tho-racic appendages) and pleopods visible.

IGR.GAR-89: one specimen; antero-ventral view; partially good visibility; antenna, pereopods (thoracic appendages), pleopod setation and uropods visible.

IGR.GAR-90: one specimen; ventral view; inclusion is at the surface of the amber and cracked open showing the interior surface of the cavity and features of the head morphology.

IGR.GAR-92: one specimen; lateral view from the left body side; good visibility restricted to some areas; dorsal surface including striation pattern visible.

IGR.GAR-93: one specimen; visible from two directions, latero-dorsal view from the left body side and latero-ventral view from the right body side; good visibility with exception for the pleo-

pod region; dorsal surface including striation pattern, antennular plate, antenna, oral cone, coxal plates and posterior pereopods (thoracic appendages) visible.

IGR.GAR-94: one specimen; lateral view from the right body side; good visibility, antenna, posterior pereopods (thoracic appendages) and uropods visible.

IGR.GAR-95: two specimens.

IGR.GAR-95-1: ventral view, good visibility restricted to some areas; antennula, antenna, pereopods (thoracic appendages), coxal plates and uropods visible.

IGR.GAR-95-2: lateral view from the right body side; bad visibility; only rough shape visible.

IGR.GAR-97: one specimen; ventral view; good visibility except for uropods; antennulae, pereopods (thoracic appendages) and pleopods visible.

IGR.GAR-98: one specimen; dorsal view; partially good visibility; antennae, dorsal striation pattern and uropods visible.

APPENDIX 2.

Character states of five selected characters in cryptoniscium larvae from the literature (data used in Figure 16) (available as zipped file at https://palaeo-electronica.org/content/2019/2757-cretaceous-epicaridea).

APPENDIX 3.

Body lengths of different life stages of epicarideans, aegids and cymothoids from the literature and from the herein studied specimens (data used in Figure 17) (available as zipped file at https://palaeo-electronica.org/content/2019/2757-cretaceous-epicaridea).

APPENDIX 4.

Stack of single fluorescence microscopy images of the head region of specimen IGR.GAR-28 (cf. Figure 10.2 and Figure 12.7) (available as zipped file at https://palaeo-electronica.org/content/2019/2757-cretaceous-epicaridea).

APPENDIX 5.

Stack of single fluorescence microscopy images of the head region of specimen IGR.GAR-53-1 (cf. Figure 10.2 and Figure 12.4) (available as zipped file at https://palaeo-electronica.org/content/2019/2757-cretaceous-epicaridea).

2.3 Study III: SCHÄDEL, HÖRNIG, HYŽNÝ & HAUG 2021

Authors: Schädel, M., Hörnig, M. K., Hyžný, M., & Haug, J. T.

Title: Mass occurrence of small isopodan crustaceans in 100-million-year-old amber: an extraordinary view on behaviour of extinct organisms

Journal: PalZ

Volume: 95

Issue: 3

Pages: 429-445

DOI: https://doi.org/10.1007/s12542-021-00564-9

RESEARCH PAPER

Mass occurrence of small isopodan crustaceans in 100-million-year-old amber: an extraordinary view on behaviour of extinct organisms

Mario Schädel[1] · Marie K. Hörnig[2] · Matúš Hyžný[3] · Joachim T. Haug[1,4]

Abstract

Within Isopoda (woodlice and relatives), there are lineages characterised by a parasitic lifestyle that all belong to Cymothoida and likely form a monophyletic group. Representatives of Epicaridea (ingroup of Cymothoida) are parasitic on crustaceans and usually go through three distinct larval stages. The fossil record of Epicaridea is sparse and thus little is known about the palaeoecology and the origin of the complex life cycle of modern epicarideans. We present an assemblage of over 100 epicarideans preserved in a single piece of Late Cretaceous Myanmar amber. All individuals are morphologically similar to cryptoniscium stage larvae. The cryptoniscium stage usually constitutes the third and last larval stage. In modern representatives of Epicaridea, the cryptoniscium larvae are planktic and search for suitable host animals or adult females. These fossil specimens, though similar to some extant species, differ from other fossil epicaridean larvae in many aspects. Thus, a new species (and a new genus), *Cryptolacruma nidis*, is erected. Several factors can favour the preservation of multiple conspecific animals in a single piece of amber. However, the enormous density of epicarideans in the herein presented amber piece can only be explained by circumstances that result in high local densities of individuals, close to the resin-producing tree.

Keywords Cymothoida · Epicaridea · Cryptoniscium larvae · Palaeoecology · Taphocoenosis · Taphonomy

Handling Editor: Mike Reich.

✉ Mario Schädel
mario.schaedel@palaeo-evo-devo.info

Marie K. Hörnig
marie.hoernig@palaeo-evo-devo.info

Matúš Hyžný
matus.hyzny@uniba.sk

Joachim T. Haug
joachim.haug@palaeo-evo-devo.info

1 Faculty of Biology, Ludwig-Maximilians-Universität München, Großhaderner Str. 2, 82152 Planegg-Martinsried, Germany

2 Cytology and Evolutionary Biology, Zoological Institute and Museum, University of Greifswald, Soldmannstr. 23, 17489 Greifswald, Germany

3 Department of Geology and Paleontology, Comenius University in Bratislava, Mlynská dolina, Ilkovičova 6, 842 15 Bratislava, Slovakia

4 GeoBio-Center of the LMU Munich, Richard-Wagner-Str. 10, 80333 Munich, Germany

Introduction

Isopoda is a diverse group of crustaceans and its representatives today live in a wide variety of habitats (Brandt 1999; Raupach et al. 2004; Schmidt 2008; Poore and Bruce 2012). Isopoda is a group of primarily marine animals, meaning that the direct ancestor of Isopoda was very likely marine and representatives of most ingroups of Isopoda live in marine environments (Poore and Bruce 2012). However, many ingroups of Isopoda have species that live in brackish or fresh water (Brasil-Lima and De Lima Barros 1998; Wilson and Johnson 1999). The group Oniscidea forms an extreme exception to the aquatic lifestyle found in most representatives of Isopoda as oniscideans live on land and some of them even in arid areas (Schmidt 2008).

Isopoda is an ingroup of Peracarida, which is characterised by females that have a brood pouch formed by lamellae on the legs (oostegites) (Ax 2000). Most freshly hatched immatures of Isopoda resemble the adults in many aspects of their morphology and no drastic changes appear to happen during the further development (Boyko and Wolff 2014). Specialised hatchlings are present in two ingroups of Isopoda that are both characterised by a parasitic lifestyle:

Gnathiidae and Epicaridea. Here, more drastic changes occur during the post-embryonic development (Boyko and Wolff 2014). Based on various criteria, representatives of these groups have true larva (discussed in Haug 2020).

Epicarideans mostly live in marine and brackish environments (Markham 1986). However, there are some reports on species living in fresh water (Chopra 1923; Shiino 1954). All epicaridean species parasitise other crustaceans (Markham 1986; but see Pascual et al. (2002) for a record on squids). Epicaridea is closely related to Cymothoidae (possibly a sister group relationship); representatives of Cymothoidae parasitise fishes (Wägele 1989; Dreyer and Wägele 2001). Other closely related groups such as Aegidae or Cymothoidae likewise have representatives parasitising fishes; therefore, it is likely that fishes are the ancestral hosts and the change to crustacean hosts evolved in the common ancestor of epicarideans (Dreyer and Wägele 2001).

The post-embryonic development in Epicaridea is characterised by distinct transformations. With only one exception (Miyashita 1940), epicarideans are released from the brood pouch as epicaridium larvae (Boyko and Wolff 2014). Epicaridium larvae are planktic and search for a small-sized intermediate crustacean host of the group Copepoda to which they attach (Boyko and Wolff 2014). Once an epicaridium larva has attached to its host, it will moult into the microniscium stage. The microniscium stage larvae stay on the small-sized host and feed on its haemolymph (Anderson 1975; Uye and Murase 1997). At some point, the larva moults into the cryptoniscium stage, leaves the host and is again planktic (Boyko and Wolff 2014).

Within Epicaridea, there are lineages with strictly protandric development as well as lineages in which the sex develops triggered by the presence or absence of conspecific parasites on the final host (Wägele 1989). Especially in lineages with strictly protandric development, the cryptoniscium stage is not distinctly differentiable on a morphological basis to later stages (males) in some ingroups of Epicaridea (Hosie 2008). Males are generally much smaller than the females (Shimomura et al. 2005). Female epicarideans often lose their bilateral symmetry, due to their position on the left or right side in the body of the host (Williams and An 2009). In some lineages, the female becomes endoparasitic; this can be accompanied by a drastic loss of sclerotisation (e.g. Shiino 1954). Reconstructions of the possible origin of this complex life cycle have been discussed in Schädel et al. (2019).

Until a few years ago, the fossil record of Epicaridea only consisted of trace fossils. Swellings of the branchial chambers of some shrimps, lobsters and crabs—caused by the presence of large female epicarideans—have been recorded, ranging from the Late Jurassic to the Pleistocene (Bell 1863; Markham 1986; Wienberg Rasmussen et al. 2008; Robins et al. 2013; Klompmaker et al. 2014, 2018; Klompmaker and Boxshall 2015; Robins and Klompmaker 2019). One record

(material lost) suggests that such swellings were present even earlier in the Early Jurassic (Soergel 1913).

Recently, body fossils of Epicaridea have been reported from two amber deposits. All epicaridean amber inclusions are from cryptoniscium stage larvae or later stages retaining a cryptoniscium-like morphology. Several 20-million-year-old specimens come from Chiapas, Mexico (Early Miocene, Campo La Granja amber; Serrano-Sánchez et al. 2016), about 99-million-year-old specimens come from Vendée, France (Late Cretaceous, Vendean amber, La Garnache outcrop; Néraudeau et al. 2017; Schädel et al. 2019).

Amber has the potential to preserve very fine details of even small animals (Sidorchuk et al. 2016). Although they make only a small fraction of the overall number of inclusions, aquatic animals can get preserved in amber (e.g. Gustafson et al. 2020). There are also records for supposedly marine organisms on (Mao et al. 2018) and in amber (Girard et al. 2008; Saint Martin et al. 2015; Xing et al. 2018; Yu et al. 2019). Experiments in a modern day swamp have demonstrated that it is possible for animals that are submerged in water to get trapped in resin that is also submerged in water (Schmidt and Dilcher 2007; illustrated in Schädel et al. 2019).

Mass occurrences of individuals of the same species in a single piece of amber have been reported for several amber sites and several lineages of Euarthropoda (Arillo 2007). These lineages include web spiders (Araneae; Poinar and Poinar 1994: fig. 73; Weitschat and Wichard 1998: fig. 20h), springtails (Collembola; Robin et al. 2019), plant lice (Sternorrhyncha; Wang et al. 2014; Szwedo and Drohojowska 2016; Hakim et al. 2019), termites (Isoptera; Grimaldi 1996: 85; Wu 1997: fig. 269; Martínez-Delclòs et al. 2004: fig. 3D; Wichard and Weitschat 2004: 107; Arillo 2007: fig. 1D; Vršanský et al. 2019), ants (Formicidae; Grimaldi 1996: 92; Martínez-Delclòs et al. 2004: fig. 3C; Arillo 2007: fig. 1C), beetles (Coleoptera; Poinar 1999; Martínez-Delclòs et al. 2004: fig. 3E) and flies (Diptera; Brown and Pike 1990; Grimaldi 1996: 84; Ross 1998: fig. 1).

Here, we present an amber piece with more than 100 specimens with a cryptoniscium-like morphology. We describe the fossils and discuss their relationships as well as the unusually high density of inclusions in a single amber piece.

Materials and methods

The amber piece (Myanmar amber, Kachin amber, 'Burmese' amber) was acquired from a private collection. Further information on the provenance, including the date of the excavation and export permits are not available. The amber piece is currently part of the PED research collection (Zoomorphology working group,

Ludwig-Maximilians-Universität, Munich, Germany). For a discussion on the ethical aspects of the trade of amber fossils, see Haug et al. (2020). The surface of the amber piece was polished using common metal polish (POLIBOY Brandt and Walther GmbH) applied by hand using a sponge.

Microscopic images were made using a Keyence VHX-6000 digital microscope. Overview images of the entire amber piece were recorded under transmitted light combined with cross-polarised coaxial epi-illumination. Detail images of individual specimens were recorded under transmitted light combined with ring-light epi-illumination. The depth-of-field limitations were overcome by recording stacks of images and fusing these to a single sharp image. To overcome the field-of-view limitations, several adjacent image details were recorded, each with a stack, and then stitched to a large panorama image.

For the detail images, a digital method to reduce the effect of reflections was applied (implemented in the software of the microscope). Images from slightly different angles were recorded to produce stereo images. Epi-fluorescence microscopic images were recorded using a Keyence BZ-9000 digital microscope (exciting light of 545 nm wavelength, dichroitic mirror with a wave length of 565 nm, optimised for TRITC stains; Haug et al. 2011a, b; Schädel et al. 2019). The potential of this method was limited by the accessibility of the specimens in the amber piece, as the distance of the specimens to the amber surface was too large. Stacks of images with a different level of the focal plane were recorded and fused using the software CombineZP (GPL licence) (cf. C. Haug et al. 2011a, b).

GIMP (GPL license) was used to optimise image properties (histogram optimisation, brightness, colour and contrast enhancement), to remove backgrounds, to colour-code morphological structures and to create red-cyan stereo anaglyphs.

A Zeiss Xradia XCT-200 (Carl Zeiss Microscopy GmbH, Jena, Germany) was used for micro-computed-tomography (μCT) of the amber piece. The Xradia XCT-200 is equipped with switchable scintillator-objective lens units. Tomographies were performed using 0.39×, 4× and 10× objectives, with the following X-ray source settings: 30 kV, 6 W, 3.5 s exposure time (0.39× and 4×), and 40 kV, 8 W, 4 s exposure time (10×).

Stacks of images (TIF format) were reconstructed based on projections using the XMReconstructor software (Carl Zeiss Microscopy GmbH, Jena, Germany). Image stack properties were: (1) overview scan (0.39×): system based calculated pixel size = 18 μm, 1024 by 1024 px; (2) 4× scan: system-based calculated pixel size = 3.16 μm, 1024 by 1024 px; (3) 10× scan: system-based calculated pixel size = 1.5 μm, 1005 by 1005 px. All scans were performed using 'Binning 2' and subsequently reconstructed using 'Binning 1' (full resolution).

To exclude further enclosed particles and debris in the final volume, the specimens in the focus of the 10× scan were roughly "segmented" using TrakEM2 (part of FIJI, GPL license; cf. Kypke and Solodovnikov 2018). Volume rendering was performed in Drishti 2.6.5 (on Linux, using WINE, GPL license; Limaye 2012). The three-dimensional of the specimens within the amber piece was visualised by placing points in Drishti.

The total number of specimens was counted by matching the light microscopic overview images from both sides of the amber piece to the μCT data. Data on the body lengths in Epicaridea was reused from Schädel et al. (2019). All plots were created using R (GPL license) and the packages readr, ggplot2 and gridExtra. The geological scale was added to the plot using the package deeptime (William Gearty, GPL license, https://github.com/willgearty/deeptime). A special colour palette (copyright Paul Tol, https://personal.sron.nl/~pault/) was used to map multiple groups in a single plot, whilst ensuring perceptibility for colour vision impaired readers.

The figure plates were arranged using Inkscape (GPL license). All figure plates were checked for the perceptibility by colour vision impaired readers using the software Color Oracle 1.3 (CC-BY license, Bernhard jenny and Nathaniel V. Kelso).

Taxonomic and systematic information for literature specimens (Supplementary data tables 1–2) was retrieved from the Word Register of Marine Species ("WoRMS", Boyko et al. 2008 onwards). Large parts of Supplementary data tables 1–2 are reused from Schädel et al. (2019).

Institutional abbreviations. PED, research collection of the Palaeo-Evo-Devo Research Group, Ludwig-Maximilians-Universität, Munich, Germany.

Results

Description of the amber piece

The amber piece is flat on two opposing sides and roughly oval in outline when viewed from either of the flat sides. The amber matrix contains a substantial amount of macroscopic gas-filled bubbles. The amber matrix contains few organic debris particles. Roughly, parallel to the flat sides of the amber piece is a plane within the resin that is less transparent than the surrounding resin. There are 103 small fossils of Euarthropoda (described in detail below) distributed along this plane within the amber matrix (Figs. 1b, 2f). Other organic inclusions are stellate plant trichomes and a single mite.

Description of the specimens

General body shape strictly bilateral, body with multiple segments: presumably 1 ocular segment and 19 post-ocular segments (PO in the following). Body much longer than wide. Outline of body in dorsal view elongated tear-drop shaped, tapering towards posterior end. Dorsal surface convex. Ventral side of body concave (if appendages not considered). Overall body size (without appendages) ranging from 0.45 to 1.29 mm, with mean of 0.83 mm and standard deviation of 0.19 mm (Fig. 3a–a).

Body organised into functional head (ocular segment and PO 1–6, 'cephalothorax') and trunk (PO 7–19 and telson). Trunk divided into three functional units (tagmata): posterior part of thorax (with walking or grasping appendages, PO 7–13, 'pereon'), anterior part of pleon (with swimming appendages, PO 14–18), and pleotelson (PO 19 and telson). Head segments form single dorsal sclerite (head shield) (Fig. 2a). Each trunk segment with individual dorsal sclerite (tergite). Tergite of trunk segment 1 similar in height and width to posterior margin of head shield (without neck) (Fig. 2a–c). Tergite of last trunk segment continuous with telson. Pleotelson pointed, half-oval shape in dorsal view, posterior margin smooth, without teeth. Striation pattern (shallow, fine-scaled grooves) at least on surface of tergites of trunk segments 3–5.

Antennula (appendage of PO 1) with proximal element large and flat ('antennular plate'), roughly triangular in ventral view, posterior margin with 4 large teeth. Further distal elements not visible (too small for resolution of μCT with 10×objective and not accessible by microscopy).

Antenna (appendage of PO 2) subdivided into peduncle (proximal elements) and flagellum (distal elements). 4 peduncle elements visible (likely 5 peduncle elements present, two most proximal elements likely not differentiable in μCT data). Two strong setae on ventral side of distal-most peduncle element (Fig. 2d–e, h). Flagellum much narrower than peduncle, with 5 elements.

Mouthparts not directed in anterior direction and not located between antennular plates; details of individual mouthparts (labrum, appendages of PO 3–6 and paragnaths) not visible.

Anterior trunk appendages (appendages of PO 7–13, 'pereopods') not visible, individual elements not discernible in μCT data, only most distal elements accessible in microscopic images. A subdivision into seven elements along the main axis (coxa, basipod, ischium, merus, carpus, propodus and dactylus) is assumed.

Coxa in trunk appendages 2–7 forming scale-like structure ('coxal plates') adjoining lateral sides of the tergites. Coxal plates with antero-ventral corner rounded, ventral margin straight, postero-ventral corner rounded, posterior margin straight, posterior margin without teeth, posterior margin with slight serration.

Basipod long and slender in all legs, where visible (trunk appendages 2–7). Further distal elements much shorter. Penultimate element (propodus) compressed in anterior–posterior direction, median margin straight, lateral margin convex. Propodus on trunk appendages 2 and 3 with two strong setae on median side (Fig. 2d–e, 2h). Terminal element (dactylus) much shorter and slenderer than propodus. Dactylus in trunk appendages 1 and 2 curved inwards, more straight in trunk appendages 3 and 4.

Anterior five pleopods (appendages of PO 14–18) subdivided into three elements, all elements strongly compressed in anterior–posterior direction (leaf shaped). Proximal element (basipod) broad, distinctly longer on lateral side, distal margin with distinct angle. Endopod inserting on medio-distal margin of basipod; broad, approximately 0.75 times width of basipod in proximal part; tapering towards distal margin, multiple long setae at distal margin. Exopod inserting on latero-distal margin of basipod; distinctly narrower than endopod, approximately 0.3 times width of basipod; multiple long setae at distal margin. Size of pleopods slightly decreasing from anterior to posterior.

Uropod (appendage of PO 19) subdivided into three elements. Proximal element (basipod) longer than wide, rectangular in posterior view, compressed in anterior–posterior direction (functional dorsal–ventral direction). Endopod inserting on medio-distal margin of basipod; narrow, straight, approximately half of width of basipod, approximately as long as basipod; long setae on distal margin. Exopod inserting on latero-distal margin of basipod; narrow, straight, approximately half of width of basipod, approximately as long as basipod, as long as endopod; long setae on distal margin.

Discussion

Conspecificity of the specimens

The herein presented specimens vary considerably in size (see below); however, the overall morphology is very similar throughout all specimens. We could not find any morphological differences between the specimens that cannot be explained by the size differences of the individuals or the quality of preservation. Thus, it seems likely that all specimens within this amber piece are conspecific.

Systematic affinity of the specimens

The specimens have an ocular segment followed by presumably 19 appendage-bearing body segments; the trunk has a distinct posterior tagma with six segments that appear

specialised for swimming (or ventilation). This condition is identifiable as a derived condition of a tagmatisation of the body into a 6–8–6 pattern, i.e. three tagmata: head, thorax, and pleon (the latter with six appendage-bearing segments). This is apomorphic for the eucrustacean ingroup Eumalacostraca (Walossek 1999). The presence of uropods (specialised last trunk appendages) in the herein presented specimens is likewise apomorphic for the group Eumalacostraca (Walossek and Müller 1998). For Isopoda, there is no single, unambiguous apomorphy that is visible in the herein presented fossils; however, the combination of the following character states is indicative for Isopoda: (1) body dorsoventrally flattened; (2) anterior trunk appendages without exopods (Ax 2000; Wilson 2009). The presence of fixed, scale-like coxae ('coxal plates') on trunk segments 2–7 is apomorphic for Scutocoxifera, an ingroup of Isopoda (Dreyer and Wägele 2002). Within this group, the combination of the following features is characteristic for cryptoniscium stage larvae of Epicaridea: (1) body tear-drop shaped, tapering posteriorly; (2) anterior trunk appendages with large, sometimes flattened, propodi and (3) with long, spine-like, pointed dactyli; (4) distal (ancestrally movable) claws firmly conjoined with the main part of the dactylus; (5) uropod endo- and exopod rod-shaped (Wägele 1989; Serrano-Sánchez et al. 2016). The proximal element of the antennula is enlarged and with distinct teeth on the posterior margin. This feature is only known from a small number of species within Epicaridea (Schädel et al. 2019).

Exact ontogenetic stage

The morphology of the herein presented specimens is typical for cryptoniscium stage larvae of Epicaridea. This morphology can easily be differentiated from the morphology in earlier larval stages of Epicaridea. Epicaridium larvae are much less elongated, the trunk appendage 7 is absent and the pleopods are located on the lateral margins of the animal (Dale and Anderson 1982; Boyko and Wolff 2014). In microniscium stage larvae of Epicaridea, the appendages of the trunk appear less differentiated; for example, the individual elements of the antenna are not differentiable (Anderson and Dale 1981).

Especially in lineages of Epicaridea in which the representatives show a strictly protandric development, juvenile males can retain the morphology of the cryptoniscium stage (paedomorphosis; Hosie 2008). In other lineages, where the sex is determined by the presence or absence of a female on the final host, the cryptoniscium-like morphology can be lost rapidly in both sexes (Williams and An 2009). Therefore, the exact developmental stage cannot be determined for the herein presented fossils. The fossil specimens in the centre of this study are either cryptoniscium stage larvae or paedomorphic males.

Size variation

We performed two measurement series: (1) based on scaled microscopic images ('2D'; Fig. 1); (2) based on the overview μCT data ('3D'; Supplementary image data 1). Not all specimens were measured in both series; some were only visible in the microscopic images, others only in the μCT-based images. The distributions of size classes were similar in both series (Fig. 3b–c). The '3D' measurements generally showed higher values than the '2D' measurements, due to the loss of depth information in the 2D projections. The '2D' measurements are still included, as the number of measured specimens is much higher in this series because many specimens had a weak x-ray contrast (see Supplementary data table 1).

The specimens in the herein presented amber piece vary in their body length. The smallest specimen measures only 0.45 mm, the largest measures 1.29 mm. This variation could indicate the presence of more than one stage within the sample. However, the frequencies of size classes (Fig. 3b–c) do not support this hypothesis, as there are also many specimens with a medium body length present. Whilst it is still possible that the fossils at hand are different instars (e.g. cryptoniscium stage larvae together with paedomorphic later stages), this is not apparent from the observed size distribution.

A large size variation within one stage has previously been reported for cryptoniscium stages. Representatives of *Cryptoniscus laevis* with a cryptoniscium size range from 0.8 to 2.8 mm (Schultz 1977) constitutes an even wider range than in the herein presented specimens (further ranges can be retrieved from Supplementary data table 1). A contributing factor to wide size ranges in cryptoniscium larvae and males could be the gain in body size during the microniscium stage, up to 300% gain in body length (Anderson 1975; Dale and Anderson 1982), leaving more room for size variation within one life stage than in other ingroups of Euarthropoda (cf. 'Dyar's law'/'Brook's law'; Dyar 1890; Fowler 1904).

Systematic affinity within Epicaridea

Within Epicaridea, the two groups Cryptoniscoidea (comprising Cabiropidae, Crinoniscidae, Cryptoniscidae, Cyproniscidae, Dajidae, Entophilidae and Hemioniscidae) and Bopyroidea (comprising Bopyridae, Ionidae and Entoniscidae) form a sister group relationship (Boyko et al. 2013; Boyko and Williams 2015). We were not able to determine whether the herein presented specimens belong to either of these two groups, as the characters that we observed did not provide conclusive information (see Supplementary data table 2).
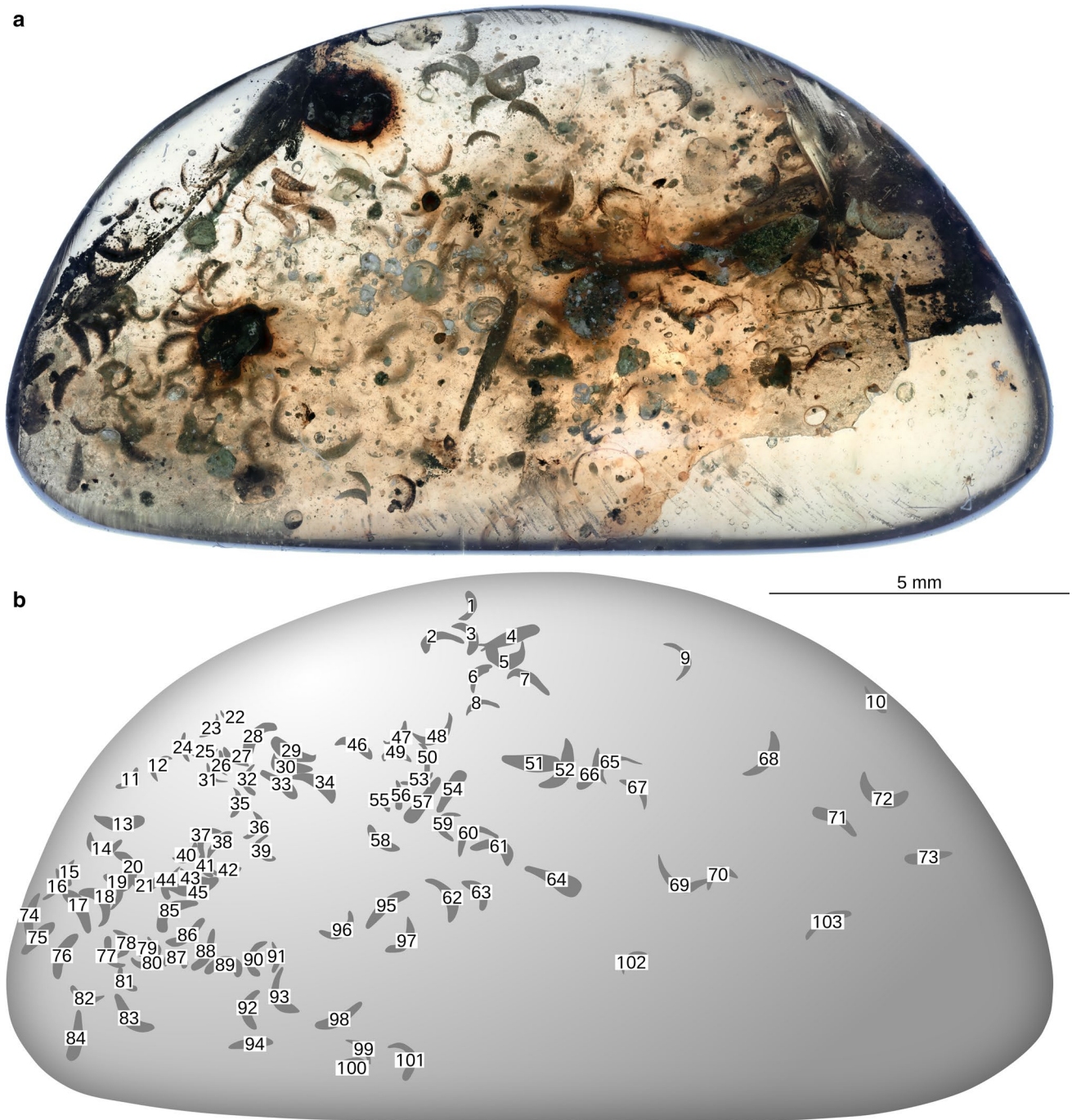
Fig. 1 **a** Overview of the amber piece, light microscopic image. **b** Drawing of the amber piece with the outlines of all counted fossil epicaridean specimens. Numbers correspond to the last part of the collection number [PED 0226-(number)]

It has been suggested (Boyko et al. 2013; Boyko and Williams 2015) that there is a connection between certain ingroups of Epicaridea and the number of flagellum elements of the antenna. Our literature review (Schädel et al. 2019; Supplementary data table 2) supports that in Cryptoniscoidea the number of antennal flagellum elements is 5, except for *Ancyroniscus bonnieri* (Holdich 1975, 4

flagellum segments). In Bopyroidea, the number of flagellum elements varies. In representatives of the Bopyroidea ingroup Bopyridae the number of flagellum elements is either 4 or 5, whereas in the supposed sister group Entoniscidae (Boyko et al. 2013) the number of flagellum elements is 3 or less. The low number of flagellum elements in Entoniscidae (Boyko et al. 2013; Boyko and Williams
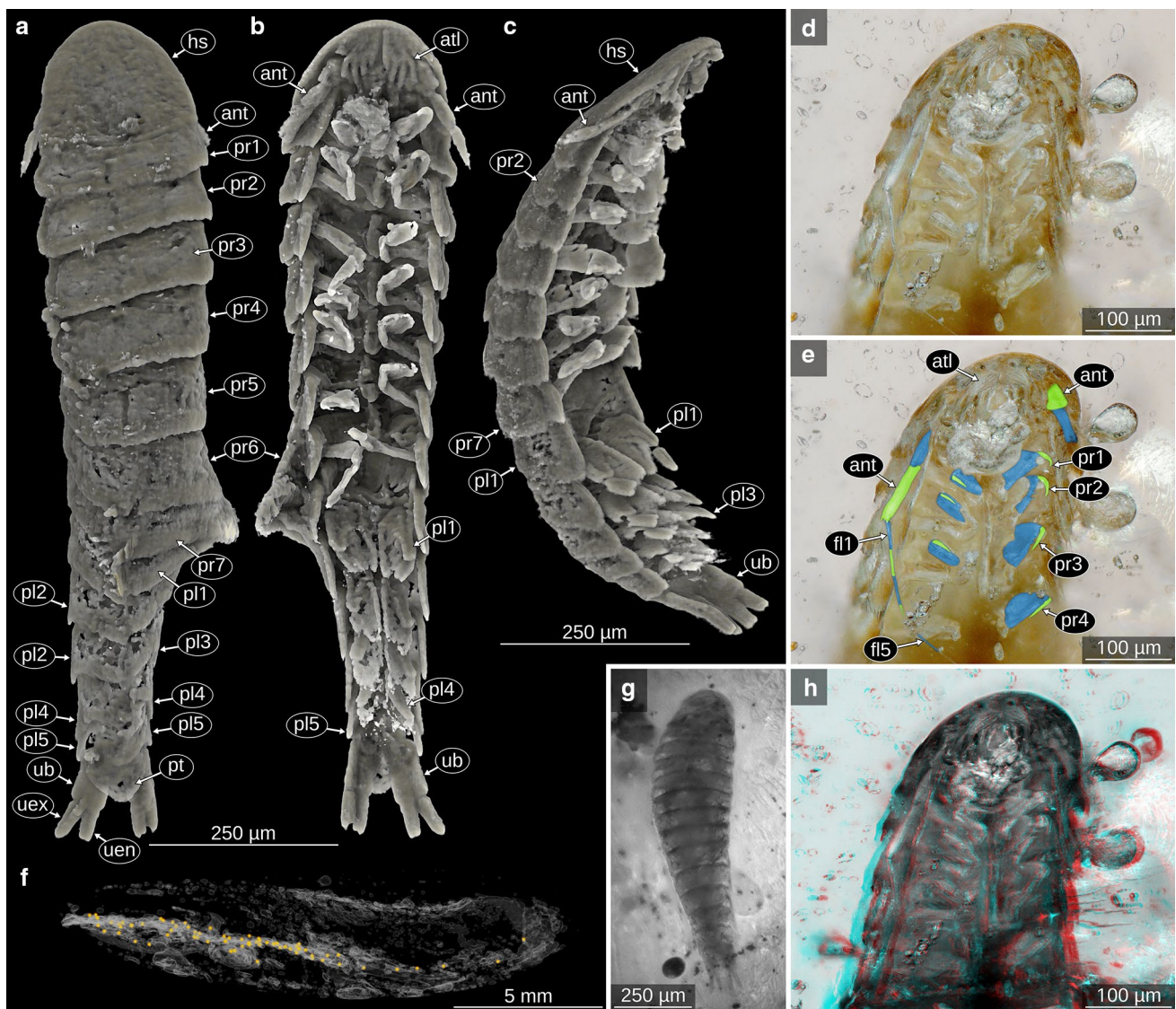
Fig. 2 **a**, **b** Holotype of *Cryptolacruma nidis* gen. et sp. nov., PED 0226-4, μCT-reconstruction, orthographic projection. **a** Dorsal view. **b** Ventral view. **c** Paratype of *Cryptolacruma nidis* gen. et sp. nov., PED 0226-5, μCT-reconstruction, latero-ventral view, orthographic projection. **d**, **e** Holotype of *Cryptolacruma nidis* gen. et sp. nov., PED 0226-4, detail of the anterior body region, ventral view, light microscopic image. **e** With colour markings. **f** μCT-reconstruction of the amber piece, yellow dots depict the position of the fossil isopo-

dans. **g** Paratype of *Cryptolacruma nidis* gen. et sp. nov., PED 0226-84, dorsal view, epifluorescence microscopic image. **h** Holotype of *Cryptolacruma nidis* gen. et sp. nov., PED 0226-4, detail of the anterior body region, ventral view, red-cyan stereo anaglyphs based on light microscopic image. *ant* antenna; *atl* antennula; *fl1–5* flagellum elements 1–5 of the antenna; *hs* head shield; *pl1–5* pleon segments 1–5; *pr1–7* trunk segments 1–7; *pt* pleotelson; *ub* uropod basipod; *uen* uropod endopod; *uex* uropod exopod

2015) could be an autapomorphy of the group making an ingroup position of the here presented fossils, which have 5 antennal flagellum elements, very unlikely. Due to the variability in the number of antennal flagellum elements in the other lineages, this character is not informative for the systematic affinity of the here presented fossils.

Comparably a position within Dajidae is very unlikely, because one apomorphy of Dajidae are the specialised mouthparts in the cryptoniscium stage larvae, which form a sucking disc. Although the individual mouthparts are not

differentiable in the μCT data or the microscopic images of the here reported fossils, the sucking disc in representatives of Dajidae is so conspicuous that it would be expected to be clearly visible in the microscopic images (e.g. Fig. 2d–e, h). The sucking discs in representatives of Dajidae can easily detach from the rest of the body (Taberly 1954), which, however, does not explain the absence in the here presented fossil specimens, given the high number of studied individuals. The herein presented specimens can, therefore, be interpreted as representatives of Epicaridea, that are
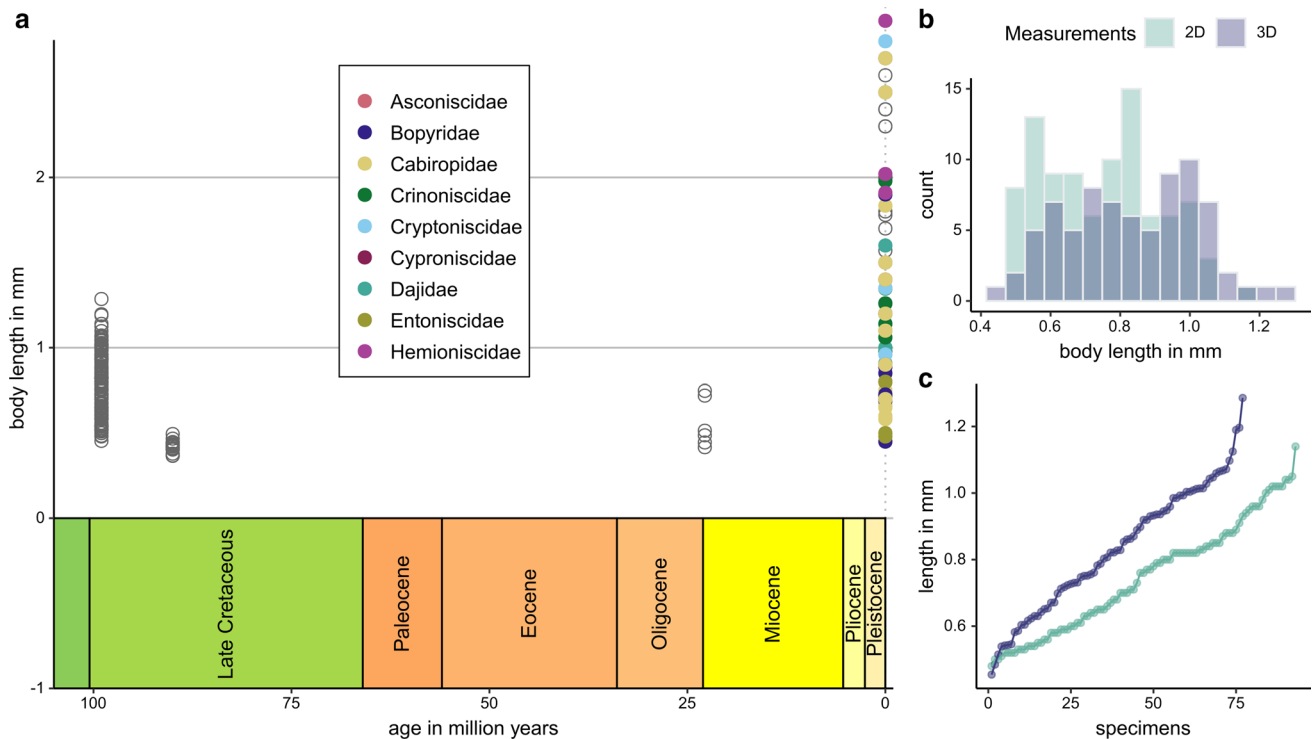
Fig. 3 a Body lengths of cryptoniscia and paedomorphic males in Epicaridea over time, empty circles depict records for which no affinity to an ingroup of Epicaridea could be identified. **b** Histogram of measurements of this study (*Cryptolacruma nidis* gen. et sp. nov., PED 0226). **c** Ranked size plot, values sorted in ascending order. Simple measurements from microscopy ('2D') vs. measurements based on volumetric data from the μCT ('3D')

not representatives of the ingroups Entoniscidae and Dajidae, hence 'Epicaridea nec Entoniscidae, nec Dajidae' (cf. Schädel et al. 2019).

Differential diagnosis

The herein presented specimens differ from the Late Cretaceous amber inclusions of *Vacuotheca dupeorum* Schädel, Perrichot and Haug, 2019 in having a pleotelson without teeth (with teeth in *V. dupeorum*). *Vacuotheca dupeorum* also has distinct teeth on the posterior margin of the coxal plates (Schädel et al. 2019: fig. 14), whereas the herein presented specimens have coxal plates with only slightly serrated posterior margins (Fig. 2b–e). The head shield in the herein presented specimens is flat, whereas in *V. dupeorum* the head shield is much higher in dorsoventral aspect (Schädel et al. 2019: figs. 5.3–5.5).

The herein presented specimens differ from the Early Miocene fossils from Campo La Granja amber (Chiapas, Mexico) in having uropod endo- and exopods that are of the same length. In the Mexican specimens, either the endopod or the exopod is distinctly longer than its corresponding other distal part of the uropod (Serrano-Sánchez et al. 2016), suggesting that they are likely representatives of at least two distinct species.

Most extant species differ in the combination of the following character states present in the herein presented fossils: (1) antenna with five flagellum elements; (2) uropod with endopod longer than exopod or equal to exopod; (3) antennula with proximal element enlarged in posterior direction (antennular plate); (4) antennular plate with distinct teeth on the posterior margin; (5) posterior margin of the pleotelson without distinct teeth.

There are three species in the literature that also have this combination of characters, but differ in some other aspects. (1) *Arturocheres gaussicola* Schultz, 1980 (Cabiropidae) differs from the herein presented specimens in having an uropod exopod that is much shorter than the endopod; also, the pleotelson in *A. gaussicola* is triangular instead of rounded as in the herein presented specimens (Schultz 1980). (2) *Dolichophryxus geminatus* Schultz, 1977 (Dajidae) differs from the herein presented specimens in having a much longer antenna (extending up to the anterior end of the pleon); also, specialised mouthparts (sucking discs) as in representatives of Dajidae are not apparent in the herein presented specimens (Schultz 1977). (3) Not formally described specimens from South America (Pascual et al. 2002) differ from the herein presented specimens in having shorter teeth on the posterior

margin of the antennular plate and in having a triangular, much more pointed pleotelson (Pascual et al. 2002).

Mass occurrence

In the here described amber piece, more than 100 fossil remains of epicarideans are enclosed, more than three times as many body fossils as known before. This raises the question: how can this mass occurrence be explained? It is unlikely that the embedment happened in a terrestrial environment. Transport by wind or spray can not explain the large number of specimens and the simultaneous low number of other syninclusions.

A passive embedment, e.g. by a resin drop dripping onto the fossilised individuals or overflowing them is also very unlikely. Resin overflowing dead specimens, either on land (e.g. in a dried-out pool) or under water would likely introduce a substantial amount of debris into the resin, which is not present in the here presented amber piece. This is unless there are recurrent resins flows and the specimens lie on a piece of resin. Resin dripping or rapidly flowing into a body of water can probably not cause small aquatic animals, such as cryptoniscium larvae to get in contact with the resin, as the resin would push away the water in which the specimens were located. However, submerged resin can act as an underwater trap in which aquatic arthropods can get stuck, as actuo-palaeontological experiments in a swamp have demonstrated (Schmidt and Dilcher 2007; Schädel et al. 2019: fig. 3).

High abundances of conspecific animals in amber pieces are not uncommon (Arillo 2007). In the following, possible reasons for such assemblages are outlined

(visualised in Fig. 4). To have many animals preserved in a piece of resin, the resin piece must act as a trap for a long time or many animals must come in contact with the resin within a short period of time.

Entrapment of many conspecific individuals

To have a high number of conspecific animals and a high relative abundance of a single species in the case of a long time trap, representatives of one species must get trapped more frequently than other species. Examples for such an enhanced selective risk of getting trapped are animals that naturally live close to resin, such as ambrosia beetles (Platypodinae; Martínez-Delclòs et al. 2004). A species can also be over-represented due to an attraction towards exposed resin. This has been shown for flying stages of insects with aquatic larvae, which are attracted to horizontally polarised light (Horváth et al. 2019). Attraction to polarised light is very unlikely for epicarideans, especially for the herein presented specimens which do not have prominent eyes.

A strong dominance of one species (or the absence of other species) in a specific habitat would promote a high relative abundance in the fossil record. Some amber deposits bear amber pieces with a high content of soil organisms, where springtails often dominate the content in the amber pieces (Robin et al. 2019). It is very unlikely that epicarideans dominate a habitat, as they are parasitic and would thus compete with very few host animals. However, preceding events (see below) could have led to this condition.

A long-term entrapment process is very unlikely for the herein presented amber piece, as all the epicarideans lie in the same plane (Fig. 2f, App. 1–2). This suggests that they
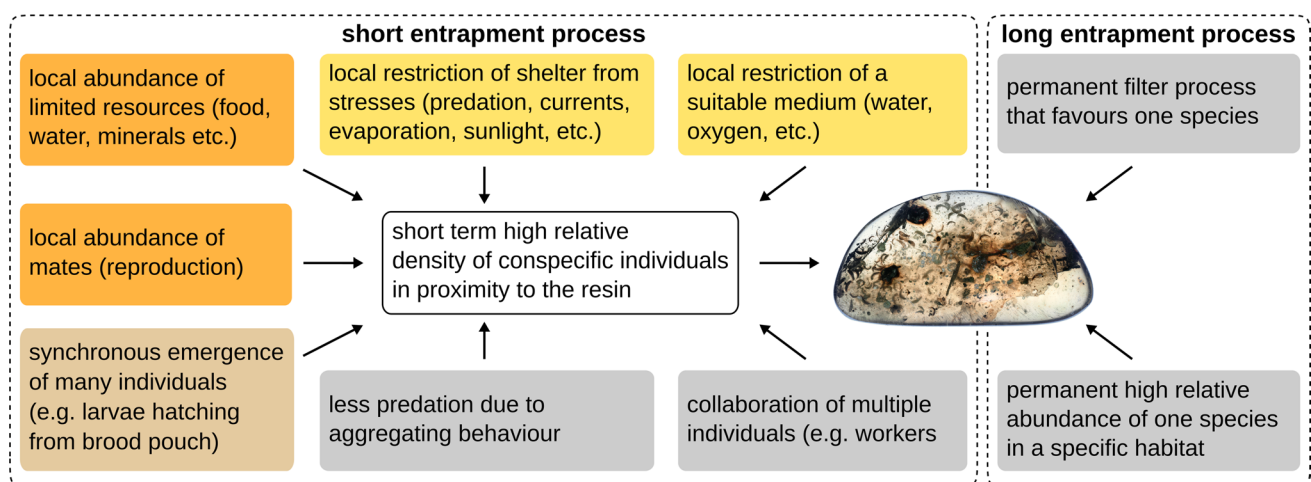
Fig. 4 Schematic depiction of factors that could have contributed to the taphonomical situation in the herein presented amber piece. Grey boxes, mechanisms that are very unlikely for representatives of Epicaridea. Yellow boxes, mechanisms that are plausible for representa- tives of Epicaridea. Orange boxes, mechanisms that are likely for representatives of Epicaridea and can explain a high density of individuals. Brown box, mechanism that could in principle explain a high density of Epicaridea individuals, but lacks modern analogues

probably became trapped on the surface of the resin drop and were then subsequently covered by more resin. In case of a long-term entrapment, the animals should be preserved more randomly throughout the amber piece and potentially even be separated by distinct layers. Such distinct layers of fossil organisms in amber are known from other amber sites with a high content of aquatic organisms (Serrano-Sanchez et al. 2015; Schädel et al. 2019). A stratification of amber in context with aquatic organisms could also be further explained by tidal influence, with the resin being periodically exposed to air and to water (Serrano-Sánchez et al. 2015).

Synchronised hatching or moulting as a factor for high abundance and density

A short-term entrapment with the outcome of a high (relative) abundance of a single species being preserved in the resin requires a temporary high (relative) abundance in proximity to the resin. This high (relative) abundance can either be on a very local scale or on a larger scale.

An example for a larger scale phenomenon would be the synchronised emergence of a specific life stage of this species (e.g. emergence of winged male ants in many colonies: Martínez-Delclòs et al. 2004). Such synchronised events could be triggered by biotic factors (e.g. pheromones, abundance of nutrients) or by abiotic factors (e.g. temperature, light, and salinity; Haug et al. 2013).

A synchronised mass moulting from the microniscium stage to the cryptoniscium stage could be triggered for example by a worsening health of an infected population of host animals or the perception of nearby final hosts. This could also explain the enormous size differences in a single life stage. If all microniscia moulted and detached from their intermediate hosts at the same time, some could have parasitised the intermediate host much longer than others. Explaining a high abundance of epicarideans requires a high abundance and density of intermediate hosts (Byron et al. 1983; Ueda et al. 1983; Ambler et al. 1991) as well as a high rate of infestation by epicaridean parasites (but see Uye and Murase 1997; Medeiros et al. 2006). Although plausible, a synchronised moulting event remains speculative, as our knowledge about the ecology of epicarideans is still very limited (Dale and Anderson 1982).

Synchronised events could potentially also play a role on a more local scale. If multiple individuals hatch or emerge at the same time close to a resin source, many of them can get trapped in the same piece of resin. A good example for such a process is a piece of Dominican amber with many small immature spiders (Poinar and Poinar 1999: fig. 73). In Epicaridea, the immatures usually hatch from the brood pouch (marsupium) of the female as epicaridium larvae, which are morphologically very distinct and different to the herein presented specimens. However, there is one species,

Entoniscoides okadai Miyashita, 1940, that has been reported to hatch larvae from the brood pouch with a morphology similar to the here presented specimens (Miyashita 1940). The systematic position of this species does not indicate that this type of development is the ancestral condition for Epicaridea (Boyko et al. 2008 onwards). Still, it is not clear exactly when and how the life cycle of most modern epicarideans evolved. This way, despite most observations of the modern fauna do not favour such an explanation, it is possible that simultaneous hatching from a brood pouch may have led to the herein presented taphocoenosis. Yet, the large variation in body sizes seen in the here presented fossil specimens cannot be easily explained by this process, as one would assume that offspring from the same brood pouch should be roughly of the same size (see, e.g. Romero-Rodríguez and Román-Contreras 2008).

Factors explaining high abundance and density of conspecific individuals

There are various other factors which could also lead to a temporary and local high (relative) abundance of a species in proximity to the resin:

(1) Social behaviour: indications of social behaviour can be found in fossils, examples are fossils of worker ants that have been found in Baltic and Dominican amber (Grimaldi 1996, 92; Weitschat and Wichard 1998: fig. 20h; Hörnig et al. 2016). Different types of (sub-) social behaviour have been reported from aquatic and terrestrial representatives of Isopoda (Broly et al. 2012; Salma and Thomson 2016, 2018). In land-living species, such a association could be coupled to the reduction of desiccation by aggregating behaviour (Allee 1926; Broly et al. 2014). In some species of Isopoda, extended parental care has also been reported as a cause for aggregation (Thiel 2003; Tanaka and Nishi 2008). However, social behaviour in epicarideans is rather unlikely due to their parasitic lifestyle that goes along with the competition over attachment sites and limited abundance and physiological capacity of the host animals. In addition, the planktic lifestyle of some of the larval stages (epicaridium and cryptoniscium) renders it unlikely that there is much social behaviour in Epicaridea beyond the maternal care within the brood pouch.

(2) Local abundance of mates: aggregating behaviour for reproductive purposes has been recorded for various ingroups of Isopoda (Holdich 1970; Shuster and Wade 1991; Tanaka and Nishi 2008). In the case of the herein presented taphocoenosis, this could mean that there was an adult female nearby. As females within Epicaridea are immobile and attached to the final host,

the search for a mate can coincide with the search for a host.

(3) Local abundance of restricted resources (nutrients, water, minerals, etc.): there are some amber taphocoenoses that indicate an aggregation of beetles around food sources (Poinar 1999; Peris et al. 2020). An aggregating behaviour around food sources can also be seen in different ingroups of Isopoda. Intertidal species of the group Oniscidea have been reported to aggregate in areas with high food content in the sand (Colombini et al. 2005). Giant representatives of Isopoda (*Bathynomus* A. Milne-Edwards, 1879) aggregate around carcasses on the ocean bottom, on which they feed as scavengers (Lowry and Dempsey 2006). Some non-parasitic representatives of the group Cymothoida are attracted by chemicals released by injured fish on which they prey (Stepien and Brusca 1985). In the case of epicaridean larvae and paedomorphic adults, the two before-mentioned factors can co-occur because mates can be attached to the food source. Within Epicaridea, a larger crustacean (potential host) could be the centre of such an aggregation behaviour. An aggregation of barnacles (Cirripedia), which in modern environments can be parasitised by epicarideans (Nielsen and Strömberg 1973), on the roots of the resin-producing tree could be a plausible explanation why so many cryptoniscium stage individuals are trapped in the amber piece. Fossils of barnacles however, have not been reported from Burmese amber.

(4) Avoidance of predation due to aggregating behaviour: aggregation behaviour is often recognised as an anti-predatory strategy, in which individuals reduce the rate of predatory attacks per individual, compared with a non-aggregation behaviour through the 'dilution effect' (Foster and Treherne 1981). This kind of behaviour is known from some species of Peracarida (Thiel 2003, 2011), including Isopoda, but not from epicarideans and thus unlikely to be the reason for the fossil assemblage.

(5) Local shelter from stresses (predation, currents, evaporation, light, etc.): aggregations in areas where there is comparably less biotic (e.g. predation) or abiotic stress (e.g. desiccation) has been reported for different species of Isopoda (Standing and Beatty 1978; Odendaal et al. 1999). In the case presented here the epicarideans could have precautiously avoided predators such as fishes by moving into shallow water areas, where they were closer to the resin-producing trees. Whilst the overall local abundance could increase by this, very high densities are unlikely to be reached and this behaviour has not been reported for epicarideans.

(6) Restriction of the habitat: the restriction of a water body can drastically increase the density of aquatic animals if they survive the chemical stress that often accompanies this process. Results of such processes can be found abundantly in the fossil record (e.g. Wings et al. 2012). Habitat restriction alone is unlikely to have caused the high density of conspecific fossils in the here studied amber piece, because other aquatic organisms would have been affected by this likewise.

A plausible scenario for the formation of the herein studied assemblage of fossil epicarideans has to explain not only a high abundance of individuals, but also a high density of individuals in closest proximity of resin. Most of the above-mentioned factors could have contributed to a high abundance of epicarideans in a habitat on a larger scale. Yet, only few factors can explain a very high density on a small scale. The aggregation due to the presence of a final host may be a plausible explanation for the high abundance of individuals in the amber piece. Yet, it is not clear whether such densities of larval epicarideans regularly occur in modern environments and observations of such in extant species would be interesting find in itself. This all the more emphasises the rarity of such a taphocoenosis preserved in fossilised tree sap. The here studied fossils could also give a hint, that there are aspects of the lifestyle in modern species of Epicaridea which would be worthwhile to investigate further.

Possible host animals in Myanmar amber

The proportion of individuals actually living in water is naturally very low in amber deposits; therefore, there are only few records of animals in Myanmar amber that could potentially have served as final hosts of the herein presented epicarideans. Epicarideans are known to parasitise other species of Isopoda (including other epicarideans; Nielsen and Strömberg 1965; Rybakov 1990). A potential host could thus be an aquatic representative of the group Cymothoida (Schädel et al. 2021 in press). Representatives of the epicaridean ingroup Cyproniscidae are parasitic on seed shrimps (Wägele 1989; Rybakov 1998), which are present in Myanmar amber (Xing et al. 2018; Wang et al. 2020). Modern epicarideans are also parasitic on amphipods (Sars 1899; Wägele 1989) and true crabs (Brachyura) (Torres Jordá 2003), which are also present in Myanmar amber (Zhang 2017).

Taxonomy

This published work and the nomenclatural acts it contains have been registered with Zoobank under the Life Science Identifier (LSID) urn:lsid:zoobank.org:pub:755965DF-B4A6-4A87-B513-1A6A26B72F5E

Isopoda Latreille, 1817
Scutocoxifera Dreyer and Wägele, 2002
Cymothoida Wägele, 1989
Epicaridea Latreille, 1825 (=Bopyridae Rafinesque, 1815 sensu Wägele 1989)

Cryptolacruma gen. nov.

Etymology. The name is derived from the cryptoniscium stage (a larval stage in Epicaridea) and from the Latin *lacruma* for 'resin' in reference to the occurrence in amber. The gender is feminine. The name also translates to 'hidden tear', in memory of the victims of commercial amber mining.

LSID. urn:lsid:zoobank.org:act:EBE923E5-E0CB-45B3-89A7-627756EEBE88.

Remark. This genus name is merely created to be compliant with the International Code of Zoological Nomenclature. Since the name stands for a monotypic (uninformative) taxonomic unit, the diagnosis is the same as for the species.

Cryptolacruma nidis sp. nov.
Figures 1, 2; Supplementary image data 1, 2, 3

Holotype. PED 0226-4.

Paratypes. PED 0226-1–PED 0226-3, PED 0226-5–PED 0226-103. Ontogenetic stage of the type specimens: cryptoniscium type larvae, paedomorphic juveniles or paedomorphic males.

Etymology. The name is derived from the Latin *nidus* for 'nest' (locative case, plural) in reference to the high number of specimens in the amber piece containing the type specimens.

LSID. urn:lsid:zoobank.org:act:5E0591E7-00B5-483C-AC8F-D0D195BB2BB3.

Type locality. Near Noje Bum, Hukawng Valley, Kachin State, Myanmar.

Type stratum and age. Unknown stratum, 98.8 million years, lowermost Cenomanian, lowermost Upper Cretaceous (Shi et al. 2012; Yu et al. 2019).

Differential diagnosis. Head shield flat, antennula with proximal element enlarged in posterior direction ('antennular plate'); antennular plate with distinct teeth on posterior margin; antenna with terminal peduncle element long and slender, five flagellum elements; mouthparts not specialised

as a sucking disc; uropod endopod as long as exopod; pleotelson posterior margin rounded, not pointed, without distinct teeth.

Systematic interpretation. Epicaridea nec Dajidae, nec Entoniscidae.

Conclusions

The herein presented piece of Myanmar amber contains more than 100 inclusions of cryptoniscium stage larvae or paedomorphic males of Epicaridea. This represents the oldest record of body fossils of the group Epicaridea (parasites of crustaceans); it is also one of only three body fossil occurrences of this group and increases the overall number of body fossil of this group by a factor of 4. The morphology of the specimens is comparable to that of extant species; however, the combination of character states is unique. The accumulation of this many specimens in a single piece of resin is a remarkable example for mass occurrences of conspecific organisms in amber.

Data availability All supplementary files are available via MorphDBase.

Supplementary image data 1: µCT data of PED 0226, 0.39x objective, 30 kV, 6 W, 3.5 s exposure time. TIF format, system based calculated pixel size = 18 µm. Available from https://www.morphdbase.de/?M_Schaedel_20200612-M-31.1

Supplementary image data 2: µCT data of PED 0226, 4x objective, 30 kV, 6 W, 3.5 s exposure time. TIF format, system based calculated pixel size = 3.16 µm. Available from https://www.morphdbase.de/?M_Schaedel_20200612-M-33.1

Supplementary image data 3: µCT data of PED 0226, 10x objective, 40 kV, 8 W, 4 s exposure time. TIF format, system based calculated pixel size = 1.5 µm. Available from https://www.morphdbase.de/?M_Schaedel_20200612-M-32.1

Supplementary data table 1: Body lengths of cryptoniscium stage representatives of Epicaridea, data for Fig. 3, csv-format (comma as separator, UTF-8 character encoding) (Fraisse 1878; Bonnier 1900; Thompson 1902; Caullery 1907; Miyashita 1940; Shiino 1954; Nielsen and Strömberg 1965; Bresciani 1966; Bourdon 1967, 1972, 1976a, 1976b, 1980, 1981, 1983, 1980; Nielsen 1967; Strömberg 1971; Holdich 1975; Schultz 1977; Kensley 1979; Bourdon and Bruce 1980; Anderson and Dale 1981; Coyle and Mueller 1981; Dale and Anderson 1982; Adkison and Collard 1990; Rybakov 1990; Shields and Ward 1998; Pascual et al. 2002; Torres Jordá 2003; Shimomura et al. 2005; Hosie 2008; Romero-Rodríguez and Román-Contreras 2013; An et al. 2015; Serrano-Sánchez et al. 2016; Schädel et al. 2019). Available from https://www.morphdbase.de/?M_Schaedel_20200812-M-36.1

Supplementary data table 2: Morphological features of fossil and extant representatives of Epicaridea, csv-format (comma as separator, UTF-8 character encoding) (Fraisse 1878; Giard and Bonnier 1887; Bonnier 1900; Thompson 1902; Caullery 1907; Miyashita 1940; Shiino 1954; Nielsen and Strömberg 1965; Bresciani 1966; Bourdon 1967, 1972, 1976a, 1976b, 1980, 1981, 1980, 2015; Holdich 1975; Schultz 1977; Kensley 1979; Bourdon and Bruce 1980; Anderson and Dale 1981; Coyle and Mueller 1981; Dale and Anderson 1982; Adkison and Collard 1990; Rybakov 1990; Pascual et al. 2002; Torres Jordá 2003; Shimomura et al. 2005; Hosie 2008; Boyko 2013; Serrano-Sánchez et al. 2016; Schädel et al. 2019). Available from https://www.morphdbase.de/?M_Schaedel_20200812-M-35.1

References

Adkison, D.L., and S.B. Collard. 1990. Description of the cryptoniscium larva of *Entophilus omnitectus* Richardson, 1903 (Crustacea: Isopoda: Epicaridea) and records from the Gulf of Mexico. *Proceedings of the Biological Society of Washington* 103(3): 649–654.

Allee, W.C. 1926. Studies in animal aggregations: causes and effects of bunching in land isopods. *Journal of Experimental Zoology* 45(1): 255–277. https://doi.org/10.1002/jez.1400450108.

Ambler, J.W., F.D. Ferrari, and J.A. Fornshell. 1991. Population structure and swarm formation of the cyclopoid copepod *Dioithona oculata* near mangrove cays. *Journal of Plankton Research* 13(6): 1257–1272. https://doi.org/10.1093/plankt/13.6.1257.

An, J., C.B. Boyko, and X. Li. 2015. A review of bopyrids (Crustacea: Isopoda: Bopyridae) parasitic on caridean shrimps (Crustacea: Decapoda: Caridea) from China. *Bulletin of the American Museum of Natural History* 399: 1–85. https://doi.org/10.1206/amnb-921-00-01.1.

Anderson, G. 1975. Larval metabolism of the epicaridian isopod parasite *Probopyrus pandalicola* and metabolic effects of *P. pandalicola* on its copepod intermediate host *Acartia tonsa*. *Comparative Biochemistry and Physiology* 50(4): 747–751. https://doi.org/10.1016/0300-9629(75)90140-1.

Anderson, G., and W. Dale. 1981. *Probopyrus pandalicola* (Packard) (Isopoda, Epicaridea): morphology and development of larvae in culture. *Crustaceana* 41(2): 143–161.

Arillo, A. 2007. Paleoethology: fossilized behaviours in amber. *Geologica Acta* 5(2): 159–166.

Ax, P. 2000. The phylogenetic system of the Metazoa. In *Multicellular Animals*, ed. S. Kinsey. Berlin: Springer.

Bell, T. 1863. A monograph of the fossil malacostracous Crustacea of Great Britain. Part II, Crustacea of the Gault and Greensand. *Monographs of the Palaeontographical Society* 14(63): 1–40.

Bonnier, J. 1900. Contribution à l'étude des épicarides les Bopyridae. *Travaux de la Station Zoologique de Wimereux* 8: 1–476.

Bourdon, R. 1967. Sur quelques nouvelles espèces de Cabiropsidae (Isopoda Epicaridea). *Bulletin du Muséum National d'Histoire Naturelle* 38(6): 846–868.

Bourdon, R. 1972. Epicarides de la Galathea expedition. *Galathea Report* 12: 101–112.

Bourdon, R. 1976a. Épicarides de Madagascar I. *Bulletin du Muséum National d'Histoire Naturelle (3e Série)* 371(3): 353–392.

Bourdon, R. 1976b. Les Bopyres des Porcellanes. *Bulletin du Muséum National d'Histoire Naturelle (3e Série)* 359(3): 353–392.

Bourdon, R. 1980. *Aporobopyrus dollfusi* n. sp. (Crustacea, Epicaridea, Bopyridae) parasite de Porcellanes de la mer Rouge. *Bulletin du Muséum National d'Histoire Naturelle (4e Série)* 2: 237–244.

Bourdon, R. 1981. Trois nouveaux Cryptoniscina antarctiques abyssaux (Isopoda, Epicaridea). *Bulletin du Muséum National d'Histoire Naturelle* 3: 603–613.

Bourdon, R., and N.L. Bruce. 1980. *Ancyroniscus orientalis* sp. nov. (Isopoda: Epicaridea), nouveau cabiropside parasite de la great barrier reef. *Bulletin de l'Academie et de la Societe Lorraines des Sciences* 19(1): 21–26.

Boyko, C.B. 2013. Toward a monophyletic Cabiropidae: a review of parasitic isopods with female *Cabirops*-type morphology (Isopoda: Cryptoniscoidea). *Proceedings of the Biological Society of Washington* 126: 103–119. https://doi.org/10.2988/0006-324X-126.2.103.

Boyko, C.B. 2015. A revision of *Danalia* Giard, 1887, Faba Nierstrasz & Brender à Brandis, 1930 and *Zeuxokoma* Grygier, 1993 (Crustacea: Isopoda: Epicaridea: Cryptoniscoidea: Cryptoniscidae) with description of a new genus and four new species. *Bishop Museum Bulletin in Zoology* 9: 65–92.

Boyko, C.B., and J.D. Williams. 2015. A new genus for *Entophilus mirabiledictu* Markham & Dworschak, 2005 (Crustacea: Isopoda: Cryptoniscoidea: Entophilidae) with remarks on morphological support for epicaridean superfamilies based on larval characters. *Systematic Parasitology* 92(1): 13–21. https://doi.org/10.1007/s11230-015-9578-8.

Boyko, C.B., and C. Wolff. 2014. Isopoda and Tanaidacea. In *Atlas of crustacean Larvae*, eds. J.W. Martin, J. Olesen, and J.T. Hoeg, 210–212. Baltimore: Johns Hopkins University Press.

Boyko, C.B., N.L. Bruce, K.A. Hadfield, K.L. Merrin, Y. Ota, G.C.B. Poore, S. Taiti, M. Schotte, and G.D.F. Wilson 2008 onwards. World Marine, Freshwater and Terrestrial Isopod Crustaceans database. Epicaridea. http://www.marinespecies.org/aphia.php?p=taxdetails&id=13795 on 2018–08–07. Accessed 3 October 2020.

Boyko, C.B., J. Moss, J.D. Williams, and J.D. Shields. 2013. A molecular phylogeny of Bopyroidea and Cryptoniscoidea (Crustacea: Isopoda). *Systematics and Biodiversity* 11(4): 495–506. https://doi.org/10.1080/14772000.2013.865679.

Brandt, A. 1999. On the origin and evolution of Antarctic Peracarida (Crustacea, Malacostraca). *Scientia Marina* 63: 261–274. https://doi.org/10.3989/scimar.1999.63s1261.

Brasil-Lima, I.M., and C.M. De Lima Barros. 1998. Malacostraca - Peracarida Freshwater Isopoda Flabellifera and Asellota. In

Catalogue of Crustacea of Brazil, ed. P.S. Young, 645–651. Rio de Janeiro: Museu Nacional.

Bresciani, J. 1966. *Aegophila socialis* gen. et. sp. nov., an epicaridean parasitic on the isopod *Aega ventrosa* Sars. *Ophelia* 3(1): 99–112. https://doi.org/10.1080/00785326.1966.10409636.

Broly, P., R. Mullier, J. Deneubourg, and C. Devigne. 2012. Aggregation in woodlice: social interaction and density effects. *ZooKeys* 176: 133–144. https://doi.org/10.3897/zookeys.176.2258.

Broly, P., L. Devigne, J. Deneubourg, and C. Devigne. 2014. Effects of group size on aggregation against desiccation in woodlice (Isopoda: Oniscidea). *Physiological Entomology* 39(2): 165–171. https://doi.org/10.1111/phen.12060.

Brown, B.V., and E.M. Pike. 1990. Three new fossil phorid flies (Diptera: Phoridae) from Canadian Late Cretaceous amber. *Canadian Journal of Earth Sciences* 27(6): 845–848. https://doi.org/10.1139/e90-087.

Byron, E.R., P.T. Whitman, and C.R. Goldman. 1983. Observations of copepod swarms in Lake Tahoe1. *Limnology and Oceanography* 28(2): 378–382. https://doi.org/10.4319/lo.1983.28.2.0378.

Caullery, M. 1907. Recherches sur les Liriopsidae, Épicarides cryptonisciens parasites des Rhizocéphales. *Mittheilungen aus der Zoologischen Station zu Neapel* 18: 583–643.

Chopra, B. 1923. Bopyrid isopods parasitic on Indian Decapoda Macrura. *Records of the Indian Museum* 25(2): 411–550.

Colombini, I., M. Fallaci, and L. Chelazzi. 2005. Micro-scale distribution of some arthropods inhabiting a Mediterranean sandy beach in relation to environmental parameters. *Acta Oecologica* 28(3): 249–265. https://doi.org/10.1016/j.actao.2005.05.006.

Coyle, K.O., and G.J. Mueller. 1981. Larval and juvenile stages of the isopod *Holophryxus alaskensis* (Epicarida, Dajidae) parasitic on decapods. *Canadian Journal of Fisheries and Aquatic Sciences* 38(11): 1438–1443. https://doi.org/10.1139/f81-190.

Dale, W.E., and G. Anderson. 1982. Comparison of morphologies of *Probopyrus bithynis*, *P. floridensis*, and *P. pandalicola* larvae reared in culture (Isopoda, Epicaridea). *Journal of Crustacean Biology* 2(3): 392–409.

Dreyer, H., and J.W. Wägele. 2001. Parasites of crustaceans (Isopoda: Bopyridae) evolved from fish parasites: molecular and morphological evidence. *Zoology* 103(3/4): 157–178.

Dreyer, H., and J.W. Wägele. 2002. The Scutocoxifera tax. Nov. and the information content of nuclear ssu rDNA sequences for reconstruction of isopod phylogeny (Peracarida: Isopoda). *Journal of Crustacean Biology* 22(2): 217–234.

Dyar, H.G. 1890. The number of molts of lepidopterous larvae. *Psyche A Journal of Entomology* 5: 420–422. https://doi.org/10.1155/1890/23871.

Foster, W.A., and J.E. Treherne. 1981. Evidence for the dilution effect in the selfish herd from fish predation on a marine insect. *Nature* 293: 466–467. https://doi.org/10.1038/293466a0.

Fowler, G.H. 1904. Biscayan plankton collected during a cruise of H.M.S. "Research" 1900. Part xii. The Ostracoda. *Transactions of the Linnean Society of London* 2(10): 219–336.

Fraisse, P. 1878. Die Gattung *Cryptoniscus* Fr. Müller. *Arbeiten aus dem Zoologisch-Zootomischen Institut in Würzburg* 4: 239–296.

Giard, A., and J.J. Bonnier. 1887. Contributions à l'étude des Bopyriens. *Travaux de la Station Zoologique de Wimereux* 5: 1–252.

Girard, V., A.R. Schmidt, S. Saint Martin, S. Struwe, V. Perrichot, J.P. Saint Martin, D. Grosheny, G. Breton, and D. Néraudeau. 2008. Evidence for marine microfossils from amber. *Proceedings of the National Academy of Sciences* 105(45): 17426–17429. https://doi.org/10.1073/pnas.0804980105.

Grimaldi, D.A. 1996. Amber, window to the past. New York: American Museum of Natural History, published by Harry N. Abrams Inc.

Gustafson, G.T., M.C. Michat, and M. Balke. 2020. Burmese amber reveals a new stem lineage of whirligig beetle (Coleoptera: Gyrinidae) based on the larval stage. *Zoological Journal of the Linnean Society* 189(4): 1–17. https://doi.org/10.1093/zoolinnean/zlz161.

Hakim, M., D. Azar, and D. Huang. 2019. Protopsyllidioids, and their behaviour "frozen" in mid-Cretaceous Burmese amber. *Palaeoentomology* 2(3): 271–278. https://doi.org/10.11646/palaeoentomology.2.3.12.

Haug, J.T. 2020. Why the term "larva" is ambiguous, or what makes a larva? *Acta Zoologica* 101(2): 167–188. https://doi.org/10.1111/azo.12283.

Haug, C., G. Mayer, V. Kutschera, D. Waloszek, A. Maas, and J.T. Haug. 2011a. Imaging and documenting gammarideans. *International Journal of Zoology* 2011: 1–9. https://doi.org/10.1155/2011/380829.

Haug, J.T., C. Haug, V. Kutschera, G. Mayer, A. Maas, S. Liebau, C. Castellani, U. Wolfram, E.N.K. Clarkson, and D. Waloszek. 2011b. Autofluorescence imaging, an excellent tool for comparative morphology. *Journal of Microscopy* 244(3): 259–272. https://doi.org/10.1111/j.1365-2818.2011.03534.x.

Haug, J.T., J.B. Caron, and C. Haug. 2013. Demecology in the Cambrian: synchronized molting in arthropods from the Burgess Shale. *BMC Biology* 11(1): 64. https://doi.org/10.1186/1741-7007-11-64.

Haug, C., J.W.F. Reumer, J.T. Haug, A. Arillo, D. Audo, D. Azar, V. Baranov, R. Beutel, S. Charbonnier, R. Feldmann, C. Foth, R.H.B. Fraaije, P. Frenzel, R. Gašparič, D.E. Greenwalt, D. Harms, M. Hyžný, J.W.M. Jagt, E.A. Jagt-Yazykova, E. Jarzembowski, H. Kerp, A.G. Kirejtshuk, C. Klug, D.S. Kopylov, U. Kotthoff, J. Kriwet, L. Kunzmann, R.C. McKellar, A. Nel, C. Neumann, A. Nützel, V. Perrichot, A. Pint, O. Rauhut, J.W. Schneider, F.R. Schram, G. Schweigert, P. Selden, J. Szwedo, B.W.M. van Bakel, T. van Eldijk, F.J. Vega, B. Wang, Y. Wang, L. Xing, and M. Reich. 2020. Comment on the letter of the Society of Vertebrate Paleontology (SVP) dated April 21, 2020 regarding "Fossils from conflict zones and reproducibility of fossil-based scientific data": the importance of private collections. *PalZ. Paläontologische Zeitschrift* 94: 413–429. https://doi.org/10.1007/s12542-020-00522-x.

Holdich, D.M. 1970. The distribution and habitat preferences of the Afro-European species of *Dynamene* (Crustacea: Isopoda). *Journal of Natural History* 4(3): 419–438. https://doi.org/10.1080/00222937000770401.

Holdich, D.M. 1975. *Ancyroniscus bonnieri* (Isopoda, Epicaridea) infecting British populations of *Dynamene bidentata* (Isopoda, Sphaeromatidae). *Crustaceana* 28(2): 145–151.

Hörnig, M.K., A. Sombke, C. Haug, S. Harzsch, and J.T. Haug. 2016. What nymphal morphology can tell us about parental investment: a group of cockroach hatchlings in Baltic Amber documented by a multi-method approach. *Palaeontologia Electronica* 19.1.6A: 1–20. https://doi.org/10.26879/571.

Horváth, G., A. Egri, V.B. Meyer-Rochow, and G. Kriska. 2019. How did amber get its aquatic insects? Water-seeking polarotactic insects trapped by tree resin. *Historical Biology* 33: 846–856. https://doi.org/10.1080/08912963.2019.1663843.

Hosie, A.M. 2008. Four new species and a new record of Cryptoniscoidea (Crustacea: Isopoda: Hemioniscidae and Crinoniscidae) parasitising stalked barnacles from New Zealand. *Zootaxa* 1795: 1–28.

Kensley, B. 1979. Redescription of *Zonophryxus trilobus* Richardson, with notes on the male and developmental stages (Crustacea: Isopoda: Dajidae). *Proceedings of the Biological Society of Washington* 92(3): 665–670.

Klompmaker, A.A., and G.A. Boxshall. 2015. Fossil crustaceans as parasites and hosts. *Advances in Parasitology* 90: 233–289.

Klompmaker, A.A., P. Artal, B.W.M. van Bakel, R.H.B. Fraaije, and J.W.M. Jagt. 2014. Parasites in the fossil record: a Cretaceous

fauna with isopod-infested decapod crustaceans, infestation patterns through time, and a new ichnotaxon. *PLoS ONE* 9(3): 1–17.

Klompmaker, A.A., C.M. Robins, R.W. Portell, and A. De Angeli. 2018. Crustaceans as hosts of parasites throughout the Phanerozoic. *bioRxiv*. https://doi.org/10.1101/505495.

Kypke, J.L., and A. Solodovnikov. 2018. Every cloud has a silver lining: X-ray micro-CT reveals *Orsunius* rove beetle in Rovno amber from a specimen inaccessible to light microscopy. *Historical Biology* 32: 940–950. https://doi.org/10.1080/08912963.2018.1558222.

Limaye, A. 2012. Drishti: a volume exploration and presentation tool. *Proceedings of SPIE the International Society for Optical Engineering*. https://doi.org/10.1117/12.935640.

Lowry, J., and K. Dempsey. 2006. The giant deep-sea scavenger genus *Bathynomus* (Crustacea, Isopoda, Cirolanidae) in the Indo-West Pacific. In *Tropical deep-sea benthos, vol. 24*, eds. B. Richer de Forges and J.L. Justine. *Memoires du Museum national d'Histoire naturelle* 193: 163–192.

Mao, Y., K. Liang, Y. Su, J. Li, X. Rao, H. Zhang, F. Xia, Y. Fu, C. Cai, and D. Huang. 2018. Various amberground marine animals on Burmese amber with discussions on its age. *Palaeoentomology* 1(1): 91–103. https://doi.org/10.11646/palaeoentomology.1.1.11.

Markham, J.C. 1986. Evolution and zoogeography of the Isopoda Bopyridae, parasites of Crustacea Decapoda. In *Crustacean Issues 4. Crustacean Biogeography*, eds. H.G. Robert and L.H. Kenneth, 143–164. Rotterdam: A.A Balkema.

Martínez-Delclòs, X., X. Briggs, and X. Peñalver. 2004. Taphonomy of insects in carbonates and amber. *Palaeogeography, Palaeoclimatology, Palaeoecology* 203: 19–64. https://doi.org/10.1016/S0031-0182(03)00643-6.

Medeiros, G.F., L.S. Medeiros, D.M.F. Henriques, M.T. Lima e Carlos, G.V.F. Benigna de Souza, and R.M. Lopes. 2006. Current distribution of the exotic copepod *Pseudodiaptomus trihamatus* Wright, 1937 along the northeastern coast of Brazil. *Brazilian Journal of Oceanography* 54(4): 241–245. https://doi.org/10.1590/S1679-87592006000300008.

Miyashita, Y. 1940. On an entoniscid with abbreviated development, *Entoniscoides okadai*, n. g., n. sp. *Annotationes Zoologicae Japonenses* 19(2): 149–157.

Néraudeau, D., V. Perrichot, D.J. Batten, A. Boura, V. Girard, L. Jeanneau, Y.A. Nohra, F. Polette, S. Saint Martin, and J.P. Saint Martin. 2017. Upper Cretaceous amber from Vendée, north-western France: age dating and geological, chemical, and palaeontological characteristics. *Cretaceous Research* 70: 77–95.

Nielsen, S.O. 1967. *Cironiscus dahli* gen. et sp. nov. (Crustacea, Epicaridea) with notes on host-parasite relations and distribution. *Sarsia* 29(1): 395–412. https://doi.org/10.1080/00364827.1967.10411096.

Nielsen, S.O., and J.O. Strömberg. 1965. A new parasite of *Cirolana borealis* Lilljeborg belonging to the Cryptoniscinae (Crustacea Epicaridea). *Sarsia* 18(1): 37–62. https://doi.org/10.1080/00364827.1965.10409547.

Nielsen, S., and J. Strömberg. 1973. Morphological characters of taxonomical importance in Cryptoniscina (Isopoda Epicaridea) A scanning electron microscopic study of Cryptoniscus Larvae. *Sarsia* 52(1): 75–96.

Odendaal, F.J., S. Eekhout, A.C. Brown, and G.M. Branch. 1999. Aggregations of the sandy-beach isopod, *Tylos granulatus*: adaptation or incidental-effect? *African Zoology* 34(4): 180–189.

Pascual, S., M.A. Vega, F.J. Rocha, and A. Guerra. 2002. First report of an endoparasitic epicaridean isopod infecting cephalopods. *Journal of Wildlife Diseases* 38: 473–477. https://doi.org/10.7589/0090-3558-38.2.473.

Peris, D., C.C. Labandeira, E. Barrón, X. Delclòs, J. Rust, and B. Wang. 2020. Generalist pollen-feeding beetles during the mid-Cretaceous. *iScience*. https://doi.org/10.1016/j.isci.2020.100913.

Poinar, G.O. 1999. Chrysomelids in fossilized resin: behavioural inferences. In *Advances in chrysomelidae biology 1*, ed. M.L. Cox, 1–16. Leiden: Backhuys Publishers.

Poinar, G.O., and R. Poinar. 1994. *The quest for life in amber*. Massachusetts: Addison-Wesley Publishing Company.

Poinar, G.O., and R. Poinar. 1999. *The amber forest*. Princeton: Princeton University Press.

Poore, G.C.B., and N.L. Bruce. 2012. Global diversity of marine isopods (except Asellota and crustacean symbionts). *PLoS ONE* 7(8): e43529. https://doi.org/10.1371/journal.pone.0043529.

Raupach, M.J., C. Held, and J.W. Wägele. 2004. Multiple colonization of the deep sea by the Asellota (Crustacea: Peracarida: Isopoda). *Deep Sea Research Part II* 51(14–16): 1787–1795. https://doi.org/10.1016/j.dsr2.2004.06.035.

Robin, N., C. D'Haese, and P. Barden. 2019. Fossil amber reveals springtails' longstanding dispersal by social insects. *BMC Evolutionary Biology* 19: 213. https://doi.org/10.1186/s12862-019-1529-6.

Robins, C.M., and A.A. Klompmaker. 2019. Extreme diversity and parasitism of Late Jurassic squat lobsters (Decapoda: Galatheoidea) and the oldest records of porcellanids and galatheids. *Zoological Journal of the Linnean Society* 187(4): 1131–1154. https://doi.org/10.1093/zoolinnean/zlz067.

Robins, C.M., R.M. Feldmann, and C.E. Schweitzer. 2013. Nine new genera and 24 new species of the Munidopsidae (Decapoda: Anomura: Galatheoidea) from the Jurassic Ernstbrunn Limestone of Austria, and notes on fossil munidopsid classification. *Annalen des Naturhistorischen Museums in Wien (A: Mineralogie und Petrographie, Geologie und Paläontologie, Anthropologie und Prähistorie)* 115: 167–251.

Romero-Rodríguez, J., and R. Román-Contreras. 2008. Aspects of the reproduction of *Bopyrinella thorii* (Richardson, 1904) (Isopoda, Bopyridae) a branchial parasite of *Thor floridanus* Kingsley, 1878 (Decapoda, Hippolytidae) in Bahía de la Ascensión, Mexican Caribbean. *Crustaceana* 81(10): 1201–1210. https://doi.org/10.1163/156854008X374522.

Romero-Rodríguez, J., and R. Román-Contreras. 2013. Prevalence and reproduction of *Bopyrina abbreviata* (Isopoda, Bopyridae) in Laguna de Términos, SW Gulf of Mexico. *Journal of Crustacean Biology* 33(5): 641–650. https://doi.org/10.1163/1937240X-00002182.

Ross, A. 1998. *Amber*. Cambridge: Harvard University Press.

Rybakov, A.V. 1990. *Bourdonia tridentata* gen n., sp. n. (Isopoda: Cabiropsidae) a hyperparasite of *Bopyroides hippolytes* Kroyer [sic] from the shrimp *Pandalus borealis*. *Parazitologiia* 24(5): 408–416.

Rybakov, A.V. 1998. *Onisocryptus kurilensis* sp. n. (Crustacea, Isopoda, Cyproniscidae), a parasite of the ostracod Vargula norvegica orientalis. *Russian Journal of Marine Biology* 24(5): 337–339 (in Russian).

Saint Martin, S., J.P. Saint Martin, A.R. Schmidt, V. Girard, D. Néraudeau, and V. Perrichot. 2015. The intriguing marine diatom genus *Corethron* in Late Cretaceous amber from Vendée (France). *Cretaceous Research* 52: 64–72. https://doi.org/10.1016/j.cretres.2014.07.006.

Salma, U., and M. Thomson. 2016. Gregarious aggregative behavior in the marine isopod *Cirolana harfordi*. *Invertebrate Biology* 135(3): 225–234. https://doi.org/10.1111/ivb.12134.

Salma, U., and M. Thomson. 2018. Social aggregation of the marine isopod *Cirolana harfordi* does not rely on the availability of light-reducing shelters. *Physiological Entomology* 43(1): 60–68. https://doi.org/10.1111/phen.12229.

Sars, G.O. 1899. *An account of the Crustacea of Norway, with short descriptions and figures of all the species. Volume II. Isopoda*. Bergen: Bergen Museum.

Schädel, M., V. Perrichot, and J.T. Haug. 2019. Exceptionally preserved cryptoniscium larvae: morphological details of rare isopod crustaceans from French Cretaceous Vendean amber. *Palaeontologia Electronica* 22.3.71: 1–46. https://doi.org/10.26879/977.

Schädel, M., M. Hyžný, and J.T. Haug. 2021. Ontogenetic development captured in amber: the first record of aquatic representatives of Isopoda in Cretaceous amber from Myanmar. *Nauplius* 29: e2021003, 1–29. https://doi.org/10.1590/2358-2936e2021003.

Schmidt, C. 2008. Phylogeny of the terrestrial Isopoda (Oniscidea): a review. *Arthropod Systematics and Phylogeny* 66(2): 191–226.

Schmidt, A.R., and D.L. Dilcher. 2007. Aquatic organisms as amber inclusions and examples from a modern swamp forest. *Proceedings of the National Academy of Sciences* 104(42): 16581–16585. https://doi.org/10.1073/pnas.0707949104.

Schultz, G.A. 1977. Bathypelagic isopod Crustacea from the Antarctic and Southern Seas. In *Biology of the Antarctic Seas*, ed. G.A. Schultz, 69–128. Washington: American Geophysical Union.

Schultz, G.A. 1980. *Arcturocheres gaussicola* n. sp. (Cabiropsidae) parasite on *Antarcturus gaussianus* Vanhöffen (Arcturidae) from Antarctica (Isopoda). *Crustaceana* 39(2): 153–156. https://doi.org/10.1163/156854080X00058.

Serrano-Sánchez, M.L., T.A. Hegna, P. Schaaf, L. Pérez, E. Centeno-García, and F.J. Vega. 2015. The aquatic and semiaquatic biota in Miocene amber from the Campo La Granja mine (Chiapas, Mexico): paleoenvironmental implications. *Journal of South American Earth Sciences* 62: 243–256. https://doi.org/10.1016/j.jsames.2015.06.007.

Serrano-Sánchez, M.L., C. Nagler, C. Haug, J.T. Haug, E. Centeno-García, and F.J. Vega. 2016. The first fossil record of larval stages of parasitic isopods: cryptoniscus larvae preserved in Miocene amber. *Neues Jahrbuch für Geologie und Paläontologie, Abhandlungen* 279(1): 97–106. https://doi.org/10.1127/njgpa/2016/0543.

Shi, G., D.A. Grimaldi, G.E. Harlow, J. Wang, J. Wang, M. Yang, W. Lei, Q. Li, and X. Li. 2012. Age constraint on Burmese amber based on U-Pb dating of zircons. *Cretaceous Research* 37: 155–163. https://doi.org/10.1016/j.cretres.2012.03.014.

Shields, J.D., and L.A. Ward. 1998. Tiarinion texopallium, new species, an entoniscid isopod infesting majid crabs (*Tiarinia* spp.) from the Great Barrier Reef, Australia. *Journal of Crustacean Biology* 18(3): 590–596.

Shiino, S.M. 1954. A new fresh-water entoniscid isopod, *Entionella okayamaensis* n. sp. *Report of the Faculty of Fisheries, Prefectural University of Mie* 1(3): 239–246.

Shimomura, M., S. Ohtsuka, and K. Naito. 2005. *Prodajus curviabdominalis* n. sp. (Isopoda: Epicaridea: Dajidae), an ectoparasite of mysids, with notes on morphological changes, behaviour and life-cycle. *Systematic Parasitology* 60(1): 39–57. https://doi.org/10.1007/s11230-004-1375-8.

Shuster, S.M., and M.J. Wade. 1991. Female copying and sexual selection in a marine isopod crustacean *Paracerceis sculpta*. *Animal Behaviour* 41(6): 1071–1078. https://doi.org/10.1016/S0003-3472(05)80645-1.

Sidorchuk, E.A., V. Perrichot, and E.E. Lindquist. 2016. A new fossil mite from French Cretaceous amber (Acari: Heterostigmata: *Nasutiacaroidea superfam.* nov.), testing evolutionary concepts within the Eleutherengona (Acariformes). *Journal of Systematic Palaeontology* 14(4): 297–317. https://doi.org/10.1080/14772019.2015.1046512.

Soergel, W. von. 1913. Lias und Dogger von Jefbei und Fialpopo (Misólarchipel). In *Geologische Mitteilungen aus dem Indo-Australischen Archipel*, ed. G. Boehm. *Neues Jahrbuch für Mineralogie etc.* 36: 586–650.

Standing, J.D., and D.D. Beatty. 1978. Humidity behaviour and reception in the sphaeromatid isopod *Gnorimosphaeroma oregonensis*

(Dana). *Canadian Journal of Zoology* 56(9): 2004–2014. https://doi.org/10.1139/z78-270.

Stepien, C.A., and R.C. Brusca. 1985. Nocturnal attacks on nearshore fishes in southern California by crustacean zooplankton. *Marine Ecology Progress Series* 25(1): 91–105.

Strömberg, J.O. 1971. Contribution to the embryology of bopyrid isopods with special reference to *Bopyroides, Hemiarthrus*, and *Peseudione* [sic] (Isopoda, Epicaridea). *Sarsia* 47(1): 1–46. https://doi.org/10.1080/00364827.1971.10411191.

Strömberg, J.O. 1983. A redescription of *Onisocryptus sagittus* Schultz 1977 (Epicaridea, Cryptoniscina) with notes on hosts, distribution and family relationships. *Polar Biology* 2(2): 87–94.

Szwedo, J., and J. Drohojowska. 2016. A swarm of whiteflies—the first record of gregarious behavior from Eocene Baltic amber. *The Science of Nature* 103(35): 1–6. https://doi.org/10.1007/s00114-016-1359-y.

Taberly, G. 1954. Etude morphologique d'un Dajidae peu connu: *Prodajus lobiancoi* Bonnier (Crust. Isop. Epicaridea) II. —Le cryptoniscium de *P. lobiancoi* et sa mue formes connues de cryptoniscium de Dajidae. *Bulletin d'Institut Océanographique* 1049: 1–15.

Tanaka, K., and E. Nishi. 2008. Habitat use by the gnathiid isopod *Elaphognathia discolor* living in terebellid polychaete tubes. *Journal of the Marine Biological Association of the United Kingdom* 88(1): 57–63. https://doi.org/10.1017/S0025315408000039.

Thiel, M. 2003. Reproductive biology of *Limnoria chilensis*: another boring peracarid species with extended parental care. *Journal of Natural History* 37(14): 1713–1726. https://doi.org/10.1080/00222930210125416.

Thiel, M. 2011. *The evolution of sociality: peracarid crustaceans as model organisms. New Frontiers in Crustacean Biology. Proceedings of the TCS Summer Meeting, Tokyo, 20-24 September 2009. Crustaceana Monographs* 15: 285–297.

Thompson, M.T. 1902. A new isopod parasitic on the hermit crab. *Bulletin of the U.S Fisheries Commission* 21: 53–56.

Torres Jordá, M. 2003. Estudio de la relación entre el parásito *Leidya distorta* (Isopoda: Bopyridae) y su hospedador *Uca uruguayensis* (Brachyura: Ocypodidae), y descripción de los estadíos larvales de *L. distorta*. Unpublished PhD thesis. Buenos Aires: Universidad de Buenos Aires.

Ueda, H., A. Kuwahara, N. Tanaka, and M. Azeta. 1983. Underwater observations on copepod swarms in temperate and subtropical waters. *Marine Ecology Progress Series* 11: 165–171. https://doi.org/10.3354/meps011165.

Uye, S., and A. Murase. 1997. Infertility of the planktonic copepod *Calanus sinicus* caused by parasitism by a larval epicaridian isopod. *Plankton Biology and Ecology* 44(1/2): 97–99.

Vršanský, P., I. Koubová, L. Vršanská, J. Hinkelman, M. Kúdela, T. Kúdelová, J.H. Liang, F. Xia, X. Lei, X. Ren, Ľ Vidlička, T. Bao, S. Ellenberger, L. Šmídová, and M. Barclay. 2019. Early wood-boring 'mole roach' reveals eusociality "missing ring." *AMBA Projekty* 9(1): 1–28.

Wägele, J.W. 1989. *Evolution und phylogenetisches System der Isopoda: Stand der Forschung und neue Erkenntnisse. Zoologica*. Stuttgart: Schweizerbart.

Walossek, D. 1999. On the Cambrian Diversity of Crustacea. In *Crustaceans and the Biodiversity Crisis*, eds. F.R. Schram, and J.C. von Vaupel Klein, 3–27. *Proceedings of the Fourth International Crustacean Congress*. Leiden: Brill.

Walossek, D., and K.J. Müller. 1998. Cambrian 'Orsten'-type arthropods and the phylogeny of Crustacea. In *Arthropod relationships*, eds. R.A. Fortey and R.H. Thomas, 139–153. Dordrecht: Springer.

Wang, B., J. Rust, M.S. Engel, J. Szwedo, S. Dutta, A. Nel, Y. Fan, F. Meng, G. Shi, E.A. Jarzembowski, T. Wappler, F. Stebner, Y. Fang, L. Mao, D. Zheng, and H. Zhang. 2014. A diverse

paleobiota in early Eocene fushun amber from China. *Current Biology* 24(14): 1606–1610. https://doi.org/10.1016/j.cub.2014.05.048.

Wang, H., M. Schädel, B. Sames, and D.J. Horne. 2020. New record of podocopid ostracods from Cretaceous amber. *PeerJ* e10134: 1–10. https://doi.org/10.7717/peerj.10134.

Weitschat, W., and W. Wichard. 1998. *Atlas der Pflanzen und Tiere im Baltischen Bernstein*. München: Verlag Dr. Friedrich Pfeil.

Wichard, W., and W. Weitschat. 2004. *Im Bernsteinwald*. Hildesheim: Gerstenberg.

Wienberg Rasmussen, H., S.L. Jakobsen, and J.S.H. Collins. 2008. Raninidae infested by parasitic Isopoda (Epicaridea). *Bulletin of the Mizunami Fossil Museum* 34: 31–49.

Williams, J.D., and J. An. 2009. The cryptogenic parasitic isopod *Orthione griffenis* Markham, 2004 from the eastern and western Pacific. *Integrative and Comparative Biology* 49(2): 114–126.

Wilson, G.D.F. 2009. The phylogenetic position of the Isopoda in the Peracarida (Crustacea: Malacostraca). *Arthropod Systematics and Phylogeny* 67(2): 159–198.

Wilson, G.D.F., and R.T. Johnson. 1999. Ancient endemism among freshwater isopods (Crustacea, Phreatoicidea). In *The other 99%: the conservation and biodiversity of invertebrates*, ed. W. Ponder, 264–268. New South Wales: Royal Zoological Society of New South Wales. https://doi.org/10.7882/0958608512.

Wings, O., M. Rabi, J.W. Schneider, L. Schwermann, G. Sun, C.F. Zhou, and W.G. Joyce. 2012. An enormous Jurassic turtle bone bed from the Turpan Basin of Xinjiang, China. *Naturwissenschaften* 99(11): 925–935. https://doi.org/10.1007/s00114-012-0974-5.

Wu, R.J.C. 1997. *Secrets of a lost world. Dominican amber and its inclusions*. Santo Domingo

Xing, L., B. Sames, R.C. McKellar, D. Xi, M. Bai, and X. Wan. 2018. A gigantic marine ostracod (Crustacea: Myodocopa) trapped in mid-Cretaceous Burmese amber. *Scientific Reports* 8(1): 1365. https://doi.org/10.1038/s41598-018-19877-y.

Yu, T., R. Kelly, L. Mu, A. Ross, J. Kennedy, P. Broly, F. Xia, H. Zhang, B. Wang, and D. Dilcher. 2019. An ammonite trapped in Burmese amber. *Proceedings of the National Academy of Sciences* 116(23): 11345–11350. https://doi.org/10.1073/pnas.1821292116.

Zhang, W.W. 2017. *Frozen dimensions. The fossil insects and other invertebrates in amber*. Chongqing: Chongqing University Press.

2.4   Study IV: VAN DER WAL, SCHÄDEL, EKRT & HAUG 2021

Description and ontogeny of a 40-million-year-old parasitic isopodan crustacean: *Parvucymoides dvorakorum* gen. et sp. nov.

Serita Van der Wal[1], Mario Schädel[1], Boris Ekrt[2] and
Joachim T. Haug[1,3]

[1] Zoomorphology Group, Faculty of Biology, LMU Munich, Planegg-Martinsried, Germany
[2] Department of Paleontology, National Museum, Prague, Czech Republic
[3] GeoBio-Center, LMU Munich, Munich, Germany

ABSTRACT

A collection of exceptionally well-preserved fossil specimens of crustaceans, clearly representatives of Isopoda, is presented here. Excavated from the late Eocene (approximately 40 million years ago) freshwater sediments of the Trupelník hill field site near Kučlín, Czech Republic, these specimens are preserved with many details of the appendages. The morphological characteristics of the fossils were documented using macro-photography with polarised light, as well as stereo imaging. These characteristics, especially including the trunk appendage morphology, were compared to those of related extant groups from different ontogenetic stages. All specimens are conspecific, representing a single species *Parvucymoides dvorakorum* gen. et sp. nov. Morphometric analysis of body shapes and sizes of the reconstructed fossils and related extant species were performed. These analyses provided insight into the ontogenetic stages of each reconstructed fossil specimen. In combination with the morphological assessment, the results indicate that the fossils represent at least two (possibly three) developmental stages, including immatures. The morphology of the appendages suggests that these fossils were parasites. The fossils are interpreted as either representatives of Cymothoidae or at least closely related to this group.

INTRODUCTION

Isopoda is an extremely species-rich and diverse group of organisms (*Wilson, 2009*; *Poore & Bruce, 2012*). Among the marine forms of Isopoda, Cymothoida *Wägele, 1989* is a morphologically and distributionally diverse group, with a variety of life strategies, ranging from scavengers and predators (see *Holdich, 1981*; *Wilson, Sims & Grutter, 2011*; *Robin et al., 2019*; *Youssef et al., 2020*) to highly specialised temporary and permanent parasitic individuals (see *Hadfield, Smit & Avenant-Oldewage, 2009*; *Williams & Boyko, 2012*; *Alves-Júnior et al., 2019*). Despite the large number of species and the morphological diversity within extant representatives of Cymothoida (*Boyko et al., 2019*), the current

fossil record does not reflect this diversity (*Hyžný, Bruce & Schlögl, 2013*; *Smit, Bruce & Hadfield, 2014*). In most cases, only the dorsal sclerites (tergites) of the posterior body region are preserved as fossils, likely as a result of the biphasic moulting process that characterises Isopoda (*Wieder & Feldmann, 1992*; *Feldmann & Goolaerts, 2005*; *Hansen & Hansen, 2010*; *Hyžný, Bruce & Schlögl, 2013*; *Etter, 2014*). Fossil remains of Isopoda are also mostly preserved without complete or accessible appendages, impeding their further systematic interpretation and comparison to extant groups (*Hyžný, Bruce & Schlögl, 2013*; *Smit, Bruce & Hadfield, 2014*; *Maguire et al., 2018*).

The majority of fossil specimens that can be interpreted as representatives of Cymothoida seem to be predatory or scavenging forms. Several of the ingroups of Cymothoida have species that exhibit parasitic strategies (temporarily or permanently) during some stage of development, or for a specific duration of time. Species with parasitic life strategies are found in the following groups: Corallanidae *Hansen, 1890* (see *Gentil-Vasconcelos & Tavares-Dias, 2015*; *Nagasawa, Imai & Saito, 2018*), Aegidae *White, 1850* (see *Nair & Nair, 1983*; *Cavalcanti et al., 2012*), Cymothoidae *Leach, 1818* (see *Kottarathil et al., 2019*; *Mahmoud, Fahmy & Abuowarda, 2020*), Epicaridea (including Bopyroidea *Rafinesque, 1815* and Cryptoniscoidea *Kossmann, 1880*; see *Roccatagliata & Jordá, 2002*; *Alves-Júnior et al., 2019*), Gnathiidae *Leach, 1814* (see *Smit, Basson & Van As, 2003*; *Marino et al., 2004*) and possibly *Urda Münster, 1840* (see *Nagler, Hyžný & Haug, 2017*).

Direct indications of parasitic behaviour by representatives of Isopoda (*e.g.*, body fossils of parasites on the suspected host) are scarce. *Nagler et al. (2016)* described and presented a direct parasite-host interaction from 150 million years old fossils, containing both the host and the interpreted parasitic representatives of Cymothoida attached to it. Less direct indications of parasitic behaviour for Cymothoida include:

(1) Deformations of the host, such as swellings on the shields of fossil crustaceans, can serve as an indication for parasitic behaviour of representatives of Bopyridae (ingroup of Cymothoida; *Morris, 1981*; *Boyko, Williams & Markham, 2012*). Records and photographs of these deformations have been provided in, for example, *Bachmayer (1948)*, *Radwański (1972)*, *Klompmaker et al. (2014)*, *Klompmaker et al. (2018)* and *Robins & Klompmaker (2019)*.

(2) The reconstructed functional morphology of the fossil remains as an indication for possible parasitic behaviour (*Nagler & Haug, 2016*; *Nagler et al., 2016*). If the quality of preservation is sufficient, the functional morphology can be reconstructed for isolated fossil remains of representatives of Cymothoida. Here, the attaching appendages, such as the anterior trunk appendages (thoracopods) and mouthparts, are particularly informative.

(3) A specific and distinct life stage, such as a dispersal stage, if it is only known in parasitic species of the modern fauna, is also an indication for parasitic behaviour. For example, the distinct, dispersal larval stages of Epicaridea (epicaridium, microniscium and cryptoniscium), which are unique to the group. *Serrano-Sánchez et al. (2016)* reported the first direct body fossils (without the host) of cryptoniscium larvae from Miocene Chiapas Amber, originating from Mexico. Shortly thereafter, *Néraudeau et al. (2017)* and *Schädel, Perrichot & Haug (2019)* reported on separate additional specimens of epicaridean

larvae from Cretaceous French Vendean amber. The latest report of such an indication of parasitic behaviour is provided in *Schädel et al. (2021)*.

(4) A phylogenetic position of which all representatives exhibit a parasitic behaviour is another indication for parasitic behaviour, provided that the supporting morphological characters for parasitism are also accessible. Some previous publications have reported on fossil finds of specimens that might be closely related to Cymothoidae (*Bowman, 1971*; *Nagler et al., 2016*), or that could be early forms of Cymothoidae.

Some fossils have been described as species of or closely related to Aegidae, based on similarities with extant species (*e.g.*, *Van Straelen, 1930*; *Hessler, 1969*; *Polz, 2005*; *Hansen & Hansen, 2010*). *Urda*, a group of species associated with fossil fish, has recently been interpreted as an ingroup of Cymothoida, based on the functional morphology of its representatives (*Nagler, Hyžný & Haug, 2017*).

Here we present exceptionally well-preserved fossil representatives and describe a new species of Cymothoida that provide clear indications for parasitic behaviour, based on morphology and systematic interpretation. We compare the morphological characters, body shapes and sizes of these fossils, with those of extant genera and species. These comparisons provide some insight into the possible behaviour and ontogenetic variability of the fossils.

MATERIALS & METHODS

Material

The examined fossil specimens were collected from Kučlín, Czech Republic (Fig. 1), during 1995–2010 by Zdeněk Dvořák and Pavel Dvořák. A total of 11 fossil specimens were examined, photographed and illustrated in detail (Figs. 2–18). All specimens are deposited at the National Museum, Prague, under collection numbers P2338–P2348.

The electronic version of this article in Portable Document Format (PDF) will represent a published work according to the International Commission on Zoological Nomenclature (ICZN), and hence the new names contained in the electronic version are effectively published under that Code from the electronic edition alone. This published work and the nomenclatural acts it contains have been registered in ZooBank, the online registration system for the ICZN. The ZooBank LSIDs (Life Science Identifiers) can be resolved and the associated information viewed through any standard web browser by appending the LSID to the prefix http://zoobank.org/. The LSID for this publication is: urn:lsid:zoobank.org:pub:C38FC926-EEC4-45F8-8CBB-3639D845C4DA. The online version of this work is archived and available from the following digital repositories: PeerJ, PubMed Central and CLOCKSS.

Geological setting and palaeoenvironment

The herein presented fossils come from the so called 'upper pothole quarry' of the Trupelník hill field site, near Kučlín (České středohoří mountain range, North Bohemia, Czech Republic; see Fig. 1). This fossil site was first mentioned in publications at the end of the 18th century and throughout the 19th–21st centuries. It afforded rich palaeontological material. Private and particularly commercial collecting was focused
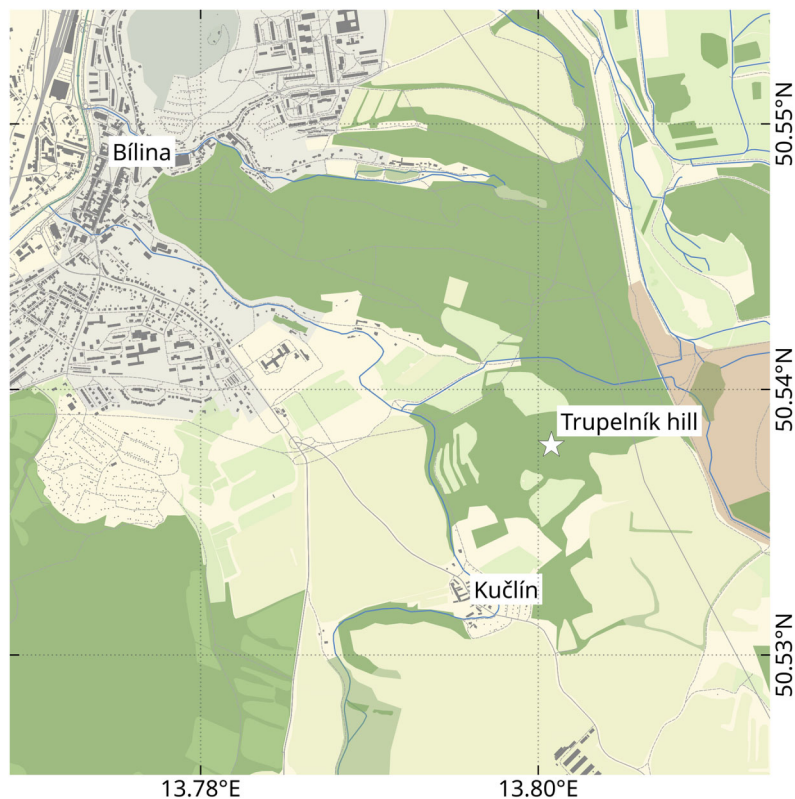
Figure 1 Location of the Trupelník hill field site (denoted by a white star), southeast of the town Bílina (Teplice District) and northwest of the village Kučlín, Northwestern Bohemia, Czech Republic. Map data from OpenStreetMap (openstreetmap.org, ODbL license).

Full-size ⬚ DOI: 10.7717/peerj.12317/fig-1

mostly on decorative fish skeletons, plant particles and sometimes certain insects. Small, non-decorative fossils, such as those presented herein, have usually been neglected. Comprehensive collecting was done by Zdeněk and Pavel Dvořák over the last 25 years.

The sediments in which the fossils were found are late Eocene in age (see *Fejfar & Kvaček, 1993*). Basaloid rock (sodalite tephrite) that overlie the sediments have been dated to an age of 38.3 ± 0.9 million years (*Bellon et al., 1998*). Subsequently, the sedimentary rocks below this, including the herein presented fossils, are only slightly older. The late Eocene age of the sedimentary rocks, which contain the fossils herein presented, is also corroborated *via* biostratigraphy of pollen of *Compositoipollenites rhizophorus* (R.Pot., 1934) R. Pot., 1960 and *Striatricolpites catatumbus* Gonzalez, 1967 (*Konzalová, 1981*).

The fossils were excavated from finely laminated diatomites. The exact composition of the rock matrix and the degree of compaction and diagenesis between the individual layers of sediment, varies considerably. The sediments were most likely deposited in a freshwater lake within a geological basin (*Mach & Dvořák, 2011*). Even though there is no geological indication for a connection of the depositional environment with the ocean (*Mach & Dvořák, 2011*), such a connection can be suggested by the presence of temperate basses (Moronidae). These fish have been assumed to have populated the environment

via a river system or that they represent primarily marine animals with anadromous behaviour (*Micklich, 1990*; *Micklich & Böhme, 1997*; *Přikryl, 2008*). Except for the relatively rare representatives of *Morone*, three abundant species of ray-finned fishes have been collected from this site (*Properca prisca* (*Agassiz, 1834*); *Thaumaturus furcatus Reuss, 1844*; *Cyclurus macrocephalus Reuss, 1844*). The presence of possible parasites, *in situ*, was carefully checked for all of the collected fish fossils, but none were found. Parasitic representatives of Isopoda can easily be overlooked during the preparation of a fossil, especially since re-crystallisation of the crustacean can appear as an insignificant crystalline blob (*Nagler et al., 2016*). The most likely connection to the ocean would have been towards the north into the Atlantic Ocean (*Micklich & Böhme, 1997*; *Scotese, 2014*). Palaeoclimate reconstructions, based on the fossil flora and fauna of the Trupelník Hill field site, suggest a seasonal warm-temperate to subtropical palaeoenvironment during the late Eocene (*Kvaček, 2002*; *Kvaček & Teodoridis, 2011*; *Chroust, Mazuch & Hernández Luján, 2019*).

Documentation methods

Fossil specimens were photographed under white light using a Keyence VHX-6000 digital microscope. The built-in focus fusion technique of the digital microscope was used to achieve full focus images. Stereo images were created by tilting the microscope seven degrees to the left and to the right, respectively, and recording full focus images (*Wheatstone, 1838*). The stereo images were converted into red-cyan stereo anaglyphs (*Rollmann, 1853*) using Affinity Photo (Serif Europe Ltd). In case the stereo anaglyphs cannot be perceived by the reader, they can be converted into wiggle images using free software such as kataglyph (GPL licence, available from https://github.com/mcranium/kataglyph). Image editing and enhancement was done using Affinity Photo. Line drawings, colour markings of body parts, and assembly of figure plates were prepared using a combination of Adobe Illustrator (Adobe Inc.) and Affinity Designer. All drawings are available from the 'MorphDBase' online repository *via* the permanent link www.morphdbase.de/. Exact links to the figures of each respective specimen are provided in *Material examined*.

Field site map

The map depicting the location of the 'Trupelník hill' field site was created using QGIS v.3.14 (qgis.org, GPL license). The map data comes from OpenStreetMap (openstreetmap.org, ODbL licence) and was retrieved using the QuickOSM plugin for QGIS (GPL v.2 licence).

Terminology

Specialised terminology often prohibit communication beyond a specific taxonomic border. In order to avoid the confusion regarding terms used for specific structures, these are provided here. Descriptions comprise terminology used for the general Eumalacostraca body organisation and articulation (based on *Walossek, 1999*) which can be compared to Isopoda specific terms as used by for example *Jackson (1926)*, *Kensley (1978)* and

Hoffman (2019). A further comparison between preferred terms among isopod- and other crustacean workers is provided in *Nagler, Eiler & Haug (2019)*. The descriptions herein comprise the following terminology: a functional head (in literature also referred to as cephalon or cephalothorax), bearing the ocular segment and six post-ocular segments, including the corresponding appendages (antennula, antenna, mandible, maxillula, maxilla and maxilliped); an anterior trunk (in literature also referred to as the posterior thorax or pereon) of seven segments (thoracomeres, also referred to as pereonites), each with one pair of appendages (thoracopods, also referred to as pereopods); a posterior trunk (pleon) comprising five anterior segments (pleomeres, or also pleonites), each with one pair of appendages (pleopods) and the sixth pleon segment conjoined to the telson forming the pleotelson, with one pair of appendages (uropods). Additionally, species of the group Cymothoidae are protandric, meaning that a "male" will eventually develop into a female and is therefore regarded as a separate ontogenetic stage.

Measurements, descriptions and morphometrics

Measurements of the examined fossils include the following distances, measured using ImageJ (public domain): The total length and width of the complete specimen, where completely preserved; maximum length and maximum width of the head, each completely preserved anterior trunk segment, each completely preserved element of trunk appendages, each completely preserved pleon segment, and pleotelson (where preserved). These measurements were used to calculate ratios of the completely preserved structures, used in the descriptions. Only structures that were complete and preserved without distortion, were measured (in mm) to avoid inaccuracy due to perspective. Measurements were rounded to two decimal points, ratios were rounded to one decimal point. Specimen descriptions were made with structures in the direction from anterior to posterior and from proximal to distal.

A comparative overall body outline analysis was done using: (1) the reconstructed illustrations of examined specimens from which a complete and undistorted dorsal side was preserved; (2) and those of different ontogenetic stages of various extant species. This provided information on the variation in body shape between the examined fossils, among the examined fossils and extant species, as well as between different ontogenetic stages.

From literature, the body outlines of 18 extant species (dorsoventral projection) were included in the analysis. The selection of species was made based on: (1) the availability of dorsal view illustrations or photographs of at least three different ontogenetic stages of a species (*i.e.*, female, male and immature stage), and (2) the site of attachment (*i.e.*, mouth, gill and externally attaching parasitic groups). A total of 76 individual outlines were included in the analysis, along with five reconstructed outlines of completely preserved examined fossils.

The reconstructions were done manually with the aid of the software program Affinity Designer. Interpretive digital illustrations were made of specimens P2338, P2339, P2347, P2344 and P234 as these specimens have the best preservation in terms of orientation (accessible in dorsal view) in order to avoid or reduce the degree of idealisation when creating reconstructions. From the fossils it is evident that the specimens had a bilaterally

symmetrical body, which was used as a guideline for reconstruction. Undistorted body segments were arranged and distorted segments symmetrized (idealised) in a way that would provide a complete and smoother body outline, with minimum alteration in the shape and proportions of the segment. For this, the best preserved lateral side of a segment was chosen to serve as a guide. This side (left or right from the medial symmetry line of the specimen) was then mirrored on the opposite side to create a complete segment which is bilaterally symmetrical.

For the list of species included and publications from which the additional illustrations were redrawn, see Doc. S1. Illustrations of curved specimens were straightened by deforming a vectorised copy of the outline in Inkscape (GPL-2 licence) using the 'bend from clipboard' function with a mirrored midline of the shape. ImageMagick (Apache 2.0 licence) was used for batch resizing and converting raster image files. The quantitative analysis of the outline shapes was performed using the R programming language (*R Core Team, 2020*, v.3.6.3). Momocs (GPL-3 licence; *Bonhomme et al., 2014*) was used to read the raster image files. The outlines were automatically centred, scaled and aligned using functions from the Momocs package. The 'efourier' function from Momocs was used to convert the shape information from a coordinate based format to Fourier coefficients (elliptic Fourier transformation). For this, 10 harmonics were used and the Fourier coefficients were automatically normalized. The Fourier coefficients were then ordinated using the Principle Component Analysis (PCA) function implemented in Momocs. Linear models ('lm' function, base R) were fitted to the first two principle components relative to the total body length.

Additional R packages were used for data manipulation ('dplyr', 'magrittr', 'reshape2') (*Wickham, 2007*; *Bache & Wickham, 2014*; *Wickham et al., 2020*). The web application 'iWantHue' (GPL-3 licence, https://medialab.github.io/iwanthue/) was used to choose colours used in the plots that are suitable for colour vision impaired persons. The colours were additionally checked, using the software Color Oracle 1.3 (CC-BY licence, Bernhard jenny and Nathaniel V. Kelso). The R code used for this analysis is available from Doc. S2.

The dataset imported to R, is given in Doc. S1, with the code created and applied for visualising the results as plots, given in Doc. S2. A total of 76 dorsal view body shapes were analysed together. To visualise the variation in the outline shapes and to simplify the data, a principal component analysis (PCA) was done. The variation in the principle components (PC1–PC10) is given in Fig. S1. The mean shapes of each ontogenetic stage (immature, male and female) are presented and compared in Fig. S2.

RESULTS

Systematic palaeontology
Cymothoida *Wägele, 1989*
Cymothoidae *Leach, 1814*

Parvucymoides gen. nov. ZooBank LSID: urn:lsid:zoobank.org:act:DE6F26BC-87E1-43B8-BDF9-47B25537627C.

Type species: *Parvucymoides dvorakorum* sp. nov.; by monotypy.

Diagnosis: As for the type species, as it is monotypic.

Etymology: The genus name is derived from a combination of the Latin words *parvus*, meaning little or tiny and *cymoides*, emphasizing the presumed systematic affinity of the species. The gender is male (masculine).

Parvucymoides dvorakorum sp. nov. ZooBank LSID: urn:lsid:zoobank.org:act:485FBA58-F578-48A0-AD3C-D93991C6A8D3.

Type locality and age: Trupelník hill near Kučlín u Bíliny (late Eocene)

Etymology: The species name is derived from the family name of the two brothers that collected the specimens (noun in the genitive case, gender: male (masculine), plural). Zdeněk Dvořák and Pavel Dvořák both collected numerous fossils in Kučlín since their childhood, and have largely contributed to the abundance of fossils available from this site.

Species diagnosis
Immature/male. *Body* elongate, bilaterally symmetrical. *Head* visible from dorsal view, roughly triangular in shape. *Compound eyes* visible in dorsal view (when preserved and accessible). *Antennula* with minimum of 12 articles; *antenna* with minimum of 10 articles, bases not in contact. *Anterior trunk* (pereon) *segment 1* narrowest, posterior margin evenly rounded, not encompassing the head. *Anterior trunk segment 7* wider than posterior trunk segment 1, posterolateral margins not overlapping lateral margins of posterior trunk segments. *Posterior trunk* (pleon) *segments* subequal in width, all narrower than pereon segments, posterior margins concave in dorsal view. *Pleotelson* narrower than pleon, wider than long. *Uropod* endopod and exopod sub-equal in length, extending past pleotelson posterior margin, apices narrowly rounded.

Female. Same as immature/male. *Body* longer and wider than males/immatures; *anterior trunk* (pereon) *segment 1* triangular, anterior margin encompassing the head.

Remarks
As the genus that has been created to accommodate this species is monotypic, this diagnosis contains a set of characters that distinguish the species from other extant and extinct species. This set of characters includes also those characters that could later serve as diagnostic characters of the genus or 'genus diagnosis', if a con-generic species to the herein presented species is described. This extensive diagnosis is referenced above according to ICZN Code Act 13.1.2.

Material examined:
Holotype. 1 male. P2339a/b as part and counterpart (8.44 mm TL; 4.04 mm W), collected at Kučlín, Czech Republic, during 1995–2010. Coll. Zdeněk Dvořák and Pavel Dvořák. Deposited at the National Museum, Prague, Figs. 2–3 (www.morphdbase.de/?S_VanderWal_20210812-M-154.1, www.morphdbase.de/?S_VanderWal_20210812-M-147.1).

Paratypes. 9 additional specimens. 2 males. P2346a/b part and counterpart (total body length & width not preserved), Figs. 6–7 (www.morphdbase.de/?S_VanderWal_20210812-M-153.1, www.morphdbase.de/?S_VanderWal_20210812-M-145.1). P2348 (7 mm TL, total width cannot be accurately determined), Fig. 8 (www.morphdbase.de/?S_VanderWal_20210812-M-152.1). 4 immatures? P2338a/b part and counterpart (7.41 mm TL, 2.95 mm W), Figs. 9–10 (www.morphdbase.de/?S_VanderWal_20210812-M-144.1, www.morphdbase.de/?S_VanderWal_20210812-M-151.1). P2347(at least 5.20 mm TL, 2.36 mm W), Fig. 11 (www.morphdbase.de/?S_VanderWal_20210812-M-143.1). P2344 (4.68 mm TL, 2.12 mm W), Fig. 12 (www.morphdbase.de/?S_VanderWal_20210812-M-149.1). P2343 (at least 6.12mm TL, at least 2.70 mm W), Fig. 13 (https://www.morphdbase.de/?S_VanderWal_20210812-M-142.1). 3 females? P2345a/b part and counterpart (at least 9.42 mm TL, 4.95 mm W), Figs. 14–16 (www.morphdbase.de/?S_VanderWal_20210812-M-150.1, www.morphdbase.de/?S_VanderWal_20210812-M-141.1, www.morphdbase.de/?S_VanderWal_20210812-M-148.1). P2341 (at least 9.39 mm TL, 6.20 mm W), Fig. 17 (www.morphdbase.de/?S_VanderWal_20210812-M-140.1). P2340 (at least 6.80 mm TL, total width cannot be accurately determined), Fig. 18 (www.morphdbase.de/?S_VanderWal_20210812-M-20.1). Same data as holotype.

Additional material. Male? P2342a/b part and counterpart (9.50 mm TL, total width cannot be accurately determined), Figs. 4–5 (www.morphdbase.de/?S_VanderWal_20210812-M-155.1, www.morphdbase.de/?S_VanderWal_20210812-M-146.1). Same data as holotype.

Description of holotype male (P2339a/b, Figs. 2–3)
One specimen as part (Fig. 2 with mostly dorsal features visible, P2339a) and counterpart (Fig. 3 with mostly ventral features visible, P2339b). Total body length 8.44 mm, total width 4.04 mm.

Body expanding in width posteriorly; longer than wide, 2.1x; widest at anterior trunk segment 5. *Head* triangular; wider than long, 1.5x; anterior margin narrowly rounded. *Eyes* not accessible.

Some articles of antennulae and antennae accessible. *Antennula* with at least nine articles; *antenna* with at least seven articles.

All *anterior trunk* (pereon) *segments* wider than long (Fig. 2), segment 1, 3.1x, not encompassing functional head; segment 2, 5.2x; segment 3, 6.2x; segment 4, 6.0x; segment 5 (widest), 5.7x; segment 6 (longest), 4.7x; segment 7 (posterior margin concave), 4.2x; all with at least one, partly preserved appendage.

Anterior trunk appendages (pereopods), distal region with 6 articles well accessible. *Proximal article* (coxa) accessible (Fig. 3C), as long as, or shorter than trunk segment.

Trunk appendage 1 (thoracopod 2, right), basipod longer than wide, 1.9x; ischium longer than wide, 2.7x; merus twice as wide as long; carpus longer than wide, 1.7x; propodus wider than long, 2.2x; dactylus longer than wide, 2.1x.
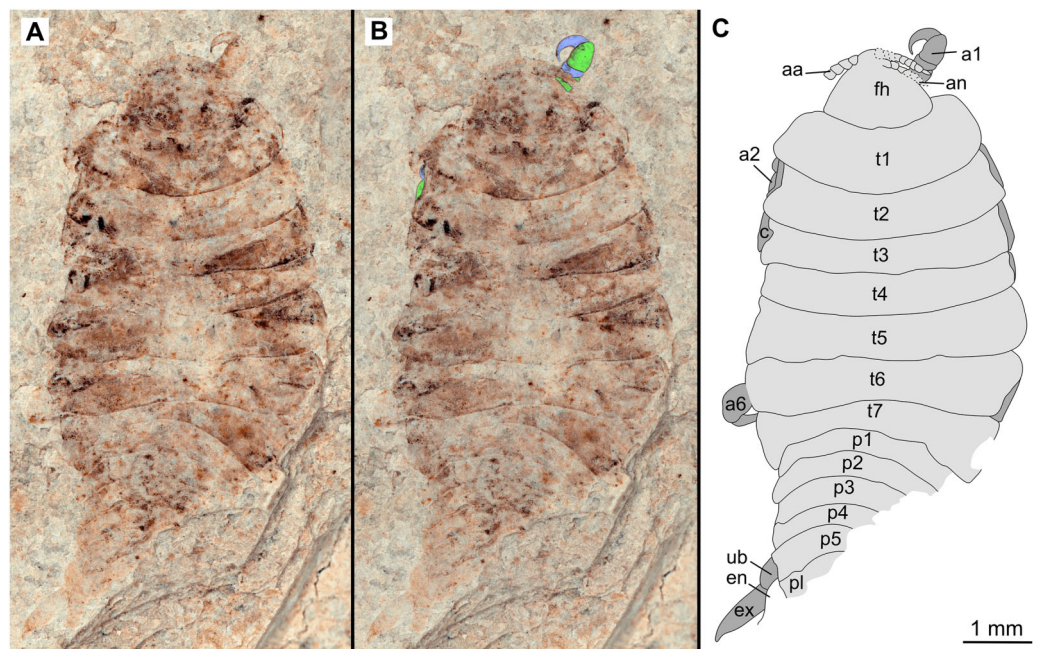
Figure 2 Holotype male (P2339a). (A–C) same scale. (A) Light microscope image with dorsal features and structures visible. (B) With colour marked trunk appendages, (C) Line drawing. Abbreviations: a1–2, trunk appendages 1–2; aa, antennula; ex, uropod exopod; fh, functional head; p1–5, pleon segments 1–5; pl, pleotelson; t1–7, trunk segments 1–7; ub, uropod basipod.

Full-size ☑ DOI: 10.7717/peerj.12317/fig-2

Trunk appendage 3 (thoracopod 4, right), basipod longer than wide, 2.2x; ischium longer than wide, 1.3x; merus as long as wide; carpus wider than long, 1.6x; propodus wider than long, 1.1x; dactylus twice as long as wide.

Trunk appendage 3 (thoracopod 4, left), basipod longer than wide, 1.7x; ischium longer than wide, 1.7x; merus as long as wide; carpus wider than long, 1.4x; propodus wider than long, 1.6x; dactylus longer than wide, 2.7x.

Trunk appendage 4 (thoracopod 5, right), basipod longer than wide, 1.5x; ischium wider than long, 2.4x; merus wider than long, 1.8x; carpus longer than wide, 1.5x; propodus longer than wide, 2.5x; dactylus twice as long as wide.

Trunk appendage 6 (thoracopod 5, right), basipod twice as long as wide; ischium wider than long, 2.2x; merus wider than long, 1.2x; carpus wider than long, 1.1x; propodus longer than wide, 1.2x; dactylus longer than wide, 2.6x.

Posterior trunk (pleon) *segments* posterior margins concave (Fig. 2); all wider than long (Fig. 3), segment 1, 4.9x; segment 2 lateral margins not visible; segment 3, 7.0x; segment 4, 7.3x; segment 5 (longest), 4.5x; posterior trunk appendage insertion areas visible (Fig. 3).

Pleotelson (Fig. 3), converging to postero-medial point (possibly distorted); wider than long, 1.4x. *Uropods* with basipods extending past lateral margins of pleotelson; exo-and endopods distal margins not preserved/accessible, extending past pleotelson posterior margin.
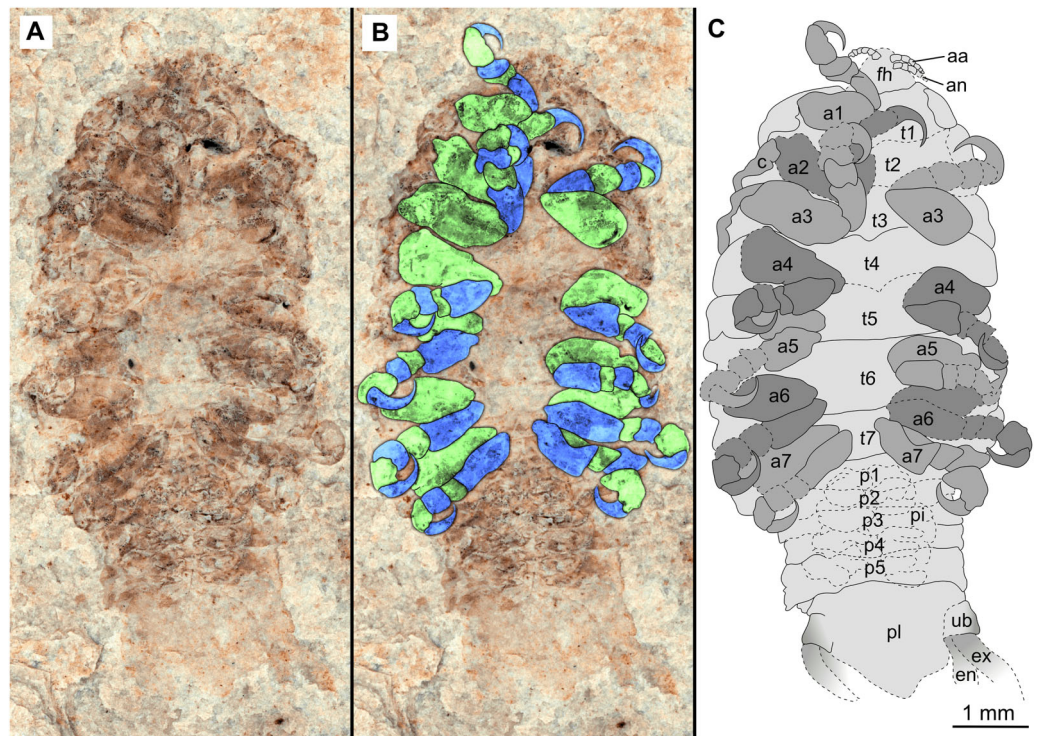
Figure 3 Holotype male (P2339b). (A–C) same scale. (A) Light microscope image with ventral features and structures visible. (B) With colour marked trunk appendages, (C) Line drawing. Abbreviations: a1–7, trunk appendages 1–7; aa, antennula; an, antenna; c, coxa; en, uropod endopod; ex, uropod exopod; fh, functional head; p1–5, pleon segments 1–5; pi, pleon attachment; pl, pleotelson; t1–7, trunk segments 1–7; ub, uropod basipod. Full-size 🖼 DOI: 10.7717/peerj.12317/fig-3

Variation. The shape of the anterior margin of the functional head of specimen P2342 (Figs. 4 and 5) is broadly rounded. *Posterior trunk* (pleon) *segments* with lateral margins slightly extended. *Pleotelson* evenly rounded. Specimen P2346 (Figs. 6 and 7) have compound eyes visible, with at least six rows of ommatidia. Accessible antennula articles vary between at least five to six articles.

Description of immature (P2338a/b, Figs. 9–10)
One specimen as part (Fig. 9 with mostly dorsal features visible, P2338a) and counterpart (Fig. 10 with mostly ventral features visible, P2338b).

Body elongated; longer than wide, 2.5x; anterior trunk segments lateral margins subparallel.

Head sub-truncate oval; wider than long, 1.1x; anterior margin blunt, slightly rounded. *Eyes* not accessible.

Some elements of antennulae and antennae accessible (Fig. 10). *Antennula* with at least 12 articles; *antenna* with at least 10 articles.

All *anterior trunk* (pereon) *segments* wider than long (Fig. 9), segment 1, 3.5x, not encompassing functional head; segment 2, 4.8x; segment 3, 4.5x; segment 4, 4.3x; segment 5 (longest), 2.9x; segment 6, 4.0x; segment 7, 3.9x; all with at least one, partly preserved appendage (Fig. 10). *Trunk appendages* (pereopods), distal region with 6 articles well
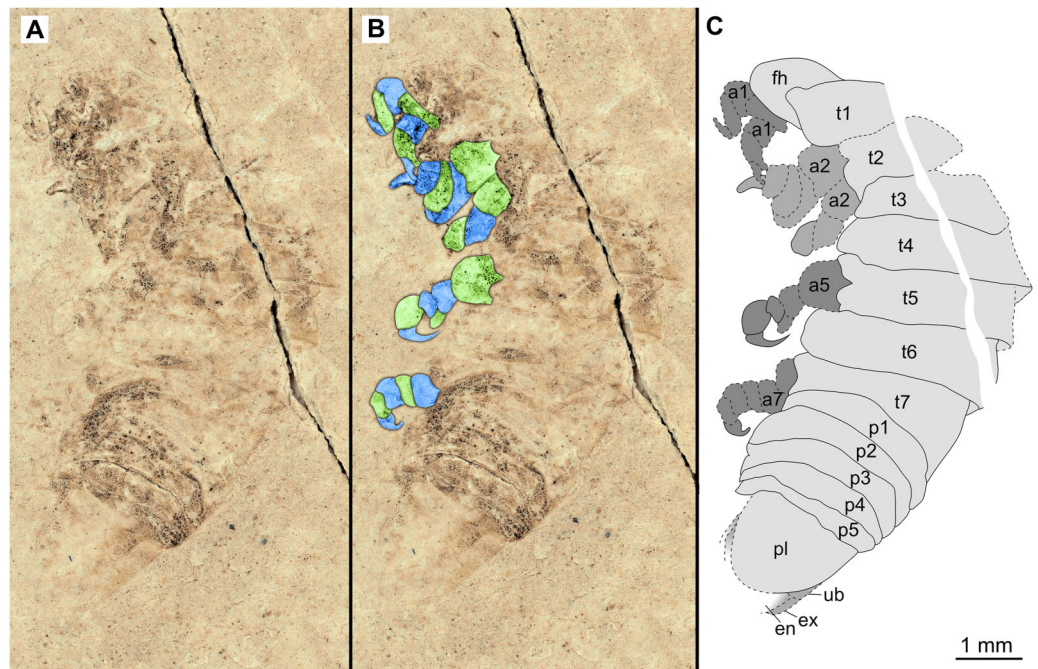
Figure 4 Specimen P2342a. (A–C) Same scale. (A) Light microscope image with dorso-lateral features and structures visible. (B) With colour marked trunk appendages. (C) Line drawing. Abbreviations: a1–2, trunk appendages 1–2; a5, trunk appendage 5; a7, trunk appendage 7; en, uropod endopod; ex, uropod exopod; fh, functional head; p1–5, pleon segments 1–5; pl, pleotelson; t1–7, trunk segments 1–7; ub, uropod basipod. Full-size ☒ DOI: 10.7717/peerj.12317/fig-4

accessible. *Proximal article* (coxa) accessible (Fig. 10C), as long as, or shorter than trunk segment.

Trunk appendage 1 (thoracopod 2, right) completely preserved without distortion, basipod longer than wide, 1.4x; ischium longer than wide, 1.2x; merus longer than wide, 1.2x; carpus longer than wide, 1.1x; propodus wider than long, 1.5x; dactylus longer than wide, 2.2x.

Trunk appendage 1 (thoracopod 2, left) basipod longer than wide, 1.8x; ischium as long as wide; merus longer than wide, 1.1x; carpus as long as wide; propodus as long as wide; dactylus longer than wide, 3.1x.

Posterior trunk (pleon) segments with posteriorly angled, rounded, sub-parallel lateral margins; all wider than long, segment 1, 4.7x; segment 2, 4.5x; segment 3, 5.8x; segment 4 (shortest), 7.5x; segment 5, 5.1x; insertion areas of pleon appendages (pleopods) accessible (Fig. 10).

Pleotelson posteriorly evenly rounded; wider than long, 1.4x. *Uropods* endo-and exopod distal margins not clear, extending past pleotelson posterior margin.

Variation. The functional head of specimen P2347 (Fig. 11) is more sub-triangular than sub-truncate oval, with at least 6 antennulae articles accessible. Specimen P2344 (Fig. 12) have at least seven articles accessible. Specimen P2343 (Fig. 13) and specimen P2344 (Fig. 12) both have somewhat shorter posterior trunk segments with pleotelson shape
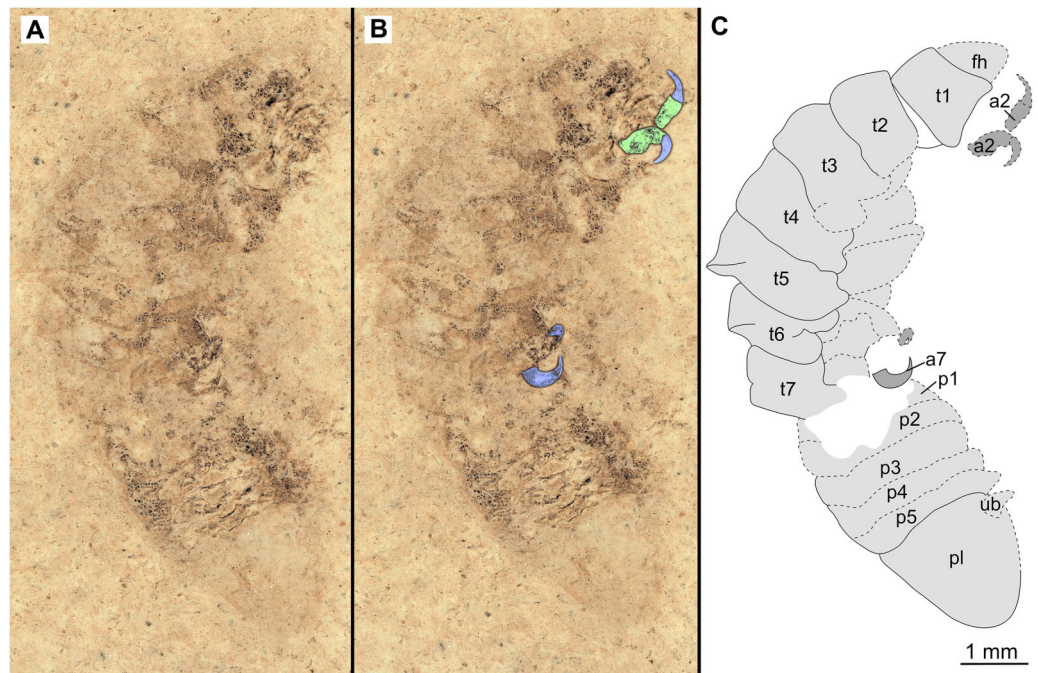
Figure 5 Specimen P2342b. (A–C) Same scale. (A) Light microscope image with dorso-lateral features and structures visible. (B) with colour marked trunk appendages. (C) Line drawing. Abbreviations: a2, trunk appendage 2; a7, trunk appendage 7; en, uropod endopod; ex, uropod exopod; fh, functional head; p1–5, pleon segments 1–5; pl, pleotelson; t1–7, trunk segments 1–7; ub, uropod basipod.

Full-size 🖼 DOI: 10.7717/peerj.12317/fig-5
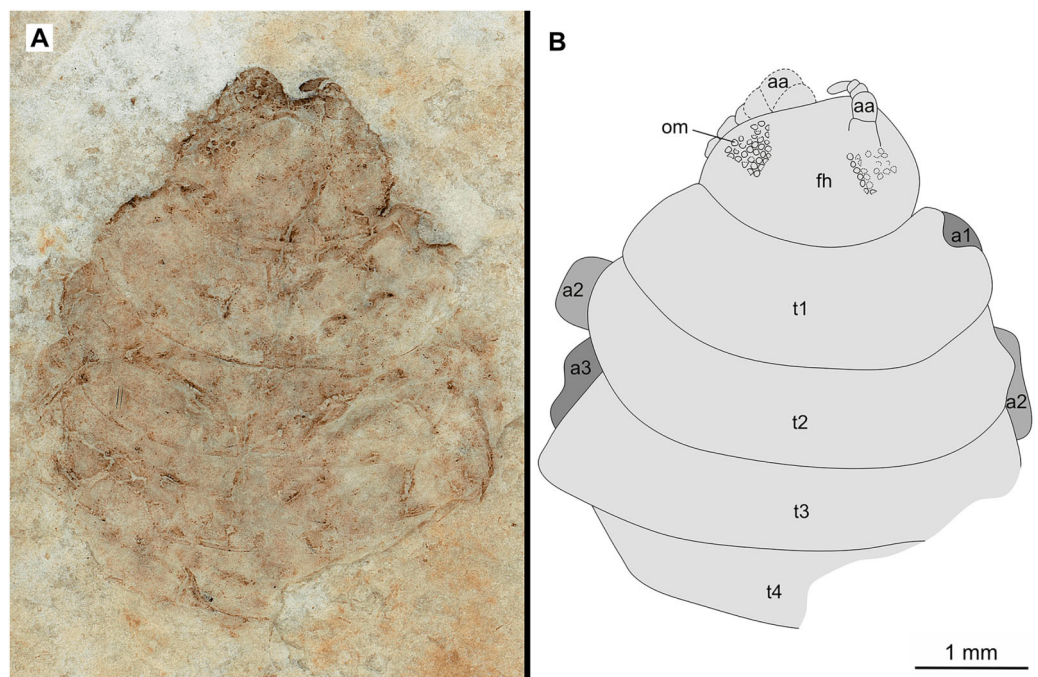
Figure 6 Specimen P2346a. (A–B) Same scale. (A) Light microscope image with dorsal features and structures visible. (B) Line drawing. Abbreviations: a1–3, trunk appendages 1–3; aa, antennula; om, ommatidium of compound eye; fh, functional head; t1–4, trunk segments 1–4.

Full-size 🖼 DOI: 10.7717/peerj.12317/fig-6
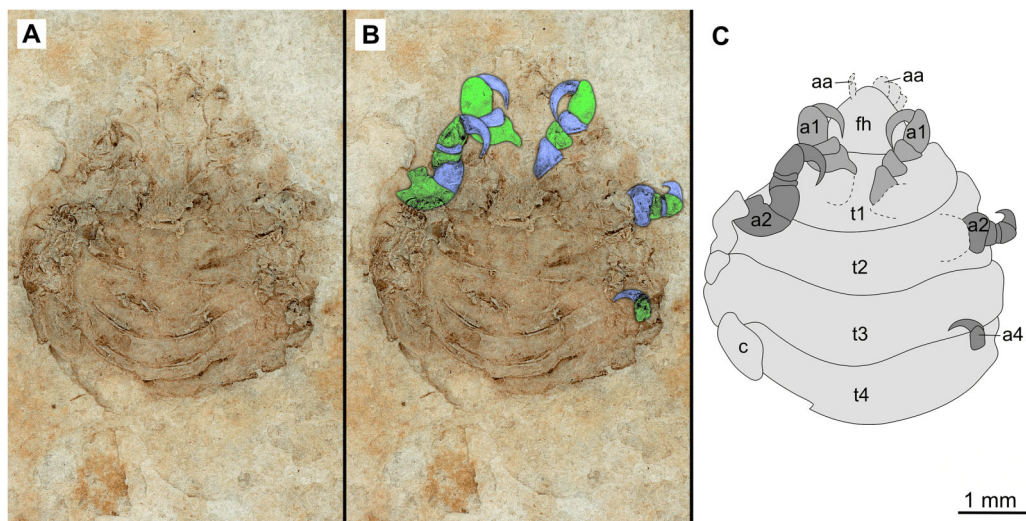
Figure 7 Specimen P2346b. (A–C) Same scale. (A) Light microscope image with ventral features and structures visible. (B) With colour marked trunk appendages. (C) Line drawing. Abbreviations: a1–2, trunk appendages 1–2; a4, trunk appendage 4; aa, antennula; c, coxa; fh, functional head; t1–4, trunk segments 1–4.   Full-size ⬛ DOI: 10.7717/peerj.12317/fig-7
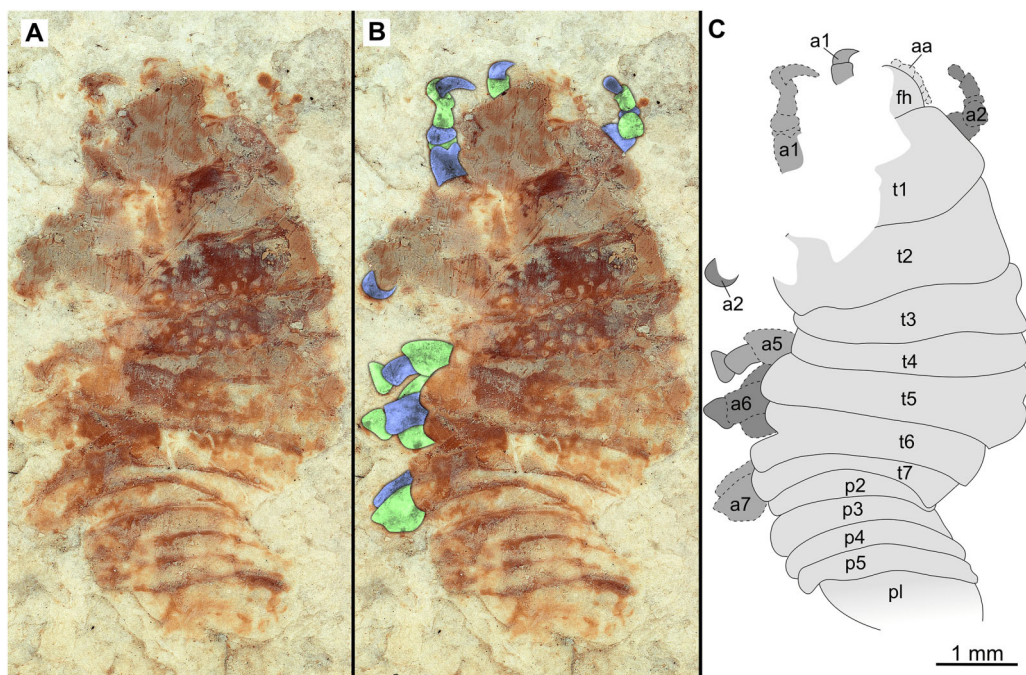
Figure 8 Specimen P2348. (A–C) Same scale. (A) Light microscope image with dorso-lateral features and structures visible. (B) With colour marked trunk appendages. (C) Line drawing. Abbreviations: a1–2, trunk appendages 1–2; a5–7, trunk appendages 5–7; aa, antennula; fh, functional head; p1–5, pleon segments 1–5; pl, pleotelson; t1–7, trunk segments 1–7.   Full-size ⬛ DOI: 10.7717/peerj.12317/fig-8

varying between evenly rounded and sub-triangular. All pleotelsons are wider than long. The uropods of specimen P2343 (Fig. 13) extend only just past the pleotelson posterior margin.
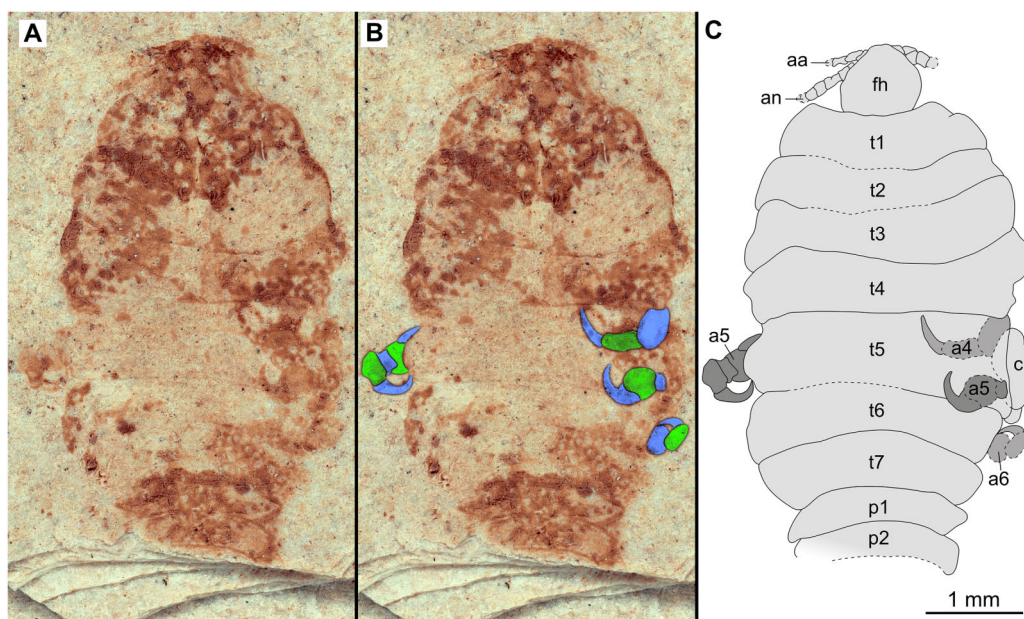
Figure 9 Paratype immature (P2338a). (A–C) Same scale. (A) Light microscope image with dorsal features and structures visible. (B) With colour marked trunk appendages. (C) Line drawing. Abbreviations: a4–6, trunk appendages 4–6; aa, antennula; an, antenna; c, coxa; fh, functional head; p1–2, pleon segments 1–2; t1–7, trunk segments 1–7. Full-size ☒ DOI: 10.7717/peerj.12317/fig-9
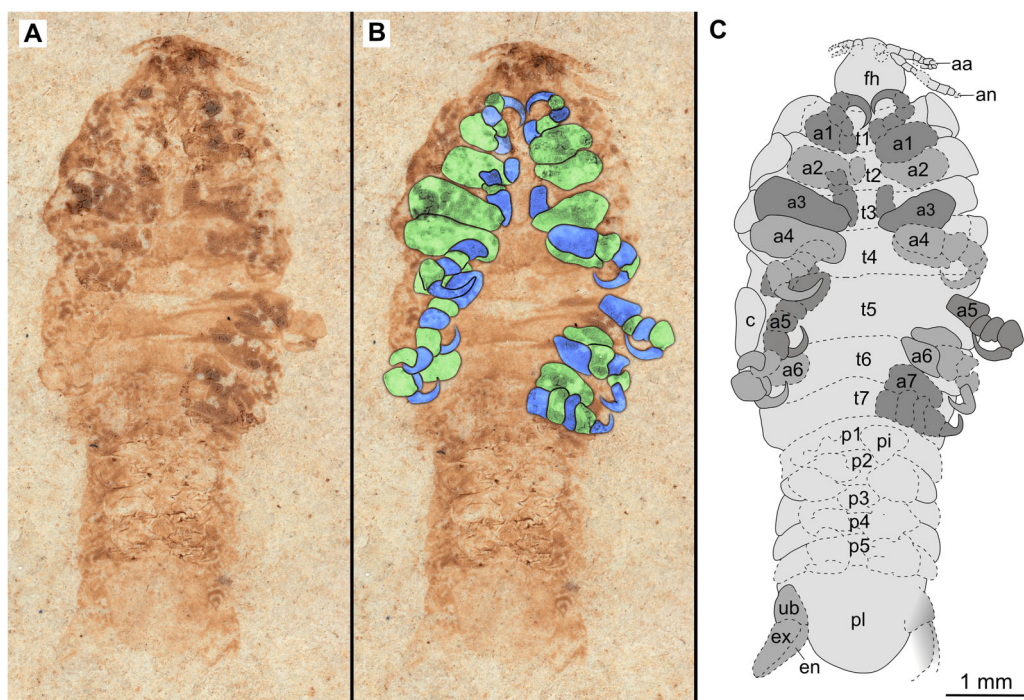
Figure 10 Paratype immature (P2338b). (A–C) Same scale. (A) Light microscope image with ventral features and structures visible. (B) With colour marked trunk appendages. (C) Line drawing. Abbreviations: a1–7, trunk appendages 1–7; aa, antennula; an, antenna; c, coxa; en, uropod endopod; ex, uropod exopod; fh, functional head; p1–5, pleon segments 1–5; pi, pleon attachment; pl, pleotelson; t1–7, trunk segments 1–7; ub, uropod basipod. Full-size ☒ DOI: 10.7717/peerj.12317/fig-10
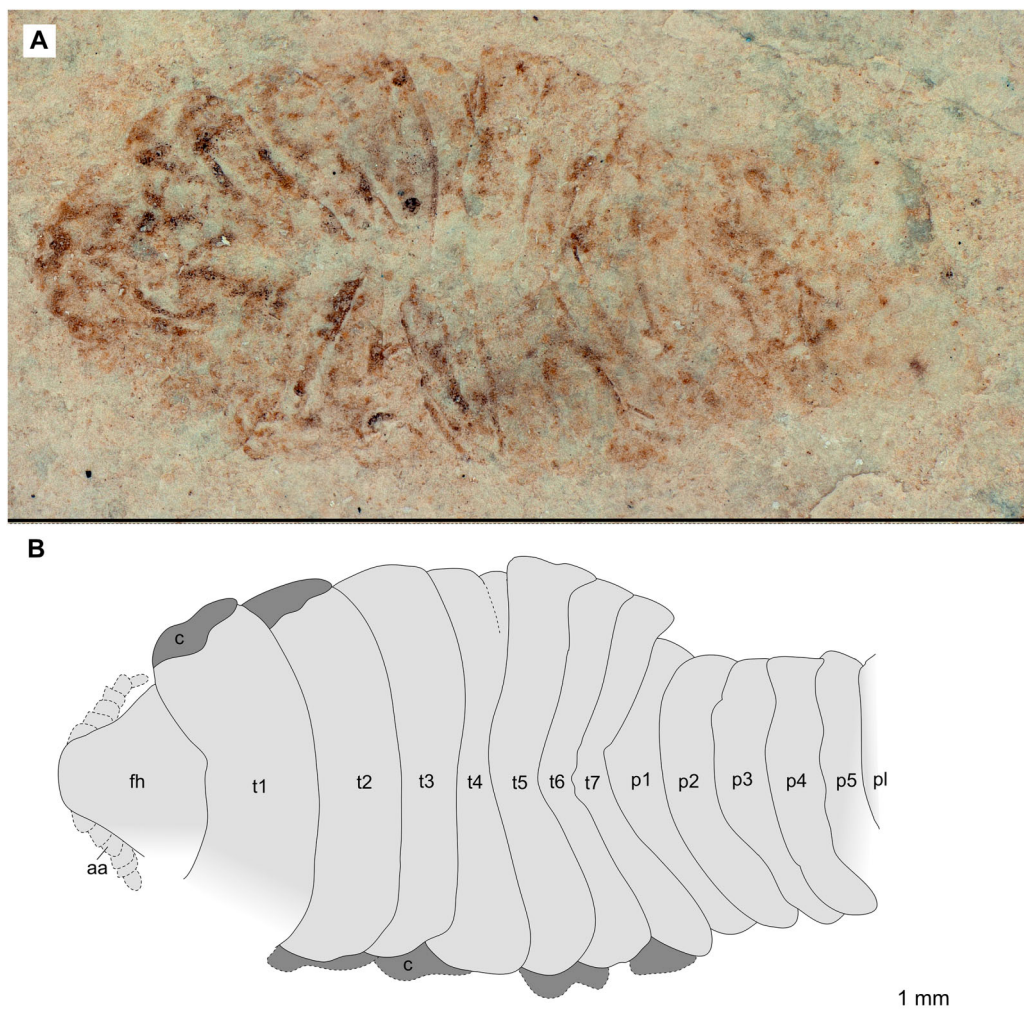
Figure 11 Specimen P2347. (A–B) Same scale. (A) Light microscope image with dorsal features and structures visible. (B) Line drawing. Abbreviations: a7, trunk appendage 7; aa, antennula; c, coxa; fh, functional head; p1–5, pleon segments 1–5; pl, pleotelson; t1–7, trunk segments 1–7.

Full-size ⬓ DOI: 10.7717/peerj.12317/fig-11

Description of female (P2345a/b, Figs. 14–16)

One specimen as part (Fig. 14 with mostly dorsal features visible, P2345a) and counterpart (Figs. 15 and 16 with mostly ventral features visible, P2345b).

Body oval, longer than wide; widest at anterior trunk segment 4/5.

Head triangular; wider than long, 1.1x; with anterior margin narrowly rounded. *Eyes* not accessible.

Some articles of antennulae and antennae accessible. *Antennula* with at least six articles; *antenna* with at least four articles.

All *anterior trunk* (pereon) *segments* wider than long, segment 1 (longest), 2.4x, encompassing the functional head; segment 2, 3.3x; segment 3 (widest), 3.7x; segment 4, 5.1x; segment 5, 7.0x; segment 6, 5.7x; segment 7 left lateral margin not visible; segments 1–4 with at least one, partly preserved appendage.
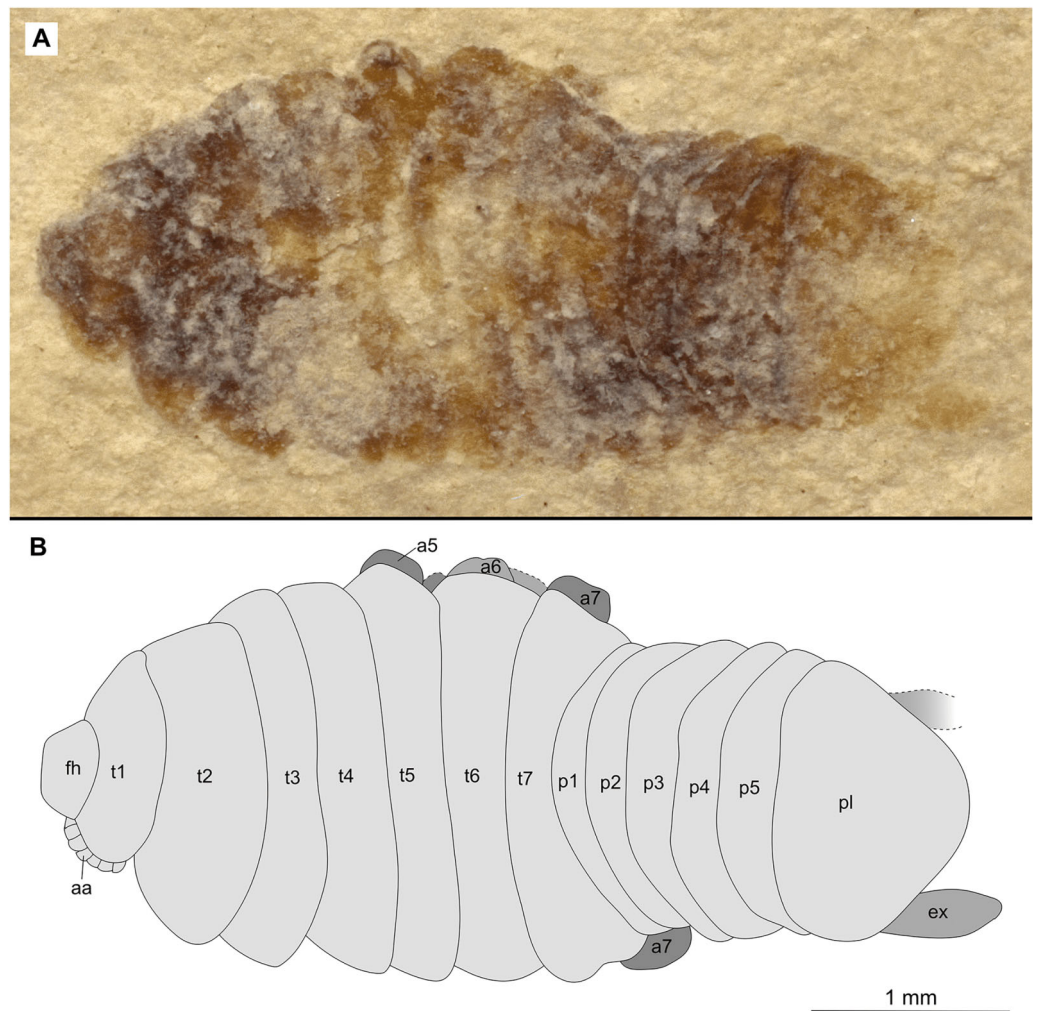
Figure 12 Specimen P2344. (A–B) Same scale. (A) Light microscope image with dorsal features and structures visible. (B) Line drawing. Abbreviations: a7, trunk appendage 7; aa, antennula; ex, uropod exopod; fh, functional head; p1–5, pleon segments 1–5; pl, pleotelson; t1–7, trunk segments 1–7.

Full-size ☒ DOI: 10.7717/peerj.12317/fig-12

Trunk appendages (pereopods) distal region with six articles well accessible. *Proximal article* (coxa) accessible (Fig. 16B).

Trunk appendage 2 (thoracopod 3, right), basipod longer than wide, 1.7x; ischium wider than long, 1.2x; merus wider than long, 1.8x; carpus wider than long, 1.6x; propodus as long as wide; dactylus longer than wide, 3.3.

Trunk appendage 3 (thoracopod 4, right), basipod longer than wide, 1.3x; ischium wider than long, 1.2x; merus wider than long, 3.7x; carpus wider than long, 3.0x; propodus as long as wide; dactylus longer than wide, 2.7x.

Posterior trunk (pleon) *segments* posterior margins slightly concave; segments 1, 2 & 5 lateral margins not visible; segments 1 and 2 lateral margins not visible; all segments wider than long, segment 3, 5.4x; segment 4, 7.9x; segment 5, 6.7x.
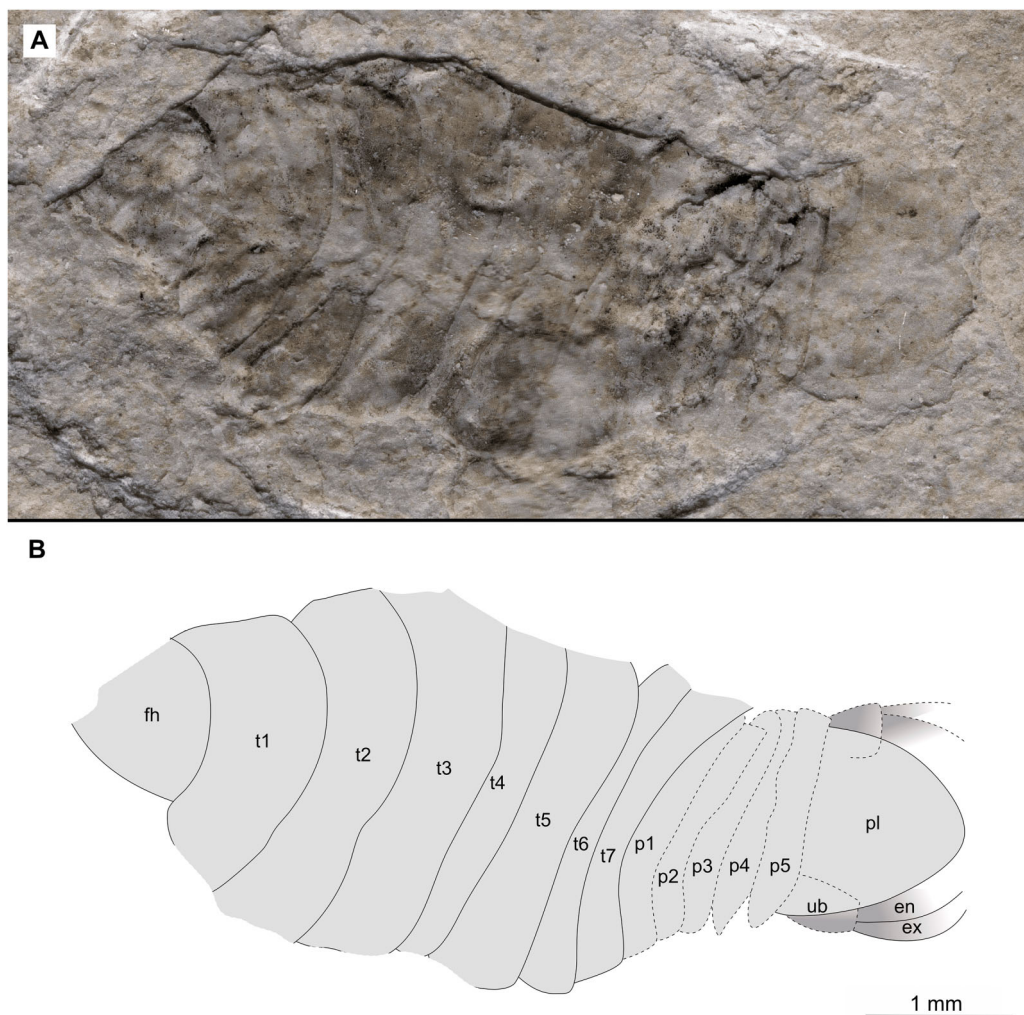
Figure 13 Specimen P2343. (A–B) Same scale. (A) Light microscope image with dorsal features and structures visible. (B) Line drawing. Abbreviations: en, uropod endopod; ex, uropod exopod; fh, functional head; p1–5, pleon segments 1–5; pl, pleotelson; t1–7, trunk segments 1–7; ub, uropod basipod.

Full-size ☒ DOI: 10.7717/peerj.12317/fig-13

Pleotelson, uropods not preserved.

Variation. Specimen P2341 (Fig. 17) has the body widest at anterior trunk segment 4. The posterior trunk segments of specimen P2341 (Fig. 17) has slightly more extended lateral margins.

Morphometric analyses

The body outline variation for all analysed specimens, according to ontogenetic stage, is presented in Figs. 19 and 20. Only specimens P2338–P2339 and P2343–P2345 were reconstructed and used for the analyses, as these were preserved with complete length and width. These reconstructions are not perfect replications of the true shape of the specimens, but rather an idealised representation thereof, based on the interpretive
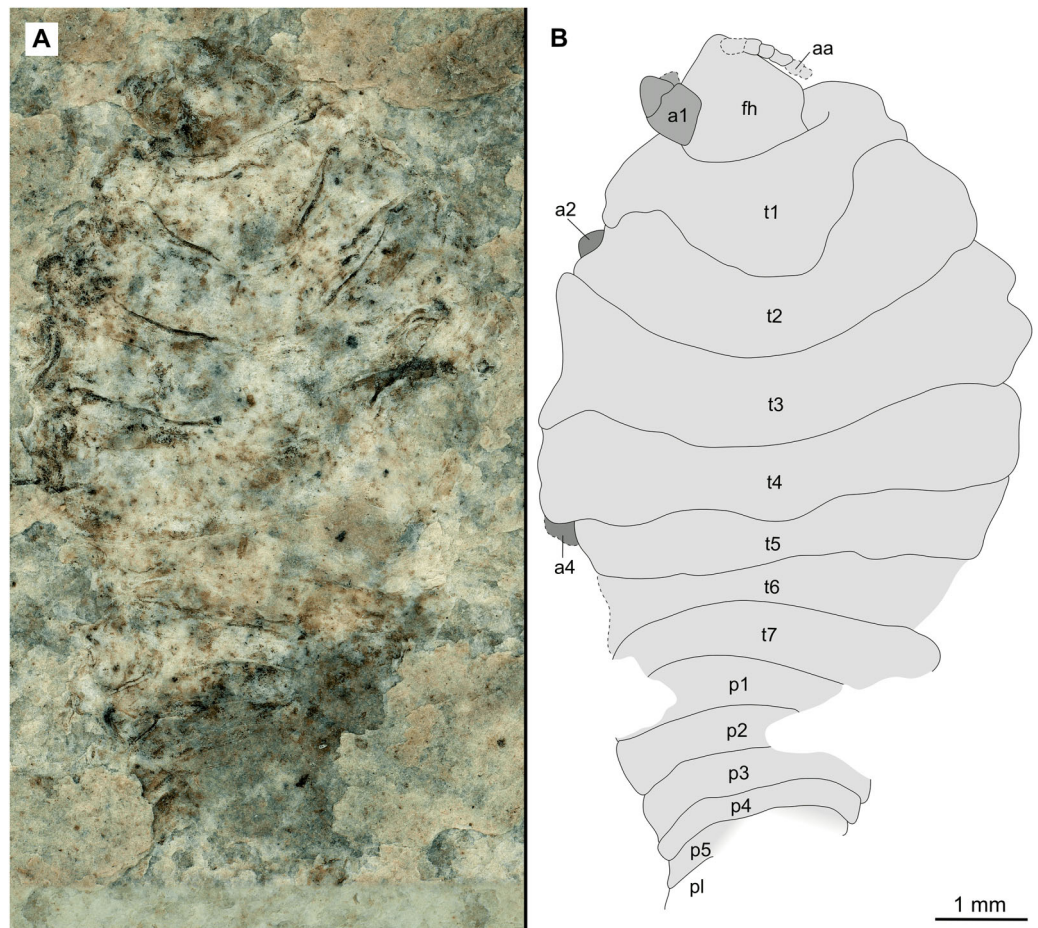
Figure 14 Paratype female (P2345a). (A–B) Same scale. (A) Light microscope image with dorsal features and structures visible. (B) Line drawing. Abbreviations: a1–2, trunk appendages 1–2; a4, trunk appendage 4; aa, antennula; fh, functional head; p1–5, pleon segments 1–5; pl, pleotelson; t1–7, trunk segments 1–7. Full-size ⬛ DOI: 10.7717/peerj.12317/fig-14

drawings. For the presentation of results, only PC1 and PC2 were of interest, as they account for the most variation (see Fig. S1). PC1 and PC2 account for 84.2% of the total variation, with PC1 explaining 76.6% of the variation and PC2 explaining 7.6% of the variation. PC1 is largely influenced by the total body width, where the body is wider towards the positive values and narrower towards the negative values. PC2 is largely influenced by the region of the anterior trunk, where the body is most expanded in width. Positive values indicate a narrower anterior end and wider posterior end, while negative values indicate a narrower posterior end and wider anterior end. The general body shapes at specific PC values are visualised in the background of Figs. 19 and 20. The shape parameters are also visualised in relation to the total body length (size, in mm) of each analysed specimen. The relationship between PC1, PC2 and total body length is visualised in Fig. 21. Specimens from literature with no size data available, were excluded from the analysis (see Doc. S1).
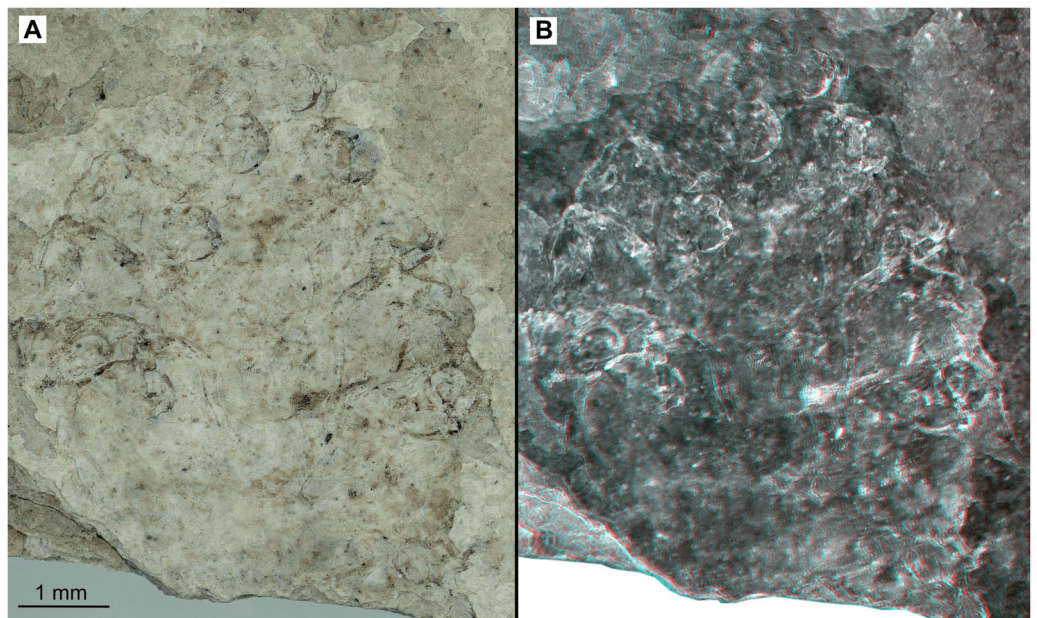
Figure 15 Paratype female (P2345b). (A–B) Same scale. (A) Light microscope image with ventral features and structures visible. (B) Three dimentional stereo-photograph.

Full-size ⬜ DOI: 10.7717/peerj.12317/fig-15
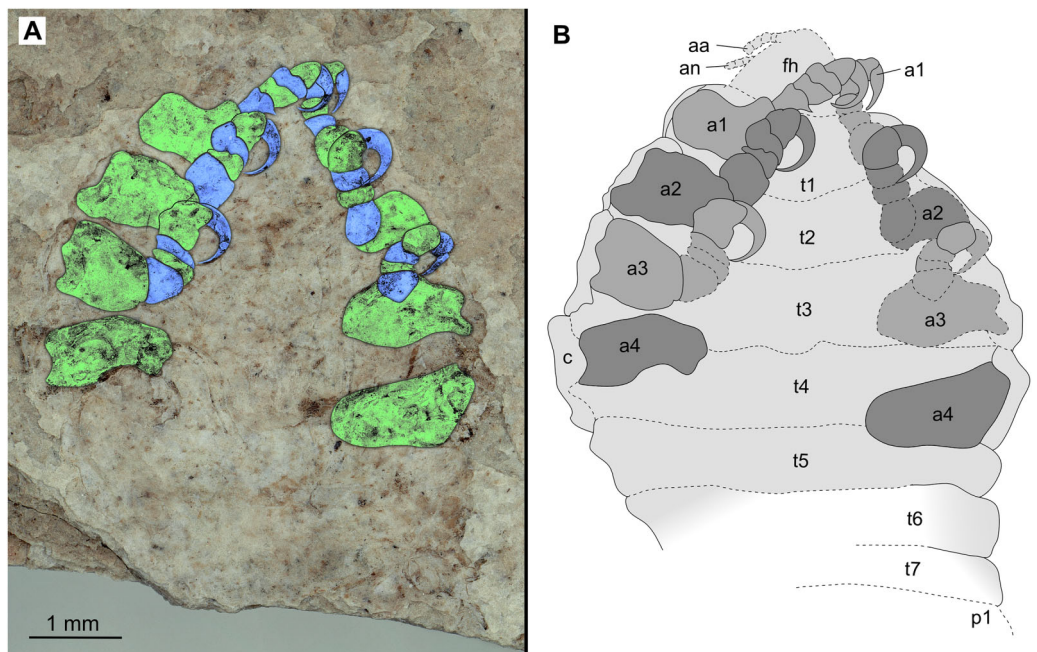
Figure 16 Paratype female (P2345b). (A–B) Same scale. (A) Light microscope image with ventral features and structures visible. (B) Line drawing. Abbreviations: a1–4, trunk appendages 1–4; aa, antennula; an, antenna; c, coxa; fh, functional head; p1, pleon segment 1; t1–7, trunk segments 1–7.

Full-size ⬜ DOI: 10.7717/peerj.12317/fig-16
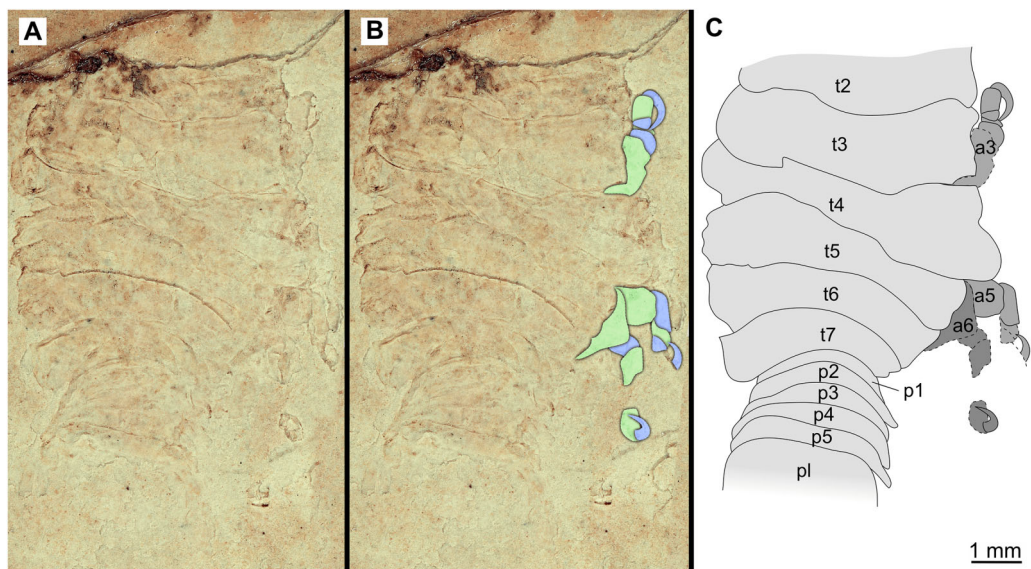
Figure 17 Specimen P2341. (A–B) Same scale. (A) Light microscope image with dorsal features and structures visible. (B) With colour marked trunk appendages. (C) Line drawing. Abbreviations: a3, trunk appendage 3; a5, trunk appendage 5; a6, trunk appendage 6; p1–5, pleon segments 1–5; pl, pleotelson; t2–7, trunk segment 2–7. Full-size ☑ DOI: 10.7717/peerj.12317/fig-17
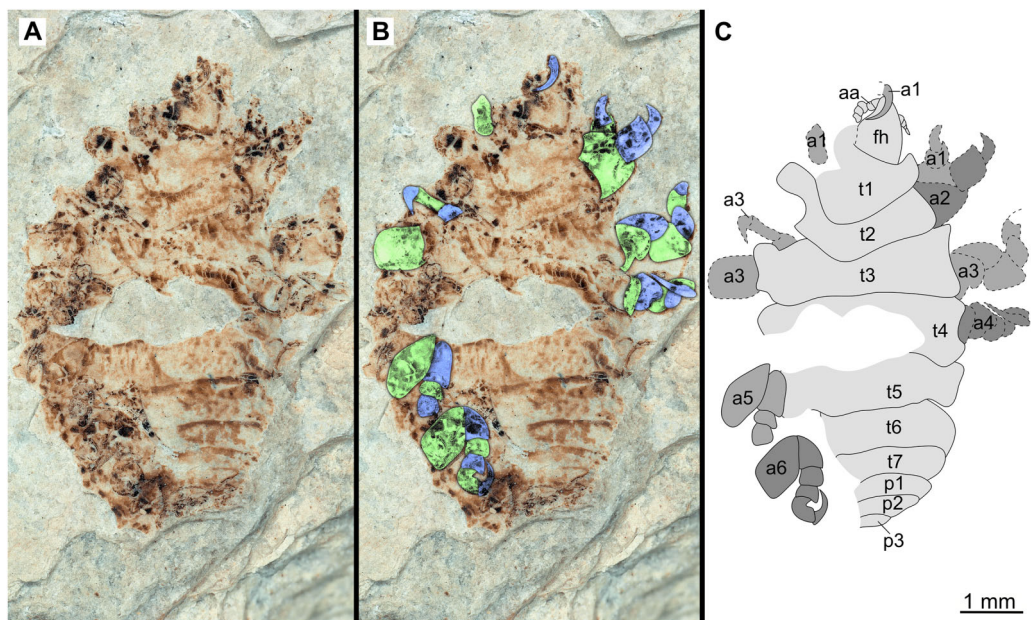
Figure 18 Specimen P2340. (A–B) Same scale. (A) Light microscope image with dorsal features and structures visible. (B) With colour marked trunk appendages (C) Line drawing. Abbreviations: a1–6, trunk appendage 1–6; aa, antennula; fh, functional head; p1–3, pleon segments 1–3; t1–7, trunk segments 1–7. Full-size ☑ DOI: 10.7717/peerj.12317/fig-18
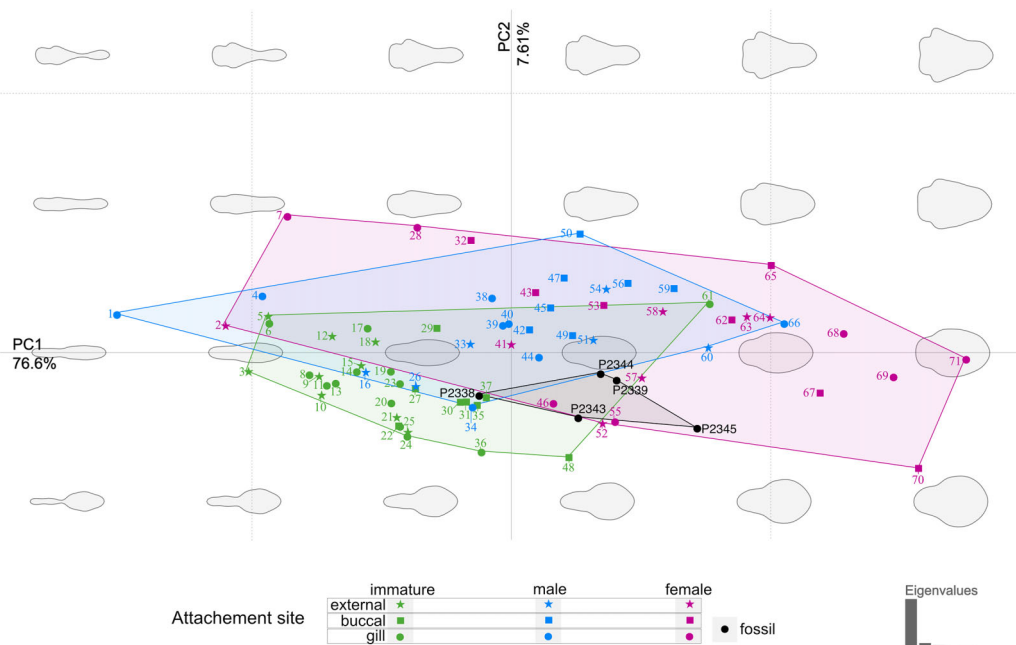
Figure 19 Principle component analysis representation of the body outline variation for all analysed specimens. Colour-coded according to their ontogenetic stage and shape-coded according to their attachment site. Numbers correspond to extant species included in the analysis: **1, 2, 10.** *Anilocra pilchardi Bariche & Trilles, 2006.* **3, 16, 57.** *Anilocra frontalis* Milne Edwards, 1840. **4, 6, 7, 13.** *Olencira praegustator* (Latrobe, 1802). **5, 54, 58.** *Nerocila acuminata* Schioedte & Meinert, 1881. **8, 11, 19, 34, 55.** *Mothocya renardi* (*Bleeker, 1857*). **9, 15, 33, 41.** *Anilocra physodes* (Linnaeus, 1758). **12, 21, 26, 52.** *Anilocra pomacentri* Bruce, 1987. **14, 51, 64.** *Nerocila orbignyi* (*Guérin-Méneville, 1832*). **17, 40, 68.** *Agarna malayi* Tiwari, 1952. **18, 25, 60, 63.** *Nerocila bivittata* (Risso, 1816). **20, 24, 28, 38.** *Glossobius hemiramphi* Williams & Bunkley-Williams, 1985. **22, 47, 53.** *Ceratothoa gaudichaudii* (*Milne Edwards, 1840*). **23, 44, 71.** *Ryukyua circularis* (*Pillai, 1954*). **27, 32, 56.** *Ceraothoa* sp. **29, 30, 43, 50.** *Cymothoa liannae Sartor & Pires, 1988.* **31, 41, 70.** *Cinusa tetrodontis Schioedte & Meinert, 1884.* **35, 45, 65.** *Cymothoa catarinensis Thatcher et al., 2003.* **36, 39, 46.** *Norileca indica* (*Milne Edwards, 1840*). **37, 42, 67.** *Ichthyoxenos puhi* (Bowman, 1962). **48, 59, 62.** *Ceratothoa steindachneri Koelbel, 1879.* **61, 66, 69.** *Elthusa vulgaris* (*Stimpson, 1857*). Full-size 🖼 DOI: 10.7717/peerj.12317/fig-19

DISCUSSION

The body segmentation and appendage pattern of *Parvucymoides dvorakorum* gen. et sp. nov. follows that of the group Eumalacostraca (6–8–6) (see *Walossek, 1999*). The uropods (specialised last trunk appendages) are apomorphic for Eumalacostraca (*Walossek & Müller, 1998*). There is no single apomorphic condition apparent in the examined fossils, which is not present in closely related groups. However, the following character states are indicative for Isopoda: body dorsoventrally flattened (*Ax, 2000*), and anterior trunk appendages without exopods (*Ax, 2000*; *Wilson, 2009*). The coxae are scale-like and fixed on the trunk (forming 'coxal plates') on trunk segments 2–7. This character state is apomorphic for Scutocoxifera (*Dreyer & Wägele, 2002*).

From representatives of *Urda*, the fossils of *P. dvorakorum* gen. et sp. nov. differ in having a much larger tergite of the anterior-most trunk segment (*e.g.*, *Feldmann, Wieder & Rolfe, 1994*). From representatives of Gnathiidae, the herein presented fossils differ in having seven pairs of well-developed appendages of the anterior trunk (see *Boxshall &*
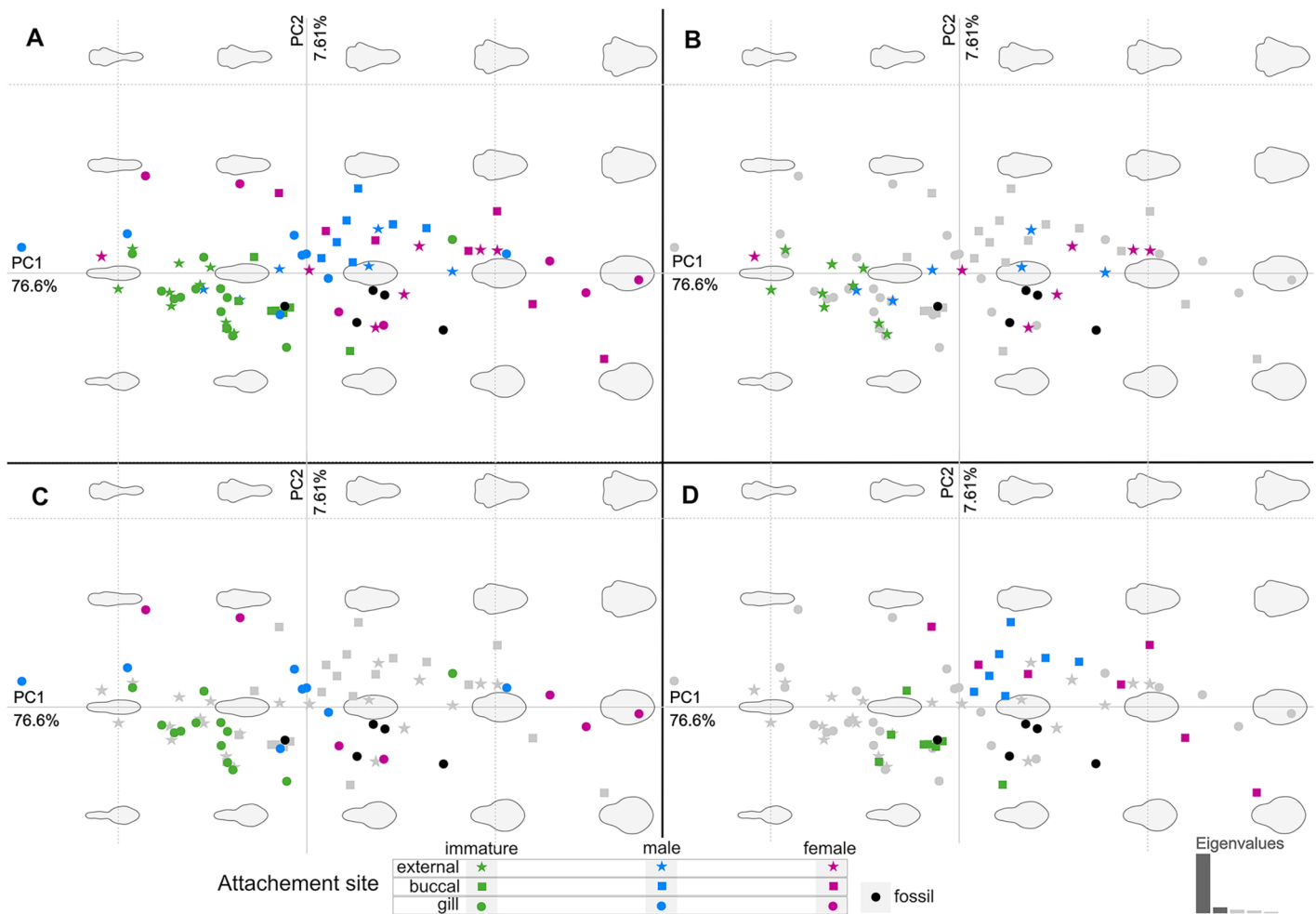
Figure 20 Principle component analysis representation of the body outline variation for all analysed specimens. Colour-coded according to their ontogenetic stage and shape-coded according to their attachment site. (A) Individuals of different ontogenetic stages and sites of attachment from extant species in colour. (B) Externally attaching individuals from extant species in colour. (C) Gill-attaching individuals from extant species in colour. (D) Buccal-attaching individuals from extant species in colour. Full-size ☑ DOI: 10.7717/peerj.12317/fig-20

Montú, 1997; *Smit & Davies, 2004*). The examined fossils have well developed antennulae, unlike the shortened and modified antennulae of Epicaridea; uropods that are not styliform; and a morphology not reminiscent of epicaridium, microniscium, or cryptoniscium larvae (see *Wägele, 1989*; *Brusca & Wilson, 1991*; *Schädel, Perrichot & Haug, 2019*), therefore, excluding Epicaridea as having possible systematic affinity to the examined fossils.

Based on these systematically informative morphological characters, these specimens are interpreted as possible representatives of Cymothoidae, or at least closely related to Cymothoidae, during different developmental stages and are consequently interpreted as parasites.

Specimens examined herein range between a minimum length of 4.68 mm and a maximum of at least 9.50 mm, with larger, incompletely preserved specimens likely
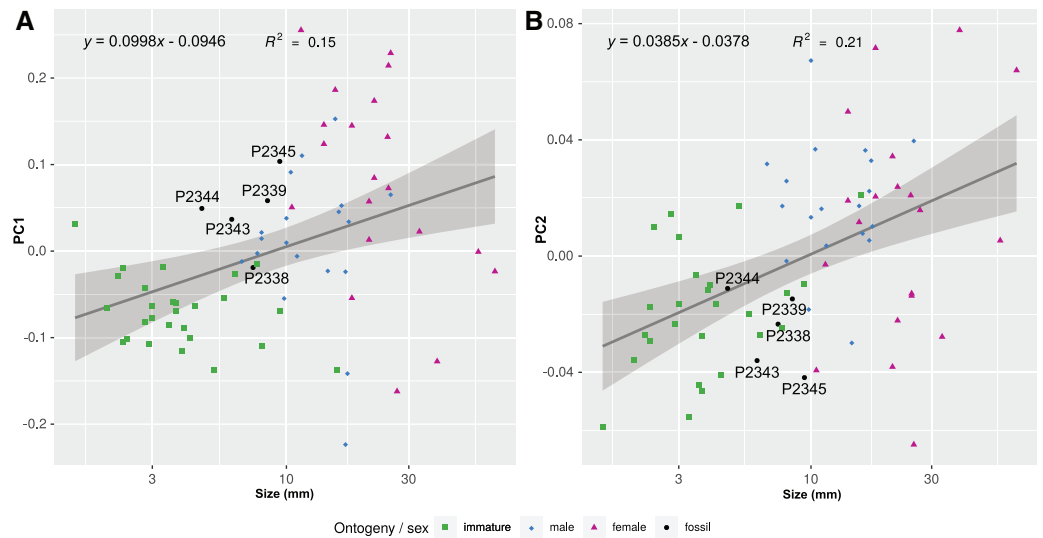
Figure 21 **Shape parameters visualised in relation to the total body length (size, in mm) of each analysed specimen, extant and fossil.** Linear models fitted to the first two principle components relative to the total body length. (A) PC1 to total body length. (B) PC2 to total body length.

reaching a total body length of just slightly over 10 mm. The size comparison between the examined specimens is shown in Fig. 22. Mouthparts are not visible in the examined fossils. For the same reason, characters regarding setae can also not be assessed. In one specimen, P2346, compound eyes with clearly preserved ommatidia are preserved and located laterally on each side of the head. The eyes are not accessible from any of the remaining specimens. Similar to representatives of Cymothoidae, the examined specimens have anterior trunk appendages (thoracopods 2–8, pereopods 1–7) that each consist of seven articles and are prehensile, *i.e.*, specialised for attachment, with the distalmost article being a sharp, hook-like, curved dactylus (as seen from specimens P2338, P2339, P2340, P2341 and P2342). It is not possible to evaluate this aspect completely in the case of specimens P2345 and P2346, where only the anterior trunk appendages are preserved, and of specimen P2343, P2344, P2347 and P2348, where the trunk appendages are incompletely preserved or not visible. Even so, it is very likely that all herein studied specimens have 7 pairs of appendages with curved, hook-like dactyli, further inferring a parasitic life habit. In the specimens where they are preserved, the pleon segments 1–5 are free, with biramous uropods located antero-laterally on the pleotelson.

Conspecificity

All herein studied type specimens are interpreted to be conspecific, as there are no apparent diagnostic characters that would suggest that they belong to separate species and all specimens were collected at the same location from within the same layers of rock. Some variation between specimens was noted to a similar degree in which extant conspecific individuals vary, and is therefore expected. Specimen P2342a/b seems to differ from the remainder of the specimens in the morphology of the pleon; however, this difference might be due to the mode of preservation (slightly distorted sclerites) rather than to a
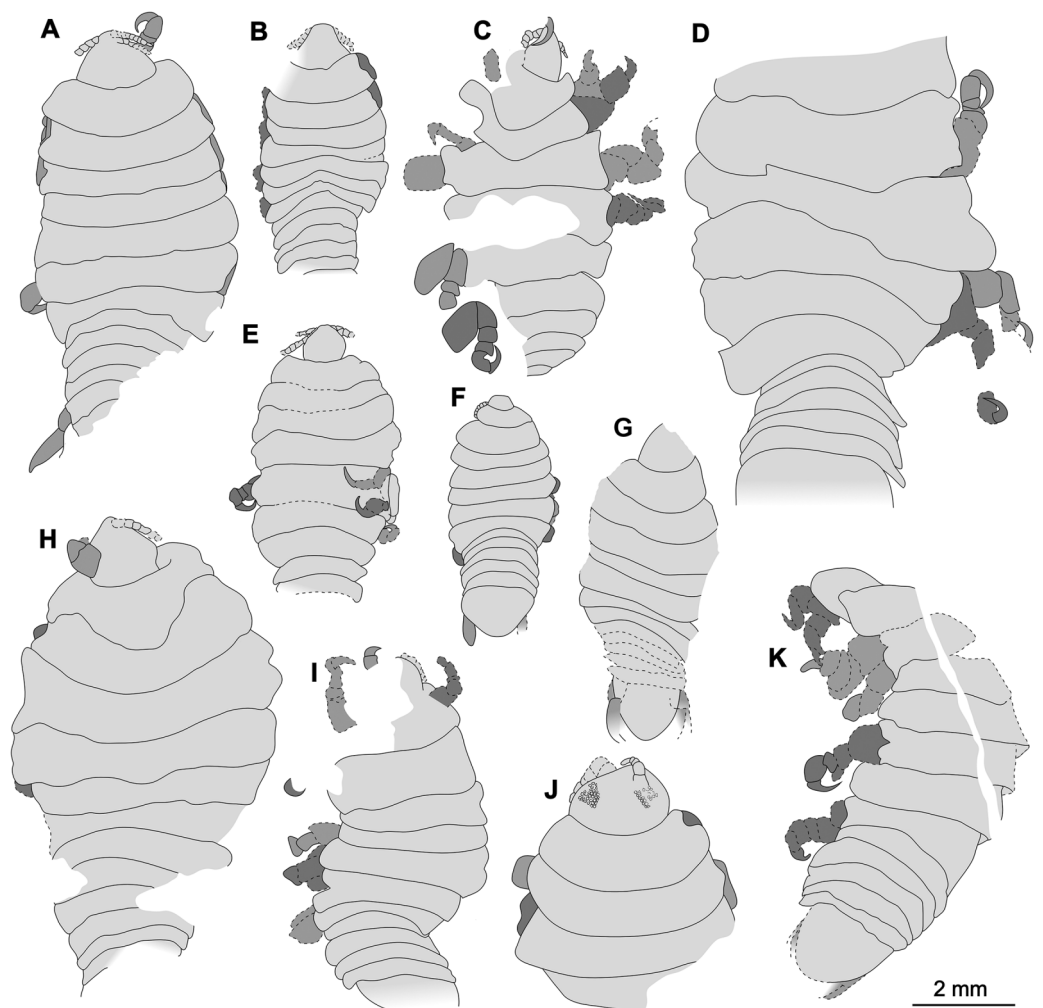
Figure 22 Comparison of the body size of examined fossils, same scale. (A) Specimen P2339. (B) Specimen P2347. (C) Specimen P2340. (D) Specimen P2341. (E) Specimen P2338. (F) Specimen P2344. (G) Specimen P2343. (H) Specimen P2345. (I) Specimen P2348. (J) Specimen P2346. (K) Specimen P2342. Full-size ☐ DOI: 10.7717/peerj.12317/fig-22

difference in the morphology of the once living animal. For this reason, this specimen is not included in the type series as a paratype, but rather as additional material examined.

Morphological differences to other groups and species

The specimens examined herein share characters with many ingroups of Cymothoidae, but also lack, or vary from many diagnostic characters provided of extant groups, especially for different ontogenetic stages. *Parvucymoides dvorakorum* sp. nov. can be distinguished from extant species of Cymothoidae by: its small overall body length, especially immature and male stages, not exceeding much more than 10.0 mm, adult female specimens might be somewhat larger; an ovoid, but symmetrical body shape of larger (adult) specimens; having 12 or more antennulae articles.

Only a few extant species of Cymothoidae have a comparable, small body length as adult females, such as: *Artystone minima Thatcher & Carvalho, 1988* (5.2–6.9 mm);

Catoessa ambassae Bruce, 1990 (7.5–9. 3 mm); *Joryma brachysoma* (Pillai, 1964) (10.5–13.6 mm, *Aneesh, Helna & Kumar, 2019*); *Elthusa samariscii* (*Shiino, 1951*) (10–13.4 mm, *Kumar & Bruce, 1997*, *Aneesh et al., 2020* and *Elthusa sigani Bruce, 1990* (9.5–13.0 mm)); *Mothocya argenosa Bruce, 1986* (5.5–9.8 mm); *Mothocya bertlucy Hadfield, Sikkel & Smit, 2014* (7.0–9.0 mm); *Mothocya epimerica Costa, 1851* (5.5–11.5 mm, *Bruce, 1986*); *Mothocya powelli Van der Wal et al., 2021* (7 mm), *Mothocya waminda Bruce, 1986* (5.6–8.9 mm); *Mothocya bermudensis Bruce, 1986* (8.8–9.8 mm); *Mothocya rosea Bruce, 1986* (6.2–8.4 mm); *Nerocila lomatia* Bruce, 1987 (7.0 mm (male)–16.0 mm); *Norileca triangulata* (*Richardson, 1910*) (9.2–18 mm, *Rameshkumar & Ravichandran, 2015*, *Bruce, 1990*); *Telotha henselli* (*von Martens, 1869*) (6.0–14 mm, *Taberner, Volonterio & De León, 2003*).

Parvucymoides dvorakorum gen. et sp. nov. can be distinguished from the genera of the above mentioned, similar-sized species. The ovoid and laterally symmetrical body shape of *P. dvorakorum* gen. et sp. nov. distinguishes it from the asymmetrical or strongly twisted body shapes of female individuals of *Joryma Bowman & Tareen, 1983* (see *Aneesh et al., 2019*.), *Norileca Bruce, 1990* (see original description) and *Mothocya* Costa in Hope, 1851 (see *Bruce, 1986*; *Aneesh et al., 2016*). The subtriangular to truncate functional head distinguishes *P. dvorakorum* gen et sp. nov. from *Nerocila Leach, 1818* (see *Bruce, 1987a*; *Nagler & Haug, 2016*) and *Telotha*.

Schioedte & Meinert, 1884 (see original description and *Taberner, Volonterio & De León, 2003*) as representatives of the latter two groups both have a broadly rounded functional head anterior margin. A closer relationship to *Nerocila* can immediately be excluded, based on numerous characters including: larger size; pleon morphology; and slender uropod exopods which are longer than the endopods.

Telotha and *Artystone Schioedte, 1866* (see *Thatcher & Carvalho, 1988*; *Thatcher & Schindler, 1999*) both have antennulae and antennae with between eight to nine articles, compared to the 10–12 minimum of the genus described here. The antennulae in species of *Catoessa Schioedte & Meinert, 1884* (see *Bruce, 1990*) and *Mothocya* are thicker ('more stout') than the antennae, where these are subequal in thickness in *P. dvorakorum* gen. et sp. nov. Regarding anterior trunk segments, *Joryma* can be excluded based on the largely produced anterolateral margins of anterior trunk segment 1 in the adult females, as well as the anterior trunk segment 7 that overlaps posterior trunk segment 1 lateral margins. The latter character difference is also noticeable in *Mothocya* and *Elthusa Schioedte & Meinert, 1884* (see *Bruce, 1990*; *Kumar & Bruce, 1997*). The coxae in the examined fossils are not well accessible and visible in all specimens, but from what is accessible, these differ from the large, rounded coxae of *Mothocya* and the posteriorly produced, acute coxae in *Nerocila*; in both groups extending to, or past the corresponding trunk segment posterior margin.

The trunk appendages of the examined fossils of *P. dvorakorum* gen. et sp. nov. all have long, acute dactyli, in contrast to the trunk appendage 7 of *Artystone*, of which the dactylus is short (less than half the length of the propodus) and distally round. Considering posterior trunk segments (pleon), those of *Catoessa* and *Elthusa* are notably different. Species of *Elthusa* have a wide pleon (mostly equal in width or wider than anterior trunk

segment 7); while representatives of *Catoessa* have laterally extended pleon segments, with gaps between the segments. Representatives of the group *Catoessa* additionally have a unique, rotationally twisted posterior trunk. Posterior trunk (pleon) segments (pleonites) of *P. dvorakorum* gen. et sp. nov. are narrow with no gaps. Many of these extant groups have notable differences in pleotelson morphology. The posterior margins of the pleotelson of *P. dvorakorum* gen. et sp. nov. are subtriangular to broadly rounded in all specimens where it is accessible; slightly and wider than long. Representatives of *Joryma* (males), *Telotha* (immatures and males) and *Artystone* have a pleotelson that is longer than wide, with that of *Telotha* converging to a posteromedial point (in immatures and males) and that of representatives of *Artystone* being subtriangular to heart shaped. Lastly, the shape of uropods provides clear distinctions. *Parvucymoides dvorakorum* gen. et sp. nov. has uropods with the endopod and exopod subequal in length, longer than uropod basipod, extending slightly past pleotelson posterior margin. Representatives of both *Mothocya* and *Artystone* also have the exopods longer than the endopods, with representatives of *Artystone* additionally having uropod basipods longer or as long as the rami.

From the results of the body shape analysis (Figs. 19 and 20), it is clear that most of the body shape data points of the examined fossils are in close to very close proximity of those of various developmental stages of extant species. The body shapes of the *P. dvorakorum* sp. nov. specimens included in the analysis, can further be compared to various extant species with similar body shapes in order to further substantiate its interpretation as a separate species.

The extant species and their representative ontogenetic stages that have the most similar body shapes (according to Figs. 19 and 20) to the examined fossil specimens are: the externally attaching *Anilocra frontalis* Milne Edwards, 1840 (female), *Anilocra pomacentri* Bruce, 1987 (female), and *Nerocila orbignyi* (Guérin-Méneville, 1832) (male); the gill attaching *Mothocya renardi* (Bleeker, 1857) (male, female) and *Norileca indica* (Milne Edwards, 1840) (female, twisted body shape straightened); and the buccal attaching immature stage 2 (manca) of *Cinusa tetrodontis* Schioedte & Meinert, 1884; *Cymothoa catarinensis* Thatcher et al., 2003; *Cymothoa liannae* Sartor & Pires, 1988; *Ichthyoxenos puhi* (Bowman, 1960).

Norileca, *Nerocila* and *Mothocya* have already been excluded as possible affinities for the examined specimens of *P. dvorakorum* gen. et sp. nov. (above). Specimens P2339 and P2343 plot within close proximity of two species of *Anilocra* Leach, 1818 (females) (Figs. 19 and 20), which can be differentiated by having a larger overall body size; a pleotelson that is longer than wide; trunk appendage 7 notably longer than trunk appendage 6; and with antennulae usually with eight articles.

Specimen P2338, interpreted as immature (stage 3, juvenile), has a body shape similar to the immatures of *C. tetrodontis*, *C. catarinensis*, *C. liannae* and *I. puhi* and to the male stage of *M. renardi*. During immature stage 2, the anterior trunk segment 7 is underdeveloped and with underdeveloped trunk appendages. The illustration and descriptive characters available for immatures of *C. tetrodontis* do not allow for a sufficient comparison between this ontogenetic stage and specimen P2338. Even so, the later

developmental stages of *C. tetrodontis* can be compared to and distinguished from *P. dvorakorum* sp. nov. by having the proximal articles of the antennae close together, almost in contact; a short anterior trunk segment 1; posterior trunk segment 1 (pleon segment 1) notably narrower than the remaining pleon segments; and uropods that do not reach the posterior margin of the pleotelson. The immature stage 2 of *C. catarinensis* can be distinguished from specimen P2338 by having fewer antennulae and antennae articles (eight, *vs.* 10–12 minimum) and uropods that extend well past the pleotelson posterior margin. The body shapes of adult stages of *C. catarinensis* (male and female) do not compare to those of any of the examined specimens. Even though specimen P2338 plots close to the immature stage 2 of *C. liannae*, its body shape outline is not similar to that of the immature stage 3 (juvenile) or adult stages of the latter species. The immature stage 2 of *C. liannae* has uniquely long antennae, reaching to anterior trunk segment 6. These antennae are much shorter during all later developmental stages. It further has uropod rami that extend far beyond the pleotelson posterior margin. The immature stage 2 of *Ichthyoxenus puhi* can be differentiated from specimen P2338 by having a larger, broadly rounded functional head and shorter, wider, broadly rounded uropod rami that don't extend to the pleotelson posterior margin. Specimen P2338 is in close proximity of the male representative of *M. renardi*, but not of the immature stages 1–2. *Mothocya renardi* male stages have narrower and longer uropod rami that extend well beyond the pleotelson posterior margin and pleon segments wider than anterior trunk segment 7. Therefore, the examined fossils cannot be interpreted as representatives of these species.

Ontogenetic interpretation

The life cycle and developmental stages of representatives of Cymothoidae are consistent (see *Smit, Bruce & Hadfield, 2014*), and have been described and illustrated for various extant groups, for example *Anilocra Leach, 1818*; *Agarna Schioedte & Meinert, 1884*; *Ceratothoa Dana, 1852*; *Glossobius Schioedte & Meinert, 1883*; *Mothocya* Costa in Hope, 1851; *Nerocila Leach, 1818*; and *Norileca Bruce, 1990* (see *Brusca, 1978*; *Adlard & Lester, 1995*; *Mladineo, 2003*; *Bakenhaster, McBride & Price, 2006*; *Aneesh et al., 2016, 2018*; *Kottarathil et al., 2019*). Species of Cymothoidae are protandrous hermaphrodites, where males develop and moult into adult females under certain conditions (*Legrand, 1952*; *Trilles, 1991*; *Bunkley-Williams & Williams, 1998*). This change in sex during ontogeny differentiates adult male and adult female specimens as two different ontogenetic stages. This sexual dimorphism, that also affects the general shape of the body, is well documented for Cymothoidae in terms of primary sexual characters and apart from appendage dimorphism (*Bunkley-Williams & Williams, 1998*; *Bruce, 2002*; *Poore & Bruce, 2012*). Thus, adult male and female specimens can be well differentiated. More recently, detailed morphological descriptions and differentiating characters of different immature stages have been presented (*Bakenhaster, 2004*; *Jones et al., 2008*; *Aneesh et al., 2016*; *Van der Wal & Haug, 2020*). A tentative restoration of the ontogenetic sequence of the examined fossils (Fig. 23) appears very similar to that in modern day representatives of Cymothoidae.
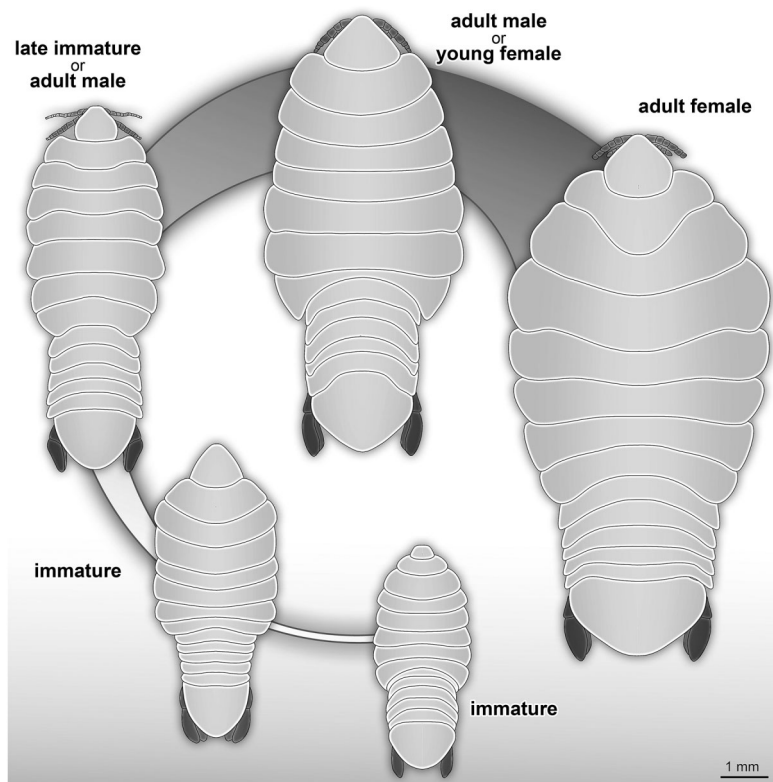
Figure 23 Reconstruction drawings of interpreted ontogenetic stages of the examined fossil specimens. (A) Specimen P2344 (immature). (B) Specimen P2343 (immature). (C) Specimen P2338 (immature/young male). (D) Specimen P2339 (adult male/young female). (E) Specimen P2345 (adult female). Full-size 🖼 DOI: 10.7717/peerj.12317/fig-23

Possible immature representatives

The term 'immature' is used here to refer to all stages after hatching (post-marsupial development), but before maturation (*sensu Van der Wal & Haug, 2020*). Immatures of extant species have a larger body length to width ratio (more elongated) that decreases over ontogenetic development (Fig. S2). This results in adults that have a smaller length to width ratio (more rounded) (for example, see figures and illustrations from *Trilles, Colorni & Golani, 1999*, fig. 4; *Thatcher, de Lima & Chellappa, 2007*, figs. 23, 46; *Aneesh et al., 2019*, fig. 1; *Van der Wal & Haug, 2020*, figs. 1, 4, 7,11, 14, 17, 20, 26, 29). Even though the body shape is highly variable among extant representatives of these groups, there seems to be a trend throughout, that adults are less elongated than immatures of the same species (see interpretation: attachment site). The source of this variation is seen at the mid-to posterior region of the anterior trunk, including the anterior region of the posterior trunk. The anterior and posterior ends of the specimens show variation to a much lesser extent (Fig. S2). Immature and adult male specimens of Cymothoidae have not been as thoroughly documented (described, photographed or illustrated) as adult female specimens, even though changes in body shape and size are prominent through these developmental stages.

The examined fossil specimens P2338, P2343, P2344 and P2347 have the same type of slender and elongated body, most prominent in specimen P2338 (Figs. 9 and 10), as in many immature stages of extant species. The body ratio trend is also noted with the specimens studied here. Specimens P2338, P2343, P2344 and P2347 have a body length range of 4.68–7.41 mm and a width range of 2.12–2.95 mm, resulting in an average body length to width ratio of 2.38. This ratio is notably higher than the body ratio of the specimens herein interpreted as adult representatives (see discussion 'Possible adult representatives').

Considering the ordinated (PCA) values of the body shapes (Figs. 19 and 20), the reconstructed body shapes of specimens P2338, P2343 and P2344 fall well within the shape variation of immatures, with specimen P2338 notably close to extant immature representatives *Cinusa tetrodontis Schioedte & Meinert, 1884*; *Cymothoa catarinensis Thatcher et al., 2003*; *Cymothoa liannae Sartor & Pires, 1988*; *Ichthyoxenos puhi* (*Bowman, 1960*); and a gill attaching male of *Mothocya renardi* (*Bleeker, 1857*). The body shape of specimen P2343 is similar to some extant female representatives: *Anilocra pomacentri* Bruce, 1987 (*Bruce, 1987b*, external attaching) and *Norileca indica* (*Milne Edwards, 1840*) (gill attaching), requiring further consideration regarding the substantiation of the interpreted ontogenetic stage. The same is true for the shape of specimen P2344, which is similar in thickness to those of extant males (*Ryukyua circularis* (*Pillai, 1954*) and *Nerocila orbignyi* (*Guérin-Méneville, 1832*)) and a female (*Anilocra frontalis Milne Edwards, 1840*). The body shape most similar to this is that of specimen P2339 (herein interpreted as a male), which is only slightly wider (relative to body size) than specimen P2344. In order to further substantiate the ontogenetic interpretation of specimens P2343 and P2344, the total body length (size) of all analysed specimens is considered.

With regards to size, the body measurements for specimens P2338, P2343, P2344 and P2347 are the smallest of the examined specimens. With regards to body width, the reconstructed body shapes of specimen P2343 and P2344 are relatively wider than most example immatures analysed (Figs. 19 and 20), but with the area of greatest width (widest in the medial region of the body, PC2), similar to those of extant immatures. The results from both body shape and size analyses support the interpretation of specimen P2338 as an immature individual. The interpretation of specimen P2343 and P2344 as immatures is supported by the size comparison and region of greatest body width (PC2), but partially supported by the total body width analysis (PC1). The interpretation of specimen P2347 as immature is based on general body shape and size comparison among the examined specimens.

Immature forms of Cymothoidae have different developmental stages (*e.g.,* pre-mancae, mancae and juveniles/natatory-stage individuals, *sensu Van der Wal & Haug, 2020*). These can be differentiated based on characters such as the presence or absence of developed appendages on trunk segment 7, the presence of yolk and the presence of setae on the pleopods and uropods. Since the latter two characters are not visible in the examined fossils, due to the mode of preservation, the exceptionally preserved trunk appendages allowed for a more accurate interpretation.

Specimens P2338, P2343, P2344 and P2347 are interpreted as representing the final immature stage (immature stage 3 *sensu Van der Wal & Haug, 2020*; 'juvenile' *sensu Brusca, 1978*; *Segal, 1987*; *Kottarathil et al., 2019*; 'natatory-stage' *sensu Jones et al., 2008*) for the following reasons. Immature stages prior to immature stage 3 (*i.e.*, immature stage 1 and 2, also referred to as pre-manca and manca stage respectively) lack fully developed appendages on the posterior-most segment of the anterior trunk (thoracopod 8, pereopod 7). The appendages on this segment are fully developed at immature stage 3 (*Aneesh et al., 2018*; *Boyko & Wolff, 2014*; *Sartor & Pires, 1988*; *Jones et al., 2008*). These seven pairs of well-developed trunk appendages are best visible from specimen P2338 as immature (Fig. 10).

Possible adult representatives

Examined specimens P2339–P2342, P2345–P2346 and P2348 are interpreted as at least immature adults (immature males or immature females). Since neither adult male characters (*e.g.*, appendix masculina on pleon appendage 2 and penes), nor adult female characters (*e.g.*, developed brood pouch, no penes) are visible on the fossils, this interpretation is based on the body shape and size.

When considering the overall body shape and individual size of these specimens (Figs. 19 and 20), a further differentiation between possible male and female specimens can be made. Specimens P2339, P2342, P2346, P2348 are herein interpreted as possible male or transitional stage individuals, while specimens P2340, P2341 and P2345 are interpreted as possible female specimens. The body shape variation that suggests this distinction, is most prominent from comparing the reconstructed body shapes of specimen P2339 and specimen P2345. The remaining fossil specimens were either incompletely preserved or preserved at an angle so that no reconstruction could be done. Therefore, the interpretation of the remaining specimens is based on general body shape and size comparison.

Specimen P2339 has a slightly less elongated, pear-like body shape, widening towards the posterior end, widest at trunk segments 5 or 6 (Fig. 2). Preserved with minimal dorsal and ventral feature distortion, this specimen has a similar body shape to that of extant male representatives of Cymothoidae. When considering the results of the shape analysis (Fig. 19), the reconstructed body shape of the supposed male specimens group between data points of male and female representatives. This indicates that specimen P2339 has a body shape comparative to males or small females of extant, externally attaching species (*Anilocra frontalis* and *Nerocila orbignyi*), suggesting a possible transitional stage from male to female. With regards to the body width, specimen P2339 is comparable to most herein analysed males (Fig. 21A) with the area of greatest width (Fig. 21B) still within the range of extant males (Figs. 19–21). The results from both body shape and size analyses support the interpretation of specimen P2339 as a transitional stage specimen, between the stages of adult male and becoming an adult female.

The possible male/transitional stage individuals (specimens P2339, P2342, P2346 and P2348) have a body length range of 7.0–9.5 mm and a width of 4.0 mm (with only the width of specimen P2339 available). This results in an average body length to width ratio of

2.04, corresponding to the trend of a smaller ratio of adult male specimens compared to that of immatures.

Possible female specimens P2340, P2341and P2345 have body proportions that are somewhat different to those interpreted as male representatives. These specimens have an oval to rounded anterior trunk region, with the body widest at trunk segment 3 or 4. This oval body shape is especially prominent within adult female stages of many extant species, suggesting that these specimens might be female representatives. With a body length range of >6.80–>9.42 mm and a width range of 4.95–6.20 mm, these specimens are the largest among the examined fossils, when incomplete length preservation are taken into consideration. These measurements result in an average body length to width ratio of 1.46, which is smaller than that of the fossil specimens interpreted as adult males and immatures.

According to the body shape analysis results from Fig. 19, the possible female reconstructed body shape (P2345) plot within the group of female representatives of extant species, surrounded only by other adult female body shapes (*A. pomacentri*, *A. frontalis*, external attaching; *M. renardi*, gill attaching). Even though its overall body size is smaller than that of the analysed extant females, specimen P2345 has a similar relative body width to extant species (Fig. 21A), but with the area of greatest width more toward the anterior region (Fig 21B) than most extant females included in the analysis.

In addition to these characters, another female specific feature was noted: specimens interpreted as possible females have a rather distinct trunk segment 1 shape. This structure is almost triangular in shape, with the posterior margin medially elongated; and encompassing the head from the lateral sides (as seen in specimens P2340 and P2345, Figs. 18, 14). Specimens interpreted as possible immatures, males and transitional stages, have a trunk segment 1 with narrowly rounded antero-lateral angles and with an evenly rounded posterior margin (as seen in specimens P2339, P2342, P2343 and P2346, Figs. 2, 4, 13, 6). This structure is incompletely preserved in specimens P2341 and P2348.

Body shape as a proxy for ontogenetic stage

The comparison of body shapes (Fig. 19) show no distinct separation between ontogenetic stages among various extant species of Cymothoidae. These results may be different for an intra-species analysis. Even so, when body shape is compared relative to actual size (Fig. 21), a general but weak trend becomes visible. These trends were noticed for the individuals included in the analysis from literature: 18 extant species, with representatives that attach to different sites on the host (mouth, gills, external). A larger dataset would be needed to further support these trends:

(1) Immature individuals of extant species tend to have a smaller range in body width, generally having slender/narrow body outlines (grouping mostly within the negative PC1 values in Figs. 19–21). This narrow body shape is characteristic of most externally attaching forms, independent of their ontogenetic stage. The immature specimens included here, range in size between 1–10 mm, with only one individual (*Nerocila acuminata Schioedte & Meinert, 1881*) grouping outside of this size range, with an average

body length of 15.7 mm, as calculated from *Segal (1987)*. The latter individual also plots in close proximity (shape and size) to two other male representatives of *Anilocra*.

(2) Body shapes tend to become more diverse through development, with adult males having a larger range in body width than immatures. Their body size range is between 7.7–17.5 mm, with only the male representative of *Ceratothoa* reaching a size of 25.5 mm. This is not surprising, since species of *Ceratothoa* are some of the largest in size, if not the largest, among the ingroups of Cymothoidae.

(3) Female individuals are highly diverse in body shape and size, even more so than male representatives, supporting the notion of wide morphological variability among ingroups of Cymothoidae. In species of Cymothoidae, the body size ranges between 10.5–65.0 mm and the body shape ranges (in body width, PC1) from long, slender individuals, as seen with *Anilocra pilchardi*, to strongly oval to round individuals, as seen with *R. circularis* and *C. tetrodontis*.

Not surprisingly, adult females occupy the largest area in our ordinations, indicating that this ontogenetic stage is the most morphologically variable. This can be explained by the ecology and life habit of adult females of Cymothoidae as permanent parasites of mainly fish hosts. The site of attachment to the host plays a distinct role in the final body shape of female individuals due the space available for growth (*Kensley, 1978*; *Brusca, 1981*; *Hadfield, 2012*).

Possible site of attachment

The body shape outline analysis of the included extant species can provide insight into the possible site of attachment of *P. dvorakorum* sp. nov. (Fig. 20). Even though there is no obvious trend, it is noticeable that all immatures have long, slender bodies (with only two exceptions: *E. vulgaris* (*Stimpson, 1857*) and *C. steindachneri Koelbel, 1879*) and how, throughout development, species that attach to different sites develop differently shaped, wider bodies. According to the results (Fig. 20), externally attaching species have the most constant length to width ratio and only slightly gain some width through development along the midline of the body (with *A. pilchardi Bariche & Trilles, 2006* as exception). Even though attaching to the external surface of a host does not pose any growth restrictions, it causes the resulting adult body shape to be streamlined, in order to withstand the water current and flow. Gill-attaching species have more variation in midline width, according to the available space in the gill cavity of the host. Gill-attaching species usually have rounded and strongly twisted body shapes in order to take on the shape of the space available in the gill cavity. Buccal-attaching species do not show as much variation in width, but the most variation in where the increase in body width takes place (*i.e.*, towards the anterior part of anterior trunk or toward the posterior part of anterior trunk). The growth in width of buccal-attaching species are restricted in the mouth cavity of the fish, resulting in elongated slender (almost cylindrical) adults, that gain body width depending on available space.

The position of the examined fossil specimens in Fig. 20 does not clearly suggests a possible site of attachment. It does, however, show that especially the fossils interpreted as adult male and female are less likely to have been buccal-attaching, as the body shapes

of buccal-attaching species are the least similar to the reconstructed fossil body shapes. Extant male and female individuals of externally-attaching groups seem to have the most similar body shapes to the interpreted male and female specimens examined here. The isolated finds of these specimens support the possibilities that they might have been either buccal-attaching or externally-attaching, based on the ability of extant buccal- and externally-attaching species to abandon their host when it is dying. Gill-attaching species cannot easily detach from the host and leave the gill cavity, therefore, dying *in situ*. Although not conclusive, it is most likely that the examined specimens were externally-attaching individuals, based on this ecological strategy and the results presented in Fig. 20.

Palaeoecology

All examined fossil specimens are isolated, showing no interaction or closeness to other macro-organisms. Immatures of Cymothoidae are free-swimming, in search of an appropriate fish host to attach to. This might explain why the immature specimens are preserved isolated from potential hosts. The lack of a fish host in close proximity to the fossils does not exclude the possibility that the studied specimens were permanent parasites, but is likely a result of their ontogenetic stage as immature individuals. Adult representatives are usually permanently attached to a host. Yet, the specimens interpreted here as possible adult representatives are also isolated. Even though it is unlikely for adult specimens of Cymothoidae to be encountered without a host, it is not impossible. The death of a host could result in the parasitic individual detaching from it, in order to find a new host. Alternatively, the individuals might have accidentally become detached from its host. If the studied fossils were permanent parasites, isolated discoveries are certainly not unlikely.

To date, no possible specimen of Cymothoidae has been discovered attached to a fish fossil at this collection site. Preserved fish bones are small, and if there was to be a parasite preserved in the mouth or gill areas of a fish, in most cases it would be hard to recognise.

By considering the reconstructed palaeoenvironment from which the fossils were collected, it is possible to speculate on the life habit of the studied individuals, based on the ecology of extant animals (actualism). The presence of temperate basses (Moronidae, ray-finned fish) in the depositional environment indicates a possible connection to the sea *via* rivers (*Micklich, 1990*; *Micklich & Böhme, 1997*; *Přikryl, 2008*) and additionally points out possible hosts for the studied individuals. Today, temperate basses occur in marine, fresh- and brackish water habitats (*Wallace, 1971*; *Whittier, Halliwell & Daniels, 1999*; *Jobling, Peruzzi & Woods, 2010*), with some records of species infested with species of Cymothoidae (*Sadzikowski & Wallace, 1974*; *Papapanagiotou, Trilles & Photis, 1999*; *Charfi-Cheikhrouha et al., 2000*; *Bariche & Trilles, 2006*; *Hata et al., 2017*). If Cymothoidae-like parasites were associated with representatives of Moronidae from this collection site, such findings are expected to be rare, as there are only two representatives of Moronidae fossils recorded, where the mouth and/or pharyngeal region of the fish is preserved.

Records and origin of freshwater parasitic isopods

The sediments from which the fossils were collected were most probably deposited in a freshwater lake (see Geological setting and palaeoenvironment). This suggests that the fossil specimens collected from these sediments were freshwater inhabitants. Even though a large majority of extant species of Cymothoida are distributed in marine environments, many ingroups, including Cymothoidae, have been recorded from freshwater and brackish water habitats (*Smit, Bruce & Hadfield, 2014*; *Tavares-Dias et al., 2014*; *Hata et al., 2017*).

There is no concise distribution pattern for representatives of Cymothoidae in freshwater. Yet, the majority of cases have been reported from South American freshwater sources (*Huizinga, 1972*; *Bowman, 1986*; *Bastos & Thatcher, 1997*; *Lins et al., 2008*; *Tavares-Dias et al., 2014*), with some species recorded from central African (see *Moore, 1898*; *Van Name, 1920*; *Fryer, 1965, 1968*; *Lincoln, 1971*) and Asian freshwater environments (*Tsai & Dai, 1999*; *Yamano, Yamauchi & Hosoya, 2011*). Some species have been reported from estuaries in North America (*Lindsay & Moran, 1976*) with one record from southern Europe (Mediterranean) (see *Leonardos & Trilles, 2004*).

The occurrence of the examined fossil specimens in sediments from a fossil freshwater lake not only suggests the presence of freshwater forms of Cymothoidae in Europe, it also suggests that the transition between the marine and the freshwater lifestyle happened during or even before the Eocene. The co-occurrence of temperate basses (Moronidae) as possible fish hosts provides a possible scenario how this transition might have happened: through the colonisation of freshwater habitats by fishes from the ocean. Alternatively, the fossil specimens could represent remains of individuals that were transported to the lake by anadromous migrating fish.

CONCLUSIONS

The examined fossils are conspecific and interpreted as ingroup representatives of, or close relatives to, the group Cymothoidae. Fossils of the newly described species, *Parvucymoides dvorakorum* gen. et sp. nov., possibly represent different developmental stages. The examined fossil specimens (and subsequently the new species) have been interpreted as parasites based on their close affinity to Cymothoidae as well as the presence of seven pairs of thoracopods with prehensile, curved and hook-like dactyli. Ray-finned fishes occurring in the same palaeoenvironment might possibly have been the hosts of these parasites. The interpretation of the ontogenetic stage of the fossils is based on an analysis of the body sizes and different morphological characters of extant representatives of Cymothoidae and the fossils. The palaeoenvironment suggests that these individuals once lived in a freshwater lake, which contributes a well-dated fossil record to the ongoing research about the origin of freshwater species of Cymothoidae.

ACKNOWLEDGEMENTS

as Niel L. Bruce and two anonymous reviewers for their comments and input on the manuscript.

ADDITIONAL INFORMATION AND DECLARATIONS

Competing Interests

The authors declare that they have no competing interests.

Author Contributions

- Serita Van der Wal conceived and designed the experiments, performed the experiments, analyzed the data, prepared figures and/or tables, authored or reviewed drafts of the paper, and approved the final draft.
- Mario Schädel conceived and designed the experiments, performed the experiments, analyzed the data, prepared figures and/or tables, authored or reviewed drafts of the paper, and approved the final draft.
- Boris Ekrt conceived and designed the experiments, authored or reviewed drafts of the paper, and approved the final draft.
- Joachim T. Haug conceived and designed the experiments, analyzed the data, authored or reviewed drafts of the paper, and approved the final draft.

Data Availability

The following information was supplied regarding data availability:

The raw data is available in the Supplemental Files.

New Species Registration

The following information was supplied regarding the registration of a newly described species:

Publication LSID: urn:lsid:zoobank.org:pub:C38FC926-EEC4-45F8-8CBB-3639D845C4DA.

Parvucymoides gen. nov. LSID: urn:lsid:zoobank.org:act:DE6F26BC-87E1-43B8-BDF9-47B25537627C.

Parvucymoides dvorakorum sp. nov. LSID: urn:lsid:zoobank.org:act:485FBA58-F578-48A0-AD3C-D93991C6A8D3.

Supplemental Information

Supplemental information for this article can be found online at http://dx.doi.org/10.7717/peerj.12317#supplemental-information.

REFERENCES

Adlard RD, Lester RJG. 1995. The life-cycle and biology of *Anilocra pomacentri* (Isopoda, Cymothoidae), an ectoparasitic isopod of the coral-reef fish, *Chromis nitida* (Perciformes, Pomacentridae). *Australian Journal of Zoology* **43(3)**:271–281 DOI 10.1071/ZO9950271.

Agassiz L. 1834. Recherches sur les poissons fossiles. Volumes I – V. Neuchatel. Biodiversity Heritage Library. *Available at https://www.biodiversitylibrary.org/item/23070.*

Alves-Júnior FA, Bertrand A, de Carvalho Paiva RJ, de Souza-Filho JF. 2019. First report of the ectoparasitic isopod, *Holophryxus acanthephyrae* Stephensen 1912 (Cymothoida: Dajidae) in the South Atlantic: Recovered from a new host, the deep-sea shrimp, *Acanthephyra acanthitelsonis* Spence Bate, 1888. *Thalassas: An International Journal of Marine Sciences* **35(1)**:13–15 DOI 10.1007/s41208-018-0072-3.

Aneesh PT, Helna AK, Kumar AB. 2019. Redescription and neotype designation for the poorly known fish parasitic cymothoid *Joryma brachysoma* (Pillai, 1964) (Crustacea: Isopoda) from India. *Folia Parasitologica* **66**:1–6 DOI 10.14411/fp.2019.014.

Aneesh PT, Helna AK, Kumar AB, Trilles JP. 2020. A taxonomic review of the branchial fish parasitic genus *Elthusa* Schioedte & Meinert, 1884 (Crustacea: Isopoda: Cymothoidae) from Indian waters, with the description of three new species. *Marine Biodiversity* **50(5)**:1–38 DOI 10.1007/s12526-020-01084-6.

Aneesh PT, Helna AK, Trilles J-P, Chandra K. 2019. A taxonomic review of the genus *Joryma* Bowman and Tareen, 1983 (Crustacea: Isopoda: Cymothoidae) parasitizing the marine fishes from Indian waters, with a description of a new species. *Marine Biodiversity* **49**:1449–1478 DOI 10.1007/s12526-018-0920-7.

Aneesh PT, Sudha K, Helna AK, Anilkumar G. 2016. *Mothocya renardi* (Bleeker, 1857) (Crustacea: Isopoda: Cymothoidae) parasitising *Strongylura leiura* (Bleeker) (Belonidae) off the Malabar coast of India: redescription, occurrence and life-cycle. *Systematic Parasitology* **93(6)**:583–599 DOI 10.1007/s11230-016-9646-8.

Aneesh PT, Sudha K, Helna AK, Anilkumar G. 2018. *Agarna malayi* Tiwari 1952 (Crustacea: Isopoda: Cymothoidae) parasitising the marine fish, *Tenualosa toli* (Clupeidae) from India: re-

description/description of parasite life cycle and patterns of occurrence. *Zoological Studies* **57**:1–22 DOI 10.6620/ZS.2018.57-25.

Ax P. 2000. *Multicellular animals: the phylogenetic system of the Metazoa, Volume II. (S. Kinsey, Tran.).* Berlin, Heidelberg: Springer-Verlag, 396.

Bache SM, Wickham H. 2014. magrittr: a forward-pipe operator for R (1.5) [R]. *Available at* *https://CRAN.R-project.org/package=magrittr*.

Bachmayer F. 1948. Pathogene Wucherungen bei jurassischen Dekapoden. Sitzungsber. *Österreichische Akademie der Wissenschaften* **157**:263–266.

Bakenhaster MD. 2004. External morphological features of mancas of four parasitic isopod species (Cymothoidae) in the northern Gulf of Mexico. Ms. thesis, University of Southern Mississippi.

Bakenhaster MD, McBride RS, Price WW. 2006. Life history of *Glossobius hemiramphi* (Isopods: Cymothoidae): development, reproduction, and symbiosis with its host *Hemiramphus brasiliensis* (Pises: Hemiramphidae). *Journal of Crustacean Biology* **26(3)**:283–294 DOI 10.1651/C-2573.1.

Bariche M, Trilles J-P. 2006. Preliminary check-list of cymothoids (Crustacea: Isopoda) parasitic on marine fishes from Lebanon. *Zoology in the Middle East* **34**:53–60 DOI 10.1080/09397140.2005.10638082.

Bastos PB, Thatcher VE. 1997. A redescription of *Riggia paranensis* Szidat, 1948 (Isopoda, Cymothoidae) based on thirty-two specimens from curimatid fish of Rio de Janeiro, Brazil, with an emendation of the genus. *Memórias do Instituto Oswaldo Cruz* **92**:755–760 DOI 10.1590/S0074-02761997000600005.

Bellon H, Bůžek Č, Gaudant J, Kvaček Z, Walter H. 1998. The Česke Středohoří magmatic complex in Northern Bohemia 40K-40Ar ages for volcanism and biostratigraphy of the Cenozoic freshwater formations. *Newsletters on Stratigraphy* **36(2–3)**:77–103 DOI 10.1127/nos/36/1998/77.

Bleeker P. 1857. Recherches sur les Crustacés de L'Inde Archipelagique. II. Sur les Isopodes Cymothoadiens de L'Archipel Indien. *Natuurkundige vereeniging in Nederlandsche-Indie, Batavia, Verhandelingen* **2**:20–40.

Bonhomme V, Picq S, Gaucherel C, Claude J. 2014. Momocs: outline analysis using R. *Journal of Statistical Software* **56**:1–24 DOI 10.18637/jss.v056.i13.

Bowman TE. 1960. Description and notes on the biology of *Lironeca puhi*, n. sp. (Isopoda: Cymothoidae), parasite of the Hawaiian moray eel, *Gymnothorax eurostus* (Abbott). *Crustaceana* 84–91.

Bowman TE. 1971. *Palaega lamnae*, new species (Crustacea; isopoda) from the upper Cretaceous of Texas. *Journal of Paleontology* **45(3)**:540–541.

Bowman SE. 1986. *Paracymothoa tholoceps*, a new freshwater parasitic isopod from southern Venezuela. *Proceedings of the Biological Society of Washington* **99**:753–756.

Bowman TE, Tareen IU. 1983. Cymothoidae from fishes of Kuwait Arabian Gulf (Crustacea: Isopoda). *Smithsonian Contributions to Zoology* **382(382)**:1–30 DOI 10.5479/si.00810282.382.

Boxshall GA, Montú MA. 1997. Copepods parasitic on Brazilian coastal fishes: a handbook. *Nauplius* **5(1)**:1–225.

Boyko CB, Bruce NL, Hadfield KA, Merrin KL, Ota Y, Poore GCB, Taiti S, Schotte M, Wilson GDF. 2019. World marine, freshwater and terrestrial isopod crustaceans database. Cymothoida. Accessed through: World Register of Marine Species. *Available at* *http://www.marinespecies.org/aphia.php?p=taxdetails&id=292941* (accessed 30 June 2020).

Boyko CB, Williams JD, Markham JC. 2012. Recent and fossil Isopoda Bopyridae parasitic on squat lobsters and porcelain crabs (Crustacea: Anomura: Chirostyloidea and Galatheoidea), with notes on nomenclature and biogeography. *Zootaxa* **3150**:1–35 DOI 10.5281/zenodo.208724.

Boyko CB, Wolff C. 2014. Isopoda and Tanaidacea. In: Martin JW, Olesen J, Høeg JT, eds. *Atlas of Crustacean Larvae*. Baltimore: Johns Hopkins University Press, 210–215.

Bruce NL. 1986. Revision of the isopod crustacean genus *Mothocya* Costa, in Hope, 1851 (Cymothoidae: Flabellifera), parasitic on marine fishes. *Journal of Natural History* **20(5)**:1089–1192 DOI 10.1080/00222938600770781.

Bruce NL. 1987a. Australian species of *Nerocila* Leach, 1818, and *Creniola* n. gen.(Isopoda: Cymothoidae), crustacean parasites of marine fishes. *Records of the Australian Museum* **39(6)**:355–412 DOI 10.3853/j.0067-1975.39.1987.174.

Bruce NL. 1987b. Australian *Pleopodias* Richardson, 1910, and *Anilocra* Leach, 1818 (Isopoda: Cymothoidae), crustacean parasites of marine fishes. *Records of the Australian Museum* **39**:85–130 DOI 10.3853/j.0067-1975.39.1987.166.

Bruce NL. 1990. The genera *Catoessa*, *Elthusa*, *Ichthyoxenus*, *Idusa*, *Livoneca* and *Norileca*, n. gen. (Isopoda, Cymothoidae), crustacean parasites of marine fishes, with descriptions of eastern Australian species. *Records of the Australian Museum* **42**:247–300 DOI 10.3853/j.0067-1975.42.1990.118.

Bruce NL. 2002. *Tridentella rosemariae* sp. nov.(Isopoda, Tridentellidae), from northern New Zealand waters. *Crustaceana* **75(2)**:159–170.

Brusca RC. 1978. Studies on the cymothoid fish symbionts of the eastern Pacific (Crustacea: Isopoda: Cymothoidae). II. Systematics and biology of *Lironeca vulgaris* Stimpson 1857. *Allan Hancock Occasional Papers New Series* **2**:1–19.

Brusca RC. 1981. A monograph on the Isopoda Cymothoidae (Crustacea) of the eastern Pacific. *Zoological Journal of the Linnean Society* **73**:117–199 DOI 10.1111/j.1096-3642.1981.tb01592.x.

Brusca RC, Wilson GDF. 1991. A phylogenetic analysis of the Isopoda with some classificatory recommendations. *Memoirs of the Queensland Museum* **31**:143–204.

Bunkley-Williams L, Williams EH. 1998. Isopods associated with fishes: a synopsis and corrections. *The Journal of Parasitology* **84**:893–896 DOI 10.2307/3284615.

Cavalcanti ETS, do Nascimento SKS, Barros NHC, Chellappa S. 2012. Occurrence of the isopod parasite *Rocinela signata* (Isopoda: Aegidae) on marine fish *Sparisoma frondosum* (Osteichthyes: Scaridae). *Marine Biodiversity Records* **5**:1–4 DOI 10.1017/S1755267212000516.

Charfi-Cheikhrouha F, Zghidi W, Yarba LO, Trilles J. 2000. Les Cymothoidae (Isopodes parasites de poissons) des côtes tunisiennes: écologie et indices parasitologiques. *Systematic Parasitology* **46**:143–150 DOI 10.1023/A:1006336516776.

Chroust M, Mazuch M, Hernández Luján Á.. 2019. New crocodilian material from the Eocene-Oligocene transition of the NW Bohemia (Czech Republic): an updated fossil record in Central Europe during the Grande Coupure. *Neues Jahrbuch für Geologie und Paläontologie* **293(1)**:73–82 DOI 10.1127/njgpa/2019/0832.

Costa A. 1851. Caratteri di alcuni de'generi e specie nouve segnete nel presente catalogo. In: Hope FW, ed. *Catalogo dei crostacei ltaliani e di molti altri de Mediterraneo, Napoli.* 41–48. *Available at* https://www.biodiversitylibrary.org/item/21992.

Dana JD. 1852. On the classification of the Crustacea Choristopoda or Tetradecapoda. *American Journal of Science and Arts* **14(2)**:297–316.

Dreyer H, Wägele JW. 2002. The Scutocoxifera tax. nov. and the information content of nuclear ssu rDNA sequences for reconstruction of isopod phylogeny (Peracarida: Isopoda). *Journal of Crustacean Biology* **22(2)**:217–234 DOI 10.1163/20021975-99990229.

Etter W. 2014. A well-preserved isopod from the Middle Jurassic of southern Germany and implications for the isopod fossil record. *Palaeontology* **57(5)**:931–949 DOI 10.1111/pala.12095.

Fejfar O, Kvaček Z. 1993. Excursion Nr. 3, Tertiary basins in northwest Bohemia. *Paläontologische Gesellschaft* **63**:21–26.

Feldmann RM, Goolaerts S. 2005. *Palaega rugosa*, a new species of fossil isopod (Crustacea) from Maastrichtian rocks of Tunisia. *Journal of Paleontology* **79**:1031–1035.

Feldmann RM, Wieder RW, Rolfe WI. 1994. *Urda mccoyi* (Carter 1889), an isopod crustacean from the Jurassic of Skye. *Scottish Journal of Geology* **30**:87–89 DOI 10.1144/sjg30010087.

Fryer G. 1965. A new isopod of the genus *Lironeca* parasitic on a cichlid fish of Lake Tanganyika. *Revue de Zoologie et de Botanique Africaines* **71**:376–384.

Fryer G. 1968. A new parasitic isopod of the family Cymothoidae from clupeid fishes of Lake Tanganyika—a further Lake Tanganyika enigma. *Journal of Zoology* **156**:35–43 DOI 10.1111/J.1469-7998.1968.TB08577.X.

Gentil-Vasconcelos HC, Tavares-Dias M. 2015. First study on infestation of *Excorallana berbicensis* (Isopoda: Corallanidae) on six fishes in a reservoir in Brazilian Amazon during dry and rainy seasons. Embrapa Amapá-Artigo em periódico indexado (ALICE). DOI 10.3856/vol43-issue5-fulltext-13.

Guérin-Méneville FE. 1832. Crustaces. *Expedition scientifique de Moree, section des Sciences physiques* **3(1)**:30–50.

Hadfield KA. 2012. The biodiversity and systematics of marine fish parasitic isopods of the family Cymothoidae from southern Africa. D. Phil. thesis, University of Johannesburg.

Hadfield KA, Sikkel PC, Smit NJ. 2014. New records of fish parasitic isopods of the gill-attaching genus *Mothocya* Costa, in Hope, 1851 from the Virgin Islands, Caribbean, with description of a new species. *ZooKeys* **439**:109–125 DOI 10.3897/zookeys.439.8093.

Hadfield KA, Smit NJ, Avenant-Oldewage A. 2009. Life cycle of the temporary fish parasite, *Gnathia pilosus* (Crustacea: Isopoda: Gnathiidae) from the east coast of South Africa. Marine Biological Association of the United Kingdom. *Journal of the Marine Biological Association of the United Kingdom* **89(7)**:1331 DOI 10.1017/S0025315409000587.

Hansen HJ. 1890. Cirolanidæ et familiæ nonnullæ propinquæ musei hauniensis. Et bidrag til kundskaben om nogle familier af isopode krebsdyr. Kongelige Danske Videnskabernes Selskabs Skrifter, 6te Raekke. *Naturvidenskabelig Og Mathematisk Afdeling* **3**:239–426 DOI 10.5962/bhl.title.10325.

Hansen T, Hansen J. 2010. First fossils of the isopod genus *Aega* Leach, 1815. *Journal of Paleontology* **84**:141–147 DOI 10.1666/08-083.1.

Hata H, Sogabe A, Tada S, Nishimoto R, Nakano R, Kohya N, Takeshima H, Kawanishi R. 2017. Molecular phylogeny of obligate fish parasites of the family Cymothoidae (Isopoda, Crustacea): evolution of the attachment mode to host fish and the habitat shift from saline water to freshwater. *Marine Biology* **164**:105 DOI 10.1007/s00227-017-3138-5.

Hessler R. 1969. Peracarida. In: Moore RC, ed. *Treatise on Invertebrate Paleontology, Pt. R, Arthropoda 4.* Boulder, Lawrence: Geological Society of America and University Kansas Press, R360–R393.

Hoffman GL. 2019. Phylum Arthropoda: Class Crustacea: Subclass Branchiura, Orders Copepoda and Isopoda. In: *Parasites of North American Freshwater Fishes*, Ithaca: Cornell University Press, 310–331.

Holdich DM. 1981. Opportunistic feeding behaviour in a predatory isopod. *Crustaceana* **41(1)**:101–103 DOI 10.2307/20103640.

Huizinga HW. 1972. Pathology of *Artystone trysibia* Scioedte (Isopoda: Cymothoidae), an endoparasitic isopod of South American fresh water fishes. *Journal of Wildlife Diseases* **8(3)**:225–232 DOI 10.7589/0090-3558-8.3.225.

Hyžný M, Bruce NL, Schlögl J. 2013. An appraisal of the fossil record for the Cirolanidae (Malacostraca: Peracarida: Isopoda: Cymothoida), with a description of a new cirolanid isopod crustacean from the early Miocene of the Vienna Basin (Western Carpathians). *Palaeontology* **56**:615–630 DOI 10.1111/PALA.12006.

Jackson HG. 1926. The morphology of the isopod head. Part I. The head of *Ligia oceaniaa*. *Proceedings of the Zoological Society of London* **96(3)**:885–911 DOI 10.1111/j.1469-7998.1926.tb07133.x.

Jobling M, Peruzzi S, Woods C. 2010. *The temperate basses (Family: Moronidae). Finfish aquaculture diversification*. Oxfordshire: CABI, 337–360.

Jones CM, Miller TL, Grutter AS, Cribb TH. 2008. Natatory-stage cymothoid isopods: description, molecular identification and evolution of attachment. *International Journal for Parasitology* **38**:477–491 DOI 10.1016/j.ijpara.2007.07.013.

Kensley BF. 1978. *Guide to the marine isopods of Southern Africa*. Cape Town: South African Museum, 173.

Klompmaker AA, Artal P, van Bakel BW, Fraaije RH, Jagt JW. 2014. Parasites in the fossil record: a Cretaceous fauna with isopod-infested decapod crustaceans, infestation patterns through time, and a new ichnotaxon. *PLOS ONE* **9**:1–17 DOI 10.1371/journal.pone.0092551.

Klompmaker AA, Robins CM, Portell RW, De Angeli A. 2018. Crustaceans as hosts of parasites throughout the Phanerozoic. *BioRxiv* DOI 10.1101/505495.

Koelbel K. 1879. Über einige neue Cymothoiden. *Sitzungberichte der Mathematisch-Nautwissenschaftlichen Klasse der Kaiserlichen Akademie der Wissenschaften* **78(1)**:401–416.

Konzalová M. 1981. Boehlensipollis und andere Mikrofossilien des Boehmischen Tertiaers (Vulkanogene Schichtenfolge). *Sborník Geologicktfytfch Věd, Geologie* **24**:135–162.

Kossmann R. 1880. Zoologische Ergebnisse einer im auftrage der königlichen Academie der Wissenschaften zu Berlin ausgeführten Reise in die Küstengebiete des Rothen Meeres. Herausgegeben mit Unterstützung der königlichen Academie von Robby Kossmann, Dr. Phil. und Privatdocent, Universität Heidelberg. Zweite Hälfte, erste lieferung. Malacostraca (2. Theil: Anomura). Verlag von Wilhelm Engelmann, Leipzig, 67–140. *Available at* https://ia802800.us.archive.org/28/items/zoologischeergeb12koss/zoologischeergeb12koss.pdf.

Kottarathil HA, Sahadevan AV, Kattamballi R, Kappalli S. 2019. *Norileca indica* (Crustacea: Isopoda, Cymothoidae) infects *Rastrelliger kanagurta* along the Malabar Coast of India-seasonal variation in the prevalence and aspects of host-parasite interactions. *Zoological Studies* **58**:1–12 DOI 10.6620/ZS.2019.58-35.

Kumar AB, Bruce NL. 1997. *Elthusa samariscii* (Shiino, 1951)(Isopoda, Cymothoidae) parasitizing *Samaris cristatus* Gray, 1831, off the Kerala coast, India. *Crustaceana* **70(7)**:780–787.

Kvaček Z. 2002. Late Eocene landscape, ecosystems and climate in northern Bohemia with particular reference to the locality of Kučlín near Bílina. *Bulletin of the Czech Geological Survey* **77(3)**:217–236.

Kvaček Z, Teodoridis V. 2011. The Late Eocene flora of Kučlín near Bílina in North Bohemia revisited. *Acta Musei Nationalis Pragae* **67(3–4)**:83–144.

Leach WE. 1814. Crustaceology. In: *Brewster's Edinburgh Encyclopaedia. Vol.VII, Pt. II.* 385–437. *Available at* https://www.biodiversitylibrary.org/item/114403.

Leach WE. 1818. Cymothoadées, Dictionnaire des Sciences Naturelles. In: Cuvier F, ed. *Paris and Strasbourg.* Vol. 12. 338–354. *Available at* https://www.biodiversitylibrary.org/item/74437.

Legrand JJ. 1952. Contribution a l'etude experimentale et statistique de la biologie d' *Anilocra physodes* L. *Archives de Zoologie experimentale et generale* **89**:1–56.

Leonardos I, Trilles J-P. 2004. Reproduction of *Mothocya epimerica* (Crustacea: Isopoda: Cymothoidae), parasitic on the sand smelt *Atherina boyeri* (Osteichthyes: Atherinidae) in Greek lagoons. *Diseases of Aquatic Organisms* **62**:249–253.

Lincoln RJ. 1971. A new species of *Lironeca* (Isopoda; Cymothoidae) parasitic on cichlid fishes in Lake Tanganyika: British Museum (Natural History). *Available at* https://www.biodiversitylibrary.org/page/2283403.

Lindsay JA, Moran RL. 1976. Relationships of parasitic isopods *Lironeca ovalis* and *Olencira praegustator* to marine fish hosts in Delaware Bay. *Transactions of the American Fisheries Society* **105**:327–332 DOI 10.1577/1548-8659(1976)105<327:ROPILO>2.0.CO;2.

Lins DC, Meirelles ME, Malm O, Lima NR. 2008. Mercury concentration in the freshwater bonefish *Cyphocharax gilbert* (Curimatidae) and its parasite the crustacean *Riggia paranensis* (Cymothoidae). *Neotropical Ichthyology* **6**:283–288 DOI 10.1590/S1679-62252008000200017.

Mach K, Dvořák Z. 2011. Geology of the site Kučlín, Trupelník hill near Bílina in North Bohemia. *Acta Musei Nationalis Pragae* **67(3–4)**:77–82.

Maguire EP, Feldmann RM, Jones WT, Schweitzer CE, Casadío S. 2018. The first fossil isopod from Argentina: a new species of Cirolanidae (Crustacea: Peracarida) from the Miocene of Patagonia. *Journal of Crustacean Biology* **38(1)**:34–44 DOI 10.1093/jcbiol/rux100.

Mahmoud NE, Fahmy MM, Abuowarda MM. 2020. Additional morphometric and phylogenetic studies on *Mothocya melanosticta* (Isopoda: Cymothoidae) parasitizing the Red Sea *Nemipterus randalli* fish in Egypt. *Journal of Parasitic Diseases* **44(2)**:1–10 DOI 10.1007/s12639-020-01194-9.

Marino F, Giannetto S, Paradiso ML, Bottari T, De Vico G, Macri B. 2004. Tissue damage and haematophagia due to praniza larvae (Isopoda: Gnathiidae) in some aquarium seawater teleosts. *Diseases of Aquatic Organisms* **59(1)**:43–47 DOI 10.3354/dao059043.

Micklich N. 1990. Ein neuer Percoide (Pisces, Perciformes) aus den tertiären Süßwasser-Diatomiten von Kučlín in Böhmen. *Senckenbergiana Lethaea* **70(1–3)**:199–208.

Micklich N, Böhme M. 1997. Wolfsbarsch-Funde (Perciformes, Moronidae) aus den Süßwasser-Diatomiten von Kučlín (Böhmen) nebst Anmerkungen zur taxonomischen Stellung von 'Perca' lepidota aus den Süßwasser-Kalken von Öhningen (Baden). *Paläontologische Zeitschrift* **71(1–2)**:117–128 DOI 10.1007/BF03022553.

Milne Edwards H. 1840. *Histoire Naturelle des Crustacés III, Comprenent l'anatomie, la physiologie et la classification de ces animaux.* Vol. 3. Paris: Roret.

Mladineo I. 2003. Life cycle of *Ceratothoa oestroides*, a cymothoid isopod parasite from sea bass *Dicentrarchus labrax* and sea bream *Sparus aurata*. *Diseases of Aquatic Organisms* **57**:97–101 DOI 10.3354/dao057097.

Moore J. 1898. *The Marine Fauna in Lake Tanganyika, and the advisability of further exploration in the great African lakes.* Berlin: Nature Publishing Group, 404–408.

Morris SC. 1981. Parasites and the fossil record. *Parasitology* **82(3)**:489–509 DOI 10.1017/S0031182000067020.

Münster GG. 1840. Ueber einige Isopoden in den Kalkschiefern von Bayern. *Beiträge zur Petrefacten-kunde* **3(4)**:19–23.

Nagasawa K, Imai T, Saito H. 2018. *Tachaea chinensis* (Isopoda: Corallanidae), an ectoparasite of freshwater shrimps and prawns, from western Japan, with a list of its known collection localities and hosts. *Crustacean Research* **47**:73–88 DOI 10.18353/crustacea.47.0_73.

Nagler C, Eiler SM, Haug JT. 2019. Examination of functional morphology of dajiid isopods using *Arthrophryxus* sp. parasitising a mysid shrimp as an example. *Acta Zoologica* **10(4)**:1–14 DOI 10.1111/azo.12298.

Nagler C, Haug JT. 2016. Functional morphology of parasitic isopods: understanding morphological adaptations of attachment and feeding structures in *Nerocila* as a pre-requisite for reconstructing the evolution of Cymothoidae. *PeerJ* **4**:e2188 DOI 10.7717/peerj.2188.

Nagler C, Haug C, Resch U, Kriwet J, Haug JT. 2016. 150 million years old isopods on fishes: a possible case of palaeo-parasitism. *Bulletin of Geosciences* **91(1)**:1–12 DOI 10.3140/bull.geosci.1586.

Nagler C, Hyžný M, Haug JT. 2017. 168 million years old marine lice and the evolution of parasitism within isopods. *BMC Evolutionary Biology* **17**:76 DOI 10.1186/s12862-017-0915-1.

Nair GA, Nair NB. 1983. Effect of infestation with the isopod, *Alitropus typus* M. Edwards (Crustacea: Flabellifera: Aegidae) on the haematological parameters of the host fish, *Channa striatus* (Bloch). *Aquaculture* **30(1–4)**:11–19 DOI 10.1016/0044-8486(83)90147-3.

Néraudeau D, Perrichot V, Batten DJ, Boura A, Girard V, Jeanneau L, Nohra YA, Polette F, Saint Martin S, Saint Martin J-P, Thomas R. 2017. Upper Cretaceous amber from Vendée, north-western France: age dating and geological, chemical, and palaeontological characteristics. *Cretaceous Research* **70**:77–95 DOI 10.1016/j.cretres.2016.10.001.

Papapanagiotou E, Trilles J-P, Photis G. 1999. First record of *Emetha audouini*, a cymothoid isopod parasite, from cultured sea bass *Dicentrarchus labrax* in Greece. *Diseases of Aquatic Organisms* **38**:235–237 DOI 10.3354/dao038235.

Pillai NK. 1954. A preliminary note on the Tanaidacea and Isopoda of Travancore. *Bulletin of the Central Research Institute, University of Travancore, Trivandrum, Natural Sciences* **3(1)**:1–21.

Polz H. 2005. Zwei neue Asselarten (Crustacea: Isopoda: Scutocoxifera) aus den Plattenkalken von Brunn (Oberkimmeridgium, Mittlere Frankenalb). *Archaeopteryx* **23**:67–81.

Poore GC, Bruce NL. 2012. Global diversity of marine isopods (except Asellota and crustacean symbionts). *PLOS ONE* **7**:e43529 DOI 10.1371/journal.pone.0043529.

Přikryl T. 2008. Sea bass fish *Morone* sp. (Teleostei) from the north Bohemian Palaeogene (Tertiary, Czech Republic). *Bulletin of Geosciences* **83(1)**:117–122 DOI 10.3140/bull.geosci.2008.01.117.

R Core Team. 2020. *R: a language and environment for statistical computing (3.6.3)*. Vienna: The R Foundation for Statistical Computing. *Available at* https://www.R-project.org/.

Radwański A. 1972. Isopod-infected prosoponids from the Upper Jurassic of Poland. *Acta Geologica Polonica* **22(3)**:499–506.

Rafinesque CS. 1815. Analyse de la nature, ou tableau de l'univers et des corps organises. (Self-published). 244. *Available at* https://www.biodiversitylibrary.org/bibliography/106607.

Rameshkumar G, Ravichandran S. 2015. First occurrence of *Norileca triangulata* (Crustacea: Isopoda: Cymothoidae) from Indian marine fishes. *Journal of Parasitic Diseases* **39(1)**:33–36 DOI 10.1007/s12639-013-0274-9.

Reuss AE. 1844. Die Kreidegebilde des westlichen Böhmens, ein monographischer Versuch. Nebst Bemerkungen über die Braunkohlenlages jenseits der Elbe und eine Übersicht der fossilen Fischreste Böhmens. C.W. Medau, Prague, 303. *Available at* https://books.google.co.za/books?hl=en&lr=&id=mtJTAAAAcAAJ&oi=fnd&pg=PA3&ots=6RAhosmKRq&sig=ghT0J0fz0xkRIvZsFZhAkqLj4Us#v=onepage&q&f=false.

Van der Wal et al. (2021), *PeerJ,* **DOI 10.7717/peerj.12317**

43/46

Richardson H. 1910. Marine isopods collected in the Philippines by the U.S. Fisheries steamer Albatross in 1907-8. *Bureau of Fisheries Document* **736**:1–44 DOI 10.5962/bhl.title.82673.

Robin N, Marramà G, Vonk R, Kriwet J, Carnevale G. 2019. Eocene isopods on electric rays: tracking ancient biological interactions from a complex fossil record. *Palaeontology* **62(2)**:287–303 DOI 10.1111/pala.12398.

Robins CM, Klompmaker AA. 2019. Extreme diversity and parasitism of Late Jurassic squat lobsters (Decapoda: Galatheoidea) and the oldest records of porcellanids and galatheids. *Zoological Journal of the Linnean Society* **187(4)**:1131–1154 DOI 10.1093/zoolinnean/zlz067.

Roccatagliata D, Jordá MT. 2002. Infestation of the fiddler crab *Uca uruguayensis* by *Leidya distorta* (Isopoda, Bopyridae) from the Río de la Plata estuary. *Argentina Journal of Crustacean Biology* **22(1)**:69–82 DOI 10.1163/20021975-99990210.

Rollmann W. 1853. Zwei neue stereoskopische Methoden. *Annalen Der Physik* **90(1)**:186–187 DOI 10.1002/andp.18531660914.

Sadzikowski MR, Wallace DC. 1974. The incidence of *Lironeca ovalis* (Say) (Crustacea, Isopoda) and its effects on the growth of white perch, *Morone americana* (Gmelin), in the Delaware River near Artificial Island. *Chesapeake Science* **15**:163–165 DOI 10.2307/1351036.

Sartor SM, Pires AMS. 1988. The occurrence of *Cymothoa liannae*, a new species of cymothoid isopod from Brazil, with a comparative study of its post-marsupial development. *Crustaceana* **55**:147–156 DOI 10.1163/156854088x00483.

Schioedte JC. 1866. Krebsdyrenes Sugemund. I. Cymothoae. *Naturhistorisk Tidsskrift* 168–206.

Schioedte JC, Meinert FW. 1881. Symbolae ad monographiam Cymothoarum Crustaceorum Isopodum Familiae 2. Anilocridae. *Naturhistorisk Tidsskrift* **13**:1–166 DOI 10.5962/bhl.title.10300.

Schioedte JC, Meinert F. 1883. Symbolæ ad monographium Cymothoarum crustaceorum familiæ. III. Saophridæ. IV. Ceratothoinæ. *Naturhistorisk Tidsskrift, Kjøbenhavn* **13**:281–378.

Schioedte JC, Meinert F. 1884. Symbolæ ad monographium Cymothoarum crustaceorum isopodum familiæ, III: Livonecinæ. *Naturhistorisk Tidsskrift, Kjøbenhavn* **14**:221–454.

Schädel M, Hörnig MK, Hyzny M, Haug JT. 2021. Mass occurrence of small isopodan crustaceans in 100-million-year-old amber: an extraordinary view on behaviour of extinct organisms. *PalZ* **95(3)**:429–445 DOI 10.1007/s12542-021-00564-9.

Schädel M, Perrichot V, Haug JT. 2019. Exceptionally preserved cryptoniscium larvae: morphological details of rare isopod crustaceans from French Cretaceous Vendean amber. *Palaeontologia Electronica* **22**:1–46 DOI 10.26879/977.

Scotese CR. 2014. Atlas of Paleogene paleogeographic maps (Mollweide Projection). In: *PALEOMAP Atlas for ArcGIS. Evanston, Illinois, Maps 8–15*.

Segal E. 1987. Behavior of juvenile *Nerocila acuminata* (Isopoda, Cymothoidae) during attack, attachment and feeding on fish prey. *Bulletin of Marine Science* **41**:351–360.

Serrano-Sánchez MDL, Nagler C, Haug C, Haug JT, Centeno-García E, Vega FJ. 2016. The first fossil record of larval stages of parasitic isopods: cryptoniscus larvae preserved in Miocene amber. *Neues Jahrbuch für Geologie und Paläontologie-Abhandlungen* **279**:97–106 DOI 10.1127/njgpa/2016/0543.

Shiino SM. 1951. On the cymothoid Isopoda parasitic on Japanese fishes. *Bulletin of the Japanese Society of Scientific Fisheries* **16**:81–89 DOI 10.2331/suisan.16.12_81.

Smit NJ, Basson L, Van As JG. 2003. Life cycle of the temporary fish parasite, *Gnathia africana* (Crustacea: Isopoda: Gnathiidae). *Folia Parasitologica* **50(2)**:135–142 DOI 10.14411/fp.2003.024.

Smit NJ, Bruce NL, Hadfield KA. 2014. Global diversity of fish parasitic isopod crustaceans of the family Cymothoidae. *International Journal for Parasitology: Parasites and Wildlife* **3**:188–197 DOI 10.1016/j.ijppaw.2014.03.004.

Smit NJ, Davies AJ. 2004. The curious life-style of the parasitic stages of gnathiid isopods. *Advances in Parasitology* **58**:289–391 DOI 10.1016/s0065-308x(04)58005-3.

Stimpson W. 1857. The Crustacea and Echinodermata of the Pacific shores of North America. *Boston Society of Natural History* **6**:503–513.

Taberner R, Volonterio O, De León RP. 2003. Description of the pulli stages of *Telotha henselii* (Von Martens, 1869)(Isopoda, Cymothoidae), with new hosts and locality records from Uruguay and Argentina. *Crustaceana* 27–37.

Tavares-Dias M, Araújo CSO, Barros MS, Viana GM. 2014. New hosts and distribution records of *Braga patagonica*, a parasite cymothoidae of fishes from the Amazon. *Brazilian Journal of Aquatic Science and Technology* **18(1)**:91–97 DOI 10.14210/bjast.v18n1.p91-97.

Thatcher VE, Carvalho ML. 1988. *Artystone minima* n. sp.(Isopoda, Cymothoidae) a body cavity parasite of the pencil fish (*Nannostomus beckfordi* Guenther) from the Brazilian Amazon. *Amazoniana: Limnologia et Oecologia Regionalis Systematis Fluminis Amazonas* **10(3)**:255–265.

Thatcher VE, de Lima JT, Chellappa S. 2007. *Cymothoa spinipalpa* sp. nov.(Isopoda, Cymothoidae) a buccal cavity parasite of the marine fish, *Oligoplites saurus* (Bloch & Schneider) (Osteichthyes, Carangidae) of Rio Grande do Norte State, Brazil. *Revista Brasileira de Zoologia* **24(1)**:238–245.

Thatcher VE, de Loyola e Silva J, Jost GF, Souza-Conceiçao JM. 2003. Comparative morphology of *Cymothoa* spp. (Isopoda, Cymothoidae) from Brazilian fishes, with the description of *Cymothoa catarinensis* sp. nov. and redescriptions of *C. excisa* Perty and *C. oestrum* (Linnaeus). *Revista Brasileira de Zoologia* **20(3)**:541–552 DOI 10.1590/S0101-81752003000300028.

Thatcher VE, Schindler I. 1999. *Artystone bolivianensis* n. sp.(Isopoda, Cymothoidae) from a loricariid catfish of the Bolivian Amazon. *Amazoniana: Limnologia et Oecologia Regionalis Systematis Fluminis Amazonas* **3(4))**:183–191.

Trilles J-P. 1991. Present researches and perspective on Isopoda (Cymothoidae and Gnathiidae) parasites of fishes (systematics, faunistics, ecology, biology and physiology). *Wiadomości Parazytologiczne* **37(1)**:141–143.

Trilles J-P, Colorni A, Golani D. 1999. Two new species and a new record of cymothoid isopods from the Red Sea. *Cahiers de biologie marine* **40(1)**:1–14.

Tsai M-L, Dai C-F. 1999. *Ichthyoxenus fushanensis*, new species (Isopoda: Cymothoidae), parasite of the fresh-water fish *Varicorhinus barbatulus* from northern Taiwan. *Journal of Crustacean Biology* **19**:917–923 DOI 10.2307/1549311.

Van der Wal S, Haug JT. 2020. Shape of attachment structures in parasitic isopodan crustaceans: the influence of attachment site and ontogeny. *PeerJ* **8(3)**:e918 DOI 10.7717/peerj.9181.

Van der Wal S, Smit NJ, Bruce NL, Olaosebikan B, Hadfield KA. 2021. Two new species of branchial fish parasitic isopod of the genus *Mothocya* Costa, in Hope, 1851 (Isopoda, Cymothoidae) from Nigeria. *International Journal for Parasitology: Parasites and Wildlife* **15**:1–11 DOI 10.1016/j.ijppaw.2021.03.001.

Van Name WG. 1920. Isopods collected by the American Museum Congo Expedition. *Bulletin of the American Museum of Natural History* **43**:42–108.

Van Straelen V. 1930. Présentation d'un Isopode de l'Yprésien du Jutland. *Bulletin de la Sociéte Belge de Géologie de Paléontologie et d'Hydrologie* **39**:1929.

von Martens E. 1869. Südbrasilische Süss-und Brackwasser-Crustaceen nach den Sammlungen des Dr. Reinh. Hensel. *Archiv für Naturgeschichte* **35**:1–37 pls 1-2.

Wallace DC. 1971. Age, growth, year class strength, and survival rates of the white perch, *Morone americana* (Gmelin) in the Delaware River in the vicinity of Artificial Island. *Chesapeake Science* **12**:205–218 DOI 10.2307/1350907.

Walossek D. 1999. On the Cambrian diversity of Crustacea. In: Schram FR, Von Vaupel Klein JC, eds. *Crustaceans and the Biodiversity Crisis*. Leiden: Brill, 3–27.

Walossek D, Müller KJ. 1998. Cambrian 'Orsten'-type arthropods and the phylogeny of Crustacea. In: Fortey RA, Thomas RH, eds. *Arthropod Relationships*. Dordrecht: Springer Netherlands, 139–153.

Wheatstone C. 1838. On some remarkable, and hitherto unobserved, phenomena of binocular vision. *Philosophical Transactions of the Royal Society of London* **128**:371–394.

White A. 1850. List of the specimens of British animals in the collection of the British Museum. Part IV.– Crustacea. British Museum (Natural History), London. 141. *Available at https://www.biodiversitylibrary.org/item/192895*.

Whittier TR, Halliwell DB, Daniels RA. 1999. Distributions of lake fishes in the Northeast: I: Centrarchidae, Percidae, Esocidae, and Moronidae. *Northeastern Naturalist* **6(4)**:283–304 DOI 10.2307/3858271.

Wickham H. 2007. Reshaping data with the reshape package. *Journal of Statistical Software* **21(12)**:1–20 DOI 10.18637/jss.v021.i12.

Wickham H, François R, Henry L, Müller K. 2020. Dplyr: a grammar of data manipulation (1.0.2) [R]. *Available at https://CRAN.R-project.org/package=dplyr*.

Wieder RW, Feldmann RM. 1992. Mesozoic and Cenozoic fossil isopods of North America. *Journal of Paleontology* **66(6)**:958–972 DOI 10.1017/S0022336000021041.

Williams JD, Boyko CB. 2012. The global diversity of parasitic isopods associated with crustacean hosts (Isopoda: Bopyroidea and Cryptoniscoidea). *PLOS ONE* **7(4)**:1–9 DOI 10.1371/journal.pone.0035350.

Wilson GD. 2009. The phylogenetic position of the Isopoda in the Peracarida (Crustacea: Malacostraca). *Arthropod Systematics & Phylogeny* **67(2)**:159–198.

Wilson GD, Sims CA, Grutter AS. 2011. Toward a taxonomy of the Gnathiidae (Isopoda) using juveniles: the external anatomy of *Gnathia aureamaculosa* zuphea stages using scanning electron microscopy. *Journal of Crustacean Biology* **31(3)**:509–522 DOI 10.1651/10-3432.1.

Wägele JW. 1989. Evolution und phylogenetisches System der Isopoda: Stand der Forschung und neue Erkenntnisse. Stuttgart, Schweizerbart. 262. *Available at https://www.schweizerbart.de/publications/detail/isbn/9783510550265/%23*.

Yamano H, Yamauchi T, Hosoya K. 2011. A new host record of *Ichthyoxenus amurensis* (Crustacea: Isopoda: Cymothoidae) from the Amur bitterling *Rhodeus sericeus* (Cypriniformes: Cyprinidae). *Limnology* **12(1)**:103–106 DOI 10.1007/s10201-010-0325-1.

Youssef F, Mansour L, Quilichini Y, Tlig SZ, Benmansour B. 2020. Morphology and scavenging behaviour of two species of the genus *Natatolana* (Crustacea: Isopoda: Cirolanidae) attacking elasmobranchs from the Tunisian coast. *Cahiers de Biologie Marine* **61**:1–10 DOI 10.21411/CBM.A.1836C515.

2.5 Study V: SCHÄDEL, HYŽNÝ, NAGLER & HAUG

Authors: Schädel, M., Hyžný, M., Nagler, C. & Haug, J. T.

Title: Fossil relatives of extant parasitic crustaceans from the Mesozoic of Europe

Status: ready to submit

Fossil relatives of extant parasitic crustaceans from the Mesozoic of Europe

Mario Schädel[1,] Matúš Hyžný[2], Christina Nagler[1] Joachim T. Haug[1,3]

[1]Zoomorphology group, Department of Biology II, Ludwig-Maximilians-Universität München, Großhaderner Straße 2, 82152 Planegg-Martinsried, Germany.

[2]Department of Geology and Paleontology, Comenius University in Bratislava, Mlynská dolina, Ilkovičova 6, 842 15 Bratislava, Slovakia.

[3]GeoBio-Center, Ludwig-Maximilians-Universität München, Richard-Wagner-Str. 10, 80333 München, Germany.

Short title: Fossil relatives of extant parasitic crustaceans

Keywords: Isopoda, *Urda*, Gnathiidae, parasitism, mouthparts

Abstract

Isopoda is a diverse group of crustaceans that live in various habitats from the deep sea to arid terrestrial landscapes. The fossil record of Isopoda is not as rich as for example that of crabs (Brachyura) or seed shrimps (Ostracoda), nevertheless fossil remains of its representatives occur in various field sites. The fossil record of Isopoda includes remains of presumed parasites. Among the fossils which have been discussed as potential parasites are those with the name *Urda* Münster, 1840. Fossils associated with this name have been recorded from a few outcrops of Jurassic and Cretaceous sediments from all over the world. Some of these fossils have been discussed as possibly related to an extant group of parasites, Gnathiidae Leach, 1814. The type species of *Urda* – *Urda rostrata* Münster, 1840 – is herein interpreted as a close relative of the group Gnathiidae, based on the shared occurrence of a number of apomorphic features. This is with *Urda punctata* (Münster, 1842) herein being declared as a junior subjective synonym of *U. rostrata*. However, not all of the fossils associated with the name *Urda* can safely be identified as close relatives of Gnathiidae. Moreover, it is unclear whether the extinct species, which can be identified as close relatives of *U. rostrata* and Gnathiidae form a monophyletic group, as we could not identify an autapomorphy for a natural group *Urda*. A new species of close relatives of *Urda rostrata* and Gnathiidae – *Urda buechneri* n. sp. – is formally described based on μCT image data. *Palaega suevica* Reiff, 1936 and *Palaega*

kessleri Reiff, 1936 are found to be subjective synonyms and are here presented as *Urda suevica* n. comb. – as species closely related to *U. rostrata*. Another already described species *Eobooralana rhodanica* gen. et comb. nov. is interpreted as a more distant relative, which is likely to be closer related to other extant species than those within Gnathiidae.

Three species are not found to be closely related to *U. rostrata* and Gnathiidae and are declared as *nomina dubia* because of the absence of characters that would allow to distinguish the type material from other species: "*Urda*" *liasica* Frentzen, 1937 nom. dub., "*Urda*" *moravica* Remeš, 1912 nom. dub. and "*Urda*" *zelandica* Buckeridge and Johns, 1996 nom. dub.

1. Introduction

Isopoda is a morphologically diverse and species-rich group of eucrustaceans (Brandt and Poore, 2003). Most widely known to the general public by its terrestrial forms – 'woodlice' – many lineages of Isopoda have representatives that live in aquatic habitats, which is also assumed for the earliest representatives of Isopoda (e.g. Lins et al., 2012). The feeding modes within Isopoda vary extremely between its different ingroups. There are highly specialised herbivores (e.g., wood boring species of the group Limnorioidea) (Daniel et al., 1991), generalists, predators, parasites and even hyperparasites (parasites of parasites) (e.g. Rybakov, 1990). Parasites within Isopoda come from a number of different groups; how closely these groups are related to each other or if they form a monophyletic group is still a matter of ongoing research (Brusca and Wilson, 1991; Dreyer and Wägele, 2001; Brandt and Poore, 2003; Nagler et al., 2017). Hosts of these parasites are either fishes (Chondrichthyes and Actinopterygii) (e.g. Abd El-Atti, 2020) or different kinds of aquatic crustaceans such as shrimps, crabs, barnacles and other representatives of Isopoda (e.g. An et al., 2015). There is a substantial variation in the degree of dependence between the parasites and their hosts, ranging from ectoparasites that hide in reefs when not feeding (Brandt and Poore, 2001) to endoparasites that drastically reduce the sclerotization of their exoskeletons once entered the host (e.g. Shiino, 1954) but are thought to be closely related to each other if not forming a monophyletic group. Overall, compared to other ingroups of Eucrustacea, remains of representatives of Isopoda are rather rare in the fossil record (cf. Luque et al., 2017). On the other hand, in some deposits fossil remains of Isopoda can be frequent (Walther, 1904; Haack, 1933). The oldest fossils of Isopoda are from the Upper Carboniferous (Pennsylvanian) (Schram, 1970, 1974), with an almost continuous record during the

Mesozoic and the Cenozoic (Wieder and Feldmann, 1992; Feldmann et al., 2008; Hyžný et al., 2013; Schädel et al., 2020). Although many fossil representatives of Isopoda are quite similar in their overall appearance, the fossil record of Isopoda covers a wide range of body shapes and sizes (Wieder and Feldmann, 1989; Polz, 1998; Serrano-Sánchez et al., 2016). The fossil record of Isopoda also comprises species for which a parasitic lifestyle can be assumed based on their phylogenetic position and on morphological features of the body, such as claws and mouth cones that would allow the animal to cling to a host and suck body fluids from it (Schädel et al., 2019; van der Wal et al., 2021)

Fossils attributed to the name *Urda* Münster, 1840, in contrast to most other representatives of Isopoda, seemingly lack extant analogues with a similar body shape and similar morphological features (Taylor, 1972). The first finding of such fossils is from the lithographic limestone deposits of the Solnhofen area in Southern Germany (Münster, 1840, p. 184, 1842; Kunth, 1870). These fossils are strongly compressed and there is not much brightness- or colour-contrast between preserved cuticle and the sediment. For a long time, it was not clear how many trunk segments there are in the type species of *Urda – Urda rostrata* Münster 1840 – and its relatives (Münster, 1840; Ammon, 1882; Stolley, 1910). This and the lack of well-preserved mouthparts and locomotory legs have led to disparate assumptions regarding the phylogenetic position and the feeding mode of *U. rostrata* and related species (Ammon, 1882; Carter, 1889; Monod, 1926; Menzies, 1962). Studies on well-preserved fossils (Feldmann et al., 1994; Nagler et al., 2017) could show that the number of trunk segments is the same as in the ground pattern of Isopoda and in representatives of most of its ingroups (Wägele, 1989). Nagler et al. (2017) studied multiple well-preserved fossil specimens of *Urda* from the Middle Jurassic of Germany with the aid microcomputer tomography (μCT). This has revealed many aspects of the morphology and allowed for a much more detailed comparison to extant representatives of Isopoda.

In this study we compare fossils of the type species of *Urda*, i.e., *Urda rostrata*, to other fossils that have been attributed to the name *Urda,* with the goal to find autapomorphies for a group *Urda* and to identify which fossils actually can be attributed to the group based on apomorphic character states. By this we also re-examine the μCT scans from Nagler *et al.* (2017). Our new findings are discussed with regard to their implications on the functional morphology and the phylogenetic relationship of the fossils within Isopoda.

2. Material and methods

2.1. MATERIAL

The fossil and extant specimens presented in this study come from multiple collections, including those of museums and universities as well as those of private collectors. The fossils come from Mesozoic sediments of Central Europe and Great Britain.

2.2. INSTITUTIONAL ABBREVIATIONS

AM – Australian Museum, Sydney, Australia.

CeNak – Centre for Natural History, Hamburg, Germany.

ES – Natural History Musem, Bielefeld (NaMU), Germany.

GPIT – University of Tübingen, geological collection, Tübingen, Germany.

GSE – British Geological Survey, Edinburgh, UK.

JME – Jura Museum Eichstätt, Eichstätt, Bavaria, Germany.

KG – British Antarctic Survey, Station KG, Fossil Bluff, Alexander Island.

PIMUZ – Palaeontological Institute and Museum of the University of Zurich, Switzerland.

SMNK – State Museum of Natural History, Karlsruhe, Germany.

SNSB – BSPG – Bavarian State Collection for Palaeontology and Geology (part of the Bavarian Natural History Collections), Munich, Germany.

SM – Sedgwick Museum of Earth Sciences (University of Cambridge), Cambridge, UK.

2.3. DATA SOURCES

Three μCT data sets were obtained from MorphDBase (Grobe and Vogt, 2009). They are available under creative commons licences at https://www.morphdbase.de/?C_Nagler_20170221-M-130.1 (SNSB – BSPG 2011 I 50, permalink) and at https://www.morphdbase.de/?C_Nagler_20170221-M-131.1 (SNSB – BSPG 2011 I 51, permalink) along with the publication of Nagler *et al.* (2017).

Information about the correlation of (bio-) stratigraphic units was retrieved from Hopson *et al.* (2008), Owen (2002), from the databank of the Sedgwick Museum of Earth Sciences, University of Cambridge (http://www.3d-fossils.ac.uk/fossilType.cfm?typSampleId=20003067, accessed 22.03.2021), and from Ogg *et al.* (2016). Numerical ages are according to Ogg *et al.* (2016).

2.4. IMAGING

Images of the fossils were recorded using different macro photography setups including a Canon Rebel T3i DSLR camera in combination with a Canon EF 18-55 mm f/3.5-5.6 objective and a Canon MP-E 65 mm f/2.8 1-5x objective and a Nikon D7200 DSLR camera in combination with a Laowa 100mm f/2.8 2x objective. Additionally, microscopic images were recorded using a Keyence VHX 6000 digital microscope and a Keyence BZ 9000 digital fluorescence microscope. For the digital fluorescence microscope an emitting light source with a mean wavelength of 360 nm and a band width of 40 nm (used for DAPI stains) and an emitting light source with a mean wavelength of 470 nm and a band width of 40 nm (used for GFP stains) were used (Eklund et al., 2018). To obtain fluorescence images with the macro photography setup, a 10 W TATTU U2S ultraviolet light torch with a ZWB2 filter (emitting light of 365 nm wavelength) was used in combination with a UV light filter mounted on the camera objective (e.g. Tischlinger and Arratia, 2013). For one specimen fluorescence was induced by equipping white-light sources with cyan filters and the image was captured using a red filter mounted onto the camera objective ("green-orange fluorescence" Haug et al., 2009; Haug and Haug, 2011). Where possible diffuse lighting conditions (e.g., using flash diffusers) or cross-polarised light (Bengtson, 2000) was used to obtain images with fewer reflections. Some objects were imaged using an EPSON Perfection 1640SU flatbed scanner. The objects were placed in different left-right positions onto the surface of the scanner to obtain images of different viewing angles (Schubert, 2000).

X-ray computer tomography (μCT) was performed at the Zoological State Collection in Munich using a Baker Hughes (General Electrics) 'phoenix nanotom m' computer tomograph with a wolfram target on a cvd diamond, along with the acquisition software 'datos|x' (provided by the manufacturer). All objects scanned for this study were rotated 360 degrees in steps of 0.25 degrees, resulting in total scan times of 48 minutes for each object. The scans were performed with the following x-ray source settings: 120 kV, 100 μA. The volumetric data were computed with the software VGStudio MAX 2.2.6.80630 (Volume Graphics, proprietary). The resulting voxel sizes of the volumetric data are
4.55246 μm for the specimen from Reiff (1936, 'Fundstück F', GPIT without collection number), 13.86661 μm for ES/jb – 8744 and 18.44640 μm for the specimens ES/jb – 30755 and ES/jb – 30756 (scanned together).

2.5. Image processing

Images of different focal planes were fused ('extended depth of field') (Pieper and Korpel, 1983; Itoh et al., 1989) using either CombineZP/CZBatch (Alan Hadley, GPL) in combination with WINE (for running Windows applications on Linux, LGPL) or enfuse (GPL) in combination with Hugin (image alignment, GPL v.2.0). In some cases, the blue colour channel was removed using ImageMagick (Apache 2.0 license) prior to the focus merging to eliminate glow effects around highly fluorescent particles in the final images. Example scripts for the use of the command line tools are available at https://github.com/mcranium/merfoc (personal repository of the first author). Panoramic stitching was performed either manually using the unified transform tool and layer masks in GIMP v.2.10.14 (GPL v.3.0) or automatically using the 'Grid/ Collection stitching' plugin (Preibisch et al., 2009, GPL v.2.0) for ImageJ (public domain).

The red-cyan stereo anaglyph images included in this publication were either obtained as such (creative commons license) or created manually from images of slightly different viewing angles (Wheatstone, 1838; Rollmann, 1853) using GIMP. Red-cyan stereo anaglyph images can be converted to other formats such as paired stereo images or to wiggle images using free software such as GIMP or kataglyph (GPL v.3.0, available at https://github.com/mcranium/kataglyph).

For images from microscopy setups with fixed magnifications, scale bars were created from known pixel lengths, using ImageJ (public domain). In some cases, enfuse or MacroFusion (graphical interface for enfuse, GPL) were used to combine the dynamic range of multiple images of the same view, resulting in images without under- or overexposed areas (HDR, high dynamic range) (Fraser et al., 2009). The images were optimised for colour, brightness, contrast ('levels' and 'curves') and sharpness ('unsharp mask') using GIMP. In some cases, uninformative background was removed (layer masks) or simulated ('clone' tool, marked by dotted lines and explicitly stated in the figure captions. This was also done using GIMP.

2.6. 3D reconstruction

Volume rendering of the μCT data was performed using Drishti 2.6.5 (MIT licence) (Limaye, 2012). Additionally, biological structures in 2D slices of the μCT data were labelled manually using TrakEM2 (Cardona et al., 2012) in Fiji (GPL v.2.0) (Schindelin et al., 2012). In one case Biomedisa (Lösel et al., 2020) was used to compute interspersed labels based on the available image data. The label maps were processed using the 'joint', 'gaussian' and 'median' smoothing algorithms in 3DSlicer (BSD style license) (Fedorov et al., 2012; Kikinis et al., 2014) and subsequently exported as 3D meshes.

Some of the meshes were post-processed with the decimate, subdivision surface and remesh modifiers in Blender 2.8.3 (GPL v.2.0) (e.g. Sutton et al., 2014). Two-dimensional images were rendered using the 'Cycles' raytracing engine and a combination of 'sun' and 'world' lighting in Blender.

2.7. DATA VISUALISATION AND GRAPHIC DESIGN

The visualisation of the age of the fossils and their geographical distribution were created using R v.4.04 (GPL v.2) and the packages dplyr (Wickham et al., 2020), reshape2 (Wickham, 2007), ggplot2 (Wickham, 2009), ggtext (Wilke, 2020), deeptime (Gearty, 2021), sf (Pebesma, 2018), rnaturalearth (South, 2017) and tmap (Tennekes, 2018). The visualisation of the ages parallels a 'Gantt chart' (Gantt, 1910). The drawings and the arrangement of the figure plates and labels were done in Inkscape v.1.0.1 (GPL v.3.0).

2.8. BODY ORGANISATION AND TERMINOLOGY WITHIN ISOPODA

The body of most representatives of Isopoda is composed of one ocular segment and 19 post-ocular segments (PO 1–19). It consists of a head (PO 1–6) and a trunk (PO 7–19). The trunk is divided into an anterior part (pereon, PO 7–13) with walking/grasping appendages, a posterior part (pleon PO 14–18) with swimming/ventilation appendages (pleopods) and the last trunk segment that is conjoined with the telson (pleotelson, PO 19) and has swimming/steering appendages (uropods).

In some representatives of Isopoda, such as in adults of Gnathiidae, postocular segment 7 is functionally incorporated into the head. The anterior-most appendages of the head are the antennula (PO1) and the antenna (PO2). The subsequent appendages form the mouthparts: mandible, maxillula, maxilla and maxilliped. In many representatives of Isopoda there is a complex of three structures anterior or antero-dorsal to the mouthpart appendages: frontal lamina, clypeus and labrum (from anterior to posterior). In representatives of Gnathiidae the frontal lamina is not developed as a distinct structure and the labrum is either not developed (Monod, 1926; Wilson et al., 2011) or conjoined with the clypeus. The clypeus or a conjoined structure, consisting of clypeus and labrum, functionally forms an 'upper lip'. Posterior to the mandible but arising from the same segment there is a pair of sternal lobes (paragnaths) that are functionally part of the mouthparts.

The legs of postocular segments 7–13 consist of 7 elements, each: coxa, basipod, ischium, merus, carpus, propodus and dactylus (from proximal to distal). In representatives of Scutocoxifera (ingroup of Isopoda) the coxae of the anterior trunk are conjoined with the lateral parts of the tergite and form a scale-like sclerite lateral to the

rest of the tergite (coxal plate) (Dreyer and Wägele, 2002). In many representatives of Scutocoxifera the coxal plate of postocular segment 7 is conjoined with the rest of the tergite. In larval forms of Gnathiidae and *Urda* it is not clear whether there is a coxal plate in postocular segment 7. In the larval forms of Gnathiidae the coxa (or the coxal plate) of this segment is separated from the tergite (or from the rest of the tergite) and in the adult forms the coxa is (as is the tergite) conjoined with the head capsule. In Gnathiidae the first leg of the anterior is functionally part of the mouthparts. In Gnathiidae this leg (PO7) is often referred to as 'gnathopod' (larval forms) and 'pylopod' (adults).

3. Results

3.1. UPPER JURASSIC REMAINS FROM THE SOLNHOFEN AREA – TYPE MATERIAL OF *URDA ELONGATA* MÜNSTER, 1840

Material: 1 specimen, complete body, SNSB BSPG AS 493, holotype of *Urda elongata* Münster, 1840, figured in Münster, 1840, pl. 1 fig. 3, lower Tithonian, *Hybonoticeras hybonotum* Zone, Solnhofen, Bavaria, Germany.

Important morphological features: Total body length 43 mm, body slender (Figures 1B, 1C). Eyes large, extending to the posterior margin of the head (Figures 1B, 1D). Upper lip large, with rounded antero-lateral corners (Figure 1D). Mandibular incisor large, projected in anterior direction, curved 90 degrees inwards, distal part of the incisor slender and with a pointed tip, distal parts of the left and right incisor extensively overlapping (Figures 1B, 1D). Pleon tergite 3 slightly narrower than pleon tergite 2, posterior margin with distinct convex mid part (Figure 1E). Pleotelson posterior margin straight. Uropod endopod extending to the level of the posterior margin of the pleotelson. Uropod exopod narrower and shorter than the endopod (Figures 1B, 1C).

Remarks: In this specimen there is no indication of a long antenna or antennula, as it is drawn in Münster (1840, pl. 1 fig. 3). In contrast to the drawings in Kunth (1870, pl. 18 figs. 1–2, depicting a different specimen of the same species), the mandibles do not appear to be forked and the upper lip extends much more in anterior direction (Figure 1D).

3.2. UPPER JURASSIC REMAINS FROM THE SOLNHOFEN AREA – TYPE MATERIAL OF *RECKUR PUNCTATUS* MÜNSTER, 1842

Material: 1 specimen (part and counterpart), holotype of *Urda punctata* (*Reckur punctatus)* Münster, 1842, SNSB BSPG AS 496 and MB.A.0921 (part and counterparts are in different museums), figured in Münster, 1842, pl. 4 fig. 10 as '*Reckur punctatus'* and in Kunth, 1870, pl. 18 figs. 3, 3a as '*Urda punctata*' (clearly depicting MB.A.0921), Upper Jurassic, lower Tithonian, *Hybonoticeras hybonotum* Zone, Daiting, Bavaria, Germany.

Important morphological features: Total body length 52 mm. Eyes large, extending to the posterior margin of the head (Figure 2). Upper lip large. Mandibular incisor large, projected in anterior direction, curved 90 degrees inwards (Figure 1A). Pleon tergite 3 posterior margin with distinct convex mid part (Figure 2A). Pleotelson posterior margin straight to slightly concave (Figure 2B).

Remarks: The upper lip in this specimen is not well preserved and the structures that are interpreted by Kunth (1870, pl. 18 fig. 3) as the anterior and lateral margins could also be parts of the mandibles (Figure 1A). The triangular structure on the ventral side of the head, as depicted in Kunth (1870, pl. 18 fig. 3a) corresponds to a gap between the proximal parts of the mandibular incisor, the sclerite in this place is not delimited posteriorly and likely corresponds to the dorsal part of the head capsule (the fossil appears to be accessible in ventral view).

3.3. UPPER JURASSIC REMAINS FROM THE SOLNHOFEN AREA – ADDITIONAL MATERIAL

Material: 11 specimens figured herein, many of them complete bodies in various qualities of preservation, Upper Jurassic, lower Tithonian, *Hybonoticeras hybonotum* Zone or lacking further information, from the Solnhofen/Eichstätt area, Bavaria, Germany. Not figured but inspected are: 6 specimens of the collection Redenbacher (MB.A.922a-b – MB.A.927), 1 specimen of the collection Edinger (MB.A.4219) and 1 specimen figured in Kunth (1870, pl. 18 fig. 1–2, MB.A.920).

Important morphological features: Total body lengths (complete specimens only): 36.6 mm (Figure 3C), 39 mm (Figure 4A), 42 mm (Figure 5B), 44.4 (Figure 6A), 60–67 mm (Figure 7, specimen slightly distorted). Body slender, widest in the mid-part at the level of post-ocular segments 10–11 (Figures 3, 4A, 5A, 5B). Eyes large and elongate, extending to the posterior margin of the head, consisting of at least 5 rows of ommatidia, slightly tapering towards the posterior end (Figures 4D, 5C, 5D). Upper lip with proximal joint straight and wide, distal part wider than proximal part, latero-distal corners rounded (Figure 6). Antennula or antenna elements longer than wide (Figure 6D). Mandibles

sturdy, with longitudinal edges (Figures 5F–5G). Tergite of PO7 short and narrower than the head, with distinct convex posterior margin (Figures 3D, 7A, 7B). Pleon with lateral outline straight and about parallel, slightly tapering towards the posterior end. Pleon tergites 1–3 with posterior margin overall concave, convex in the mid-part and concave in the lateral parts (Figures 3B, 3C). Pleotelson on the ventral side with transverse rounded ridges in the anterior half, from the lateral sides of the anterior margin to the mid-part of the lateral margin (Figure 3C). Pleotelson posterior margin straight to slightly concave in the mid-part (Figure 6).

3.4. LOWER CRETACEOUS FOSSIL REMAINS FROM CAMBRIDGE, UK

Material: 3 specimens, syntypes of *Urda mccoyi* (*Palaega McCoyi*) (Carter, 1889), partially preserved bodies including head, trunk and pleotelson, SM B 23295, SM B 23296, and SM B 23297, figured in Carter (1889, pl. 6 figs. 1–2, 4–7) as '*Palaega McCoyi'* and in Feldmann, Wieder and Rolfe (1994, fig. 2.3–2.4, 2.6) as '*Urda mccoyi'*, Lower Cretaceous, Albian, Cambridge, Cambridgeshire, England, UK.

Important morphological features: Total body length about 30 mm (reconstructed from Figure 8A, 8C, 8E). Body elongate, with about parallel lateral outlines. Head roughly rectangular, posterior side of the head straight. Eyes on the lateral sides of the head, with posterior end at about two thirds of the length of the head. Tergite of PO7 very short, narrower than the head, posterior side convex. Tergite of PO8 much longer than that of PO7 and wider than the head. Coxal plates of PO8–9 with straight lateral margin parallel to the lateral margin of the tergite (Figures 8A, 8B). Coxal plate of PO10 anterior part wide, posterior part narrower. Coxal plates of PO11–13 anterior part narrow, posterior part wider. Tergite of PO13 postero-lateral corner pointed or tightly rounded (Figures 8C, 8D). Pleon tergites with lateral parts curved ventrally. Pleon tergites 3–4 with posterior margins evenly concave. Pleotelson gradually tapering towards the posterior side, posterior-most part not preserved in the syntypes (Figures 8E, 8F).

3.5. LOWER CRETACEOUS REMAINS FROM ALGERMISSEN, GERMANY

Material: 3 specimens, syntypes of *Urda cretacea* Stolley, 1910, one of them almost complete, two partially preserved, all of them no longer available (destroyed in a museum fire), results based on the detailed description and the figures Stolley (1910, pl. 6 figs. 2–4) as , Lower Cretaceous, Aptian, 'middle Gault', 'Acanthoplites Schichten', Algermissen (Hildesheim), Lower Saxony, Germany.

Important morphological features: Total body length about 50 mm. Head rectangular, anterior margin with a straight median portion (proximal joint of the upper lip) and

paired concave rounded incisions lateral to it (space for the proximal elements of the antennula). Eyes large and elongate, posterior end at about two thirds of the length of the head. Upper lip large, elongate bulge along the midline, anterior margin with a rounded median process. Tergite of PO7 very short, narrower than the head. Subsequent tergites of the anterior trunk much longer than that of PO7. Coxal plate of PO8 triangular. Coxal plate of PO9 parallelogram shaped. Coxal plates of PO11–12 large, with straight lateral sides parallel to the lateral margins of the tergites, antero-lateral corner angled, postero-lateral corner rounded. Pleon tergites with straight posterior margins, lateral parts curved to to ventral side. Pleon tergites 2–5 with pointed postero-lateral corners. Pleotelson about as wide as long, lateral margins in the anterior part curved to the ventral side, posterior margin evenly rounded.

Remarks: In the original description Stolley (1910) listed only 6 tergites of the anterior trunk, as opposed to 7 (PO7–13) in the ground pattern of Isopoda. However, in one of the original photographs (Stolley, 1910, pl. 6 fig. 2) a very short and wide structure is visible between the head and the subsequent tergite, most likely corresponding to the tergite of PO7.

3.6. Middle Jurassic remains from the Chřiby mountains, Czech Republic

Material: 1 specimen, partially preserved (posterior body region), collection of the University of Vienna, specimen not accessed, results based on the description and the figures, figured in Remeš (1912, pl. 1 figs. 1–3) as '*Urda moravica*', Middle Jurassic, Bathonian, 'Braunjura epsilon', Chřiby mountain region, near Koryčany, Zlín Region, Czech Republic.

Important morphological features: Body elongate, much longer than wide. Length of preserved body parts (PO11?–pleotelson) 23 mm. Segments of the anterior trunk long. Pleon segments much shorter than the segments of the anterior trunk, posterior margins about straight, with slightly convex mid part and concave lateral parts, based on the drawing (Remeš, 1912, pl. 1 fig. 4). Pleotelson longer than wide, posterior margin with narrow straight mid part.

Remarks: Remeš (1912) interpreted the fossil to represent the complete body of the animal. The head in their reconstruction (cf. drawing style in Remeš, 1912, pl. 1 fig. 4) likely corresponds to the fourth or the fifth segment of the anterior trunk, the eyes being coxal plates and the large mandibles being the lateral margins of the trunk segment.

3.7. Middle Jurassic remains from Aubenas, France

Material: 1 specimen, holotype of *Urda rhodanica* (Van Straelen, 1928), partially preserved (posterior body region, PO9–pleotelson), Institut de Géologie de I'Université de Lyon, Callovian, Aubenas, Ardèche, France. Specimen not accessed, results based on the description and the figures (Van Straelen, 1928, p. 13, text fig. 1, pl. 1 fig. 1).

Important morphological features: Body large, about 90–100 mm (estimation by Straelen 1928), longer than wide. Coxal plates of PO9–13 with transverse furrow in the anterior part. Coxal plates of 10–11 of about the same size; coxal plates of PO11–13 increasing in size. Pleon segment 2 narrower than pleon segment 1. Pleotelson about as long as coxal plate of PO13, in the anterior part with an elevation orthogonal to the midline, with a carina along the midline posterior to the elevation, posterior margin concave in the median part. Uropod endopod and exopod distally extending up to the level of the pleotelson posterior margin.

3.8. Lower Jurassic remains from Reutlingen, Göppingen and Aalen, Germany

Material: 1 specimen, paratype of *Palaega kessleri* Reiff, 1936, figured in Reiff (1936, 'Fundstück A', fig. 1a–c, pl. 1 figs. 4–5), GPIT-PV-76947, Lower Jurassic, Pliensbachian, 'Lias delta', Amaltheenton Formation, Reutlingen, Baden-Württemberg, Germany. 1 specimen, paratype of *Palaega kessleri* Reiff, 1936, figured in Reiff (1936, 'Fundstück B', fig. 2), collection of the municipal museum of Natural History in Göppingen, without accession number, Lower Jurassic, Pliensbachian, 'Lias delta', Amaltheenton Formation, Holzheim (Göppingen), Baden-Württemberg, Germany. 2 specimens, holotype of *Palaega kessleri* Reiff, 1936, figured in Reiff (1936, 'Fundstück C', figs. 3–4, pl. 1 figs. 1–3, pl. 2 figs. 1–2), paratype of *Palaega kessleri* Reiff, 1936, figured in Reiff (1936, 'Fundstück D', fig. 5), collection of the State Museum of Natural History Karlsruhe, destroyed during World War II (E. Frey, 2020, pers. comm.), Lower Jurassic, Pliensbachian, 'Lias delta', Amaltheenton Formation, Reichenbach (Aalen), Baden-Württemberg, Germany.

Important morphological features: Total body length roughly 30 mm (Figures 9C, 9D). Body elongate, widest at trunk segment 5. Head widest in the posterior part, anterior margin with a straight median portion (proximal joint of the upper lip) and paired concave rounded incisions lateral to it (space for the proximal elements of the antennula). Eyes large, elongate, posterior end extending to the posterior margin of the head, dorsal margin straight, ventral shorter than the dorsal margin (Figure 9A). Prominent dorsoventral ridge on the lateral side of the head directly anterior to the eyes (Figures 10A, 10B). Upper lip large, along the midline with slight elongate bulge,

anterior margin with a rounded median process (Reiff, 1936, fig. 3b). Antennula with proximal-most element about as wide as long and with a flat dorsal surface (Figures 10A, 10B). Tergite of PO7 very short, barely visible in the photograph, not depicted in the original drawings (Reiff, 1936 pl. 2 figs 1–2, fig). PO8 with distinct concave anterior margin (Figures 9C, 9D, 9F). PO11–13 longer than the preceding segments (Figures 9C–F, 10A, 10B). Uropod exopod narrow, distal end acute with a rounded tip (Figures 9C, 9D).

3.9. LOWER JURASSIC REMAINS FROM GÖPPINGEN AND KIRCHEIM UNTER TECK, GERMANY

Material: 1 specimen, holotype of *Palaega suevica* Reiff, 1936, figured in Reiff (1936, 'Fundstück E', figs. 7–9, pl. 1 figs. 6–9, pl. 2 fig. 3), collection of the State Museum of Natural History Karlsruhe, destroyed during World War II (E. Frey, 2020, pers. comm.), Lower Jurassic, Pliensbachian, 'Lias delta', Amaltheenton Formation, Holzheim (Göppingen), Baden-Württemberg, Germany. 1 specimen, paratype of *Palaega suevica* Reiff, 1936, figured in Reiff (1936, 'Fundstück F', fig. 10, pl. 2 fig. 4–6) as '*Palaega suevica*', GPIT-PV-76948, Lower Jurassic, Pliensbachian, 'Lias delta', Amaltheenton Formation, Kirchheim unter Teck, Baden-Württemberg, Germany.

Important morphological features: Total body length roughly 55 mm (Figures 10C, 10D). Body elongate, widest at PO11. Head widest in the posterior part, anterior margin with a straight median portion (proximal joint of the upper lip) and paired concave rounded incisions lateral to it (space for the proximal elements of the antennula). Eyes large, elongate, posterior end extending to the posterior margin of the head, dorsal margin straight in lateral view, ventral margin straight and shorter than the dorsal margin, anterior margin slightly convex in lateral view, posterior margin oblique and straight in lateral view (Figures 10D, 10J, 11A, 11F). Prominent dorsoventral ridge on the lateral side of the head directly anterior to the eyes (Figures 10C, 10J). Upper lip large, along the midline with slight elongate bulge, anterior margin with a rounded median process, proximal-most part with a distinct transverse ridge on the dorsal side (Reiff, 1936, fig. 10; Figures 10E–I, 11B–F). Mandible incisor large strongly curved inwards, with a pointed tip (Reiff, 1936, figs. 7b, 8, 10, pl. 2 fig. 6), lateral side of the incisor with a longitudinal ridge (Figures 11B, 11F), ventral side of the incisor with a curved ridge (Figures 11B, 11C). Maxillula about as long as the anterior-posterior extent of the mandibles, slender, straight, tapering towards the distal end, dorsal side with a curved longitudinal ridge (Figures 10F, 10G). Maxilliped wider than the maxillula, proximal part possibly with a leaf shaped lateral expansion (Figures 10F, 10G); alternatively, this

structure could be part of the head capsule. Tergite of PO7 short (Figure 11E), see also the gap along the midline between the posterior margin of the head and the anterior margin of the subsequent tergite (Fig 10C). Tergite of PO8 with distinct concave anterior margin (Reiff, 1936, fig. 5; Figure 10C).

3.10. Lower Jurassic remains from Östringen, Germany

Material: 1 specimen, holotype of *Urda liasica* Frentzen, 1937, posterior part of the body, figured in Frentzen (1937, text fig. 1b), collection of the State Museum of Natural History Karlsruhe, destroyed during World War II (E. Frey, 2020, pers. comm.), Lower Jurassic, Toarcian, *Phlyseogrammoceras dispansum* Zone, 'Lias zeta', Dinkelberg, small hill north of Östringen, Baden-Württemberg, Germany.

Important morphological features:

Body elongate, length of the preserved part 15 mm (PO11–pleotelson). PO11–12 long, with large coxal plates. Pleon tergites much shorter and of about the same width than the tergites of the anterior trunk region. Pleotelson elongate, about as wide as long, with an evenly rounded posterior margin.

Remarks: From the drawing it is not completely apparent to which segments some of the sclerites belong. The presence of 3 pairs of coxal plates suggests that the anterior-most sclerite belongs to PO11.

3.11. Lower Cretaceous remains from Stemmerberg (Hannover), Germany

Material: 1 specimen, holotype of *Palaega stemmerbergensis* Malzahn, 1968, massively affected by pyrite decay to the time of the original description, figured in Malzahn (1968 pl.58, figs. 1, 2, 4–6), collection of the Niedersächsisches Landesamt für Bodenforschung, specimen lost or misplaced (C. Heunisch, 2019, pers. comm.), Lower Cretaceous, Hauterivian, *Endemoceras noricum* Zone, drill core 'Stemmerberg 7', Stemmerberg (Hannover), Lower Saxony, Germany.

Important morphological features: Body elongate, total body length about 27 mm (Malzahn, 1968, p. 828). Head wider than long (Malzahn, 1968, fig. 4), anterior margin of the head with a straight median portion (proximal joint of the upper lip) and paired concave rounded incisions lateral to it (space for the proximal elements of the antennula) (Malzahn, 1968, figs. 1–2). Eyes large, on the lateral side of the head, elongate, kidney shaped, with pentagonal and hexagonal ommatidia (Malzahn, 1968, p. 829). Antennula with proximal article about as wide as long and dorsal surface flat to slightly bulged (Malzahn 1968, figs. 1–2). Upper lip large (Malzahn, 1968, figs. 1–2). Mandible incisor large, curved inwards (Malzahn, 1968, p. 829). Tergite of PO7 short and narrow

(Malzahn, 1968, fig. 4). Leg of PO7 on the ventral side of the head and projected anteriorly (Malzahn, 1968, p. 829). PO8 with coxal plate about rectangular (Malzahn, 1968, p. 830). Pleon tergite 5 longer along the midline than preceding tergites (Malzahn, 1968, fig. 5). Pleotelson about as wide as long (Malzahn, 1968, fig. 5).

3.12. Upper Jurassic remains from the Huriwai River, New Zealand

Material: 1 specimen, holotype of *Urda zelandica* Buckeridge and Johns, 1996, posterior part of the body, figured in Grant-Mackie *et al.* (1996 figs. 3–5), A406 collection of the Geology Department, University of Auckland, Upper Jurassic, middle to upper Tithonian, locality R13/f7080, Huriwai River, near Port Waikato, North Island, New Zealand.

Important morphological features: Body elongate, length of the preserved part (trunk segment 6 to pleotelson) 15.1 mm (Grant-Mackie et al., 1996, p. 36). Pleotelson slightly wider than long, posterior margin evenly rounded.

Remarks: The description in Grant-Mackie *et al.* (1996) rests upon the assumption that there are only 6 tergites of the anterior trunk. Therefore, their PO11 is herein interpreted as PO12.

3.13. Middle Jurassic remains from Bielefeld, Germany – material presented in Nagler et al. (2017)

Material: 2 specimens, SNSB – BSPG 2011 I 50a,b figured in Nagler *et al.* (2017, fig. 1A–B, D, G, fig. 3A–C, fig. $4A_6$, fig. 6) as '*Urda rostrata*' and SNSB – BSPG 2011 I 51, figured in Nagler *et al.* (2017, fig. 1C, E, fig. 2, fig. 3D–F, fig. $4A_{1–5, 7}$, $B_{1–7}$, $C_{1–3}$, fig. 5) as '*Urda rostrata*', Middle Jurassic, Bajocian, *Parkinsonia parkinsoni* Zone, quarry 'Bethel 1', Bielefeld, North Rhine-Westphalia, Germany.

Important morphological features: Body elongate, much longer than wide, total body length about 35 mm (Figure 12A). Head anterior margin with a straight median portion (proximal joint of the upper lip) and paired shallow concave rounded incisions lateral to it (space for the proximal elements of the antennula), posterior margin straight (Figures 12A–C, 13C, 13D). Eyes on the lateral side of the head, elongate, posterior end at about ¾ of the heads length (Figures 12A, 13A, 13C, 13D). Lateral side of the head on the anterior end with distinct dorsal-ventral ridge (anterior to the eye) (Figures 12A–C). Antennula proximal-most element with flat dorsal surface, subsequent elements about cylindrical, much narrower than the proximal-most element. Antenna short, two elongate cylindrical elements ('peduncle'), followed by multiple much shorter elements ('flagellum'; Figure 14). Upper lip large, wider than long, trapezoid, distal part wider

than proximal part, anterior margin with a rounded median process (Figures 12B, 12C). Mandible incisor large, about 90 degrees curved inward, with a pointed tip (Figures 12B, 12C, 14C, 14D, 14G, 14H, 15K, 15L). Tergite of PO7 very short and narrower than the head, posterior margin straight (Figures 12A, 13A). Leg of PO7 parallel to the ventral side of the head, its distal end pointing in anterior direction (to the mouth parts), coxa short, not visible in lateral view, basipod widening towards the distal end, ischium about as long as the preceding element, widening towards the distal end, merus much shorter than the preceding element, carpus triangular, shorter than the preceding element, propodus large, much longer and wider than the preceding element, lateral surface convex, median surface flat, dactylus thin, gently curved inwards, about as long as the preceding element (Figures 14C, 14D, 14G, 14H, 16G, 16H). Tergite of PO8 much longer than the preceding tergite and wider, about as wide as the head (Figures 12A, 13 A, 14E, 14F).

Coxal plates of PO8–9 with straight lateral margin parallel to the lateral margins of the tergites (Figures 13A, 14E, 14F). Leg of PO8 much larger than the leg of the preceding segment, ischium proportionally shorter than in the leg of the preceding segment, merus lateral surface convex, larger than in the leg of the preceding segment, dactylus thin, curved inwards, about ⅔ of the length of the preceding leg element (Figures 14, 16A–D). Coxal plate 4 triangular, anterior part wide, posterior part narrow (Figures 14E, 14F). Coxal plates of PO11–13 anterior part narrow and posterior part wider (Figures 12A, 12E, 14E, 14F). Legs of PO11–13 ischium slenderer than in leg of PO8, merus flattened in anterior-posterior direction, lateral side straight, carpus widening in towards the distal end, proportionally longer than in leg of PO8, distal end with 2 spines on the median side, propodus slender, curved inwards, dactylus thin, curved inwards, about ½ of the length of the preceding element (Figures 14A–F, 16A, 16B, 16E, 16F). Tergite of PO13 shorter than preceding tergite, postero-lateral corner widely rounded (Figures 12A, 12E). Coxal plate of PO13 with posterolateral corner extending posterior to tergite of PO13, the posterior part being lateral to the anterior-most pleon tergites (Figure 12A). Pleon tergites 2–5 with lateral parts curved to the ventral side, postero-lateral corners pointed and distinctly projecting posteriorly (Figures 14A, 14B). Pleon tergite 5 longer along the midline than the preceding tergites (Figures 12A, 12E). Pleotelson about as wide as long, posterior margin evenly rounded (Figure 12D). Uropod endopod lateral margin with denticles (Figure 12D).

3.14. MIDDLE JURASSIC REMAINS FROM BIELEFELD, GERMANY – ADDITIONAL MATERIAL

Material: 3 specimens, ES/jb-8744, ES/jb-30755, and ES/jb-30756, Middle Jurassic, Bajocian, *Parkinsonia parkinsoni* Zone, quarry 'Bethel 1', Bielefeld, North Rhine-Westphalia, Germany.

Important morphological features: Body elongate, much longer than wide, total length about 34 mm (Figure 17A). Head anterior margin with a straight median portion (proximal joint of the upper lip) and paired concave rounded incisions lateral to it (space for the proximal elements of the antennula), posterior margin straight (Figures 17A, 17B). Eyes on the lateral side of the head, elongate, posterior end at about three quarters of the length of the head (Figures 17A, 17B). Tergite of PO7 very short and narrower than the head, posterior margin straight (Figures 17A, 17B). Tergite of PO8 much longer than the preceding tergite and wider, about as wide as the head (Figures 17A, 17B). Coxal plate of PO8 with straight lateral margin parallel to the lateral margins of the tergites. Coxal plates of PO12–13 anterior part narrow and posterior part wider (Figures 17C, 17D, 18C–F). Tergite of PO13 shorter than preceding tergite (Figures 17A–D). Coxal plate of PO13 with posterolateral corner extending posterior to tergite of PO13, the posterior part being lateral to the anterior-most pleon tergites (Figures 17A–D). Pleon tergites 2–5 with lateral parts curved to the ventral side, postero-lateral corners pointed and distinctly projecting posteriorly (Figure 18). Pleon tergite 5 longer along the midline than the preceding tergites (Figures 17A–D, 17F).

4. Discussion

4.1. THE TYPE MATERIAL OF *URDA* AND ADDITIONAL FOSSILS FROM SOLNHOFEN

There are numerous fossil remains of the group *Urda* from the lithographic limestones of the Solnhofen area in Southern Germany, which are all early Tithonian (Late Jurassic) in age. Initially, Münster (1840) described 4 species of *Urda* from Solnhofen, shortly afterwards Münster (1842) and Meyer (1856) described two additional species of Isopoda with a similar appearance under the generic name *Reckur*, which was later synonymised with *Urda* (Oppel, 1862; Kunth, 1870). Although it was possible to explain most of the species differences listed by Münster (1840, 1842) and Meyer (1856) as artefacts of preservation or negligent mistakes (e.g., the type specimen of *Urda cincta* is the counterpart of the type specimen of *Urda decorata*), Kunth (1870) did not venture to synonymise the remaining species *Urda rostrata* and *Urda punctata*, because of the morphology of the mouthparts, which seemingly differed between the species.

With the aid of fluorescence microscopy and macro photography using fluorescent light settings, we could show that the differences in the interpretation of the mouthparts (Kunth, 1870, pl. 18 figs. 1–2 vs. fig. 3) in the type material of *U. elongata (= U. rostrata)* (Figure 1D) and *U. punctata* (Figure 2A) can easily be explained by misinterpretation due to different modes of preservation. Kunth (1870) interpreted the mandible in the type specimen of *U. rostrata* to be bifurcate; however, in the fluorescence image (Figure 1D) it is apparent that the mandible is not bifurcate and the upper lip is much larger than depicted by Kunth (1870, pl. 18 fig. 1). Also, it is apparent from the fluorescence images that the conspicuous triangular sclerite of *U. punctata* depicted in Kunth (1870, pl. 18 fig. 3a) is in fact a part of the head capsule and not a distinct sclerite (Figure 2A). The upper lip morphology in the type material of *U. rostrata* and *U. punctata* is also consistent with the upper lip morphology in the herein presented additional material (Figures 5F, 5G, 6B, 6D).

There seems to be a variation in the proportional length of the anterior trunk region (cf. Figures 1 A, 5A, 5B, 7A, 7B vs. 2, 6A–C). However, it is not clear, whether this variation is due to a variation in the living animal – where it could be interpreted as a possible sexual dimorphism – or due to a post-mortem distortion. Therefore, we conclude, that there is only a single species of *Urda* from the lower Tithonian of Solnhofen. In this case, *U. punctata* is considered a junior subjective synonym of *U. rostrata* (see taxonomy section below).

4.2. MORPHOLOGICAL CHARACTERISTICS OF *URDA*

The type species of *Urda – Urda rostrata* Münster, 1840 – has a series of morphological features that are derived (not part of the ground pattern of Isopoda) and not present in other species of Isopoda, except for those within the group Gnathiidae Leach, 1814 (see discussion below).

The upper lip in *U. rostrata* is large and, despite the good preservation, neither the frontal lamina, which in other representatives of Isopoda is located dorsal to the clypeus, nor the labrum, which in other representatives of Isopoda is located ventral to the clypeus, is recognisable as a distinct structure in the fossil remains. The mandible is large, its incisor is projected towards the anterior side of the head, in dorsal view protruding from the rest of the head and strongly curved (about 90 degrees). The tergite of postocular segment 7 (the one directly posterior to the head) is very short (the subsequent tergites are much longer) and it is also not as wide as the head or the subsequent tergites.

Additional characteristics, which can also be seen also in other lineages of Isopoda, comprise the elongate shape of the body (e.g. Brandt and Poore, 2003 fig.

1A,D,G), the large eyes on the lateral sides of the head (Delaney, 1989 fig. 1C,E) and the shape of the pleotelson, which lateral sides are about parallel in the anterior part (e.g. Camp and Heard, 1988; Bruce and Olesen, 2002 fig. 8A; Bruce, 2005; Thamban et al., 2015 fig. 8A). A concave part of the posterior margin of the pleotelson as present in some individuals of *U. rostrata* (Figures 2B, 6A) can also be seen in other lineages of Isopoda, such as in Aegidae (e.g. Bruce, 2009 fig. 19A,E).

4.3. REINTERPRETATION OF FOSSILS FROM THE LITERATURE (IN HISTORICAL ORDER)

Urda mccoyi *(Carter, 1889) – type material only*

The type specimens of *Urda mccoyi* differ from *U. rostrata* in having considerably shorter eyes, a proportionally longer tergite of PO8 than in *U. rostrata* (cf. Figures 8A, 8B vs. Figures 7A, 7C) and rounded posterior margin of the pleotelson instead of a straight or slightly concave posterior margin as in *U. rostrata* (cf. Figures 8E, 8F vs. 1A, 5E). Additionally, the remains of *U. rostrata* are about 40 million years older than the type specimens of *U. mccoyi*.

      Urda mccoyi and *U. rostrata* share a similar body shape. The rectangular shape of the head is also very similar, which is likely due to a similar arrangement of the mouthparts (wide upper lip joint and protruding mandibles), which is not apparent from the fossils itself (Figures 8A, 8B). The eyes in both species are elongate and located on the lateral sides of the head (cf. Figures 8A, 8B vs. 5C, 5D). In both species, the tergite of PO7 is very short (the subsequent tergites are much longer) and narrower than the head (Figures 8A, 8B vs. 5C, 5D, 7), which is dissimilar to other representatives of Isopoda (except for those within Gnathiidae, see discussion below). Thus, it is most likely that *U. mccoyi* is a close relative of *U. rostrata*.

Urda cretacea *Stolley, 1910*

The type specimens of *Urda cretacea* have shorter eyes than representatives of *U. rostrata*. In *U. cretacea* the anterior margin of the upper lip has a median process (Stolley, 1910 pl. 6 fig. 4), whereas in *U. rostrata* the anterior margin appears to be straight or slightly convex (Figures 1D, 5F, 5G). Unlike in *U. rostrata*, the pleotelson in *U. cretacea* is evenly rounded (Stolley, 1910 pl. 6 fig. 2). In *U. cretacea* the head is about as wide as the tergite of PO8 and the straight portion of the posterior margin of the head in dorsal view is wide (Stolley, 1910 pl. 6 figs. 2,4), whereas in the slightly younger (Figure 19) fossils of *U. mccoyi* the head is markedly narrower than the tergite of PO8 and the straight portion of the posterior margin of the head in dorsal view is narrower (Figures 8A, 8B). Additionally, the type specimens of *U. cretacea* are about 30 million

years younger than the type specimens of *U. rostrata* and at least 3.6 million years younger than those of *U. mccoyi*.

The head morphology in *U. cretacea* is very similar as in *Urda rostrata*; in both species the upper lip is large and its proximal joint in wide and straight. Lateral to the upper lip joint, in both species there are concave incisions on the dorsal side of the head capsule, where the proximal element of the antennula is located. In both species the tergite of PO7 is very short (Stolley, 1910, pl. 6 fig. 2, not mentioned in the original description). Thus, it is most likely that *U. cretacea* is a close relative of *U. rostrata* and *U. mccoyi*.

Urda moravica *Remeš, 1912*

Although the holotype of *Urda moravica* resembles *U. rostrata* and the other two above mentioned species in some characters (elongate body, shape of the pleotelson; Remeš, 1912 fig. 1–3), similar expressions of those characters can also be found in other lineages of Isopoda as well (see discussion above). It is important to note, that the interpretation in Remeš (1912) unlikely reflects the body organisation of the fossil, most notably the large mandibles described in Remeš (1912) are probably either lateral margins of a tergite or coxal plates. The allegedly present eyes are most likely coxal plates. Therefore, despite some similarities, *U. moravica* cannot reliably be interpreted as a close relative of *U. rostrata*.

Furthermore, the preservation of the specimen does not allow to differentiate the species from other species such as for example *Urda cretacea* or the fossil remains from Bielefeld (*U. rostrata* sensu Nagler *et al.*, 2017). Therefore, we suggest treating *Urda moravica* as a *nomen dubium* until further material becomes available.

Urda rhodanica *Van Straelen, 1928*

Urda rhodanica can safely be identified as a species within the group Scutocoxifera based on the presence of coxal plates (Dreyer and Wägele, 2002). The head and the anterior part of the trunk are not preserved in the holotype of *U. rhodanica*. Consequently, it cannot be affirmed, whether the distinct morphological features that are shared between *U. rostrata*, *U. mccoyi* and *U. cretacea* (see discussion above) are present in representatives of *U. rhodanica*. *Urda rhodanica* also differs from the above-mentioned species in features of posterior body part. In *U. rhodanica* the coxal plate of PO12 is much larger than the coxal plate of PO11 and the coxal plate of PO13 is even larger than the coxal plate of PO12, whereas in *U. rostrata* the coxal plate of PO13 is smaller than the preceding coxal plates (Figures 3B, 3C, 4A). The size of the coxal plates in *U.*

rhodanica is also different from that in *U. mccoyi* (Figures 8C, 8D) and *U. cretacea* (Stolley, 1910, pl. 6 figs. 2a,3a), the latter two species being more similar to *U. rostrata* in this aspect. The posterior margin of the pleotelson in *U. rhodanica* has a distinct concave notch, which is much more prominent than in the few specimens of *U. rostrata*, where the posterior margin of the pleotelson also has a concave portion (Figures 2B, 6A). Ultimately, *U. rhodanica* cannot be reliably interpreted as a close relative of *U. rostrata*. Moreover, the differences between *U. rhodanica* and the above-mentioned species make it also unlikely that *U. rhodanica* is closely related *U. rostrata*.

Close relatives of Urda rostrata *hiding within* Palaega *Woodward, 1870*

Reiff (1936) noticed differences in the shape of the upper lip between specimens of *Palaega kessleri* (pentagonal shape, Reiff, 1936 fig. 3b, 4) and *Palaega suevica* (hexagonal shape, Figures 11A, 10E–G). However, the shape of the clypei only differs in the distal-most part. In the specimen 'Fundstück C' (*P. kessleri*, specimen destroyed) a transverse ridge is depicted at the place where in the specimens of *P. suevica* there is the distal margin. This makes it likely that the overall hexagonal upper lip shape in *P. suevica* is an artefact of the preservation rather than an original morphological feature that distinguishes the two species.

Reiff (1936) listed a different proportional length of the pleon between *Palaega kessleri* (Figures 9C–F) and *Palaega suevica* (Figures 10C, 10D). However, this difference is probably described by the different proportional lengths of the tergites of PO10–12 (cf. Fig 10A, 10B vs. 10C, 10D). A similar variability in the lengths of these tergites can also be found in *Urda rostrata* (cf. Figures 6, 7) and can well be explained by sexual dimorphism (longer tergites in females due to the presence of a brood pouch). Therefore, we conclude, that the type material of *Palaega kessleri* and *Palaega suevica* comes from the same biological species. In this case, *P. kessleri* should be seen as the subjective synonym of *P. suevica* (see taxonomy section below).

The head morphology in *P. suevica* (incl. *P. suevica* in the following) is very similar to that in *Urda rostrata*. The upper lip is large and its proximal joint is wide and straight; lateral to the upper lip joint, there are concave incisions on the dorsal side of the head capsule (insertion point of the proximal antennula elements; Figures 11A, 10B, 10J). The mandibles are large, projected in anterior direction and strongly curved (Figures 10E–I, 11B, 11C, Reiff, 1936, pl. 2 fig. 6).

Even though not recognised by Reiff (1936), in representatives of *P. suevica* there is a very short tergite visible (PO7) anterior to the much longer ones of the rest of the anterior trunk region (Figure 11E, Reiff, 1936, pl. 2 figs. 1–2). Here, the morphology of

the tergite of PO8 seemingly speaks against a short first tergite being present, because in PO8 the coxal plates are conjoined with the tergite (Figures 9C–F, 11A). In many representatives of Scutocoxifera, which is a monophyletic group characterised by the presence of coxal plates (Dreyer and Wägele, 2002), in PO7 the coxal plate is conjoined with the tergite. However, in larval forms of some species of Gnathiidae, where the tergite of PO7 is also very short, post-ocular segment 8 has coxal plates that are conjoined with the tergite – the morphological feature is shifted one segment posterior (Monod, 1926 fig. 13; Smit et al., 1999 fig. 31, 2003 fig. 14; Manship et al., 2011 fig. 4G). Considering the morphological features, especially those of the head, shared with *U. rostrata*, which are, except for representatives of Gnathiidae and the above-mentioned species, not present in other lineages of Isopoda, we interpret *P. suevica* as being closely related to *U. rostrata*.

Palaega suevica differs from *U. rostrata*, *U. mccoyi* and *U. cretacea* in having the coxal plate of PO8 conjoined with the tergite. *Palaega suevica* has a convex posterior margin of the head instead of a straight margin as in *U. mccoyi* and *U. cretacea*. The distal margin of the upper lip in *U. rostrata* is stout and evenly rounded (Figures 1D, 5F, 5G, 6B, 6D), whereas in *P. suevica* it has a distinct median convexity (Reiff, 1936, fig. 3b, 4). In addition, the remains of *P. suevica* are at least 30 million years older than the type material of *U. rostrata* and even older than the type material of *U. mccoyi* and *U. cretacea*. Therefore, it is unlikely that *P. suevica* is conspecific with *U. rostrata* or its close relatives.

Keupp and Mahlow (2017 p. 167, fig. 10) identified a fossil specimen from the Amaltheenton Formation of Buttenheim (Lower Jurassic, upper Pliensbachian, *Pleuroceras spinatum* Zone) as a representative of *Palaega suevica* sensu Reiff (1936). Being of about the same age as the specimens from Reiff (1936), the specimen in Keupp and Mahlow (2017, SNSB BSPG 2016 I 32) resembles the type specimens in having a broad straight upper lip joint and eyes that are located on the lateral sides of the head (visible in an unpublished μCT scan, Keupp and Mahlow, 2017, p. 167). Because many body parts are not exposed to the rock surface, only a detailed study of the μCT scan or further mechanical preparation will reveal further information about the possible conspecificity with the material from Reiff (1936) and the relationship to *U. rostrata* and the extant group Gnathiidae.

Urda liasica Frentzen, 1937 sensu Frentzen (1937)
In some respects, the holotype of *Urda liasica* resembles other fossils that have been associated with the name *Urda*. For example, the tergites of the anterior trunk are long

and the coxal plates are large; also, the pleotelson is longer than wide, its lateral margins are parallel in the anterior part and its posterior margin is evenly rounded (Frentzen, 1937 text fig. 1b). However, because only the posterior part of the body is known, the key morphological features of the type species of Urda – *Urda rostrata* – are not known to be present in the holotype of *U. liasica*. A close relationship between the type specimen of *U. liasica* and *U. rostrata* is possible, as there are no morphological features that would suggest otherwise. Yet, because the features present in the type specimen of *U. liasica* also occur in other lineages (see discussion above), such a close relationship cannot be inferred from the holotype.

The holotype (and only type) of *U. liasica* was destroyed in World War II. Therefore, only a single drawing is available. Based on this drawing, which appears to be a rather stylised than detailed depiction, it is not possible to clearly distinguish the fossil from other fossil occurrences (cf. Figures 12A, 12D). Therefore, we suggest treating *Urda liasica* as a *nomen dubium* and its holotype as a representative of Scutocoxifera of uncertain systematic position.

Palaega stemmerbergensis Malzahn, 1968 sensu Malzahn (1968)
The holotype of *Palaega stemmerbergensis* shares multiple morphological features with *U. rostrata*, that otherwise only occur in representatives of Gnathiidae and fossil remains of close relatives of *U. rostrata*. The joint between the dorsal surface of the head capsule and the upper lip is wide and straight, lateral to it are concave rounded incisions, where the proximal element of the antennula is located (Malzahn, 1968 figs. 1–2). The mandible incisors are large and curved inwards (Malzahn, 1968, p. 829). The tergite of PO7 is short and narrow (Malzahn, 1968, fig. 4). The leg of PO7 is located on the ventral side of the head with its distal part pointing anteriorly (Malzahn, 1968, p. 829). The morphology of the leg of PO7 is not apparent in any of the fossils of *U. rostrata* from Solnhofen. However, the orientation of the first trunk leg as described by Malzahn (1968, p. 829) is very similar to that in representatives of Gnathiidae (see discussion below). Additional similarities between the type material of *P. stemmerbergensis* and *U. rostrata*, that are also present in other lineages of Isopoda, comprise the elongated body shape, the position of the eyes on the lateral sides of the head (Malzahn, 1968 fig. 4, p. 829).

The holotype of *P. stemmerbergensis* has already been strongly deformed due to pyrite decay when it was described (Malzahn, 1968), rendering many features of the body incomparable to other specimens. Furthermore, it could not be located in the collection, where it should have been deposited (C. Heunisch, 2020, pers. comm.). This makes it impractical to differentiate *P. stemmerbergensis* from other species based on its

morphological features. For example, the morphology of the *P. stemmerbergensis* type material is similar to the about 20 million years younger fossils of *U. cretacea* (both Early Cretaceous in age, Figure 19), yet most of the body parts where there could be differences between the type of *P. stemmerbergensis* and representatives of *U. cretacea* have not been described in detail nor visible in the figurers of Malzahn (1968). Therefore, we suggest treating the name *Palaega stemmerbergensis* as a *nomen dubium* and its holotype as *Urda* sp. (see taxonomic part).

Urda zelandica Buckeridge & Johns, 1996 sensu Buckeridge & Johns (1996)
The holotype of *Urda zelandica* can safely be identified as a representative of the group Scutocoxifera based on the presence of coxal plates (Dreyer and Wägele, 2002). It resembles other fossils that have been associated with the name *Urda* in the body parts which are preserved in the specimen. Namely, this resemblance comprises the elongate body shape, the pleon tergites, which lateral parts are either stout or curved towards the ventral side (Grant-Mackie *et al.,* 1996, figs. 3–4, p. 36), and the shape of the pleotelson, which lateral margins are about parallel in the anterior part and its posterior margin is evenly rounded or with a narrow straight mid-part (Grant-Mackie et al., 1996, fig. 5).

While the holotype of *U. zelandica* resembles representatives of *U. rostrata* in some aspects, it consists only of strongly compressed remains of the posterior body region and therefore lacks the body parts in which *U. rostrata* differs from other representatives of Isopoda (see discussion above). Thus, a close relationship between *U. zelandica* and *U. rostrata* can not be reliably inferred based on morphological features. The compressed nature of the fossil and that only the posterior body region is preserved make it difficult to morphologically distinguish the type specimen of *U. zelandica* from other fossils and from extant representatives of Isopoda. Therefore, we suggest to treat *Urda zelandica* as a *nomen dubium* and its holotype as a representative of Scutocoxifera of uncertain systematic position, until further material becomes available.

The fossils from the Middle Jurassic of Bielefeld, Germany
The fossil material from Bielefeld presented in Büchner (1971) and Nagler *et al.* (2017) differs from the remains of *Urda rostrata* from Solnhofen in many aspects. In the Solnhofen material the eyes extend to the posterior end of the head (Figures 3, 4C), whereas in the material from Bielefeld the eyes end at about three quarters of the length of the head (Figures 12A, 13C, 17A). In the Solnhofen fossils the tergite of PO7 is narrow and its posterior margin is distinctly convex (Figures 3D, 7A); in the Bielefeld fossils the corresponding tergite is wider and its posterior margin is less convex (Figures

17A, 12A). The pleotelson in the Solnhofen fossils has a straight posterior margin, in some cases even with a slightly concave mid-part (Figures 1A, 1B, 5E); in the fossils from Bielefeld, however, the posterior margin is evenly rounded (Figure 12D). Additionally, the occurrence of *U. rostrata* from Solnhofen is about 16 million years younger than the fossils from Bielefeld (Figure 19). Therefore, it is unlikely that fossils of both localities come from a single species.

As in the fossils of *U. rostrata* from Solnhofen, the upper lip in the fossils from Bielefeld is also large and with a wide joint to the head capsule with rounded incision lateral to the joint, where the proximal elements of the antennula insert (Figures 12B, 12C, 13C, 13D). The mandible incisors in the Bielefeld fossils are large and strongly curved, with a pointed tip as it is the case in representatives of *U. rostrata* from Solnhofen (cf. Figures 15K, 15L vs. Figures 1D, 1E). The tergite of PO7 is also very short and narrower than the head and the tergite of PO8 in both the fossils from Solnhofen and the fossils from Bielefeld (Figures 17A vs. 7A). Therefore, we interpret the fossils from Bielefeld to be from a separate species, which is closely related to *U. rostrata*.

In the fossils from Bielefeld the legs of PO7 are preserved and their morphology, size and relative position to the head is well visible in renderings of the µCT scans (Figures 16C, 16D, 16G, 16H). The much smaller size relative to the subsequent legs and the position on the ventral side of the head, with the distal elements projected anteriorly, is very similar to the condition in larval forms of Gnathiidae (Figure 20B). A similar orientation and relative size of the legs of PO7 also occurs in some representatives of Aegidae (e.g. Nozères, 2008) and Cymothoidae (van der Wal and Haug, 2020 fig. 20).

In the here studied remains of *U. rostrata* from Solnhofen the leg of PO7 is either not preserved or overlain by other structures. In µCT renders of two of the specimens from Bielefeld the maxilliped is visible (Figures 14C, 14D, 14G, 14H, 15K, 15N). The maxilliped is notably slenderer than in representatives of Cymothoidae (Figure 15I) and adult forms of Gnathiidae (Figure 15H). The slender shape of the maxilliped is similar to larval forms of Gnathiidae (e.g. Ota, 2014 fig. 13; Figure 20B). In the remains of *U. rostrata* from Solnhofen there is only one specimen that has a paired structure on the ventral side of the head that could potentially be mains of the maxillipeds (Figures 5F, 15G). Because of the strong similarity in the body parts that are known from both occurrences, it is likely that representatives of *U. rostrata* had a similar morphology of the legs of PO7 and the maxilliped as the fossils from Bielefeld.

The fossils from Bielefeld differ from representatives of *U. mccoyi* in having a less bulged head and a less convex posterior margin of the tergite of PO7 (cf. Figures 12B,

12C, 13A, 13B vs. 8A, 8B). Additionally, the fossil material from Bielefeld is about 60 million years older than the type fossil of *U. mccoyi*. From representatives of *U. cretacea* the Bielefeld fossils differ in having a narrower head; in *U. cretacea* the second tergite of the trunk is about as wide as the head (Stolley, 1910, pl. 6 figs. 2,4), whereas in the fossils from Bielefeld the second tergite of the trunk is markedly wider than head (Figures 12A, 13B). Furthermore, the fossils from Bielefeld are more than 50 million years older than the type material of *U. cretacea*. Representatives of *P. suevica* lack distinct coxal plates in PO8 (Figures 9C–F), whereas the fossils from Bielefeld clearly have distinct coxal plates in PO8 (Figures 12B, 13A). Also, in representatives of *P. suevica* the posterior margin of the head is convex (Figures 10B, 10C, 10J), whereas in the fossils from Bielefeld the posterior margin of the head has a straight mid-part (Figures 3B, 17A). The fossils of *P. suevica* are about 15 million years older than the fossils from Bielefeld. Therefore we interpret the fossils from Bielefeld to be from a distinct species, which is closely related to *U. rostrata*; its description is presented in the taxonomy section below.

4.4. OTHER MENTIONS OF *URDA* IN THE FOSSIL RECORD

Feldmann *et al.* (1994) presented a single specimen (GSE 15083) from the Oxfordian (Upper Jurassic) of the Isle of Skye (UK). The specimen is complete, except for the appendages which are not preserved or not exposed to the surface of the sediment. The shape of the head is typical for *U. rostrata* and its close relatives, the upper lip joint is wide, there are rounded incisions where the antennula inserts and the eyes are elongate and on the lateral sides of the head. The tergite of PO7 is very short and narrower than the head (Feldmann et al., 1994 figs. 1–2,5,7). Therefore, and due to the overall similarity between the specimen, *U. rostrata* and its close relatives mentioned above, it is most likely that the fossil described by Feldmann *et al.* (1994) comes from a close relative of *U. rostrata*. Feldmann *et al.* (1994) noted the striking similarity between this specimen and the type material of *U. mccoyi* (Upper Cretaceous, UK), based on which they suggested that the specimen from Skye is a representative of *U. mccoyi* despite the age difference of at least 53 million years (Figure 19). One difference that could indicate that the specimen from the Isle of Skye might be from a different species are the dimensions of the pleotelson. In the specimen from Skye the pleotelson is wider than long (Feldmann et al., 1994, p. 89 fig. 2.7), whereas in the type material of *U. mccoyi* the pleotelson is more elongate (about as wide as long, Figures 8E, 8F).

From the mid-Bajocian (Middle Jurassic) of Velpe (near Osnabrück, Germany) there is one incomplete specimen (Ruhr Museum Essen, Germany), which has been

associated with the name *Urda* because of the shape of the pleotelson (Wittler, 2007, 2011). In this specimen only the pleon (segment 2 onwards) and the pleotelson are preserved and the specimen is lacking visible remains of appendages. This specimen is of about the same age (less than one million years older) as the fossils from Bielefeld (Büchner, 1971; Wittler, 2007). Despite the partial preservation in the fossil from Velpe, which would not allow for a robust and precise systematic interpretation of the fossil, the strong resemblance to the fossils from Bielefeld (cf. Figure 12A vs. Wittler, 2011, figs. 1– 2) and small age difference suggest that the fossil from Velpe comes from the same species as the fossils from Bielefeld.

From the lower Pliensbachian (Lower Jurassic) of Östringen (Southern Germany) there is one record of a fossil remain (SMNK, destroyed) Frentzen (1937) described as '*Urda* spec.'. The fossil consists of 3 bilateral-symmetric sclerites (Frentzen, 1937 text fig. 1a). The sclerites provide no morphological indication that they are from a representative of Isopoda (or even Eucrustacea). Also, the sclerites do not resemble those of the holotype of *U. liasica* (treated as a *nomen dubium* herein), which was found in a nearby fossil site and described by the same author (Frentzen, 1937).

There is a single fossil (PIMUZ 132a Sch 70) from the lower Aalenian (Middle Jurassic) of Schinznach-Dorf (Canton of Aargau, Switzerland), which Etter (1988) described as *Urda* sp. While the parts of the body that are preserved in the fossil resemble those of close relative of *U. rostrata* (as discussed above), the fossil consists only of remains of the posterior region of the body (Etter, 1988 fig. 6). The similarity to *U. rostrata* is apparent particularly in the pleotelson which has a concave mid-part of the posterior margin, similar to some fossils of *U. rostrata* (Figures 2B, 6). However, similar pleotelson morphologies also occur in other lineages of Isopoda, such as in representatives of Aegidae (Bruce, 2009 fig. 19A,E). Therefore, while it is possible that the fossil from Schinznach-Dorf is a close relative of *U. rostrata*, there are not enough morphological characters preserved to judge this as being most likely.

From the Aptian (Lower Cretaceous) of Alexander Island (West Antarctica) there is one fossil (KG.5.16) of a representative of Isopoda, which Taylor (1972) treated as *Urda* cf. *cretacea*. Unlike interpreted in Taylor (1972), the fossil does not comprise the head and the anterior part of the trunk (Taylor, 1972, fig. 2). What has been interpreted as the head in Taylor (1972) is most likely the tergite of PO12. In the body parts that are visible in this fossil, it strongly resembles *U. rostrata* and its close relatives. However, none of the characteristic features of *U. rostrata* and its close relatives are apparent in the fossil. Therefore, despite the resemblance, there are not enough morphological characters

available for a robust interpretation of the Antarctic fossil as a close relative of *U. rostrata*.

4.5. RELATIONSHIP BETWEEN SPECIES OF *URDA* AND GNATHIIDAE

The above mentioned extinct close relatives of *Urda rostrata* and *U. rostrata* itself can all be easily identified as representatives of Scutocoxifera due to the presence of coxal plates (modified parts of the coxae; Dreyer and Wägele, 2002). The pleotelsa in these species are relatively flat and the uropods are located on the ventral side of the pleotelson (their proximal joint is not lateral to the tergite of the pleotelson; Figures 1A, 1B, 14A–F). This can be interpreted as in indication that the species are representatives of the group Cymothoida (an ingroup of Scutocoxifera) (Brandt and Poore, 2003). While this character can serve as an indication, it cannot be seen as a clear autapomorphy of Cymothoida, since the polarity of this character with respect to the condition in Valvifera and Sphaeromatidea is unclear (Brandt and Poore, 2003).

Kunth (1870) interpreted *Urda rostrata* and its congeners, treated by him as "Urdaidae", as intermediate forms between Gnathiidae and Cymothoidae. *Urda rostrata* and its extinct close relatives (recognized as congeners here) share a number of character states with the group Gnathiidae (as already noted by Van Straelen, 1928, p. 12), which are not present in other lineages of Isopoda and can therefore be seen as autapomorphies of a group that comprises Gnathiidae, *U. rostrata* and its close relatives (Figure 21). The anterior margin of the dorsal surface of the head has a straight median portion which is formed by the proximal joint of the upper lip and two incisions lateral to it where the proximal elements of the antennulae are located. The upper lip is large, and its proximal part is directly articulated with the head capsule; a distinct frontal lamina, as present in many lineages of Isopoda, is not developed (Monod, 1926); a distinct labrum, which in many lineages of Isopoda is located on the distal side of the clypeus is also not developed (cf. Figures 12B, 12C, 11 vs. 20A) (Wilson et al., 2011). This morphology is only present in the larval forms of Gnathiidae, as in the adult males and females the upper lip as a whole is reduced (Figure 20D; figures in (Thing et al., 2015; Ota, 2019), probably due to the fact that they are no longer feeding.

The tergite of post-ocular segment 7 is very short, narrower than the head (cf. Figures 7A, 8A, 11E, 12A, 17A vs. 20A) and the legs of post-ocular segment 7 (corresponding to the first trunk legs in other representatives of Isopoda) are functionally incorporated into the head (Nagler et al., 2017). This morphology is also only present in the larval forms of Gnathiidae, because in the adults the tergite is often fully conjoined

with the head capsule (Figure 20D), but sometimes a suture is visible in the adults (e.g. Manship et al., 2011 fig. 1D).

Urda rostrata and its above discussed extinct relatives can be distinguished from representatives of Gnathiidae by a series of autapomorphies of Gnathiidae (Figure 21). In adult representatives of Gnathiidae there is no well-developed leg in post-ocular segment 13 (Figures 20C, 20E, 20F) (Wilson, 1996), which seems to be a paedomorphy as in all representatives of Isopoda this appendage is not yet developed in young (manca stage) individuals (Watling, 1981; Ax, 2000, p. 176; Boyko and Wolff, 2014). On the other hand, in fossils of extinct close relatives of *U. rostrata* have a well-developed leg in this segment is preserved (Figures 10C, 10D, 14A–D, 16A, 16B, 16E, 16F, 18C–F), which indicates that the fossils are remains of adult (or late immature) individuals that are more plesiomorphic with respect to Gnathiidae regarding this character. The absence of well-developed legs of PO13 in adults of Gnathiidae is a paedomorphic feature, as the leg is also missing in manca-stage immature individuals of all species of Isopoda and other related ingroups of the more inclusive group Mancoida.

In adults of the group Gnathiidae there is an extreme sexual dimorphism and the mouthparts not used for feeding Wägele, 1989, fig. 93). This seems to be reflected in the morphology of the mouthparts. The appendages of post-ocular segments 6 and 7 – maxilliped and trunk leg 1 ('pylopod' in Gnathiidae literature) are flattened and in adults of most, but not all (Figure 15H), species of Gnathiidae the dactylus of PO7 is reduced (Cohen and Poore, 1994).

In larval forms of Gnathiidae the mandible is thin, straight and has a pointed tip (Wägele, 1989 fig. 93). In adult males of Gnathiidae the mandible is often very large and strongly curved, extending far beyond the anterior margin of the head capsule; in this, the condition in adults of Gnathiidae is more similar to the condition in *U. rostrata* (Monod, 1926). However, representatives of *U. rostrata*, *P. suevica* and the specimens from Bielefeld lack the blade (flat median expansion of the mandible) which is present in many males of Gnathiidae (e.g. Ota and Hirose, 2009). The shape of the mandibles in the here presented fossils is more similar to that in representatives of other lineages of Cymothoida, such as Corallanidae (Delaney, 1989 fig. 22A–B) or *Protognathia* (Wägele and Brandt, 1988; Kussakin and Rybakov, 1995), in which the mandibles do not extend beyond the anterior margin of the head and a well-developed labrum is present.

The fossils from Bielefeld and the fossils of *U. rostrata* and *P. suevica*, where the mouthparts are preserved, give no indication that they are from larval or immature individuals; specifically, the legs on post-ocular segment 13 are well developed, as opposed to being not yet developed or very short as in (manca stage) immature

representatives of Isopoda (Ax, 2000, p. 176). Therefore, the mandibles in immature stages of the extinct relatives of Gnathiidae could either have been similar to those of the adults (large and inwards curved; Figure 15H) or more similar to larval forms of Gnathiidae (straight or slightly outwards curved; Figure 15A, 15C).

The shape of the eyes is another character in which *U. rostrata* and its extinct relatives are similar to representatives of Gnathiidae, however mostly to larval individuals of the group. In adult forms of Gnathiidae the eyes are still located on the lateral sides of the head but are much smaller compared to the size of the head than in the larvae (e.g. Ota and Hirose, 2009). Nevertheless, in some adults of Gnathiidae the eyes remain large and similar to those in the herein presented fossils (Tanaka, 2005; Ota, 2019). As there is no drastic reduction of the size of the eyes apparent in most representatives of Isopoda, the reduction of the eye size from larval to adult individuals within Gnathiidae likely represents a hypermorphosis, which is not shared by the extinct relatives presented herein.

The shape of pleotelson in most species of Gnathiidae is approximately triangular, with a narrow posterior end (Figures 20A, 20B, 20E, 20F, 22E–F), yet there are also exceptions to that in extant species (e.g., Figure 22D). In that it is very different from that in *U. rostrata* and its herein presented extinct relatives, where the width of the pleotelson decreases significantly only in the posterior half and the posterior margin is either rounded or truncate (Figures 22G, 22H). Since both conditions occur in other lineages of Cymothoida as well (Bruce, 1986 fig. 35I; Messana, 2020 fig. 2), the polarity of this character, and thus the value of the pleotelson shape as a potential autapomorphy of a monophyletic group *Urda*, is unclear.

Urda rostrata and the extinct species that are herein interpreted as close relatives of it share several apomorphies with representatives of Gnathiidae but differ from them in characters that are plesiomorphic for the extinct species or of unclear polarity. This implies a close relationship between the extinct species and the extant representatives of Gnathiidae. One possibility is that the extinct species form a monophyletic group *Urda*. In the other case (non-monophyletic *Urda*), a nomenclatural dilemma arises due to the use of binomial species names. Either the name *Urda* is used as a name of a higher group, in which case Gnathiidae would become an ingroup of *Urda*, which would cause much trouble among those who care about taxonomic ranks and their reflection in the naming of groups, or alternatively the name *Urda* is used as the first part of the binomen *Urda rostrata*, in which case all species of extinct close relatives of *U. rostrata* need to receive a separate genus name. Because of this dilemma and because uninomial nomenclature (Lanham, 1965) is currently not accepted by the ICZN, the nomenclature

herein used in the taxonomy section below is as if *Urda* forms a sister group to Gnathiidae, while pointing out that this is not necessarily the case. Therefore, Urdidae as a monotypic taxonomical entity ranked at the family level, proposed by Kunth, 1870, and adopted subsequently by some authors, e.g., Van Straelen, 1928; Taylor, 1972; Feldmann *et al.*, 1994; Etter, 2014) is not followed here.

4.6. RELATIONSHIP BETWEEN *URDA* AND OTHER LINEAGES OF ISOPODA

Coxal plates (compound structures of the lateral parts of the tergites and the proximal leg element) are well visible in representatives of Gnathiidae and the herein discussed close relatives of the group (Figures 7, 20A); this clearly identifies them as representatives of the group Scutocoxifera (Dreyer and Wägele, 2002). Within Scutocoxifera, Gnathiidae and its extinct relatives belong to the group Flabellifera (sensu Wilson, 2003) which can be characterised by the functional grouping of the legs of the anterior trunk (legs of PO7–9 are projected anteriorly and the more posterior legs are projected posteriorly), which is not present in other representatives of Scutocoxifera, such as woodlice (Brusca and Wilson, 1991).

Within Flabellifera sensu Wilson 2003, the position of Gnathiidae, and thus also its extinct relatives, has been debated for several decades. Wägele and Brandt (1988; Wägele, 1989) assumed that Gnathiidae was more closely related to the non-parasitic forms of Cymothoida. They proposed a close relationship between the group *Protognathia* Wägele and Brandt, 1988 and Gnathiidae (Wägele and Brandt, 1988). However, the most important proposed synapomorphy of *Protognathia* and Gnathiidae, the lack of a well-developed leg on post-ocular segment 13, has later been shown to be the result of an erroneous interpretation of the holotype as an adult individual, but it is a manca stage (Kussakin and Rybakov, 1995; Wilson, 1996). In all representatives of Mancoida (of which Isopoda is an ingroup) early immature stages lack a well-developed leg on post-ocular segment 13 (Ax, 2000; Boyko and Wolff, 2014). In all species of *Protognathia* the tergite of PO7 is distinctly wider than the head and about as long as the subsequent tergites at least in the lateral aspect) and the leg of PO7 resembles the subsequent legs in size and orientation; also, a well-developed labrum is present (Wägele and Brandt, 1988; Kussakin and Rybakov, 1995). Therefore, it is most likely that *Protognathia* and Gnathiidae are less closely related than Gnathiidae and *U. rostrata* and all its herein discussed extinct relatives. Consequently, the slender shape the pleotelson and the uropod rami have, shared by representatives of *Protognathia* and most representatives of Gnathiidae (Figures 20A, 20B, 20E, 20F), has to be considered a result of convergent evolution.

Similarly, another non-parasitic species of the group Cymothoida – *Gnatholana mandibularis* Barnard, 1920 – has been interpreted to be a close relative of *Urda rostrata* and closely related extinct species (Monod, 1926, p. 639 ff.; Menzies, 1962). Representatives of *Gnatholana mandibularis* have large mandibles, protruding in anterior direction (well visible in dorsal view), a distinct clypeus and a distinct labrum are also projected anteriorly, similar to the upper lip in *Urda rostrata*. However, other aspects of the morphology in *G. mandibularis* are very different from representatives of *U. rostrata* and its extinct relatives: the head is short and wide; the eyes are not elongate clypeus and labrum are both visible and not conjoined with each other; the tip of the mandible has 4 small teeth; the tergite of PO7 is long and much wider than the head (Barnard, 1920, p. 352 ff. pl. 15 fig. 24). The similar morphology of the mandible therefore has to be interpreted as a result of convergent evolution (cf. Brusca and Wilson, 1991, p. 167).

The group *Protourda* Mezzalira and Martins-Neto, 1992 has been described based on an assemblage of fossils from the Permian of the Paraná basin (São Paulo state, Brazil). The group *Protourda*, according to Mezzalira and Martins-Neto (1992), comprises two species (*Protourda tupiensis* Mezzalira and Martins-Neto, 1992 and *Protourda ? circunscriptia* Mezzalira and Martins-Neto, 1992). Mezzalira and Martins-Neto (1992) assumed a sister group relationship between *Protourda* and *U. rostrata* and its extinct relatives based on the shared presence of six (instead of seven) tergites of the anterior trunk. However, as shown herein *Urda rostrata*, has seven tergites of the anterior trunk (PO7–13), which is also true for its extinct close relatives (Feldmann et al., 1994; Nagler et al., 2017). Apart from a somewhat elongate body in the type specimens of *P. tupiensis* and *P. circunscriptia*, there seems to be not much morphological similarities between *U. rostrata* and representatives of *Protourda*. Judging from additional images available to the authors and the type of preservation, it appears doubtful, that there are multiple species of *Protourda* at the type locality and also a possible synonymy with species of the group *Pseudopalaega*, recorded from the same locality (Mezzalira and Martins-Neto, 1992; Martins-Neto, 2001), should be considered when revising the material.

Brandt and Poore (2003) interpreted Anthuridea (representatives with long cylindrical bodies) to be the sister group of Gnathiidae, without discussing potential extinct relatives of the group. The morphological features that supported their finding were a reduction of coxal plates (so that they are still present but not visible in dorsal view) and that the vestigial maxilla is conjoined with the paragnaths ('hypopharynx' in Brandt and Poore 2003). The former finding appears to be problematic, since the observed condition within Gnathiidae and Anthuridea can easily be explained as a result

of a slender body shape and the condition is clearly not true for the larval forms within Gnathiidae (Figure 22F; (Wilson et al., 2011, figs. 1A,C, 6A).

Brusca and Wilson (1991) argued for a close relationship between Gnathiidae and Epicaridea because of the similar morphology of the mandible (thin and pointed, molar process absent, palp absent). Dreyer and Wägele (2001), based on molecular data (18S rDNA) found more support for a sister group relationship between Epicaridea and Cymothoidae rather than for a sister group relationship between Gnathiidae and Epicaridea. Nagler *et al.* (2017) combined the findings of Brusca and Wilson (1991) and Dreyer and Wägele (2001), resulting in a monophyletic group that comprises Cymothoidae, Epicaridea, Gnathiidae. They argued for a closer relationship between Epicaridea and Gnathiidae based on the shared absence of a well-developed maxillula (Brusca and Wilson, 1991). With *Urda rostrata* and the other extinct species presented herein most likely being the closest known relatives of the group Gnathiidae, the morphology of the extinct relatives of Gnathiidae could provide important morphological data for future phylogenetic analyses.

4.7. PALAEOECOLOGY

Representatives of *Urda rostrata* and some of its extinct relatives have been discussed to possibly be parasites of fishes (Nagler et al., 2017). Yet so far there are no publications that could show a direct interaction or association between the crustacean animals and their fish hosts. However, there is one record of representatives of Isopoda that are in direct association with fossil fishes (Nagler et al., 2016). Just as the fossils of *Urda rostrata*, this record is also from the Tithonian (Upper Jurassic) of the Solnhofen area (southern Germany). The authors of the study did identify the fossil remains as belonging to *U. rostrata*. Despite the apomorphic characters of the group that comprises *U. rostrata*, its extinct relatives and Gnathiidae not being preserved or visible in the figures, some of the fossilized representatives of Isopoda depicted in Nagler *et al.* (2016) strikingly resemble representatives of *Urda rostrata* in many aspects.

1) The bodies are of large size compared to other representatives of Isopoda (Nagler *et al.*, 2016, fig. 1). 2) The head appears to be large (in none of the figures it shows much detail; Nagler *et al.*, 2016, fig. 4A). 3) The shape of the legs is similar to that of the herein presented remains of *U. rostrata* (cf. Nagler *et al.*, 2016, fig. 3A vs. Figure 7A). 4) The shape of the pleotelsa is very similar to that of *U. rostrata*. Based on the original images (Nagler *et al.*, 2016, figs. 3C, 4A), the pleotelsa appear to be much larger than in the colour-marked reconstructions (Nagler *et al.*, 2016, figs. 3D, 4B) appear to have a

straight mid-part of the posterior margin like in representatives of *U. rostrata* (e.g., Figure 1A).

For the fossil remains in Nagler *et al.* (2016) the tergite of PO7 ('thoracic segment 2' therein) is reconstructed to be of the same length as the subsequent tergites (their figs. 2B, 3B, 4B, 5B–C, E). This is in contrast to the herein presented reconstruction of *U. rostrata*, where this tergite is reconstructed to be short and narrow (Figure 22G). This might be due to a misinterpretation in Nagler *et al.* (2016), as this structure is not clearly visible in the not-colour-marked figures. Based on the inspection of the figures, one of the fossil remains (Nagler *et al.*, 2016, fig. 4 C–D) might represent a part of the fish rather than a representative of Isopoda, as there appears to be dark, bone-like matter where they interpreted the pleon tergite borders to be. Nagler *et al.* (2016, p. 8) interpreted the body of the presumed parasites to be 'twisted' as a result of growth response while being permanently attached to their host, similar to extant representatives of Cymothoidae (e.g. Smit et al., 2014). However, none of the 'twisted' individuals are accessible in dorsal or ventral view. Therefore, the strongly compressed fossils presented in Nagler *et al.* (2016) do not allow to unambiguously observe derivations from a strict bilateral symmetry. Additional to this published record, there are several other similar, unpublished, associations with fishes (van der Wal et al., 2021). All these associations have in common that the representatives of Isopoda are not randomly distributed on the fish fossils, but all of them are located at the fins and their head is oriented towards the anterior end of the fish (Nagler et al., 2016). With respect to the possibility of rapid oxygen deprivation that has been suggested for at least some of the Solnhofen limestone taphocoenoses (Viohl, 1994; Pan et al., 2019), the occurrences of individuals of *U. rostrata* on fishes suggests an interaction between living organisms.

As discussed above, the closest relatives of *U. rostrata* and its herein presented extinct relatives are most likely extant representatives of the group Gnathiidae. Larval forms of all species of Gnathiidae, for which live observations have been made, are parasitic to fishes (Monod, 1926). From this perspective a parasitic lifestyle seems to be a likely feeding mode for their extinct relatives. However, from a pure morphological perspective, the available information is less conclusive.

The eyes in all individuals of *U. rostrata*, *U. mccoyi*, *U. cretacea*, *P. suevica* and the specimens from the Middle Jurassic of Bielefeld are large and located on the lateral sides of the head, similar to extant larval forms of Gnathiidae, which need to find and attach to their host fishes (Monod, 1926). This suggests that the visual sense likely played an important role in the ecology of the now extinct animals (Nagler et al., 2017). Due to the large size of the fossil specimens, it is likely that they are of adult individuals.

However, in adult extant parasitic representatives of the group Cymothoidae, which are known to attach to their host for long periods of time, the eyes are often much smaller and proportionally smaller than those of immatures, with adult females having the proportionally smallest eyes, even in species that do not attach within body cavities of the host (e.g. Brusca, 1978; Thamban et al., 2015). In extant representatives of Aegidae, which have been recorded to be temporary parasites of fishes, the eyes of the adults are often very large (Bruce, 2009). This could be an indication that representatives of the above-mentioned extinct species were not permanently attached to the fishes.

Nagler *et al.* (2017, p. 9) reconstructed the mouthparts of the fossil specimens from Bielefeld ('*Urda rostrata*' therein but see discussion above). They concluded that the mouthparts formed a 'loose' mouth-cone and the individual mouthparts were similar to those of extant parasitic forms of the group Cymothoida. Our reconstruction of the mouthparts (based on the same μCT scans) shows important differences to the original reconstruction. 1) Based on our reconstruction, there is no distinct labrum present that could form the anterior confinement of the mouth cone. 2) The maxilliped in our reconstruction corresponds to the maxilla in the reconstruction of Nagler *et al.* (2017, fig. 4B3). Also, we could not find this structure to have a distal end with 3 spines (Figures 15M, 15N). Overall, in our reconstruction we could not find similar confinement structures as in the feeding apparatus of extant representatives of Cymothoidae or larval forms of Gnathiidae (cf. Figures 15K–N, 10E–I vs. 15A, 15I, 15J). Most importantly, the proportional size and the strongly curved shape of the mandible incisors are very different to the extant parasitic forms within the groups Cymothoidae and Gnathiidae. The large shape of the mandibles indicates a piercing rather than a cutting or grinding motion, however without a sealing mouth-cone, the feeding mechanism of the herein presented fossil specimens remains uncertain.

The morphology of the distal leg elements (dactyli) is different to those in representatives of Cymothoidae, which use their legs to attach to a host. The most obvious difference is that in representatives of Cymothoidae the claws are more strongly curved and the width of the claw at the base is much greater. This would suggest that at least the mechanism of attaching to a fish is different from that in representatives of Cymothoidae and possibly more similar to that in larval forms of Gnathiidae, as they are more similar to them (cf. Figures 14A–F, 16 vs. 20A–B).

4.8. Geographic and stratigraphic distribution

Urda rostrata and all its herein discussed extinct relatives come from Central and Western Europe (Figure 23). Considering the scarcity of the fossil record of the group Isopoda in general, a probably strong geographical sampling bias (intensive collecting in Europe), and the presence of fossils outside of Europe with resemblance to *U. rostrata* (Taylor, 1972; Grant-Mackie et al., 1996), as of now, the fossil record seems not to be a helpful tool for the study of the biogeographical origin of the group Gnathiidae.

The earliest fossils that can be identified as close relatives of *Urda rostrata* and Gnathiidae are from the Lower Jurassic Amaltheenton Formation (Pliensbachian) in southern Germany (Reiff, 1936; Figure 19). Slightly even older fossils – also from the Pliensbachian – have been found geographically close by (Frentzen, 1937); however, as discussed above, while there are no morphological structures that would argue against a close phylogenetic relationship to *U. rostrata*, there are not enough structures preserved in the fossils to convincingly argue for a close relationship. The youngest occurrence of a close relative of *Urda rostrata*, that does not share the above mentioned apomorphies of Gnathiidae, is Albian in age and from the East of England (Carter, 1889; Feldmann et al., 1994) (Figure 19).

When exactly the last relatives of *U. rostrata*, that are not representatives of Gnathiidae, went extinct is difficult to tell. For once, although there are intensively studied marine sediments from the Upper Cretaceous (e.g. Rathbun, 1935; Lehmann and Höll, 1989), there is no record of animals with a similar body shape, except for one poorly preserved specimen from the Santonian (Upper Cretaceous) of Texas (Bowman, 1971), that bears some resemblance to the herein discussed fossils, but does not allow for a concise systematic interpretation. On the other hand, there is no fossil record of the group Gnathiidae, which could suggest that from the Late Cretaceous on extinct relatives and representatives of Gnathiidae lived in habitats where animals with chitinous exoskeletons are unlikely to be preserved as fossils.

5. Taxonomy

Remark: Full synonymy lists are presented; their style follows Matthews (1973).

Peracarida Calman, 1904

Isopoda Latreille, 1817

Scutocoxifera Dreyer and Wägele, 2002

Urda Münster, 1840

Type species: *Urda rostrata* Münster, 1840.

Emended diagnosis: Anterior margin of the head with a straight median portion (proximal joint of the upper lip) and paired concave rounded incisions lateral to it (space for the proximal elements of the antennula); frontal lamina not developed (or conjoined with the head capsule); upper lip large, (can be) projected in anterior direction (not facing in ventro-posterior direction); labrum not distinct (likely conjoined with the clypeus, forming the upper lip); mandible incisor large, projected anteriorly (not to the ventral side), about 90 degrees curved inward, with a pointed tip; tergite of PO7 very short, subsequent tergites much longer; leg of PO7 short and located on the ventral side of the head; pleotelson with lateral sides about parallel in the anterior part, posterior margin semicircular, straight or with a slight concave median notch.

Remarks: The genus *Urda* was originally described to accommodate four different species (Münster, 1840), all of them recognized later as representing a single species (Oppel, 1862; Kunth, 1870). The genus *Reckur* was erected by Münster (1842), only to be found synonymous with *Urda* several decades later (Oppel, 1862; Kunth, 1870). Since then, various isopod fossils from Mesozoic strata were assigned to the genus *Urda*.

Urda rostrata Münster, 1840
Figures 1–7, 22G

       1839 'Isopoden' – Münster in Münster, p. 2.

*   1840 *Urda rostrata* – Münster in Meyer and Münster, p. 21, pl. 1, fig. 2.

       1840 *Urda decorata* – Münster in Meyer and Münster, p. 21, pl. 1, fig. 4.

       1840 *Urda cincta* – Münster in Meyer and Münster, p. 22, pl. 1, fig. 5.

       1840 *Urda elongata* – Münster in Meyer and Münster, p. 22, pl. 1, fig. 3.

.   1842 *Reckur punctatus* – Münster in Meyer and Münster, p. 77, pl. 9, fig. 10. **syn. nov**.

       1846 'Les *Urda*' [sic] – Pictet, p. 55, pl. 3, fig. 2.

       1846 Reckur affinis – Meyer, p. 598.

       1853 *Urda decorata* Münster – Pictet, atlas, pl. 43, fig. 13.

       1854 Urda rostrata Münster – Pictet, p. 467.

       1854 Urda decorata Münster – Pictet, p. 467.

1854 Urda cincta Münster – Pictet, p. 467.

1854 Urda elongata Münster – Pictet, p. 467.

1856 *Reckur affinis* Meyer – Meyer in Dunkler and Meyer, p. 50, pl. 10, fig. 2.

1862 *Urda punctata* Münster – Oppel in Boehm, Cotteau and Zittel, p .116.

1862 *Urda rostrata* Münster – Oppel in Boehm, Cotteau and Zittel, p. 116.

1870 *Urda rostrata* Münster – Kunth, p .790, pl. 18, figs. 1, 1a, 2.

. 1870 *Urda punctata* Münster – Kunth, p. 796, pl. 18, figs. 3, 3a.

1882 Urda rostrata Münster – Ammon, p. 539.

1882 Urda punctata Münster – Ammon, p. 539.

1887 *Urda rostrata* Münster – Zittel, p. 664, fig. 868.

1887 Urda punctata Münster – Zittel, p. 664.

1889 Urda rostrata Münster – Carter, p. 194.

1889 Urda punctata Münster – Carter, p. 194.

1904 Urda punctata Münster – Walther, p. 172.

1904 Urda rostrata Münster – Walther, p. 172.

1910 Urda rostrata Münster – Stolley, p. 191.

1910 Urda punctata Münster – Stolley, p. 191.

1912 Urda rostrata Münster – Remeš, p. 176.

1912 Urda punctata (Münster) – Remeš, p. 176.

1928 *Urda rostrata* Münster – Van Straelen, p. 14.

1928 *Urda punctata* Münster – Van Straelen, p. 15.

1937 Urda rostrata Münster – Frentzen, p. 102.

1937 Urda punctata Münster – Frentzen, p. 102.

1969 Urda rostrata Münster – Hessler, p. R387.

1971 Urda rostrata Münster – Büchner, p. 32.

1971 Urda punctata Münster – Büchner, p. 32.

1972 Urda rostrata Münster – Taylor, p. 101.

1972 Urda punctata Münster – Taylor, p. 101.

1988 Urda rostrata Münster – Etter, p. 867.

1988 Urda punctata Münster – Etter, p. 867.

1992 Urda rostrata Münster – Mezzalira and Martins-Neto, p. 55.

1992 Urda punctata Münster – Mezzalira and Martins-Neto, p. 55.

1996 Urda rostrata Münster – Grant-Mackie, Buckeridge and Johns, p. 37.

1999 Urda rostrata Münster – Brandt, Crame, Polz and Thomson, p. 666, tab. 1.

1999 Urda punctata Münster – Brandt, Crame, Polz and Thomson, p. 666, tab 1.

2014 Urda rostrata Münster – Etter, tab. 1.

2014 Urda punctata Münster – Etter, tab. 1.

2017 Urda rostrata Münster – Nagler, Hyžný and Haug, p. 3, tab. 1.

2017 Urda punctata Münster – Nagler, Hyžný and Haug, p. 3, tab. 1.

Type material studied: Holotype considered lost, not found in the collections in Munich and Berlin, (M. Reich, 2020, pers. comm.; A. Abele-Rassuly, 2021, pers. comm.); holotype of *Urda elongata* Münster, 1840 (SNSB BSPG AS 493); holotype of *Reckur punctatus* Münster, 1842 (SNSB BSPG AS 496).

Other material studied: JME SOS 1794; 10 additional specimens from private collections of the German private collector 'Leptolepides' (Figure 3), Herbert Gratt (Figure 4A), Manfred Ehrlich (Figure 4B, 4D), Udo Resch (Figures 4C, 5A – E), Falk Starke (Figure 4E), Daniel Fauser (Figure 6), and Norbert Winkler (Figure 7).

Diagnosis: Upper lip distal part wider than proximal part, latero-distal corners rounded; eyes narrow and elongate, tapering towards the posterior end; posterior ends of the eyes close to the level of the posterior margin of the head; tergite of PO7 with convex posterior margin; pleon tergites 1–3 with posterior margin overall concave, convex in the mid-part and concave in the lateral parts; pleotelson posterior margin straight in the median portion.

Remarks: Originally, Meyer (1840) described four different species of *Urda*, i.e., *U. rostrata*, *U. decorata*, *U. cincta*, and *U. elongata*. All of them were found synonymous with each other by Oppel (1862). Kunth (1870) recognized *Reckur affinis* as a junior subjective synonym of *U. rostrata*. Since then, consistently two species of *Urda* have been recognized from lithographic limestones of the Solnhofen area, i.e., *U. rostrata* and *U. punctata*. Alleged differences are considered as a result of taphonomy (for more details see the text further above). Consequently, both taxa are treated as a single valid species herein. Thus, *U. punctata* (originally as *Reckur punctatus*) is herein recognized a junior subjective synonym of *U. rostrata*.

Occurrence: Upper Jurassic (Tithonian) of Bavaria, Germany.

Urda mccoyi (Carter, 1889)
Figure 8

(1875) Squilla McCoyi – Seeley: museum label. (*nomen nudum*)

1875 Squilla McCoyi – Jukes-Browne, p. 277. (*nomen nudum*)

1881 Squilla McCoyi – Jukes-Browne, p. 153. (*nomen nudum*)

*   1889 *Palaega McCoyi* – Carter, p. 195, pl. 6, figs. 1–7.

    1897 Squilla McCoyi – Cowper Reed, p. 120.

    1928 *Palaega Mac Coyi* Carter – Van Straelen, p. 20.

    1994 *Urda mccoyi* (Carter) – Feldmann, Wieder and Rolfe, p. 88, fig. 2.3, 2.4, 2.6.

non   1994 *Urda mccoyi* (Carter) – Feldmann, Wieder and Rolfe, p. 88 fig. 2.1, 2.2, 2.5, 2.7.

    1999 Urda mccoyi (Carter) – Brandt, Crame, Polz and Thomson, tab. 1.

    2006 ?Palaega mccoyi Carter – Feldmann and Rust, tab. 1.

    2014 Urda mccoyi (Carter) – Etter, p. 935, tab. 1.

Type material studied: Three syntypes: SM B 23295, SM B 23296, SM B 23297.

Emended diagnosis: Eyes with posterior end at about ⅔ of the heads length; coxal plates of PO8–9 with straight lateral margin parallel to the lateral margin of the tergite; coxal plate of PO10 anterior part wide, posterior part narrower; coxal plates of PO11–13 anterior part narrow, posterior part wider; tergite of PO13 postero-lateral corner pointed or tightly rounded; pleon tergites with lateral parts curved ventrally; pleon tergites 3–4 with posterior margins evenly concave; pleotelson posterior margin rounded (or with a very narrow straight median part, distal-most part not well preserved).

Remarks: The species, originally described as a representative of *Palaega*, was interpreted to be a representative of *Urda* by Feldmann *et al*. (1994), based on the restudy of the type material; we concur with this interpretation. *Urda mccoyi* differs from the type species, *U. rostrata*, in having considerably smaller eyes, a proportionally longer tergite of PO8 and rounded posterior margin of the pleotelson. The pleotelson of *U. mccoyi* is more elongate than in *U. buechneri*.

Occurrence: Lower Cretaceous (Albian) of England (UK).

Urda aff. *mccoyi* (Carter, 1889)

    1994 *Urda mccoyi* (Carter) – Feldmann, Wieder and Rolfe, p. 88, fig. 2.1, 2.2, 2.5, 2.7.

Material: One specimen, GSE 15083.

Remarks: There are morphological differences between the specimen from the Isle of Skye and the type material from England. Additionally, the specimen from the Isle of

Skye is more than 53 million years older than the type material of *U. mccoyi* (see discussion above).

Occurrence: Upper Jurassic (early Oxfordian) of the Isle of Skye (Scotland, UK).

Urda cretacea **Stolley, 1910**

*   1910 *Urda cretacea* – Stolley, p. 204, pl. 6. figs. 2–4, 2a–4a.

        1914 Urda cretacea Stolley – Calman, p. 325.

        1928 *Urda cretacea* Stolley – Van Straelen, p. 17.

        1937 Urda cretacea Stolley – Frentzen, p. 102.

        1969 Urda cretacea Stolley – Hessler, p. R387.

        1971 Urda cretacea Stolley – Büchner, p. 32.

        1972 Urda cretacea Stolley – Taylor, p. 101.

non   *1972 Urda* cf. *cretacea* Stolley – Taylor, p. 97, figs. 2.

        1988 Urda cretacea Stolley – Etter, p. 865.

        1992 Urda cretacea Stolley – Mezzalira and Martins-Neto, p. 55.

        1994 Urda cretacea Stolley – Feldmann, Wieder and Rolfe, p. 89.

        2017 Urda cretacea Stolley – Nagler, Hyžný and Haug, p. 3, tab. 1.

Type material studied: None. The type material is lost, most likely destroyed in World War II (Nägelke, 2000).

Diagnosis: Eyes with posterior end at about two thirds of the length if the head; upper lip with median process; coxal plates of PO11–12 large, with straight lateral sides parallel to the lateral margins of the tergites, antero-lateral corner angled, postero-lateral corner rounded; pleon tergites with straight posterior margins, lateral parts curved to ventral side; pleon tergites 2–5 with pointed postero-lateral corners.

Remarks: *Urda cretacea* differs from the type species, *U. rostrata*, in having shorter eyes, the anterior margin of the upper lip with a median process, the pleotelson with evenly rounded posterior margin. *Urda cretacea* differs from *U. mccoyi* in having the head as wide as the tergite of PO8 and the posterior margin of the head in dorsal view being wide.

        Taylor (1972) presented a specimen from the Lower Cretaceous of Antarctica, which he identified as *Urda* cf. *cretacea*. Feldmann *et al.* (1994) already noted that they could not confirm this identification. We concur with Feldmann *et al.* (1994): the poor preservation of the material from Antarctica precludes an identification of the specimen

as a representative of *U. cretacea* and also as a representative of the group *Urda* (see discussion above).

Occurrence: Lower Cretaceous (Aptian) of Lower Saxony, Germany.

Urda suevica (Reiff, 1936) n. comb.
Figures 9–11

*   1936 *Palaega suevica* – Reiff, p. 67, figs. 7a–c, 8, 9; pl. 1, fig. 6–9; pl. 2, fig. 3; fig. 10; pl.   9, figs. 4–6.

.   1936 *Palaega kessleri* – Reiff, p. 51, fig. 1a–e; pl. 1, figs. 4–5, fig. 2, figs. 3–4; pl. 1, figs. 1–   3; pl. 9, figs. 1–9; fig. 5.b **syn. nov.**

  1937 Palaega kessleri Reiff – Frentzen, p. 101.

  1968 Palaega kessleri Reiff – Malzahn, p. 832.

  1968 Palaega suevica Reiff – Malzahn, p. 832.

  1982 Palaega kessleri Reiff – Quayle, p. 31.

  1988 Palaega kessleri Reiff – Etter, p. 859.

  1988 Palaega suevica Reiff – Etter, p. 859.

  1993 Palaega kesslei [sic] Reiff – Obata and Omori, p. 60.

  2005 Palaega kessleri Reiff – Feldmann and Goolaerts, p. 1031.

  2005 Palaega suevica Reiff – Feldmann and Goolaerts, p. 1031.

  2006 Palaega kessleri Reiff – Feldmann and Rust, p. 412, tab. 1.

  2006 ?Palaega suevica Reiff – Feldmann and Rust, p. 412, tab. 1.

  2013 Palaega kessleri Reiff – Hyžný, Bruce and Schlögl, p. 620.

  2013 Palaega suevica Reiff – Hyžný, Bruce and Schlögl, p. 620.

  2014 Palaega kessleri Reiff – Etter, p. 935, tab. 1

  2013 Palaega suevica Reiff – Etter, p. 935, tab. 1

  2014 Palaega kessleri Reiff – Jones, Feldmann and Garassino, p. 740.

  2017 Palaega kessleri Reiff – Keupp and Mahlow, p. 162.

  2017 Palaega suevica Reiff – Keupp and Mahlow, p. 162.

Neotype: Kirchheimer Exemplar (Fundstück F) in Reiff (1936) collection of the University of Tübingen, GPIT-PV-76948, Lower Jurassic, Pliensbachian, 'Lias delta', Amaltheenton Formation, Kirchheim unter Teck, Baden-Württemberg, Germany.

Other material studied: 1 specimen figured in Reiff (1936, 'Fundstück A', fig. 1a–c, pl. 1 figs. 4–5) as '*Palaega kessleri*', GPIT-PV-76947, Reutlingen, Baden-Württemberg,

Germany. 1 specimen, figured in Reiff (1936, 'Fundstück B', fig. 2) as '*Palaega kessleri*', collection of the municipal museum of Natural History in Göppingen, without accession number, Holzheim (Göppingen), Baden-Württemberg, Germany. 2 specimens, figured in Reiff (1936; 'Fundstück C', figs. 3–4, pl. 1 figs. 1–3, pl. 2 figs. 1–2; 'Fundstück D', fig. 5) as '*Palaega kessleri*', collection of the State Museum of Natural History Karlsruhe, destroyed during World War II (E. Frey, 2020, pers. comm.), Reichenbach (Aalen), Baden-Württemberg, Germany. 1 specimen, figured in Reiff (1936, 'Fundstück E', figs. 7–9, pl. 1 figs. 6–9, pl. 2 fig. 3) as '*Palaega suevica*', collection of the State Museum of Natural History Karlsruhe, destroyed during World War II (E. Frey, 2020, pers. comm.), Holzheim (Göppingen), Baden-Württemberg, Germany. All from the Lower Jurassic, Pliensbachian, 'Lias delta', Amaltheenton Formation.

Diagnosis: Eyes with posterior end at about ¾ of the heads length; upper lip with a distinct median convexity; posterior margin of the head convex, without a straight median part; coxal plate of PO8 conjoined with the tergite of PO8.

Remarks: The two names *suevica* and *kessleri* were both published in the same publication (Reiff, 1936) with different name bearing types. As discussed above, we find that the two names belong to the same species, making one of the names a subjective synonym of the other. Based on the availability of suitable type specimens we designate GPIT-PV-76948 ('Fundstück F') to be the neotype of this species. According to ICZN Art. 24.2.2 we give the species *suevica* precedence over *kessleri* because GPIT-PV-76948 (within the type series of suevica) is the only remaining specimen of the type series (there are no additional specimens) where the head is preserved. This makes the name *kessleri* a subjective synonym of *suevica*. The holotype of *Palaega suevica* has been destroyed in WW2 (E. Frey, 2020, pers. comm.). To clarify the taxonomic status of the species, we decided to designate GPIT-PV-76948 to be the neotype of the species *Urda suevica*. Judging from the original description and illustrations, the head morphology in GPIT-PV-76948 is consistent with the head morphology of the (lost) holotype of *suevica* and the (lost) holotype of *kessleri*. The holotype of *suevica* and the neotype of *suevica* come from rocks of the same (suggested by the similar preservation) or about the same age (both are specified as 'Lias alpha') and come from a narrow geographical region (the field sites are less than 20 km apart).

Occurrence: Lower Jurassic (Pliensbachian) of Baden-Württemberg, Germany.

Urda buechneri n. sp.

Figures 12–14, 15K–15N, 16–18
urn:lsid:zoobank.org:act:XXX

1971 *Urda* sp. Büchner, p. 28, figs. 1–5.

. 2007 *'Flabellifera'* Wittler, p. 19, fig. 1.

. 2011 *'Flabellifera'* Wittler, p. 19, figs. 1–2.

v . 2017 *Urda rostrata* Nagler, Hyžný and Haug, p. 5, figs. 1A–E, 1G, 2, 3, 4A–C, 5, 6.

Etymology: In honour of Martin Büchner, the former director of the Natural History Museum Bielefeld, who described some of the type specimens in 1971, without formally describing the species.

Holotype: SNSB – BSPG 2011 I 50.

Paratypes: SNSB – BSPG 2011 I 51, ES/jb-8744, ES/jb-30755, ES/jb-30756.

Type location and stratum: Middle Jurassic, Bajocian, *Parkinsonia parkinsoni* Zone, quarry 'Bethel 1', Bielefeld, North Rhine-Westphalia, Germany.

Diagnosis: Eyes with posterior end at about ¾ of the heads length; antenna short; tergite of PO7 posterior margin straight; coxal plates of PO8–9 with straight lateral margin parallel to the lateral margins of the tergites; coxal plate of PO10 anterior part wide and much narrower in the posterior part; coxal plates of PO11–13 anterior part narrow and posterior part wider; tergite of PO13 with postero-lateral corner widely rounded; pleon tergites with about straight posterior margins; pleon tergites 2–5 with lateral parts curved to the ventral side, postero-lateral corners pointed and projecting posteriorly; pleotelson posterior margin rounded; uropod endopod lateral margin with denticles.

Remarks: The type material of *U. buechneri* n. sp. has previously been figured as *U. rostrata* (Nagler et al., 2017); the same material is herein interpreted as a belonging to a species distinct from *U. rostrata*. *Urda buechneri* n. sp. differs from *U. rostrata* in having distinctly shorter eyes (relative to the length of the head) and from *U. mccoyi* in having a less bulged head and a less convex posterior margin of the tergite of PO7. *Urda buechneri* n. sp. differs from *U. cretacea* in having a narrower head and from *U. suevica* n. comb. in having a straight mid-part in the posterior margin of the head and in having distinct coxal plates in PO8.

Occurrence: Middle Jurassic (Bajocian) of North Rhine-Westphalia, Germany.

Urda **sp.**

*   1968 *Palaega?* *stemmerbergensis* Malzahn, p. 828, pl. 58, figs. 1–2, 4–5.

1975 Palaega stemmerbergensis Malzahn – Secretan, p. 320.

2005 ?*Palaega stemmerbergensis* Malzahn – Feldmann and Goolaerts, p. 1031.

2006 ?*Palaega stemmerbergensis* Malzahn – Feldmann and Rust, p. 412, tab. 1.

2015 Palaega stemmerbergensis Malzahn – Vonk, Latella and Zorzin, p. 543.

Type material studied: None. The material was lost or misplaced (C. Heunisch, 2019, pers. comm.).

Remarks: The affinity of the fossil with other representatives of *Palaega* (collective group) has already been doubted in its original description (Malzahn, 1968) – e.g. the pleotelson in *P. stemmerbergensis* lacks a spinose posterior margin which is one of the most important characters for the assignment to *Palaega* (Hyžný et al., 2013). The holotype of *P. stemmerbergensis* shares multiple characters with species of *Urda* as characterised herein (for more details see the discussion above). Nevertheless, most of the body parts where important diagnostic characters could be present are not sufficiently described nor depicted in figures of Malzahn (1968) due to the poor preservation of the holotype. Therefore, *P. stemmerbergensis* is considered a *nomen dubium* here.

Occurrence: Lower Cretaceous (Hauterivian) of Lower Saxony, Germany.

<div align="center">

Scutocoxifera incertae sedis

Eobooralana **n. gen.**
urn:lsid:zoobank.org:act:XXX

</div>

Etymology: Prefix *eo* (from Greek ēōs, meaning *dawn*) refers to the age of the holotype of the type species; -*booralana* indicates the superficial resemblance to the extant species *Booralana tricarinata* Camp and Heard, 1988, which etymological origin is the aboriginal word *booral*, meaning *large* reflecting the size of the holotype of the type species; the gender is feminine.

Type species: *Urda rhodanica* Van Straelen, 1928.

Diagnosis: as for the species/not applicable, since monotypic.

Remark: The holotype of the type species can not be identified to a group ranked at genus level based on apomorphic character states. To be consistent with the recommendations of the ICZN, this new generic name is provided.

<div align="center">(45)</div>

Eobooralana rhodanica (Van Straelen, 1928) n. comb.

*   1928 *Urda rhodanica* – Van Straelen, p. 13, text fig. 1, pl. 1, fig. 1.
        1988 Urda rhodanica Van Straelen – Etter, p. 867.
        1992 Urda rhodanica Van Straelen – Mezzalira and Martins-Neto, p. 55.
        1999 Urda rhodanica Van Straelen – Brandt, Crame, Polz and Thomson, tab. 1.
        2014 *Urda rhodanica* Van Straelen – Etter, tab. 1.
        2017 Urda rhodanica Van Straelen – Nagler, Hyžný and Haug, p. 3, tab. 1.

Type material studied: Interpretation based on Van Straelen text fig. 1 (drawing) and pl. 1, fig. 1 (photograph); type material should be located in the collection of the Institut de Géologie de I'Université de Lyon.

Diagnosis: Coxal plates of PO10–13 (all that are preserved) with transverse furrow in the anterior part; coxal plates of PO10–11 of about the same size; coxal plates of PO11–13 increasing in size; pleotelson about as long as coxal plate of PO13, in the anterior part with an elevation orthogonal to the midline, with a carina along the midline posterior to the elevation, posterior margin concave in the median part; uropod endopod and exopod distally extending to the level of the pleotelson posterior margin.

Remarks: Although the only known specimen of *Eobooralana rhodanica* n. comb. does not possess the head and the anterior portion of the trunk, the coxal plate of PO12 is much larger than the coxal plate of PO11 and the coxal plate PO13 is even larger than the coxal plate of PO12, whereas in the type species of *Urda* (*U. rostrata*) and its congeners (*U. buechneri* n. sp., *U. cretacea*, *U. mccoyi*) the coxal plate of PO13 is smaller than the preceding coxal plates. Additionally, the posterior margin of the pleotelson in *E. rhodanica* n. comb. has a distinct concave notch, which is much more prominent than that in the type species of *Urda*, *U. rostrata*.

Occurrence: Middle Jurassic (Callovian) of France.

Scutocoxifera incertae sedis (*nomina dubia*)

Remarks: The three species discussed below are based on incomplete material, the classification of which is difficult. They are treated as *nomina dubia* with uncertain affinities within Scutiocoxifera.

"Urda" liasica **Frentzen, 1937 nom. dub.**

*   1937 *Urda liasica* – Frentzen, p. 101, text fig. 1b.

       1972 Urda liasica Frentzen – Taylor, p. 101.

       1988 Urda liasica Frentzen – Etter, p. 867.

       1992 Urda liasica Frentzen – Mezzalira and Martins-Neto, p. 55.

       1999 Urda liasica Frentzen – Brandt, Crame, Polz and Thomson, tab. 1.

       2014 Urda liasica Frentzen – Etter, tab. 1.

       2017 Urda liasica Frentzen – Nagler, Hyžný and Haug, p. 3, tab. 1.

Type material studied: None. The type material was destroyed during World War II (E. Frey, 2020, pers. comm.).

Remarks: Only a single, rather stylised drawing is available. It does not show any important characters, which would differentiate unequivocally *Urda liasica* from other representatives of Scutocoxifera. Consequently, *U. liasica* is considered a *nomen dubium* herein.

Occurrence: Lower Jurassic (Toarcian) of Baden-Württemberg, Germany.

"Urda" moravica **Remeš, 1912 nom. dub.**

*   1912 *Urda moravica* Remeš, p. 173, pl. 1, figs. 1–4.

       1928 *Urda moravica* Remeš – Van Straelen, p. 14.

       1972 Urda moravica Remeš – Taylor, p. 101.

       1988 Urda moravica Remeš – Etter, p. 867.

       1992 Urda moravica Remeš – Mezzalira and Martins-Neto, p. 55.

       1999 Urda moravica Remeš – Brandt, Crame, Polz and Thomson, tab. 1.

       2014 Urda moravica Remeš – Etter, tab. 1.

       2017 *Urda moravica* Remeš – Nagler, Hyžný and Haug: p. 3, tab. 1.

Type material studied: None. The type material was supposed to be deposited in the palaeontological collections of the University of Vienna. The search at respective institution of one of us (MH) was not successful; hence, the type material of *Urda moravica* is considered lost.

Remarks: The preservation of a single known specimen consisting of a posterior portion does not allow to reliably differentiate the species from other taxa within Scutocoxifera.

Occurrence: Middle Jurassic (Bathonian) of Czech Republic.

"Urda" zelandica **Buckeridge and Johns in Grant-Mackie, Buckeridge and Johns, 1996 nom. dub.**

*   1996 *Urda zelandica* Buckeridge and Johns in Grant-Mackie, Buckeridge and Johns, p. 35, figs. 3–5.

1999 Urda zelandica Buckeridge and Johns – Brandt, Crame, Polz and Thomson, tab. 1.

2014 Urda zelandica Buckeridge and Johns – Etter, tab. 1.

2017 Urda zelandica Buckeridge and Johns – Nagler, Hyžný and Haug, p. 3, tab. 1.

Type material studied: Holotype: A406 in collection of the Geology Department, University of Auckland.

Remarks: Although the holotype of *Urda zelandica* resembles *U. rostrata*, the type species of *Urda*, in some respects it represents a strongly compressed fossil of a posterior body region only. Thus, it cannot be reliable compared with other representatives of *Urda* and its affinities to *U. rostrata* are doubtful. Therefore, *U. zelandica* is considered a *nomen dubium* and its holotype as a representative of Scutocoxifera incertae sedis.

Occurrence: Upper Jurassic (Tithonian) of North Island, New Zealand.

6. Conclusions

– There is only a single species – *Urda rostrata* – that occurs in the Late Jurassic limestones of the Solnhofen area (southern Germany).

– The fossil specimens from the Middle Jurassic of Bielefeld are not conspecific with *U. rostrata* but can be attributed to a new species: *Urda buechneri* n. sp.

– Several species that have been attributed with the name *Urda* cannot be safely identified as close relatives of the type species *U. rostrata* or cannot be distinguished from other species.

– *Urda rostrata* and its extinct relatives are closely related to the group Gnathiidae.

– There is no autapomorphy for a monophyletic group *Urda*, but there are apomorphic characters for an unnamed group that comprises all species attributed with the name *Urda* and the extant group Gnathiidae.

– Well preserved fossils as the ones presented herein could play an important role to determine the phylogenetic position of the group Gnathiidae within its parent group Scutocoxifera.

– All fossil remains that can clearly be identified as belonging to close relatives of *U. rostrata* are from Europe with a stratigraphic range spanning from the Early Jurassic to the Early Cretaceous (ca. 185–105 million years before now).

Author contributions
MS designed the study, contributed photographs and µCT data, performed 3D reconstructions, designed the figures and contributed large parts of the main text. MH contributed to the discussion and to the taxonomy section. CN contributed photographs and µCT data. JTH helped to design the study and contributed to all parts of the manuscript. All authors reviewed the final manuscript.

Figures
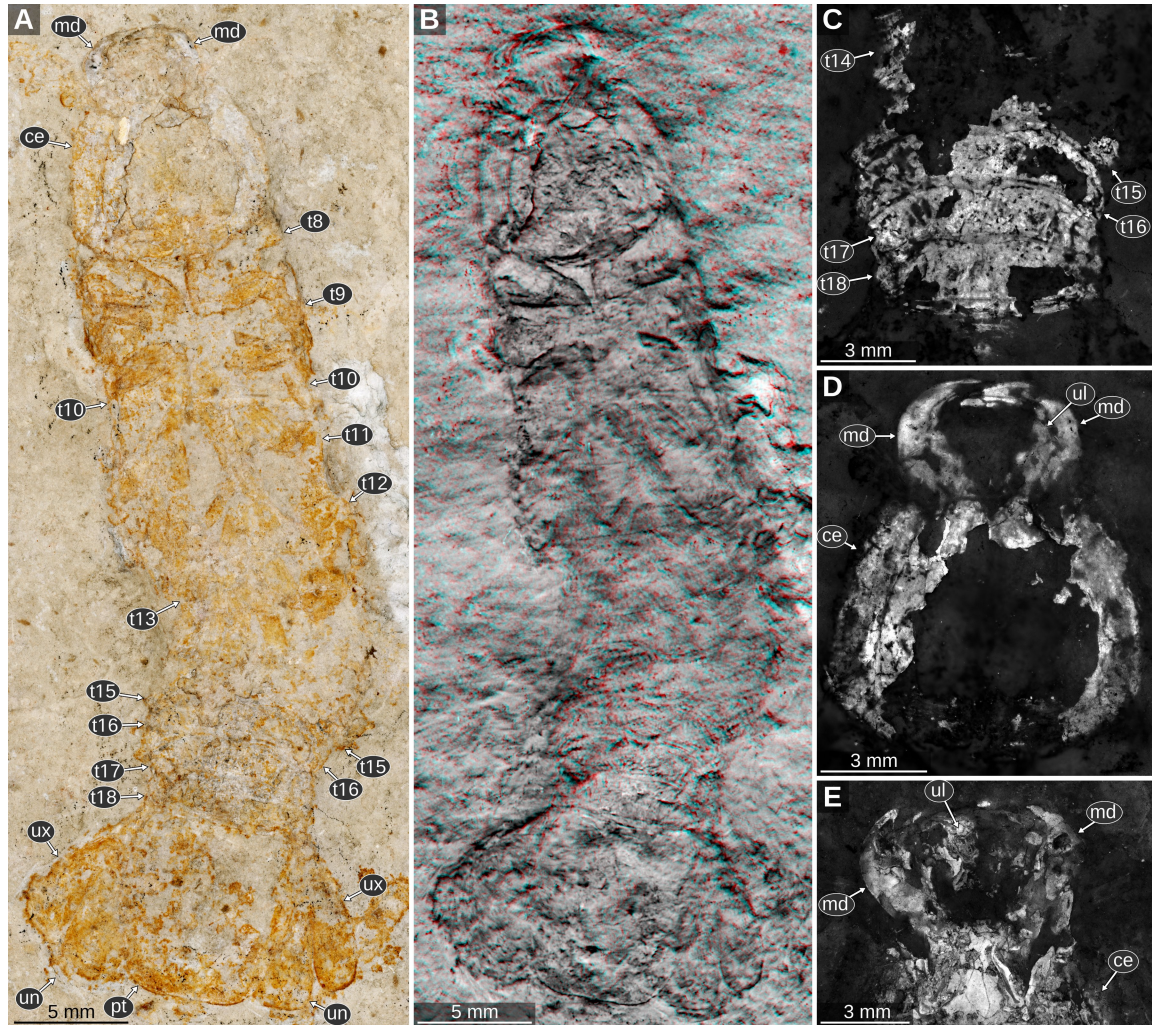
Figure 1: *Urda rostrata* Münster, 1840. **A–D:** SNSB BSPG AS 493 syntype of '*Urda elongata*' (Münster 1840 pl. 1 fig. 3), Late Jurassic, early Tithonian, *Hybonoticeras hybonotum* Zone, Solnhofen, Bavaria, Germany. **A:** white light microscopy. **B:** red-cyan stereo anaglyph. **C:** pleon region, epifluorescence microscopy. **D:** head region, epifluorescence microscopy. **E:** SNSB BSPG AS 496 syntype of '*Reckur punctatus*' (Münster 1842 pl. 10 fig. 10; Kunth 1870 pl. 18 figs. 3, 3a), Late Jurassic, early Tithonian, *Hybonoticeras hybonotum* Zone, Daiting, Bavaria, Germany, anterior region of the head, epifluorescence microscopy. **ce**, compound eye; **md**, mandible; **pt**, pleotelson; **t8–18**, tergites of post-ocular segments 8–18; **ub**, uropod basipod; **ul**, upper lip; **un**, uropod endopod; **ux**, uropod exopod.
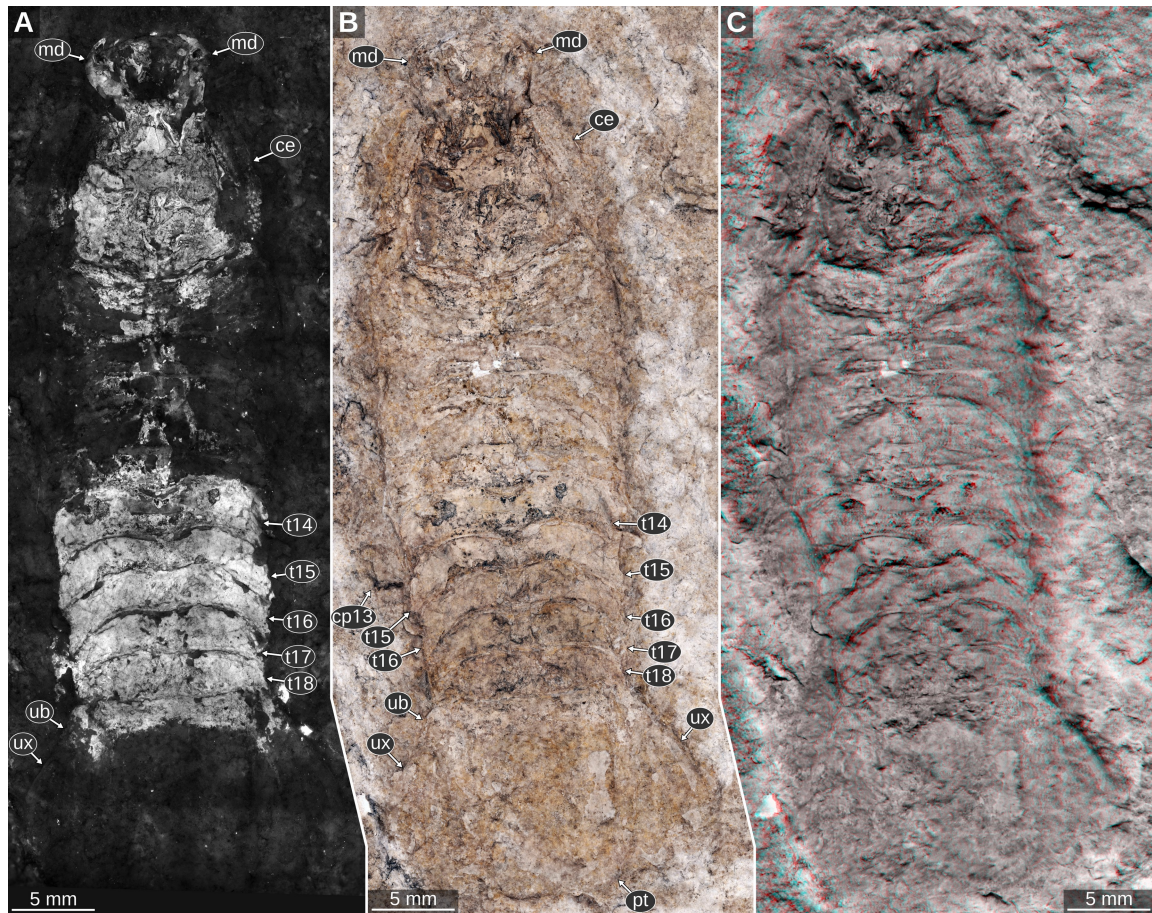
Figure 2: *Urda rostrata* Münster, 1840 (*Urda punctata* sensu Kunth 1870), SNSB BSPG AS 496 syntype of '*Reckur punctatus*' (Münster, 1842 pl. 4 fig. 10; Kunth, 1870 pl. 18 figs. 3, 3a), Late Jurassic, early Tithonian, *Hybonoticeras hybonotum* Zone, Daiting, Bavaria, Germany. **A:** epifluorescence microscopy. B: white light microscopy. red cyan stereo anaglyph. **ce**, compound eye; **cp13**, coxal plate of post-ocular segment 13; **md**, mandible; **pt**, pleotelson; **t14–18**, tergites of post-ocular segments 14–18; **ub**, uropod basipod; **ux**, uropod exopod.
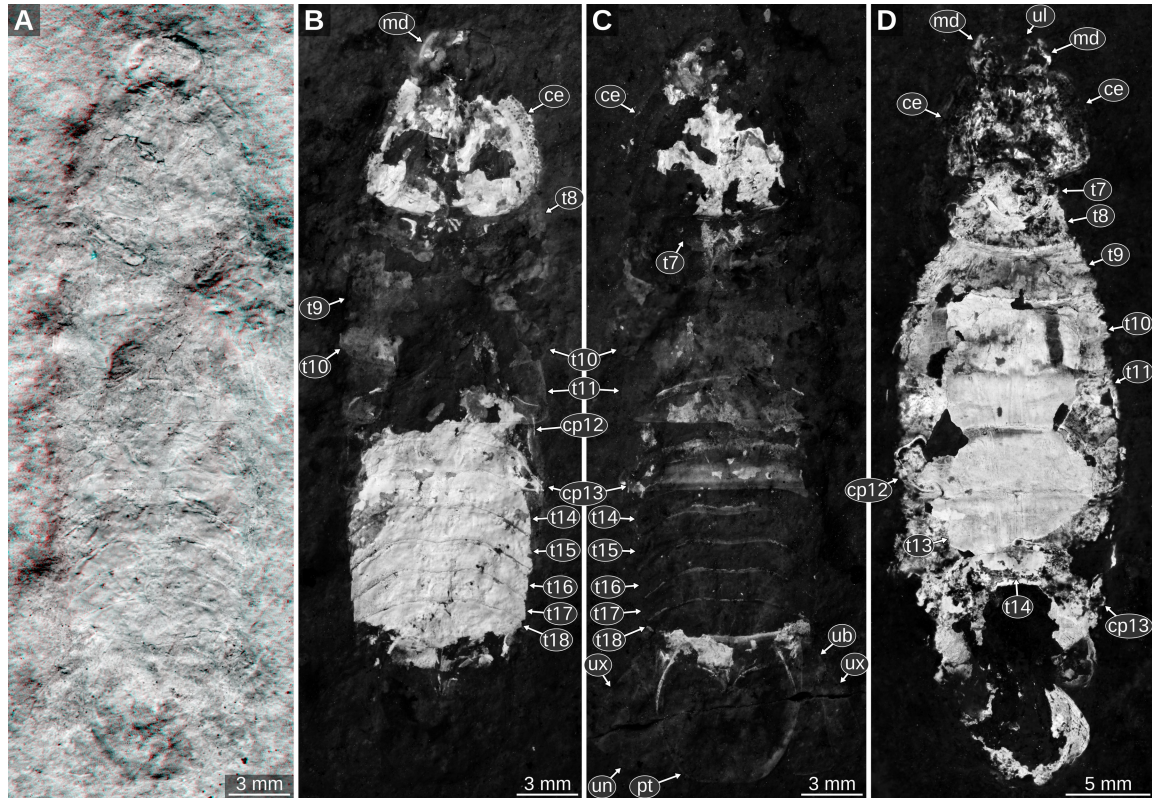
Figure 3: *Urda rostrata* Münster, 1840, private collection of 'Leptolepides' (German private collector), Late Jurassic, early Tithonian. **A–C:** specimen 1, Schernfeld (Eichstätt), Bavaria, Germany. **A:** red-cyan stereo anaglyph. **B–C:** UV light (365 nm) macro photography. **B:** specimen 1 **C:** specimen 1, counterpart to A and B. **D:** specimen 2, Blumenberg (Eichstätt), Bavaria, Germany, UV light (365 nm) macro photography, composite image of part and counterpart. **ce**, compound eye; **cp 12–13**, coxal plates of post-ocular segments 12–13; **md**, mandible; **pt**, pleotelson; **t7–18**, tergites of post-ocular segments 7–18; **ub**, uropod basipod; **ul**, upper lip; **un**, uropod endopod; **ux**, uropod exopod.
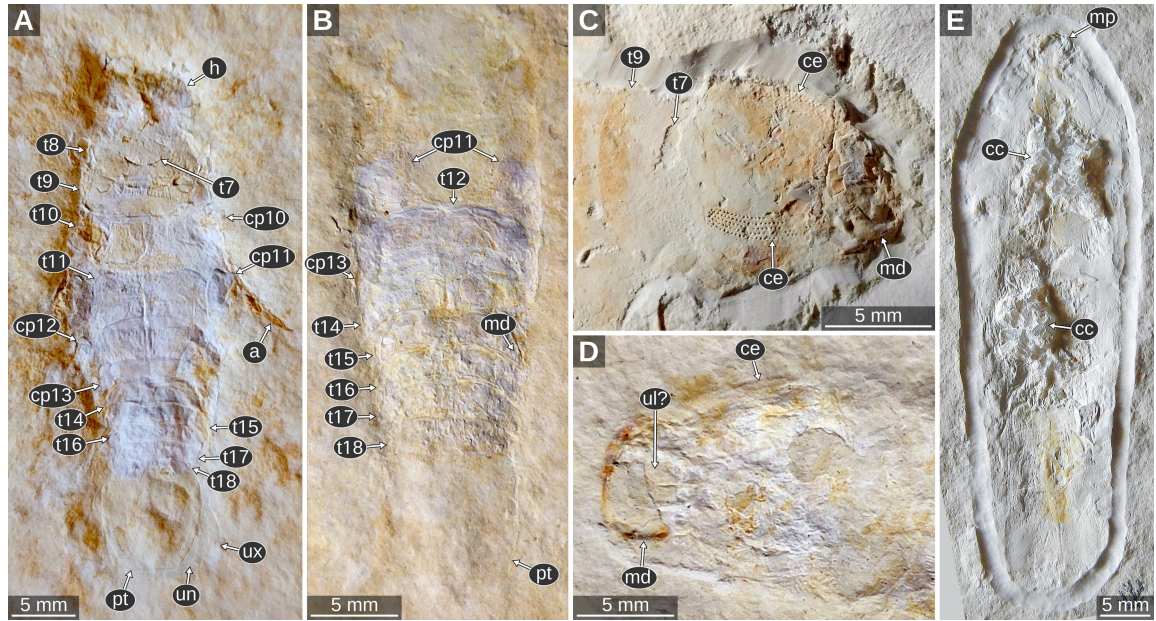
Figure 4: *Urda rostrata* Münster, 1840, macro photography, images are courtesies of the collectors. **A:** private collection of Herbert Gratt (Brixlegg, Austria), Late Jurassic, early Tithonian, *Hybonoticeras hybonotum* Zone, Wegscheid (Eichstätt), Bavaria, Germany. **B:** private collection of Manfred Ehrlich (Böhl-Iggelheim, Germany), Late Jurassic, early Tithonian, Blumenberg, Eichstätt, Bavaria, Germany. **C:** private collection of Udo Resch (Eichstätt, Germany), Late Jurassic, early Tithonian, Schernfeld (Eichstätt), Bavaria, Germany. **D:** private collection of Manfred Ehrlich (Böhl-Iggelheim, Germany), Late Jurassic, early Tithonian, Blumenberg, Eichstätt, Bavaria, Germany. **E:** private collection of Falk Starke (Bodenwerder, Germany), Late Jurassic, early Tithonian, Schernfeld, Bavaria, Germany. **cc**, calcite crystal, **ce**, compound eyes; **cp10–13**, coxal plates of post-ocular segments 10–13; **h**, head; **md**, mandible; **t7–18**, tergites of post-ocular segments 7–18; **pt**, pleotelson; **ul?**, possible remain of the upper lip; **un**, uropod endopod; **ux**, uropod exopod.
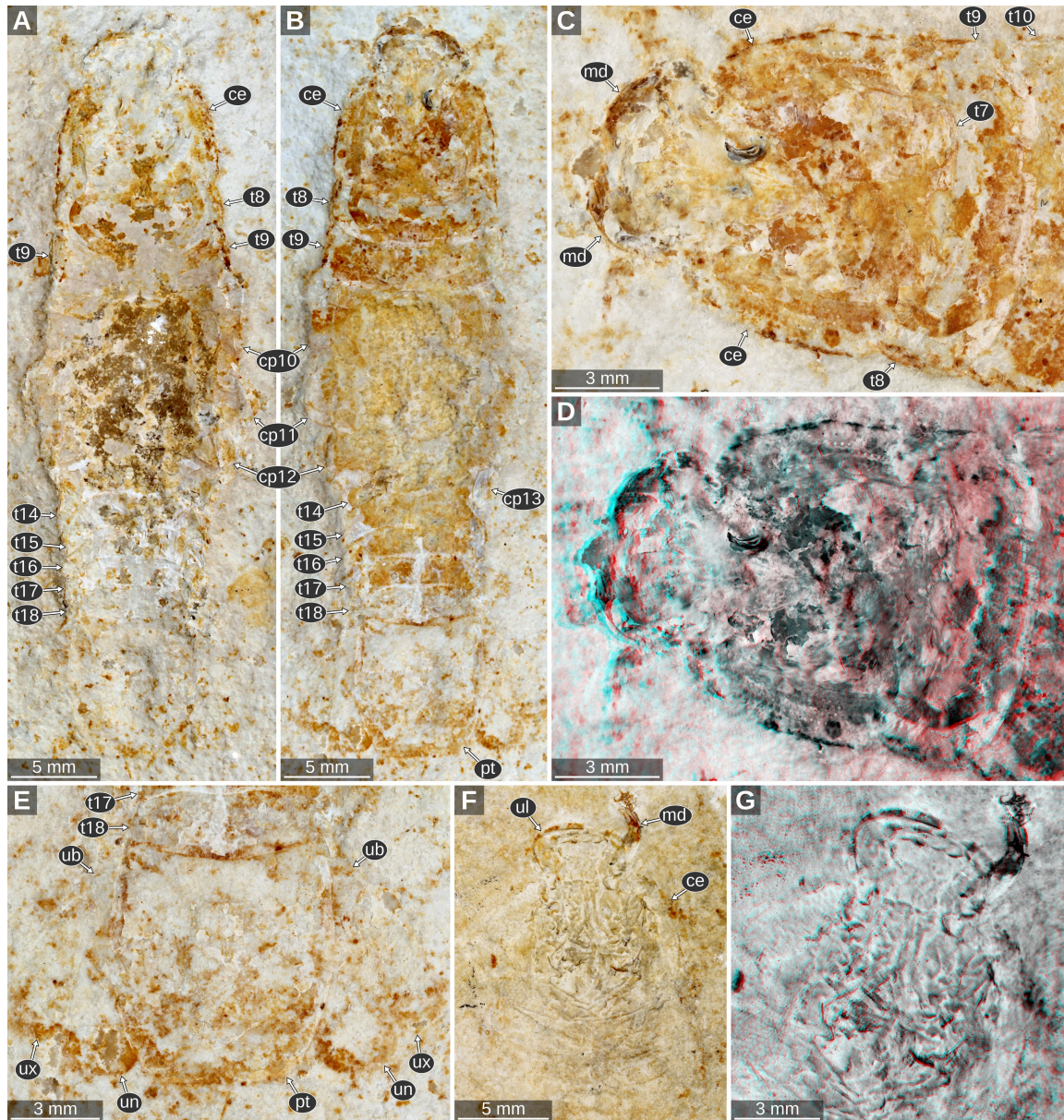
Figure 5: *Urda rostrata* Münster, 1840, macro photography. **A–E:** JMS-288, private collection of Udo Resch (Solnhofen), Late Jurassic, early Tithonian, Blumenberg (Eichstätt), Bavaria, Germany. **B:** counterpart of A. **C:** counterpart of A, head region. **D:** same view as C, red-cyan stereoanaglyph. **E:** counterpart of A, pleotelson region. **F–G:** JME SOS 1794, early Tithonian, Late Jurassic, greater Solnhofen area, Bavaria, Germany. **G:** red-cyan stereo anaglyph. **ce**, compound eye; **cp 10–13**, coxal plates of post-ocular segments 10–13; **md**, mandible; **pt**, pleotelson; **t7–18**, tergites of post-ocular segments 7–18; **ub**, uropod basipod; **ul**, upper lip; **un**, uropod endopod; **ux**, uropod exopod.
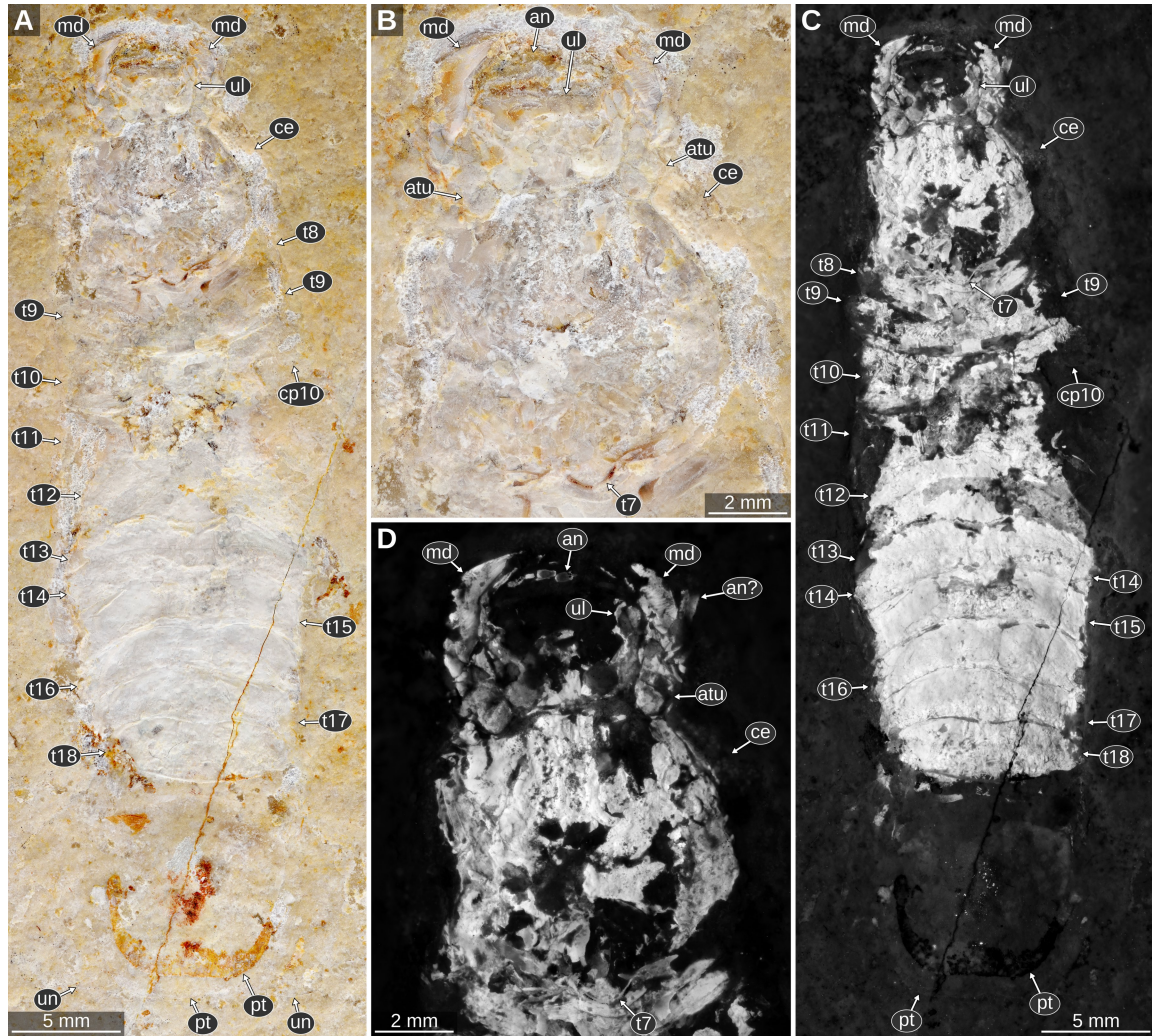
Figure 6: *Urda rostrata* Münster, 1840, private collection of Daniel Fauser (Schwäbisch Gmünd, Germany), Late Jurassic, early Tithonian, Wegscheid (Eichstätt), Bavaria, Germany. Note the preservation of the pleotelson and the uropod endopod. **A–B:** macro photography, diffused white light illumination. **B:** detail of the head region. **C–D:** UV light (365 nm) macro photography. **D:** detail of the head region. **an**, element of either antennula or antenna; **an?**, possible remain of either antennula or antenna; **atu**, antennula; **ce**, compound eye; **cp10**, coxal plate of post-ocular segment 10; **md**, mandible; **pt**, pleotelson; **t7–18**, tergites of post-ocular segments 7–18; **ul**, upper lip; **un**, uropod endopod.
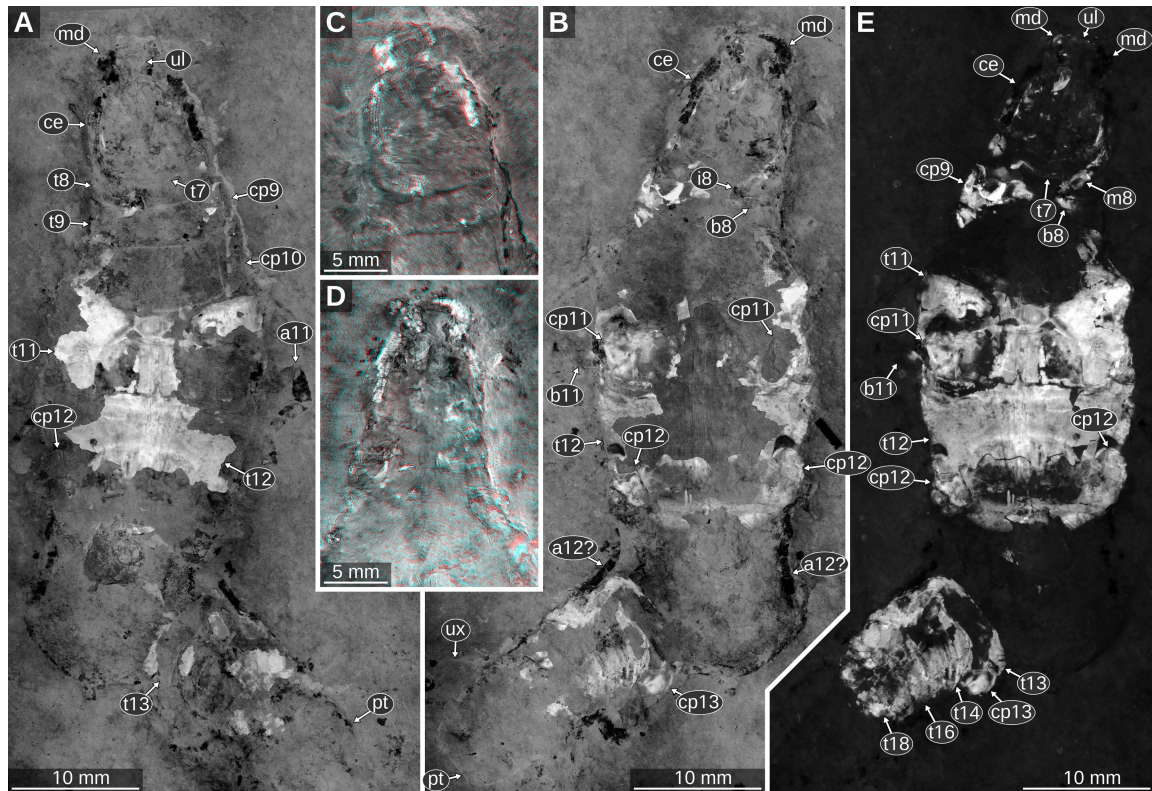
Figure 7: *Urda rostrata* Münster, 1840, private collection of Norbert Winkler (Stahnsdorf, Germany), Late Jurassic, early Tithonian, *Hybonoticeras hybonotum* Zone, Wegscheid (Eichstätt), Bavaria, Germany, green-orange fluorescence macro photography, desaturated. **A:** positive side. **B:** negative side. **C–D:** details of the head and anterior-most trunk region, red-cyan stereo anaglyphs based on luminescence-inverted fluorescence images, details of the. **C:** positive side. **D:** negative side. **E:** composite image of the positive and the negative side with focus on the fluorescent body parts. **a11**, appendage of post-ocular segment 11; **a12?**, possible appendage of post-ocular segment 12; **b8–11**, basipods of post-ocular segments 8–11; **ce**, compound eye; **cp9–13**, coxal plates of post-ocular segments 9–13; **i8**, ischium of post-ocular segment 8; **m8**, merus of post-ocular segment 8; **md**, mandible; **pt**, pleotelson; **t7–18**, tergites of post-ocular segments 7–18; **ul**, upper lip; **ux**, uropod exopod.
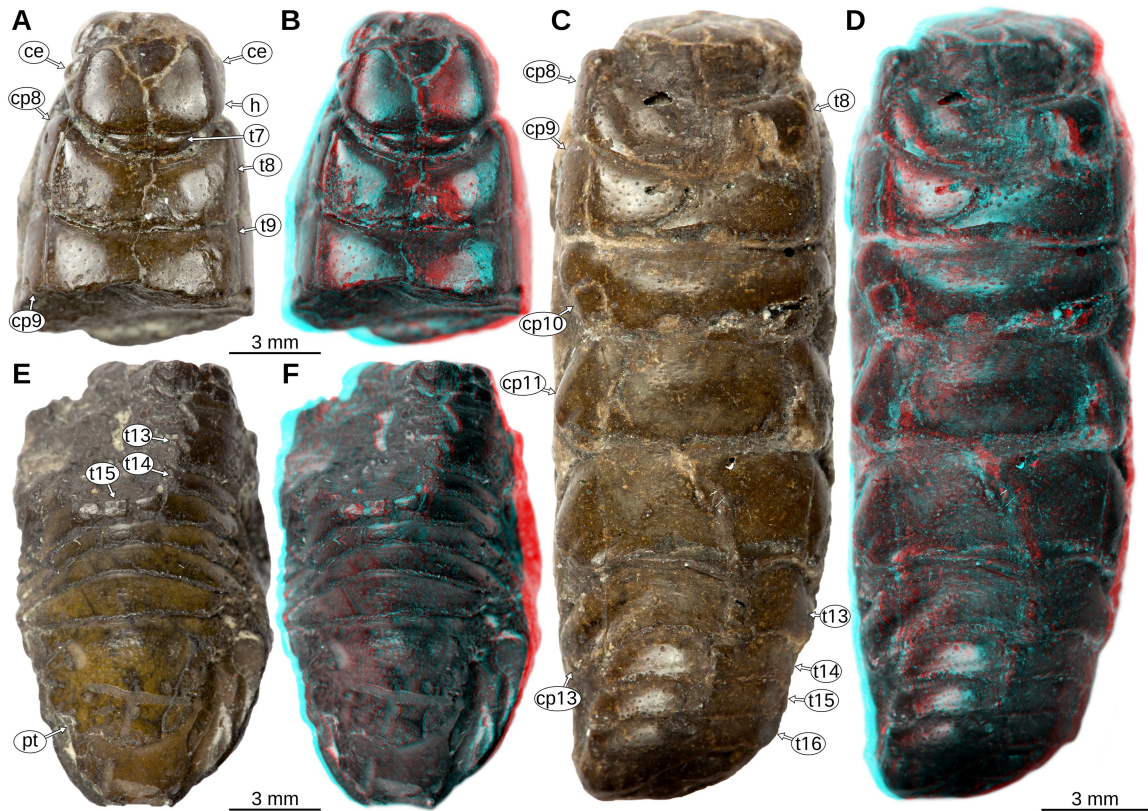
Figure 8: *Urda mccoyi* (Carter, 1889) sensu Feldmann, Wieder, and Rolfe (1994), syntypes, Early Cretaceous, Albian, Cambridge, Cambridgeshire, England, UK, images from 3d-fossils.ac.uk (CC BY-NC-SA 3.0). **A–B:** SM B 23295, dorsal view. **A:** macro photography. **B:** red-cyan stereo anaglyph. **C–D:** SM B 23296, dorsal view. **C:** macro photography. **D:** red-cyan stereo anaglyph. **E–F:** SM B 23297, dorsal view. **E:** macro photography. **F:** red-cyan stereo anaglyph. **ce**, compound eye; **cp8–13**, coxal plates of post-ocular segments 8–13; **h**, head; **pt**, pleotelson; **t7–16**, tergites of post-ocular segments 7–16.
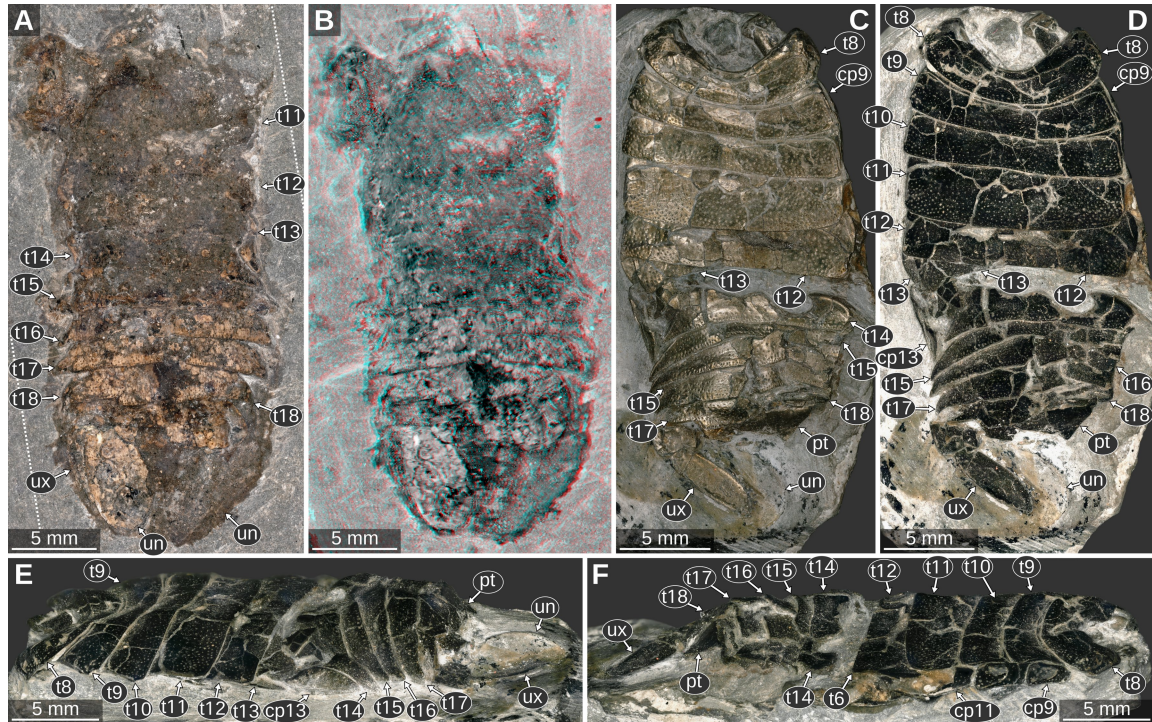
Figure 9: *Urda suevica* (Reiff, 1936) n. comb. **A–B:** syntype of '*Palaega kessleri*' (Reiff 1936, fig. 2, 'Fundstück B'), Natural History Museum Göppingen, without accession number, Early Jurassic, Pliensbachian, Göppingen, Germany. **A:** cross-polarised light microscopy, areas left and right to dotted lines are added digitally. **B:** macrophotography, red-cyan stereo anaglyph. **C–F:** syntype of '*Palaega kessleri*' (Reiff 1936, fig. 1, pl. 1, fig 4–5, 'Fundstück A'), GPIT, without accession number, Early Jurassic, Pliensbachian, Reutlingen, Germany. **C:** dorsal view, white light microscopy, HDR. **D:** dorsal view, cross-polarised light microscopy. **E:** lateral view from the left body side, cross-polarised light microscopy. **F:** lateral view from the right body side. **cp9–13**, coxal plates of post-ocular segments 9–13; **pt**, pleotelson; **t8–13**, tergites of post-ocular segments 8–13; **ub**, uropod basipod; **un**, uropod endopod; **ux**, uropod exopod.
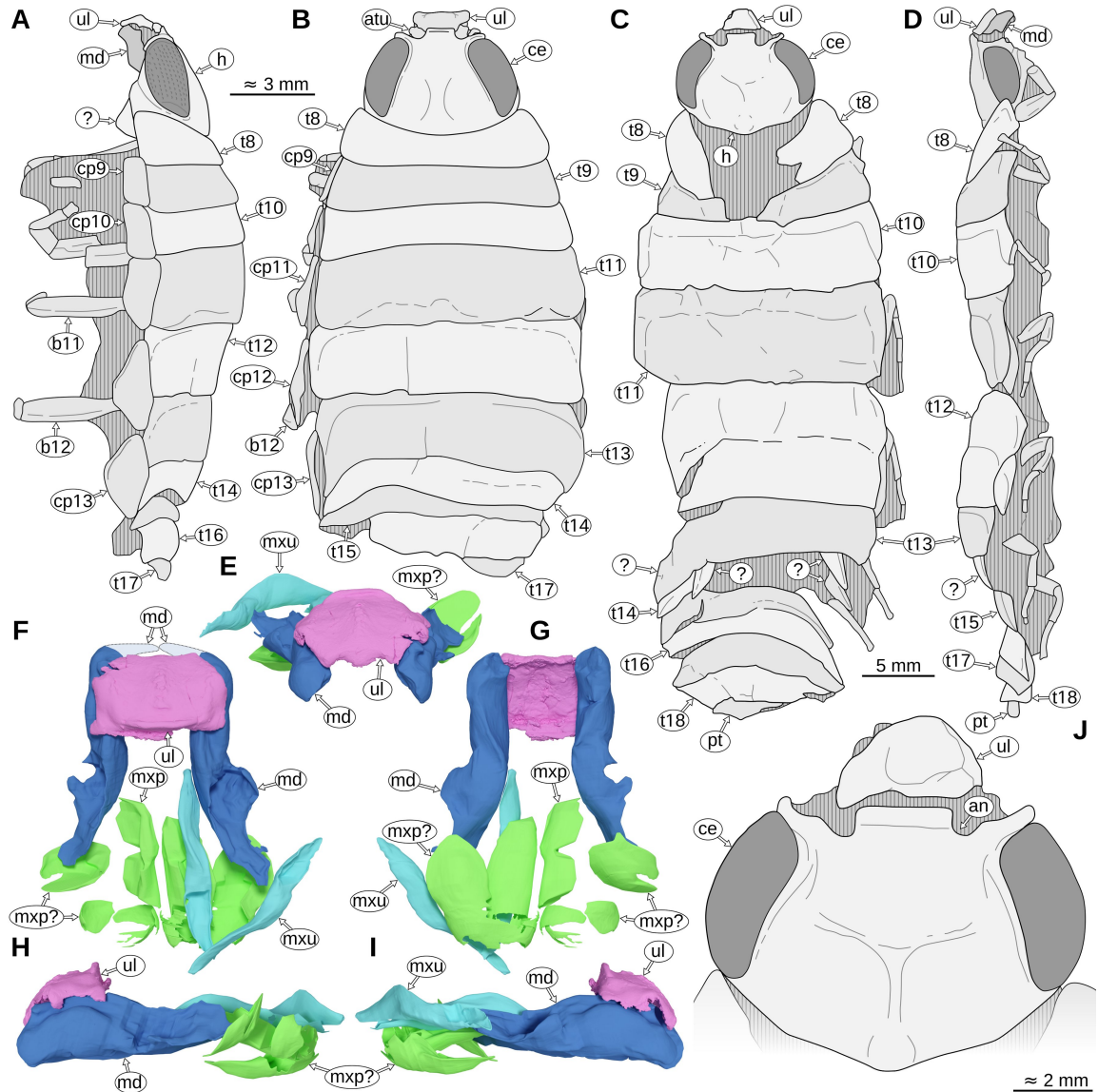
Figure 10: *Urda suevica* (Reiff, 1936) n. comb. **A–B:** syntype of '*Palaega kessleri*' (Reiff, 1936, fig. 3, pl. 1 figs 1–3, pl. 2 figs 1–2, 'Fundstück C'), SMNK, object destroyed, Early Jurassic, Pliensbachian, Reichenbach (Aalen), Germany. **A:** lateral view from the left body side, redrawn from Reiff (1936, fig. 3c). **B:** dorsal view, redrawn from Reiff (1936, fig. 3a). **C–D, J:** syntype of '*Palaega suevica*' (Reiff, 1936, fig. 7, pl. 1 figs. 6–9, pl. 2 fig. 3, 'Fundstück E'), SMNK, object destroyed, Early Jurassic, Pliensbachian, Holzheim (Göppingen), Germany, redrawn from Reiff (1936). **C:** dorsal view, redrawn from Reiff (1936, fig. 7a). **D:** lateral view from the right body side, redrawn from Reiff (1936, fig. 7c). **E–I:** syntype of '*Palaega suevica*' (Reiff 1936, fig. 10, pl. 3, fig. 4−6, 'Fundstück F'), GPIT, without accession number, Early Jurassic, Pliensbachian, Kirchheim unter Teck, Germany, 3D models based on μCT scanning data. **E:** frontal view. **F:** dorsal view, light blue area with dotted outline depicts broken-off parts that are visible in the original figures (Reiff 1936). **G:** ventral view. **H:** lateral view from the left body side. **I:** lateral view from the right body side. **J:** same specimen as in C–D, detail of the head in dorsal view, redrawn from

Reiff (1936, fig. 8a). **an**, antennular notch; **atu**, antennula; **b11–12**, basipods of post-ocular segments 11–12; **ce**, compound eye; **cp9–13**, coxal plates of post-ocular segments 9–13; **h**, head; **md**, mandible; **mxp**, maxilliped; **mxp?**, possibly part of the maxilliped; **mxu**, maxillula; **pt**, pleotelson; **t8–18**, tergites of post-ocular segments 2–7; **ul**, upper lip; **?**, unknown body part.
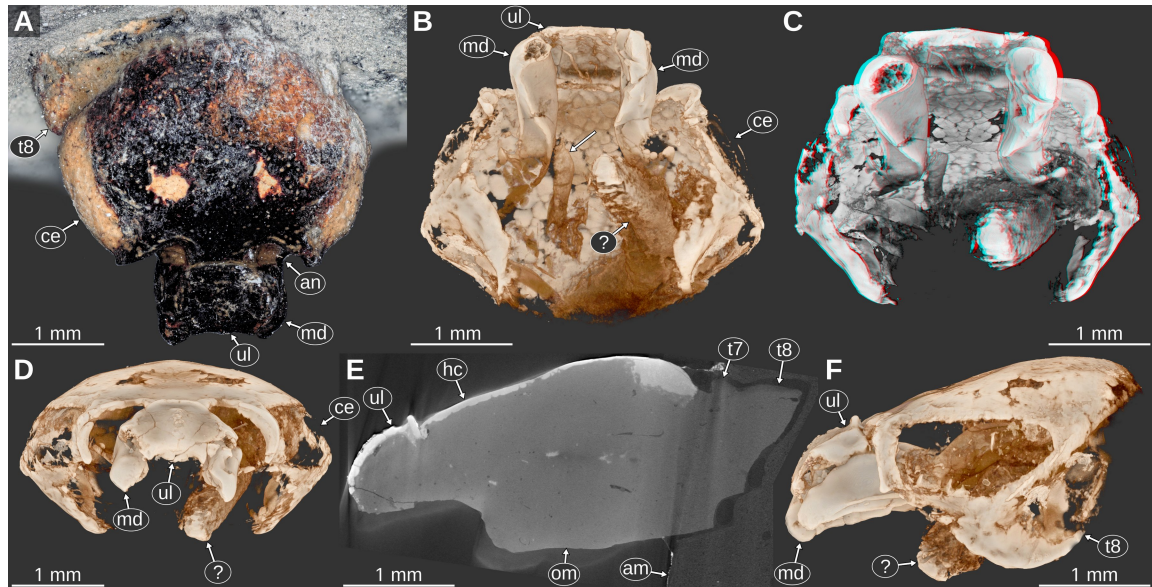
Figure 11: *Urda suevica* (Reiff, 1936) n. comb., syntype of '*Palaega suevica*' (Reiff 1936, fig. 10, pl. 3, fig. 4−6, 'Fundstück F'), GPIT, without accession number, Early Jurassic, Pliensbachian, Kirchheim, Germany. **A:** dorsal view, cross-polarised light microscopy, high dynamic range. **B–D, F:** volume rendered images from µCT scanning data, orthographic projection.

B–C: fronto-ventral view. **C:** red-cyan stereo anaglyph. **D:** frontal view. **E:** raw µCT volume, median-sagittal plane. **F:** lateral view from the rigt body side, mirrored. **am**, artificial matrix (likely gypsum); **an**, antennular notch; **ce**, compound eye; **hc**, head capsule; **md**, mandible; **om**, original sediment matrix; **t7–8**, tergites of post-ocular segments 7–8; **ul**, upper lip; **?**, unknown body part or sediment structure.
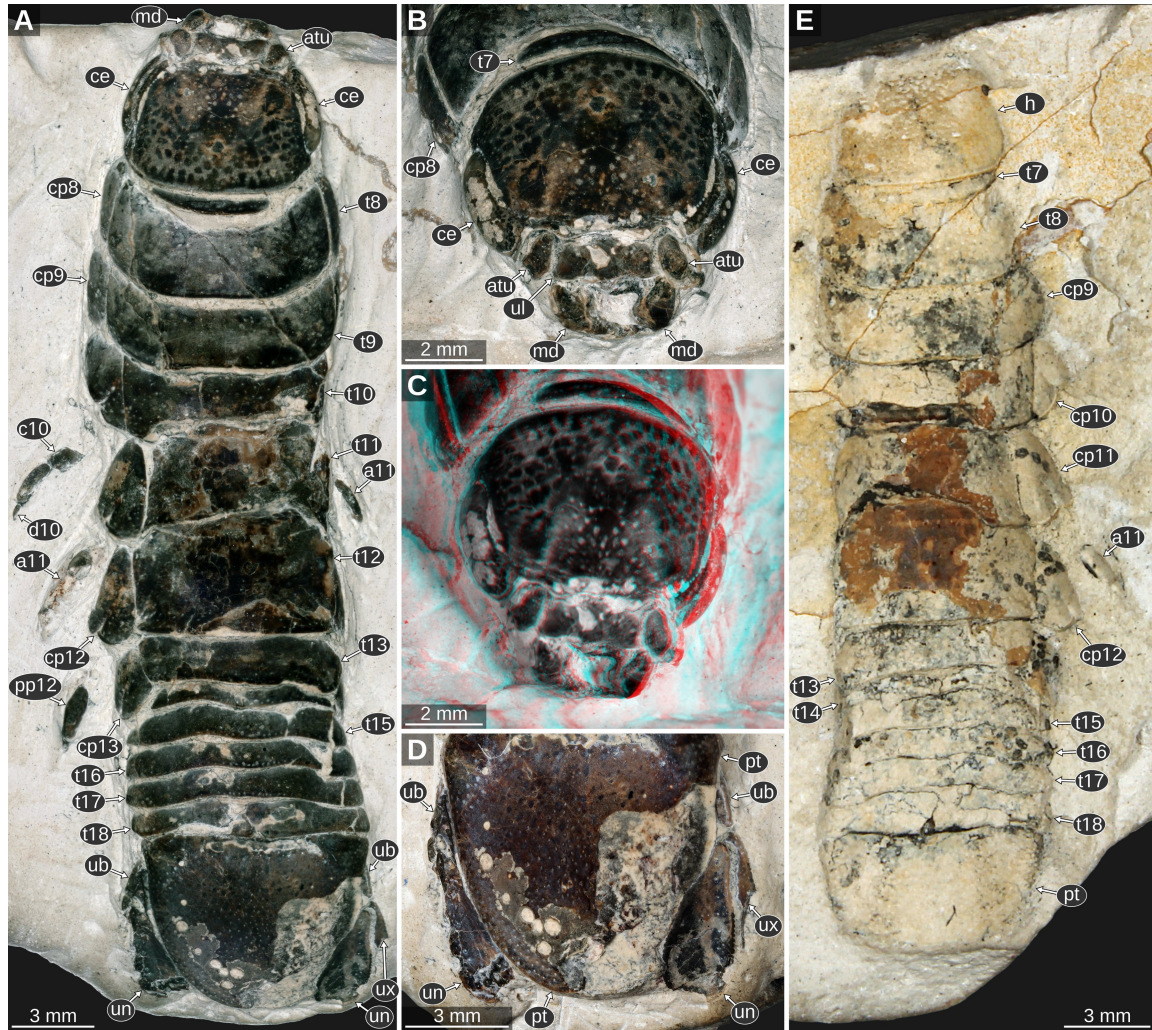
Figure 12: *Urda buechneri* n. sp., Middle Jurassic, Bajocian, quarry 'Bethel 1', Bielefeld, North Rhine-Westphalia. **A–D:** SNSB – BSPG 2011 I 50a (figured in Nagler *et al.*, 2017 as '*Urda rostrata*'). **A:** dorsal view, cross polarised light microscopy. **B:** head in antero-dorsal view, cross polarised light microscopy. **C:** red-cyan stereo anaglyph version of B. **E:** SNSB – BSPG 2011 I 50b (counterpart of A–D, figured in Nagler *et al.*, 2017 as '*Urda rostrata*'), macro photography. **a5**, appendage of post-ocular segment 5; **atu**, antennula; **c10**, carpus of post-ocular segment 10; **ce**, compound eye; **cp8–13**, coxal plates of post-ocular segments 8–13; **d10**, dactylus of post-ocular segment 10; **md**, mandible; **pp10–12**, propodi of post-ocular segments 10–12; **pt**, pleotelson; **t7–18**, tergites of post-ocular segments 7–18; **ub**, uropod basipod; **ul**, upper lip; **un**, uropod endopod; **ux**, uropod exopod.
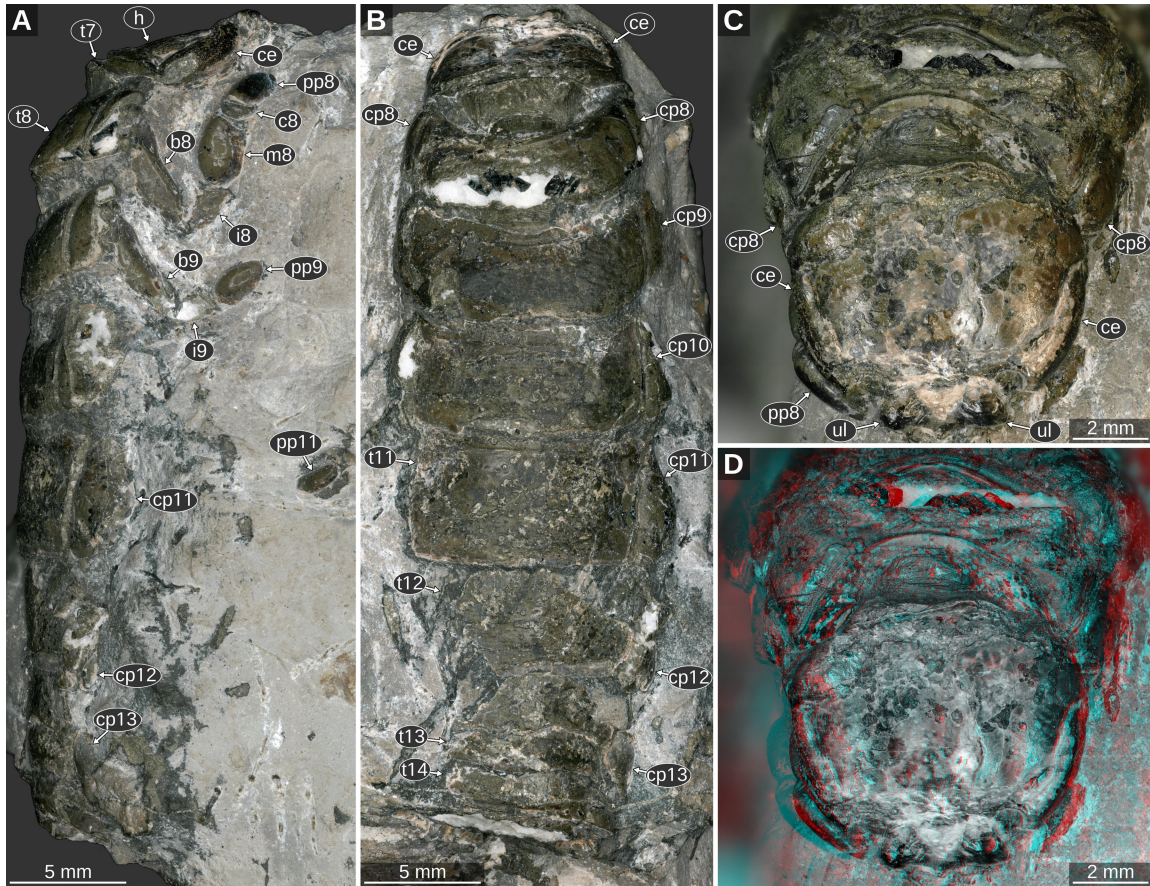
Figure 13: *Urda buechneri* n. sp. SNSB – BSPG 2011 I 51 (figured in Nagler *et al.*, 2017 as '*Urda rostrata*'), Middle Jurassic, Bajocian, quarry 'Bethel 1', Bielefeld, North Rhine-Westphalia, Germany, cross-polarised light microscopy. **A:** lateral view. **B:** dorsal view. **C–D:** head and anterior trunk region in anterodorsal view. **D:** red-cyan stereo anaglyph. **c8**, carpus of post-ocular segment 8; **ce**, compound eye; **cp8–13**, coxal plates of post-ocular segments 8–13; **h**, head; **i8–9**, ischia of post-ocular segments 8–9; **m8**, merus of post-ocular segment 8; **pp8–11**, propodi of post-ocular segments 8–11; **t7–14**, tergites of post-ocular segments 7–14; **ul**, upper lip.
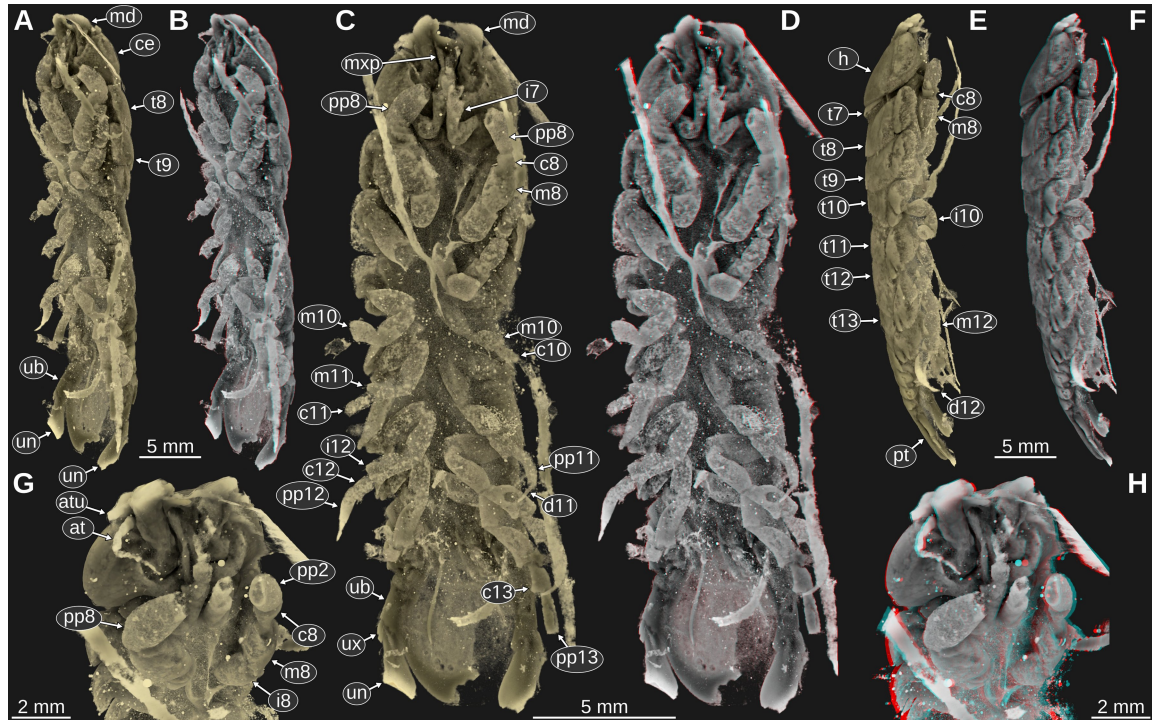
Figure 14: *Urda buechneri* n. sp. SNSB – BSPG 2011 I 50a (figured in Nagler *et al.*, 2017 as '*Urda rostrata*'), Middle Jurassic, Bajocian, quarry 'Bethel 1', Bielefeld, North Rhine-Westphalia, Germany, volume rendered images from μCT scanning data. **A–B:** ventro-lateral view from the left body side. **B:** red-cyan stereo anaglyph. **C–D:** ventral view. **D:** red-cyan stereo anaglyph. **E–F:** lateral view from the right body side. **F:** red-cyan stereo anaglyph. **G–H:** head and anterior trunk region in antero-ventro-lateral view from the right body side. **H:** red-cyan stereo anaglyph. **at**, antenna; **atu**, antennula; **c8–13**, carpi of t post-ocular segments 8–13; **ce**, compound eye; **d11–12**, dactyli of post-ocular segments 11–12; **h**, head; **i7–12**, ischia of post-ocular segments 7–12; **m8–11**, meri of post-ocular segments 8–11; **md**, mandible; **mxp**, maxilliped; **t7–13**, tergites of post-ocular segments 7–13; **pp8–13**, propodi of post-ocular segments 8–13; **pt**, pleotelson; **ub**, uropod basipod; **un**, uropod endopod; **ux**, uropod exopod.
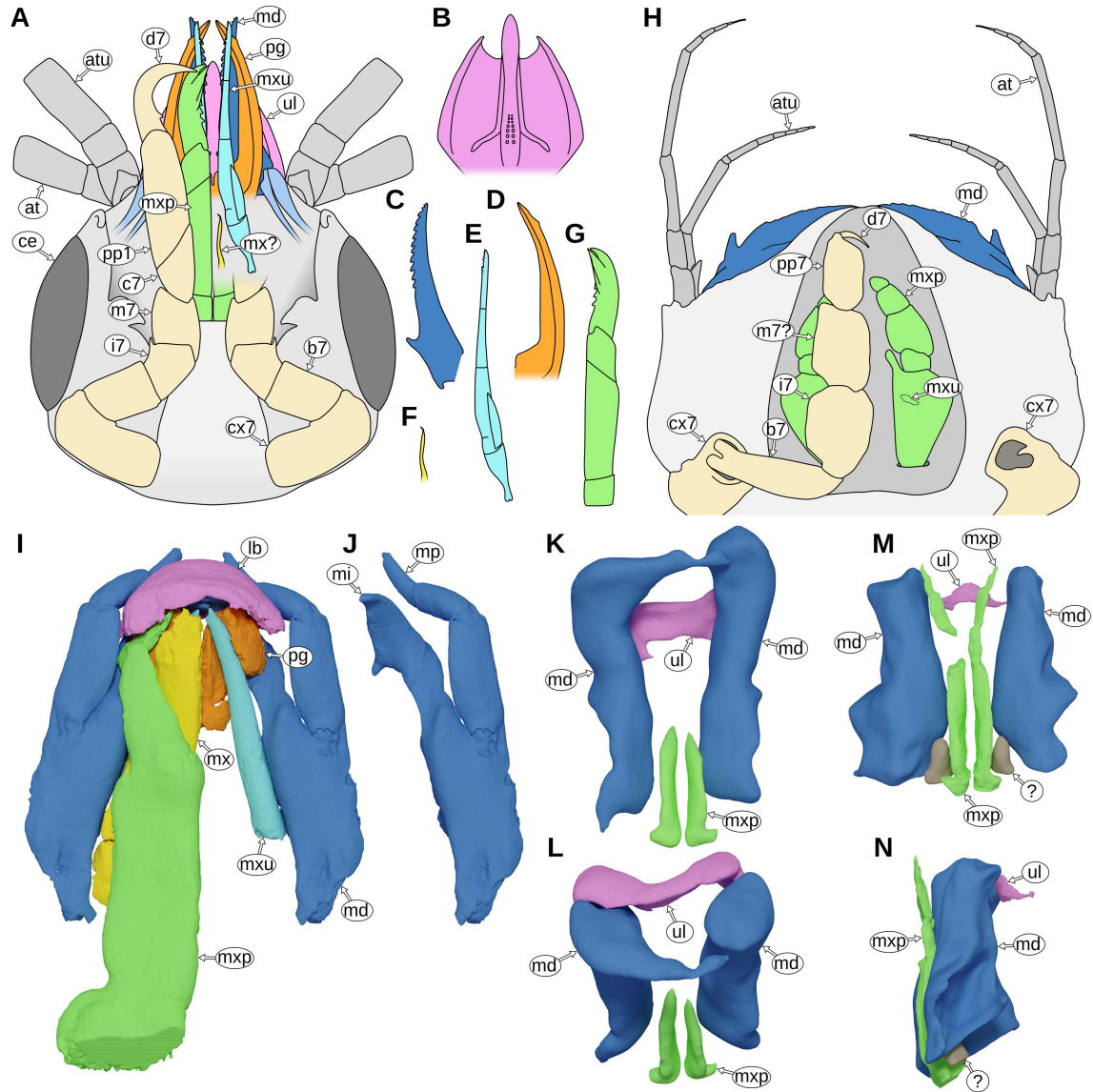
Figure 15: A: *Paragnathia formica* (Hesse, 1864), head in ventral view, redrawn after Monod (1926, p. 75 figs. 30, 33, 34). **B–G:** details of A, ventral view. **B:** upper lip. **C:** mandible. **D:** paragnath. **E:** maxillula. **F:** possible maxilla. **G:** maxilliped. **H:** *Bythognathia yucatanensis* Camp, 1988 head in ventral view, redrawn from Camp (1988, pp. 670–671 figs. 1–2). **I–J:** *Nerocila acuminata* Schiödte and Meinert, 1881, 3D reconstruction based on µCT data from Nagler *et al.* (2017). **I:** mouthparts in ventral view. **J:** left mandible in ventral view. **K–N:** *Urda buechneri* n. sp. (*Urda rostrata* sensu Nagler *et al.* 2017), 3D reconstruction of the mouthparts based on µCT data from Nagler *et al.* (2017). **K–L:** SNSB – BSPG 2011 I 50. **K:** ventral view. **L:** antero-ventral view. **M–N:** SNSB – BSPG 2011 I 51, note that the distal parts of the mandibles are missing. **M:** ventral view. **N:** lateral view from the left side of the body. **at**, antenna; **atu**, antennula; **b7**, basipod of post-ocular segment 7; **c7**, carpus of post-ocular segment 7; **ce**, compound eye; **cx7**, coxa of post-ocular segment 7; **d7**, dactylus of post-ocular segment 7; **i7**, ischium of post-ocular segment 7; **m7**, merus of post-ocular segment 7; **m7?**, possible merus (and/or carpus) of post-ocular segment 7; **md**,

mandible; **mx**, maxillula; **mx?**, possible maxillula; **mxp**, maxilliped; **mxu**, maxillula; **pg**, paragnath; **pp7**, propodus of post-ocular segment 7; **ul**, upper lip.
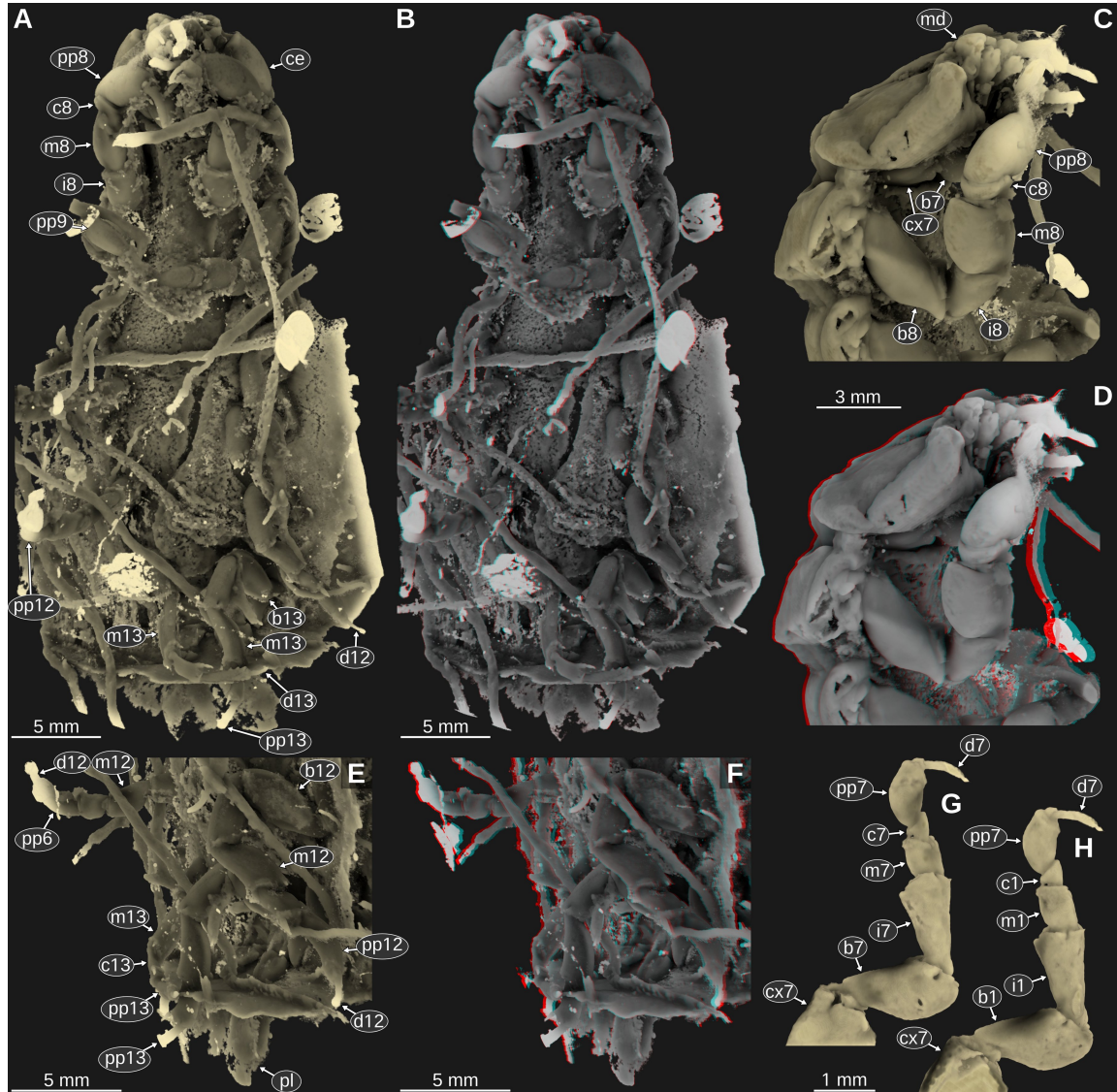
Figure 16: *Urda buechneri* n. sp. SNSB – BSPG 2011 I 51 (figured in Nagler *et al.*, 2017 as '*Urda rostrata*'), Middle Jurassic, Bajocian, quarry 'Bethel 1', Bielefeld, North Rhine-Westphalia, Germany, volume rendered images from µCT scanning data. **A–B:** ventral view, pleon region is missing. **B:** red-cyan stereo anaglyph. **C–D:** head and anterior trunk region in lateral view from the right body side. **D:** red-cyan stereo anaglyph. **E–F:** mid-body region in ventrolateral view from the left body side. **F:** red-cyan stereo anaglyph. **G–H:** appendage of post-ocular segment 7; **G:** posterior (functional lateral) view. **H:** anterior (functional median) view, mirrored. **b7–13**, basipods of post-ocular segments 7–13; **c7–13**, carpi of post-ocular segments 7–13; **ce**, compound eye; **cx7**, coxa of post-ocular segment 7; **d7–13**, dactyli of post-ocular segments 7–13; **i7–8**, ischia of post-ocular segments 7–8; **m7–13**, meri of post-ocular segments 7–13; **md**, mandible; **pl**, pleopod; **pp7–13**, propodi of post-ocular segments 7–13.
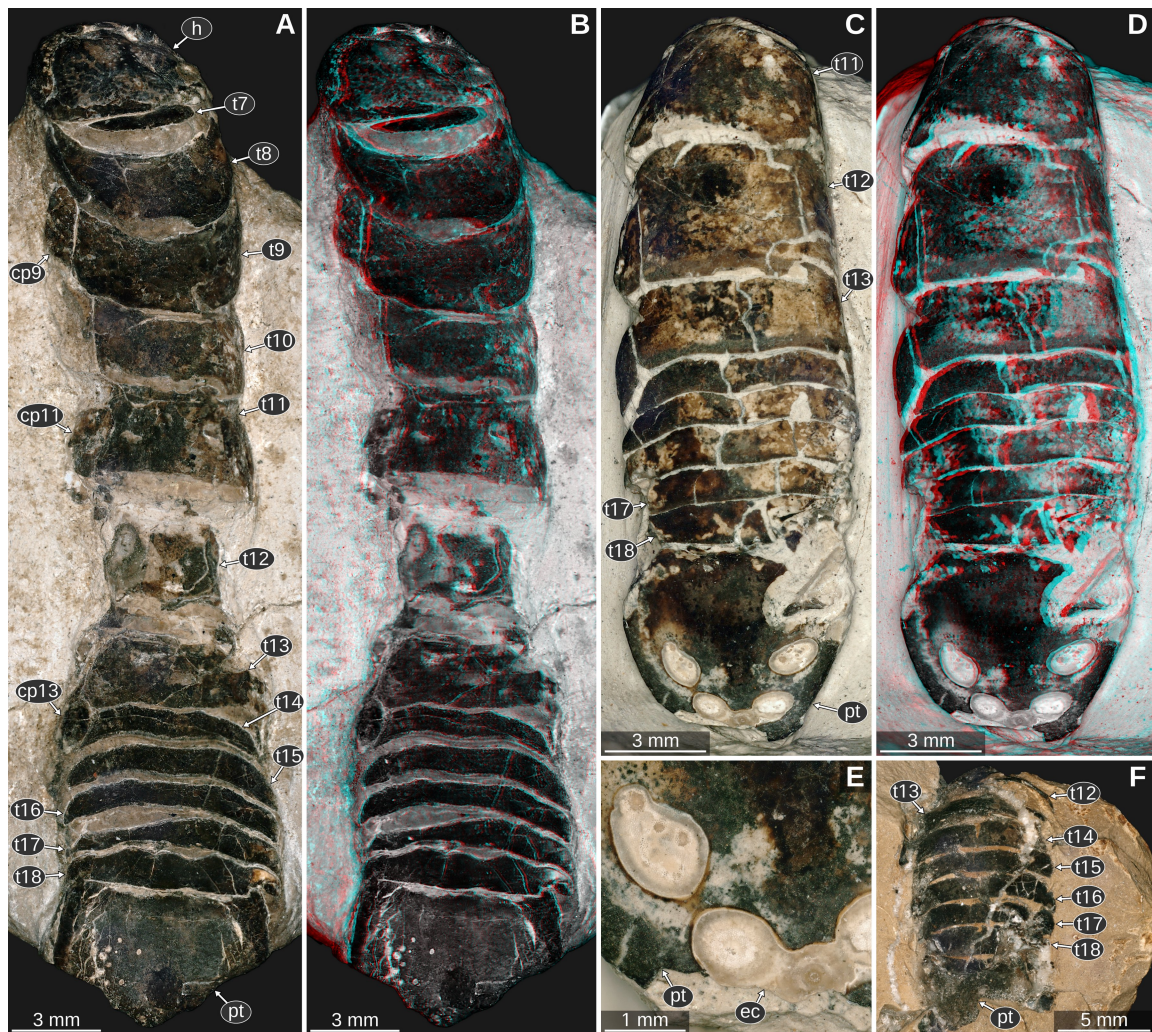
Figure 17: *Urda buechneri* n. sp., Middle Jurassic, Bajocian, quarry 'Bethel 1', Bielefeld, North Rhine-Westphalia, Germany, cross polarised light microscopy. **A–B:** ES/jb-8744, dorsal view. **B:** red-cyan stereo anaglyph. **C–E:** ES/jb-30755, dorsal view. **D:** red-cyan stereo anaglyph. **E:** detail of the posterior part of the pleotelson. **F:** ES/jb-30756, posterior trunk region in dorsal view. **cp9–13**, coxal plates of post-ocular segments 9–13; **ec**, encrustation; **h**, head; **pt**, pleotelson; **t7–18**, tergites of post-ocular segments 7–18.
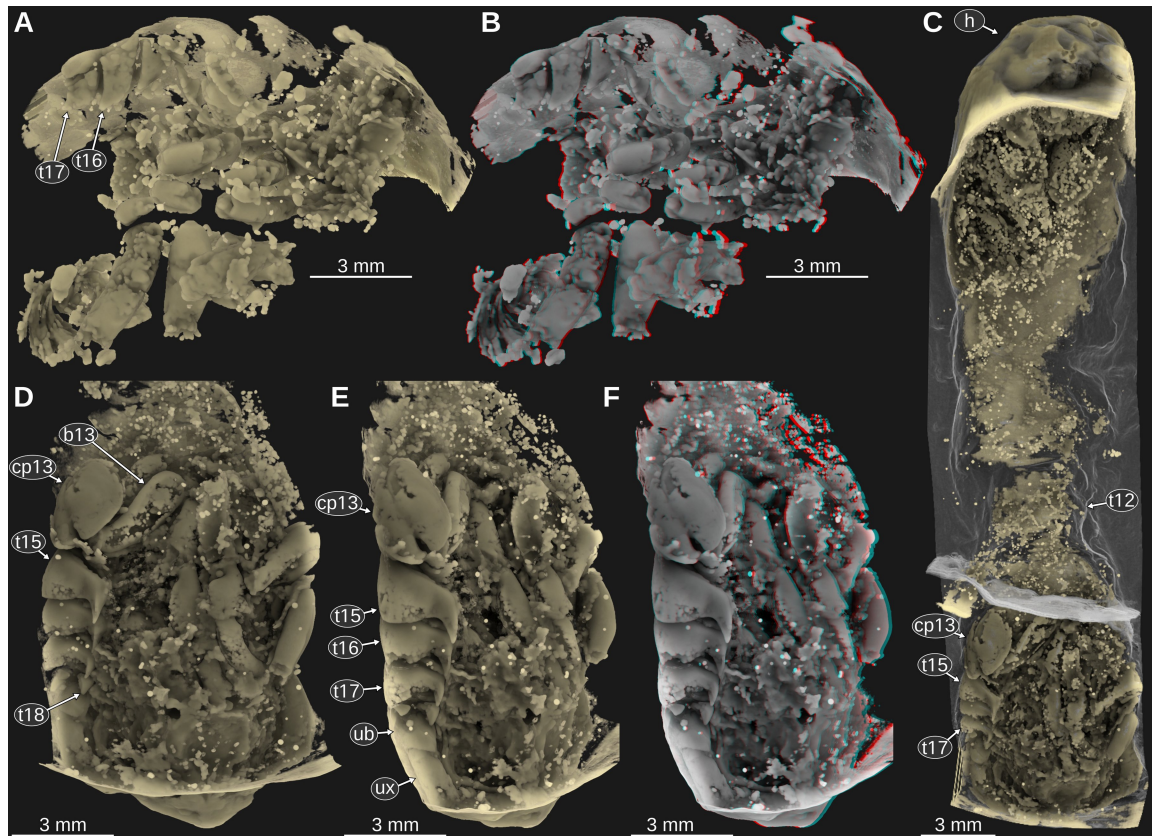
Figure 18: *Urda buechneri* n. sp., Middle Jurassic, Bajocian, quarry 'Bethel 1', Bielefeld, North Rhine-Westphalia, Germany, volume rendered images from µCT scanning data. **A–B:** ES/jb-30756, mid-body region in ventro-lateral view from the right body side (right side is anterior). **B:** red-cyan stereo anaglyph. **C–F:** ES/jb-8744. **C:** ventral view. **D:** pleon region in ventral view. **E:** pleon region in ventro-lateral view from the left body side. **F:** red-cyan stereo anaglyph version of E. **b13**, basipod of post-ocular segments 13; **cp13**, coxal plate of post-ocular segment 13; **h**, head; **t12–18**, tergites of post-ocular segments 12–18; **ub**, uropod basipod; **ux**, uropod exopod.
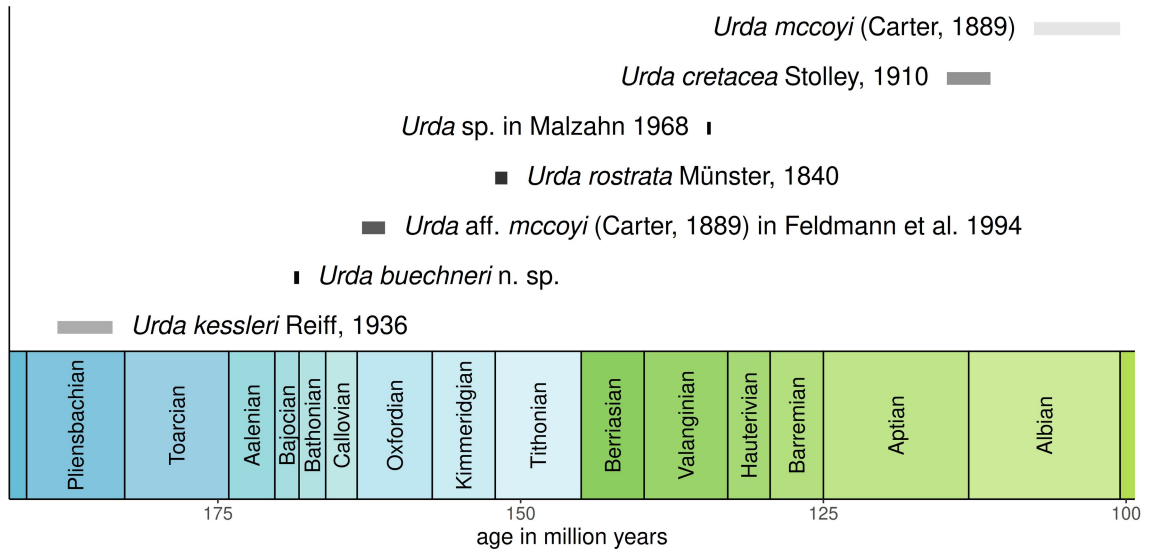
Figure 19: Stratigraphic distribution of representatives of *Urda* Münster, 1840 ('Gantt chart'). The depicted timespans (horizontal grey bars) do not refer to the longevity of the species but represent the possible age range of each occurrence. The grey values of the horizontal lines additionally correlate with the uncertainty of the occurrence: short dark lines for precisely and long light lines for less precisely dated occurrences. The colours of the geological scale are according to the International Chronostratigraphic Chart (v 2020/01).
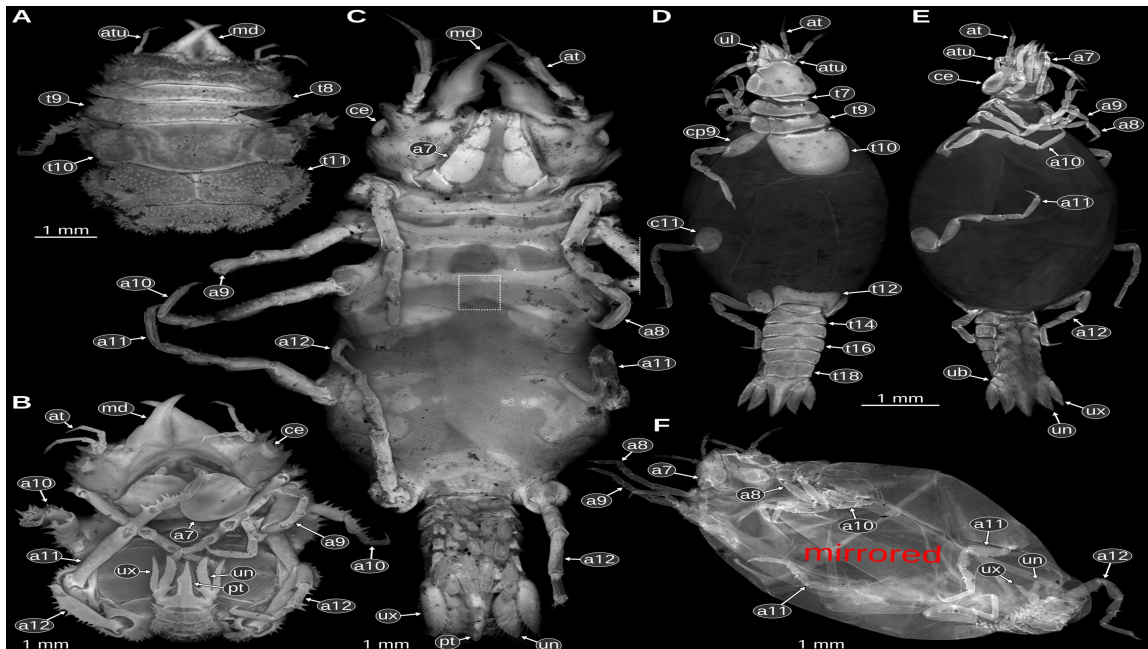
Figure 20: Extant representatives of Gnathiidae, epifluorescence microscopy, 360 ± 20 nm excitation wavelength. **A–B:** *Gnathia* sp., praniza, CeNak K 38945-1. **A:** dorso-lateral view. **B:** ventro-lateral view. **C:** *Gnathia* sp., adult female, eggs removed from marsupium, CeNak K 38945-2, ventral view. **D–E:** Gnathiidae sp., adult male, CeNak K 38947-1. **D:** head and anterior part of the trunk in dorsal view. **E:**

ventral view, dotted rectangle encompasses area with artificially generated image. **F:** *Euneognathia* sp., adult male, CeNak K 40059, ventral view. **a7–12**, appendages of post-ocular segments 7–12; **at**, antenna; **atu**, antennula; **ce**, compound eye; **cp10–11**, coxal plates of post-ocular segments10–11; **md**, mandible; **pt**, pleotelson; **t7–18**, tergites of post-ocular segments 7–18; **ub**, uropod basipod; **ul**, upper lip; **un**, uropod endopod; **ux**, uropod exopod.
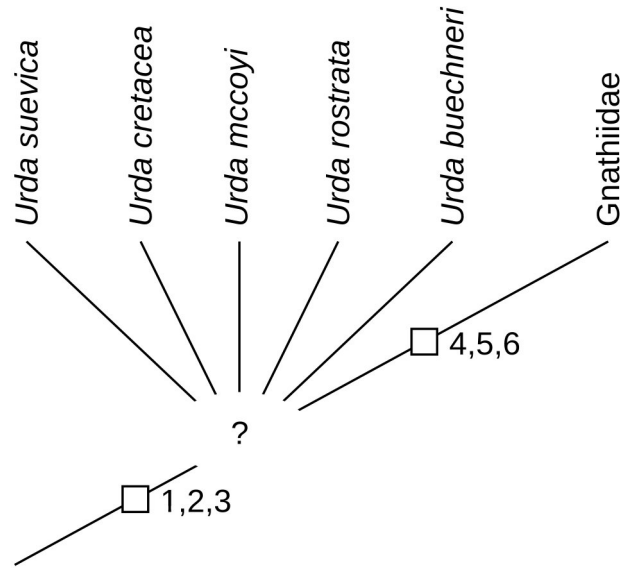
Figure 21: Proposed relationship between species of Urda and the group Gnathiidae. **1**, anterior margin of the head with a straight median portion (proximal joint of the upper lip); **2**, upper lip large, frontal lamina and labrum not developed or conjoined with other structures; **3**, tergite of post-ocular segment 7 very short; **4**, post-ocular segments 13 without well-developed appendages; **5**, maxilliped and appendage of post-ocular segments 7 with flattened elements (adult forms); **6**, mandible straight and projected anteriorly (larval forms).
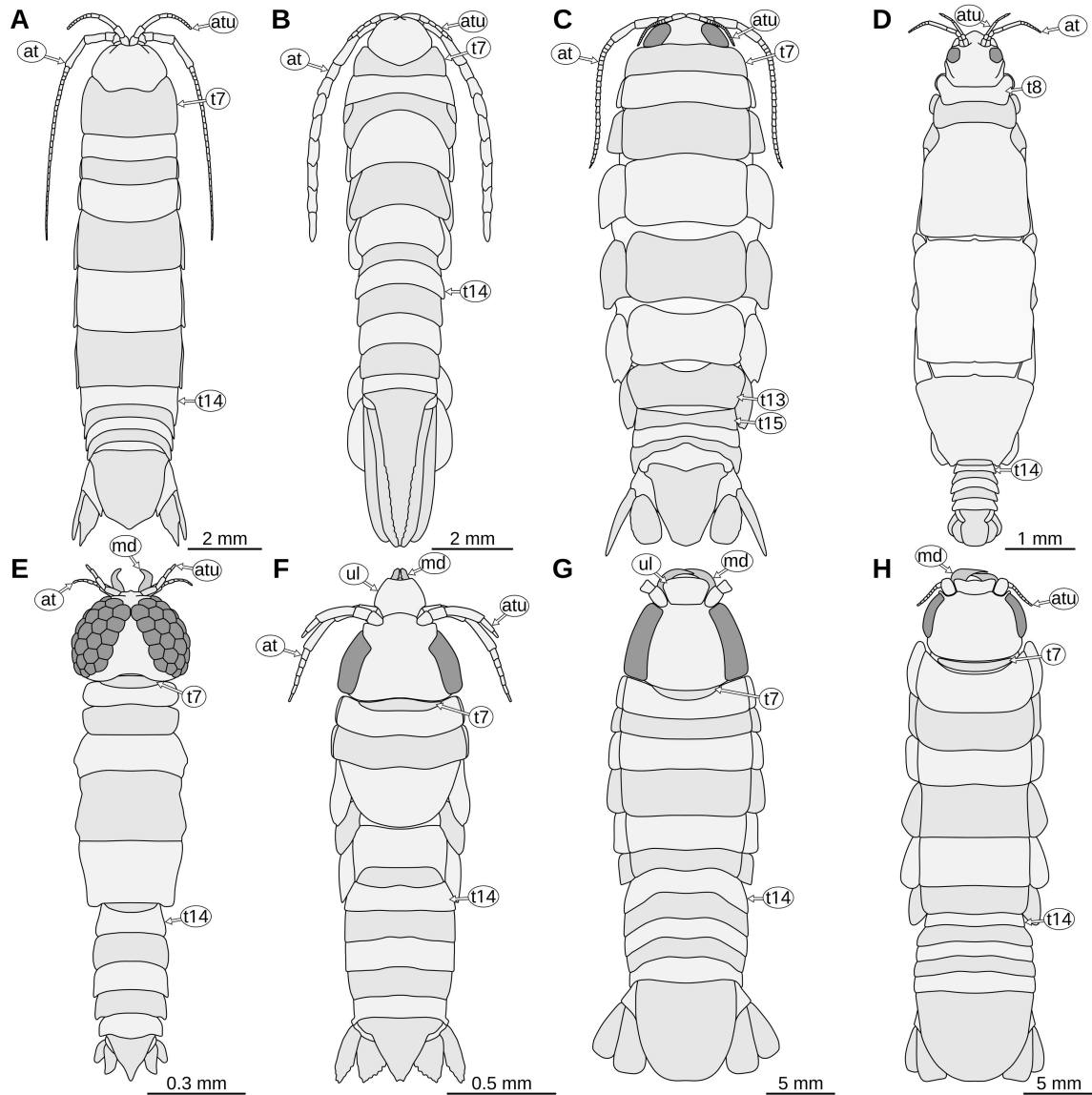
Figure 22: habitus drawings in dorsal view. **A:** *Typhlocirolana buxtoni* Racovitza, 1912, adult, redrawn from Racovitza (1912). **B:** *Protognathia bathypelagica* (Schultz, 1977), immature specimen, redrawn from Wägele and Brandt (1988). **C:** Corallana sp., Comprehensive Marine Biodiversity Survey, Singapore, JS-2675, drawn after a photograph by Arthur Anker, no scale available. **D:** *Caecognathia agwillisi* (Seed, 1979), adult female, redrawn from Seed (1979). **E:** *Tenerognathia visus* Tanaka, 2005, adult male, redrawn from Tanaka (2005). **F:** *Gnathia* sp., zuphea stage, Lizard Island, AM P.81399, drawn from SEM images in Wilson *et al.* (2011). **G:** *Urda rostrata* Münster, 1842, reconstructed from multiple fossils of the greater Solnhofen area, Germany. **H:** *Urda buechneri* n. sp., reconstructed from multiple fossils from Bethel, Germany. **at**, antenna; **atu**, antennula; **md**, mandible; **t7–15**, tergites of post-ocular segments 7–15; **ul**, upper lip.
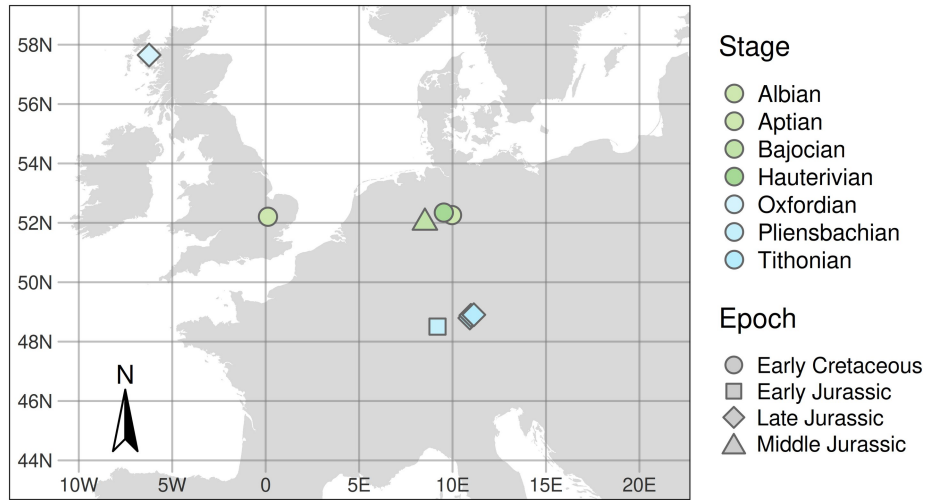
Figure 23: Map of Central Europe with the geographical occurrences of fossil representatives of *Urda* Münster, 1840 colour and shape coded after the age of the fossils. Map data from naturalearthdata.com (public domain) via 'rnaturalearth' (South, 2017).

References

Abd El-Atti, M., 2020, Light and Scanning electron microscopic investigations on gravid female *Anilocra* sp. (Isopoda: Cymothoidae) infesting *Tilapia zillii* in Qarun Lake, Egypt.: Egyptian Journal of Aquatic Biology and Fisheries 24, 183–196. https://doi.org/10.21608/ejabf.2020.104225

Ammon, L. von, 1882, Ein Beitrag zur Kenntnis der fossilen Asseln: Sitzungsberichte Der Mathemathisch- Physikalischen Classe Der Königlichen Bayerischen Akademie Der Wissenschaften 12, 507–551.

An, J., Boyko, C.B., Li, X., 2015, A Review of bopyrids (Crustacea: Isopoda: Bopyridae) parasitic on caridean shrimps (Crustacea: Decapoda: Caridea) from China: Bulletin of the American Museum of Natural History 399, 01–85. https://doi.org/10.1206/amnb-921-00-01.1

Ax, P., 2000, The Phylogenetic System of the Metazoa, Multicellular Animals. Springer-Verlag, Berlin.

Barnard, K.H., 1920, Contributions to the crustacean fauna of South Africa. No. 6.- Further additions to the list of marine Isopoda: Annals of the South African Museum 17, 319–438.

Bengtson, S., 2000, Teasing fossils out of shales with cameras and computers: Palaeontologia Electronica 3, 1–14.

Bowman, T.E., 1971, *Palaega lamnae*, new species (Crustacea: Isopoda) from the Upper Cretaceous of Texas: Journal of Paleontology 45, 540–541.

Boyko, C.B., Wolff, C., 2014, Isopoda and Tanaidacea: in Martin, J.W., Olesen, J., Hoeg, J.T. (eds.), Atlas of Crustacean Larvae, Johns Hopkins University Press, Baltimore, 210–212.

Brandt, A., Poore, G.C., 2003, Higher classification of the flabelliferan and related Isopoda based on a reappraisal of relationships: Invertebrate Systematics 17, 893–923.

Brandt, A., Poore, G.C., 2001, Two new species of *Tridentella* (Crustacea: Isopoda: Tridentellidae) from Namibia: Beaufortia 51, 199–212.

Bruce, N.L., 2009, The marine fauna of New Zealand: Isopoda, Aegidae (Crustacea), Biodiversity Memoir. National Institute of Water and Atmospheric Research, Wellington.

Bruce, N.L., 2005, Two new species of the mesopelagic isopod genus *Syscenus* Harger, 1880 (Crustacea: Isopoda: Aegidae) from the southwestern Pacific: Zootaxa 1070, 31–42. https://doi.org/10.11646/zootaxa.1070.1.2

Bruce, N.L., 1986, Cirolanidae (Crustacea: Isopoda) of Australia: Records of the Australian Museum, Supplement 6, 1–239. https://doi.org/10.3853/j.0812-7387.6.1986.98

Bruce, N.L., Olesen, J., 2002, Cirolanid isopods from the Andaman Sea off Phuket, Thailand, with description of two new species: Phuket Marine Biological Center Special Publication 23, 109–131.

Brusca, R.C., 1978, Studies on the Cymothoid fish symbionts of the eastern Pacific (Isopoda, Cymothoidae) I. Biology of *Nerocila californica*: Crustaceana 34, 141–154.

Brusca, R.C., Wilson, G.D.F., 1991, A phylogenetic analysis of the Isopoda with some classificatory recommendations: Memoirs of the Queensland Museum 31, 143–204.

Büchner, M., 1971, Eine fossile Meeresassel (Isopoda, Malacostraca) aus den Parkinsonienschichten (Mittlerer Jura) von Bethel, Kreis Bielefeld: Bericht Des Naturwissenschaftlichen Vereins Bielefeld 27–35.

Calman, W.T., 1914, Reviews. I.—Fossil Crustacea: Geological Magazine 1, 325–326. https://doi.org/10.1017/S0016756800139767

Camp, D.K.`, 1988, *Bythognathia yucatanensis*, new genus, new species, from Abyssal depths in the Caribbean Sea, with a list of gnathiid species described since 1926 (Isopoda: Gnathiidea): Journal of Crustacean Biology 8, 668–678.

Camp, D.K., Heard, R.W., 1988, *Booralana tricarinata*, A new species of isopod from the Western Atlantic Ocean (Crustacea, Isopoda, Cirolanidae): Proceedings of the Biological Society of Washington 101, 603–613.

Cardona, A., Saalfeld, S., Schindelin, J., Arganda-Carreras, I., Preibisch, S., Longair, M., Tomancak, P., Hartenstein, V., Douglas, R.J., 2012, TrakEM2 Software for Neural Circuit Reconstruction: PLOS ONE 7, e38011. https://doi.org/10.1371/journal.pone.0038011

Carter, J., 1889, On fossil isopods, with a description of a new species: The Geological Magazine. New Series 3, 193–196.

Cohen, B.F., Poore, G.C.B., 1994, Phylogeny and biogeography of the Gnathiidae (Crustacea: Isopoda) with descriptions of new genera and species, most from southeastern Australia: Memoirs of the Museum of Victoria 54, 271–397. https://doi.org/10.24199/j.mmv.1994.54.13

Cowper Reed, F.R., 1897, The Geology of Cambridgeshire. Cambridge University Press, Cambridge.

Daniel, G., Nilsson, T., Cragg, S., 1991, *Limnoria lignorum* ingest bacterial and fungal degraded wood: Holz Als Roh- Und Werkstoff 49, 488–490. https://doi.org/10.1007/BF02619480

Delaney, P.M., 1989, Phylogeny and biogeography of the marine isopod family Corallanidae (Crustacea, Isopoda, Flabellifera), Contribution in Science. Natural History Museum.

Dreyer, H., Wägele, J.-W., 2002, The Scutocoxifera tax. nov. and the information content of nuclear ssu rDNA sequences for reconstruction of isopod phylogeny (Peracarida: Isopoda): Journal of Crustacean Biology 22, 217–234.

Dreyer, H., Wägele, J.-W., 2001, Parasites of crustaceans (Isopoda: Bopyridae) evolved from fish parasites: molecular and morphological evidence: Zoology 103, 157–178.

Eklund, M.J., Aase, A., Bell, C.J., 2018, Progressive photonics: methods and applications of sequential imaging using visible and non-visible spectra to enhance data-yield and facilitate forensic interpretation of fossils: Journal of Paleontological Techniques 20, 1–36.

Etter, W., 1988, Isopoden und Tanaidaceen (Crustacea, Malacostraca) aus dem unteren Opalinuston der Nordschweiz: Eclogae geologicae Helveticae 81, 857–877. https://doi.org/10.5169/seals-166204

Fedorov, A., Beichel, R., Kalpathy-Cramer, J., Finet, J., Fillion-Robin, J.-C., Pujol, S., Bauer, C., Jennings, D., Fennessy, F., Sonka, M., Buatti, J., Aylward, S., Miller, J.V., Pieper, S., Kikinis, R., 2012, 3D Slicer as an image computing platform for the Quantitative Imaging Network: Magnetic Resonance Imaging, Quantitative Imaging in Cancer 30, 1323–1341. https://doi.org/10.1016/j.mri.2012.05.001

Feldmann, R.M., Schweitzer, C.E., Maxwell, P.A., Kelley, B.M., 2008, Fossil isopod and decapod crustaceans from the Kowai Formation (Pliocene) near Makikihi, South Canterbury, New Zealand: New Zealand Journal of Geology and Geophysics 51, 43–58. https://doi.org/10.1080/00288300809509849

Feldmann, R.M., Wieder, R.W., Ian Rolfe, W.D., 1994, *Urda mccoyi* (Carter 1889), an isopod crustacean from the Jurassic of Skye: Scottish Journal of Geology 30, 87–89. https://doi.org/10.1144/sjg30010087

Fraser, D., Mallon, J.C., Furr, R., Theodor, J.M., 2009, Improving the repeatability of low magnification microwear methods using high dynamic range imaging: PALAIOS 24, 818–825. https://doi.org/10.2110/palo.2009.p09-064r

Frentzen, K., 1937, Paläontologische Notizen aus den Badischen Landessamlungen für Naturkunde, Karlsruhe i. B. I. Neue Funde von Isopoden (Asseln) im Lias Südwestdeutschlands: Beiträge Zur Naturkundlichen Forschung in Südwestdeutschland 2, 100–103.

Gantt, H.L., 1910, Work, Wages and Profit, 2nd ed. The Engineering Magazine Co., New York.

Gearty, W., 2021, deeptime: Plotting tools for anyone working in deep time. R.

Grant-Mackie, J.A., Buckeridge, J.S., Johns, P.M., 1996, Two new Upper Jurassic arthropods from New Zealand: Alcheringa: An Australasian Journal of Palaeontology 20, 31–39. https://doi.org/10.1080/03115519608619221

Grobe, P., Vogt, P.R., 2009, Morph.D.Base 2.0: A public data base for morphological data, metadata, and phylogenetic matrices [WWW Document]. URL http://www.morphdbase.de

Haack, W., 1933, Zur Verbreitung des Asselkrebses Archaeoniscus brodiei M. EDW. im Serpulit des Teutoburger Waldes: Zeitschrift der Deutschen Geologischen Gesellschaft 85, 229–234.

Haug, C., Haug, J.T., Waloszek, D., Maas, A., Frattigiani, R., Liebau, S., 2009, New methods to document fossils from lithographic limestones of Southern Germany and Lebanon: Palaeontologia Electronica 12, 1–12.

Haug, J.T., Haug, C., 2011, Fossilien unter langwelligem Licht: Grün-Orange-Fluoreszenz an makroskopischen Objekten: Archaeopteryx 29, 20–23.

Hesse, Eugène., 1864, Les Pranizes et sur les Ancées: Mémoire sur les pranizes et les ancées et sur les moyens curieux à l'aide desquels certains crustacés parasites assurent la conservation de leur espèce, Des Mémoires Presentés Par Divers Savants à L'Institut Impérial De France, Impremerie Imperiale, Paris, 1–72.

Hessler, R.R., 1969, Peracarida: in Moore, R.C. (ed.), Treatise of Invertebrate Paleontology, Part R, Arthropoda 4, The Geological Society of America and University of Kansas, Boulder, Colorado and Lawrence, Kansas, R360–R393.

Hopson, P.M., Wilkinson, I.P., Woods, M.A., 2008, A stratigraphical framework for the Lower Cretaceous of England: British Geological Survey British Geological Survey Research Report, 1–74.

Hyžný, M., Bruce, N.L., Schlögl, J., 2013, An appraisal of the fossil record for the Cirolanidae (Malacostraca: Peracarida: Isopoda: Cymothoida), with a description of a new cirolanid isopod crustacean from the early Miocene of the Vienna Basin (Western Carpathians): Palaeontology 56, 615–630. https://doi.org/10.1111/pala.12006

Itoh, K., Hayashi, A., Ichioka, Y., 1989, Digitized optical microscopy with extended depth of field: Applied Optics 28, 3487–3493. https://doi.org/10.1364/AO.28.003487

Jukes-Browne, A.J., 1881, Appendix B. List of Gault Fossils (remaniés) found in the "Cambridge Greensand": in Penning, W.H., Jukes-Browne, A.J. (eds.), The

Geology of the Neighbourhood of Cambridge, H.M. Stationery Office, London, 149–154.

Jukes-Browne, A.J., 1875, On the relations of the Cambridge Gault and Greensand: Quarterly Journal of the Geological Society 31, 256–316.

Keupp, H., Mahlow, K., 2017, Eine neue Isopoden-Art (*Palaega johannschoberti* n. sp.) aus dem Amaltheenton (Unter-Jura, Ober-Pliensbachium) von Buttenheim in Oberfranken: Zitteliana 89, 161–170.

Kikinis, R., Pieper, S.D., Vosburgh, K.G., 2014, 3D Slicer: A Platform for Subject-Specific Image Analysis, Visualization, and Clinical Support: in Jolesz, F.A. (ed.), Intraoperative Imaging and Image-Guided Therapy, Springer, New York, NY, 277–289. https://doi.org/10.1007/978-1-4614-7657-3_19

Kunth, A., 1870, Ueber wenig bekannte Crustaceen von Solenhofen: Zeitschrift Der Deutschen Geologischen Gesellschaft 22, 771–802.

Kussakin, O.G., Rybakov, A.V., 1995, *Protognathia waegeli* sp. n. (Crustacea, Isopoda, Flabellifera), a new species from the Antarctic of the rare and poorly known family Protognathiidae: Russian Journal of Marine Biology 17–28.

Lanham, U., 1965, Uninominal nomenclature: Systematic Zoology 14, 144–144.

Lehmann, J., Höll, K., 1989, Asseln aus dem Cenoman (Oberkreide) Nordwestdeutschlands: Arbeitskreis Paläontologie Hannover 17, 1–16.

Limaye, A., 2012, Drishti: a volume exploration and presentation tool: in Stock, S.R. (ed.), Presented at the SPIE Optical Engineering + Applications, San Diego, California, USA, 1–10. https://doi.org/10.1117/12.935640

Lins, L.S.F., Ho, S.Y.W., Wilson, G.D.F., Lo, N., 2012, Evidence for Permo-Triassic colonization of the deep sea by isopods: Biology Letters 8, 979–982. https://doi.org/10.1098/rsbl.2012.0774

Lösel, P.D., van de Kamp, T., Jayme, A., Ershov, A., Faragó, T., Pichler, O., Tan Jerome, N., Aadepu, N., Bremer, S., Chilingaryan, S.A., Heethoff, M., Kopmann, A., Odar, J., Schmelzle, S., Zuber, M., Wittbrodt, J., Baumbach, T., Heuveline, V., 2020, Introducing Biomedisa as an open-source online platform for biomedical image segmentation: Nature Communications 11, 5577. https://doi.org/10.1038/s41467-020-19303-w

Luque, J., Schweitzer, C.E., Santana, W., Portell, R.W., Vega, F.J., Klompmaker, A.A., 2017, Checklist of fossil decapod crustaceans from tropical America. Part I: Anomura and Brachyura: Nauplius 25, 1–85. https://doi.org/10.1590/2358-2936e2017025

Malzahn, E., 1968, Über einen neuen Isopoden aus dem Hauterive Nordwestdeutschlands: Geologisches Jahrbuch 86, 827–834.

Manship, B.M., Walker, A.J., Davies, A.J., 2011, Brooding and embryonic development in the crustacean *Paragnathia formica* (Hesse, 1864) (Peracarida: Isopoda: Gnathiidae): Arthropod Structure & Development 40, 135–145. https://doi.org/10.1016/j.asd.2010.12.004

Martins-Neto, R.G., 2001, Review of some Crustacea (Isopoda and Decapoda) from Brazilian deposits (Paleozoic. Mesozoic and Cenozoic) with descriptions of new taxa.: Acta Geologica Leopoldensia 24, 237–254.

Matthews, 1973, Notes on open nomenclature and synonymy lists: Palaeontology 16, 713–719.

Menzies, R.J., 1962, The isopods of abyssal depths in the Atlantic ocean: Vema Research Series 1, 79–206.

Messana, G., 2020, *Catailana whitteni*, a new genus and species of stygobiotic cirolanid from a cave in Guangxi, China (Crustacea: Isopoda: Cirolanidae): Raffles Bulletin of Zoology 35, 101–108.

Meyer, H. von, 1856, Jurasische und Triasische Crustaceen: in Dunkler, W., Meyer, H. von (eds.), 123023600044252.pdf, Palaeontographica, Theodor Fischer, Kassel, 44–55.

Meyer, H. von, 1846, Mittheilungen an Professor Bronn gerichtet: Neues Jahrbuch Für Mineralogie, Geognosie, Geologie Und Petrefaktenkunde 596–599.

Mezzalira, S., Martins-Neto, R.G., 1992, Novos crustáceos Paleozóicus do estado de Sao Paulo, com descricao de novos taxa: Acta Geologica Leopoldensia 36, 49–66.

Monod, T., 1926, Les Gnathiidæ. Essai monographique (Morphologie, Biologie, Systématique): Mémoires de La Société Des Sciences Naturelles Du Maroc 13, 1–668.

Münster, G.G. zu, 1842, Beschreibung drei neuer Arten Crustaciten: in Meyer, H. von, Münster, Georg Graf zu (eds.), Beiträge zur Petrefacten-Kunde, 76–78.

Münster, G.G. zu, 1840, Ueber einige Isopoden in den Kalkschiefern von Bayern: in Meyer, H. von, Münster, G.G. zu (eds.), Beiträge Zur Petrefacten-Kunde, Buchner'sche Buchhandlung, Bayreuth, 19–23.

Münster, G.G. zu, 1839, Ueber die fossilen langschwänzigen Krebse in den Kalkschiefern von Bayern: in Münster, G.G. zu (ed.), Beiträge Zur Petrefacten-Kunde, Buchner'sche Buchhandlung, Bayreuth, 1–88.

Nägelke, H.D., 2000, Hochschulbau im Kaiserreich: historische Architektur im Prozess bürgerlicher Konsensbildung. Verlag Ludwig, Kiel.

Nagler, C., Haug, C., Resch, U., Kriwet, J., Haug, J.T., 2016, 150 million years old isopods on fishes: a possible case of palaeo-parasitism: Bulletin of Geosciences 91, 1–12.

Nagler, C., Haug, J.T., 2016, Functional morphology of parasitic isopods: understanding morphological adaptations of attachment and feeding structures in *Nerocila* as a pre-requisite for reconstructing the evolution of Cymothoidae: PeerJ 4, e2188. https://doi.org/10.7717/peerj.2188

Nagler, C., Hyžný, M., Haug, J.T., 2017, 168 million years old "marine lice" and the evolution of parasitism within isopods: BMC Evolutionary Biology 17, 76.

Nozères, C., 2008, Aega psora (Linnaeus, 1758): in Boyko, C.B., Bruce, N.L., Hadfield, K.A., Merrin, K.L., Ota, Y., Poore, G.C.B., Taiti, S., Schotte, M., Wilson, G.D.F. (eds.), World Marine, Freshwater and Terrestrial Isopod Crustaceans Database, World Register of Marine Species.

Ogg, J.G., Ogg, G., Gradstein, F.M., 2016, A concise geologic time scale 2016. Elsevier, Amsterdam.

Oppel, C.A., 1862, Ueber jurassische Crustaceen: in Boehm, G., Cotteau, G., Zittel, K.A. von (eds.), Palaeontologische Mittheilungen Aus Dem Museum Des Koeniglich-Bayerischen Staates, Ebner & Seubert, Stuttgart, 1–120. https://doi.org/10.5962/bhl.title.15040

Ota, Y., 2019, Description of female adult and praniza larva of *Tenerognathia visus* Tanaka, 2005 (Crustacea; Isopoda; Gnathiidae) with notes on mating behavior: Zootaxa 4711, 561–570. https://doi.org/10.11646/zootaxa.4711.3.7

Ota, Y., 2014, Three new gnathiid species with larvae ectoparasitic on coastal sharks from southwestern Japan (Crustacea: Isopoda): Zootaxa 3857, 478. https://doi.org/10.11646/zootaxa.3857.4.2

Ota, Y., Hirose, E., 2009, *Gnathia nubila* n. sp. and a new record of *Gnathia grandilaris* (Crustacea, Isopoda, Gnathiidae) that parasitizes elasmobranchs from Okinawan coastal waters, Japan: Zootaxa 2238, 43–55. https://doi.org/10.11646/zootaxa.2238.1.4

Owen, H.G., 2002, The base of the Albian Stage; comments on recent proposals: Cretaceous Research 23, 1–13. https://doi.org/10.1006/cres.2001.0306

Pan, Y., Fürsich, F.T., Chellouche, P., Hu, L., 2019, Taphonomy of fish concentrations from the Upper Jurassic Solnhofen Plattenkalk of Southern Germany: Neues Jahrbuch Für Geologie Und Paläontologie - Abhandlungen 292, 73–92. https://doi.org/10.1127/njgpa/2019/0809

Pebesma, E., 2018, Simple Features for R: Standardized Support for Spatial Vector Data: The R Journal 10, 439. https://doi.org/10.32614/RJ-2018-009

Pictet, F.J., 1854, Traité de paléontologie ou Histoire naturelle des animaux fossiles considérés dans leurs rapports zoologiques et géologiques, 2nd ed. Chez J.-B. Bailliere, Paris.

Pictet, F.J., 1853, Traité de paléontologie ou histoire naturelle des animaux fossiles considérés dans leurs rapports zoologiques et géologiques. J. -B. Baillière et Fils, Paris.

Pictet, F.J., 1846, Traité élémentaire de paléontologie ou histoire naturelle des animaux fossiles, considérés dans leurs rapports zoologiques et géologiques. Langlois et Leclerq, Paris. https://doi.org/10.5962/bhl.title.25238

Pieper, R.J., Korpel, A., 1983, Image processing for extended depth of field: Applied Optics 22, 1449–1453. https://doi.org/10.1364/AO.22.001449

Polz, H., 1998, *Schweglerella strobli* gen.nov. sp.nov. (Crustacea: Isopoda: Sphaeromatidea), eine Meeres-Assel aus den Solnhofener Plattenkalken: Archaeopteryx 16, 19–28.

Preibisch, S., Saalfeld, S., Tomancak, P., 2009, Globally optimal stitching of tiled 3D microscopic image acquisitions: Bioinformatics 25, 1463–1465. https://doi.org/10.1093/bioinformatics/btp184

Racovitza, E.G., 1912, Cirolanides (Premiere serie). Biospeleologica 27: Archives de Zoologie Experimentale et Generale 10, 203–329.

Rathbun, M.J., 1935, Fossil Crustacea of the Atlantic and Gulf Coastal Plain: Geological Society of America Special Papers.

Reiff, E., 1936, Isopoden aus dem Lias Delta (Amaltheenschichten) Schwabens: Paläontologische Zeitschrift 18, 49–90. https://doi.org/10.1007/BF03041710

Remeš, M., 1912, *Urda moravica* n. sp. z doggeru Chřibů: Časopisu Moravského Museo Zemeského 12, 173–177.

Rollmann, W., 1853, Zwei neue stereoskopische Methoden: Annalen Der Physik 90, 186–187.

Rybakov, A.V., 1990, *Bourdonia tridentata* gen. n., sp. n. (Isopoda: Cabiropsidae) a hyperparasite of *Bopyroides hippolytes* Kroyer from the shrimp *Pandalus borealis*: Parazitologiia 24, 408–416.

Schädel, M., Perrichot, V., Haug, J., 2019, Exceptionally preserved cryptoniscium larvae - morphological details of rare isopod crustaceans from French Cretaceous Vendean amber: Palaeontologia Electronica 22.3.71, 1–46. https://doi.org/10.26879/977

Schädel, M., van Eldijk, T., Winkelhorst, H., Reumer, J.W.F., Haug, J.T., 2020, Triassic Isopoda – three new species from Central Europe shed light on the early diversity of the group: Bulletin of Geosciences 95, 145–166.

Schindelin, J., Arganda-Carreras, I., Frise, E., Kaynig, V., Longair, M., Pietzsch, T., Preibisch, S., Rueden, C., Saalfeld, S., Schmid, B., Tinevez, J.-Y., White, D.J., Hartenstein, V., Eliceiri, K., Tomancak, P., Cardona, A., 2012, Fiji: an open-source platform for biological-image analysis: Nature Methods 9, 676–682. https://doi.org/10.1038/nmeth.2019

Schiødte, J.C., Meinert, F.W., 1881, Symbolæ ad Monographiam Cymotharum Crustaceorum Isopodum Familiæ 2. Anilocridae: Naturhistorisk Tidsskrift 3, 1–166. https://doi.org/10.5962/bhl.title.10300

Schram, F.R., 1974, Paleozoic Peracarida of North America: Fieldiana Geology 33, 95–124.

Schram, F.R., 1970, Isopod from the Pennsylvanian of Illinois: Science 169, 854–855.

Schubert, R., 2000, Using a flatbed scanner as a stereoscopic near-field camera: IEEE Computer Graphics and Applications 20, 38–45. https://doi.org/10.1109/38.824535

Schultz, G.A., 1977, Bathypelagic Isopod Crustacea from the Antarctic and Southern Seas: in Schultz, G.A. (ed.), Biology of the Antarctic Seas V, Antarctic Research Series, American Geophysical Union (AGU), Richmond, 69–128. https://doi.org/10.1029/AR023p0069

Seed, W.F., 1979, Article: The family Gnathiidae (Crustacea: Isopoda). A new Victorian species: The Victorian Naturalist 96, 56–62.

Serrano-Sánchez, M. de L., Nagler, C., Haug, C., Haug, J.T., Centeno-García, E., Vega, F.J., 2016, The first fossil record of larval stages of parasitic isopods: cryptoniscus larvae preserved in Miocene amber: Neues Jahrbuch Für Geologie Und Paläontologie-Abhandlungen 279, 97–106. https://doi.org/10.1127/njgpa/2016/0543

Shiino, S.M., 1954, A new fresh-water entoniscid isopod, *Entionella okayamaensis* n. sp.: Report of the Faculty of Fisheries, Prefectural University of Mie 1, 239–246.

Smit, N.J., Basson, L., Van As, J.G., 2003, Life cycle of the temporary fish parasite, *Gnathia africana* (Crustacea: Isopoda: Gnathiidae): Folia Parasitologica 50, 135–142. https://doi.org/10.14411/fp.2003.024

Smit, N.J., Bruce, N.L., Hadfield, K.A., 2014, Global diversity of fish parasitic isopod crustaceans of the family Cymothoidae: International Journal for Parasitology: Parasites and Wildlife 3, 188–197. https://doi.org/10.1016/j.ijppaw.2014.03.004

Smit, N.J., Van As, J.G., Basson, L., 1999, A redescription of the adult male and praniza of *Gnathia africana* Barnard, 1914 (Crustacea, Isopoda, Gnathiidae) from southern Africa: Folia Parasitologica 46, 229–240.

South, A., 2017, rnaturalearth: World Map Data from Natural Earth.

Stolley, E., 1910, Über zwei neue Isopoden aus norddeutschem Mesozoikum: Jahresbericht Der Naturhistorischen Gesellschaft Zu Hannover 60, 191–216.

Sutton, M.D., Rahman, I.A., Garwood, R.J., 2014, Techniques for virtual palaeontology, New analytical methods in earth and environmental science. Wiley Blackwell, Hoboken, NJ; Chichester, West Sussex.

Tanaka, K., 2005, A new genus and species of gnathiid isopod (Isopoda, Gnathiidae) from the Ryukyus, Southwestern Japan: Journal of Crustacean Biology 25, 565–569. https://doi.org/10.1651/C-2605.1

Taylor, B., 1972, An urdidid isopod from the Lower Cretaceous of south-east Alexander Island: British Antarctic Survey Bulletin 27, 97–103.

Tennekes, M., 2018, tmap: Thematic Maps in R: Journal of Statistical Software 84, 1–39. https://doi.org/10.18637/jss.v084.i06

Thamban, A.P., Kappalli, S., Kottarathil, H.A., Gopinathan, A., Paul, T.J., 2015, *Cymothoa frontalis*, a cymothoid isopod parasitizing the belonid fish *Strongylura strongylura* from the Malabar Coast (Kerala, India): redescription, description, prevalence and life cycle: Zoological Studies 54, 42. https://doi.org/10.1186/s40555-015-0118-7

Thing, C.Y., Ota, Y., Hatai, K., Ransangan, J., 2015, Redescription of *Caecognathia coralliophila* (Monod, 1926) (Crustacea, Isopoda, Gnathiidae), collected from a fish hatchery in Sabah, Borneo Island, Malaysia: Proceedings of the Biological Society of Washington 128, 51–62. https://doi.org/10.2988/0006-324X-128.1.51

Tischlinger, H., Arratia, G., 2013, Ultraviolet light as a tool for investigating Mesozoic fishes, with a focus on the ichthyofauna of the Solnhofen archipelago: Mesozoic Fishes – Global Diversity and Evolution, Verlag Dr. Friedrich Pfeil, München, 549–560.

van der Wal, S., Haug, J.T., 2020, Shape of attachment structures in parasitic isopodan crustaceans: the influence of attachment site and ontogeny: PeerJ 8, e9181. https://doi.org/10.7717/peerj.9181

van der Wal, S., Schädel, M., Ekrt, B., Haug, J.T., 2021, Description and ontogeny of a 40-million-year-old parasitic isopodan crustacean: *Parvucymoides dvorakorum* gen. et sp. nov.: PeerJ 9, 1–46. https://doi.org/10.7717/peerj.12317

Van Straelen, V., 1928, Contribution a l'etude des Isopodes Méso- et Cénozoiques: Mémoires de l'Académie Impériale et Royale des Sciences et Belles-Lettres de Bruxelles 9, 1–59.

Viohl, G., 1994, Fish taphonomy of the Solnhofen Plattenkalk - an approach to the reconstruction of the palaeoenvironment Taphonomie des poissons des Calcaires en Plaquettes de Solnhofen-intérêt pour la reconstruction du paléoenvironnement: GEOBIOS 27, 81–90.

Wägele, J.-W., 1989, Evolution und phylogenetisches System der Isopoda: Stand der Forschung und neue Erkenntnisse, Zoologica. Schweizerbart, Stuttgart.

Wägele, J.-W., Brandt, A., 1988, *Protognathia* n. gen. *bathypelagica* (Schultz, 1977) rediscovered in the Weddell Sea: A missing link between the Gnathiidae and the Cirolanidae (Crustacea, Isopoda): Polar Biology 8, 359–365. https://doi.org/10.1007/BF00442027

Walther, J., 1904, Die Fauna der Solnhofener Plattenkalke. Bionomisch betrachtet: Festschrift Zum Siebzigsten Geburtstage von Ernst Haeckel, Gustav Fischer, Jena, 135–214. https://doi.org/10.5962/bhl.title.142760

Watling, L., 1981, An Alternative Phylogeny of Peracarid Crustaceans: Journal of Crustacean Biology 1, 201–210. https://doi.org/10.2307/1548159

Wheatstone, C., 1838, On some remarkable, and hitherto unobserved, phenomena of binocular vision: Philosophical Transactions of the Royal Society of London 128, 371–394.

Wickham, H., 2009, ggplot2: Elegant Graphics for Data Analysis, Use R! Springer New York, New York, NY. https://doi.org/10.1007/978-0-387-98141-3

Wickham, H., 2007, Reshaping Data with the reshape Package: Journal of Statistical Software 21. https://doi.org/10.18637/jss.v021.i12

Wickham, H., François, R., Henry, L., Müller, K., 2020, dplyr: A Grammar of Data Manipulation. R.

Wieder, R.W., Feldmann, R.M., 1992, Mesozoic and Cenozoic fossil isopods of North America: Journal of Paleontology 66, 958–972.

Wieder, R.W., Feldmann, R.M., 1989, *Palaega goedertorum*, a fossil isopod (Crustacea) from late Eocene to early Miocene rocks of Washington State: Journal of Paleontology 63, 73–80. https://doi.org/10.1017/S0022336000040981

Wilke, C.O., 2020, ggtext: Improved Text Rendering Support for ggplot2. R.

Wilson, G.D., 1996, Of uropods and isopod crustacean trees: A comparison of "groundpattern" and cladistic methods: Vie et Milieu 46, 139–154.

Wilson, G.D.F., 2003, A new genus of Tainisopidae fam. nov. (Crustacea: Isopoda) from the Pilbara,Western Australia: Zootaxa 245, 1–20. https://doi.org/10.11646/zootaxa.245.1.1

Wilson, G.D.F., Sims, C.A., Grutter, A.S., 2011, Toward a taxonomy of the Gnathiidae (Isopoda) using juveniles: The external anatomy of *Gnathia aureamaculosa* zuphea stages using scanning electron microscopy: Journal of Crustacean Biology 31, 509–522. https://doi.org/10.1651/10-3432.1

Wittler, F.A., 2011, Ein Isopode im Mittelbajocium von Velpe bei Osnabrück (Crustacea, Dogger, NW – Deutschland): Steinkern (Online).

Wittler, F.A., 2007, Ein Isopode im Mittelbajocium von Velpe bei Osnabrück (Crustacea, Dogger, NW – Deutschland): Arbeitskreis Paläontologie Hannover 35, 15–21.

Zittel, K.A.V., 1887, Traité de Paléontologie. Tome II, Partie I. Mollusca et Arthropoda. Octave Doin, Paris.

3 Discussion

3.1 The identification of immature forms of Isopoda in the fossil record

Representatives of Isopoda throughout their life produce a sequence of exoskeletons, which might be preserved as fossils, either as moults or together with the rest of the carcass, given they are deposited under the right conditions. This leads to the possibility to find fossil remains of both the immature form as well as the adult form of the same individual. There are two situations one might find oneself in when interpreting the developmental stage a fossil remain belongs to. In the first case, there are several other remains that ideally come from the same locality, are of the same age and can be confidently be identified as conspecific. In the other case the interpretation has to be based on the specimen itself and the knowledge about the extant fauna or better understood fossils. These cases figuratively stand for two sources of information which can be used to interpret the developmental stage the animal was in when it produced the fossil remain – the information contained in the fossil itself and the information gained through the comparison of different remains. The fossil itself can contain morphological information that when compared to the morphology of different developmental stages in extant or better understood extinct, closely related species, can provide strong indications to which developmental stage a fossil should be attributed.

In Isopoda immature stages that have just hatched from the brood pouch of the female can be recognised by the absence of a well developed posterior-most walking leg (post-ocular segment 13) – the 'manca' stage (Boyko & Wolff 2014). The term 'pre-manca' refers to the stage just before the manca stage, in which the immatures have already hatched from the eggs but are still located within the brood pouch (see van der Wal & Haug 2020, also for other terminologies used in the literature). By this, the absence of legs on post-ocular segment 13 can be used as a key feature to identify a fossil specimens as an immature (Schädel et al. 2021b). While an exceptional preservation, for example in amber, is needed to tell whether a leg is present or absent, especially when there are other conspecific fossils available for comparison, in the group Scutocoxifera the absence of the leg can sometimes also be recognised when the animal is only accessible in dorsal view. This is because the coxal plates are, like the rest of the leg, not developed. Also in manca stage individuals the

tergite of the segment on which the not yet developed leg is located is relatively shorter as in later stages (Fig. 4).
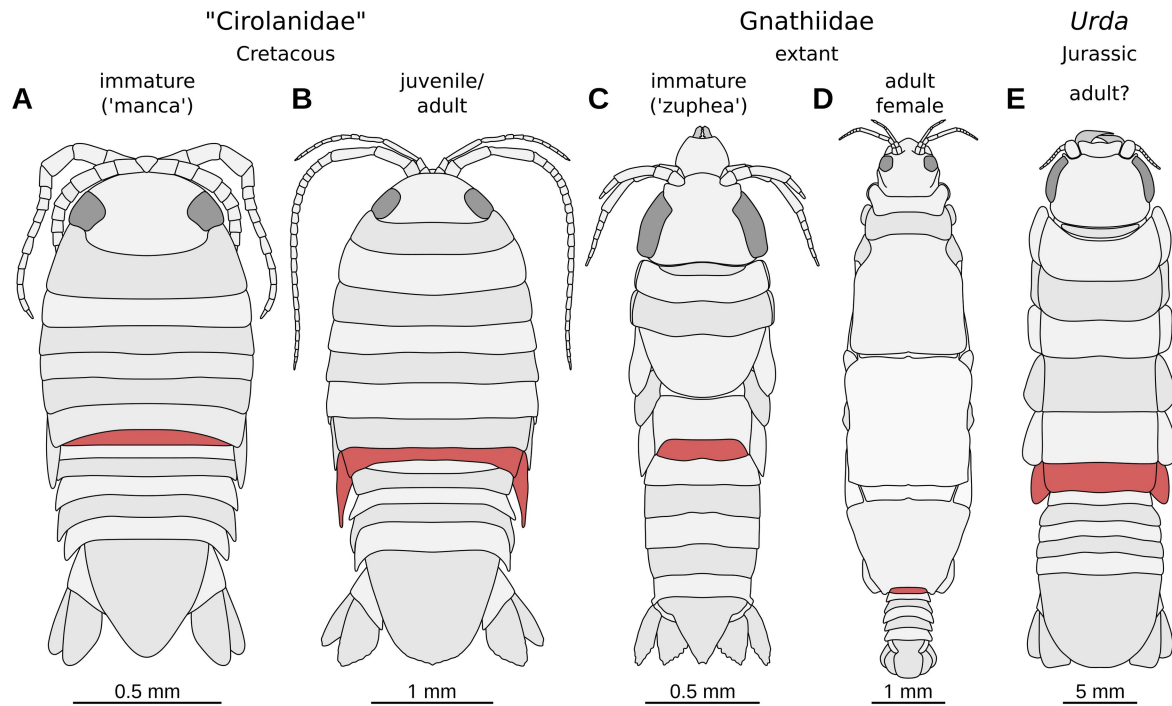
Figure 4: Development of structures of post-ocular segment 13 (highlighted in red) in different representatives of Isopoda, drawings, dorsal view. **A–B:** *Electrolana madelineae* Schädel, Hyžný & Haug (study I), collection of the Natural History Museum Vienna. **A:** NHMW 2017/0052/0002. **B:** NHMW 2017/0052/0001. **C:** *Gnathia* sp., drawn from specimen AM P.81399 in Wilson *et al.* (2011b). **D:** *Caecognathia agwillisi* (Seed, 1979), redrawn from Seed (1979). **E:** *Urda* sp., reconstructed from multiple fossils (study V), Bielefeld, Germany, Middle Jurassic.

However, in less well preserved fossils the absence of coxal plates could be not due to the delayed development but due to the preservation and distortion could make individual tergites appear shorter or longer. Apart from preservational factors, also biological factors could lead to an incorrect interpretation of a specimen as an immature one, based on the absence of a fully developed leg on post-ocular segment 13. A heterochronic deviation from the typical development pattern can result in paedomorphic adults that also lack the mentioned leg. Within Isopoda this phenomenon occurs in several ingroups and is present in all species of Gnathiidae (Monod 1926; Brökeland & Brandt 2004). Vice versa, this has

38

already led to wrong interpretations of extant species, where the first discovered specimen, that lacked one pair of legs compared to related species, has been interpreted as a paedomorphic adult (Wägele 1989; Kussakin & Rybakov 1995) and later an additional adult male specimen without lacking paair of legs of of a closely related species has been found, suggesting that the first specimen is an immature (Kussakin & Rybakov 1995; Wilson 1996). However, the leg on post-ocular segment 7 can also be missing for reasons other than heterochronic development. In some species of Epicaridea this pair of legs can be missing despite in the immature stages of the same species it is present (in the cryptoniscium stage) (Wägele 1989).

In many lineages of Isopoda, without specific knowledge about the species, immature stages that are later than the manca stage can only be differentiated from the adults when the reproductive organs can be inspected (e.g. Bruce 1986). In females, the presence of oostegites and in males the presence of penile papillae (penes) and appendices masculinae (modified endopods of the second pleopods) can be used to recognize specimens as adults (Wilson 1991). While there is no published record of male genitalia in the fossil record of Isopoda, oostegites are more conspicuous and have been described in fossil representatives of Isopoda (Broly et al. 2017) as well as from other ingroups of Peracarida (Pazinato et al. 2016; Jones et al. 2016; Sánchez-García et al. 2017), for which oostegites are an apomorphy (Ax 2000). However, the absence of both some of the male (Messana 2004) and female sexual characters, such as the oostegites (Wägele 1982) can be problematic as a criterion to identify immature forms, as some of the characters may be missing in adults of some extant species. In fossils, additionally, all of the adult sexual characters, except for the oostegites, often are not preserved or covered by other body parts, sediment or debris.

Individual fossils can also be interpreted as immatures when they strongly resemble immature forms of extant species, where the adults differ drastically from the earlier stages (morpho-larvae). However, also here paedomorphosis can be a factor that might lead to wrong interpretations, as especially in species with protandric development, the sexually mature stages can retain the morphology of the immature forms (e.g. Hosie 2008). Especially in lineages where paedomorphosis occurs in extant species, this has to be considered when interpreting fossil specimens (Schädel et al. 2019, 2021a).

When there is more than one fossil of the same species the comparison between specimens can add further information about the developmental state of individual specimens. Generally, larger specimens can be interpreted as later in their developmental

state. However, even such a simple conclusion relies on a set of assumptions that might not be trivial in practice. First, the specimens actually have to come from the same species, which in practice, especially when there are only few specimens available, strongly depends on the expectations about the intra-species variability. Second, it depends on the body size variation within each developmental stage within the species – two specimens of different body sizes can come either from the same or from different developmental stages, depending on the size variation within the stage. By comparing multiple specimens, factors that complicate the interpretation of the developmental state, such as paedomorphosis, can be ruled out when the smaller specimen has features that are indicative for an earlier stage or the larger specimen has features indicative for later immature stages or adults (Schädel et al. 2021b). With larger numbers of specimens at hand (e.g. Schädel et al. 2021a), the distribution of body sizes within the fossil assemblage can be informative about the variation of body sizes within developmental stages. In many species within Eurthropoda the growth of highly sclerotised body parts between developmental stages can be approximated using a constant growth coefficient ('Dyar's rule'/'Brooks' rule') (Dyar 1890). This growth coefficient can then, together with the distribution of body sizes within the fossil assemblage, be used to estimate the number of moults between different stages (Baranov et al. 2019; Schädel et al. 2021b). Using data on the development of extant closely related species, also other morphological features of the body, such as the overall body shape, can be informative about the developmental stage of specimens (van der Wal et al. 2021).

Morphological features of immature individuals of Isopoda that can be recognised in the fossil record:
- absence of features that are only present in adults, such as oostegites
- the absence of a fully developed leg on post-ocular segment 13
- strong resemblance to morphologically distinct immature forms of extant species (morpho-larvae)
- smaller size than other conspecific individuals

3.2   The fossil record of immature forms of Isopoda

The published fossil record of immature forms of Isopoda is so far very limited. Despite immature forms could be recognised in most field sites that yield complete and un-distorted remains, all published immatures are preserved in amber. For land-dwelling forms of Isopoda (Oniscidea) there is one record of an immature form from Miocene Chiapas amber (Mexico), where many small individuals are preserved in close vicinity to adults of the same species, some of which being located on the underside of the adults between the legs as if been carried in the brood pouch (Broly et al. 2017). Apart from the direct association between the smaller and larger specimens, the smaller specimens can be interpreted as immatures based on the typical morphology of the manca stage (post-ocular segment 13 shorter and lacking fully developed legs) (Broly et al. 2017). Poinar (2018 p. 3) claimed the presence of 'some newly hatched juveniles' in the 'marsupium' of a fossil woodlouse (Oniscidea) from mid-Cretaceous Kachin amber from Myanmar; however, neither the alleged immatures nor structures indicating a marsupium are visible in the photographs.

From Kachin amber (Myanmar, mid-Cretaceous) there is one immature specimen, belonging to the group Cymothoida, which strongly resembles extant forms of "Cirolanidae" (predatory and scavenging forms of Cymothoida). The specimen can be recognised as an immature because of it being much smaller than a second, conspecific, specimen from the same locality as well as the typical manca morphology (Fig. 4A–B). In this case the second specimen not only provides an indication that the smaller specimen has not reached the size associated with adult specimens, it further renders the possibility that the smaller specimen could be a paedomorphic adult as extremely unlikely, as the larger specimen has fully developed legs (including coxal plates) on post-ocular segment 13, suggesting a typical development. It was also possible to estimate the number of moults, which lie between the instars, to which the two fossils correspond; by comparing the potential growth coefficients with actual growth coefficients of other, extant, species of Isopoda, three or four moults appear to be the most likely number (Schädel et al. 2021b). This also represents the currently oldest record of a manca stage individual. As the manca stage is already present in the ground pattern of Isopoda (Ax 2000), stratigraphically older records of manca stages are likely to be reported in the future. The lack of older records might be due to practical reasons: Few fossil-rich amber sites are older than Kachin amber and outside of amber small arthropod fossils are far less likely to be spotted by collectors in the field.

For the group Epicaridea there are fossils from three different localities that might represent immature forms. From Miocene Chiapas amber (Mexico) there are multiple minute

specimens with a cryptoniscium type morphology, which most likely come from two or more species (Serrano-Sánchez et al. 2016). From Late Cretaceous Vendean amber from France there are several fossils with a cryptoniscium-like morphology (Néraudeau et al. 2017; Schädel et al. 2019). The oldest record of immature forms of Epicaridea – and of body fossils of the group as well – is from the mid-Cretaceous, from Kachin amber (Myanmar), where more than 100 individuals with a cryptoniscium morphology are preserved in a single piece of amber (Schädel et al. 2021a). In all of the cases the morphology is similar to cryptoniscium stage larvae of extant species within Epicaridea. However, as there are many extant species where the male retains the cryptoniscium morphology (e.g. Hosie 2008), the similarity to larval stages of extant species does not rule out the possibility that the fossil specimens could be paedomorphic males rather than immatures. The occurrence of paedomorphic males in the extant fauna is limited to some of the ingroups of Epicaridea; however, none of the fossils could be identified as belonging to any of the ingroups of Epicaridea where in all extant species the males do not retain the larval morphology. Therefore, all so far reported fossils with a cryptoniscium morphology, which are at the same time all body fossils of the group Epicaridea, should be interpreted as either cryptoniscium stage larvae or paedomorphic adults (Schädel et al. 2019, 2021a). Nevertheless, the fossils from the mid-Cretaceous of Myanmar (Schädel et al. 2021a) provide the oldest record of larval morphology for the entire group Isopoda.

3.3   The identification of parasites within the fossil record

Parasitism in animals as a form of interaction between individuals can leave traces in the fossil record. As morphology is often the only available source of information about the life style of the studied organisms, distinguishing fossil specimens that are remains of parasites from those of animals with a different life style requires a careful assessment of the information that can be retrieved from the fossil itself and from what is known about extant or extinct closely related species (Conway Morris 1981). The way in which the term parasitism is applied by different authors strongly depends on the degree of dependence of the parasite to its host and the length of the interactions between them. Especially the distinction between parasitism and micro-predation, that is made by some authors (Lafferty & Kuris 2002), can be particularly hard to make when interpreting fossils. How long an interaction between a feeding and a being-fed-on organism lasted can only be estimated

when the interaction itself has left traces, which properties depend on the length of the interaction. Also, for most species that are only known from fossils not much is known about their development. Therefore, even if one particular life stage can be regarded as parasitic, other life stages of the same species might not be parasitic. For example, if only immature representatives of Gnathiidae were known, the conclusion that also the adults were parasites would be tempting but ultimately wrong.

There are multiple ways in which fossils can be recognised as coming from parasitic animals. The interaction between the parasite and its host can leave traces on the host. In this case the parasite itself does not have to be preserved alongside with the host; consequently, also parasitism through animals with low preservation potential, such as parasitic barnacles (Rhizocephala) (Klompmaker & Boxshall 2015), can be found in the fossil record. When many specimens are available, the measured reduced growth of the host can serve as an indication for the negative impact o the parasites on their host (Zhang et al. 2020), however in fossil traces of parasitism that are interpreted to be caused by representatives of Isopoda (more specifically those of Epicaridea) a reduced growth (approximated by the size of the host animals) could not be measured (Klompmaker et al. 2021).

The systematic positions of fossils are often used to infer parasitic behaviour. Ideally, the interpretation of the systematic position of a fossil should be based on apomorphic characters that are visible in the fossil (Hennig 1965). However, unfortunately in many publications on fossils of the group Isopoda the systematic position, which is often reflected in the taxonomic treatments, has been determined based on the overall similarity to extant species, rather than based on unique features (Bruce et al. 2021). The conclusion that a fossil remain comes from a parasite because it is from a representative of a group in which all extant species are parasites is based on the assumption that the parasitic lifestyle was already present in the last common ancestor of all representatives of the group. The parasitic life style can be either plesiomorphic ('extant phylogenetic bracket' method) (Witmer & Thomason 1995) or an apomorphy of the group ('taxonomic uniformitarism') (Nützel 2021), the former having a stronger epistemological backing while being not applicable in many cases.

Apart from the characters of systematic value, also other aspects of the morphology of a fossil organism can provide information about the lifestyle of the organism that it comes from. The shape and relative size of body parts can be associated with a parasitic behaviour in extant species. This can include piercing-sucking mouth parts that in the extant

counterparts are used for feeding on body fluids or structures that allow the animal to firmly attach to a host, such as strongly curved distal elements of the legs (Nagler & Haug 2016). However, such or similar structures can also occur in species with a different lifestyle. Piercing-sucking mouth parts, for example, also occur in predatory forms of Isopoda, for example within the group Paranthuridae (ingroup of Anthuridea), as well as strongly curved distal-most leg elements, which can not only be used to cling to a host but also to grab prey (Wägele 1985).

A position on, in or close to a potential host can be a strong indication of a parasitic relationship. However, unlike when dealing with living organisms, in fossil assemblages of animals (taphocoenoses) it is often not directly apparent, whether the animals are preserved together because they interacted when all animals were still alive and died together or shortly after each other. Alternatively, one animal could have been scavenging on the carcass of another animal (Leung 2017, 2021) and then died or both animals died while not directly interacting and agglomerated post-mortem for example through subsequently getting stuck on a piece of liquid resin (see discussion in Schädel et al. 2021a). Presumed both animals were alive and interacted with each other, parasitism still is not the only form of interaction that could have produced the fossil assemblage. The animals could have interacted in a mutualistic fashion or only one animal benefited from the interaction without feeding on the non-benefiting animal, for example through phoresis (travel on a larger animal) (Robin et al. 2019), which can be hard to distinguish even in extant species (Leung & Poulin 2008). The exact position of the smaller animal on its potential host is an iportant factors when interpreting fossil assemblages where the potential parasite is located on its potential host are – whether it is located in a position where extant parasites are located, where for a fast moving potential host there would be the least drag or where body fluids are best accessible (Robin et al. 2018). Also the relative orientation can give additional information about whether an assemblage comes from an interaction of two living animals; elongated parasites or commensals of fast moving fishes are for example unlikely to find perpendicular to the drag or, if the attachment is through the mouthparts, with the head towards the tail of the fish (Nagler et al. 2016).

The occurrence of parasites in coprolites represents another way, in which parasitic interactions can get preserved as fossils, with only the parasite but not the host being preserved (De Baets et al. 2021). However, as there are no extant forms of Isopoda that are parasites that inhabit the digestive tract of their host (without destroying it) (Stepien &

Brusca 1985), the occurrence of remains of representatives of Isopoda inside a coprolite would be rather uninformative regarding the a possible parasitic life style of their producer.

There are instances where isolated fossils have been identified as parasites or micro-predators based on the presence of host tissue in their gut (Wappler et al. 2004). Blood can be identified in fossils on morphological grounds (preservation of erythrocytes), similar to how pollen can be found in fossils of pollen-feeding animals (Wedmann et al. 2021) or through chemical analyses (Yao et al. 2014; Greenwalt 2021). While there is no report of fossils belonging to Isopoda with blood preserved in the gut, the inspection of gut contents could be possible in exceptionally well preserved fossils.

When dealing with potential parasitic animals in the fossil record, often it is a combination of ways in which parasitism can manifest itself in a particular fossil, rather than in a single way and often the individual factors that are indicative for a parasitic life style in themselves are equivocal, while their combination produce a much more persuasive image and a parasitic life style can be inferred from an 'analogy based on associated phenomena' (Nützel 2021 p. 224).

Following features help to recognise parasitic forms of Isopoda in the fossil record:
- swellings of branchial chambers of crustaceans (growth responses of the hosts)
- systematic positions within a group for which the common ancestor is assumed to be a parasitic form
- morphological features that in extant species are associated with behaviour that is part of a parasitic life style
- proximity to or position on or in a potential host in a death assemblage
- orientation on a potential host in a death assemblage that suggests a syn-vivo interaction
- presence of blood or haemolymph in the gut of the potential parasite (not yet reported for fossils of the group Isopoda)

3.4 The fossil record of parasitism in Isopoda

As noted in the introduction ('Parasitic forms of Isopoda in the fossil record'), there are some fossil occurrences of representatives of Isopoda that have been linked with parasitic behaviour. These occurrences include also fossils that are interpreted to belong to "Cirolanidae" – a potentially non-monophyletic group of representatives of the larger group Cymothoida (Wägele 1989). "Cirolanidae" lacks morphological characteristics, that can unambiguously interpreted as apomorphic (see discussion in Schädel et al. 2021b). Robin et al. (2018) presented several specimens from the Eocene of Italy, interpreted as representatives of *Cirolana* Leach, 1818, which is a genus-ranked 'group' that also lacks convincing apomorphies (see discussion in Schädel et al. 2021b) – a problem that is largely ignored by many authors (e.g. Bruce et al. 2021). The fossil specimens presented in Robin et al. (2018) have been interpreted as either coming from scavengers or from parasites/micro-predators due to their location on many two specimens of fossil electric rays (Torpediniformes). However, as the morphology of the specimens gives no further indication for parasitic behaviour, the nature of the interaction and whether the fish were still alive when the representatives of Isopoda arrived on their bodies is unclear. The occurrence of another species of Isopoda belonging to not very closely related lineage (Sphaeromatidea: *Dynamenella* sp.) can be seen as a hint towards scavenging as the cause of the fossil assemblage (Robin et al. 2018).

The presence of a single individual of a species of Isopoda on a fossil mackerel shark from the Upper Cretaceous of Texas (USA) (Bowman 1971), which systematic position is unclear due to the poor preservation of the fossil, represents a similar case, where the nature of the interaction, and in this case if there has been an interaction at all, is unclear (Klompmaker & Boxshall 2015). *Brunnaega roeperi* Polz, 2005 from the Late Jurassic of Bavaria (Germany) has originally been interpreted as a representative of Aegidae White, 1850, a group of micro-predatators/temporary parasites, which monophyletic property has been questioned by some authors (Wägele 1989; Dreyer & Wägele 2001) and for which there is no convincing apomorphy (Brandt & Poore 2003). However, this systematic interpretation is based on the similarity to some species of *Palaega* a non-monophyletic group ('form genus') of extinct species that share some superficial similarities (e.g. Feldmann & Rust 2006), which in works of early authors has been said to belong to the group Aegidae (e.g. Zittel 1887). The species has later been interpreted as a representative of Cirolanidae (Wilson et al. 2011a). Furthermore, specimens of *B. roeperi* do not show any morphological

indications for a parasitic or micro-predatory behaviour and therefore different life styles are equally if not more likely for this species. Hansen and Hansen (2010) interpreted two specimens from the Miocene of Denmark as representatives of *Aega* (an ingroup of Aegidae) based on the overall similarity of the preserved body parts, which in this case are remains of the posterior body region comprising tergites of the trunk, the pleotelson and parts of the uropods. The authors coded characters visible in the fossils, of which none is unique to the groups they included into their analysis, into a matrix of zeros and ones and concluded based in statistical measures of similarity and a 2D ordination plot that their fossils is a representative of the most similar group *Aega*. Despite the numerically recognised similarity with representatives of Aegidae (Hansen & Hansen 2010), the fossils are still very similar to representatives of "Cirolanidae" (representatives of Cymothoida that lack apomorphic features of its ingroups).

Nagler et al. (2016) reported fossil remains of representatives of Isopoda on fossil fishes from the Late Jurassic Solnhofen limestones of Bavaria (Germany), which they tentatively interpreted as close relatives of the group Cymothoidae (parasites of fishes). However, the fossil specimens they presented are very similar to representatives of a species, that occur at the same locality in the same layers of rock – *Urda rostrata* Münster, 1840 (study V). The differences that appear when comparing the colour marked figures in Nagler et al. (2016) with specimens of *U. rostrata* are not apparent in the non colour marked versions. For example in the colour-marked version the pleotelson is with a rounded posterior margin (Nagler et al. 2016, fig. 3D), whereas in the image itself a straight mid-portion is visible (Nagler et al. 2016, fig. 3C) (for a more detailed discussion see study 5). Therefore at least some of the specimens presented by Nagler et al. (2016) can be interpreted as coming from *U. rostrata*. The palaeoecological implications of the fossils are thus discussed below.

Very recently a fossil specimen from the Cretaceous of Mexico has been reported (Stinnesbeck et al. 2022), which by the authors of the study has been interpreted to be a parasite of the fish on which fossil remains it has been found. Their interpretation as a parasite is based on the location of the specimen on a fossil fish. They argued for a parasitic interaction as the reason for the death assemblage because of multiple factors. The specimen is the only animal preserved together with the fish, which they with reference to the discussion in (Nagler et al. 2016), saw as a point against scavenging together with the absence of visible traces of decay, which they suggested to be caused by rapid burial or

anoxic conditions near the sediment surface (Stinnesbeck et al. 2022). A 'twisted body position', which they argued could be the result of a growth response resulting from the parasite living permanently on its host, is not directly apparent from the photographs nor their drawing. In order to recognise a growth response there would have to be asymmetries in body parts which can not be explained by a distortion of sclerites relative to each other. Stinnesbeck et al. (2022), based on the photographs, which are available in the manuscript at full resolution, interpreted the reported specimen to have seven pairs of legs (post-ocular segments 7-13) to have strongly curved distal-most elements as in extant species of Cymothoidae. This would make a strong case for the proposed life style as well as for a position closely related or within Cymothoidae (van der Wal et al. 2021). However, in the photograph details of the legs are not visible and the legs in the drawings are untypical in shape compared to those in extant species of Cymothoidae and Aegidae and also are different on the two sides of the body, suggesting an over-interpretation of the visible structures.

In Eocene fossils from Kučlín (Czech Republic) (van der Wal et al. 2021) the distal-most elements of the legs of the anterior trunk region (post-ocular segments 7-13) are well preserved in several specimens and very similar to those in extant representatives of Cymothoidae, allowing to interpret the specimens either as closest relatives to or representatives of the group Cymothoidae. This indiscrimination is because there is no single-apomorphy based characterisation of Cymothoidae in the literature and other characters might be eligible as well; also it has not been possible to identify the specimens as belonging to any of the ingroups of Cymothoidae (van der Wal et al. 2021). The systematic position of the fossils from Kučlín make a strong case for a parasitic/micro-predatory life style of the extinct organisms, as representatives of Cymothoidae are permanently attaching parasites and representatives of Aegidae, which are closely related to Cymothoidae, are temporary parasites/micropredators. The main character used for the systematic interpretation of the fossils, the presence of robust, strongly curved, distal leg elements, also hints towards a syn-vivo interaction with a larger animal by attaching to it. The, compared to the entire body, small head is a feature present in many species of Cymothoidae which permanently attach to fishes. The presence in immatures or absence in adults of swimming setae on the pleopods, which can be seen in extant species of Cymothoidae, which could be a good argument for parasitism in the narrow sense as opposed to micro-predation, due to the mode of preservation is not assessable in the fossils. In summary it can be said that,

despite no specimens could be found on potential hosts (Van der Wal 2019, pers. comm.) the fossil specimens from Kučlín are very likely the remains of parasites, at least in the broader sense (including the possibility that the animals were only temporarily feeding on larger animals).

The fossil record of Epicaridea can be divided into two categories: occurrences of trace fossils and occurrences of body fossils. Fossil traces of parasitism caused by representatives of Epicaridea have so far only been found without the parasite itself (Robin 2021). The known traces consist of swellings of the thoracic shields of crustaceans usually in the region where the respiratory apparatus is located. In the extant fauna adult representatives of Epicaridea are the only known source for such swellings (Klompmaker et al. 2014). The swellings are the result of a growth response of the host because of the presence of a parasite (Wägele 1989). This makes the swellings traces of parasitism in a strict sense, meaning that the parasites have had to stay on their host for a long period of time; also the size of the swellings indicates a quite large size of the parasite relative to its host, preventing the parasite to leave the inhabited swollen gill chamber through its natural opening.

Trace fossils associated with Epicaridea have been known for a long time (e.g. Bachmayer 1948). But only since a few years there are fossil remains that can be attributed to the group. The first record of such fossils is from the Miocene of Mexico from Chiapas amber (Serrano-Sánchez et al. 2016). In these fossils the distinct morphology of the cryptoniscium larval stage is apparent, allowing the fossils to be interpreted as representatives of Epicaridea through a number of morphological features that are unique to the group (Serrano-Sánchez et al. 2016). As most extant representatives of Epicaridea are believed to be parasites of crustaceans ('taxonomic uniformitarism') and under many phylogenetic hypotheses the common ancestor of Epicaridea can, through the extant phylogenetic bracket method, be reconstructed to be parasitic or at least temporary parasitic (cf. Fig. 2), the systematic affinity of the fossils is a strong link to parasitism. There are two further occurrences of body fossils that are interpreted to belong to representatives of Epicaridea, from the Late Cretaceous of France (Vendean amber) (Néraudeau et al. 2017; Schädel et al. 2019) and from the mid-Cretaceous Kachin amber of Myanmar (Schädel et al. 2021a). In both of these occurrences in addition the systematic affinity, also the morphology visible in the fossils itself provides an indication for parasitic behaviour. The mouthparts in the fossils from France form a distinct cone shaped structure with a small apical opening (Schädel et al. 2019), which is also present in extant

cryptoniscium larvae, where the mouthparts are used for piercing through the body wall of their hosts and to feed on the body fluids of it (Nagler et al. 2020). The thin moderately curved distal-most leg elements visible in the fossils (Schädel et al. 2019, 2021a), which are also present in extant species and together with the penultimate leg element form a subchela, could be used to cling to a larger animals in order to feed on them; however, not much is available in the literature about the behaviour of the larvae in the extant fauna.

As of now, the group Gnathiidae lacks a fossil record. There are however fossils which are morphologically distinct from extant forms of Gnathiidae but share systematically important characters with representatives of Gnathiidae. Fossils of *Urda* Münster, 1840 have a straight portion of the dorsal side of the head that likely serves as a joint between the upper lip and the head; the upper lip itself is large and there is no distinct frontal lamina or labrum; the tergite of the anteriormost trunk segment is very short and the legs are projected in anterior direction, adjoining the mouthparts (study 5). All of these features are also present in immature forms of Gnathiidae; in adult forms of Gnathiidae the lip is missing and the segment which is the anterior-most trunk segment in the immatures (post-ocular segment 7) is conjoined with the head (a suture is visible in adults of some species) (Monod 1926).

There are multiple species with a similar morphology to the type species of *Urda* – *Urda rostrata* Münster, 1840 – which differ in their overall body shape from the extant representatives of Gnathiidae; yet, there are no apparent morphological features in the fossils that can be seen as an apomorphy of a group *Urda*. Instead the *Urda* fossils might be a good model for the common ancestor of all species of Gnathiidae that still lacked the apomorphic features by which representatives of Gnathiidae differ from the *Urda* fossils (post-ocular segments 13 without well-developed appendages (paedomorphosis); non-feeding adults with flattened mouthparts; sexual dimorphism in which males have large mandibles).

50
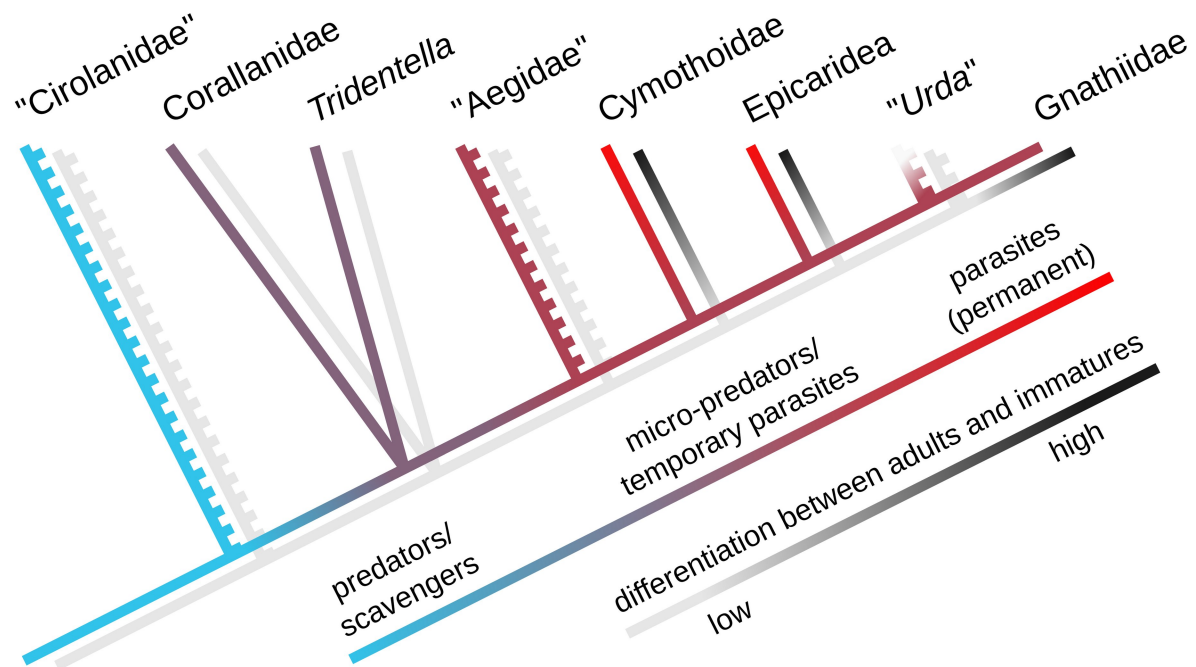
Figure 5: Phylogenetic tree depicting the possible relationships between groups with parasitic and micro-predatory representatives (cf. Nagler et al. 2017), along with the proposed evolution of the feeding modes/life styles and the degree of differentiation between adults and immatures – a high degree of differentiation implying the presence of larvae in a morphological and ecological sense.

Depending on which extant group forms the sister group of Gnathiidae (Fig. 2, Fig. 5), the systematic position of the *Urda* fossils could be an indication for a parasitic life style. Apart from that, the morphology of the fossil specimens can provide indications about the behaviour of the once living organisms. Nagler et al. (2017) argued for a parasitic life style based on characteristics of the mouth parts and the legs. They interpreted the individual mouth parts to form a cone-like structure which they saw as an indication for piercing-sucking food uptake. However, the morphology of the mouth parts as reconstructed by Nagler et al. (2017) based on μCT data (manual segmentation) could only partly be reproduced and crucial aspects of the repeated reconstruction (also manual segmentation; study 5) differed from the findings in Nagler et al. (2017). Instead of being part of a cone-like assembly of mouthparts, the mandibles are large and strongly curved, with a pointy tip and protruding beyond the anterior margin of the head. By this the mandibles are very similar to those found in strongly compressed fossils of *Urda rostrata* from the Late Jurassic Solnhofen

51

Limestones of southern Germany. The curved mandibles could have been used to cling to fishes, which is very likely, as specimens of *U. rostrata* have been found on fish fossils, seemingly attaching with structures that are located in the anterior-most part of the body. The mandibles in extant immatures of Gnathiidae are, however, not strongly curved but straight and with a serrated median side (Monod 1926, fig. 30), which clearly indicates a different mechanism for attachment. The distal-most elements of the legs in the *Urda* fossils from the middle Jurassic of Bielefeld (Germany; study 5, fig. A–B), which were studied in Nagler et al. (2017), are not as robust (with a thick base) and not as strongly curved as in species of Cymothoidae or Aegidae (cf. Nagler et al. 2017, fig. 7), but are instead much more similar to the distal leg elements in immature individuals of Gnathiidae which are distinctly less curved than in representatives of Cymothoidae and Aegidae (study 5, fig. 20).

Figure 6: Fossil death assemblage of a fish together with one or possibly two, crustacean remains (arrows), likely representing specimens of *Urda rostrata* Münster, 1840, from the Upper Jurassic Solnhofen Limestones (Bavaria, Germany). Composite of ultraviolet light fluorescence photographs, images courtesy of Falk Starke (Bodenwerder, Germany), private collection of Falk Starke.

As briefly noted above, specimens of *Urda rostrata* have been found on fossils of fishes (Fig. 6). Nagler et al. (2016) reported several such fossil assemblages, however, without identifying the arthropod fossils as repesentatives of *U. rostrata* but as potential close relatives of Cymothoidae (see discussion above; study 5). As Nagler et al. (2016) noted, the position of the *U. rostrata* specimens is not as one would expect for a post-mortem agglomeration through bottom currents or by the *U. rostrata* specimens feeding on carcasses

of fish and dying on their food item. Instead, most specimens are located near the fins (e.g. Fig. 6) with the head towards the anterior side of the fish. This suggests a syn-vivo interaction. Theoretically, also a mutualistic or commensalistic relationships could result in such constellations of fossils. The representatives of *U. rostrata* could for example have used the fish as a means of transportation (phoresy). Although micro-predation or parasitism seem to be the most compatible interactions to have produced the fossil assemblages, more information in the form of new and restudied fossils is needed in order to support or dismantle this assumption.

3.5   Larval development as a result of effective parasitism

Parasites exploit the resources of their host for their benefit – usually, or by most characterisations of the term parasitism, through feeding on the hosts resources. To do so most efficiently, the parasite needs to develop an efficient way to retrieve nutrients from the host body, whilst diminishing the possibility to be removed from the host or to get killed by a predator. Parasites therefore often have morphological adaptions that allow them to be more efficient in these aspects. Such adaptions can, for example, comprise specialised mouthparts, attachment structures and a flat body shape (e.g. van der Wal & Haug 2020). Being located underneath sheltering structures of the host, in the body cavity of the host or outside the hosts body underneath robust body parts, such as exoskeletal shields of euarthropods or gill plates of fishes, drastically increases the security of the parasite, using mostly resources of the host for this purpose. Especially when such a shelter on the host can be used, staying on the host permanently is a viable option for the parasite if the host is long-lived. A good example for such a strategy are species of Cymothoidae that are located in the mouth or the gills of their fish hosts (Brusca 1981). If a parasite stays on its host permanently, the reproductive stage is consequently immobile relative to the host and the offspring has to be mobile relative to the host and able to attach to a new host. The reproductive stage being immobile and the immatures serving as a dispersal stage qualifies the immatures to be larvae from an ecological viewpoint ('ecolarvae' sensu Haug 2020). This requirement is comparable to other non parasitic sessile organisms, such as for example corals or barnacles. The more the reproductive stage of the parasite is morphologically adapted to live on its host, the more the immatures have to differ from their adult counterparts in order to stay mobile and fit in their environment, which fundamentally differs from the environment of the

immobile adults. This then qualifies the immature forms also as larvae in a morphological sense ('morpholarvae' sensu Haug 2020). Such developments can be expected to have evolved in the groups Cymothoidae and Epicaridea, where in some species the adults are immobile relative to the hosts and unable to continue to survive without their host in natural environments; in those species the immature forms can be clearly identified as eco- and morpholarvae.

In Gnathiidae effective (temporary) parasitism is linked with the development of larvae in a different way. Within Gnathiidae the immature stages both serve as dispersal stages and are at the same time the only parasitic stages in the life cycle. The energy for the production of offspring is derived from the meal of the last immature stage; the adults are thought to be non-feeding (Upton 1987). The immature stages are able to take up enormous amounts of nutrients through very few and short feeding processes by stretching out strongly wrinkled parts of their body in a similar way as ticks (Ixodida) do when feeding on mammals (Wilson et al. 2011b; Starck et al. 2018). Ecologically this separates the immature stages from the adults ('ecolarvae') and additionally there are numerous morphological differences between immature and adult forms of Gnathiidae that qualify the immatures as morpholarvae: e.g. flattened maxillipeds and appendages of post-ocular segment 7 (first pair of trunk legs in many representatives of Isopoda, functional mouthparts in Gnathiidae), reduced mandibles in females, large and curved mandibles in males (opposed to thin and straight in the immature stages), reduced eyes in most species (Monod 1926).

There are circumstances where there is less need for specialised dispersal stages despite a pronounced dependence of the parasite on its host animal. In hair lice of mammals the immature stages differ little from their their adult counterparts in their mode of life and their appearance (Nuttall 1917). This is likely due to the close interactions between the host animals and their high mobility which allows for a dispersal between host animals and within the habitat of the hosts. In all parasites within Isopoda that permanently attach to their host the dispersal happens through the immature stages, which in all cases differ at least in some degree from their parents (Brusca 1981; Boyko & Wolff 2014). Also, within Isopoda there are no records of larvae in species without a parasitic lifestyle. This renders a coincidental nature of the occurrence of larvae associated with parasitism unlikely. Given the lack of larvae in some lineages where a similar mode of life (micropredation/parasitism without permanent attachment) is prevalent such as in Aegidae, Corallanidae and *Tridentella* (Bunkley-Williams & Williams 1998), the development of larvae seems not to be a necessary

precursor for parasitism, but rather the effect of an increase in dependence of the parasites to their host.

The fossil record of Epicaridea can be subdivided into fossil traces of its representatives (Klompmaker et al. 2021) and the actual fossil remains of its representatives (Serrano-Sánchez et al. 2016; Schädel et al. 2019, 2021a). The trace fossils attributed to representatives of Epicaridea are not only much more abundant than the body fossils but the earliest trace fossils are also considerably older (ca. 160 million years; Klompmaker et al. 2014) than the oldest body fossils, which are from the mid Cretaceous (Schädel et al. 2021a). The body fossils of representatives of Epicaridea all come from individuals with an appearance similar to extant cryptoniscium stage larvae. This clearly shows that larvae or at least the morphology typical for larvae within Epicaridea was already present before the Late Cretaceous. From the geologically older trace fossils it can be concluded that at least some species of Epicaridea had a parasitic lifestyle to the time from which the oldest fossils of larvae stem (ca. 99 million years ago). Consequently, the fossil record of Epicaridea can, as of now, add little to our understanding how parasitism and larval development are interlinked within the group other than providing minimal ages for the specialised larval morphology and for the parasitic lifestyle.

There are fossils from the Eocene of Kučlín (Czech Republic), which can be interpreted as representatives of Cymothoidae or as close relatives of the group (van der Wal et al. 2021). From this fossil occurrence 11 specimens have been documented, from which the smallest specimens are presumed to come from immature stages of the species. The presumed immatures do differ in their body shape from the largest presumably adult female specimens; however, apart from the overall body shape, which seems to change rather gradually as the individuals grow, there are no distinct differences which would qualify the immature stages as larvae in a morphological sense. However, in extant species of Cymothoidae the immatures differ from the adults in the presence of long swimming setae on the pleopods – a feature that can not be observed in the available fossils due to their mode of preservation. By this, the development of the extinct species from Kučlín appears to be similar to those extant species of the group Cymothoidae which are externally attached to their host, meaning they are not located within the gill chamber or inside the mouth of the fish host. An external attachment to the host can be reconstructed to be the plesiomorphic condition for the group Cymothoidae , as the most basal extant species of Cymothoidae are externally attaching (Brusca 1981, fig. 4) and representatives of Aegidae, Corallanidae and

Tridentella, which are thought to be closely related to Cymothoidae, are also externally attaching (Brandt & Poore 2003). Consequently, the fossil record of Cymothoidae – the only compelling fossils coming from the Eocene of the Czech Republic (van der Wal et al. 2021; see discussion above) – does not provide additional information about the evolution of larvae and their relation to parasitism.

Similar to the fossil assemblage from Kučlín, fossils of *Urda rostrata* and closely related extinct species (see study 5) show no signs of a presence of larvae. The studied fossils are relatively large for representatives of Isopoda (many specimens are longer than 30 mm; study 5). Where preserved fossils comprise a combination of morphological features resembling larval as well as adult representatives of the extant group Gnathiidae, which is the closest related group to the fossils (study 5). Therefore, there is little reason to assume that the fossil remains of *U. rostrata* and related extinct species (study 5) come from immature stages or that the extinct species had true larval forms. Instead the mixture of features that are characteristic for larval and adult forms of the closest modern relatives suggests that the morphological distinction between immatures and adults had intensified in the lineage between the last common ancestor of *U. rostrata* and Gnathiidae and the last common ancestor of extant representatives of Gnathiidae and that even though no immature forms of *Urda* fossils are known, the distinction them and the adults is smaller than in extant representatives of Gnathiidae. There are specimens of *U. rostrata* that clearly show a close interaction with fishes (Nagler et al. 2016; Fig. 6). As discussed above, it is not entirely clear whether these interactions represent parasitism or another form of close interaction such as commensalism. Nevertheless, the fossil record of close interaction with fishes – the hosts of the closest extant relatives – probably being older than the presence of larval forms is an important information for understanding the origin of the parasitism that is present in extant species of Gnathiidae. In this respect the evolution of larval forms in Gnathiidae seems very similar to the evolution of larval forms in Cymothoidae, suggesting similar constraints despite very different life cycles.

3.6 Outlook

The continuation of the study of the fossil record and the evolution of parasitism and larval development in Isopoda relies on multiple factors. The discovery of new fossils as well as the thorough documentation of already formally described fossils have the potential to provide unique character combinations that are not present in extant species and to provide minimum ages of morphological features that can be used to infer information about the temporal aspect of the studied evolutionary process. Modern imaging technologies such as μCT or synchroton scanning as well as fluorescence imaging have the potential to unearth morphological features in newly discovered fossils as well as old type material from many field sites. Many key steps in the evolution of both parasitism and larval development happened prior to the mid-Cretaceous, from where the oldest fossil-rich ambers come from. This highlights the necessity to apply imaging techniques that have the potential to recover fine morphological details of the legs and mouthparts, such as μCT scanning, more widely, in order to retrieve valuable characters from fossils that are preserved in a sediment matrix, as these are not as limited in their age as fossils from amber. Fluorescence techniques also show a great potential to gain new information about fossils, even from well-studied localities. A wide application of fluorescence imaging (maybe even in the field) could be the key to finding and studying small fossils of immature representatives of Isopoda. In fossil sites such as the Solnhofen limestones of southern Germany, which yield a plethora of exceptionally well preserved specimens, the search for gut contents could solve long-standing questions about the diet of extinct species that have been hypothesised as parasites. The correspondence with fossil collectors and amateur palaeontologist has shown that many interesting specimens are currently housed outside of public museum collections, making the collaboration with the owners of privately housed collections essential for the discovery of new fossils that could contribute valuable information about the history of parasitism and larval development in Isopoda.

4 References

ALAŞ, A., ÖKTENER, A. & YILMAZ, M. 2009. *Gnathia* sp. (Gnathiidae) Infestations on marine fish species from Turkey. *Kafkas Üniversitesi Veteriner Fakültesi Dergisi 15(2),* 201–204.

ANDERSON, G. 1975. Larval metabolism of the epicaridian isopod parasite *Probopyrus pandalicola* and metabolic effects of *P. pandalicola* on its copepod intermediate host *Acartia tonsa. Comparative Biochemistry and Physiology Part A: Physiology 50(4),* 747–751. DOI 10.1016/0300-9629(75)90140-1

ANDERSON, G. & DALE, W.E. 1981. *Probopyrus pandalicola* (Packard)(Isopoda, Epicaridea): morphology and development of larvae in culture. *Crustaceana 41(2),* 143–161.

ANEESH, P.T., HELNA, A.K., KUMAR, A.B. & TRILLES, J.-P. 2020. A taxonomic review of the branchial fish parasitic genus Elthusa Schioedte & Meinert, 1884 (Crustacea: Isopoda: Cymothoidae) from Indian waters, with the description of three new species. *Marine Biodiversity 50(5).* DOI 10.1007/s12526-020-01084-6

ARRONTES, J. 1990. Diet, food preference and digestive efficiency in intertidal isopods inhabiting macroalgae. *Journal of Experimental Marine Biology and Ecology 139(3),* 231–249. DOI 10.1016/0022-0981(90)90149-7

ARTIM, J.M., SELLERS, J.C. & SIKKEL, P.C. 2015. Micropredation by gnathiid isopods on settlement-stage reef fish in the eastern Caribbean Sea. *Bulletin of Marine Science 91(4),* 479–487. DOI 10.5343/bms.2015.1023

ATKINS, D. 1933. 20. *Pinnotherion vermiforme* Giard and Bonnier, an entoniscid infecting *Pinnotheres pisum. Proceedings of the Zoological Society of London 103(2),* 319–363. DOI 10.1111/j.1096-3642.1933.tb01598.x

AUGUIE, B. & ANTONOV, A. 2017. *GridExtra: Miscellaneous Functions for 'Grid' Graphics.*

AX, P. 2000. *The Phylogenetic System of the Metazoa.* 154 pp. Springer-Verlag, Berlin, Multicellular Animals, 1.

BACHMAYER, F. 1948. Pathogene Wucherungen bei jurassischen Dekapoden. *Sitzungsberichte der Österreichische Akademie der Wissenschaften 157,* 263–266.

BAPST, D.W. & WAGNER, P.J. 2019. *Paleotree: Paleontological and Phylogenetic Analyses of Evolution.* R.

BARANOV, V.A., SCHÄDEL, M. & HAUG, J.T. 2019. Fly palaeo-evo-devo: immature stages of bibionomorphan dipterans in Baltic and Bitterfeld amber. *PeerJ 7,* e7843. DOI 10.7717/peerj.7843

BARTLOW, A.W. & AGOSTA, S.J. 2021. Phoresy in animals: review and synthesis of a common but understudied mode of dispersal. *Biological Reviews 96(1),* 223–246. DOI 10.1111/brv.12654

BECK, J.T. 1980. Life history relationships between the bopyrid isopod *Probopyrus pandalicola* and of its freshwater shrimp hosts *Palaemonetes paludosus*. *American Midland Naturalist 104(1),* 135. DOI 10.2307/2424966

BELL, T. 1863. *A Monograph of the Fossil Malacostracous Crustacea of Great Britain, Part II, Crustacea of the Gault and Greensand*. 40 pp. Palaeontographical Society, London, Palaeontographical Society Monograph.

BENGTSON, S. 2000. Teasing fossils out of shales with cameras and computers. *Palaeontologia Electronica 3(1(4)),* 1–14.

BONHOMME, V., PICQ, S., GAUCHEREL, C. & CLAUDE, J. 2014. Momocs: Outline Analysis Using *R. Journal of Statistical Software 56(13)*. DOI 10.18637/jss.v056.i13

BOWMAN, T.E. 1971. *Palaega lamnae*, new species (Crustacea: Isopoda) from the Upper Cretaceous of Texas. *Journal of Paleontology 45(3),* 540–541.

BOWMAN, T.E. 1977. Isopod crustaceans (except Anthuridae) collected on the Presidential Cruise of 1938. *Proceedings of the Biological Society of Washington 89(4),* 653–666.

BOYKO, C.B. & WOLFF, C. 2014. Isopoda and Tanaidacea. In: Martin, J.W., Olesen, J. & Hoeg, J.T. (eds) *Atlas of Crustacean Larvae*. Johns Hopkins University Press, Baltimore, 210–212.

BOYKO, C.B., BRUCE, N.L., HADFIELD, K.A., MERRIN, K.L., OTA, Y., POORE, G.C.B., TAITI, S., SCHOTTE, M. & WILSON, G.D.F. (EDS). 2008. World Marine, Freshwater and Terrestrial Isopod Crustaceans database. Epicaridea.

BRANDT, A. & POORE, G.C. 2003. Higher classification of the flabelliferan and related Isopoda based on a reappraisal of relationships. *Invertebrate Systematics 17(6),* 893–923.

BRASIL-LIMA, I.M. & DE LIMA BARROS, C.M. 1998. Malacostraca - Peracarida Freshwater Isopoda Flabellifera and Asellota. In: Young, P.S. (ed.) *Catalogue of Crustacea of Brazil*. Museu Nacional, Rio de Janeiro, Série Livros, 6, 645–651.

BREED, M.D., COOK, C. & KRASNEC, M.O. 2012. Cleptobiosis in Social Insects. *Psyche 2012(e484765),* 1–7. DOI 10.1155/2012/484765

BROCKMANN, H.J. & BARNARD, C.J. 1979. Kleptoparasitism in birds. *Animal Behaviour 27,* 487–514. DOI 10.1016/0003-3472(79)90185-4

BRÖKELAND, W. & BRANDT, A. 2004. Two new species of Ischnomesidae (Crustacea: Isopoda) from the Southern Ocean displaying neoteny. *Deep Sea Research Part II: Topical Studies in Oceanography 51(14–16),* 1769–1785. DOI 10.1016/j.dsr2.2004.06.034

BROLY, P., SERRANO-SÁNCHEZ, M. DE L., RODRÍGUEZ-GARCÍA, S. & VEGA, F.J. 2017. Fossil evidence of extended brood care in new Miocene Peracarida (Crustacea) from Mexico. *Journal of Systematic Palaeontology 15(12),* 1037–1049. DOI 10.1080/14772019.2016.1266525

BRUCE, N.L. 1983. Aegidae (Isopoda: Crustacea) from Australia with descriptions of three new species. *Journal of Natural History 17(5),* 757–788. DOI 10.1080/00222938300770591

BRUCE, N.L. 1984. A new family for the isopod crustacean genus *Tridentella* Richardson, 1905, with description of a new species from Fiji. *Zoological Journal of the Linnean Society 80(4),* 447–455. DOI 10.1111/j.1096-3642.1984.tb02555.x

BRUCE, N.L. 1986. Cirolanidae (Crustacea: Isopoda) of Australia. *Records of the Australian Museum, Supplement 6,* 1–239. DOI 10.3853/j.0812-7387.6.1986.98

BRUCE, N.L., DE LOURDES SERRANO-SÁNCHEZ, M., CARBOT-CHANONA, G. & VEGA, F.J. 2021. New species of fossil Cirolanidae (Isopoda, Cymothoida) from the Lower Cretaceous (Aptian) Sierra Madre Formation plattenkalk dolomites of El Espinal quarries, Chiapas, SE Mexico. *Journal of South American Earth Sciences 109,* 103285. DOI 10.1016/j.jsames.2021.103285

BRUSCA, R.C. 1981. A monograph on the Isopoda Cymothoidae (Crustacea) of the eastern Pacific. *Zoological Journal of the Linnean Society 73(2),* 117–199. DOI 10.1111/j.1096-3642.1981.tb01592.x

BRUSCA, R.C. & IVERSON, E.W. 1985. A Guide to the Marine Isopod Crustacea of Pacific Costa Rica. *Universidade Costa Rica Revista de Biologia Tropical 33(Supplement 1),* 1–77.

BRUSCA, R.C. & WILSON, G.D.F. 1991. A phylogenetic analysis of the Isopoda with some classificatory recommendations. *Memoirs of the Queensland Museum 31,* 143–204.

BRUSCA, R.C., COELHO, V.R. & TAITI, S. 2001. Suborder Oniscidea (Terrestrial Isopods). *Tree of life web project*. World Wide Web Address: http://tolweb.org/notes/? note_id=4179

BUNKLEY-WILLIAMS, L. & WILLIAMS, E.H. 1998. Isopods Associated with Fishes: A Synopsis and Corrections. *Journal of Parasitology 84(5),* 893–896. DOI 10.2307/3284615

BUSCHINGER, A. 2009. Social parasitism among ants: a review (Hymenoptera: Formicidae). *Myrmecological News 12,* 219–235.

CARDONA, A., SAALFELD, S., SCHINDELIN, J., ARGANDA-CARRERAS, I., PREIBISCH, S., LONGAIR, M., TOMANCAK, P., HARTENSTEIN, V. & DOUGLAS, R.J. 2012. TrakEM2 Software for Neural Circuit Reconstruction. *PLOS ONE 7(6),* e38011. DOI 10.1371/journal.pone.0038011

CAROLI, E. 1928. La fase 'micronisci' di Ione thoracica (Montagu) ottenuta per allevamento sui copepodi. *Accademia Nazionale dei Lincei Rendiconti 6(8),* 321–326.

CONWAY MORRIS, S. 1981. Parasites and the fossil record. *Parasitology 82`(3),* 489–509.

DALE, W.E. & ANDERSON, G. 1982. Comparison of morphologies of *Probopyrus bithynis*, *P. floridensis*, and *P. pandalicola* larvae reared in culture (Isopoda, Epicaridea). *Journal of Crustacean Biology 2(3),* 392–409.

DALEY, A.C. & DRAGE, H.B. 2016. The fossil record of ecdysis, and trends in the moulting behaviour of trilobites. *Arthropod Structure & Development 45(2),* 71–96. DOI 10.1016/j.asd.2015.09.004

DANIEL, G., NILSSON, T. & CRAGG, S. 1991. Limnoria lignorum ingest bacterial and fungal degraded wood. *Holz als Roh- und Werkstoff 49(12),* 488–490. DOI 10.1007/BF02619480

DE ANGELI, A. & QUAGGIOTTO, E. 2014. *Eosphaeroma obtusum* (von Meyer, 1858) Ermanno Quaggiotto** (Isopoda, Sphaeromatidae) dell'Oligocene inferiore della Valle del Ponte (Laverda, Vicenza, Italia nordorientale). *Societa Veneziana di Scienze Naturali Lavori 39,* 39–67.

DE BAETS, K., DENTZIEN-DIAS, P., HARRISON, W.M., TIMOTHY, D., LITTLEWOOD, J. & PARRY, L.A. 2021. Chapter 7 Fossil constraints on the timescale of parasitic helminth evolution. In: De Baets, K. & Huntley, J.W. (eds) *The Evolution and Fossil Record of Parasitism: Identification and Macroevolution of Parasites*. Springer International Publishing, Cham, Topics in Geobiology, 231–271. DOI 10.1007/978-3-030-42484-8

DE LIMA, J.T.A.X., CHELLAPPA, S. & THATCHER, V.E. 2005. *Livoneca redmanni* Leach (Isopoda, Cymothoidae) e *Rocinela signata* Schioedte & Meinert (Isopoda, Aegidae), ectoparasitos de *Scomberomorus brasiliensis* Collette, Russo & Zavala-Camin (Ostheichthyes, Scombridae) no Rio Grande do Norte, Brasil. *Revista Brasileira de Zoologia 22(4),* 1104–1108. DOI 10.1590/S0101-81752005000400041

DELANEY, P.M. 1984. Isopods of the genus *Excorallana* stebbing, 1904 from the Gulf of California, Mexico (Crustacea, Isopoda, Corallanidae). *Bulletin of Marine Science 34(1),* 1–20.

DELANEY, P.M. 1989. *Phylogeny and Biogeography of the Marine Isopod Family Corallanidae (Crustacea, Isopoda, Flabellifera).* 75 pp. Natural History Museum, Contribution in Science, 409.

DELANEY, P.M. & BRUSCA, R.C. 1985. Two new species of *Tridentella* Richardson, 1905 (Isopoda: Flabellifera: Tridentellidae) from California, with a rediagnosis and comments on the family, and a key to the genera of Tridentellidae and Corallanidae. *Journal of Crustacean Biology 5(4),* 728–742. DOI 10.2307/1548249

DREYER, H. & WÄGELE, J.-W. 2001. Parasites of crustaceans (Isopoda: Bopyridae) evolved from fish parasites: molecular and morphological evidence. *Zoology 103(3/4),* 157–178.

DREYER, H. & WÄGELE, J.-W. 2002. The Scutocoxifera tax. nov. and the information content of nuclear ssu rDNA sequences for reconstruction of isopod phylogeny (Peracarida: Isopoda). *Journal of Crustacean Biology 22(2),* 217–234.

DUCHÁČEK, L. & LAMKA, J. 2003. Dicrocoeliosis – the Present State of Knowledge with Respect to Wildlife Species. *Acta Veterinaria Brno 72(4),* 613–626. DOI 10.2754/avb200372040613

DYAR, H.G. 1890. The number of molts of lepidopterous larvae. *Psyche: A Journal of Entomology 5(175–176),* 420–422. DOI 10.1155/1890/23871

EKLUND, M.J., AASE, A. & BELL, C.J. 2018. Progressive photonics: methods and applications of sequential imaging using visible and non-visible spectra to enhance data-yield and facilitate forensic interpretation of fossils. *Journal of Paleontological Techniques 20,* 1–36.

FEDOROV, A., BEICHEL, R., KALPATHY-CRAMER, J., FINET, J., FILLION-ROBIN, J.-C., PUJOL, S., BAUER, C., JENNINGS, D., FENNESSY, F., SONKA, M., BUATTI, J., AYLWARD, S., MILLER, J.V., PIEPER, S. & KIKINIS, R. 2012. 3D Slicer as an image computing platform for the Quantitative Imaging Network. *Magnetic Resonance Imaging 30(9),* 1323–1341. DOI 10.1016/j.mri.2012.05.001

FELDMANN, R.M. & RUST, S. 2006. *Palaega kakatahi* n. sp.: The first record of a marine fossil isopod from the Pliocene of New Zealand. *New Zealand Journal of Geology and Geophysics 49(4),* 411–415. DOI 10.1080/00288306.2006.9515177

FRAAIJE, R.H.B., LÓPEZ-HORGUE, M.A., BRUCE, N.L., VAN BAKEL, B.W.M., ARTAL, P., JAGT, J.W.M. & KLOMPMAKER, A.A. 2019. New isopod and achelatan crustaceans from mid–Cretaceous reefal limestones in the Basque-Cantabrian Basin, northern Spain. *Cretaceous Research 101,* 61–69. DOI 10.1016/j.cretres.2019.04.012

FRAISSE, P. 1878. Die Gattung *Cryptoniscus* Fr. Müller. *Arbeiten aus dem Zoologisch-Zootomischen Institut in Würzburg 4,* 239–296.

FRASER, D., MALLON, J.C., FURR, R. & THEODOR, J.M. 2009. Improving the repeatability of low magnification microwear methods using high dynamic range imaging. *PALAIOS 24(12),* 818–825. DOI 10.2110/palo.2009.p09-064r

GEARTY, W. 2021. *Deeptime: Plotting Tools for Anyone Working in Deep Time*.

GEORGE, R.Y. 1972. Biphasic moulting in Isopod Crustacea and the finding of an unusual mode of moulting in the antarctic genus *Glyptonotus*. *Journal of Natural History 6(6),* 651–656. DOI 10.1080/00222937200770591

GIRARD, V., SCHMIDT, A.R., MARTIN, S.S., STRUWE, S., PERRICHOT, V., MARTIN, J.-P.S., GROSHENY, D., BRETON, G. & NÉRAUDEAU, D. 2008. Evidence for marine microfossils from amber. *Proceedings of the National Academy of Sciences 105(45),* 17426–17429. DOI 10.1073/pnas.0804980105

GRASSINI, C.M. 1994. Estudios preliminares de *Telotha henselii* (Crustacea: Isopoda: Cymothoidae) parasito de camarones palemonidos. *An. Mus. Hist. Nat. Valparaíso 22,* 81.

GREENWALT, D. 2021. Blood to Molecules: The Fossil Record of Blood and Its Constituents. In: De Baets, K. & Huntley, J.W. (eds) *The Evolution and Fossil Record of Parasitism: Coevolution and Paleoparasitological Techniques*. Springer International Publishing, Cham, Topics in Geobiology, 377–416. DOI 10.1007/978-3-030-52233-9_12

GUZMAN, H.M., OBANDO, V.L. & DELANEY, P.M. 1988. Aspects of the population biology of the marine isopod *Excorallana tricornis occidentalis* Richardson, 1905 (Crustacea: Isopoda: Corallanidae) at Cano Island, Pacific Costa Rica. *Bulletin of Marine Science 43(1),* 77–87.

HAACK, W. 1933. Zur Verbreitung des Asselkrebses *Archaeoniscus brodiei* M. EDW. im Serpulit des Teutoburger Waldes. *Zeitschrift der Deutschen Geologischen Gesellschaft 85,* 229–234.

HANSEN, T. & HANSEN, J. 2010. First fossils of the isopod genus *Aega* Leach, 1815. *Journal of Paleontology 84(01),* 141–147. DOI 10.1666/08-083.1

HAUG, C., HAUG, J.T., WALOSZEK, D., MAAS, A., FRATTIGIANI, R. & LIEBAU, S. 2009. New methods to document fossils from lithographic limestones of Southern Germany and Lebanon. *Palaeontologia Electronica 12(3(6)),* 1–12.

HAUG, J.T. 2019. Categories of developmental biology: Examples of ambiguities and how to deal with them. In: Fusco, G. (ed.) *Essays for Alessandro Minelli.* Padova University Press, Padova, Festschrift, 2, 93–102.

HAUG, J.T. 2020. Why the term "larva" is ambiguous, or what makes a larva? *Acta Zoologica 101(2),* 167–188. DOI 10.1111/azo.12283

HAUG, J.T. & HAUG, C. 2011. Fossilien unter langwelligem Licht: Grün-Orange-Fluoreszenz an makroskopischen Objekten. *Archaeopteryx 29,* 20–23.

HENNIG, W. 1965. Phylogenetic Systematics. *Annual Review of Entomology 10,* 97–116.

HOLDICH, D.M. 1975. *Ancyroniscus bonnieri* (Isopoda, Epicaridea) infecting British populations of *Dynamene bidentata* (Isopoda, Sphaeromatidae). *Crustaceana 28(2),* 145–151.

HOSIE, A.M. 2008. Four new species and a new record of Cryptoniscoidea (Crustacea: Isopoda: Hemioniscidae and Crinoniscidae) parasitising stalked barnacles from New Zealand. *Zootaxa 1795,* 1–28.

HUSSON, F., JOSSE, J., LE, S. & MAZET, J. 2020. *FactoMineR: Multivariate Exploratory Data Analysis and Data Mining.*

HYŽNÝ, M., BRUCE, N.L. & SCHLÖGL, J. 2013. An appraisal of the fossil record for the Cirolanidae (Malacostraca: Peracarida: Isopoda: Cymothoida), with a description of a new cirolanid isopod crustacean from the early Miocene of the Vienna Basin (Western Carpathians). *Palaeontology 56(3),* 615–630. DOI 10.1111/pala.12006

ITOH, K., HAYASHI, A. & ICHIOKA, Y. 1989. Digitized optical microscopy with extended depth of field. *Applied Optics 28(16),* 3487–3493. DOI 10.1364/AO.28.003487

JONES, W.T., FELDMANN, R.M., SCHRAM, F.R., SCHWEITZER, C.E. & MAGUIRE, E.P. 2016. The Proof is in the Pouch: *Tealliocaris* is a Peracarid. *Palaeodiversity 9(1),* 75–88. DOI 10.18476/pale.v9.a5

KARASAWA, H., NOBUHARA, T. & MATSUOKA, K. 1992. Fossil and living species of the giant isopod genus *Palaega* Woodward, 1870 of Japan. *Scientific Reports of the Toyohashi Museum of Natural History 2,* 1–12.

KASSAMBARA, A. & MUNDT, F. 2020. *Factoextra: Extract and Visualize the Results of Multivariate Data Analyses*.

KIKINIS, R., PIEPER, S.D. & VOSBURGH, K.G. 2014. 3D Slicer: A Platform for Subject-Specific Image Analysis, Visualization, and Clinical Support. In: Jolesz, F.A. (ed.) *Intraoperative Imaging and Image-Guided Therapy*. Springer, New York, NY, 277–289. DOI 10.1007/978-1-4614-7657-3_19

KLOMPMAKER, A.A. & BOXSHALL, G.A. 2015. Fossil crustaceans as parasites and hosts. In: *Advances in Parasitology*. Elsevier, 233–289.

KLOMPMAKER, A.A., ARTAL, P., VAN BAKEL, B.W., FRAAIJE, R.H. & JAGT, J.W. 2014. Parasites in the fossil record: a Cretaceous fauna with isopod-infested decapod crustaceans, infestation patterns through time, and a new ichnotaxon. *PLoS One 9(3),* 1–17.

KLOMPMAKER, A.A., ROBINS, C.M., PORTELL, R.W. & ANGELI, A.D. 2018. Crustaceans as hosts of parasites throughout the Phanerozoic. *bioRxiv,* 1–27. DOI 10.1101/505495

KLOMPMAKER, A.A., ROBINS, C.M., PORTELL, R.W. & DE ANGELI, A. 2021. Crustaceans as Hosts of Parasites Throughout the Phanerozoic. In: De Baets, K. & Huntley, J.W. (eds) *The Evolution and Fossil Record of Parasitism: Coevolution and Paleoparasitological Techniques*. Springer International Publishing, Cham, Topics in Geobiology, 121–172. DOI 10.1007/978-3-030-52233-9_5

KOCSIS, A.T. & RAJA, N.B. 2020. *Chronosphere: Earth System History Variables*. R.

KUSSAKIN, O.G. & RYBAKOV, A.V. 1995. *Protognathia waegeli* sp. n. (Crustacea, Isopoda, Flabellifera), a new species from the Antarctic of the rare and poorly known family Protognathiidae. *Russian Journal of Marine Biology(1),* 17–28.

LABANDEIRA, C.C. & LI, L. 2021. Chapter 11 The history of insect parasitism and the mid-mesozoic parasitoid revolution. In: De Baets, K. & Huntley, J.W. (eds) *The Evolution and Fossil Record of Parasitism: Identification and Macroevolution of Parasites*. Springer International Publishing, Cham, Topics in Geobiology, 377–533. DOI 10.1007/978-3-030-42484-8

LAFFERTY, K.D. & KURIS, A.M. 2002. Trophic strategies, animal diversity and body size. *Trends in Ecology & Evolution 17(11),* 507–513. DOI 10.1016/S0169-5347(02)02615-0

LANG, C., KRAPP, T. & MELZER, R.R. 2007. Postembryonal development in Caprellidae: SEM description and comparison of ready-to-hatch juveniles and adults of two Mediterranean skeleton shrimps (Crustacea: Amphipoda). *Zootaxa 1605(1),* 1–32. DOI 10.11646/zootaxa.1605.1.1

LAVOUÉ, S., ARNEGARD, M.E., RABOSKY, D.L., MCINTYRE, P.B., ARCILA, D., VARI, R.P. & NISHIDA, M. 2017. Trophic evolution in African citharinoid fishes (Teleostei: Characiformes) and the origin of intraordinal pterygophagy. *Molecular Phylogenetics and Evolution 113,* 23–32. DOI 10.1016/j.ympev.2017.05.001

LEMOS DE CASTRO, A. 1985. Ectoparasitism of *Telotha henselii* (Von Martens) (Isopoda, Cymothoidae) on *Macrobrachium brasiliense* (Heller) (Decapoda, Palaemonidae). *Crustaceana 49(1),* 200–201.

LEUNG, T.L.F. 2017. Fossils of parasites: what can the fossil record tell us about the evolution of parasitism? *Biological Reviews 92(1),* 410–430. DOI 10.1111/brv.12238

LEUNG, T.L.F. 2021. Chapter 1 Parasites of fossil vertebrates: what we know and what can we expect. In: De Baets, K. & Huntley, J.W. (eds) *The Evolution and Fossil Record of Parasitism: Identification and Macroevolution of Parasites*. Springer International Publishing, Cham, Topics in Geobiology, 1–27. DOI 10.1007/978-3-030-42484-8

LEUNG, T.L.F. & POULIN, R. 2008. Parasitism, commensalism, and mutualism: exploring the many shades of symbioses. *Vie Milieu - Life and environment 58(2),* 107–115.

LIMAYE, A. 2012. Drishti: a volume exploration and presentation tool. In: Stock, S.R. (ed.) SPIE Optical Engineering + Applications. San Diego, California, USA, 1–10. DOI 10.1117/12.935640

LINS, L.S.F., HO, S.Y.W., WILSON, G.D.F. & LO, N. 2012. Evidence for Permo-Triassic colonization of the deep sea by isopods. *Biology Letters 8(6),* 979–982. DOI 10.1098/rsbl.2012.0774

LÖSEL, P.D., VAN DE KAMP, T., JAYME, A., ERSHOV, A., FARAGÓ, T., PICHLER, O., TAN JEROME, N., AADEPU, N., BREMER, S., CHILINGARYAN, S.A., HEETHOFF, M., KOPMANN, A., ODAR, J., SCHMELZLE, S., ZUBER, M., WITTBRODT, J., BAUMBACH, T. & HEUVELINE, V. 2020. Introducing Biomedisa as an open-source online platform for biomedical image segmentation. *Nature Communications 11(1),* 5577. DOI 10.1038/s41467-020-19303-w

LOWRY, J. & DEMPSEY, K. 2006. The giant deep-sea scavenger genus *Bathynomus* (Crustacea, Isopoda, Cirolanidae) in the Indo-West Pacific. In: Richer de Forges, B. & Justine, J.L. (eds) *Tropical Deep-Sea Benthos*. Paris, Mémoires du Muséum national d'Histoire naturelle, 193, 163–192.

LUQUE, J., SCHWEITZER, C.E., SANTANA, W., PORTELL, R.W., VEGA, F.J. & KLOMPMAKER, A.A. 2017. Checklist of fossil decapod crustaceans from tropical America. Part I: Anomura and Brachyura. *Nauplius 25(e2017025),* 1–85. DOI 10.1590/2358-2936e2017025

MARKHAM, J.C. 1986. Evolution and zoogeography of the Isopoda Bopyridae, parasites of Crustacea Decapoda. In: Gore, R.H. & Heck, K.L. (eds) *Crustacean Biogeography*. A.A. Balkema, Rotterdam, Crustacean Issues, 143–164.

MARTIN, J.W., OLESEN, J. & HØEG, J. (EDS). 2014. *Atlas of Crustacean Larvae*. 370 pp. Johns Hopkins University Press, Baltimore.

MESSANA, G. 2004. How can I mate without an appendix masculina? The case of *Sphaeroma terebrans* Bate, 1866 (Isopoda, Sphaeromatidae). *Crustaceana 77(4)*, 499–505.

MONOD, T. 1926. Les Gnathiidæ. Essai monographique (Morphologie, Biologie, Systématique). *Mémoires de la Société des Sciences Naturelles du Maroc 13,* 1–668.

MOREIRA, P.S. 1971. Species of Serolis (Isopoda, Flabellifera) from Southern Brazil. *Boletim do Instituto Oceanográfico 20(1),* 85–144.

MORIN, P.J. 2011. Communities. In: *Community Ecology*. Wiley, Chichester, West Sussex ; Hoboken, NJ, 3–23.

NAGEL, L. 2009. The role of vision in host-finding behaviour of the ectoparasite *Gnathia falcipenis* (Crustacea; Isopoda). *Marine and Freshwater Behaviour and Physiology 42(1),* 31–42. DOI 10.1080/10236240902781456

NAGLER, C. & HAUG, J.T. 2016. Functional morphology of parasitic isopods: understanding morphological adaptations of attachment and feeding structures in *Nerocila* as a pre-requisite for reconstructing the evolution of Cymothoidae. *PeerJ 4,* e2188. DOI 10.7717/peerj.2188

NAGLER, C., HAUG, C., RESCH, U., KRIWET, J. & HAUG, J.T. 2016. 150 million years old isopods on fishes: a possible case of palaeo-parasitism. *Bulletin of Geosciences 91(1),* 1–12.

NAGLER, C., HYŽNÝ, M. & HAUG, J.T. 2017. 168 million years old "marine lice" and the evolution of parasitism within isopods. *BMC evolutionary biology 17(1),* 76.

NAGLER, C., EILER, S.M. & HAUG, J.T. 2020. Examination of functional morphology of dajiid isopods using *Arthrophryxus* sp. parasitising a mysid shrimp as an example. *Acta Zoologica 101(4),* 339–352. DOI https://doi.org/10.1111/azo.12298

NÉRAUDEAU, D., PERRICHOT, V., BATTEN, D.J., BOURA, A., GIRARD, V., JEANNEAU, L., NOHRA, Y.A., POLETTE, F., SAINT MARTIN, S. & SAINT MARTIN, J.-P. 2017. Upper Cretaceous amber from Vendée, north-western France: age dating and geological, chemical, and palaeontological characteristics. *Cretaceous Research 70,* 77–95.

NICHOLSON, M.D., ARTIM, J.D., HENDRICK, G.C., PACKARD, A.J. & SIKKEL, P.C. 2019. Fish-parasitic gnathiid isopods metamorphose following invertebrate-derived meal. *Journal of Parasitology 105(5),* 793. DOI 10.1645/19-59

NIELSEN, S.-O. & STRÖMBERG, J.-O. 1965. A new parasite of *Cirolana borealis* Lilljeborg belonging to the Cryptoniscinae (Crustacea Epicaridea). *Sarsia 18(1),* 37–62. DOI 10.1080/00364827.1965.10409547

NIELSEN, S.-O. & STRÖMBERG, J.-O. 1973. Morphological characters of taxonomical importance in Cryptoniscina (Isopoda Epicaridea) A scanning electron microscopic study of Cryptoniscus Larvae. *Sarsia 52(1),* 75–96.

NUTTALL, G.H.F. 1917. The Biology of Pediculus humanus. *Parasitology 10(1),* 80–185. DOI 10.1017/S0031182000003747

NÜTZEL, A. 2021. Chapter 6 Gastropods as parasites and carnivorous grazers: a major guild in marine. In: De Baets, K. & Huntley, J.W. (eds) *The Evolution and Fossil Record of Parasitism: Identification and Macroevolution of Parasites.* Springer International Publishing, Cham, Topics in Geobiology, 209–229. DOI 10.1007/978-3-030-42484-8

ÖKTENER, A., ŞIRIN, M. & YURDIGÜL, E. 2020. Micropredator behaviour of *Rocinela dumerilii* (Isopoda, Aegidae) on *Trachurus trachurus* in the Sea of Marmara (Turkey). *Transylvanian Review of Systematical and Ecological Research 22(2),* 57–72. DOI 10.2478/trser-2020-0011

OTA, Y. 2019. Habitat utilization and seasonal occurrence of *Tachaea chinensis* (Isopoda: Corallanidae) infesting freshwater shrimps in Lake Biwa, central Japan. *Crustacean Research 48,* 133–143. DOI 10.18353/crustacea.48.0_133

OWENS, L. & ROTHLISBERG, P.C. 1991. Vertical migration and advection of bopyrid isopod cryptoniscid larvae in the Gulf of Carpentaria, Australia. *Journal of plankton research 13(4),* 779–787.

PANAKKOOL-THAMBAN, A. & KAPPALLI, S. 2020. Occurrence of life cycle dependent monophasic and biphasic molting in a parasitic isopod, *Mothocya renardi. Thalassas: An International Journal of Marine Sciences.* DOI 10.1007/s41208-019-00188-6

PARADIS, E., BLOMBERG, S., BOLKER, B., BROWN, J., CLARAMUNT, S., CLAUDE, J., CUONG, H.S., DESPER, R., DIDIER, G., DURAND, B., DUTHEIL, J., EWING, R.J., GASCUEL, O., GUILLERME, T., HEIBL, C., IVES, A., JONES, B., KRAH, F., LAWSON, D., LEFORT, V., LEGENDRE, P., LEMON, J., LOUVEL, G., MARCON, E., MCCLOSKEY, R., NYLANDER, J., OPGEN-RHEIN, R., POPESCU, A.-A., ROYER-CARENZI, M., SCHLIEP, K.,

STRIMMER, K. & VIENNE, D. DE. 2021. *Ape: Analyses of Phylogenetics and Evolution*. R.

PASCUAL, S., VEGA, M.A., JOSÉ ROCHA, F. & GUERRA, A. 2002. First report of an endoparasitic epicaridean isopod infecting cephalopods. *Journal of Wildlife Diseases 38(2),* 473–477. DOI 10.7589/0090-3558-38.2.473

PAWLOWSKI, Z.S. 2002. *Taenia solium*: basic biology and transmission. In: Singh, G. & Prabhakar, S. (eds) *Taenia Solium Cysticercosis: From Basic to Clinical Science*. CABI Publishing, Wallingford, 1–13.

PAZINATO, P.G., SOARES, M.B. & ADAMI-RODRIGUES, K. 2016. Systematic and palaeoecological significance of the first record of Pygocephalomorpha females bearing oöstegites (Malacostraca, Peracarida) from the lower Permian of southern Brazil. *Palaeontology 59(6),* 817–826. DOI 10.1111/pala.12260

PEBESMA, E. 2018. Simple Features for R: Standardized Support for Spatial Vector Data. *The R Journal 10(1),* 439. DOI 10.32614/RJ-2018-009

PENFOLD, R., GRUTTER, A.S., KURIS, A.M., MCCORMICK, M.I. & JONES, C.M. 2008. Interactions between juvenile marine fish and gnathiid isopods: predation versus micropredation. *Marine Ecology Progress Series 357,* 111–119. DOI 10.3354/meps07312

PENNEY, D. (ED.). 2010. *Biodiversity of Fossils in Amber from the Major World Deposits*. 304 pp. Siri Scientific Press, Manchester.

PIEPER, R.J. & KORPEL, A. 1983. Image processing for extended depth of field. *Applied Optics 22(10),* 1449–1453. DOI 10.1364/AO.22.001449

POINAR, G. 2018. A new genus of terrestrial isopods (Crustacea: Oniscidea: Armadillidae) in Myanmar amber. *Historical Biology,* 1–6. DOI 10.1080/08912963.2018.1509964

POLZ, H. 2005. Zwei neue Asselarten (Crustacea: Isopoda: Scutocoxifera) aus den Plattenkalken von Brunn (Oberkimmeridgium, Mittlere Frankenalb). Two new isopods (Crustacea: Isopoda: Scutocoxifera) from Brunn (Upper Kimmeridgian, Franconian Alb, South Germany). *Archaeopteryx 23,* 67–81.

POORE, G.C.B. & BRUCE, N.L. 2012. Global diversity of marine isopods (except Asellota and crustacean symbionts). *PLOS ONE 7(8),* e43529. DOI 10.1371/journal.pone.0043529

R CORE TEAM. 2021. *R: A Language and Environment for Statistical Computing*. R Foundation for Statistical Computing, Vienna, R.

RABELING, C. 2020. Social Parasitism. In: Starr, C.K. (ed.) *Encyclopedia of Social Insects*. Springer International Publishing, Cham, 1–23. DOI 10.1007/978-3-319-90306-4_175-1

RACHEBOEUF, P.R., SCHRAM, F.R. & VIDAL, M. 2009. New malacostracan Crustacea from the Carboniferous (Stephanian) Lagerstätte of Montceau-les-Mines, France. *Journal of Paleontology 83(4),* 624–629. DOI 10.1666/08-171R.1

RADWAŃSKI, A. 1972. Isopod-infected prosoponids from the Upper Jurassic of Poland. *Acta Geologica Polonica 22(3),* 499–506.

REVELL, L.J. 2017. *Phytools: Phylogenetic Tools for Comparative Biology (and Other Things)*. R.

ROBIN, N. 2021. Importance of Data on Fossil Symbioses for Parasite–Host Evolution. In: De Baets, K. & Huntley, J.W. (eds) *The Evolution and Fossil Record of Parasitism: Coevolution and Paleoparasitological Techniques*. Springer International Publishing, Cham, Topics in Geobiology, 51–73. DOI 10.1007/978-3-030-52233-9_2

ROBIN, N., MARRAMÀ, G., VONK, R., KRIWET, J. & CARNEVALE, G. 2018. Eocene isopods on electric rays: tracking ancient biological interactions from a complex fossil record. *Palaeontology,* 1–17. DOI 10.1111/pala.12398

ROBIN, N., D'HAESE, C. & BARDEN, P. 2019. Fossil amber reveals springtails' longstanding dispersal by social insects. *BMC Evolutionary Biology 19(213),* 1–12. DOI 10.1186/s12862-019-1529-6

ROBINS, C.M. & KLOMPMAKER, A.A. 2019. Extreme diversity and parasitism of Late Jurassic squat lobsters (Decapoda: Galatheoidea) and the oldest records of porcellanids and galatheids. *Zoological Journal of the Linnean Society 187(4),* 1131–1154. DOI 10.1093/zoolinnean/zlz067

ROBINS, C.M., FELDMANN, R.M. & SCHWEITZER, C.E. 2013. Nine new genera and 24 new species of the Munidopsidae (Decapoda: Anomura: Galatheoidea) from the Jurassic Ernstbrunn Limestone of Austria, and notes on fossil munidopsid classification. *Annalen des Naturhistorischen Museums in Wien. Serie A für Mineralogie und Petrographie, Geologie und Paläontologie, Anthropologie und Prähistorie 115,* 167–251.

ROLLMANN, W. 1853. Zwei neue stereoskopische Methoden. *Annalen der Physik 90(1),* 186–187.

RYBAKOV, A.V. 1990. *Bourdonia tridentata* gen. n., sp. n. (Isopoda: Cabiropsidae) a hyperparasite of *Bopyroides hippolytes* Kroyer from the shrimp *Pandalus borealis*. *Parazitologiia 24(5),* 408–416.

RYBAKOV, A.V. 1998. *Onisocryptus kurilensis* sp. n. (Crustacea, Isopoda, Cyproniscidae), a parasite of the ostracod *Vargula norvegica orientalis*. *Russian Journal of Marine Biology 24(5),* 337–339.

SAINT MARTIN, S., SAINT MARTIN, J.-P., SCHMIDT, A.R., GIRARD, V., NÉRAUDEAU, D. & PERRICHOT, V. 2015. The intriguing marine diatom genus *Corethron* in Late Cretaceous amber from Vendée (France). *Cretaceous Research 52,* 64–72. DOI 10.1016/j.cretres.2014.07.006

SAITO, N. & SAITO, T. 2011. New record of *Aegiochus spongiophila* (Semper) (Isopoda: Aegidae), inhabiting the hexactinellid sponge *Euplectella oweni* Herklots & Marshall from off Makurazaki, southern Kyushu, Japan. *Crustacean Research 40(0),* 33–40. DOI 10.18353/crustacea.40.0_33

SÁNCHEZ-GARCÍA, A., DELCLÒS, X., ENGEL, M.S., BIRD, G.J., PERRICHOT, V. & PEÑALVER, E. 2017. Marsupial brood care in Cretaceous tanaidaceans. *Scientific Reports 7(1).* DOI 10.1038/s41598-017-04050-8

SARS, G.O. 1899. *An Account of the Crustacea of Norway, with Short Descriptions and Figures of All the Species. Isopoda.* 270 pp. Bergen Museum, Bergen.

SCHÄDEL, M., PERRICHOT, V. & HAUG, J. 2019. Exceptionally preserved cryptoniscium larvae - morphological details of rare isopod crustaceans from French Cretaceous Vendean amber. *Palaeontologia Electronica 22.3.71,* 1–46. DOI 10.26879/977

SCHÄDEL, M., VAN ELDIJK, T., WINKELHORST, H., REUMER, J.W.F. & HAUG, J.T. 2020. Triassic Isopoda – three new species from Central Europe shed light on the early diversity of the group. *Bulletin of Geosciences 95(2),* 145–166.

SCHÄDEL, M., HÖRNIG, M.K., HYŽNÝ, M. & HAUG, J.T. 2021a. Mass occurrence of small isopodan crustaceans in 100-million-year-old amber: an extraordinary view on behaviour of extinct organisms. *PalZ 95(3),* 429–445. DOI 10.1007/s12542-021-00564-9

SCHÄDEL, M., HYŽNÝ, M. & HAUG, J.T. 2021b. Ontogenetic development captured in amber - the first record of aquatic representatives of Isopoda in Cretaceous amber from Myanmar. *Nauplius 29(e2021003),* 1–29. DOI 10.1590/2358-2936e2021003

SCHMALFUSS, H. 2003. World catalog of terrestrial isopods (Isopoda: Oniscidea). *Stuttgarter Beiträge zur Naturkunde, Serie A 654,* 1–296.

SCHMIDT, A.R. & DILCHER, D.L. 2007. Aquatic organisms as amber inclusions and examples from a modern swamp forest. *Proceedings of the National Academy of Sciences 104(42),* 16581–16585. DOI 10.1073/pnas.0707949104

SCHMIDT, C. 2008. Phylogeny of the terrestrial Isopoda (Oniscidea): a review. *Arthropod Systematics & Phylogeny 66(2),* 191–226.

SCHNEIDER, C.A., RASBAND, W.S. & ELICEIRI, K.W. 2012. NIH Image to ImageJ: 25 years of image analysis. *Nature Methods 9(7),* 671–675. DOI 10.1038/nmeth.2089

SCHRAM, F.R. 1970. Isopod from the Pennsylvanian of Illinois. *Science 169(3948),* 854–855.

SCHUBERT, R. 2000. Using a flatbed scanner as a stereoscopic near-field camera. *IEEE Computer Graphics and Applications 20(2),* 38–45. DOI 10.1109/38.824535

SCOTESE, C.R. 2016. PALEOMAP PaleoAtlas for GPlates and the PaleoData plotter programm, PALEOMAP Project.

SEED, W.F. 1979. Article: The family Gnathiidae (Crustacea: Isopoda). A new Victorian species. *The Victorian Naturalist 96,* 56–62.

SEGAL, E. 1987. Behavior of juvenile *Nerocila acuminata* (Isopoda, Cymothoidae) during attack, attachment and feeding on fish prey. *Bulletin of Marine Science 41(2),* 351–360.

SERRANO-SÁNCHEZ, M. DE L., HEGNA, T.A., SCHAAF, P., PÉREZ, L., CENTENO-GARCÍA, E. & VEGA, F.J. 2015. The aquatic and semiaquatic biota in Miocene amber from the Campo La Granja mine (Chiapas, Mexico): paleoenvironmental implications. *Journal of South American Earth Sciences 62,* 243–256. DOI 10.1016/j.jsames.2015.06.007

SERRANO-SÁNCHEZ, M. DE L., NAGLER, C., HAUG, C., HAUG, J.T., CENTENO-GARCÍA, E. & VEGA, F.J. 2016. The first fossil record of larval stages of parasitic isopods: cryptoniscus larvae preserved in Miocene amber. *Neues Jahrbuch für Geologie und Paläontologie-Abhandlungen 279(1),* 97–106. DOI 10.1127/njgpa/2016/0543

SHIINO, S.M. 1954. A new fresh-water entoniscid isopod, *Entionella okayamaensis* n. sp. *Report of the Faculty of Fisheries, Prefectural University of Mie 1(3),* 239–246.

SHIMOMURA, M., OHTSUKA, S. & NAITO, K. 2005. *Prodajus curviabdominalis* n. sp. (Isopoda: Epicaridea: Dajidae), an ectoparasite of mysids, with notes on morphological changes, behaviour and life-cycle. *Systematic Parasitology 60(1),* 39–57. DOI 10.1007/s11230-004-1375-8

SHODIPO, M.O., GOMEZ, R.D.C., WELICKY, R.L. & SIKKEL, P.C. 2019. Apparent kleptoparasitism in fish—parasitic gnathiid isopods. *Parasitology Research 118(2),* 653–655. DOI 10.1007/s00436-018-6152-8

SI, A., BELLWOOD, O. & ALEXANDER, C. 2002. Evidence for filter-feeding by the wood-boring isopod, *Sphaeroma terebrans* (Crustacea: Peracarida). *Journal of Zoology 256,* 463–471. DOI 10.1017/S095283690200050X

SIDORCHUK, E.A. 2013. A new technique for the preparation of small-sized amber samples with application to mites. In: Azar, D., Engel, M.S., Jarzembowski, E.A., Krogmann, L., Nel, A. & Santiago-Blay, J.A. (eds) *Insect Evolution in an Amberiferous and Stone Alphabet*. Brill, Leiden, 189–201.

SKAWINA, A. 2021. Chapter 5 Evolutionary History of Bivalves. In: De Baets, K. & Huntley, J.W. (eds) *The Evolution and Fossil Record of Parasitism: Identification and Macroevolution of Parasites*. Springer International Publishing, Cham, Topics in Geobiology, 153–2007. DOI 10.1007/978-3-030-42484-8

SLOWIKOWSKI, K. 2019. *Ggrepel: Automatically position non-overlapping text labels with 'Ggplot2'*. R.

SMIT, N.J. & DAVIES, A.J. 2004. The curious life-style of the parasitic stages of gnathiid Isopods. *Advances in Parasitology 58,* 289–391. DOI https://doi.org/10.1016/S0065-308X(04)58005-3

SMIT, N.J., BASSON, L. & VAN AS, J.G. 2003. Life cycle of the temporary fish parasite, *Gnathia africana* (Crustacea: Isopoda: Gnathiidae). *Folia Parasitologica 50(2),* 135–142. DOI 10.14411/fp.2003.024

SOUTH, A. 2017. *Rnaturalearth: World Map Data from Natural Earth*.

STARCK, J.M., MEHNERT, L., BIGING, A., BJARSCH, J., FRANZ-GUESS, S., KLEEBERGER, D. & HÖRNIG, M. 2018. Morphological responses to feeding in ticks (Ixodes ricinus). *Zoological letters 4(1),* 1–19.

STEPIEN, C.A. & BRUSCA, R.C. 1985. Nocturnal attacks on nearshore fishes in southern California by crustacean zooplankton. *Marine Ecology Progress Series 25(1),* 91–105.

STINNESBECK, E.S., WÄGELE, J.W., HERDER, F., RUST, J. & STINNESBECK, W. 2022. A fish-parasitic isopod (Cymothoidae) on the pachyrhizodont *Goulmimichthys roberti* from the lower Turonian (Upper Cretaceous) Vallecillo plattenkalk, NE Mexico. *Cretaceous Research 129(105019)*. DOI 10.1016/j.cretres.2021.105019

SUTTON, M.D., RAHMAN, I.A. & GARWOOD, R.J. 2014. *Techniques for Virtual Palaeontology*. 200 pp. Wiley Blackwell, Hoboken, NJ; Chichester, West Sussex, New analytical methods in earth and environmental science.

TAIT, J. 1918. V.—Experiments and Observations on Crustacea: Part II. Moulting of Isopods. *Proceedings of the Royal Society of Edinburgh 37,* 59–68. DOI 10.1017/S0370164600023506

TANAKA, K. 2007. Life history of gnathiid isopods-current knowledge and future directions. *Plankton and Benthos Research 2(1),* 1–11. DOI 10.3800/pbr.2.1

TENNEKES, M. 2018. tmap: Thematic Maps in R. *Journal of Statistical Software 84(6),* 1–39. DOI 10.18637/jss.v084.i06

THAMBAN, A.P., KAPPALLI, S., KOTTARATHIL, H.A., GOPINATHAN, A. & PAUL, T.J. 2015. *Cymothoa frontalis*, a cymothoid isopod parasitizing the belonid fish *Strongylura strongylura* from the Malabar Coast (Kerala, India): redescription, description, prevalence and life cycle. *Zoological Studies 54,* 42. DOI 10.1186/s40555-015-0118-7

THING, C.Y., OTA, Y., HATAI, K. & RANSANGAN, J. 2015. Redescription of *Caecognathia coralliophila* (Monod, 1926) (Crustacea, Isopoda, Gnathiidae), collected from a fish hatchery in Sabah, Borneo Island, Malaysia. *Proceedings of the Biological Society of Washington 128(1),* 51–62. DOI 10.2988/0006-324X-128.1.51

TISCHLINGER, H. & ARRATIA, G. 2013. Ultraviolet light as a tool for investigating Mesozoic fishes, with a focus on the ichthyofauna of the Solnhofen archipelago. In: *Mesozoic Fishes – Global Diversity and Evolution.* Verlag Dr. Friedrich Pfeil, München, 549–560.

TORRES JORDÁ, M. 2003. *Estudio de La Relación Entre El Parásito* Leidya Distorta *(Isopoda: Bopyridae) y Su Hospedador* Uca Uruguayensis *(Brachyura: Ocypodidae), y Descripción de Los Estadíos Larvales de* L. Distorta. doctoral thesis, Universidad de Buenos Aires, 158 pp.

UPTON, N.P.D. 1987. Asynchronous male and female life cycles in the sexually dimorphic, harem-forming isopod *Paragnathia formica* (Crustacea: Isopoda). *Journal of Zoology 212(4),* 677–690. DOI 10.1111/j.1469-7998.1987.tb05964.x

UYE, S. & MURASE, A. 1997. Infertility of the planktonic copepod *Calanus sinicus* caused by parasitism by a larval epicaridian isopod. *Plankton Biology & Ecology 44(1/2),* 97–99.

VAN DER WAL, S. & HAUG, J.T. 2019. Letter to the editor referencing "The apparent kleptoparasitism in fish-parasitic gnathiid isopods" 10.1007/s00436-018-6152-8. *Parasitology Research 118(5),* 1679–1682. DOI 10.1007/s00436-019-06281-2

VAN DER WAL, S. & HAUG, J.T. 2020. Shape of attachment structures in parasitic isopodan crustaceans: the influence of attachment site and ontogeny. *PeerJ 8,* e9181. DOI 10.7717/peerj.9181

VAN DER WAL, S., SCHÄDEL, M., EKRT, B. & HAUG, J.T. 2021. Description and ontogeny of a 40-million-year-old parasitic isopodan crustacean: *Parvucymoides dvorakorum* gen. et sp. nov. *PeerJ 9(e1231),* 1–46. DOI 10.7717/peerj.12317

VÁSQUEZ-YEOMANS, L., MORALES, S., SUÁREZ-MORALES, E. & COHUO, J.A. 2011. *Eurydice personata* Kensley (Isopoda, Cirolanidae) on a Caribbean *Leptocephalus* fish larva: an intriguing case report. *Crustaceana 84(8),* 1013–1018. DOI 10.1163/001121611X584307

WÄGELE, J.-W. 1981. *Zur Phylogenie Der Anthuridea (Crustacea, Isopoda).* 127 pp. Schweizerbart, Stuttgart.

WÄGELE, J.-W. 1982. Isopoda (Crustacea: Peracarida) ohne Oostegite: Über einen *Microcerberus* aus Florida. *Mitteilungen des Zoologischen Museums der Universität Kiel 1(9),* 19–23.

WÄGELE, J.-W. 1985. Observations on nutrition and ultrastructure of digestive tract and fat body of the giant paranthurid *Accalathura gigantissima* Kussakin. *Polar Biology 4(1),* 33–43. DOI 10.1007/BF00286815

WÄGELE, J.W. 1987. The feeding mechanism of *Antarcturus* and a redescription of *A. spinacoronatus* Schultz, 1978 (Crustacea: Isopoda: Valvifera). *Philosophical Transactions of the Royal Society of London. B, Biological Sciences 316,* 429–458. DOI 10.1098/rstb.1987.0031

WÄGELE, J.W. 1988. Aspects of the life-cycle of the Antarctic fish parasite *Gnathia calva* Vanhöffen (Crustacea: Isopoda). *Polar Biology 8(4),* 287–291. DOI 10.1007/BF00263177

WÄGELE, J.-W. 1989. *Evolution und phylogenetisches System der Isopoda: Stand der Forschung und neue Erkenntnisse.* 262 pp. Schweizerbart, Stuttgart, Zoologica, 140 = Bd. 47.

WALTHER, J. 1904. Die Fauna der Solnhofener Plattenkalke. Bionomisch betrachtet. In: *Festschrift Zum Siebzigsten Geburtstage von Ernst Haeckel.* Gustav Fischer, Jena, 135–214. DOI 10.5962/bhl.title.142760

WANG, H., SCHÄDEL, M., SAMES, B. & HORNE, D.J. 2020. New record of podocopid ostracods from Cretaceous amber. *PeerJ 8,* e10134. DOI 10.7717/peerj.10134

WAPPLER, T., SMITH, V.S. & DALGLEISH, R.C. 2004. Scratching an ancient itch: an Eocene bird louse fossil. *Proceedings of the Royal Society of London. Series B: Biological Sciences 271(Suppl.),* S255–S258. DOI 10.1098/rsbl.2003.0158

WATLING, L. 1981. An Alternative Phylogeny of Peracarid Crustaceans. *Journal of Crustacean Biology 1(2),* 201–210. DOI 10.2307/1548159

WEDMANN, S., HÖRNSCHEMEYER, T., ENGEL, M.S., ZETTER, R. & GRÍMSSON, F. 2021. The last meal of an Eocene pollen-feeding fly. *Current Biology 31(9),* 2020-2026.e4. DOI 10.1016/j.cub.2021.02.025

WETZER, R. 1990. A new species of isopod, *Aega* (*rhamphion*) *francoisae* (Flabellifera: Aegidae), from the cloaca of an ascidian from the Galapagos Islands. *Proceedings of the Biological Society of Washington 103(3),* 655–662.

WHEATSTONE, C. 1838. On some remarkable, and hitherto unobserved, phenomena of binocular vision. *Philosophical Transactions of the Royal Society of London 128,* 371–394.

WHITE, P.S., MORRAN, L. & DE ROODE, J. 2017. Phoresy. *Current Biology 27(12),* R578–R580. DOI 10.1016/j.cub.2017.03.073

WICKHAM, H. 2007. Reshaping Data with the reshape Package. *Journal of Statistical Software 21(12).* DOI 10.18637/jss.v021.i12

WICKHAM, H. 2009. *Ggplot2: Elegant Graphics for Data Analysis.* 212 pp. Springer New York, New York, NY, Use R! DOI 10.1007/978-0-387-98141-3

WICKHAM, H., FRANÇOIS, R., HENRY, L. & MÜLLER, K. 2020. *Dplyr: A Grammar of Data Manipulation.* R.

WICKHAM, H., HESTER, J., FRANCOIS, R. 2021. *Readr: Read Rectangular Text Data.* R.

WIEDER, R.W. & FELDMANN, R.M. 1989. *Palaega goedertorum,* a fossil isopod (Crustacea) from late Eocene to early Miocene rocks of Washington State. *Journal of Paleontology 63(01),* 73–80. DOI 10.1017/S0022336000040981

WIEDER, R.W. & FELDMANN, R.M. 1992. Mesozoic and Cenozoic fossil isopods of North America. *Journal of Paleontology 66(6),* 958–972.

WIENBERG RASMUSSEN, H., JAKOBSEN, S.L. & COLLINS, J.S.H. 2008. Raninidae infested by parasitic Isopoda (Epicaridea). *Bulletin of the Mizunami Fossil Museum 34,* 31–49.

WILKE, C.O. 2020. *Ggtext: Improved Text Rendering Support for Ggplot2.* R.

WILLIAMS, J.D. & AN, J. 2009. The cryptogenic parasitic isopod *Orthione griffenis* Markham, 2004 from the eastern and western Pacific. *Integrative and Comparative Biology 49(2),* 114–126.

WILLIAMS, J.D. & BOYKO, C.B. 2012. The global diversity of parasitic isopods associated with crustacean hosts (Isopoda: Bopyroidea and Cryptoniscoidea). *PLoS One 7(4),* e35350. DOI 10.1371/journal.pone.0035350

WILSON, G.D. 1996. Of uropods and isopod crustacean trees: A comparison of 'groundpattern' and cladistic methods. *Vie et Milieu 46(2),* 139–154.

WILSON, G.D.F. 1991. THIRTEEN. Functional Morphology and Evolution of Isopod Genitalia. In: Bauer, R.T. & Martin, J.W. (eds) *Crustacean Sexual Biology.* Columbia University Press, New York, 228–245. DOI 10.7312/baue90796-014

WILSON, G.D.F. 2009. The phylogenetic position of the Isopoda in the Peracarida (Crustacea: Malacostraca). *Arthropod Systematics & Phylogeny 67(2),* 159–198.

WILSON, G.D.F., PATERSON, J.R. & KEAR, B.P. 2011a. Fossil isopods associated with a fish skeleton from the Lower Cretaceous of Queensland, Australia - direct evidence of a scavenging lifestyle in Mesozoic Cymothoida: Scavenging sopod Crustaceans from the Lower Cretaceous. *Palaeontology 54(5),* 1053–1068. DOI 10.1111/j.1475-4983.2011.01095.x

WILSON, G.D.F., SIMS, C.A. & GRUTTER, A.S. 2011b. Toward a taxonomy of the Gnathiidae (Isopoda) using juveniles: The external anatomy of *Gnathia aureamaculosa* zuphea stages using scanning electron microscopy. *Journal of Crustacean Biology 31(3),* 509–522. DOI 10.1651/10-3432.1

WITMER, L.M. & THOMASON, J.J. 1995. The extant phylogenetic bracket and the importance of reconstructing soft tissues in fossils. *Functional morphology in vertebrate paleontology 1,* 19–33.

WUNDERLICH, A.C., TRILLES, J.-P. & HATTORI, G.Y. 2011. A new host record, *Palaemonetes* Carteri (Gordon, 1935) (Decapoda, Palaemonidae), for *Telotha Henselii* (Von Martens, 1869) (Isopoda, Cymothoidae). *Crustaceana 84(11),* 1403–1409. DOI 10.1163/156854011X603794

XING, L., SAMES, B., MCKELLAR, R.C., XI, D., BAI, M. & WAN, X. 2018. A gigantic marine ostracod (Crustacea: Myodocopa) trapped in mid-Cretaceous Burmese amber. *Scientific Reports 8(1),* 1365. DOI 10.1038/s41598-018-19877-y

YAO, Y., CAI, W., XU, X., SHIH, C., ENGEL, M.S., ZHENG, X., ZHAO, Y. & REN, D. 2014. Blood-Feeding True Bugs in the Early Cretaceous. *Current Biology 24(15),* 1786–1792. DOI 10.1016/j.cub.2014.06.045

YU, T., KELLY, R., MU, L., ROSS, A., KENNEDY, J., BROLY, P., XIA, F., ZHANG, H., WANG, B. & DILCHER, D. 2019. An ammonite trapped in Burmese amber. *Proceedings of the National Academy of Sciences 116(23),* 11345–11350. DOI 10.1073/pnas.1821292116

ZELMER, D.A. 1998. An evolutionary definition of parasitism. *International Journal for Parasitology 28(3),* 531–533. DOI 10.1016/S0020-7519(97)00199-9

ZHANG, ZHIFEI, STROTZ, L.C., TOPPER, T.P., CHEN, F., CHEN, Y., LIANG, Y., ZHANG, ZHILIANG, SKOVSTED, C.B. & BROCK, G.A. 2020. An encrusting kleptoparasite-host interaction from the early Cambrian. *Nature Communications 11(1),* 2625. DOI 10.1038/s41467-020-16332-3

ZITTEL, K.A.V. 1887. *Traité de Paléontologie. Tome II, Partie I. Mollusca et Arthropoda.* Octave Doin, Paris.

5 Acknowledgements

I would like to express my gratitude to the German Research Foundaation (DFG, grant number DFG 6300/3-2) which funded most of the the research that became part of this thesis. I also have to thank the German Federal Employment Agency for providing me with a stable income during the last year of my studies, allowing me to continue my research and to work on the thesis itself.

I would like to thank Joachim T. Haug for supervising my doctoral studies and for many inspirational discussions and specifically for introducing me to a critical view on taxonomic practices. I thank Carolin Haug for helping me on many occasions with a variety of bureaucratic and personal problems. Carolin, together with Joachim, created a safe and friendly environment, which allowed for personal growth, for which I am very grateful. I would also like to thank my co-workers in the Haug lab, which filled the lab with people to which I could come with both academic as well as personal matters and which provided the much needed support I received over the four years of working on my doctoral project. I want to thank Matúš Hyžný for his help on the projects on which we worked together and for long and fruitful discussions, as well as for mediating in difficult situations with colleagues.

Much of the work that I conducted would not have been possible without the help of friendly and cooperative curators of natural history collections, including those housing their own personal collection in their spare time, many of which I met as members in the 'Steinkern' online forum. The publication of the manuscripts included in this thesis would not have been possible without the hard, but unpaid, work of reviewers and editors, for which I am very grateful. Annett Junginger and Oliver Betz (both University of Tübingen) provided me with a convenient work space and a social environment that I needed much during the time I worked living in Tübingen.

I would like to thank my family for providing me with much needed personal support and helping me with practical tasks during my time as a doctoral student. From my heart I thank Margarita Yavorskaya for her loving and caring support and her conceptual as well as practical help, without which, writing this dissertation would have been a much harder task.

7 Publication list

VAN DER WAL, S., **SCHÄDEL, M.**, EKRT, B., HAUG, J. T. 2021. Description and ontogeny of a 40-million-year-old parasitic isopodan crustacean: *Parvucymoides dvorakorum* gen. et sp. nov. *PeerJ*. https://doi.org/10.7717/peerj.12317

SCHÄDEL, M., HÖRNIG, M. K., HYŽNÝ, M., & HAUG, J. T. 2021. Mass occurrence of small isopodan crustaceans in 100-million-year-old amber: an extraordinary view on behaviour of extinct organisms. *PalZ*, 1-17. https://doi.org/10.1007/s12542-021-00564-9

SCHÄDEL, M., HYŽNÝ, M. & HAUG, J. T. 2021. Ontogenetic development captured in amber - the first record of aquatic representatives of Isopoda in Cretaceous amber from Myanmar. *Nauplius* 29, e2021003. https://doi.org/10.1590/2358-2936e2021003

HAUG, J. T., BARANOV, V., **SCHÄDEL, M.**, MÜLLER, P., GRÖHN, C., & HAUG, C. 2020. Challenges for understanding lacewings: how to deal with the incomplete data from extant and fossil larvae of Nevrorthidae?(Neuroptera). *Fragmenta entomologica* 52(2), 137-168. https://doi.org/10.13133/2284-4880/472

WANG, H., **SCHÄDEL, M.**, SAMES, B. & HORNE, D. J. 2020. New record of podocopid ostracods from Cretaceous amber. *PeerJ* 8:e10134. https://doi.org/10.7717/peerj.10134

SCHÄDEL, M. & HAUG J. T. 2020. A new interpretation of the enigmatic fossil arthropod *Anhelkocephalon handlirschi* Bill, 1914 – important insights in the morphology of Cyclida. *Palaeodiversity* 13, 69–81. https://doi.org/10.18476/pale.v13.a7

SCHÄDEL, M., VAN ELDIJK, T., WINKELHORST, H., REUMER, J. W. F. & HAUG, J. T. 2020. Triassic Isopoda – three new species from Central Europe shed light on the early diversity of the group. *Bulletin of Geosciences* 95(2). https://doi.org/10.3140/bull.geosci.1773

HAUG, J. T., **SCHÄDEL, M.**, BARANOV, V. A. & HAUG, C. 2020. An unusual 100-million-year old holometabolan larva with a piercing mouthcone. *PeerJ* 8, e8661. https://doi.org/10.7717/peerj.8661

SCHÄDEL, M., MÜLLER, P. & HAUG J. T. 2020. Two remarkable fossil insect larvae from Burmese amber suggest the presence of a terminal filum in the direct stem lineage of dragonflies and damselflies (Odonata). *Rivista Italiana di Palaeontologia e Stratigrafia* 126(1), 13-35. https://doi.org/10.13130/2039-4942/12720

BARANOV, V. A., **SCHÄDEL, M.** & HAUG, J. T. 2019. Fly palaeo-evo-devo: immature stages of bibionomorphan dipterans in Baltic and Bitterfeld amber. *PeerJ* 7:e7843. https://doi.org/10.7717/peerj.7843

SCHÄDEL, M., PERRICHOT, V. & HAUG, J. T. 2019. Exceptionally preserved cryptoniscium larvae - morphological details of rare isopod crustaceans from French Cretaceous Vendean amber. *Palaeontologia Electronica*, 22.3.71, 1-45. https://doi.org/10.26879/977

BRAIG, F., HAUG, J. T., **SCHÄDEL, M.** & HAUG, C. 2019. A new thylacocephalan crustacean from the Upper Jurassic lithographic limestones of southern Germany and the diversity of Thylacocephala. *Palaeodiversity* 12, 69–87. https://doi.org/10.18476/pale.v12.a6

SCHÄDEL, M., PAZINATO, P. G., VAN DER WAL, S. & HAUG, J. T. 2019. A fossil tanaidacean crustacean from the Middle Jurassic of southern Germany. *Palaeodiversity* 12, 13–30. https://doi.org/10.18476/pale.v12.a2

SCHÄDEL, M. & LECHNER, T. S. 2017. Two new dragonflies (Odonata: Anisoptera) from the Miocene of Carinthia (Austria). *Zootaxa*, 4243(1), 153-164. https://doi.org/10.11646/zootaxa.4243.1.7

SCHÄDEL, M. & BECHLY, G. 2016. First record of Anisoptera (Insecta: Odonata) from mid-Cretaceous Burmese Amber. *Zootaxa*, 4103(6), 537-549. https://doi.org/10.11646/zootaxa.4103.6.4

8   Conference contributions

SCHÄDEL, M. HYŽNÝ, M., NAGLER, C. & HAUG, J. T. 2021. Close relatives of extant parasitic forms of crustaceans from the Mesozoic of Europe. 92th *Annual Meeting of the Paläontologische Gesellschaft*, Vienna, 27.09.2021–01.10.2021 (talk)

SCHÄDEL, M. HYŽNÝ, M. & HAUG, J. T. 2019. From a systematic waste basket to the fossil record of giant isopods. *Annual Meeting of the Palaeontological Association*, Valencia, 19.12.2019–20.12.2019. (poster)

SCHÄDEL, M. & LECHNER, T. S. 2019. Schaßbach – eine neue Fundstelle für gut erhaltene Insektenfossilien aus dem Miozän von Kärnten (Österreich). Schaßbach – a new field site for well preserved insect fossils from the Miocene of Carinthia (Austria). *Palaeoentomology meeting*, Frankfurt am Main, 25.10.2019–27.10.2019 (talk)

SCHÄDEL, M. HYŽNÝ, M. & HAUG, J. T. 2019. How to dispose a systematic waste basket – Revision of the fossil isopod form genus "Palaega". 90th *Annual Meeting of the Paläontologische Gesellschaft*, Munich, 15.09.2019–18.09.2019 (talk)

SCHÄDEL, M. & LECHNER, T. S. 2019. Schaßbach - A new locality for abundant and well preserved fossil insects from the Miocene of Carinthia (Austria). 90th *Annual Meeting of the Paläontologische Gesellschaft*, Munich, 15.09.2019–18.09.2019 (poster)

SCHÄDEL, M. HYŽNÝ, M. & HAUG, J. T. 2019. Upper Cretaceous misfits – cirolanid-like isopodans in Burmese Amber. *International Conference on Fossil Insects, Arthropods & Amber*, St. Domingo, 07.04.2019–11.04.2019 (talk)

SCHÄDEL, M. & HAUG, J. T. 2019. New insights in the character evolution in the lineage towards modern dragonflies and damselflies. *20th Annual Meeting of the Society for Biogical Systematics, Jahrestagung der Gesellschaft für Biologische Systematik*, München, 24.04.2019–27.04.2019 (poster)

SCHÄDEL, M., MÜLLER, P. & HAUG, J. T. 2018. 100 million years old insect larvae shed light on the ancestral morphology of Odonata (dragonflies and damselflies). Annual meeting of the German Zoological Society (DZG), Greifswald, 10.09.2018–.09.2018 (talk)

SCHÄDEL, M., MÜLLER, P. & HAUG, J. T. 2018. Fossil aquatic insect larvae in Burmese amber with important implications on the ground pattern of Odonata (dragonflies

and damselflies). *GeoBonn* (Annual meeting of the Paläontologische Gesellschaft), Bonn, 02.09.2018–06.09.2018 (talk)

SCHÄDEL, M., PERRICHOT, V. & HAUG, J. T. 2018. Marine larvae in Cretaceous amber-important insight into the evolution of parasitic life habits of epicaridean isopods. *GeoBonn* (Annual meeting of the Paläontologische Gesellschaft), Bonn, 02.09.2018– 06.09.2018 (poster)

SCHÄDEL, M., PERRICHOT, V. & HAUG, J. T. 2018. Marine life captured in amber - Exceptional preservation of small aquatic isopod larvae in Cretaceous amber from France. *5th International Paleontological Congres*s, Paris, 09.10.2018–13.10.2018 (talk)

SCHÄDEL, M., VAN ELDIJK, T. & HAUG, J. T. 2018.Isopod diversity in deep time-Assessing the morphological diversity of isopod crustaceans back in the Triassic. 5t*h International Paleontological Congress*, Paris, 09.10.2018–13.10.2018 (poster)

SCHÄDEL, M., PERRICHOT, V. & HAUG, J. T. 2018. Exceptionally Preserved Fossils of Minute Infective Larvae – 90 Million Years Old Window Into the Evolution of the Parasitism of Epicaridean Isopods. *9th International Crustacean Congress*, Washington (DC), 22.05.2018–25.05.2018 (talk)

SCHÄDEL, M., NAGLER, C. & HAUG, J. T. 2018.Taking a Deeper Look-A Fossil Isopod Revisited By 'Virtual Paleontology'. *9th International Crustacean Congress*, Washington (DC), 22.05.2018–25.05.2018 (poster)